

GEOLOGICA HUNGARICA

FASCICULI INSTITUTI GEOLOGICI HUNGARIAE
AD ILLUSTRANDAM NOTIONEM GEOLOGICAM
ET PALAEONTOLOGICAM

SERIES GEOLOGICA

TOMUS 24

Editors:

LÁSZLÓ ÓDOR and RICHARD B. MCCAMMON

**DEPOSIT MODELING AND MINING-INDUCED ENVIRONMENTAL
RISKS**

Editors:

LÁSZLÓ KORPÁS and ALBERT H. HOFSTRA

CARLIN GOLD IN HUNGARY

BUDAPEST, 1999

©Copyright Geological Institute of Hungary, 1999
All rights reserved

Revised by

L. KORPÁS, L. ÓDOR, R. B. MCCAMMON and A. H. HOFSTRA

Technical edition and DTP by

PÁL KASZAI

Published by the Geological Institute of Hungary
H-1143 Budapest, Stefánia út 14., Hungary

Responsible editor
KÁROLY BREZSNYÁNSZKY
director

HU ISSN 0367-4150
ISBN 963 671 222 0



CONTENTS

Contents	3
Preface	15
Introduction	17
About the participants of the projects	19
PROJECT J. F. NO. 415: DEPOSIT MODELING, ASSESSMENT OF MINERAL RESOURCES AND MINING-INDUCED ENVIRONMENTAL RISKS	25
R. B. MCCAMMON–L. ÓDOR: Deposit modeling, assessment of mineral resources and mining-induced environmental risks	27
Abstract	27
1. Introduction	27
2. Assessment of undiscovered deposits	27
3. Mineral-deposit models	28
4. Assessment of undiscovered deposits in the Mátra, Börzsöny and Visegrád Mountains, Northern Hungary	28
5. Geoenvironmental models	28
6. Environmental signatures of mineral deposits	29
7. Conclusions	29
8. Acknowledgements	29
9. References	29
L. J. DREW–D. A. SINGER–W. D. MENZIE–B. R. BERGER: Mineral-resource assessment – state of the art	31
Abstract	31
1. Introduction	31
2. The body of literature	32
3. Recent developments	33
3.1. A metric for mineral-deposit occurrence probabilities	33
3.2. Application of neural network analysis	35
3.3. Analysis of favorable regions within permissive terranes	35

3.4. Computation of economic cost filters	36
4. Conclusion	38
5. References	38
B. R. BERGER–L. J. DREW–D. A. SINGER: Quantifying mineral-deposit models for resource assessment	41
Abstract	41
1. Introduction	41
2. A frame of thinking about mineral deposits	42
3. Improving the predictive capabilities of models	43
3.1. Lithotectonic terranes	43
3.1.1. Current USGS approach to regional classification	44
3.1.2. Example of lithotectonic terrane: Magmatic arcs	44
3.2. Dynamic deposit landscapes	46
3.2.1. A hypothetycal landscape/dynamics model	46
3.2.2. Implications of the hypothetical model for mineral-resource assessment	48
3.3. Quantified mineral-deposit model attributes	51
3.3.1. Frequency of occurrence of deposit attributes	51
3.3.2. Metrics that predict associated (linked) deposit types	52
4. Conclusions	52
5. References	53
GY. CSIRIK–L. ÓDOR–J. KISS–S. RÓZSAVÖLGYI: Regional geologic, geophysical, and geochemical data used in the assessment of undiscovered deposits in the Mátra, Börzsöny and Visegrád Mountains, Northern Hungary	55
Abstract	55
1. Location	55
2. Geologic data	55
3. Geophysical data	55
3.1. Aerial magnetic data	57
3.2. Gravity data	57
4. Regional geochemical data	60
4.1. Mátra Mountains	60
4.2. Börzsöny Mountains	60
5. Low density national geochemical survey	60
6. Stream sediment geochemical survey	61
7. Summary	61
8. References	62
É. VETŐ-ÁKOS: Alpine deposit models for the Mátra and Börzsöny Mts. Northern Hungary	63
Abstract	63
1. Introduction	63

2. Geotectonic setting and Alpine mineralization in the Carpathian realm	65
3. Alpine mineralization in Hungary	66
3.1. Mátra Mountains	67
3.1.1. Geological setting	67
3.1.2. Paleogene mineralizations	67
3.1.2.1. Epithermal high sulfidation Au-Cu deposit of Recsk-Lahóca	67
3.1.2.2. Base metal deposit "Recsk-deep"	70
3.1.2.3. Porphyry copper deposit "Recsk-deep"	70
3.1.2.4. Cu-Zn-skarn and replacement deposit "Recsk-deep"	70
3.1.3. Neogene mineralizations	70
3.1.3.1. Base metal deposit of GyöngyöSOROSZI	70
3.1.3.2. Geochemistry and rock alterations	71
3.1.3.3. Ore controls	72
3.2. Börzsöny Mountains	72
3.2.1. Geological setting	72
3.2.2. Neogene mineralizations	74
3.2.2.1. Epithermal low sulfidation precious and base metal deposit of Kuruc-patak-Rózsa-hegy-Bánya-puszta	74
3.2.2.2. Geochemistry and rock alterations	74
3.2.2.3. Ore controls	75
4. Conclusions	75
5. References	76
L. J. DREW–B. R. BERGER–W. J. BAVIEC–D. M. SUTPHIN–GY. CSIRIK–L. KÖRPÁS– É. VETŐ-ÁKOS–L. ÓDOR–J. KISS: Mineral-resource assessment of the Mátra and Börzsöny–Visegrád Mountains, North Hungary	79
Abstract	79
1. Introduction	79
2. Mineral-deposit models	79
3. Tectonic model of porphyry copper/polymetallic vein kin-deposit system	82
4. Geological setting and tectonic history of the study area	86
5. Assessment of the undiscovered deposits in the study area	87
5.1. Previous exploration data	87
5.2. Assessment of the Mátra Mountains	90
5.3. Assessment of the Börzsöny and Visegrád Mountains	92
6. Aggregate resource estimates	92
7. Conclusions	94
8. References	94
R. B. WANTY–B. R. BERGER–G. S. PLUMLEE: Environmental models of mineral deposits a state of the art	97
Abstract	97

1. What is the problem?	97
1.1. Enhancement of weathering rates by mining	98
1.2. Natural and manmade contamination of the environment	99
2. How have we tried to solve it in the past?	99
2.1. Acid-base accounting	99
2.2. Geoenvironmental maps	99
2.3. Geoenvironmental models	101
3. Uses for geoenvironmental models	102
4. New directions	102
5. How are these models generated?	103
6. Conclusions	104
7. References	104
L. ÓDOR–R. B. WANTY–I. HORVÁTH–U. FÜGEDI: Environmental signatures of mineral deposits and areas of regional hydrothermal alteration in Northeastern Hungary	107
Abstract	107
1. Introduction	107
2. General definitions	108
3. Methods and area description	108
4. Geochemical background based on a low-density survey	108
5. Environmental signatures of mineral deposits using stream sediment surveys for Northern Hungary ...	110
5.1. Zemplén Mountains	110
5.1.1. Polymetallic veins, hot-spring precious metals and Hg mineralizations	110
Geological setting, results of earlier investigations	110
Deposit models	110
5.1.2. Stream sediment survey of the Zemplén Mountains	111
5.1.3. Environmental considerations	112
Environmental effects	112
Potential environmental considerations	116
5.2. Mátra Mountains	118
5.2.1. Polymetallic veins, volcanic-hosted Cu, porphyry copper and Cu-Zn-Pb skarn mineralizations	118
Geological setting, main results of earlier investigations	118
Deposit models	118
5.2.2. Stream sediment survey of the Mátra Mountains	118
5.2.3. Environmental considerations	119
Environmental effects	119
Potential environmental considerations	123
5.3. Börzsöny Mountains	123
5.3.1. Polymetallic veins and replacement mineralizations	123

Geological setting and main results of earlier investigations	123
Deposit models	123
5.3.2. Stream sediment survey of the Börzsöny Mountains	124
5.3.3. Environmental considerations	124
Environmental effects	124
Potential environmental considerations	126
6. Conclusions	126
7. References	127
PROJECT J. F. NO. 435: POTENTIAL FOR CARLIN-TYPE GOLD DEPOSIT IN HUNGARY	131
L. KORPÁS–A. H. HOFSTRA: Potential for Carlin-type gold deposit in Hungary	133
Abstract	133
1. Model for Carlin-type gold deposits	133
2. The development of the Carlin gold project in Hungary	133
3. Geological and tectonic models	133
4. The Carlin gold potential of Hungary	134
5. Conclusions	134
6. Acknowledgements	134
7. References	134
A. H. HOFSTRA: Descriptive model of Carlin-type gold deposits	137
1. Introduction	137
2. Overview	137
3. Origin of the Carlin Trend and Battle Mountain–Eureka Trend	139
4. Mineral association and transfer	140
5. Methods of exploration	145
6. Genesis and model of the deposits	145
7. Bibliography	146
L. KORPÁS–A. H. HOFSTRA–L. ÓDOR–I. HORVÁTH–J. HAAS–J. LEVENTHAL: The Carlin gold project in Hungary (1995–1998)	151
Abstract	151
1. Introduction	151
2. Preliminary evaluation–geological and geochemical criteria	152
3. Project developments	165
4. References	166
É. BERTALAN–A. BARTHA: Analytical background of Carlin-type gold prospection in Hungary	169
Abstract	169
1. Introduction	169
2. Instrumentation	170
3. Chemicals and reagents	170

4. Analytical methods	171
4.1. Sample decomposition methods	171
4.2. ICP-MS determinations	171
4.3. Analysis of gold	172
4.4. Analysis of mercury	172
4.5. ICP-OES determinations	174
4.6. Analysis of arsenic and antimony	174
4.7. Analysis of silver	174
5. Comparison with different analytical methods	175
6. Conclusion	178
7. References	178
J. HAAS–G. HÁMOR–L. KÖRPÁS: Geological setting and tectonic evolution of Hungary	179
Abstract	179
1. Introduction	180
2. Tectonic setting and stages of evolution	180
2.1. Pre–Alpine evolution	180
2.2. Alpine evolution	183
2.2.1. Pre–rifting stage (P ₃ –T ₂)	184
2.2.2. Rifting stage (T ₂)	184
2.2.3. Stabilisation of the passive margins (T ₃)	184
2.2.4. Late rifting stage (J ₁₋₂)	186
2.2.5. Early Tethys subduction and collision stage (J ₃ –Cr)	186
2.2.6. Late Tethys subduction and collision stage, formation of the Paratethys Basins (E–O)	188
2.2.7. Pannonian basin stage (M–Q)	188
3. Conclusions	194
4. References	194
L. KÖRPÁS–A. H. HOFSTRA–L. ÓDOR–I. HORVÁTH–J. HAAS–T. ZELENKA: Evaluation of the prospected areas and formations	197
Abstract	197
1. Introduction	197
2. Main features of our geochemical treatment	197
2.1. Processing of the data	198
2.2. Anomaly patterns of the stream sediment surveys	198
3. Description of the prospected areas and formations	214
3.1. Kőszeg Mountains	214
3.1.1. Mesozoic	214
3.1.1.1. Jurassic	214
Kőszeg Quartz Phyllite (37)	214

Cák Conglomerate (38)	217
Velem Calc Phyllite (39)	217
3.1.1.2. Cretaceous	217
Felsőcsatár Greenschist (40)	217
Summary for the Kőszeg Mountains	218
3.2. Transdanubian Range	218
3.2.1. Palaeozoic	218
3.2.1.1. Ordovician-Silurian-Devonian	218
Balatonfőkajár Quartz Phyllite (41)	218
Lovas Slate (42)	220
Litér Metabasalt (43)	220
Úrhida Limestone (44)	227
Polgárdi Limestone (1)	227
3.2.1.2. Carboniferous	227
Szababattyán Limestone (45)	227
Füle Conglomerate (46)	228
Velence Granite (47)	228
3.2.2. Mesozoic	229
3.2.2.1. Triassic	229
Hidegkút Formation (48)	229
Csopak Marl (8)	229
Aszófő Dolomite (9)	229
Iszkahegy Limestone (10)	230
Megyehegy Dolomite (11)	230
Budaörs Dolomite (49)	230
Vashegy Dolomite (50)	231
Felsőörs Limestone (12)	231
Buchenstein Formation (13)	231
Füred Limestone (14)	232
Veszprém Marl (15)	232
Mátyáshegy Formation (16)	233
Sándorhegy Formation (17)	233
Fődolomit Formation (51)	234
Rezi Dolomite (19)	234
Kössen Formation (20)	234
Feketehegy Formation (21)	235
Dachstein Limestone (52)	235
3.2.2.2. Triassic–Jurassic	236

Csövár Limestone (18)	236
3.2.2.3. Jurassic	236
Pisznice Limestone (53)	236
Úrkút Manganese Ore (33)	237
Kisgerecse Marl (54)	238
Eplény Limestone (55)	238
Lókút Radiolarite (56)	238
3.2.2.4. Cretaceous	239
Budakeszi Picrite (57)	239
3.2.3. Cenozoic	239
3.2.3.1. Cretaceous–Eocene	239
Bauxite Formation (58)	239
3.2.3.2. Eocene	239
Nadap Andesite (59)	239
Szépvölgy Limestone (60)	240
3.2.3.3. Eocene–Oligocene	240
Buda Marl (34)	240
3.2.3.4. Oligocene	241
Tard Clay (35)	241
Hárshegy Sandstone (36)	241
Mány Formation (61)	242
3.2.3.5. Miocene	242
Börzsöny and Visegrád Andesite (62)	242
Kálla Gravel (63)	243
Zámor Gravel (64)	243
Szák Marl (65)	243
3.2.3.6. Pliocene–Pleistocene	243
Travertine Formation. (66)	243
Summary for the Transdanubian Range	244
3.3. Mecsek Mountains	249
3.3.1. Mesozoic	249
3.3.1.1. Triassic	249
Patacs Siltstone (67)	249
Hetvehely Dolomite (27)	249
Lapis Limestone (28)	250
Zuhánya Limestone (29)	250
Csukma Formation / Kozár Limestone (30)	250
Kantavár Formation (31)	253

3.3.1.2. Triassic–Jurassic	253
Mecsek Coal (68)	253
3.3.1.3. Jurassic	254
Vasas Marl (69)	254
Hosszúhetény Marl (70)	254
Mecseknádasd Sandstone (71)	254
Óbánya Siltstone (32)	255
Summary for the Mecsek Mountains	255
3.4. Northeastern Range	257
3.4.1. Palaeozoic	257
3.4.1.1. Silurian–Devonian–Carboniferous	257
Tapolcsány Formation (4)	257
Strázsahegy Formation (72)	257
Irota Formation (73)	258
Szendrőlád Limestone (2)	258
Uppony Limestone (3)	258
Abod Limestone (74)	263
Szendrő Phyllite (75)	263
Rakaca Marble (76)	263
Lázberc Formation (77)	263
Szilvásvár Formation (6)	264
Mályinka Formation (6)	264
Tarófő Conglomerate (78)	264
3.4.1.2. Permian	265
Perkupa Anhydrite (79)	265
Szentlélek Formation (80)	265
Nagyvisnyó Limestone (5)	265
3.4.2. Mesozoic	266
3.4.2.1. Triassic	266
Gerennavár Limestone (81)	266
Ablakoskővölgy Limestone (82)	266
Rudabánya Iron Ore (7)	266
Gutenstein Dolomite (24)	267
Bodvarákó Formation (25)	268
Tornaszentandrás Shale (26)	268
Hámor Dolomite (22)	268
Szentistvánhegy Metaandesite (83)	268
Parád Complex (84)	268

Fehérkő Limestone (85)	269
Berva Limestone (86)	269
Szinva Metabasalt (87)	270
Kisfennsík Limestone (88)	270
Vesszős Shale (23)	270
Felsőtárkány Limestone (89)	270
Répáshuta Limestone (90)	271
Rónabükk Limestone (91)	271
3.4.2.2. Jurassic	271
Darnóhegy Shale (92)	271
Darnó Radiolarite (93)	272
Szarvaskő Basalt (94)	272
Bányahegy Radiolarite (95)	272
Lökvölgy Shale (96)	273
Mónosbél Formation (97)	273
Oldalvölgy Formation (98)	273
3.4.3. Cenozoic	274
3.4.3.1. Miocene	274
Edelény Clay (99)	274
3.4.3.2. Holocene	274
Rudabánya Mine Dump (100)	274
Martonyi Mine Dump (101)	274
Summary for the Northeastern Range	274
4. Discussion	278
4.1. Establishing anomaly thresholds	279
4.2. Influence of certain factors on the distribution of elements	280
4.2.1. Lithology	282
4.2.2. Geological age	283
4.2.3. Geotectonic position	283
5. Perspective areas and formations for further explorations	284
5.1. Velence Hills–Balatonfő area, Transdanubian Range	287
5.1.1. Velence Hills	287
5.1.2. Balatonfő	287
5.2. Darnó Zone area, Northeastern Range	287
5.2.1. Rudabánya Mountains	287
5.2.2. Recsk area	288
5.2.3. Uppony Mountains	288

5.2.4. Szendrő Mountains	288
5.3. East Alpine units in West Hungary	288
6.3.1. Vas-hegy, Transdanubia	288
5.3.2. Kőszeg Mountains, Transdanubia	288
5.4. Pilis Mountains, Transdanubian Range	289
5.5. Mecsek Mountains, Transdanubia	289
6. Conclusions	289
7. References	289
A. H. HOFSTRA–L. KORPÁS–I. CSALAGOVITS–C. A. JOHNSON–W. D. CHRISTIANSEN: Stable isotopic study of the Rudabánya iron mine. A carbonate-hosted siderite, barite, base-metal sulfide replacement deposit	295
Abstract	295
1. Introduction	295
2. Geologic setting and tectonic evolution	297
3. Deposit description	297
4. Stable isotopes	298
5. Processes of ore formation	300
6. Summary	301
7. References	301
Appendix	303

PREFACE

Ten years ago, on October 4, 1989 the US and Hungarian governments signed a new agreement on scientific and technological cooperation, in which the two countries agreed to contribute equal amounts of financial support annually for establishing a joint fund.

The bilateral agreement stipulates the purpose of the US-Hungarian Science and Technology Joint Fund to encourage and support a wide range of scientific and technological cooperation between the two countries, based on the principles of equality, reciprocity, and mutual benefit. International science and technology cooperation, the agreement states, would strengthen the bonds of friendship and understanding between the US and Hungarian scientific communities and would advance the state of science and technology to the benefit of both countries, as well as mankind generally.

Within the scope of the bilateral program, US and Hungarian scientists may receive support from the Fund for (1) cooperative research projects, (2) bilateral scientific symposia and (3) project development visits. Researchers from US and Hungarian governmental agencies, scientific institutes and societies, universities, and other national research and development centers are eligible to apply for Joint Fund support. Applications to the Joint Fund must propose collaborative US-Hungarian scientific research and/or technological development activity, involving researchers from both countries. All projects must contribute to the advancement of mutually beneficial scientific knowledge. Research results must be publishable in open source journals.

The resources of the Joint Fund has been allocated among mutually agreed priority areas as follows:

Basic Sciences	20%
Environmental Protection	20%
Biomedical Sciences	14%
Agriculture	14%
Engineering	14%
Energy and Natural Resources	14%
Others	4%

Total number of the supported projects is nearly 300, while the amount of the distributed grant payments between 1990 and 1998 comes to almost 550 million HUF and more than 5 million USD, respectively.

Earth sciences (geology and geophysics) were represented between 1990 and 1998 by 19 projects with a financial support of about 28 million HUF and 370,000 USD. The cooperating institutions have been the following: Eötvös Loránd Geophysical Institute, Eötvös Loránd University, Geological Institute of Hungary, Hungarian Academy of Sciences, Hungarian Geological Survey, National Oil and Gas Company Ltd. from Hungary, and Defense Mapping Agency, Halliburton Logging Services, Howard University, Ohio State University, United States Bureau of Mines, United States Geological Survey, University of Wisconsin, Virginia Polytechnic Institute, from the USA. The number of the participating investigators from both side amounts to 100. The investigations cover a broad range of topics, including sedimentology, stratigraphy, geochemistry, mineral exploration, deposit modeling, hydrogeology, ecology and environment, gravimetry, geomagnetism, well logging and geographical information system.

The Geological Institute of Hungary and the United States Geological Survey have played a decisive role in the cooperation. A great part of the projects above were carried out by researchers of both institutions and two of those are the subject of the present volume. The Joint Fund Project 415 entitled "Deposit modeling, assessment of

mineral resources and mining-induced environmental risks” integrates both the results of quantitative assessment for undiscovered ore deposits in NE Hungary, and at the same time the ways to predict and prevent the environmental effects and risks induced by mining. The Carlin gold project (“Potential for Carlin-type gold deposit in Hungary, Joint Fund Project No. 435”) summarizes how can the experiences and results of US researchers be applied in the exploration of unknown and undiscovered gold deposits in Hungary.

This special issue is a milestone in the history of the US-Hungarian Joint Fund. As a first publication supported by the Joint Fund it commemorates worthily the 10th anniversary of its establishment.

Budapest, 4th of October, 1999.

Dr. István Takács
Hungarian co-chairman of
the US–Hungarian Science and Technology Joint Board

INTRODUCTION

It was 84 years ago, in 1915 that the first volume of *Geologica Hungarica* was published as a "Bulletin for the acquaintance of geology and paleontology of the Hungarian Empire". The aim of its authors and editors (formulated in German) is valid up to the present: "Publication in close translation of summing up works in foreign languages in order to make the results of our activities understood and taken into consideration all over the world." 76 volumes of the series have since appeared more or less regularly. Since 1928 paleontological descriptions and studies have been separately published in Series *Palaeontologica* and geological monographs have appeared in Series *Geologica*. 53 volumes of Series *Palaeontologica* have been published, the last one came out in 1992. 23 volumes of Series *Geologica* have come out since that time, the last one was published in 1986.

Since to be founded in 1896 the early nineties of this century resulted to be one of the most conflictive periods of our Institute. Radical changes in profile, organization and reduction of staff have occurred. After that painful transformation our Institute became a modern, capable survey ready to face the challenges of the new century. In our new publishing strategy the two Series of *Geologica Hungarica* are destined to bring out the most outstanding scientific results of our activity in form of both articles or monographs.

Tradition and renewal are the keywords of this series restarted now at the turn of the century. The rich heritage of our past is preserved and taken care of, we rely on it and take courage from it. The new challenges of the changing and more and more globalising environment are continuously testing our readiness and ability for renewal. Is it possible to preserve the capacity of the Earth to maintain mankind? Can we balance the use of natural resources available to us? Are we ready to protect and rehabilitate the state and values of our environment? As geologists, our responsibility is increased because we know it very well that the geological environment is a determining factor of our existence. We know that in this environment irreversible harmful processes have already been generated from time to time measurable even in our individual lifetime. The recognition of these facts and the formulation of new answers are not enough in themselves. Our permanent aim is to help society to recognise these facts and accept the conclusions.

This volume summarises the results of investigations carried out by Hungarian and American researchers in the period 1994–1998. During the last decade the US–Hungarian Joint Fund as the only supporter of common geological investigations helped a lot in the realisation of the projects of the Geological Institute of Hungary (MÁFI) and it helped to gain new experiences to the United States Geological Survey (USGS) scientists. But this is the first occasion that the results of these common researches by Hungarian (MÁFI) and American (USGS) co-authors appear collected in the *Geologica Hungarica* reflecting the ideas of the editors who started the Series. This collection of papers contains the results of two projects. One is Joint Fund No. 415 project: "Deposit modeling, assessment of mineral resources and mining-induced environmental risks" (1994–1998), and the other is JFNo. 435 project: "Potential for Carlin-type gold deposit in Hungary" (1995–1998).

The leaders of the project "Deposit modeling, assessment of mineral resources and mining-induced environmental risks" were László ÓDOR and Richard B. MCCAMMON. Hungarian participants and USGS counterpart scientists were: György CSIRIK, Éva VETŐ-ÁKOS, Byron R. BERGER, Lawrence J. DREW, Richard B. WANTY and Walter J. BAWIEC. Co-authors of the contributions were: István HORVÁTH, Ubul FÜGEDI, László KORPÁS, János KISS, Sándor RÓZSAVÖLGYI, W. David MENZIE, Geoffrey S. PLUMLEE, Donald A. SINGER and David M. SUTPHIN. A wide range of geologic, petrographic and mineralogic data were used to prepare mineral deposit models. A pilot mineral-resource assessment for a study area in north-central Hungary was used to transfer the assessment

methodology from the USGS to the MÁFI. Environmental effects of old and recent mining activities were investigated using the new concepts of geoenvironmental models.

Leaders of the other project: "Potential for Carlin-type gold deposit in Hungary" were László KORPÁS and Albert H. HOFSTRA. Hungarian participants and USGS counterpart scientists were: László ÓDOR, István HORVÁTH, János HAAS, György CSIRIK and Joel S. LEVENTHAL. Co-authors of the contributions were: Éva BERTALAN, Géza HÁMOR, Tibor ZELENKA, Imre CSALAGOVITS, András BARTHA, William D. CHRISTIANSEN and Craig A. JOHNSON. The analytical data were arranged in data bases by Sándor LAJTOS. The contributions are summarising how the experiences of the American researchers could be used and applied in the study of the potential of a so far unknown and not investigated type of mineralization in Hungary, that is the Carlin-type gold.

Finally I would like to express my thanks for the support of the US–Hungarian Science & Technology Joint Fund given to our investigations. Thanks are also due to the participants for their successful work. It is our belief that the publication in English of the results of these investigations promoted the geological knowledge of Hungary both here and abroad.

Budapest, 14th of September, 1999.

Károly Brezsnayánszky
Director

ABOUT THE PARTICIPANTS OF THE PROJECTS



László ÓDOR was the leader and one of the Hungarian Counterpart Scientists for the US-Hungarian Joint Fund Projects 415 (Deposit modeling, assessment of mineral resources and mining-induced environmental risks) and 435 (Potential for Carlin-type gold deposit in Hungary). He has now retired, was employed at the Hungarian Geological Survey from 1966 to 1999. Born in 1938 he studied geology at the Eötvös Loránd University of Budapest, graduated in 1961. Spent one year in the USA, studying at the University of Minnesota. Started working at the Hungarian Geological Survey in 1966, taking part in a survey for rare elements. Spent one year in Mongolia, doing geological mapping. Participated in research going on in the Great Hungarian Plain. Worked with hydrocarbon prognostics for mountainous regions. Spent many years with geological and geochemical research of the Velence–Balatonfő region. In recent years was leader of a geochemical project dealing with low density and stream sediment surveys. His main interest has been environmental geochemistry: the establishing of baseline values, the study of the effects of recent and historical ore mining.



Dr. Richard B. MCCAMMON was the co-leader and one of the US Counterpart Scientists for the US-Hungarian Joint Fund Project 415 on Deposit modeling, assessment of mineral resources and mining-induced environmental risks. Dr. MCCAMMON, now retired, was employed at the US Geological Survey from 1975 to 1998. During his career, Dr. MCCAMMON was active in regional mineral resource assessments, multivariate methods applied to resource assessment, and application of computers in geology. He served as Chief of the Branch of Resource Analysis from 1992 to 1995 and was Project Chief of the 1998 National Mineral Resource Assessment. Dr. MCCAMMON served as President of the International Association for Mathematical Geology and in 1992 received the William Christian Krumbein Medal. He was Editor of *Mathematical Geology* and the founding Editor of *Nonrenewable Resources*. Most recently, he was a Co-Director of the NATO Advanced Study Institute on Deposit and Geoenvironmental Models for Resource Exploitation and Environmental Security held September 6-18, 1998, Mátraháza, Hungary.



I, **Dr. Byron R. BERGER** was one of the US Counterpart Scientists for the US-Hungarian Joint Fund Project 415 on Deposit modeling, assessment of mineral resources and mining-induced environmental risks. I attended Occidental College, Los Angeles, California, where I received a Bachelor of Arts degree in economics in 1966. I studied geology at the University of California, Los Angeles, where I received a Master of Science degree in geology in 1975. My thesis was on the origin of layering in the San Marcos gabbro, Southern California batholith. While a student, I worked for the Standard Oil Company, California, in petroleum exploration (1968-70) in southern California. I joined the USGS in 1977 as a research geologist working on regional resource assessments and the geology and geochemistry of epithermal Au-Ag deposits. In 1983 I became Chief, Branch of Geochemistry and in 1988 Deputy Chief, Office of Mineral Resources. In 1992 I returned to science working on new mineral-resource assessment methods and the relation of stress to fluid flow in the genesis of Au and Cu deposits. Prior to joining the Survey, I worked for the Continental Oil Company (1971-77) in their Research and Development Department, Exploration Research Division on various projects including Carlin-style gold deposits, the effects of metamorphism on primary geochemical zoning, and the applicability of mercury vapor to minerals exploration.



György CSIRIK was one of the Hungarian Counterpart Scientists for the US-Hungarian Joint Fund Project 415 on Deposit modeling, assessment of mineral resources and mining-induced environmental risks. He was born in 1958. He studied geology at Eötvös Loránd University Budapest, was graduated in 1983. He has been working for the Geological Institute since 1983. Between 1983 and 1992 he participated in the compiling of Metallogenic Map of Hungary, scale 1:500000. He has been the Project Manager of the Mineral Resource Assessment Project at the Department of Natural Resources since 1996. He was involved in the investigation of mineral reserves deposited in maar lakes (bentonite and oil shale). Between 1993 and 1995 he compiled pre-bid documentation. From 1997 on, he was the leader of The Usage of Amorphous Silica and Hydrous Aluminosilicates for the Production of Construction Materials with Improved Mechanical Properties INCO-Copernicus Project, sponsored by the EU. His fields of interests are mineral resource assessment and industrial minerals.



Dr. Lawrence J. DREW was one of the US Counterpart Scientists for the US-Hungarian Joint Fund Project 415 on Deposit modeling, assessment of mineral resources and mining-induced environmental risks. Lawrence J. DREW, geologist, US Geological Survey, Reston, Virginia, USA, has specialized in oil-, gas-, and mineral-resource assessment for over 25 years. He is an expert in the development and application of oil and gas discovery process models, field-size distributions, and the phenomenon of field growth and developed the Mark3 model, which calculates the aggregate metal resources in an assessment tract. DREW's recent research developed the tectonic model for the porphyry copper/polymetallic vein kin-deposits system. He has published summary studies on two of the world's giant mineral deposits—Bayan Obo (iron and rare earths, China) and Muruntau (the world's largest mesothermal vein gold deposit, Uzbekistan). He has written over 100 papers of resource assessment and economic geology and two books and writes a column covering resources and the environment for *Nonrenewable Resources*. DREW holds a Ph.D. from The Pennsylvania State University.



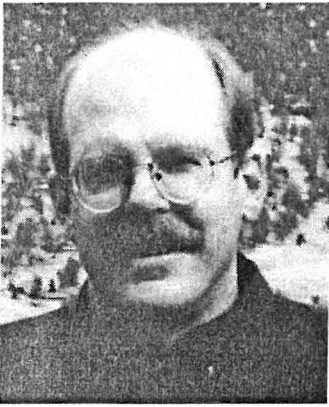
Dr. Éva VETŐ-ÁKOS was one of the Hungarian Counterpart Scientists for the US-Hungarian Joint Fund Project 415 on Deposit modeling, assessment of mineral resources and mining-induced environmental risks. She graduated in geology at the Eötvös Loránd University, Budapest in 1964. First, she was in charge of the exploration for non/metallic raw/materials. Between 1971-76 beside the petrographical works she was associated with a porphyry copper and base-metal exploration in Hungary as well as abroad and began the application of fluid-inclusion studies in these investigations. She obtained her Ph.D. at the Eötvös Loránd University in 1982 and made a comparative study of Carpathian and Alpine Mesozoic magmatites. Since 1993 she has been dealing with the connection between the Alpine plate tectonics and metallogeny in the Carpatho-Balkan area and now she is preparing a Metallogenic/Plate-tectonic Map and descriptive deposit models.



Dr. Richard B. WANTY was one of the US Counterpart Scientists for the US-Hungarian Joint Fund Project 415 on Deposit modeling, assessment of mineral resources and mining-induced environmental risks. He has a Bachelor's degree in geochemistry from the State University of New York at Binghamton, and Master's and Ph.D. degrees, both in geochemistry, from the Colorado School of Mines. His primary research interests revolve around environmental geochemistry, and have included such topics as natural radionuclides in drinking water, quality of waters produced with hydrocarbon resources, and the geochemistry of vanadium. Recently, his research has centered around the geochemistry of mineralized areas, the environmental effects of mining, and the determination of regional background and baseline geochemistry.



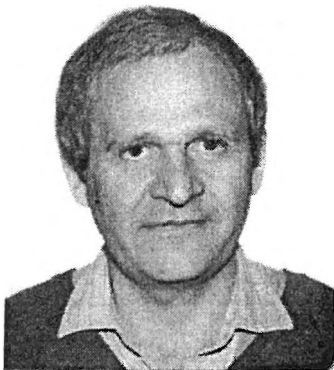
Dr. László KÖRPÁS was the leader and one of the Hungarian Counterpart Scientist for the US-Hungarian Joint Fund Project 435 on Potential for Carlin-type gold deposit in Hungary. He was born in 1943. He studied geology and cartography at the Eötvös Loránd University of Budapest, graduated in 1966 and became a Ph. D. in 1979. He is working at the Geological Institute of Hungary since 1966. His main field of research are: geological mapping (1966-1972 and 1981-1983), exploration of bauxites (1972-1974 and 1983-1987) and hydrothermal ore deposits (1976-1981), sedimentology and source rocks of bauxites (1987-1989), study of paleokarstic reservoir systems (since 1989) and exploration of Carlin-type gold deposits (1995-1998). He is author and co-author of more than 100 publications, including four books. As adviser or short term consultant he spent about ten years during various rounds in 22 countries of the world. He is member of the Geological Commission at the Hungarian Academy of Sciences, the Geological Society of Hungary, the Geophysical Society of Hungary, the Geological Society of America, honorary member of the Geological Society of Cuba and president of the Hungarian Karst and Speleological Society.



Dr. Albert H. HOFSTRA was the co-leader and one of the US Counterpart Scientist for the US-Hungarian Joint Fund Project 435 on Potential for Carlin-type gold deposit in Hungary. He works in the Mineral Resource Program of the US Geological Survey in Denver where he has made important contributions to genetic models for Carlin-type gold deposits, mesothermal Ag-Pb-Zn veins, and Mississippi Valley-Type Pb-Zn deposits. Al has also developed new techniques for the analysis of gases and ionic species in fluid inclusions and application of these data to studies of ore deposits. His Ph.D. was on the geology and genesis of the Carlin-type gold deposits in the Jerritt Canyon district, Nevada. He has since been involved in detailed studies of Carlin-type deposits in the Getchell district and Carlin Trend and reconnaissance investigations of similar deposits in the western United States. His publications on Carlin-type deposits address topics such as their geochronology and relation to tectonics, mineral paragenesis, alteration, litho-geochemistry, P-T-X and source of ore fluids, chemical modeling of ore formation, and environmental aspects of mining and mineral processing.



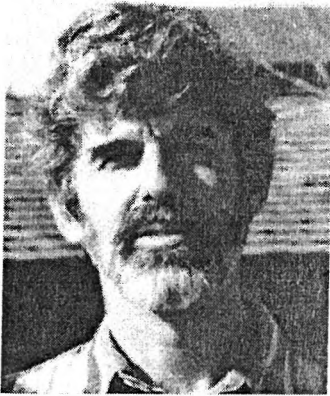
István HORVÁTH, head of the Geochemistry Division of the Geological Institute of Hungary has participated in both Joint Fund projects. He was born in 1938, studied geology at the Eötvös Loránd University of Budapest, graduated in 1963. Started his career at the Mecsek Uranium Ore Company then he had been doing geological mapping and prospection for raw materials in Mongolia for four years. He has been working at the Geological Institute since 1971. Here, he has been active in the investigation of the Great Hungarian Plain, in the hydrocarbon prognostic works for the mountainous areas of the country and in ore geological mapping. In the past decade he participated in geochemical surveys conducted for prospection and environmental purposes. He has also participated in the research to find depository for radioactive waste material. Besides that the study of the geochemical properties of subsurface waters in Hungary has been the most important part of his professional activity.



Dr. János HAAS was one of the Hungarian Counterpart Scientist for the US-Hungarian Joint Fund Project 435 on Potential for Carlin-type gold deposit in Hungary. He was born in 1947 in Budapest. He took his M.S. degree in Geology in 1972, became a University Doctor in 1977 and earned a D.Sc. degree in 1990 at the Hungarian Academy of Sciences. He carried on his research activity at the Hungarian Geological Institute for 15 years. Since 1994, he has been the Head of the Geological Research Group of the Hungarian Academy of Sciences as a Research Professor.

His main fields of research are sedimentology, stratigraphy and regional geology. In the last 10 years, more than 100 of his publications appeared, out of them 70 in foreign languages, mainly in English. He wrote separate chapters to manuals published abroad as well as to the manual series "Sedimentology"; edited 3 separate volumes; compiled 2 lecture notes and 1 textbook; contributed to the editing of several geological maps, atlases. His research work is closely connected with his educational activity. He is a Professor of the Eötvös Loránd University, Budapest. He teaches the courses "Sedimentology" and "Geology of Hungary".

He is a member of the Triassic Subcommittee of the International Stratigraphic Commission. In 1990, he was elected as a member of the scientific board of the International Association of Sedimentologists (IAS) for 4 years. He is a member of the IUGS and the National Committee for the IGCP and was a President of the latter body between 1987 and 1994. In 1985, he was elected as the Secretary of the Hungarian Geological Commission of the Hungarian Academy of Sciences and held this office till 1996. He is a President of the Triassic Subcommittee of the Hungarian Stratigraphic Commission and President of the Hungarian Sedimentological Commission. Since 1991, he has been the Editor-in-Chief of *Acta Geologica Hungarica*.



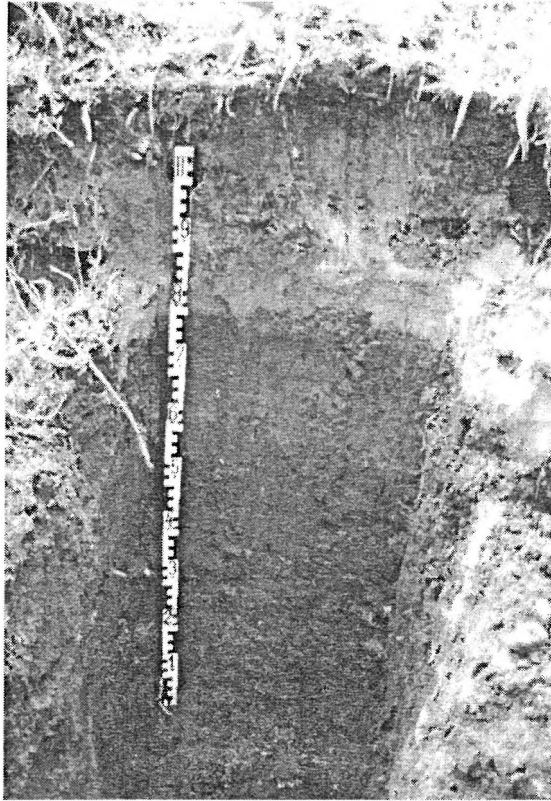
Dr. Joel S. LEVENTHAL organic geochemist was one of the US Counterpart Scientist for the US-Hungarian Joint Fund Project 435 on Potential for Carlin-type gold deposits in Hungary. He was at the USGS Denver for 24 years before his early retirement in 1997. He is now Emeritus Scientist at the USGS and a private consultant. Most of LEVENTHAL's research is related to natural organic matter in mineral deposits and black shales and the role of organic matter in mineral deposits. He worked on uranium (sandstone-type, Africa) and metaliferous black shales (world-wide), MVT Pb-Zn, disseminated Au (Nevada), and Sedex type deposits. Leventhal is the author/co-author of more than 90 papers. LEVENTHAL received a Ph. D. from the University of Arizona.

LÁSZLÓ ÓDOR and RICHARD B. MCCAMMON editors:

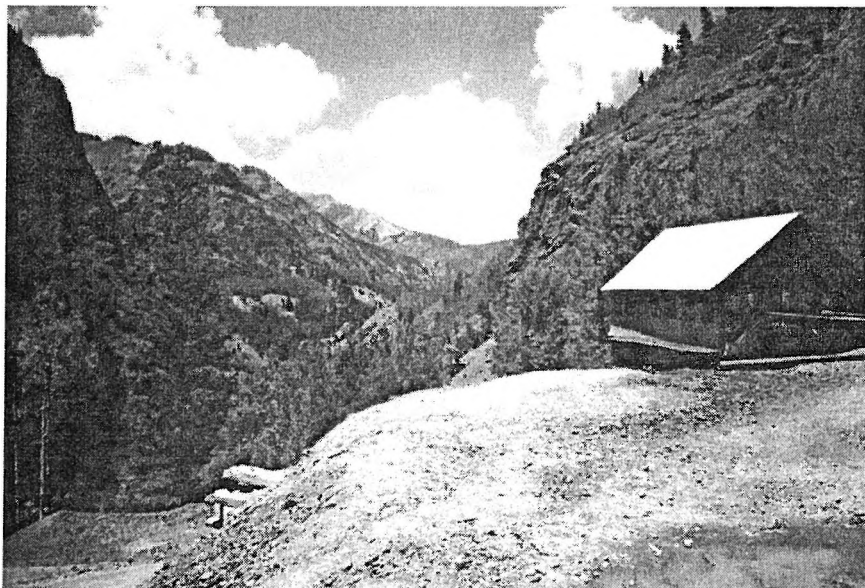
DEPOSIT MODELING AND MINING-INDUCED ENVIRONMENTAL RISKS



Field trip in Colorado State, USA
(from left to right: RICHARD B. WANTY, BYRON R. BERGER (USGS), LÁSZLÓ ÓDOR (GIH)
(É. VETŐ-ÁKOS, 1996)



„Yellow sand” in the soil profile of the flood-plain deposits of Toka Creek, Gyöngyösroszi, Mátra Mts., Hungary. It is originated from the flotation waste. (L. ÓDOR, 1996)



Colorado State, USA. Looking back to Engineers' Pass. (É. VETŐ-ÁKOS, 1996)

DEPOSIT MODELING, ASSESSMENT OF MINERAL RESOURCES AND MINING–INDUCED ENVIRONMENTAL RISKS

RICHARD B. MCCAMMON¹ and LÁSZLÓ ÓDOR²

¹US Geological Survey, 20192 Reston, Virginia, USA

²Geological Institute of Hungary, H–1143 Budapest, Stefánia út 14., Hungary

ABSTRACT

The results of a 3-year joint effort in assessing the undiscovered deposits in the Mátra and the Börzsöny-Visegrád Mountains in Northern Hungary and evaluating the environmental signatures of mineral deposits and areas of regional hydrothermal alteration in northeastern Hungary are included in this special issue. This study was made possible through the US-Hungarian Science and Technology Joint Fund Program. In addition to these results, recent advances in the fields of resource assessment and geoenvironmental modeling are described in companion articles in this special issue

1. INTRODUCTION

The US-Hungarian Science and Technology Joint Fund Project 415 entitled “Deposit modeling, assessment of mineral resources and mining-induced environmental risks” was proposed as a 3-year joint effort between research scientists at the Geological Institute of Hungary (MÁFI) and research scientists at the US Geological Survey (USGS). The proposed activities were to apply the three-part assessment method that had been developed at the USGS to a pilot area of northern Hungary, to evaluate the efficacy of the existing deposit model for alpine-type mineral deposits, and to establish the environmental signatures of mineral deposits and areas of regional hydrothermal alteration in northeastern Hungary. The project was begun in 1995 and completed in 1998. The papers in this special issue describe the results that were obtained in the project.

2. ASSESSMENT OF UNDISCOVERED DEPOSITS

The method used to estimate the quantity and quality of undiscovered deposits is based on the three-part form of quantitative assessment described by SINGER (1993). In three-part assessments, areas are delineated according to the types of deposits permitted by the geology, the amount of metal in typical deposits is estimated by using grade and tonnage models, and the number of undiscovered deposits of each type is estimated by using a variety of subjective methods. Estimates of the number of undiscovered deposits are internally consistent in that the geologic settings of the delineated areas are consistent with the geologic settings for the descriptive models, as well as with the identified deposits in the area and the deposits that comprise the grade and tonnage models. Every effort is made to incorporate the available information in the estimates, and the uncertainty is explicitly represented. The three-part form of quantitative assessment has been applied by the USGS since 1975.

In the paper by DREW, SINGER, MENZIE, and BERGER, the authors review the state of the art in mineral-resource assessment. Mineral-resource assessment is a robust, highly quantified, and active field of research; moreover, quantitative assessments of undiscovered deposits are an important tool for policy decisions in land-use planning. In reviewing the state of the art, the authors look ahead to promising new approaches such as a metric for mineral-deposit occurrence probabilities, probabilistic neural networks, and economic filters. These approaches reaffirm the dynamic quality of mineral-resource assessment.

3. MINERAL-DEPOSIT MODELS

Mineral-deposit models are an integral component of any mineral-resource assessment methodology. In the paper by BERGER, DREW, and SINGER, the authors provide a frame of thinking about mineral deposits by focusing on ore-forming systems which leads to a consistent set of describable dynamic processes and results in a hierarchical scheme that can improve the predictive capabilities of mineral-deposit models. An example that illustrates the efficacy of such a scheme is that of magmatic arcs. This led the authors to construct a hypothetical landscape/dynamics model of a geologic terrane permissive for the occurrence of porphyry- and epithermal-style mineral deposits in a continental-arc setting that is similar to the setting expected to occur in northern Hungary. This raises the possibility that both the localization of deposits and likely economic outcomes in such settings may be predictable. Because the full dimension of components in mineral-deposit models are needed to be effective, the authors conclude by suggesting that approaches to quantify terrane characteristics, mineral-district characteristics, and deposit characteristics be explored more fully, particularly in the context of the fundamental principles important in ore-forming processes.

4. ASSESSMENT OF UNDISCOVERED DEPOSITS IN THE MÁTRA, BÖRZSÖNY AND VISEGRÁD MOUNTAINS, NORTHERN HUNGARY

Critical to the assessment of undiscovered deposits in a region is the collection and description of regional geologic, geophysical, and geochemical data. In the paper by CSIRIK, ÓDOR, KISS, and RÓZSAVÖLGYI, the authors provide a description of the regional geologic, geophysical, and geochemical data that were used to assess the undiscovered deposits in the Mátra, Börzsöny and Visegrád Mountains, located in the western part of the Northern Hungarian Range. For the purpose of the assessment, the authors created a digital geologic map that was used to identify potential host rocks for undiscovered deposits and digital geophysical maps that were used to assess the areal extent of the potential host rocks. To assist in evaluating the nature and composition of the potential host rocks, the authors prepared a variety of geochemical maps based on a reconnaissance (low-density) geochemical survey of Hungary. This information was critical for a proper interpretation of the geologic setting in which undiscovered deposits may occur.

Before an assessment can be made, it is necessary to identify the type or types of mineral deposits permitted by the geology in the area. For this purpose, the paper by VETŐ-ÁKOS reviews the metallogeny of the study area and offers deposit models of the types of deposits that may occur. The author describes the different Alpine type deposit models in Hungary. By considering the different geologic settings in which the known deposits occur, it is possible to constrain the types of undiscovered deposits that may occur. To assist in the assessment of undiscovered deposits, the author has prepared a chart, which lists the deposits in the Börzsöny and Mátra Mountains according to location, host rock, rock alteration, age of mineralization, and structure. The author concludes that the main ore controls are the faults and the subvolcanic andesites and dacites.

The paper by DREW, BERGER, BAWIEC, SUTPHIN, CSIRIK, KÖRÖSI, VETŐ-ÁKOS, ÓDOR and KISS presents the mineral-resource assessment of the Mátra and Börzsöny–Visegrád Mountains, Northern Hungary. The assessment confirms that the Middle Miocene volcanic complexes in the study area are permissive for the occurrence of mineral deposits that belong to the porphyry copper/polymetallic vein kin-deposit system. Estimated undiscovered resources are reported for each volcanic complex.

The thoroughness with which the assessment was carried out and the effort evidenced by the extensive data that were collected, interpreted, and analyzed as a part of the assessment is testimony to the successful collaboration between the research scientists at the MÁFI and the research scientists at the USGS.

5. GEOENVIRONMENTAL MODELS

Geoenvironmental models have been recently developed which include characteristics of the ore and associated waste rocks in terms of the environmental risks. Such risks are related to the biotic, climatic, and topographic settings. Such models serve as guides for evaluating potential environmental impacts. An important goal in the continued development of geoenvironmental models is the integration of empirical data to produce more quantitative models which can be used to predict the costs of environmental mitigation and the risks associated with mineral extraction. In their paper, WANTY, BERGER, and PLUMLEE describe the advancements made in environmental models of mineral deposits in which they stress the importance of baseline and natural backgrounds in assessing

mined areas and areas where future mining may occur. The authors argue for a strategy for developing geoenvironmental models to include climatic and ecoregional effects embodying such physical environmental characteristics as precipitation, evaporation, temperature, and ground water-surface water interactions. The development of geoenvironmental models represents a new direction in the environmental geosciences.

6. ENVIRONMENTAL SIGNATURES OF MINERAL DEPOSITS

A final objective of Joint Fund Project 415 was to evaluate the mining-induced environmental risks in northeastern Hungary, a region that has been mined intermittently since the Middle Ages. The paper by ÓDOR, WANTY, HORVÁTH, and FÜGEDI establishes the environmental signatures of the mineral deposits and areas of regional hydrothermal alteration that occur in the region. The generalised geochemical features associated with the mineral deposits and prospects that occur are categorized according to the corresponding deposit model. Such information is invaluable for evaluating environmental effects due to past mining or the potential effects of future mining.

7. CONCLUSIONS

The scientific value of the results obtained during the course of Project 415 have far surpassed the costs involved as part of the US-Hungary Science and Technology Joint Fund. By allowing the joint collaboration of research scientists from two National Surveys, it has been possible not only to transfer the knowledge and expertise from one institution to another, but more importantly, by the publication of this special issue, to make the science of resource assessment and geoenvironmental models available to a wider professional audience which, in turn, makes it possible for the science to be applied worldwide.

8. ACKNOWLEDGEMENTS

We would like to give special thanks to Janet S. SACHS, US Geological Survey, for her help in editing the manuscripts that were prepared for this special issue, and also, to Dr. Gábor GAÁL, former Director of the Geological Institute of Hungary, for his support and leadership in initiating the project in 1994.

9. REFERENCE

- SINGER, D. A. 1993: Basic concepts in three-part quantitative assessments of undiscovered mineral resources. — *Nonrenewable Resources*, 2(2): 69–81.
- DREW, L. J.–SINGER, D. A.–MENZIE, W. D.–BERGER, B. R. 1999: Mineral resource assessment — state of the art. — *Geologica Hungarica Series Geologica* 24: 31–40.
- BERGER, B. R.–DREW, L. J.–SINGER, D. A. 1999: Quantifying mineral-deposit models for resource assessment. — *Geologica Hungarica Series Geologica* 24: 41–54.
- CSIRIK, GY.–ÓDOR, L.–KISS, J.–RÓZSAVÖLGYI, S. 1999: Regional geologic, geophysical, and geochemical data used in the assessment of undiscovered deposits in the Mátra, Börzsöny and Visegrád Mountains, northern Hungary. — *Geologica Hungarica Series Geologica* 24: 55–62.
- VETŐ-ÁKOS, É. 1999: Alpine deposit models for the Mátra and Börzsöny Mts. Northern Hungary. — *Geologica Hungarica Series Geologica* 24: 63–77.
- DREW, L. J.–BERGER, B. R.–BAWIEC, W. J.–SUTPHIN, D. M.–CSIRIK, GY.–KORPÁS, L.–VETŐ-ÁKOS, É.–ÓDOR, L.–KISS, J. 1999: Mineral-resource assessment of the Mátra and Börzsöny-Visegrád Mountains, North Hungary. — *Geologica Hungarica Series Geologica* 24: 79–96.
- WANTY, R. B.–BERGER, B. R.–PLUMLEE, G. S. 1999: Environmental models of mineral deposits — a state of the art. — *Geologica Hungarica Series Geologica* 24: 97–106.
- ÓDOR, L.–WANTY, R. B.–HORVÁTH, I.–FÜGEDI, U. 1999: Environmental signatures of mineral deposits and areas of regional hydrothermal alteration in northeastern Hungary. — *Geologica Hungarica Series Geologica* 24: 107–129.

MINERAL-RESOURCE ASSESSMENT – STATE OF THE ART

LAWRENCE J. DREW¹, DONALD A. SINGER², W. DAVID MENZIE¹, and BYRON R. BERGER³

¹US Geological Survey, 12201 Sunrise Valley Drive, Reston, VA 20192, USA

²US Geological Survey, 345 Middlefield Road, Menlo Park, CA 94025, USA

³US Geological Survey, P. O. Box 25046 Denver, CO 80225, USA

ABSTRACT

Mineral-resource assessment is a field of research and application that has expanded rapidly during the past 25 years. Today, it is a robust, highly quantified, and active field of research that describes mineral deposits, measures their grade and tonnage, estimates the occurrence of the undiscovered deposits, and aggregates the grade and tonnage data to estimate resources in the undiscovered deposits in a form useful for quantitative decisionmaking in mineral exploration, mineral-resource assessment, and policy decisionmaking in land-use planning.

1. INTRODUCTION

The notion that the state of the art of a scientific field can be reckoned is far simpler to desire than to achieve. It is not a historical summation of the field with all the important building blocks identified and placed in temporal order, properly referenced and evaluated. Instead, the state of the art of a scientific field is typically reflected by the extent of recent achievements in the field. In a sense, it is an attempt to forecast what the field will look like in the future. Consequently, this assessment is based on the recent developments in the field. While using such a measure, we will not forget the major contributions of the past 25 years. Many of the fundamental building blocks that make up the structure of mineral-resource assessment were reviewed by DREW (1990) and SINGER (1993b).

In passing, we will briefly touch on the historical development of the field of mineral-resource assessment before examining significant recent developments that bear on where the field is today; that is, its state of the art. Unlike the other, more-typical subfields of geology, mineral-resource assessment directly bridges the gap between the geological sciences and the economic and public policy sectors. The process of assessment integrates data from a variety of sources (Fig. 1) that range from the purely physical, such as geological, geochemical, and geophysical properties of the rocks in study area, to the economic, such as the possible grades and tonnages and numbers, and to the financial attractiveness of undiscovered mineral deposits

Delineation of terranes that are permissive for mineral deposits (LASKY 1948), which is a complex integrative activity, is a fundamental element in the assessment process (SINGER 1993a). Early developments included the identification of mineral belts (such as tin in Cornwall, England, pyrite in Spain, and molybdenum in the Rocky Mountains) and the description of host rocks and their plate tectonic settings (GUILD 1971). At about this same time, the common occurrence of associated mineral deposits was suggested by HOSKING (1969) for greisen, vein, stockwork, and replacement tin deposits and by SILLITOE (1972, 1973) for porphyry copper and polymetallic veins, skarns, and replacement deposits. Soon thereafter, the notion that certain deposits (porphyry copper and volcanogenic massive sulfides) could not occur together in the same time-stratigraphic packages of rocks was suggested by ISHIHARA (1974) and SILLITOE (1980). Many descriptive mineral-deposit models have been developed to characterize the association (and nonassociation) of deposits with host rocks, proximity to heat sources, and other types of geological data, as well as other types of deposits (COX 1983a, b, COX and SINGER 1986, BLISS 1992, KIRKHAM et al. 1993).

During this same period, SINGER and his colleagues (SINGER et al. 1975; SINGER and MOSIER 1983a, b, and COX and SINGER 1986) developed grade and tonnage models, which are statistical characterizations of the con-

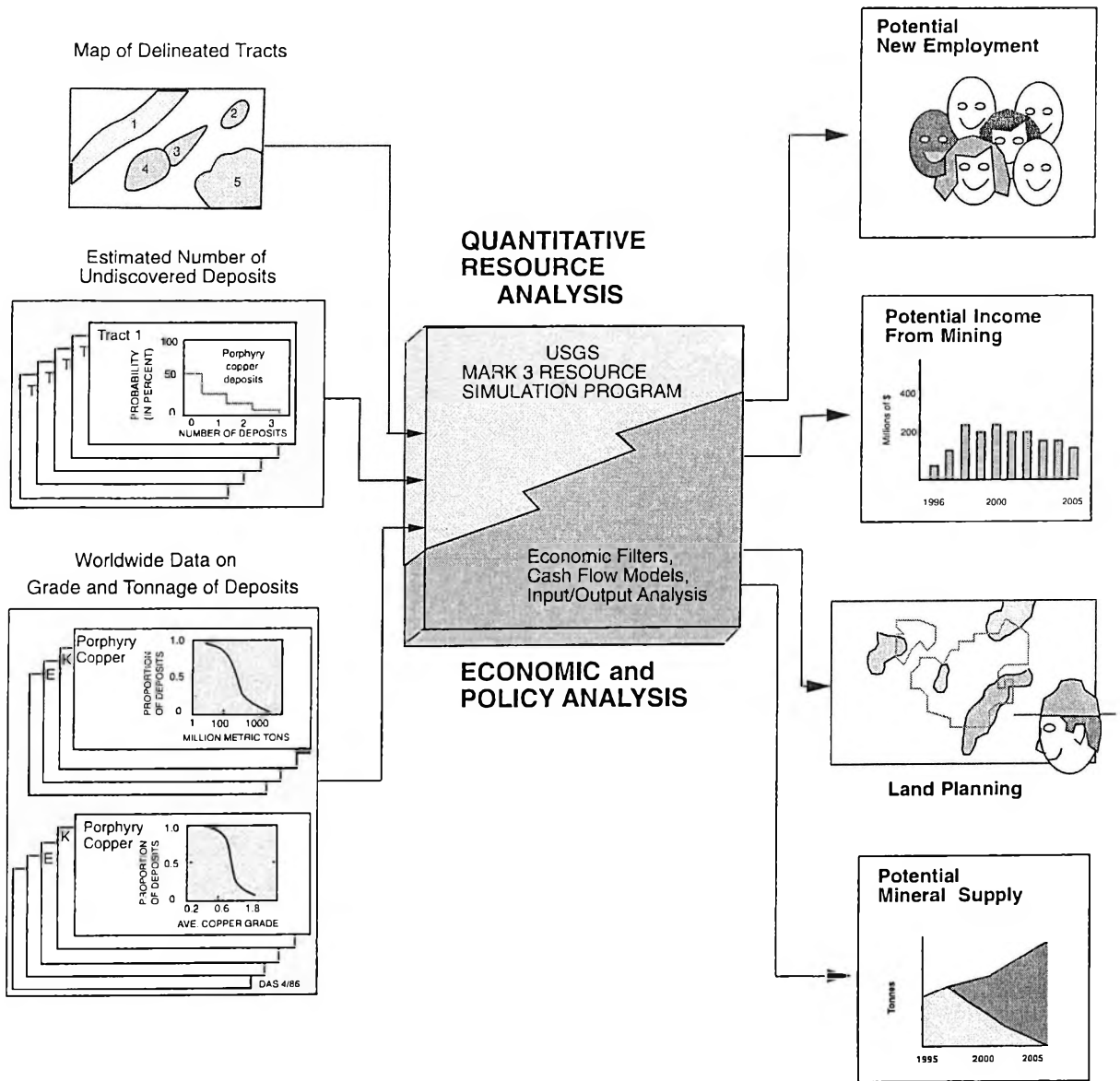


Fig. 1: Description of the elements of a mineral-resource assessment

centration (quantity and quality) of the useful constituents in mineral deposits. Our goal is to construct a grade and tonnage model for each descriptive mineral-deposit model so that the assessment process can proceed from a qualitative to a quantitative (probabilistic) estimation of undiscovered mineral resources. Grade and tonnage models are central building blocks in an assessment as they describe statistically the probable distributions of grade and tonnages for the undiscovered mineral deposits forecast to occur in the study area. These models are, in turn, linked in the Mark3 Monte Carlo computer simulator (DREW et al. 1986, ROOT et al. 1992; Fig. 1) with the estimated probability of occurrence of these mineral deposits. Frequency distributions and statistics are produced that describe the expectations and probability ranges for deposit occurrence in the delineated tracts in the study area. These statistical measures may be used in land-management and other decisions associated with the social costs and benefits of development and use of mineral deposits or, contrarily, their nondevelopment and nonuse.

2. THE BODY OF LITERATURE

An early compilation by SINGER and MOSIER (1981) of about 100 contributions is helpful when surveying the literature. Since then, the number has nearly doubled. Today, contributions range from expositions on descriptive

models (for example, ECKSTRAND 1984, COX and SINGER 1986, and KIRKHAM et al. 1993), grade and tonnage model development (SINGER 1993b), Monte Carlo aggregation models (ROOT et al. 1992) to applications of these methods, such as the assessment of the undiscovered resources in large areas (for example, the 27,000-square-mile Tongass National Forest, Alaska; BREW et al. 1991) to small land tracts (for example, the assessment of the 60-square-mile Redcloud Peak and Handies Peak Wilderness study area in Colorado (MCCAMMON et al. 1991). GUNTHER (1992) has used Monte Carlo simulation and simplified cost models to analyze the possible economic effects of land-use alternatives in the Kootenai National Forest. Similar methods are routinely used in planning mineral exploration programs (ANDERSON 1982).

3. RECENT DEVELOPMENTS

During the past few years, four noteworthy contributions have been made to the field of mineral-resource assessment. These are the development of a metric for mineral-deposit occurrence probabilities, the application of neural network analysis to deposit model classification and permissive terrane identification, the analysis of favorable regions (small areas) within large regions identified as permissive for deposit occurrence, and the computation of economic cost filters for mineral deposits by type.

3.1. A metric for mineral-deposit occurrence probabilities

The metric for mineral-deposit occurrence probabilities is a set of inequalities that ordinarily specify the probability of occurrence of the kin deposits created by hydrothermal systems. The types of deposits that can be formed by hydrothermal systems (for example, porphyry, skarn, greisen, vein, and replacement) are determined, for the most part, as a function of the characteristics of fluid-focusing structures and the composition of wallrock. Many factors, such as the depth of emplacement of igneous complexes and the environment into which the complexes have been emplaced, can affect the metric. During the past two to three decades, it had become apparent to many resource analysts that certain forms of deposits occur less frequently than others; for example, across systems, vein deposits outnumber replacement deposits. To account for such factors, the following metric is used for the suite of kin deposits associated with important sources of metal, such as a porphyry copper deposit system:

$$E(\text{PMR}) < E(\text{SK}) < E(\text{PPY}_{\text{Cu}}) < E(\text{PMV}),$$

where:

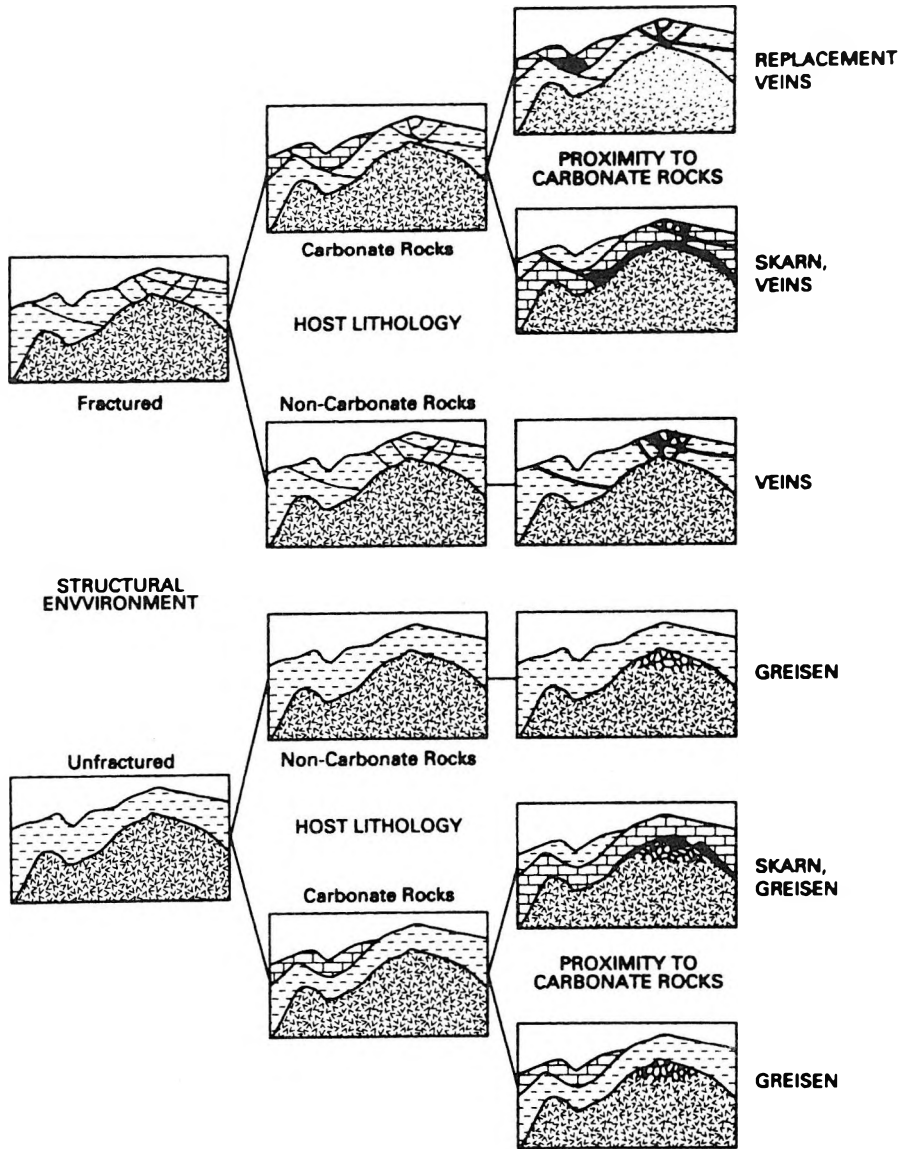
- $E(\)$ = the expected number of deposits,
- PMR = polymetallic replacement deposits
- SK = skarn deposits,
- PPY_(Cu) = porphyry copper deposits, and
- PMV = polymetallic vein deposits.

The metric is based on the idea that the types of kin deposits that will occur are determined by the degree to which the conduits for convective flow (faults and fractures) and the types of wallrock that are present interact within hydrothermal systems (DREW and MENZIE 1993). This metric was confirmed empirically by DREW and MENZIE (1993) by examining the frequencies of occurrence of these kin deposits as recorded in the US Geological Survey's Mineral Resource Data System (MRDS).

We cannot describe here the lengthy calculus used to develop this metric, but we can illustrate its development by showing how several of its elements were assembled (ordered). Briefly, the reasoning is as follows. Skarn deposits, in general, occur more frequently than replacement deposits. Although both deposit types require carbonate wallrock, the replacement deposit also requires that the wallrock be well fractured. Such fractures are necessary so that the hydrothermal fluid can "leak off" into the carbonate wallrock far enough for the proper temperature regime (lower than for a skarn deposit) to be encountered, for deposition of a replacement deposit. With each additional requirement, a degree of freedom is lost, and we assert that, on average, the deposit occurrence probability must diminish. And if we argue additionally that porphyry systems are emplace more commonly into an environment with fractured country rocks than into an environment in which the country rocks adjacent to the intrusion are of carbonate composition, then we can state that polymetallic veins occur more frequently in the permissive area than do skarn deposits.

When REED et al. (1989) assessed the undiscovered lode tin resources of the Seward Peninsula, Alaska, they used the decision-tree equivalent of this metric (Fig. 2). In this assessment, the geology and geophysics of each subarea of the study area was examined (with specific emphasis on identifying the locations of plutons). The decision tree was then used to determine the probable types and locations of targets for undiscovered lode tin depos-

Fig. 2: Decision tree showing diagrammatic cross section of possible relations of granite plutons, structural features, wallrock, and permissiveness for lode tin deposits



Estimated number of deposits at different confidence levels

Table 1

Deposit type	Probability, in percent		
	90	50	10
Skarn	5	9	15
Replacements	1	2	4
Greisen	2	3	5
Vein	1	2	4

(Chance that at least the indicated number of deposits are present)

its. The number of undiscovered tin deposits (Table 1) was then estimated (in probability) on the basis of expected numbers of targets of each type which was influenced by the implicit metric (probability structure) represented in the decision tree. Notice that at each of the three probability levels, the estimated number of undiscovered deposits follows the same order as specified by the metric shown above. For example, there are more skarns than replacement deposits.

3.2. Application of neural network analysis

One way to measure the progress of a scientific research field, such as mineral-resource assessment, is to note its change in activity level from qualitative and descriptive to quantitative and predictive. As a field, mineral-resource assessment has witnessed rapid movement along this path as is demonstrated by the widespread application of quantitative data-integration techniques. Within these techniques, two categories or types of analysis are commonly distinguished: the knowledge- and data-driven systems. The knowledge-driven systems include those that use expert systems, fuzzy logic, and Dempster-Shafer functions. The data-driven systems (that is, the inductive learning systems) include those that use logistic regression, weights of evidence, decision trees, statistical pattern recognition, and neural network analysis. One of the newest methods that is currently being investigated to classify mineral deposits into homogenous, hopefully genetic, groups is the probabilistic neural network.

Like its namesake, a neural network learns by example from a training set of data where weights are estimated and loaded into its neurons. New data are processed through this set of weights stored in the neurons for the purpose of classification. We are concerned here with the ability of a probabilistic neural network to be trained for the purpose of objectively classifying mineral deposits into groups that form the basis for predictive models. SINGER and KOUDA (1997) showed that a probabilistic neural network can classify 98 percent of 267 mineral deposits into 8 different deposit types by using mineralogy and 2 rock types. In a later paper, probabilistic neural networks were shown to excel at integrating geoscience data when the training data were representative of the groups to be classified (SINGER and KOUDA 1997). The neural network was trained to recognize 28 deposit types by using 1005 deposits from around the world. In one test, 2,751 deposits and occurrences not used in training were classified by the neural network into one of the learned deposit types that were then grouped into broad categories, such as pluton-related and epithermal. The pluton-related deposits are shown in Fig. 3 with terranes that were independently determined by experts to be permissive for pluton-related deposits. Most mineral sites not within a tract delineated as permissive for pluton-related deposits (Fig. 3), such as the deposits in southeastern Nevada, are correctly classed as replacement Mn or W vein deposits. However, these were not delineated by COX et al. (1996) because they either were not economically important or were associated with Proterozoic plutons. A few deposits apparently outside delineated tracts, such as the one in northeastern Nevada, are within tracts too small to be seen at the scale of the figures. Because of the scale, many of the sites plot on other sites. When these apparent errors are properly counted, the probabilistic neural network successfully classified 99 percent of the 907 deposits and occurrences grouped as pluton-related in COX et al. (1996). Similar results were obtained for epithermal mineral sites.

Current, ongoing research is being expanded to include the use of a probabilistic neural network to integrate more geologic variables and related deposit types and the identification and classification of permissive terranes (Fig. 4).

3.3. Analysis of favorable regions within permissive terranes

Some of the users of assessment maps (such as Fig. 3 and Fig. 4), most often land-management agencies, have requested more-detailed information, especially on small target areas that have higher probabilities of occurrence in tracts permissive for deposit occurrence. To address the requests, we believe that the research should move from resource assessment per se toward identification of smaller subareas within permissive tracts. We have begun to investigate several situations that will allow us to identify those subareas that are more favorable for mineral deposit occurrence within permissive tracts. One geological environment that is now being studied is that of extension along strike-slip fault systems, such as the Walker Lane area in Nevada. The Walker Lane is a region characterized by a large strike-slip fault system (transcurrent fault) with associated syntectonic/synigneous intrusive events in the far-field stress regime of the San Andres Fault System. Within the Walker Lane system, many strike-slip faults have moved differentially with respect to each other, which has produced releasing and restraining offsets, as well as extensional and contractual duplexes. Within these and their associated structures, we can identify the location of small areas that are favorable for a variety of different epithermal mineral deposits. Fig. 5 shows a collection of these areas in relation to various configurations of strike-slip faults. For example, the large

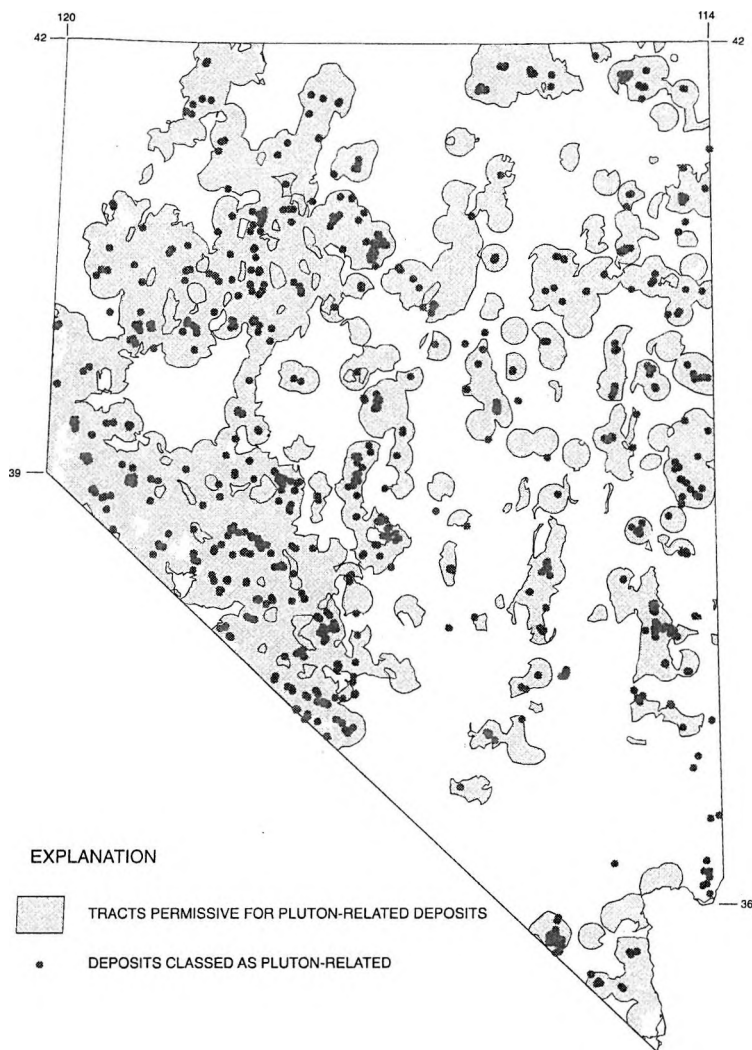


Fig. 3: Map of Nevada showing areas permissible for pluton-related deposits (after COX et al. 1996) and deposits and occurrences classified by a probabilistic neural network as pluton-related

Bonanza districts are preferentially located at the intersection of reactivated basement shear zones and strike-slip faults that have moved in such a manner as to form an extensional zone.

3.4. Computation of economic cost filters

The fourth noteworthy development in mineral-resource assessment is the formulation of simplified engineering cost models for mining and mining operations (CAMP 1991). Although detailed engineering cost models have been available for some time, they were not suitable for application to undiscovered resources. The simplified cost models, such as those developed by CAMP (1991), provide a practical means of developing cost equations and economic filters useful for resource-assessment and exploration planning (HARRIS 1990). Fig. 6 is a plot of the copper grades and tonnages of porphyry copper deposits from Alaska, USA, and British Columbia, Canada, that have been evaluated by applying engineering cost models (MENZIE and SINGER 1993). In this figure, deposits are classified as follows: **E** producers (deposits that are being or have been produced) that have positive estimated net present values (calculated at a 10-percent interest rate), **E** nonproducers that have positive estimated net present values, **N** producers that have negative estimated net present values, and **N** nonproducers that have negative estimated net present values. In grade and tonnage space, the line separates deposits that would be "economic" (have positive net present values) at stated conditions of depth (at surface), price, and interest rate from "noneconomic" deposits. Because many of the deposits contain multiple metals (Cu, Mo, Au, and Ag) complete separation of "economic" and "noneconomic" deposits is not apparent in a bivariate plot. The relative proportions of E's, E's, N's, and N's measure the effectiveness of the engineering cost models at estimating which de-

Fig. 4: Diagram showing integration of various kinds of earth science data to delineate mineral-resource tracts

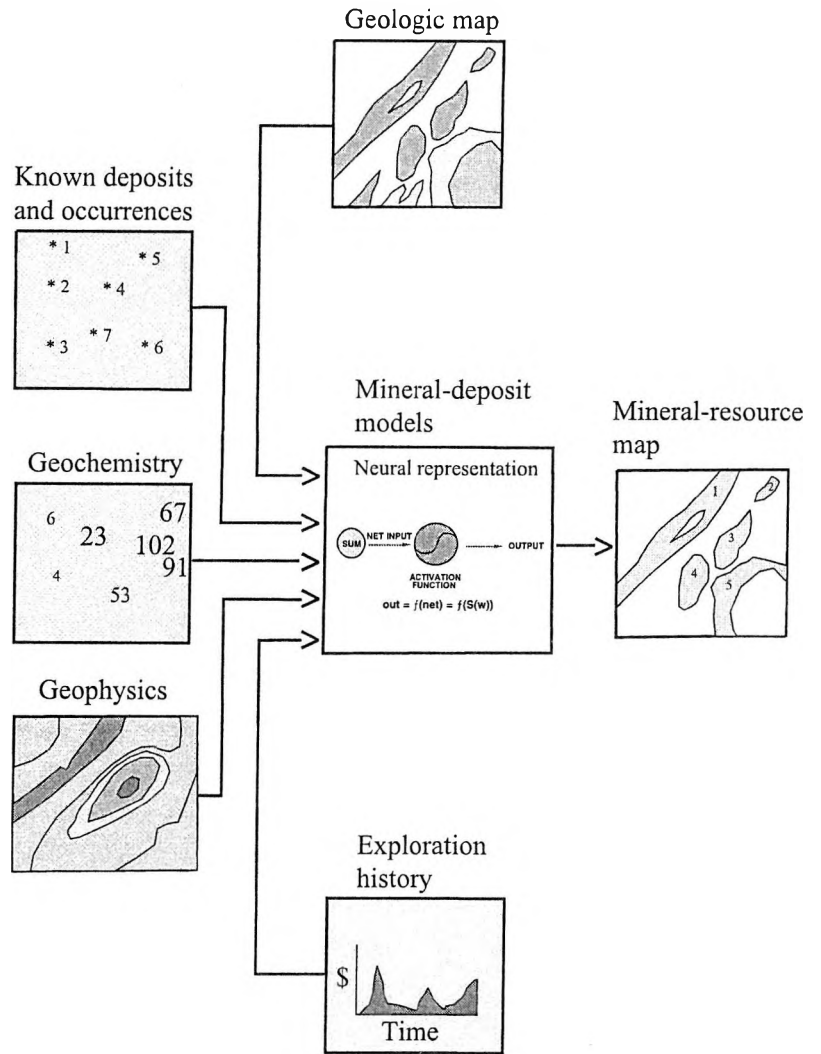
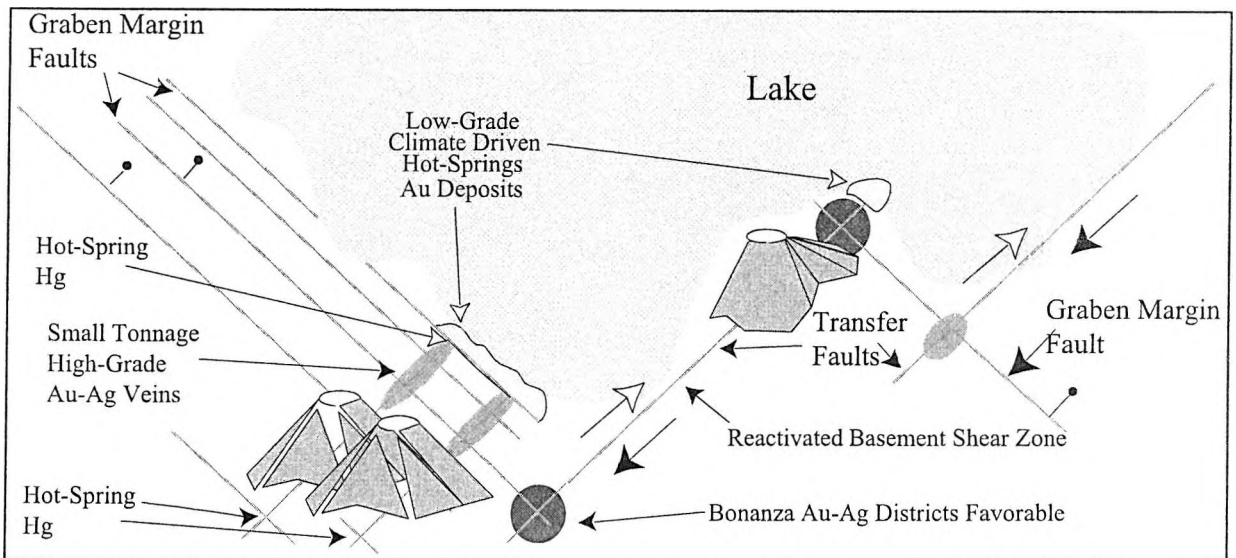


Fig. 5: Areas favorable for the occurrence of epithermal mineral deposits in a larger permissive area created by a strike-slip fault system associated with a collision orogen



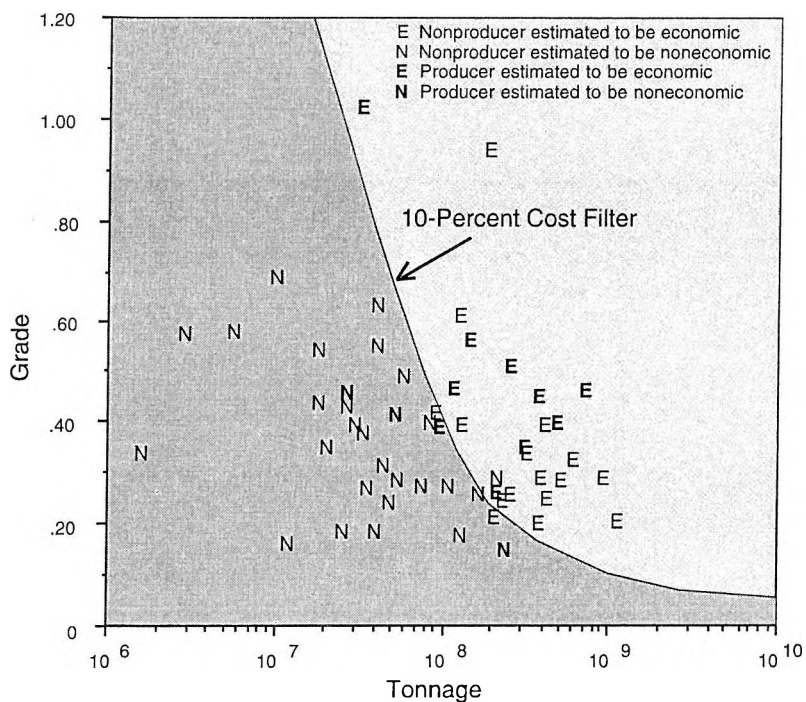


Fig. 6: Economic cost filter for porphyry copper deposits in Alaska, USA, and British Columbia, Canada

posits would be produced at conditions similar to those prevailing now and in the recent past. In general, the models “correctly” classify most producers as “economic”. The models, however, “incorrectly” classify about 40 percent of the nonproducers as “economic”. This asymmetry in misclassification may reflect the fact that a number of the nonproducers represent on-the-shelf deposits that are currently being considered for production.

4. CONCLUSION

Mineral-resource assessment is an ever-expanding and mature activity that produces a public good for government and industry officials who must make mineral-exploration, resource-assessment, and land-use decisions. Major advances have been made in the description of mineral deposits, the construction of grade and tonnage models, and the application of Monte Carlo aggregation methods as a basis for the assessment of undiscovered mineral resources. In recent years, advancement has continued with the identification of metrics for mineral-deposit occurrence probabilities, data-integration methods (such as probabilistic neural networks), the identification of favorable areas within permissive tracts for mineral-deposit occurrences, and the computation of economic cost filters for mineral deposits. Each of these advances has moved the field onto higher levels of quantification and predictive capability. These methods are accurate and flexible enough that they can be applied to a wide range of situations – from regions that cover tens of thousands of square miles to areas that cover only a few tens of square miles.

5. REFERENCES

- ANDERSON, J. A. 1982: Gold—its history and role in the US economy and the US exploration of Homestake Mining Company. — Mining Congress Journal, January 1982: 51–58.
- BLISS, J. D. ed. 1992: Developments in mineral deposit modeling. — US Geological Survey Bulletin 2004: 168 p.
- BREW, D. A.—DREW, L. J.—SCHMIDT, J. M.—ROOT, D. H.—HUBER, D. F. 1991: Undiscovered locatable mineral resources on the Tongass National Forest and adjacent lands, southwestern Alaska. — US Geological Survey Open-File Report 91–10: 340 p.

- CAMM, T. W. 1991: Simplified cost models for prefeasibility mineral evaluations. — US Bureau of Mines Information Circular 9298: 35 p.
- COX, D. P. ed. 1983a: U. S. Geological Survey-INGEOMINAS mineral resource assessment of Colombia—Ore deposit models. — US Geological Survey Open-File Report 83-423: 74 p.
- COX, D. P. ed. 1983b: U. S. Geological Survey-INGEOMINAS mineral resource assessment of Colombia – Additional ore deposit models. — US Geological Survey Open-File Report 83-901: 32.
- COX, D. P.–BERGER, B. R.–LUDINGTON, S.–MORING, B. C.–SHERLOCK, M. G.–SINGER, D. A.–TINGLEY, J. V. 1996: Delineation on mineral resource assessment tracts and estimation of numbers of undiscovered deposits in Nevada. — *in* SINGER, D. A. ed.: An analysis of Nevada's metal-bearing mineral resources: Nevada Bureau of Mines and Geology Open-File Report 96-2, Chapter 12: 12.1-12.25, 3 sheets, scale 1:1,000,000 (also available at: www.nbmj.unr.edu/ofr/962.)
- COX, D. P.–SINGER, D. A. eds. 1986: Mineral deposit models. — US Geological Survey Bulletin 1693: 379 p.
- DREW, L. J. 1990: Oil and gas forecasting. — Oxford University Press, New York: 252 p.
- DREW, L. J. (and 11 others) 1986: Quantification of undiscovered mineral-resource assessment. The case study of the U.S. Forest Service wilderness. — *Economic Geology*, 81: 80–88.
- DREW, L. J.–MENZIE, W. D. 1993: Is there a metric for mineral deposit occurrence probabilities. — *Nonrenewable Resources*, 2(2): 92–104.
- ECKSTRAND, O. R. ed. 1984: Canadian mineral deposit types, a geological synopsis. — Geological Survey of Canada, Economic Geology Report 36: 86 p.
- GUILD, P. W. 1971: Metallogeny – A key to exploration. — *Mining Engineering*, 23: 69–72.
- GUNTHER, T. M. 1992: Quantitative assessment of future development of copper/silver resources in the Kootenai National Forest, Idaho/Montana. Part 2 – Economic and policy analysis. — *Nonrenewable Resources*, 1(4): 267–280.
- HOSKING, K. F. G. 1969: The nature of the primary tin ores of southwest England. — *in* A second technical conference on tin. International Tin Council, 1: 1157–1243.
- KIRKHAM, R. V.–SINCLAIR, R. V.–THORPE, W. D.–DUKE J. M. eds. 1993: Mineral deposit modeling. — Geological Association of Canada Special Paper 40: 798 p.
- HARRIS, D. P. 1990: Mineral exploration decisions. — New York, John Wiley and Sons: 436 p.
- ISHIHARA, S. 1974: Magmatism of the Green Tuff tectonic belt, northeast Japan. — *in* ISHIHARA S. et al. eds.: Geology of Kuroko deposits. *Mining Geology Special Issue* 6: 235–249.
- LASKY, S. G. 1948: Trends in technology and outlook for improvement in mineral position: Search for new mineral supplies. — *in* Staffs Bureau of Mines and Geological Survey, Mineral Position of the United States, Public Affairs Press, Washington D. C.: 1–10.
- MCCAMMON, R. B.–MENZIE, W. D.–MAST, R. F.–CARTER, D. M. 1991: Quantitative assessment of energy and mineral resources within eighteen wilderness study areas in the states of Colorado, Nevada, and Utah. — US Geological Survey Open-File Report 91-384: 47 p.
- MENZIE, W. D.–SINGER, D. A. 1993: Grade and tonnage model of porphyry Cu deposits in British Columbia, Canada, and Alaska, USA — US Geological Survey Open-File Report 93-275: 8 p.
- REED, B. L.–MENZIE, W. D.–MCDERMOTT, M.–ROOT, D. H.–SCOTT, W.–DREW, L. J. 1989: Undiscovered lode tin resources of the Seward Peninsula, Alaska. — *Economic Geology*, 84: 1936–1947.
- ROOT, D. H.–MENZIE, W. D.–SCOTT, W. A. JR. 1992: Computer Monte Carlo simulation in quantitative resource estimation. — *Nonrenewable Resources*, 1: 125–138.
- SILLITOE, R. H. 1972: A plate tectonic model for the origin of porphyry copper deposits. — *Economic Geology*, 67: 184–197.
- SILLITOE, R. H. 1973: The tops and bottom of porphyry copper deposits. — *Economic Geology*, 68: 799–815.
- SILLITOE, R. H. 1980: Are porphyry copper and Kuroko massive sulfide deposits incompatible? — *Geology*, 8: 11–14.
- SINGER, D. A. 1993a: Basic concepts in three-part quantitative assessments of undiscovered mineral resources. — *Nonrenewable Resources*, 2(2): 69–81.
- SINGER, D. A. 1993b: Development of grade and tonnage models for different deposit types. — *in* KIRKHAM, R. V.–SINCLAIR, R. V.–THORPE, W. D.–DUKE, J. M. eds.: Mineral deposit modeling. Geological Association of Canada Special Paper 40: 21–30.
- SINGER, D. A.–COX, D. P.–DREW, L. J. 1975: Grade and tonnage relationships among copper deposits. — US Geological Survey Professional Paper 907A: A1–A11.
- SINGER, D. A.–KOUDA, RYOICHI 1997: Classification of mineral deposits into types using mineralogy with a probabilistic neural network. — *Nonrenewable Resources*, 6(1): 69–81

- SINGER, D. A.–KOURA, RYOICHI 1997: Use of a neural network to integrate geoscience information in the classification of mineral deposits and occurrences. — *Exploration* 97, p.
- SINGER, D. A.–MOSIER, D. L. 1981: Review of regional mineral resource assessment methods. — *Economic Geology*, 76(5): 1006–1015.
- SINGER, D. A.–MOSIER, D. L. eds. 1983a: Mineral deposit grade–tonnage models. — US Geological Survey Open–File Report 83–623: 100 p.
- SINGER, D. A.–MOSIER, D. L. eds. 1983b: Mineral deposit grade–tonnage models–II. — US Geological Survey Open–File Report 83–902: 101 p.

QUANTIFYING MINERAL-DEPOSIT MODELS FOR RESOURCE ASSESSMENT

BYRON R. BERGER¹, LAWRENCE J. DREW², and DONALD A. SINGER³

¹US Geological Survey, P. O. Box 25046 Denver, CO 80225, USA

²US Geological Survey, 12201 Sunrise Valley Drive, Reston, VA 20192, USA

³US Geological Survey, 345 Middlefield Road, Menlo Park, CA 94025 USA

ABSTRACT

Mineral-deposit models are an integral component of any mineral-resource assessment methodology. Pushing forward the frontiers of the state-of-the-art in deposit models is important in helping to meet the need for mineral-resource assessments to be carried out more efficiently and cost effectively, and become useful as predictive tools in quantitatively forecasting favorable sites for deposit occurrence. Advances in the understandings of plate-tectonic environments and the coupling of thermal, mechanical, and hydraulic phenomena in hydrothermal systems provide avenues for exploring aspects of mineral-deposit models that might improve them. These understandings underscore the importance of far- and near-field stresses on fluid flow in ore-forming systems and the potential of paleostress analysis to be integrated into models.

Hierarchical schemas are most frequently used to classify mineral deposits for assessments because they provide a mechanism for subdividing regions being assessed into permissive terranes. Three general categories of typical hierarchical schemes are both suitable and potentially amenable to applying coupled physical phenomena in the quantification of models—regional terranes, the landscapes within which deposits occur, and the attributes that describe the deposits *per se*. Using epizonal deposits in a continental-arc environment as an example, this paper explores some of the possibilities to quantify mineral-deposit models.

1. INTRODUCTION

Whether one's goal is exploration, economic development, or land-use planning, estimating where and the probable quantities of undiscovered mineral deposits¹ are important, but uncertain, undertakings. At the heart of any methodology used to estimate undiscovered deposits are mineral-deposit models. They are the basis for assuring consistency throughout all steps of an estimation process (SINGER 1993a). Minimizing uncertainties in deposit models decreases the overall uncertainty in their application.

Increasing labor and technology costs worldwide and the need to balance environmental versus resource-exploitation demands make it imperative that the analysis of geological information and its interpretation as to the undiscovered mineral deposits be done as efficiently and precisely as possible. Greater precision is accomplished by decreasing the uncertainty and improving the predictive capability from models. This may be accomplished through increased understanding about the localization of mineralizing systems, the formation of ore bodies within mineralizing systems, and the quantification of descriptive deposit information. This is the state-of-the-art in mineral-deposit modeling.

It is our purpose in this paper to propose a frame of thinking about hydrothermal mineral deposits that we believe will greatly improve the utility of models of them. Because the specific content of models depends to a certain extent on their application (HENLEY and BERGER 1993), our goal herein is on modeling for economic devel-

¹ We use the term "mineral deposit" in the context of Cox et al. (1986) wherein a mineral deposit is a mineral occurrence of sufficient size and grade that it might, under the most favorable circumstances, be considered to have economic potential.

opment and land-use planning purposes². The discussion focuses on three aspects that we believe will improve the predictive capabilities of these mineral-deposit models: (1) lithotectonic terranes, (2) dynamic landscapes and evolving mineralizing systems, and (3) the quantification of model attributes and linkages between commonly associated mineral-deposit types. The epizonal³ magmatic-hydrothermal environment is used for illustrative purposes, but the concepts discussed are based on first principles and are, therefore, applicable to other ore-forming environments.

2. A FRAME OF THINKING ABOUT MINERAL DEPOSITS

Hydrothermal mineral deposits are a natural part of petrogenetic processes. Studies of volcanoes, hot dry-rock geothermal areas, and nuclear waste disposal problems have shown that, in fluid-flow systems, thermal, mechanical, and hydraulic phenomena are interdependent (cf. NOORISHAD et al. 1984, INGEBRITSEN and SANFORD 1998). Therefore, mineralizing systems must be modeled as the totality of the complex coupled phenomena that form them, not by only one or two of the phenomena.

Although oversimplified for ore-forming systems, the coupling of forces and flows may be expressed as

$$q = -K\nabla H - K_T\nabla T - K_C\nabla C_S,$$

where the flow, q , is a function of the hydraulic conductivity (K), the hydraulic gradient (∇H), thermal conductivity (K_T), thermal gradient (∇T), chemical conductivity (K_C), and chemical concentration gradient (∇C_S). The coupled heat and chemical transport aspects of the flow equation have been the focus of ore-genesis research for several decades. However, the interdependence of flow and deformation in ore-forming systems is less well-studied. The importance of deformation to fluid flow is manifested in part through the equivalent hydraulic conductivity which, in a rock with parallel planar fractures, is

$$K = \frac{\rho_w g N b^3}{12 \mu [1 + C(x)^n]},$$

where ρ_w is the fluid density, g the acceleration of gravity, μ the dynamic viscosity, b the fracture aperture, N the number of fractures per unit distance across the planar rock face, and $C(x)$ the set of variables that describe fracture roughness (DOMENICO and SCHWARTZ 1998). The relation of aperture to hydraulic head gradient is cubic because, for a given gradient, flow through a fracture is proportional to the cube of the fracture aperture. Disregarding fracture roughness, the permeability, k_x , is

$$\frac{N b^3}{12}.$$

Deformation also triggers heat and chemical transport processes. Coseismic dilatation and decompression of a fracture network results in heat transfer from the host rock between the fractures to the fluid in the fractures and an increase in the vapor fraction in the fracture network (HENLEY and HUGHES in press). The separation of the vapor fraction potentially increases the solute concentrations in the remaining liquid fraction. The vapor fraction increases as fracture density and interconnectivity increase. In addition, the proximity to the fracture network at which the vapor fraction increases diminishes as the fracture spacing decreases. Thus, mineral deposition is dependent on deformation and fracture-network size and geometry.

Within any flow system—magmatic, hydrothermal, or groundwater—fluid flow is perpendicular to the least principal stress (σ_3) and parallel to the maximum principal stress (σ_1) (cf. NAKAMURA 1977, ZOBACK and ZOBACK 1980, TSUNAKAWA 1983). Laboratory and field experiments confirm the relation between principal stresses and fluid flow (HAIMSON 1974, BARTON et al. 1995). This relation is of considerable importance in reconstructing the paleostress conditions affecting magmatic and hydrothermal activity in mineralized areas.

² Although we do not specifically mention models for minerals exploration, the quantitative models we propose would be applicable to exploration strategies that attempt to estimate the number of targets within some terrane, rank target areas, and estimate the uncertainty of occurrence at a specific site.

³ We use the term "epizonal" in the context of all mineral deposits generally formed at ≤ 4 km depth in the earth's crust.

3. IMPROVING THE PREDICTIVE CAPABILITIES OF MODELS

3.1. Lithotectonic terranes

The plate-tectonic model of the earth provides a consistent set of describable dynamic processes and landscapes, landscapes that evolve, are modified, and come and go in time and space. This consistency of process leads to there being a correlation between mineral-deposit types and geologic terranes. Thus, lithologic/tectonic landscapes derived from plate motions make a logical framework around which to categorize each mineral-deposit type. Table 1 summarizes selected epizonal magmatic-hydrothermal deposit types in the context of plate tectonic lithotectonic terranes associated with convergent plate margins.

Classification of selected epizonal magmatic-hydrothermal mineral deposits.
Epizonal deposits herein are defined as those forming at ≤ 4 -km depth

Table 1

I. Deposits produced along convergent tectonic-plate margins

A. Magmatic arcs above subduction zones

1. Porphyry type
 - a. Porphyry Cu subtype
 - b. Porphyry Cu-Au subtype
 - c. Porphyry Cu-Mo subtype
2. Skarn type
 - a. Cu, Cu-Au subtype
 - b. Fe subtype
3. Polymetallic type
 - a. Replacements
 - b. Veins
4. Epithermal-style deposits
 - a. Quartz-adularia-illite type deposits
 - (1) Sado subtype
 - (2) Comstock subtype
 - (3) Creede subtype
 - b. Quartz-alunite-kaolinite±pyrophyllite type deposits
 - (1) Au, Au-Cu, Cu subtypes
 - (2) Polymetallic subtype

B. Back-arc environments

1. Back-arc basin spreading centers
2. Continental back-arc regions
 - a. Epithermal-style deposits
 - (1) Quartz-adularia-illite type deposits
 - i. Sado subtype
 - ii. Comstock subtype
 - iii. Creede subtype
 - (2) Quartz-alunite-kaolinite±pyrophyllite type deposits
 - i. Au, Au-Cu, Cu subtypes
 - ii. Polymetallic subtype
 - b. Porphyry type
 - (1) Porphyry Cu-Mo, Cu-Au subtypes
 - (2) Granodiorite-related porphyry Mo subtype
 - c. Skarn type
 - (1) Polymetallic, Au±Cu subtypes
 - (2) Fe subtype
 - (3) W subtype
 - (4) Sn±W subtype
 - d. Polymetallic type
 - (1) Replacement subtype
 - (2) Vein subtype

C. Tectonic-plate accretion: suture-related shear zones

1. Hg veins and replacements
2. Sb veins and replacements

D. Continental-margin transform environments

1. Porphyry type
 - a. Climax-style porphyry molybdenum deposits
 - b. W subtype
 - c. Be subtype
2. Skarn type
 - a. Sn±W subtype
 - b. W subtype
3. Sn-replacement type ± veins

3.1.1. Current USGS approach to regional classification

Since the early 1980s in US Geological Survey (USGS) mineral-resource assessments, the most common way to classify mineral deposits in a regional geologic context has been lithologic associations. For example, COX and SINGER (1986) subdivide epizonal magmatic-hydrothermal deposit models into lithologic groupings as shown for some deposit types in Table 2. Within a model, such as Comstock epithermal vein deposits (model 25c; MOSIER et al. 1986), the lithologic setting is simply calc-alkaline or bimodal volcanism, and the regional tectonic setting is “through-going fracture systems” or “major normal faults”. This lithologic approach to classification is qualitatively useful, but does not provide information on the frequency of occurrence of any of the stated attributes. In addition, this approach does not provide an explanation as to why some geologic terranes ostensibly permissive for the occurrence of undiscovered deposits of a specific type have, in fact, few or none. In section 3.1.2 we consider a plate-tectonic environment—magmatic arcs in subduction zone settings—as an example, with emphasis on those aspects which portend amenability to forming distinct populations.

Selected example of mineral-deposit models classification used by COX and SINGER (1986)

Table 2

1. Deposits related to felsic porphyrophanitic intrusions

- Model 16 Climax Mo deposits
- Model 17 Porphyry Cu deposits
- Model 18a Porphyry Cu, skarn-related deposits
- Model 20c Porphyry Cu-Au deposits
- Model 21a Porphyry Cu-Mo deposits
- Model 22b Au-Ag-Te vein deposits

2. Deposits related to subaerial felsic to mafic extrusive rocks

- Model 25a Hot-spring Au-Ag deposits
- Model 25b Creede epithermal vein deposits
- Model 25c Comstock epithermal vein deposits
- Model 25d Sado epithermal vein deposits
- Model 25e Epithermal quartz-alunite Au deposits

3.1.2. Example of lithotectonic terrane: Magmatic arcs

Subduction zones are regions along convergent tectonic-plate boundaries where relatively cold and dense lithospheric plates sink into the earth beneath an opposing overriding plate (TATSUMI and EGGINS 1995). These zones are commonly divided into subregions: forearc, volcanic arc, and back arc. The magmatism and surficial volcanism typically occur in the overriding plate in a linear belt (“volcanic front”) parallel to the convergent plate margin, and quite consistently are situated about 100-200 km above the subducting slab. The most common occurrence of epizonal magmatic-hydrothermal mineral deposits is in magmatic arc environments.

Subduction induces significant chemical change in the earth’s lithosphere, and magma formation is one consequence of the geochemical processes. Studies of subduction-related igneous rocks have shown them to be chemically distinct and many studies show there to be some systematic variations in igneous rock chemistry across arc terranes. Because of the focus of economic geology research on heat and chemical transport phenomena, the chemistry of magmas within subduction zones has been studied in an effort to find relations that could be used to determine if there are “productive” and “nonproductive” magmas. However, thus far no unique relations between deposit type and magma chemistry have been identified. Quantifying the chemistry of rocks associated with mineral deposits in magmatic arcs is probably not worthwhile.

Although subduction zones are dynamic, there are systematics across them that may produce metrics useful in mineral-deposit classification at the terrane scale and the prediction of where mineralizing systems are likely to occur in magmatic-arc terranes. There are topographic systematics (outer rise, trench, shelf, island arc), the topography and free air gravity are positively correlated, and the width of the positive gravity anomaly over the magmatic arcs is about the same width as the trenches (HAYES and EWING 1970). MELOSH and RAEFSKY (1980) suggest that the latter correlation implies a single, dynamical process, and showed through numerical modeling that the forces involved are due to viscous stresses⁴ generated by the bending of the lithosphere as it is being sub-

⁴ Viscosity is the property of a fluid or semifluid to maintain a shear stress as a function of velocity and pressure.

ducted and to a lesser extent the elasticity of the lithosphere. The stresses are propagated upward and affect tectonic phenomena and fluid flow in the overriding plate.

Another measurable attribute of arcs is the distribution and numbers of volcanoes. Distribution and numbers are affected by the thermal structure of the mantle wedge. In some arcs (e.g., Aleutian, Kamchatka, Kurile, NE Japan, Indonesia, and Scotia) there are two volcanic chains, while others have only a single chain (e.g., Mariana, Tonga-Kermadec, Central America, and Lesser Antilles) (TATSUMI and EGGINS 1995). MARSH (1979) found that the width of a volcanic arc is inversely proportional to the angle of subduction, with wider arcs forming above more shallowly dipping subducting slabs. The volume of erupted volcanic material is greatest at the volcanic front and decreases toward the back-arc side; large-volume calderas are more common along the plate boundary side of the arc. In the Northeast Japan, New Zealand, and Kurile arcs, there is a higher extent of differentiation on the plate-boundary side of the arcs than on the back arc side. Taken together with the greater volume of erupted volcanic material, these facts require that considerably more magma is produced on the plate-boundary sides of arcs, which TATSUMI and EGGINS (1995) speculate is a reflection of a greater amount of volatile flux. Also, the flux of volatiles has important implications for mineral deposit formation as discussed below. The number and density of volcanoes is positively correlated with the rate of subduction (SHIMOZURU and KUBO 1983). A greater rate of subduction increases the flux of dehydration fluids from the greater volume of material being subducted, which in turn leads to higher rates of melt production in the overlying mantle wedge (TATSUMI and EGGINS 1995).

In the Taupo Volcanic Zone, New Zealand, there are a large number of high-enthalpy geothermal systems (Fig. 1). The high-gas, metalliferous systems are considered to be most analogous to ore-bearing epithermal systems. But, these metalliferous systems are not randomly distributed with respect to the tectonic elements in the

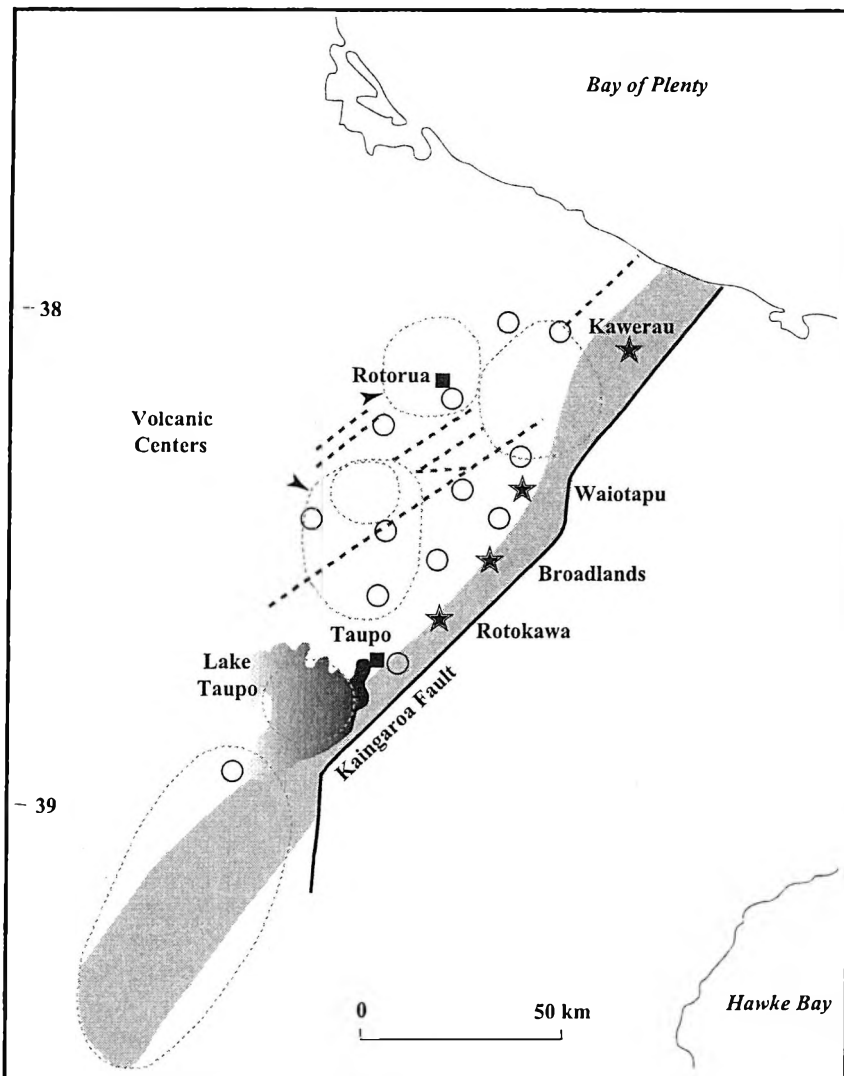


Fig. 1: The spatial relation of high-enthalpy, high-gas metalliferous geothermal systems (M) in the Taupo Volcanic Zone and the crustal-scale Kaingaroa fault and the andesitic continental-arc volcanism (shaded area). High-enthalpy, low-gas and low metal geothermal systems are shown by open circles (after BERGER and HENLEY, 1989)

Taupo zone. They all occur along a single tectonic line—the “Andesite Line”—at the front of the magmatic arc. High-enthalpy geothermal systems not along the Andesite Line are low-gas and low-metal. Dissolved gases, especially H₂S and CO₂, are important in ore formation. The implication is that deep-seated, basement penetrating fracture zones are necessary to the formation of metalliferous geothermal systems in active magmatic arcs.

Implications for mineral-resource assessments of magmatic-arc terranes. The consistency of igneous-rock chemistry in different plate-tectonic settings implies that paleo-arc terranes can be delineated. This is an important first step in drawing boundaries around terranes permissive for the occurrence of undiscovered deposits of a specific type that are known to be associated with these arc terranes. In addition, the metallogenesis of known mineral deposits within a permissive terrane provides information on the general composition and possible geochemical evolution of regions within the lithosphere where magmas are produced and on the extent of metasomatism due to devolatilization above the subducting slab. For example, within the State of Nevada, common Jurassic epizonal deposits are porphyry copper, polymetallic vein, and iron skarn types. By the Cretaceous, metasomatism of the lithosphere had been sufficient for iron skarn to diminish in abundance and tungsten skarn deposits to become common.

The links between the physical architectures of the magmatic arc and back-arc regions, the volume and localization of magmatism, localization of high-enthalpy and metalliferous geothermal activity, and the far-field stresses imply that systematics may occur in groups of terranes with characteristics having a high likelihood of predictability. Careful analysis may elucidate those aspects of modern arcs that can provide reliable population statistics. In addition to geologic variables, there are also possibilities in geochemical indicators such as across-arc variations in ⁸⁷Sr/⁸⁶Sr.

Thus, the paleogeography of arc terranes, their structural geology, and the occurrence of crustal-scale basement fracture zones may be used to further delimit areas within permissive tracts for which the undiscovered deposit potential is more favorable.

3.2. Dynamic deposit landscapes

In most mineral-deposit models, the geology of deposits is more commonly portrayed in cross-section than in plan view (cf. KIRKHAM et al. 1993). Analogs of the sedimentary-rock facies models are seldom applied to igneous-rock related mineral deposits, and the integration of tectonics and structure into evolving landscapes for models is infrequently found in the literature. However, modeled paleogeographic landscapes including indicators of stress-related dynamics have the potential to significantly improve our ability to predict where and when mineral deposits are likely to occur in any given terrane.

The analysis of the geologic settings of epizonal deposits in the western United States suggests that the settings may be divided into two groups, compressional and extensional. For deposits occurring in compressional environments, epizonal deposits appear to be preferentially localized in stepovers—extensional or contractional—within lateral fault systems. In extensional regimes, higher grade ores are related to transfer structures transverse to the direction of extension or in short length-scale extensional faults between two closely spaced transfer faults. Below, we illustrate what a time-space landscape/dynamics model might look like for a terrane with continental-arc volcanism transitioning over time from an oblique-slip plate-margin setting to a near-field hyperextending setting during volcanism-related hydrothermal activity.

3.2.1. A hypothetical landscape/dynamics model

The intrusion of large volumes of magma into the shallow crust in arc terranes results in uplift and extension. Nevertheless, strike-slip faults parallel the trend of the magmatic arc as a consequence of oblique plate convergence and/or buoyancy contrasts between converging plates (WOODCOCK and SCHUBERT 1994). In such “mixed” tectonic settings, volcanism is frequently localized at releasing bends along strike-slip faults and in transfer zones in extending regimes (GLAZNER et al. 1994).

Most geologic environments have complex histories. Capturing this complexity in generalized models is difficult. Focus must be on the environment existing at the time a mineral deposit of interest was permissive to form. Crustal-scale faults antecedent to this time are important because they affect the course of fluids in the crust (refer to section 3.1.2) and have an effect on subsequent fault tectonics by forcing releasing and/or constraining bends along strike-slip fault systems due to reactivation. In addition, changes in the far-field stresses during the time of interest have an effect on the behavior of hydrothermal systems.

Figure 2 shows a conceptual model for the time-space evolution of a continental-arc region where the near-surface fault dynamics change from strike-slip tectonics to hyperextension within a far-field driven oblique-slip

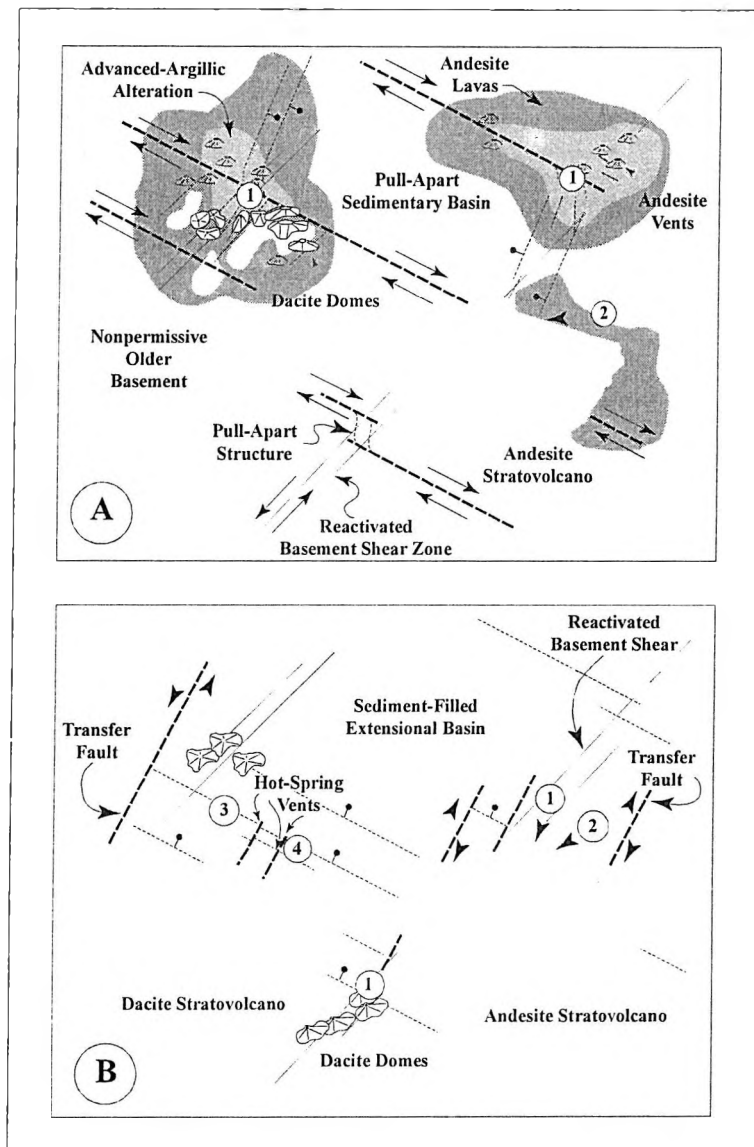


Fig. 2: Hypothetical example of an evolving time-space landscape/dynamics model of a geologic terrane permissive for the occurrence of porphyry- and epithermal-style mineral deposits in a continental-arc setting

A Stage 1. Andesitic vents and dacite to rhyodacite domes erupted on a basement that is not permissive for the occurrence of either porphyry- or epithermal-style mineral deposits. Far-field compressive stresses along the tectonic-plate margin led to the development of right-lateral strike-slip faulting (thicker dashed lines) within the magmatic arc. Strain within this terrane was largely accommodated by extension (thinner dashed lines) related to the development of a sedimentary-rock filled pull-apart basin. Releasing bends for the extensional stepovers were forced by reactivation of antecedent basement shear zones (gray lines). Advanced-argillic alteration (light grey areas) (site #1) associated with domes and small andesitic vents in the transfer zones into the duplexes are favorable for the occurrence of quartz-alunite-kaolinite \pm pyrophyllite gold deposits. The core of the large andesite stratovolcanic edifice (site #2) is favorable for the occurrence of a porphyry-style and associated vein deposits.

B Stage 2. Andesitic volcanism wanes in the large stratovolcano and dacitic volcanism becomes predominant through central-vent eruptions and domes in the southwestern part of the permissive terrane. The predominant faulting changes from strike-slip to normal with extension to the northeast. Volcanic activity is primarily in the footwalls of major normal faults. Hydrothermal convection related to the volcanic activity results in favorability for epithermal vein deposits along northeast-striking transfer faults (thicker dashed lines) (site #1) at both central vent edifices and the dacite-dome complex. There is favorability for porphyry-style deposits associated with the andesite center (site #2) as noted for Stage 1, but the dacite stratovolcanic center isn't considered as favorable because the broad area of normal faulting and extensive intrusive activity cause the region to accommodate the strain through considerable thermoelastic expansion and there is a low strain rate on the dacite magma chamber. Because of lateral hydrothermal flow northeasterly from the dacite stratocone, discharge occurs along the basin margin which migrates progressively to the east as thermoelastic expansion and normal faulting progressed. There is hot-spring Hg favorability in steaming ground surrounding the discharge vents (site #3) and, if a lake occupies the basin, there is favorability for low-grade Au in the lake margin deposits (site #4) if steam condensed in the lake waters which then collapsed across the discharge materials and acid-leached them and effectively upgraded the gold concentrations.

strain field. In Figure 2A, Stage 1, the far-field compressional stresses result in strain accommodation along northwest-striking, right-lateral strike-slip faults and associated secondary and extensional faults. This set is superimposed on a pre-existing system of northeast-striking strike-slip basement shear zones. Motion on the interacting en échelon master strike-slip faults is accommodated across stepovers through linking faults. A resulting pull-apart basin dominates the central part of the landscape depicted. Andesitic volcanic vents are widespread, with a single, large andesitic stratovolcano (Fig. 2A) localized in a releasing bend of the pull-apart basin.

During Stage 2 of the evolving landscape (Fig. 2B), a heated, strain softened shallow crust leads to near-field stresses dominating the surficial tectonics. Hyperextension is superimposed on the far-field compressional dynamics. Stretching of a rheologically uniform medium permits low-angle extensional detachments to develop. The northwest-striking faults, formerly strike-slip, serve as headwalls for the extensional detachments and continued basin evolution, and the basement shear zones which controlled the development of the extensional duplex in Stage 1 now control the localization of transfer faults.

During Stage 2, volcanism continues at the Stage 1 stratovolcano in the southeast, and a large dacitic stratoncine grows in the footwall facing the extending basin. Magma-driven thermoelastic stresses are normal to the vertical volcanic feeders; therefore, considerable strain is accommodated and the volcanic edifices are primarily in the footwalls of the normal faults. The andesitic to dacitic volcanoes in Figure 2B are localized within the footwalls of northwest-striking normal faults.

3.2.2. Implications of the hypothetical model for mineral-resource assessment

Empirically, we have found that epizonal mineral deposits are most frequently localized within fault systems in zones of releasing and restraining offsets along strike-slip faults and on transfer faults within extensional regimes. This information may be applied to conceptualizations of geothermal systems that might be expected to occur in the two landscape stages in figures 2A and 2B. Figure 3 illustrates a possible model construct for the occurrence of porphyry, epithermal vein, and hot-spring styles of mineralization related to near-neutral pH fluids (adularia stable) in the Figure 2A-B landscape. In the model the predominant hydraulic conductivity is assumed to lie in the plane of the page, and topography and prevailing winds and storms have been positioned such as to result in flow from left to right. Two synhydrothermal stress axes orientations acting on a fault in the plane of the figure are given [(a) and (b)]. Stress axes (a) imply that extension would occur on the fault whereas stress axes (b) imply the fault to be under shear. The hypothetical mineral-resource potential for each of these stress axes orientations is given in Table 3.

The critical thing that integrating dynamics into the landscape evolution brings to assessment is that there is a possibility that both the localization of deposits and likely economic outcomes may be predictable. In the scenario given above, the potential changes with time. For example, from the conceptual model in Figure 3 we predict that the large andesite stratovolcano (Fig. 2A), which is situated at the releasing bend along a northwest-striking master right-lateral, strike-slip fault, is a likely geologic setting for the occurrence of epithermal quartz-adularia-illite vein deposits and possibly porphyry-style deposits along the fault in the plane of the figure. Regarding the epithermal vein potential, however, the predominant flow in the Stage 1 landscape would be to the northeast on highly permeable, long length-scale normal faults (Fig. 3) under stress scenario (a). Highly permeable normal faults disperse rather than focus fluid flow because there are more ways for heat to be shared among randomly moving heated molecules over large volumes than ways for the energy to be restricted to a small region within the permeable zone. In such situations, one should look for higher grade ore bodies in transfer fault zones or on short length-scale normal faults. During Stage 2 (Fig. 2B) the andesite volcano is still active and hydrothermal activity continues. The flow is still along the same fracture network because the far-field σ_1 is still oriented the same, but the total mass flux is less dispersed. With the change to stress scenario (b) (Fig. 3), what was formerly a normal fault is now a strike-slip transfer fault. High permeability areas along the structure are now limited; therefore, the same mass flux is redirected through a much smaller volume of rock. It is focused. The coupling of chemical transport and mechanical deformation in the constrained volume is more conducive to rapid and more abundant mineral precipitation. Consequently, during this stage, we might predict that higher grade ores are likely to be superimposed on the earlier low-grade to economically barren vein.

In contrast, the dacite stratovolcano in Stage 2 (Fig. 2B) is constructed in the footwall of what is now a normal fault and flow is along a northeast-striking, transfer structure [Fig. 3, stress scenario (b)] and higher grade vein potential exists along this trajectory. Thus, both volcanoes have comparable potential to produce economic vein deposits, but it was the important shift in stress regimes from Stage 1 to Stage 2 that made the potential of the andesite center comparable to the dacite center. Both hypothesized hydrothermal systems discharge into a basin that may contain a lake. Although not illustrated, if a lake exists, then the condensation of acid volatiles from geother-

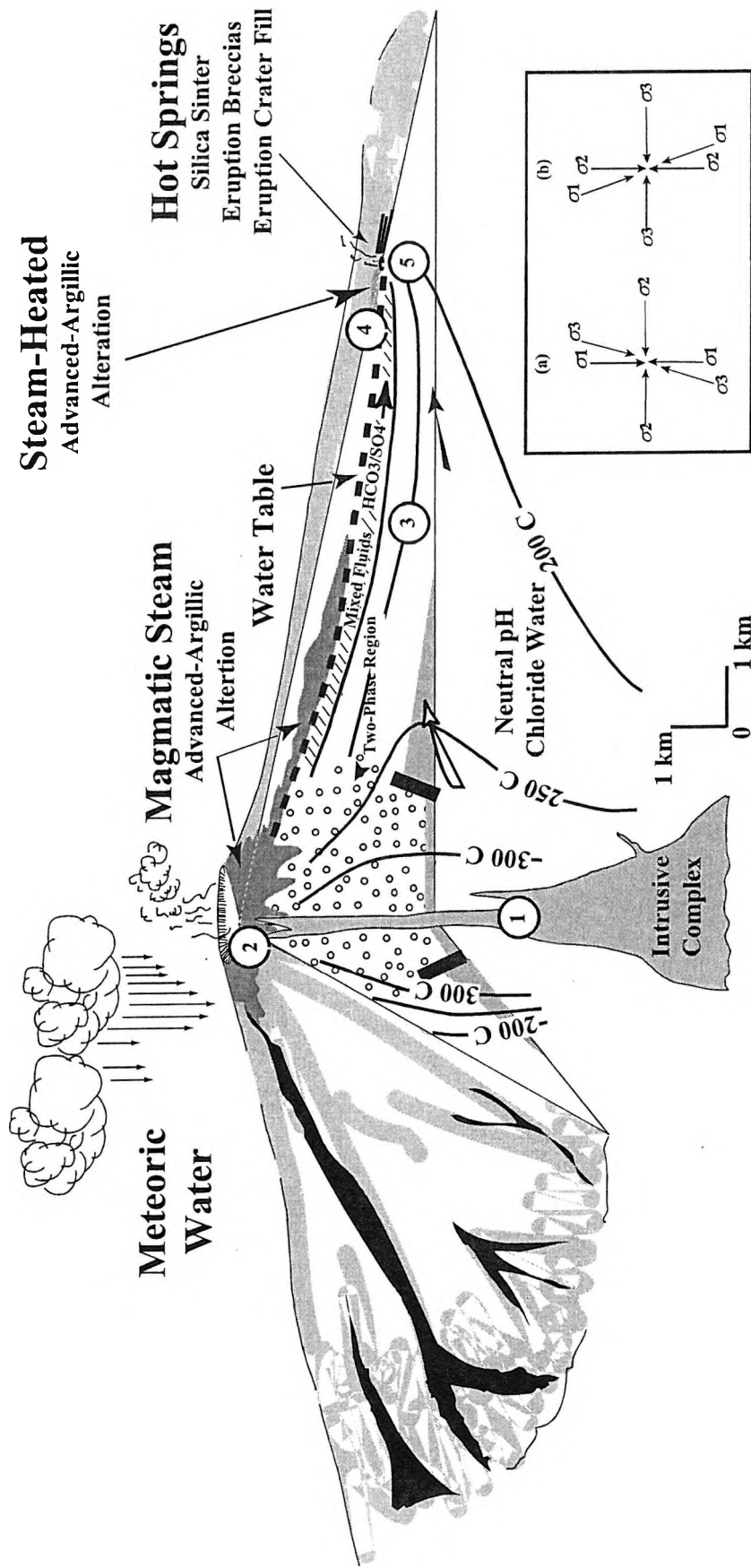


Fig. 3: Conceptual model of flow patterns within and surrounding an upwelling, near-neutral pH geothermal fluid within and adjacent to a stratovolcanic edifice. Prevailing winds are depicted as blowing from left to right; therefore climatic, rainfall, and topographic effects result in lateral flow from left to right. The amount of lateral flow is proportional to the height and slope angle of the volcanic edifice. Five styles of mineralization are depicted: 1. porphyry, 2. magmatic-steam advanced-argillic; 3. epithermal veins; 4. steam-heated hot-spring Hg; and, 5. hot-spring-related Au-Ag. Two different principal stress orientations are shown in (a) and (b). The axes are oriented to indicate the possible stresses acting on the plane of fractures controlling the left to right fluid flow; i.e., in the plane of the cross section. The favorability for the 5 styles of mineralization for the two stress orientations is given in Table 3.

Table of hypothetical favorabilities for the occurrence of porphyry-, epithermal vein-, and hot-spring-style mineralizations from near-neutral pH fluids associated with stratovolcanoes

Table 3

1. Stage 1 landscape

Landform/Deposit Style	Stress Orientation (a)	Stress Orientation (b)
Andesite Stratovolcano		
Porphyry-style	The favorability is low if the strain rate acting on the volcanic edifice is low.	The favorability is high if the strain rate acting on the volcanic edifice is high.
Epithermal-style veins	The favorability for higher grade veins is low due to unfocused flow on highly permeable NE normal faults.	The favorability for higher grade veins is high due to focused flow on NE transfer faults.
Hot-spring Hg	The favorability is high if steam-heated zone is well developed.	The favorability is high if steam-heated zone is well developed.
Hot-spring Au-Ag	The favorability for higher grade mineralization is high if flow was restricted to small rock volumes due to extensive brecciation and favorable fracture patterns. The favorability for lower grade ores is high under all circumstances.	The favorability for higher grade mineralization is high if flow was restricted to small rock volumes due to extensive brecciation and favorable fracture patterns. The favorability for lower grade ores is high under all circumstances.
Climate-controlled hot-spring Au-Ag	The favorability for low-grade deposit is high if basin occupied by lake with fluctuating surface and water table sufficiently low to produce large steam flow in discharge area.	The favorability for low-grade deposit is high if basin occupied by lake with fluctuating surface and water table sufficiently low to produce large steam flow in discharge area.

2. Stage 2 landscape

Andesite Stratovolcano		
Porphyry-style	In regions undergoing rapid extension, the strain rate is generally low on the magma chamber. The favorability is low if the strain rate in the magma chamber is low.	In regions undergoing rapid extension, the strain rate is generally low on the magma chamber. The favorability is low if the strain rate in the magma chamber is low.
Epithermal-style veins	The favorability for higher grade veins is low due to unfocused flow on highly permeable NW normal faults.	The favorability for higher grade veins is high on NE-striking fractures because the flow is focused.
Hot-spring Hg	The favorability is high if steam-heated zone is well developed.	The favorability is high if steam-heated zone is well developed.
Hot-spring Au-Ag	The favorability for higher grade mineralization is high if flow was restricted to small rock volumes due to extensive brecciation and favorable fracture patterns. The favorability for lower grade ores is high under all circumstances.	The favorability for higher grade mineralization is high if flow was restricted to small rock volumes due to extensive brecciation and favorable fracture patterns. The favorability for lower grade ores is high under all circumstances.
Climate-controlled hot-spring Au-Ag	The favorability for low-grade deposit is high if basin occupied by lake with fluctuating surface and water table sufficiently low to produce large steam flow in discharge area.	The favorability for low-grade deposit is high if basin occupied by lake with fluctuating surface and water table sufficiently low to produce large steam flow in discharge area.
Dacite Stratovolcano		
Porphyry-style	In regions undergoing rapid extension, the strain rate is generally low on the magma chamber. The favorability is low if the strain rate in the magma chamber is low.	In regions undergoing rapid extension, the strain rate is generally low on the magma chamber. The favorability is low if the strain rate in the magma chamber is low.
Epithermal-style veins	The favorability for higher grade veins on NW-striking fractures is low due to unfocused flow.	The favorability for higher grade veins on NE transfer structures is low due to no reactivated underlying basement shear.
Hot-spring Hg	The favorability is high if steam-heated zone is well developed.	The favorability is high if steam-heated zone is well developed.
Hot-spring Au-Ag	The favorability for higher grade mineralization is high if flow was restricted to small rock volumes due to extensive brecciation and favorable fracture patterns. The favorability for lower grade ores is high under all circumstances.	The favorability for higher grade mineralization is high if flow was restricted to small rock volumes due to extensive brecciation and favorable fracture patterns. The favorability for lower grade ores is high under all circumstances.
Climate-controlled hot-spring Au-Ag	The favorability for low-grade deposit is high if basin occupied by lake with fluctuating surface and water table sufficiently low to produce large steam flow in discharge area.	The favorability for low-grade deposit is high if basin occupied by lake with fluctuating surface and water table sufficiently low to produce large steam flow in discharge area.

Favorability is given for two different orientations of the stresses acting on the potentially mineralized fracture systems linked to the evolving landscape model in figures 2A and 2B.

mal steam in the lake waters may alter the discharge deposits and effectively upgrade them through acid leaching and redeposition to form a low-grade epithermal deposit at the lake water interface along the discharge zone. Adding such changes to the geologic setting changes the mineral-resource potential.

The porphyry-style mineralization potential is not equivalent for both stratovolcanoes in Figure 2. A constraint is imposed by the fault dynamics. The andesite stratovolcano is exposed to both Stage 1 and Stage 2 dynamics whereas the dacite stratovolcano is exposed only to Stage 2 dynamics. There is a higher potential for porphyry-style mineralization within the andesite edifice during the Stage 1 period than in the dacite stratovolcano of Stage 2. The andesite was initially constructed in a releasing bend where the maximum stress is focused, the total stress exceeds the far-field maximum principle stress, and the stress gradient is steepest (cf. SEGALL and POLLARD, 1980). All porphyries we have examined empirically were formed along strike-slip fault systems and most formed in such releasing bends (the remainders were in constraining bends). The dacite stratovolcano was constructed along an extensional fault zone where the stress overall would be lower than the far-field maximum principal stress. Fluids would be dispersed rather than being focused as in releasing bends of strike-slip faults reducing the expectation for deposit development.

3.3. Quantified mineral-deposit model attributes

To make deposits have a more predictive capability, two approaches are possible. The first approach is based on the observed frequency of occurrence of attributes of all deposit types consistent with the USGS models such as specific minerals, rock types, and associated deposit types. The second approach is the development of "metrics" that may be used to estimate the probabilities of occurrence of deposits as well as the different types of genetically associated deposits (DREW and MENZIE 1993).

3.3.1. Frequency of occurrence of deposit attributes

Linking observed frequency of deposit attributes to existing deposit models allows for the objective solution of several problems in quantitative resource assessment. Descriptive models in COX and SINGER (1986) have two parts. The first describes the geologic environments in which the deposits are found; the second gives the identifying characteristics of the deposits. Thus, the first part plays a primary role in the delineation process in that it describes the general geologic setting favored by a deposit type. The second part of the descriptive model helps classify known deposits and occurrences into types which can also aid in the delineation process. In some cases, geologic environments not shown on geologic maps can be identified by the types of known deposits and occurrences present.

Both quantitative and non-quantitative resource assessments require the integration of different kinds of geoscience information. A key kind of information is the classification of known deposits and occurrences in the region. In all assessments made to this day, these classifications have been subjective. The physical attribute data tabulated in the second part of the descriptive deposit model are the most appropriate quantities for this task. In a large independent test of a probabilistic neural network's ability to classify more than 2500 deposits and occurrences into 28 deposit types, SINGER and KOUDA (in press) demonstrated that mineralogy and six rock types can be used to classify the deposits into generalized groups, but not sufficient for classification into specific deposit types. These tests also showed that additional spatial information would increase the likelihood of properly classifying mineral occurrences that have sparse attribute information.

Quantifying attributes of geologic environments offers the possibility of objectively integrating different kinds of information such as that in GIS systems. Wherever spatial data such as rock types and associated deposit types prove to be predictive, it should be possible to quantitatively integrate GIS information into the classification process and link GIS data to mineral deposit models. These quantitative attributes could then be used in the identification and classification of permissive terranes in resource assessments. As noted by SINGER (1993b), data are also needed on barren areas to properly classify the population of possible mineralized environments.

Databases have already been gathered for selected attributes in a number of deposit types. MOSIER et al. (1986) compiled a comprehensive database on epithermal Au-Ag deposits, MOSIER et al. (1983) prepared one on volcanic-rock hosted massive sulfide deposits, and SINGER (1997) compiled an extensive database of minerals from a large number of deposit types. Table 4 gives an example of a small part of a quantitative mineral-deposit model.

3.3.2. Metrics that predict associated (linked) deposit types

Spatial associations of certain deposit styles have led to the long-standing concept among economic geologists of deposit zoning and associated deposit types. At the root of zoning is the assumption that hydrothermal ore deposits have magmatic origins (cf. LINDGREN 1933). Associated deposit types are typically viewed as a geochemical process, with the patterns resulting from solubility, pressure, and temperature gradients along some fluid path-line (cf. GUILBERT and PARK 1986). DREW and MENZIE (1993) and DREW (1997) suggested that a “metric”—an ordered set of occurrence probabilities specified by a set of inequalities—for zoning patterns and associated deposit types may be calculated. Working from interpretations of metallogenic information from which a density of deposits within a well-explored district or region may be calculated, they argue that within a permissive tract, each associated deposit type occurs according to some metric. Establishing such metrics is important to making deposit models more quantitative.

4. CONCLUSIONS

The outcomes resulting from mineral-resource assessments for land-use and economic development purposes are policy decisions. Therefore, assessment methodologies should be guided by the needs of policy analysis and not the whimsy of scientists. We believe that scientific research on the components of assessments, such as mineral-deposit modeling, must lead to assessment outputs that provide scientifically valid information for policy makers to consider alternative policies. In this paper, we have taken the position that quantification of attributes in mineral-deposit models is one such direction in which model development should be taken, because quantitative models contribute to more precise predictions of undiscovered resources and more precision in estimating the uncertainties in such estimates.

Because the full dimension of components in mineral-deposit models are needed to be effective, we have suggested that approaches to quantify terrane characteristics, mineral-district characteristics, and deposit characteristics should be explored, particularly in the context of the fundamental principles important in ore-forming processes.

Percentage of mineral deposits of a given type (rows) with specific minerals (columns) within them (from SINGER et al., 1997, based on models of COX and SINGER, 1986)

Table 4

Deposit Type	Mineral													
	Adularia	Bornite	Cinnabar	Chalcopyrite	Gold	Enargite/Luzonite	Galena	Kaolinite/Illite/Dickite	Molybdenite	Native Hg	Pyrite	Sericite	Sphalerite	Stibnite
Porphyry Cu (17, 141)	1	83	1	100	37	21	46	45	84	0	100	94	54	2
Porphyry Cu-Au (20c, 24)	0	96	0	100	50	17	46	42	71	0	100	96	46	0
Polymetallic Replacement (19a, 29)	3	31	14	100	48	38	97	28	24	0	93	55	93	21
Hot-Spring Au-Ag (25a, 16)	75	6	56	38	94	6	38	100	13	6	88	63	31	50
Creede Epithermal Vein (25b, 25)	32	32	8	68	60	40	88	40	8	0	80	44	100	24
Comstock Epithermal Vein (25c, 68)	65	25	9	81	87	4	69	31	10	0	84	35	63	18
Sado Epithermal Vein (25d, 29)	28	7	3	72	86	7	41	38	0	0	90	45	41	17
Epithermal quartz-alunite Au (25e, 33)	9	45	15	64	91	91	61	91	9	3	97	36	67	15
Hot-Spring Hg (27a, 39)	0	0	100	0	5	0	5	3	0	10	41	0	0	5

In parentheses next to each deposit type is the COX and SINGER (1986) model number followed by the number of deposits analyzed.

5. REFERENCES

- BARTON, C. A.—ZOBACK, M. D.—MOOS, D. 1995: Fluid flow along potentially active faults in crystalline rocks. — *Geology*, 23: 683–686.
- BERGER, B. R.—HENLEY, R. W. 1989: Advances in the understanding of epithermal gold-silver deposits, with special reference to the western United States. — in KEAYS, R. R.—RAMSAY, R. H.—GROVES D. I. (eds.): *Geology of Gold Deposits: The Perspective in 1988*. Economic Geology Monograph 6: 405–423.
- COX, D. P.—SINGER, D. A. eds. 1986: *Mineral Deposit Models*. — U. S. Geological Survey Bulletin 1693: 379 p.
- DOMENICO, P. A.—SCHWARTZ, F. W. 1998: *Physical and Chemical Hydrogeology*. — John Wiley & Sons Inc., New York: 506 p.
- DREW, L. J. 1997: *Undiscovered petroleum and mineral resources. Assessment and controversy*. — Plenum Press, New York: 149–165.
- DREW, L. J.—MENZIE, W. D. 1993: Is there a metric for mineral deposit occurrence probabilities? — *Nonrenewable Resources*, 2: 92–103.
- GLAZNER, A. F.—WALKER, J. D.—BARTLEY, J. M.—COLEMAN, D. S.—TAYLOR, W. J. 1994: Igneous activity at releasing bends and transfer zones in extensional systems: Implications for site and mode of geothermal activity — *Geothermal Resources Council Transactions*, 18: 7–9.
- GLAZNER, A. F. et al. 1994: *Reconstruction of the Mojave Block* — Geological Society of America. Cordilleran Section Guidebook. Geological Investigations of an Active Margin, Trip 1: 3–30.
- GUILBERT, J. M.—PARK, C. F. JR. 1986: *The Geology of Ore Deposits*. — W.H. Freeman and Co., New York: 217–245.
- HAIMSON, B. C. 1974: A simple method for estimating in-situ stresses at great depth, field testing and instrumentation of rock. — American Society for Testing of Material, STP 554, Philadelphia: 156–182.
- HAYES, D. E.—EWING, M. 1970: Pacific boundary structure. — in MAXWELL, A. E. (ed.): *The Sea*. Wiley & Sons, New York, : 29–72.
- HENLEY, R. W.—BERGER, B. R. 1993: What is an exploration model anyway? An analysis of the cognitive development and use of models in minerals exploration. — in KIRKHAM, R. V.—SINCLAIR, W. D.—THORPE, R. I.—DUKE, J. M. (eds.): *Mineral Deposit Modeling*. Geological Association of Canada Special Paper 40: 41–50.
- HENLEY, R. W.—HUGHES, G. O. in press: Excess heat effects in vein formation: unpublished manuscript.
- INGEBRITSEN, S.—SANFORD, W. 1998: *Ground water and geologic processes*. — New York, Cambridge University Press: 341 p.
- KIRKHAM, R. V.—SINCLAIR, W. D.—THORPE, R. I.—DUKE, J. M. (eds) 1993: *Mineral deposit modeling*. — Geological Society of Canada Special Paper 40: 798 p.
- LINDGREN, W. 1933: *Mineral deposits*. — McGraw-Hill, New York: 119–122.
- MARSH, B. D. 1979: Island arc development: Some observations, experiments, and speculations. — *Journal of Geology*, 87: 687–713.
- MELOSH, H. J.—RAEFSKY, A. 1980: The dynamical origin of subduction zone topography. — *Geophysical Journal of the Royal Astronomical Society*, 60: 333–354.
- MOSIER, D. L.—SINGER, D. A.—SALEM, B. B. 1983: Geologic and grade-tonnage information on volcanic-hosted copper-zinc-lead massive sulfide deposits. — US Geological Survey Open-File Report 83–89: 78 p.
- MOSIER, D. L.—MENZIE, W. D.—KLEINHAMPL, F. J. 1986: Geologic and grade-tonnage information on Tertiary epithermal precious- and base-metal vein districts associated with volcanic rocks. — *US Geological Survey Bulletin* 1666: 39 p.
- MOSIER, D. L.—SINGER, D. A.—BERGER, B. R. 1986: Descriptive model of Comstock epithermal veins. — *US Geological Survey Bulletin* 1693: p. 150.
- NAKAMURA, K. 1977: Volcanoes as possible indicators of tectonic stress orientation. Principle and proposal. — *Journal of Volcanology and Geothermal Research*, 2: 1–16.
- NOORISHAD, J.—TSANG, C. F.—WITHERSPOON, P. A. 1984: Coupled thermal-hydraulic-mechanical phenomena in saturated porous rocks: Numerical approach. — *Journal of Geophysical Research*, 89: 10,365–10,373.
- SEGALL, P.—POLLARD, D. D. 1980: Mechanics of discontinuous faults. — *Journal of Geophysical Research*, 85: 4337–4350.
- SHIMOZURU, D.—KUBO, N. 1983: Volcano spacing and subduction. — in SHIMOZURU, D.—YOKOYAMA, I. (eds.): *Arc Volcanism: Physics and Tectonics*. Terra Publications: 141–151.
- SINGER, D. A. 1993a: Basic concepts in three-part quantitative assessments of undiscovered mineral resources. — *Nonrenewable Resources*, 2: 69–81.

- SINGER, D. A. 1993b: Development of grade and tonnage models for different deposit types. — *in* KIRKHAM, R. V.—SINCLAIR, W. D.—THORPE, R. I.—DUKE, J. M. (eds.): Mineral Deposit Modeling: Geological Association Canada Special Paper 40: 21–30.
- SINGER, D. A.—KOUUDA, R. 1997: Use of a neural network to integrate geoscience information in the classification of mineral deposits and occurrences. — *Exploration* 97, Toronto, in press.
- SINGER, D. A.—WALLER, N.—MOSIER, D. L.—BLISS, J. D. 1997: Digital mineralogy data for 55 types of mineral deposits: Macintosh version. — US Geological Survey Open-File Report: 97–160.
- TATSUMI, Y.—EGGINS, S. 1995: Subduction zone magmatism: Blackwell Science — Cambridge, Massachusetts: 211 p.
- TSUNAKAWA, H. 1983: Simple two-dimensional model of propagation of magma-filled cracks. — *Journal of Volcanology and Geothermal Research*, 16: 335–343.
- WOODCOCK, N. H.—SCHUBERT, C. 1994: Continental strike-slip tectonics. — *in* HANCOCK, P. L. (ed.): Continental Deformation. Pergamon Press, New York: 251–263.
- ZOBACK, M. L.—ZOBACK, M. D. 1980: State of stress in the conterminous United States. — *Journal of Geophysical Research*, 85: 6113–6156.

REGIONAL GEOLOGIC, GEOPHYSICAL AND GEOCHEMICAL DATA USED IN THE ASSESSMENT OF UNDISCOVERED DEPOSITS IN THE MÁTRA, BÖRZSÖNY AND VISEGRÁD MOUNTAINS, NORTHERN HUNGARY

GYÖRGY CSIRIK¹, LÁSZLÓ ÓDOR¹, JÁNOS KISS² and SÁNDOR RÓZSAVÖLGYI²

¹ Geological Institute of Hungary, H–1143 Budapest, Stefánia út 14., Hungary

² Eötvös Loránd Geophysical Institute of Hungary, H–1145 Budapest, Kolumbusz utca 17-23., Hungary

ABSTRACT

This paper provides a description of the regional geologic, geophysical, and geochemical data that were used to assess the undiscovered deposits in the Mátra, Börzsöny and Visegrád Mountains, northern Hungary. The regional geologic data provided the basis for identifying potential host rocks for undiscovered deposits. The regional geophysical data provided the basis for assessing the areal extent of potential host rocks, and the regional geochemical data provided the basis for evaluating the nature and composition of potential host rocks.

1. LOCATION

The study area, located in the western part of the Northern Hungarian Range, comprises an area that extends from the Visegrád Mountains to the Mátra Mountains. The area extends from latitude 48 degrees, 16 minutes to 47 degrees, 38 minutes north. It extends in longitude from 18 degrees, 42 minutes to 20 degrees, 14 minutes east. Much of the middle and northern parts of the region are hilly but the southern part is flat. The highest point in Hungary is located in the Mátra Mountains (Kékes peak, 1014 m). The study area is covered by the 1:200,000-scale Hungary Geological Map Series that includes the following map sheets: Tatabánya, Budapest, Salgótarján, Miskolc, and Eger. Only the Salgótarján Map Sheet lies entirely within the study area.

2. GEOLOGIC DATA

As part of the US–Hungarian Joint Fund Project, the decision was made to create a digital geological data base for use in the assessment. The steps involved included determining the boundary of the map units to be used and the tectonic elements to be considered. Once these were decided upon, mylars were prepared from the original maps and scanned. The resulting computer files were vectorized and edited to produce a final digitized geologic map. Owing to the difficulties encountered in scanning, it became necessary to digitize the mylars manually. The initial work in preparing the digital map was done by the first author in the GIS Department of the Geological Institute of Hungary (GIH). The final editing was done by the third author at the Eötvös Loránd Geophysical Institute of Hungary (ELGI).

The original digital geological map contains 98 map units. In the hilly area, the bedrock geology is displayed, whereas in the flat plain area, the younger Pleistocene and Holocene materials are displayed. To smooth over the irregularities in coverage, a generalized digital map was produced as shown in Fig. 1. The details about the regional geology and the tectonic framework are discussed elsewhere in this volume.

3. GEOPHYSICAL DATA

Digital geophysical data were taken from the digital geophysical data bases of ELGI. Because of the size of the study area, map data rather than point or profile data were used. A large amount of data were taken from

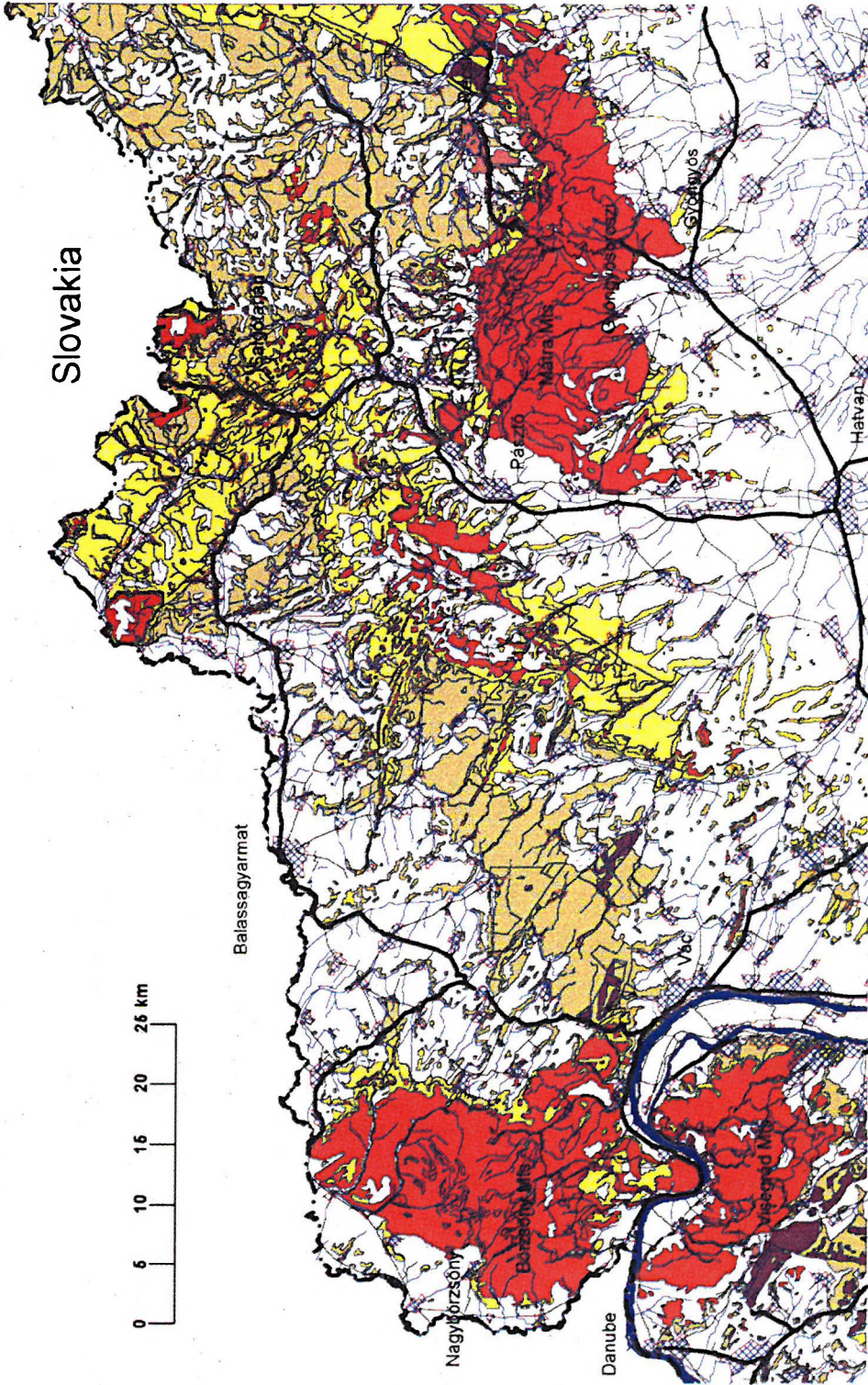


Fig. 1: Simplified geological map of NE Hungary

Miocene sediments yellow; Miocene volcanics red; Paleogene sediments pale yellow; Paleogene volcanics dark red; Mesozoic formations purple

aerial magnetic measurements, field gravity, and ground magnetic measurements, and placed into an Arc/Info data base.

3.1. Aerial magnetic data

Regional aerial geophysical measurements were carried out in Hungary between 1965 and 1969 as part of a Hungarian–USSR cooperative agreement. For the north-south flight lines, the line spacing was 250 m. The nominal flight height was 50 m, and navigation was visual. The positional accuracy was estimated to be 100 m along the flight lines and 120 m between. Only the anomalous magnetic field component (ΔT) data were digitized in 1994 from the 1:50,000 scale analogue contour maps and stacked profiles. These data were interpolated into a 100 by 100 m grid. The resolution of the aerial magnetic data is an order greater than that of the ground magnetic measurements.

The study area can be divided into two subareas by using the ΔT data shown in Fig. 2. The first subarea in the northern part of the study area shows a readily detectable, west-southwestern–east-northeastern-trending, wide magnetic anomaly zone. This anomaly defines the Diósjenő Dislocation Zone. The geologic formation that gave rise to this magnetic anomaly is unknown. The vertical shape of this anomaly is symmetrical so that a structural line can be drawn along the axis of the anomaly. Sometimes the axis is double, which indicates parallel structural lines with the main axis.

The second subarea in the southern part of the study area can be characterized by a variable magnetic field. For the most part, magnetic anomalies are associated with Miocene near-surface volcanic (andesite) rock bodies. These bodies gave rise to large magnitude, highly variable anomalies as evidenced by the magnetic fields in the Mátra, the Cserhát, the Börzsöny, and the Visegrád Mountains. Along some of these volcanic bodies, volcano-structural lines are caused by dikes, andesite veins, and the well-known Darnó Line structure. Although the late Eocene shallow intrusive and the stratovolcanic rock bodies considered to be the host for the Recsk porphyry deposit is detectable, it gives rise to only a weak anomaly because of its older age and secondary alterations of its original magnetic composition.

3.2. Gravity data

The main anomaly delineated by various gravity surveys over the years is the Diósjenő Dislocation Zone, which divides the study area into two parts—a northern part with positive anomalies and a southern part with local minima (Fig. 3). The dislocation zone, which appears as a transition gradient on the gravity map, separates basically different parts of the crust. It is this difference that creates the main gravity effect. As a consequence, structural lines cannot be drawn along this zone by using the traditional interpretation method based on the commonly accepted practice that the depth of the basement is inversely proportional to the Bouguer anomaly value.

Northward, the anomalies depend not only on the depth, but the type of basement rock. The southern anomalies are due mainly to the depth of the crust. On the southwest, a gravity high indicates the outcrop of Mesozoic basement rock in the Pilis Mountains. The gravity lows in the volcanic Börzsöny–Visegrád Mountains are associated with subsided parts of the basement. The bedrock in the Naszály–Csóvár outcrop and some parts of the Cserhát area are exposed and give rise to maxima in the gravity anomaly field. At the Zagyva graben, the minimum is greater because of the 3,000 to 4,000 m deep location of the basement. The Mátra Mountains give a maximum, but the anomalies belong not only to the volcanic bodies, but also to the basement formations with high-density contrast. The outcropping Mesozoic formations of the Bükk Mountains also give a maximum anomaly.

On the southeastern part of the study area on the Alföld, a huge minimum appears. Such an anomaly can be caused by the presence of a very thick layer of low-density young sediments that overlie the deep basement. The above-mentioned regions are limited by a gradient zone of the main geologic structure. By using the gravity anomaly map, the Darnó Line, which separates the Bükk Mountains from the Mátra Mountains can be detected. The line goes on the surface in the northeastern part of the area and under the surface, as a basement structure, in the southern part. The volcanic structural elements cannot be detected easily on the Bouguer anomaly map. Except for the center of the Börzsöny Mountains, the maximum was shaped by the emergent basement rock. This is the Magas Börzsöny Volcano (BALLA 1978), which can give rise to large gravity effects. Other volcanic structures cannot be located because the scale of the map does not show small forms of volcanism. The main causative body of gravity anomalies is the basement (or deep location of the basement). The gravity effect from the volcanic structures is an order smaller than that from the basement, consequently, it cannot be seen on the regional gravity anomalies.

Application of filtered anomaly maps provides a powerful tool for the interpretation of volcanic structural effects (BALLA 1987). The filtered anomaly map can give more information than Bouguer anomaly maps about an

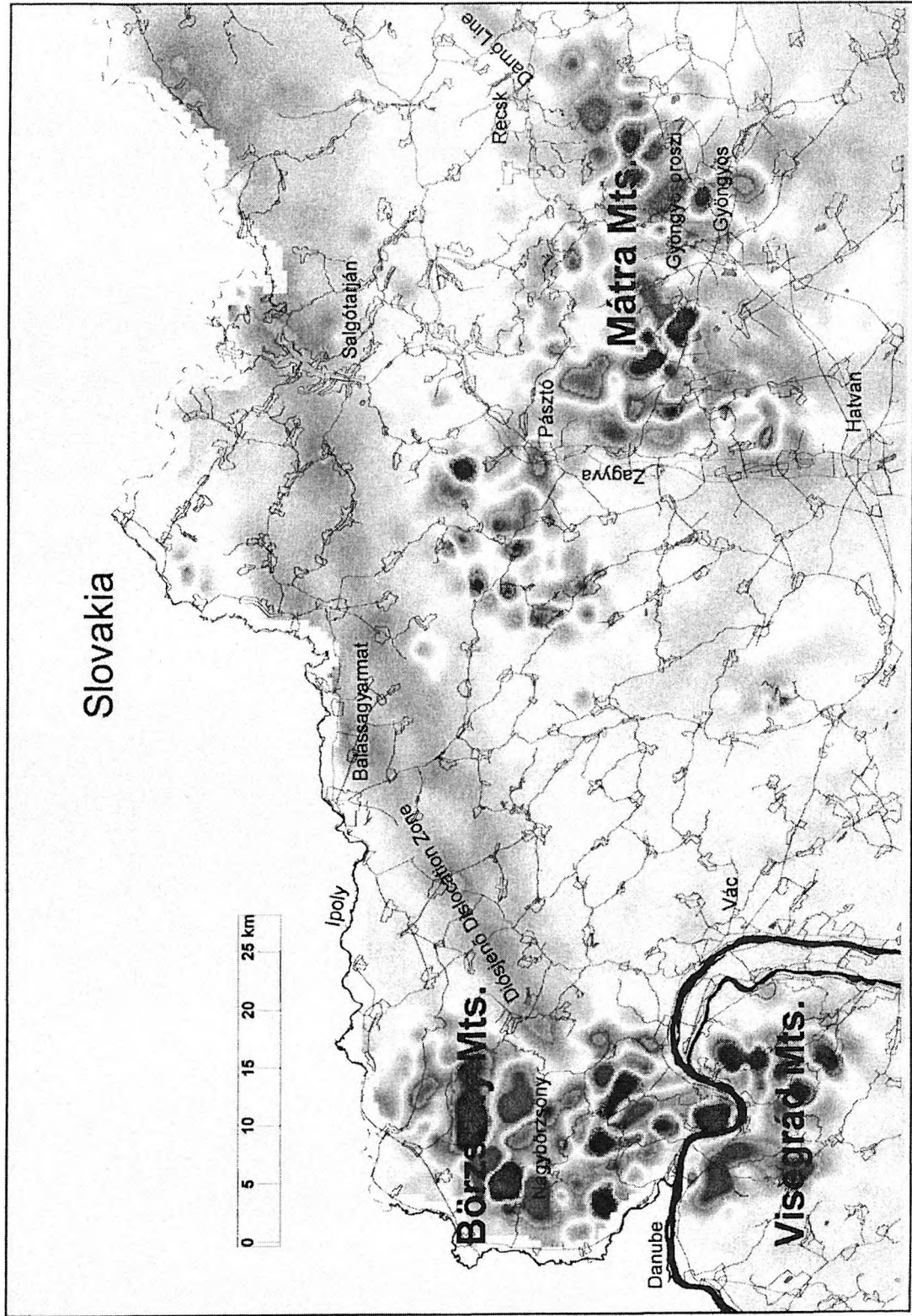


Fig. 2: Magnetic (ΔT) map of the study area

The map is coloured by linear stretching of black and white.

The light colours mean maximum values and the deep colours mean minimum values of the map.

The large areas with "0" values show the lack of magnetic consortive bodies

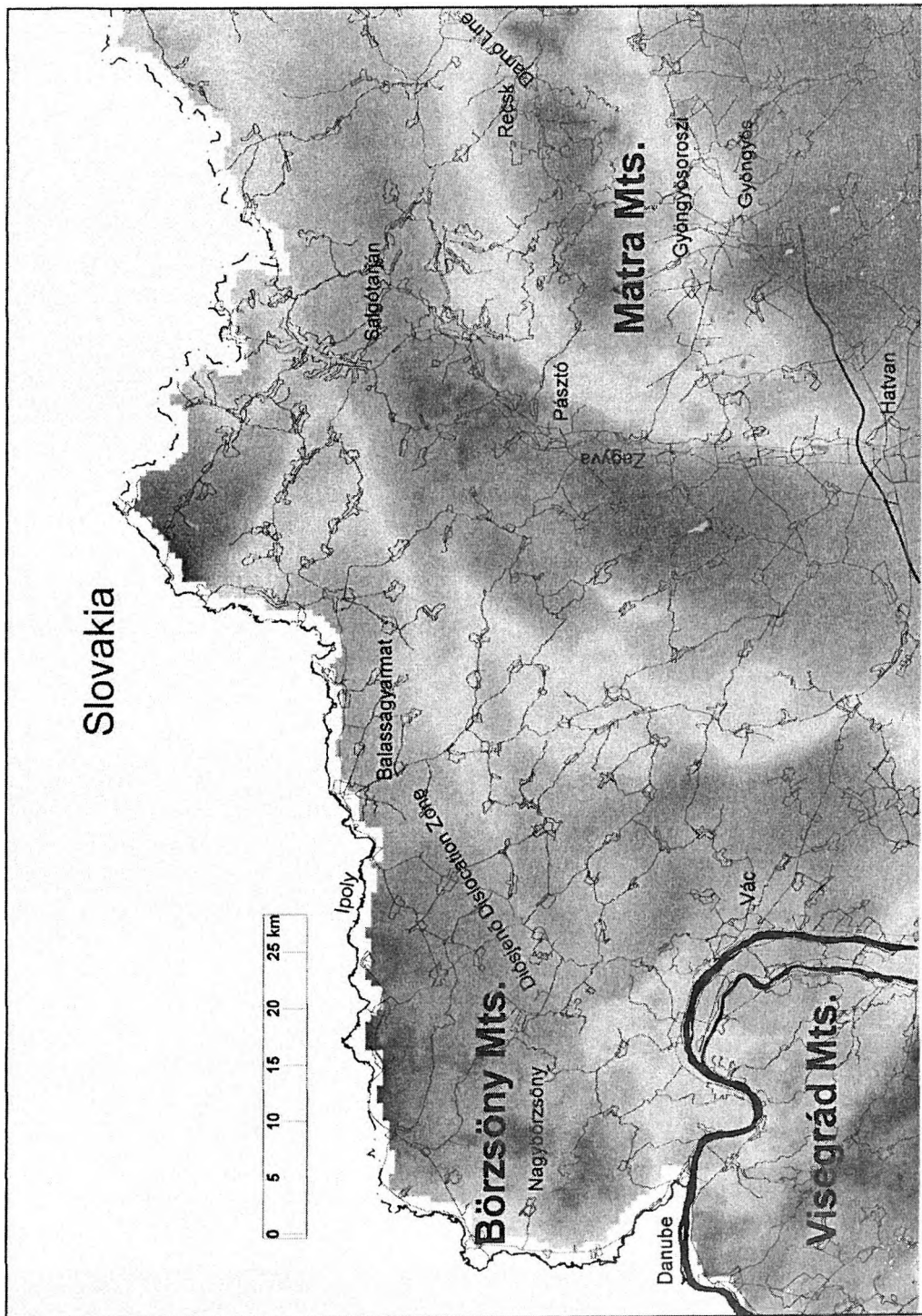


Fig. 3: Gravity map of the study area

The map is coloured by linear stretching of black and white.

The light colours mean maximum values and the deep colours mean minimum values

area of nonvolcanic formations, as the practice in gravity has shown over the last 25 years; the interpretation, however, must be done by using both of the anomaly maps simultaneously.

4. REGIONAL GEOCHEMICAL DATA

4.1. Mátra Mountains

The first geochemical studies in the Mátra and the Börzsöny Mountains were done in the 1950's. The first survey in the Mátra Mountains which covered the whole mountain was carried out by using hydrogeochemical methods (GEDEON 1964). Soil metallometry was used for follow up investigations. The total metal content (Zn + Pb + Cu) was determined by the use of dithizone. Strong hydrogeochemical anomalies were outlined in the northern part of the mountains. Detailed metallometric surveys (using a 100 by 10 m grid or sometimes less) were then conducted on these smaller (a few square kilometers) areas to detect the presence of polymetallic veins. The Middle Mátra ore mineralization zone was found this way. The study of the Mátra Mountains resumed in 1980 with the goal of discovering new ore zones of the Gyöngyösorszi base metal mine. Different sampling methods and sampling media (heavy mineral concentrates, fine fractions of stream sediments, soil A and C horizons with about 4,000 soil samples) have been used during this survey, which covered the western 23 square kilometer part of the mountain (NAGY 1988). The samples were analysed by semiquantitative optical emission spectrograph for 24 elements. These investigations resulted in the discovery of other polymetallic vein deposits.

4.2. Börzsöny Mountains

As early as 1970, 24 geological formations (including volcanic and sedimentary ones) were lithochemically sampled (1,543 samples collected and analysed by optical emission spectroscopy) and characterised in the Börzsöny Mountains (NAGY 1972). From 1968 to 1970, a hydrometallometric survey that covered the whole of the mountains was conducted, and 174 spring water samples were analysed (NAGY et al. 1973). The heavy metal content of streams was precipitated by $\text{Al}(\text{OH})_3 \cdot n\text{H}_2\text{O}$, and the precipitate was analysed by a Zeiss Quasar 24 spectograph. The following elements were analysed: Fe, Mn, Pb, Cu, Zn, Ni, Cr, Ag, V, and Mo. Eleven anomalous areas were identified, the largest areas being about 2 by 3 square km (east of Diósjenő) and 1 by 3 square km (southeast of Nagybörzsöny village).

Electrochemical methods were also applied for geochemical mapping purposes (NAGY 1973, 1976). The pH and oxidation-reduction potential were measured, and the data were analysed by statistical methods. Anomalies showing three tectonically controlled zones were outlined.

From 1976 to 1980, surveys in smaller areas, together with other ore prospecting geological and geophysical methods, IP measurements, metallometry, and rock fragment sampling were carried out (CSILLAGNÉ-TEPLÁNSZKY et al. 1983). Metallometric anomalies of Cu (>70 or >100 ppm in the Rózsa-hegy area) and Pb (>100 or >1000 ppm in the Rózsa-hegy area) were outlined, as well as IP isolines. On the basis of these investigations, three areas of mineralizations were delineated—the Kuruc-patak and the Bányapuszta and the Rózsa-hegy mineralizations. All the analyses were performed by using semiquantitative spectroscopic methods.

In the years that followed, newer quantitative analytical methods with low detection limits and better accuracy were introduced in the Laboratories of the Geological Institute of Hungary.

5. LOW DENSITY NATIONAL GEOCHEMICAL SURVEY

A reconnaissance (low-density) geochemical survey of the country was made by sampling 196 drainage basins, each with an average area of about 400 square km (ÓDOR et al. 1996, 1997a). The goal was to establish background data for environmental studies. The resulting geochemical data base has been an important contribution to the establishment of baseline values for soils in Hungary. Safe levels have been established for As, Cd, Cr, Cu, Hg, Pb and Zn. This survey has provided regional surface background geochemical data for more than 20 elements and for almost the whole country. (For baseline values and other parameters, see ÓDOR et al. 1996, 1997a, and 1999).

6. STREAM SEDIMENT GEOCHEMICAL SURVEY

Concurrent with this low density survey, a stream sediment survey was conducted to cover the hilly and mountainous parts of Hungary with one sample per 4 square km density. The data of these detailed surveys (see ÓDOR et al. 1997b, and 1999) were mainly used to outline surface geochemical anomalies and environmental signatures of ore deposits and alteration zones in the regions. The geochemical parameters are summarised for the two regions in Tables 1 and 2.

Börzsöny Mountains geochemical parameters of elements in the fine fraction of stream sediments (concentrations in ppm, unless otherwise noted, N = 91)

Table 1

Element	Geochemical parameters			
	Min.	Median	Threshold of anomaly	Max.
Au (ppb)	< 2	< 2	15	123
Ag	< 0.3	0.4	—	1.6
As	0.5	2.6	10	22.5
Cu	3	6.6	25	64
Hg (ppb)	< 20	< 20	100	284
Mn	170	640	1,600	3,194
Pb	4	9.5	20	187
Zn	19	44.5	100	583
Ba	38	93	170	2,468
Cr	5	13.3	40	73
Sb	< 0.2	< 0.2	1	1.2

Mátra Mountains geochemical parameters of elements in the fine fraction of stream sediments (concentrations in ppm, unless otherwise noted, N = 104)

Table 2

Element	Geochemical parameters			
	Min.	Median	Threshold of anomaly	Max.
Au (ppb)	< 2	< 2	16	24
Ag	< 0.4	< 0.4	—	0.4
As	1.7	5.7	50	163
Cu	2	14	50	153
Pb	7	18.5	50	288
Zn	34	65	280	12,200

7. SUMMARY

The regional geologic, geophysical, and geochemical data described in this paper provided a starting point for the three-part assessment method used by the US Geological Survey (SINGER 1992) to assess the undiscovered deposits in the Mátra and the Börzsöny Mountains, Northern Hungary. The data that were compiled for the study area allowed for the delineation of tracts that were judged to be permissive for specific mineral deposit types. This use of the data marked the first time that the three-part assessment method was applied in Hungary. Although the size of the study area was not large, this approach to resource assessment serves as a starting point for assessing the undiscovered mineral resources for the country as a whole.

8. REFERENCES

- BALLA, Z. 1978: A Magas-börzsönyi paleovulkán rekonstrukciója. (Reconstruction of the Magas-Börzsöny paleo-volcano). — *Földtani Közlemények* 108: 119–136. (In Hungarian with Russian abstract).
- BALLA, Z. 1987: A Mátra regionális vulkán szerkezeti elemzése. (Volcanostructural analysis of Mátra Mts). — *Magyar Eötvös Loránd Geofizikai Intézet Évi Jelentése 1986*: 32–60. (In Hungarian with English and Russian abstract).
- COX, D. P.–SINGER, D. A. (eds.) 1986: Mineral deposit models. — *US Geological Survey Bulletin* 1693: 379 p.
- CSILLAGNÉ–TEPLÁNSZKY, E.–CSONGRÁDI, J.–KORPÁS, L.–PENTELENYI, L.–VETÖNÉ–ÁKOS, É. 1983: A Börzsöny hegység Központi területének földtani felépítése és ércesedése. (Geology and mineralization of the Central area in the Börzsöny Mountains). — *Magyar Állami Földtani Intézet Évi Jelentése 1981*: 77–127. (In Hungarian with English abstract).
- GEDEON, A., 1964, Geokémiai mérések a Mátrahegységben, 1962. (Metallometric survey of the Mátra Mountains). — *Magyar Állami Földtani Intézet Évi Jelentése 1962*: 337–349. (In Hungarian with English abstract).
- NAGY, B. 1972: A Börzsöny hegységi földtani képződmények áttekintő geokémiai vizsgálata. (Regional geochemical investigations of the geological formations of the Börzsöny Mountains). — *Magyar Állami Földtani Intézet Évi Jelentése 1970*: 35–39. (In Hungarian with English abstract).
- NAGY, B.–PELIKÁN, P.–VIGNÉ FEJES, M. 1973: Börzsöny hegységi források hidrometallometriai vizsgálata. (Hydrometallometric surveying of the springs of the Börzsöny Mountains). — *Magyar Állami Földtani Intézet Évi Jelentése 1971*: 47–61. (In Hungarian with English abstract).
- NAGY, G. 1973: Elektrokémiai módszerek alkalmazása a Börzsöny hegység áttekintő geokémiai térképezésénél. (Electrochemical methods as applied to the general geochemical mapping of the Börzsöny Mountains). — *Magyar Állami Földtani Intézet Évi Jelentése 1971*: 237–245. (In Hungarian with English abstract).
- NAGY, G. 1976: A Börzsöny hegység áttekintő szerkezetföldtani, geokémiai és ércteleptani vizsgálata. (Review of structural, geochemical and economic-geological investigations of the ore deposits in the Börzsöny Mountains (N Hungary). — *Magyar Állami Földtani Intézet Évi Jelentése 1974*: 25–47. (In Hungarian with English abstract).
- NAGY, G. 1988: A Középső és a Nyugati Mátra ércelőkutatása (1980–85). (Ore prospecting strategies for the Central and Western Mátra areas.) — *Magyar Állami Földtani Intézet Évi Jelentése 1986*: 129–136. (In Hungarian with English abstract).
- ÓDOR, L.–HORVÁTH, I.–FÜGEDI, U. 1996: Low-density Geochemical Survey of Hungary. — Volume of Abstracts, Environmental Geochemical Baseline Mapping in Europe Conference, May 21–24, 1996, Spisska Nova Ves, Slovakia: 53–57.
- ÓDOR, L.–HORVÁTH, I.–FÜGEDI, U. 1997a: Az arany és ezüst geokémiai háttérértékei az ártéri üledékek alapján. (The geochemical background values of gold and silver on the basis of flood-plain deposits). — *Földtani Kutatás*, 34. (1): 13–17. (In Hungarian with English abstract).
- ÓDOR, L.–HORVÁTH, I.–FÜGEDI, U. 1997b: Észak-Magyarország nemesfém perspektívái a patakhordalékok geokémiai felvétele alapján. (Precious metal perspectives of northern Hungary based on stream sediment survey). — *Földtani Kutatás*, 34. (2): 9–12. (In Hungarian with English abstract).
- ÓDOR, L.–HORVÁTH, I.–FÜGEDI, U. 1997c: Low-density geochemical mapping in Hungary. — *Journal of Geochemical Exploration*. 60: 55–66.
- ÓDOR, L.–WANTY, R. B.–HORVÁTH, I.–FÜGEDI, U. 1999: Environmental signatures of mineral deposits and areas of regional hydrothermal alteration in northeastern Hungary. — *Geologica Hungarica Series Geologica* 24: 107–129.
- SINGER, D. A. 1992: Basic concepts in three-part quantitative assessments of undiscovered mineral resources: Nonrenewable Resources. 2(2): 69–81.

ALPINE DEPOSIT MODELS FOR THE MÁTRA AND BÖRZSÖNY MOUNTAINS, NORTHERN HUNGARY

ÉVA VETŐ-ÁKOS

Geological Institute of Hungary, H–1143 Budapest, Stefánia út 14., Hungary

ABSTRACT

The Hungarian segment of the Miocene Inner–Carpathian calc-alkaline volcanic arc, the Börzsöny and Mátra Mts. – built up of andesite, dacite, rhyolite, their pyroclastics and subvolcanic bodies – hosts some epithermal low sulfidation gold-bearing quartz, base metal, Cu-Zn skarn and replacement, porphyry copper and epithermal high sulfidation Au-Cu mineralizations. The main ore controls are the faults, the subvolcanic andesites and dacites.

The magmatic activity was related to the collision of the European plate and Pannonian fragment.

Significant shear zones along fault lines have been formed mainly in consequence of compression that has determined the sites of the volcanic eruptions and the pathways of ore-bearing fluids. In contrast to the Mátra Mts. there are only weakly developed tectonic zones and second order tectonic lines in the Börzsöny Mts. where the stress field is characterized by extension.

In case of the Mátra and Börzsöny Mts. as well as of the Carpathian realm, deposits of economic importance are related to localities where extension was followed by compression.

Until now, exploration has been carried out only the central part of both mountains. However, the marginal part of the Börzsöny and the southeastern part of the Mátra Mts. seem to be worthy of further exploration. The intrusions and their contact with carbonate sediments can hide porphyry copper or skarn types of mineralization.

On the basis of the deposit models it may be expected that the faults and shear zones formed and developed in the neighbourhood of the subvolcanic intrusions may also contain new deposits.

1. INTRODUCTION

The US-Hungarian Joint Fund Project No. 415. entitled “Deposit Modeling, Mineral Resource-Assessment and Mining induced Environmental Risk” was established in 1995. In the frame of this project, mineralization in the Carpathian region has been studied in the Mátra and Börzsöny Mts. in northern Hungary, and in Slovakia and Romania. Deposit models were then on the basis of the COX and SINGER method (COX and SINGER 1986) originally used in the US and Canada. A comprehensive group of mineral deposit models were assembled by COX and SINGER and Hungarian deposits were compared with them. This paper is devoted to deposit models for mineralization in the Börzsöny and Mátra Mts., mineralization in these areas is analogous to that found elsewhere in the Carpatho-Balkanide area.

The late Jurassic to Neogene–Quaternary time was an important period in the formation of the Alps, hence tectonism and mineralization connected with this period are termed Alpine type. Neogene Alpine type mineralization outcrops in the Börzsöny and Mátra Mts. of the North Hungarian Range, for example the localities of Nagy-börzsöny and Gyöngyösoroszi have been known since the Middle Age for their precious metal mining activities. In the Mátra Mts., two periods of mineralization are known, one Paleogene, the other Neogene. Beside gold, copper has also been mined here and in the 1960's a new exploration effort was launched mainly for copper.

Deposit models offer the following: indications as to whether other types of mineralization can be hidden in the neighbourhood of known but exploited deposits; indications of the potential size of the resource; assist planning of future exploration. The aim of this paper is to present the different Alpine type deposit models in Hungary.

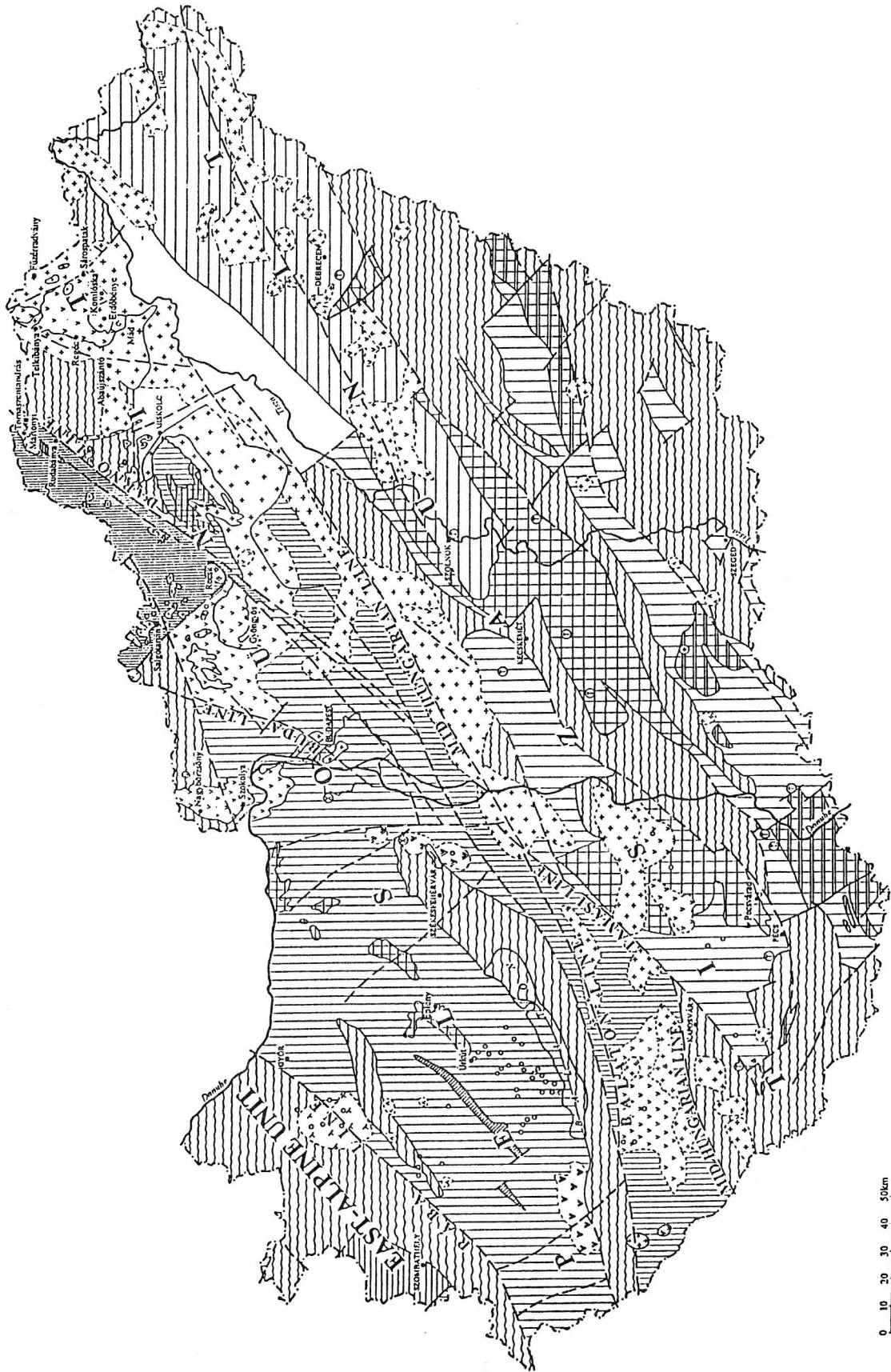


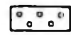
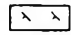

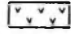
Fig. 1.: Alpine Plate-Tectonic and Metallogenic Map of Hungary

LEGEND OF THE ALPINE TECTONIC MAP OF HUNGARY

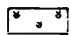

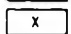
Main Plate Tectonic Units: I. Pelso Unit
II. Tisza Unit
III. East-Alpine Unit

I. PELLO UNIT

New Alpine Stage

-  1. Basalt, basanite (Pliocene)
-  2. Trachyte (Pliocene)
-  3. Rhyolite-dacite (Miocene)
-  4. Andesites, dioritic subvolcanic bodies (Miocene)

Middle- and Old-Alpine Stage


-  5. Andesites, dioritic subvolcanic bodies (Eocene)
-  6. Epicontinental molasse (Senonian)
-  7. Carbonatite (Upper Cretaceous)

Eoalpine Stage

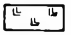

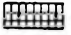
Transdanubian Subunit

-  8. Continental, shelf sediments (Perm-Triassic)

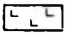

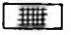
Central Transdanubian Subunit

-  9. Shelf and basin sediments (Jurassic-Lower Cretaceous)


Bükk Subunit

-  10. Ophiolitic rocks (Jurassic)
-  11. Mesozoic rocks
-  12. Shelf and basin sediments (Jurassic)

Gömör-Aggtelek-Rudabánya Subunit

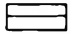
-  13. Ophiolitic rocks (Triassic)
-  14. Mesozoic rocks
-  15. Shelf and basin sediments (Triassic-Jurassic)

Prealpine Stage

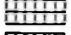
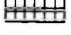

-  16. Low grade metamorphic sediments and magmatic rocks

II. TISZA UNIT

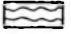
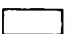
Middle- and Old-Alpine Stage

-  17. Flysch (Senonian, Paleogene)

Eoalpine Stage

-  18. Mesozoic rocks commonly
-  19. Shelf and basin sediments (Upper Triassic-Jurassic)
-  20. Shelf sediments (Jurassic-Lower Cretaceous)

Prealpine Stage

-  21. Low and high grade metamorphic rocks, granite, continental margin rhyolite, basalt continental molasse, migmatite
-  22. Terrain with unknown basement

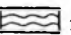
III. EAST-ALPINE UNIT

Eoalpine Stage

Penninic Subunit

-  23. Low grade metamorphic, ophiolitic sequences (Jurassic-Lower Cretaceous)

Prealpine Stage

-  24. Low and high grade metamorphic rocks, granite, continental margin rhyolite, basalt continental molasse, migmatite

2. GEOTECTONIC SETTING AND ALPINE MINERALIZATION IN THE CARPATHIAN REALM

During the Alpine period, convergent motion took place between the European and African plates along the Periadriatic-Vardar zone. This convergence resulted in the displacement of the Pannonian fragment, north-eastward overthrusting and the extension of the Pannonian Basin. Overthrusting and subduction started in the westernmost part of the outer Carpathians in early Miocene and propagated eastward. This trend of rejuvenation is reflected in the age of the calc-alkaline rocks of the Inner-Carpathian Volcanic Belt (ICVB) decreasing from Middle-Miocene in the west to Quaternary in the East (ROYDEN and HORVÁTH 1988). The continuation of the collision zone can be followed through the Balkans to the Pontides, through the countries of Slovakia, Hungary,

Ukraine, Romania, the former Yugoslavia, FYROM (Former Yugoslavian Republic of Macedonia), Bulgaria, Greece and Turkey.

On the basis of radiometric data (PÉCSKAY et al. 1996, KÖRPÁS and LANG 1991, 1993) the Inner–Carpathian volcanic belt formed over 18 my—from the Paleogene to Neogene–Quaternary, but the build-up of individual volcanic fields within the arcs lasted 1–3 my in average. This magmatism produced granodiorite, monzodiorite, diorite and granite plutons; andesitic and rhyolitic subvolcanic bodies; and subaerial and submarine stratovolcanoes.

Stratovolcanoes, and in some places sub-volcanic intrusives, host important Au, Ag and base metal mineralization in epithermal, porphyry, massive sulfide, skarn and other styles. Vein type, disseminated and massive sulfide mineralizations seem to be max. some hundreds Ka younger than their host rocks (KÖRPÁS and LANG 1993). Deposit types related to the Inner–Carpathians include: polymetallic sulfides with native gold, silver sulfides and sulfosalts; epithermal low and high sulfidation deposits; porphyry copper; skarn and metasomatic replacement type deposits. Polymetallic gold and sulfide mineralization occurring at shallow depth can grade upwards into a hot spring system and downwards into a polymetallic vein system. In vein deposits the major base metals occur as galena, sphalerite and chalcopyrite. Silver is present in a variety of sulfosalts minerals. Quartz and calcite are the predominant gangue minerals.

The most prominent geochemical features of many polymetallic gold deposits are the presence of Au–Ag tellurides, minor base metal sulfides, and fluorite as a gangue mineral (NAGY 1983). Some gold deposits in the Carpathian realm are recognized as associated with intrusive bodies, others with trachytic and andesitic explosive volcanics. Some deposits are connected with alkaline igneous rocks. Deposits are mainly confined to faults or lineaments and are controlled by the subduction related geotectonic and petrochemical setting in which they occur.

There are two main types of rock alteration. Alteration with quartz–adularia–carbonate–sericite and intense argillitisation is characteristic of low sulfidation mineralizations, while alteration with a quartz–alunite assemblage is characteristic of high sulfidation mineralization. In the study area, mineralization is commonly surrounded by chlorite-dominated propylitic alteration. Illite and/or sericite are developed close to the veins and disseminated pyrite is common in quartz-bearing host rocks.

3. ALPINE MINERALIZATION IN HUNGARY

The Börzsöny and Mátra Mts. are Neogene volcanic fields forming part of the ICVB. Both volcanic fields lie within the Pelso terrain, part of the Pannonian fragment. The Pannonian fragment is one of the two main tectonic units of Hungary that were emplaced in current position by the end of the early Miocene (NAGYMAROSY 1990, MÁRTON 1997, VETŐ–ÁKOS 1997) (Fig. 1).

Magmatic activity of two different ages are found in N–Hungary, one is of Paleogene age (Eocene), the other of Neogene age. There are indications that these are associated with two different arc systems.

Intrusives, volcanics and mineralization of Eocene (Palaeogene) age are found in the Balaton–Darnó section of a regional SW–NE tectonic zone, the Periadriatic Line which extends through the vicinity of the Recsk–Lahóca deposit. This Eocene magmatic activity may be related to a volcanic arc which developed somewhere within the Southern Alps to the SW of its current location. The arc, along with associated Palaeozoic and Mesozoic basement, was only emplaced in its present location during the Eocene–Late Oligocene when convergence between the European and African plates and consequent closure of the Vardar branch of the Tethys, resulted in part of the continental crust of the southern Alps escaping NE along the Periadriatic Line. Indications are that Palaeozoic and Mesozoic basement intruded by Paleogene volcanics originally formed part of the African plate (KÁZMÉR and KOVÁCS 1985).

In NE Hungary, the Paleogene arc is cross cut by a later Neogene–Quaternary arc which is the ICVB. Its detailed description see in the followings.

The Alpine period in the North Hungarian Range is represented by two main mineralization stages. Mineralization includes Au–Cu–epithermal, base metal, porphyry copper, porphyry skarn and metasomatic replacement deposits near Recsk in the North Hungarian Range which may be older than Neogene by the radiometric data. The younger mineralization unanimously belongs to the Neogene ICVB and includes only base metal deposit in the Mátra Mts. The mineralization has been exploited since the Middle Ages.

Genetic models of base metal-, skarn- and porphyry copper-type mineralization hosted by both volcanics and carbonates have been developed mainly by reinterpretation of old data and by using new data collected over the last few years.

3.1. Mátra Mountains

3.1.1. Geological setting

Mesozoic basement outcrops at the northeastern and southeastern part of the Mátra Mts. and its presence is also proved in boreholes on the northwestern margin of the Mátra Mts. Lithologies include bioclastic limestone, dolomites, pillow basalts, cherts and siltstones.

Paleogene intrusives, volcanics, and sediments formed within, and representing the remnants of, an Eocene volcanic arc occur in the northeastern and southeastern Mátra Mts. The Paleogene intrusives and volcanics are subduction related calc-alkaline diorites, andesites and associated pyroclastics.

The oldest Palaeogene sediments are a bituminous limestone with lithothamnium unconformably overlying the eroded surface of the Triassic and intercalated with Eocene lava flows. Younger Oligocene–Early Miocene marine sediments reach a thickness of about 1 km and consist of marls, siltstones and sandstones. Triassic and Eocene carbonate rocks are cut by a diorite intrusive. The overlying Eocene stratovolcanic sequence consists of a submarine andesite flow, dacite flows and pyroclastics as well as subvolcanic andesite. Reworked volcanic debris are also widespread in the area (FÖLDESSY 1966), (Figs. 2 and 3.).

Overlying the Oligocene and Early Miocene marine sediments are Miocene magmatics comprising subvolcanic bodies and stratovolcanic sequences the thickness of which is greater than 1200 m in the central part of the mountain. The volcanic activity started in the Early Miocene (Ottangian) with pyroxene andesite lava flows and the so-called "lower rhyolite tuff" (BAKSA et al. 1984) which deposited in a shallow marine environment. The subduction related calc-alkaline andesites are of orogenic character GILL (1981).

In the early Middle Miocene, volcanic activity was focused at the northeastern part of the Mátra Mts., here andesitic subvolcanic bodies and dikes intrude the older, Paleogene volcanics and sediments. A distinctive and regionally extensive "Middle Rhyolite Tuff" can be followed at the surface from west to east in the northern part of the Mátra Mts. The texture of this "tuff" suggests a volcanic-sedimentary origin. The tuff formed during a relatively quiet period of the volcanic history, when erosion was the dominant process and re-working of the volcanic debris of the earlier lava and pyroclastic flows took place. The rock is altered enough that it can be assumed it was at least partly water lain.

The present topography of the Mátra Mts. is determined by late Middle Miocene (Badenian) volcanic edifices. Part of a ring structure can be identified from air photos and is probably a caldera formed in the Miocene. The southern part of the structure is submerged and covered by younger sediments. The central part of the caldera consists of subvolcanic andesites.

Lava flows, tuffs and ash-and-bomb alternate over a considerable thickness, greater than 1200 m at some places. Beside the andesites, submarine rhyolite flows are also present in the area. The youngest andesite lava flow and dikes are barren of mineralization.

The caldera mentioned above could have been the centre of magmatism in the Mátra Mts. in spite of the fact that the thickest pyroclastic layers lie to the south. In the centre of the supposed caldera there are quartzite, vuggy silica formed during hydrothermal postvolcanic activities. Further indications of hydrothermal post volcanic activity is the presence of jasper and diatomite of 200 m thickness in the western part of the Mátra Mts.

3.1.2. Paleogene Mineralizations

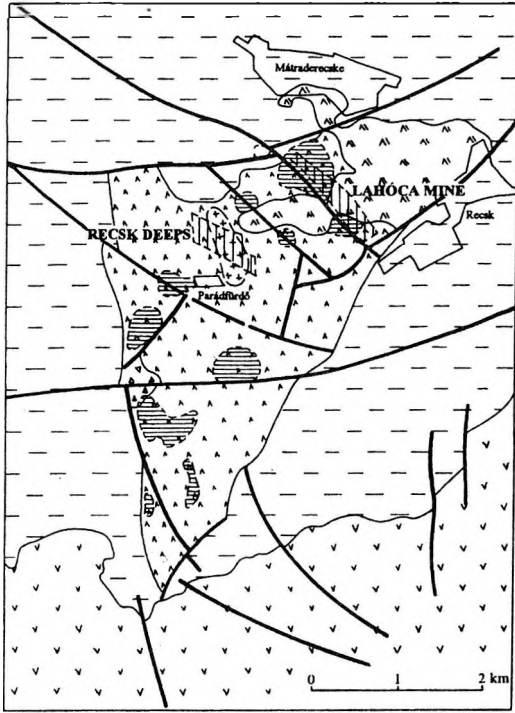
At Recsk–Lahóca, mineralization consist of: near-surface, epithermal, high sulfidation Au-Cu overprinted by low sulfidation marks on the marginal part. At the deeper ("Recsk–deep") level, mineralization comprises: porphyry copper; base metal veins; Cu-Zn skarn and replacement mineralization which are hosted by Paleogene intrusives, stratovolcanic sequences and Triassic limestones and dolomites (Fig. 4) The lithology for each mineralization type varies downwards.

3.1.2.1. Epithermal high sulfidation Au-Cu deposit of Recsk–Lahóca (22A, by COX and SINGER 1986)

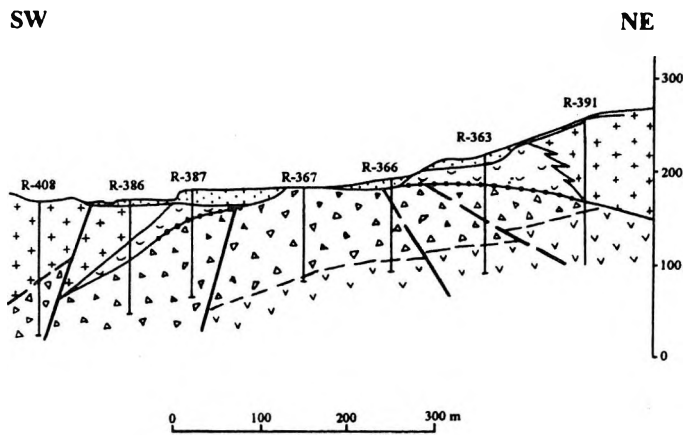
The near-surface mineralization at Recsk–Lahóca was discovered in 1852 and was mined almost continuously until 1978. Initial exploitation was for copper, not gold. In 1991, a new exploration effort tested the gold potential and resulted in the delineation of a near-surface, gold-copper deposit. The new exploration highlighted the genetic connection between the different types of mineralization.

The epithermal high sulfidation Au-Cu deposit is located in the Balaton–Darnó shear zone described earlier.

Fig. 2: Geological map Recsk (FÖLDESSY 1996)



- Miocene volcanic-sedimentary series
- Oligocene claystone, siltstone, sandstone
- Oligocene-Eocene post-ore andesite
- Eocene pre-ore andesite, dacite
- Eocene diorite-porphphy breccia pipe
- Contours of the Eocene hidden diorite porphyry intrusion
- Extreme hydrothermal alterations
- Underground mine activity



- Oligocene sediments
- Late andesite extrusives
- Late andesite tuffs
- Blueschist
- Host rock breccias
- Diorite porphyry

Fig. 3: Geological section of the Recsk-Lahóca gold mineralization (FÖLDESSY 1996)

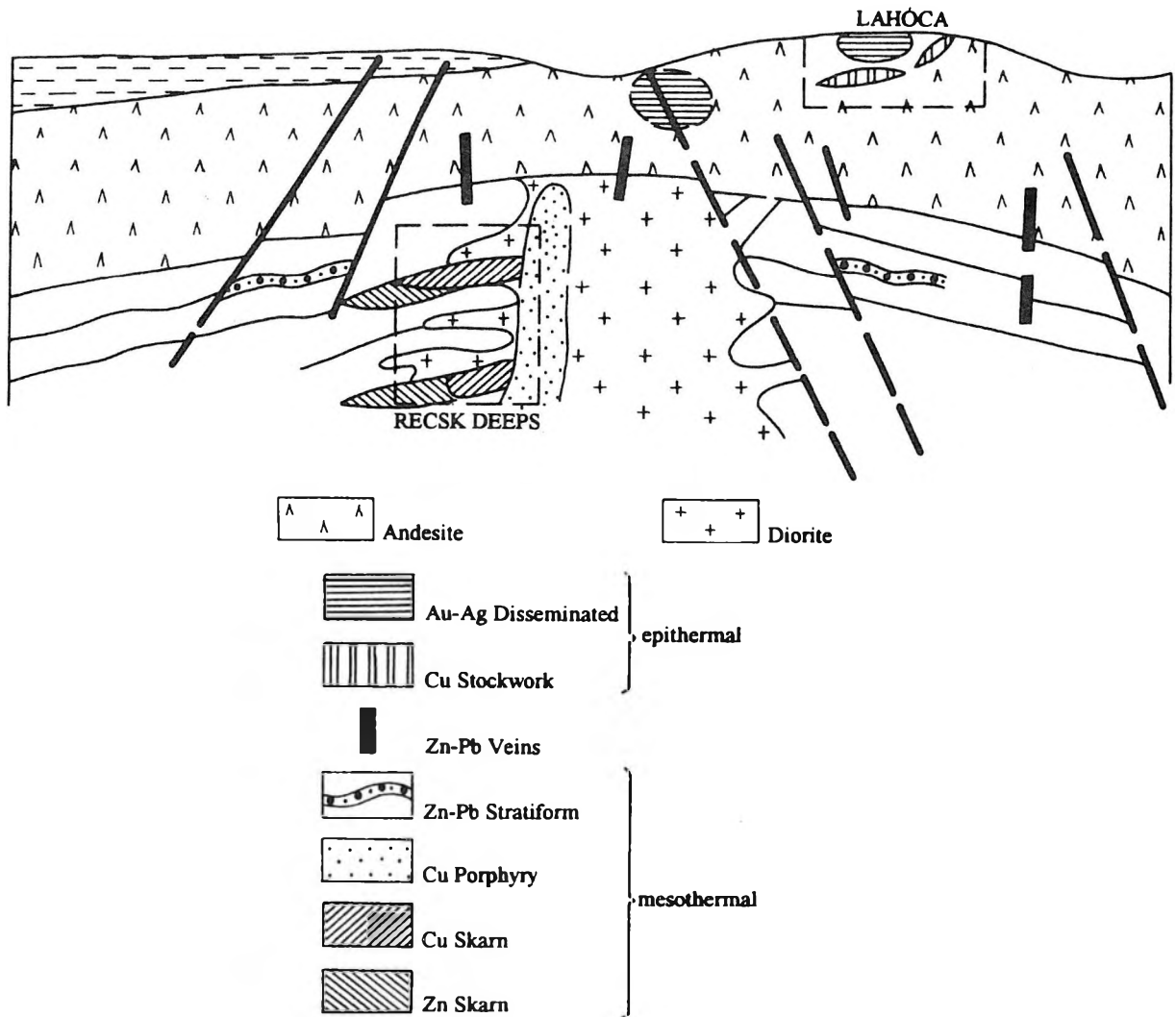


Fig. 4: Schematic section of the Recsk-Lahóca and "Recsk-deeps" ore complex. Location of ore types (FÖLDESSY 1996)

Host rocks include uppermost Eocene calc-alkaline andesitic stratovolcanic sequences, cut by a milonitized tectonic zone, composed of very altered, argillitized, brecciated andesite of the same age. Mylonite texture is mainly angular and less commonly rounded which indicates a tectonic origin.

In some places the tectonic breccia is cut by hydrothermal breccias, FÖLDESSY (1993, 1996) suggests that a pipe breccia intruded the tectonic zone. At the contact with the overlying andesite, both the tectonic and pipe breccias can be extremely siliceous and impregnated with fine grained pyrite. These parts are characterised by the presence of vuggy silica and the highest gold content. The silicified-pyritized zone is surrounded by an advanced argillic zone containing kaolinite, smectite, illite, dickite and quartz. Propylitization with biotitization is also known. The bottom of the ore zone is a high level subvolcanic andesite. Low sulfidation mineralization, with Au-Ag-tellurides, developed on the peripheries of the subvolcanic andesite.

Ore paragenesis consists of colloform pyrite, luzonite, enargite, sphalerite, tetrahedrite, chalcopyrite and Pb-, Bi- and Te-sulfosalts. Gangue minerals are calcite, quartz, barite and other sulfates.

Gold occurs in pyrite and in some cases in enargite and luzonite. As inclusion in pyrite it can occur in native form, or electrum. The average gold content is about 1.0 g/t, but 100–180 g/t was reported in the past. Gold content correlates positively with copper content but not with silver content. The silver content ranges between 1–5 g/t

only. The main rock alteration types associated with high gold contents are silicification and pyritization. Argillization is associated with low gold content. The average thickness of the mineralized zone is 30 m.

Geological resource of the high sulphidation deposit declared in 1998 was 57.4 million tons with grade ranges between 1.4–2.8 g/t. Contained gold is therefore between 760,000 and 1,430,000 ounces.

This type of mineralization seems to be younger than the mylonite and older than the subvolcanic intrusion of the younger Eocene volcanic phase (FÖLDESSY 1996). Mineralization may have been continuous until the Middle Oligocene. (ZELENKA 1994).

3.1.2.2. Base metal deposit “Recsk–deep” (22C, by COX and SINGER 1986)

At the “Recsk–deep” level, a base metal deposit of galena and sphalerite veins form above the diorite intrusion. The deposit is not of economic value.

3.1.2.3. Porphyry copper deposit “Recsk–deep” (21A, by COX and SINGER 1986)

Porphyry copper mineralization is located at a depth of 900–1200 m above and in the upper part of a diorite intrusion in a zone of strong propylitic alteration (Fig. 2). Highest copper grades are associated with highest Au contents where propylitic alteration is overprinted by skarn. Adularia-sericitic alteration is common. This deposit type is characterized by propylitic alteration.

3.1.2.4. Cu-Zn-skarn and replacement deposits “Recsk–deep” (19A, by COX and SINGER 1986)

These types developed along the contact between the diorite intrusion and the Triassic limestone and dolomite, and within the Triassic carbonates. The stratabounded Cu-Zn replacement deposit is not very significant on the upper part of the Triassic limestone.

There are genetic and spatial links between the near-surface epithermal high sulfidation Au-Cu, and the deeper base metal, porphyry copper and Cu-Zn skarn mineralizations (FÖLDESSY 1966)

3.1.3. Neogene mineralizations

In the Mátra Mts. the younger Alpine mineralization stage produced gold-bearing epithermal quartz and base metal deposits which are hosted in the Miocene calc-alkaline andesite, their pyroclastics and subvolcanic equivalents (VETŐ-ÁKOS 1994, VETŐ-ÁKOS and ZELENKA 1998) (Figs. 5 and 6).

Mining activity began in this area in the Middle Ages. There is written evidence for the presence of the gold and archeologic evidence for the presence for copper (FÜGEDI et al. 1995 and ÓDOR et al. 1999). After a long interruption, exploration took place in the 18th and 19th centuries for base metals. In the period from the 1950's until its closure in 1990, the Gyöngyösoroszi mine produced 3 Mt of Pb-Zn-ore (KUN, 1989).

3.1.3.1. Base metal deposit of Gyöngyösoroszi (22C, by COX and SINGER 1986)

Mining activities extended to a 3 km × 4 km area. The vertical extent of the mineralization is about 400 m and it consists of about 19 main ore veins. Veins, stockwork type ore bodies and impregnations containing base metals are located in the subvolcanic andesites, in the stratovolcanic sequences as well as in the pipe breccias. The subvolcanic and stratovolcanic andesites consist of 60-70% plagioclase, 30% pyroxene and hornblende and in some places biotite and minor magnetite and pyrite. The pyroclastics are mainly block and ash flows with a composition similar to that of the lava flows. The radiometric age of the host rock is 14-16 Ma.

Steeply dipping pipe breccias crosscut the andesites but only reach cm thicknesses. They are composed of fragments of andesites, underlying sediments, rhyolites, rhyolite tuffs and sometimes of the youngest vitrophyric andesite, and are associated with Hg-Sb showings. They may be the youngest postvolcanic products (CSONGRÁDI 1984).

Veins are banded or brecciated with a thickness ranging from some cm to 7 m. The ore may also be disseminated in the host rocks. Principal ore minerals are galena, sphalerite, wurtzite and chalcopyrite. Native gold, electrum, native antimony, chalcocite, covellite, malachite, anglezite, cerussite, argentite and bismuthinite have been observed as mineralogical rarities. Quartz of various types and calcite are the main gangue minerals. Current resources are 4.8 mill. tons and grades are 1.3% Pb and 3.5% Zn.

According to our current knowledge, these deposits are dissimilar to other deposits in the Carpatho-Balkan area in that they have no direct connection with intrusive rocks, and that they are hosted mainly as veins and stockworks in the stratovolcanic sequence (VETŐ-ÁKOS 1996b).

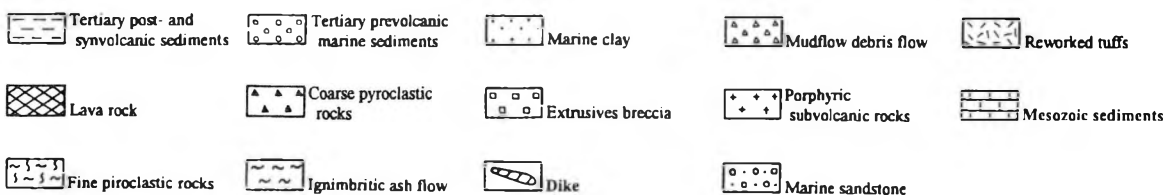
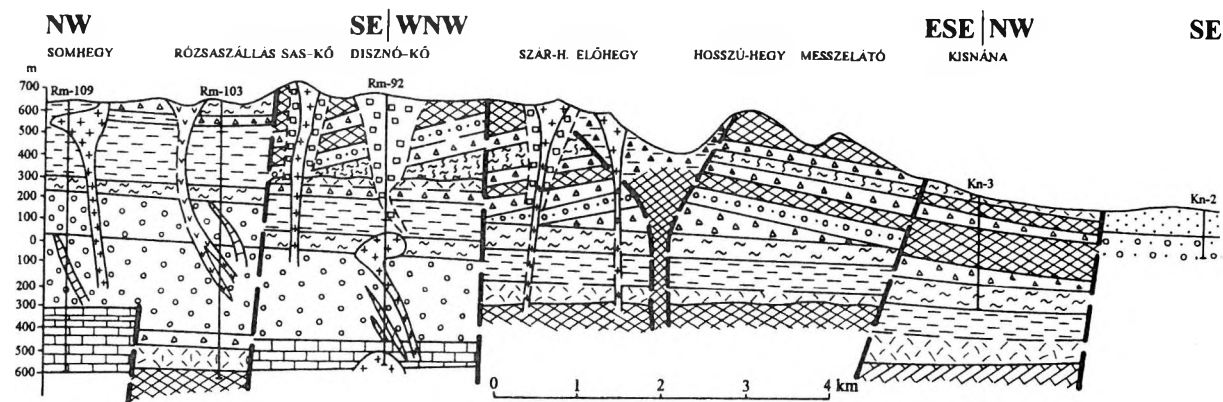
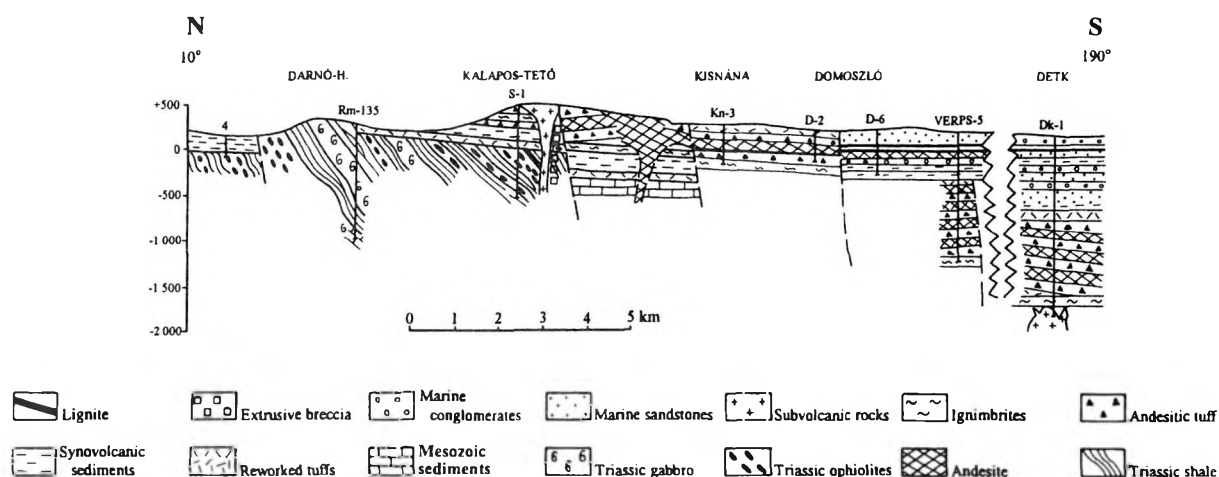


Fig. 5: Cross section illustrating the built up of the Badenian stratovolcanic sequence in the Mátra Mts. (KISS et al. 1996)

Fig. 6: Cross sections illustrating the geological built up of the E-Mátra Mts. (KISS et al. 1996)



3.1.3.2. Geochemistry and rock alterations

Based on fluid inclusion studies of quartz, calcite and transparent sphalerite in veins associated with other sulfides, the mineralization can be characterized as epithermal. The solutions responsible for precipitation of sphalerite and galena proved to be of NaCl-composition.

By fluid inclusion study – made on quartz and calcite crystals – the lowest temperature of ore-precipitation ranging between 140-245 °C practically is the same at different depth level suggesting that the upward movement of the ore forming fluids was very rapid. The main dissolved solid of the ore forming fluids was NaCl, but CaCl₂ was also present. The salinity is calculated as 0.3-12.6 wt.% NaCl equivalent.

Crystallization is believed to have taken place in an open joint and fault system at shallow depth.

Rock alteration is characterized by quartz-adularia, sericite, argillitization, biotite and pyrite which are characteristic of low sulfidation type alteration. In the vicinity of ore veins argillitization may be strong enough to obscure the distinction between subvolcanic and stratovolcanic andesites. Minor vuggy silica and alunite present in

the host rock indicates small scale, high sulfidation alteration processes were active. Different rock alteration types show distinctive paragenetic sequences (VETŐ 1988). Rock alteration suggests that the low sulfidation processes were dominant while the high sulfidation alteration is not significant in the known Gyöngyösoroszi mining area.

3.1.3.3. Ore controls

The ore veins in the Gyöngyösoroszi area follow known N–S, E–W, NE–SW, NW–SE Variscan fault directions. In the Mátra Mts. and indeed throughout the Carpathian realm, one of the most important factors controlling ore deposition is structure with mineralization best developed at fault intersections. Fault lines formed mainly by compression have focussed volcanic eruptions and the passage of the ore-bearing fluids. In the neighbourhood of the boundary between the Pelso and Tisza Unit, a significant shear zone and several fault lines of NE–SW direction have been formed serving as a channel for ore forming fluids and volcanism (FÖLDESSY 1996).

At present, only base metal mineralization is known in the Mátra Mts., but the presence of a porphyry copper or skarn type mineralization on the top of subvolcanic bodies or on their contact with carbonate sediments on the marginal part (KISS et al. 1996) cannot be excluded.

3.2. Börzsöny Mountains

The Börzsöny Mts. as the Mátra Mts. belong to the North Hungarian Range and are a segment of the Inner-Carpathian volcanic arc. Their geological setting, magmatism and mineralization are similar to those of the Mátra Mts., but there are some differences e. g. tectonics. The emphasis in the following sections is mainly on these differences.

3.2.1. Geological setting

The basement consists of Proterozoic–Paleozoic polymetamorphic, crystalline rocks, mainly micaschists in the northern part, while in the southern part it is represented by Triassic platform carbonates. In the late Oligocene, terrestrial sandstone, marine clay and terrestrial sand were deposited. A Middle Miocene (Badenian) transgression resulted in the deposition of marine limestone, marl and clay. Environment was shallow water in the NW part of the mountains and terrestrial, fluvial and marsh in the SE part of the Börzsöny Mts. In several places Badenian magmatics overlie and/or intrude these sediments, and the Proterozoic–Paleozoic or Mesozoic basement (Figs. 7 and 8).

Miocene magmatism occurred only during the Badenian. Volcanic lithologies are subvolcanic andesites, dacite bodies, extrusive dacite domes, pyroclastic surges, block and ash flows and falls and peperites of andesitic composition as well as pipe breccias. The thickness of the stratovolcanic sequence is of several hundred metres. Subvolcanic bodies and stratovolcanic sequences have the same mineralogical composition. Augite, hypersthene, hornblende with andesine and labradorite are the main minerals but quartz, goethite and magnetite occur as well. In the Börzsöny Mts., the youngest volcanic product is a hornblende bearing, leucocratic andesite which appears as lava flows or dikes. With the exception of this young andesite, all types of magmatic rocks in the Börzsöny Mts. host Alpine mineralizations.

On the basis of reinterpretation of historical data and thin sections of Oligocene sediments and Badenian magmatic host rocks, the studied central area of the Börzsöny Mts. seems to consist mainly of andesitic stratovolcanic sequences. These sequences comprise lava flows and pyroclastics, on some places alternating with coarse and fine grain sublittoral sediments and only at the lower level occurs subvolcanic andesite. The texture and chemistry of the andesites are not evidences commonly for its subvolcanic origin and the geological setting is not clear either everywhere. By this reason subvolcanic andesites are supposed to intrude the Oligocene and/or Early Miocene sediments and the lowest Badenian stratovolcanic sequence.

With respect to the stratovolcanic sequence, there are indications of periodic interaction between lavas, wet sediments (carbonates, sandstone and siltstones), and water. Evidence is given by the presence of peperites and that of the granate and epidote in the andesites and the sediments. The matrix of the andesites at the contacts with sediments consists of a fine grained glassy material indicating rapid chilling against a wet sediment. Brecciated peperites formed by the explosive interaction between lava and water often cut the recrystallized siltstone.

Carbon isotope data indicate the presence of sea water as the ore bearing fluid as in the case of the Mátra Mts. (VETŐ and ITAMAR 1991). Interaction may have been with fresh to brackish water, given the swampy to sublittoral paleo-environment area in the Börzsöny Mts. during the early Badenian.

The thickness of sediments does not exceed some ten metres, but cm thick siltstone bands occur within the stratovolcanic sequence.

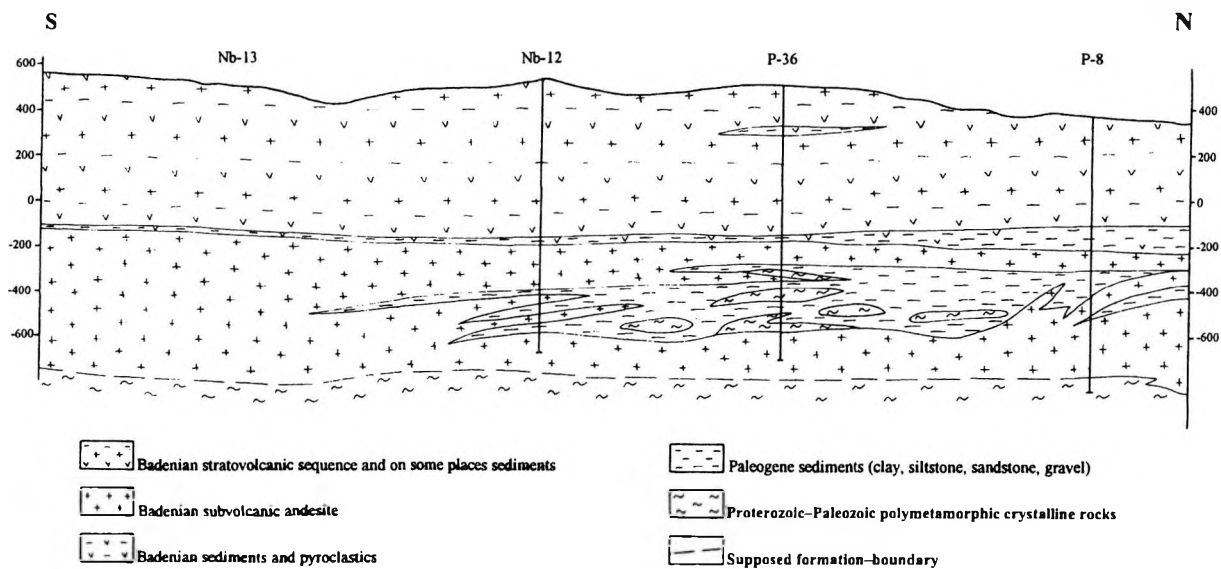
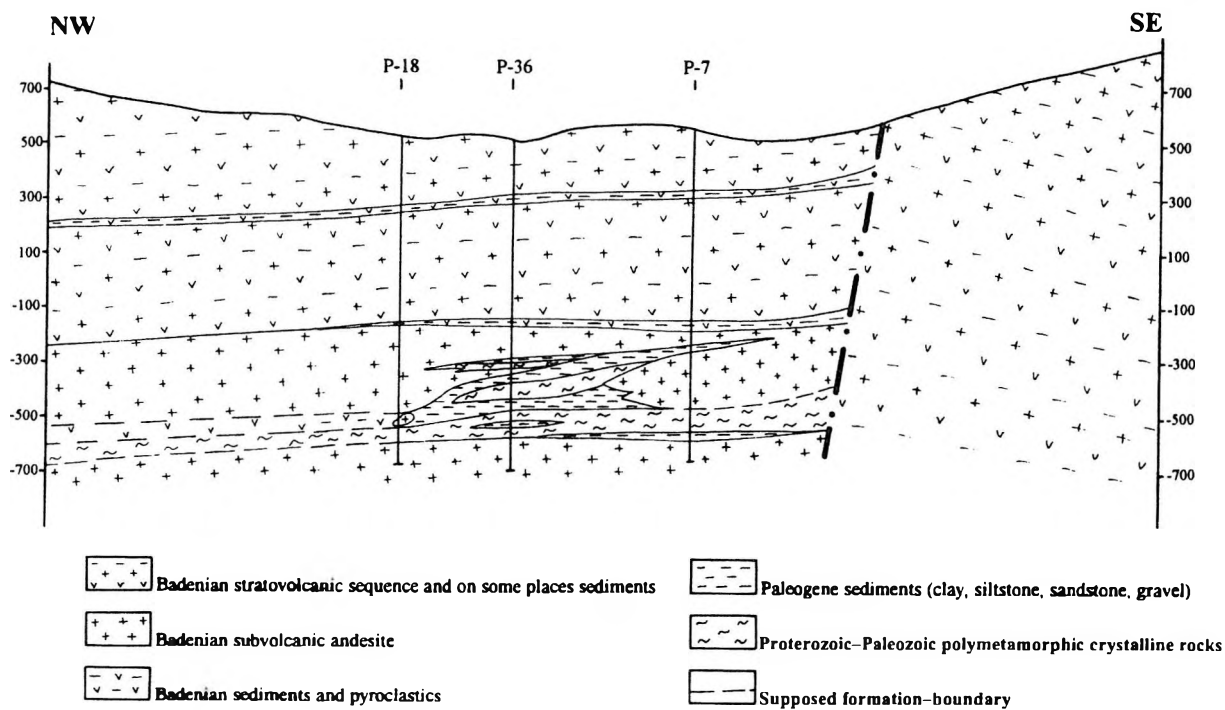


Fig. 7: Cross section of S–N, illustrating the Miocene geological built-up of the Börzsöny Mts. (VETŐ-ÁKOS 1998)

Fig. 8: Cross section of NW–SE, illustrating the Miocene geological built-up of the Börzsöny Mts. (VETŐ-ÁKOS 1998)



3.2.2. Neogene Mineralizations

During the Middle Ages, gold and silver mining at the city of Nagybörzsöny was so significant that its status was elevated to that of town. The silver of the first Hungarian national currency, the "silver mark of Vác" may have originated from the mines of the Börzsöny Mts. Besides gold and silver, iron and copper was also mined. However, by the end of the 15th century the mines were exhausted.

New exploration after the Second World War (in the 1950's and later in the 1970's) was carried out but without success. Exploration was restricted to three parts of the mountains: Kuruc-patak, Rózsa-hegy and Bányapuszta. The distance between these places is some 500–1,000 metres and the host rocks do not vary over that distance. Several drillholes and 4,266 m gallery were made during this latest exploration.

Present indications are that mineralization is restricted to the central part of the Börzsöny Mts. It consists of epithermal, low sulfidation, precious and base metal deposit (ELSPBM) types comprising mainly veins and stockworks (VETŐ-ÁKOS 1996a). In the deeper part, at the level of 900–1200 m there is weak copper mineralization (but only reaching 0.1% Cu). In the southern part of the mountains metasomatic replacement type mineralization is supposed by a single borehole (NAGY 1990). Host rocks of both types of mineralization are subvolcanic and stratovolcanic andesites, pyroclastics and pipe breccia. The pipe breccia consists only of andesitic and dacitic fragments of 2-3 mm in diameter.

A large number of K/Ar radiometric dates have been calculated for the magmatics by the Nuclear Research Institute in Debrecen and in the GSI in Jerusalem, which indicate a Gaussian distribution data ranging for 13 to 20 Ma with a peak between 13 to 15 Ma. The K/Ar ages of the fresh and altered rocks are the same. The total duration of the magmatic activity is thought to be 0.4–0.7 Ma by paleomagnetic data. The interval of magmatic and hydrothermal activities is supposed to be approximately the same. (KORPÁS and LANG 1991, 1993).

3.2.2.1. Epithermal low sulfidation precious and base metal deposit of Kuruc-patak-Rózsa-hegy-Bányapuszta (22C, by COX and SINGER 1986)

ELSPBM mineralization is found in the subvolcanic bodies, in the stratovolcanic sequences and in pipe breccias as well. Mineralization occurs as veins, stockworks and impregnations with a diameter of 60–80 m. Mineral paragenesis is very simple: major minerals are sphalerite, pyrite, chalcopyrite, galena, marcasite, pyrrhotite; minor minerals are molybdenite and bismuth-tellurides. The vertical extent of the mineralization ranges from 100 m to 1200 m. Stratigraphic and radiometric data indicate that the duration of the mineralizing episode could be only some 100 Ky. Gangue minerals are represented by quartz, calcite, adularia, manganocalcite, rhodocrosite and clay minerals.

Mineralization has been exploited historically, average Pb+Zn content is 1.40%, Cu 0.25%, Au < 1 g/t.

3.2.2.2. Geochemistry and rock alterations

The mineralizations of Kuruc-patak, Bányapuszta and Rózsa-hegy are the products of the same postvolcanic processes. Differences are that mineralization is epithermal in the area of Bányapuszta and Rózsa-hegy, and higher temperature, hypothermal in the area of Kuruc-patak.

The mineral paragenesis and coexisting rock alteration are the followings:

>260 °C	Ore paragenesis:	pyrrhotite, pyrite, magnetite, chalcopyrite, sphalerite
	Gangue minerals :	quartz, chlorite calcite
	Rock alterations :	biotite, adularia-sericite,
235–190 °C	Ore paragenesis:	pyrite, pyrrhotite, sphalerite, galena, chalcopyrite, arsenopyrite, marcasite
	Gangue minerals:	quartz, calcite, chlorite
	Rock alterations :	argillitic
<160 °C	Ore paragenesis:	pyrite, galena, sphalerite, chalcopyrite, marcasite, arsenopyrite
	Gangue mineral:	calcite
	Rock alteration:	argillitic

Fluid inclusion studies indicate that the mineralizing fluids were saline with composition ranging from 7 to 38% NaCl. In the Rózsa-hegy area the crystallization temperature seems to increase in parallel with an increase in the Cu/Pb+Zn ratio (VETŐ 1982). The possibility of element mobilization from the metamorphic basement by magmatic fluids can not be excluded.

3.2.2.3. Ore controls

In the central part of the Börzsöny Mts. two main fault systems have been developed, one WNW–ESE, the other NNE–SSW. The NNE–SSW fault system seems to be the younger. Vein and stockwork-type mineralizations are located along this NNE–SSW direction, related to the emplacement of subvolcanic intrusions.

Reinterpretation of historical data provides no clear indication that mineralization is related to a caldera structure. The centre of the volcanic activity could have been in the southern part of the Börzsöny Mts. and it cannot be excluded that the centre lay to the south in the Dunazug Mts. south of the Danube.

In contrast to the Mátra Mts. there are only weakly developed tectonic zones and second order tectonic lines in the Börzsöny Mts.. Given the prevalent compressive stress regime, hydraulic fracturing could not have been developed here. There are no large tectonic zones serving as channels for the ore-bearing solutions and there are only very weak shear zones which are not comparable to the Darnó zone in the Mátra Mts. (DREW *et al.* 1999).

4. CONCLUSIONS

The Alpine mineralization in the Börzsöny and Mátra Mts. in Hungary represents the following deposits from the deeper level to the near-surface (Table 1):

Cu-Zn skarn and replacement deposits,
Porphyry copper deposits,
Base metal deposits,
Epithermal high sulfidation Au-Cu deposits.

The main ore controls are the faults, the subvolcanic andesites and dacites. This magmatic activity was related to the collision of the European plate and Pannonian fragment. This collision resulted in a crustal escape with local extensions and compressions.

Significant shear zones along fault lines have been formed mainly in consequence of compression that has determined the sites of the volcanic eruptions and the pathways of ore-bearing fluids. In contrast to the Mátra Mts. there are only weakly developed tectonic zones and second-order tectonic lines in the Börzsöny Mts. where the stress field was characterized by extension.

In case of the Mátra and Börzsöny Mts. as well as of the Carpathian realm, deposits of economic importance are related to localities where extension was followed by compression. Since these process were not

Deposits in the Börzsöny and Mátra Mts.

Table 1

Locality	Deposit type	Host rock	Rock alteration	Age of mineralisation and paragenesis	Hydr. breccia	Controlling structure	Data source
Gyöngyös-oroszi, Mátra Mts.	Base metal	Andesitic strato-volcanic sequence	Argillitic, propylitic	NEOGENE Miocene galena–sphalerite–chalcopyrite	+	Fault zone	Vető 1988
Kuruc-patak, Rózsa-hegy, Bánya-puszta, Börzsöny Mts.	Epith. low sulfidation precious and base metal	Subvolcanic and strato-volcanic andesites,	Biotitic, adularia-sericitic, argillitic	NEOGENE Miocene sphalerite–pyrite–chalcopyrite–galena–pyrrhotite	+	Weak fault zone	Korpás and Lang 1993
Recsk deep, Mátra Mts.	Cu-Zn skarn and replacement	Triassic carbonates, diorite	Skarnic	PALEOGENE Eocene sphalerite–chalcopyrite	-	Magm. and sed. contact	Földessy 1996
Recsk deep, Mátra Mts.	Porphyry copper	Subvolcanic andesite	Adularia-sericitic propylitic skarnic	PALEOGENE Eocene sphalerite–chalcopyrite–pyrite–galena	-	Lineament	Földessy 1996
Recsk deep, Mátra Mts	Base metal	Diorite and strato-volcanic andesites	Adularia-sericitic propylitic	PALEOGENE Eocene galena–sphalerite	-	Fault zone	Földessy 1996
Recsk-Lahóca, Mátra Mts.	Epith. high sulfidation Au-Cu	Strato-volcanic andesite	Argillitic, propylitic, silicic	PALEOGENE Eocene pyrite–galena–sphalerite–luzonite–enargite–tetrahedrite	+	Lineament, fault zone	Földessy 1996

Locality	Deposit type	Host rock	Rock alteration	Age of miner. and paragenesis	Hydr. breccia	Controlling structure	Data source
Banska Stiavnica region (Slovakia)	Epith. Au-Q Base metal Porph.-Cu Magn. skarn	Granodiorite, Diorite porph., Q-porph, Granite porph., Rhyolite	Biotite, Sericite, Pyrite, Argillite	12-10 my galena-sphalerite-chalcopyrite-pyrite-electrum-sulfosalts	+	Lineament Fault zone Horst-graben structure	Stohl, Lexa, Kaliciak, Bacsó 1994
Capnik, (Baia-Mare region, Romania)	Epith. Au-Ag, Base metal	Q-diorite, Gabbro-monzo-diorite Micro-granodiorite	Quartz, zeolite, argillite, adularia	no data galena-sphalerite-chalcopyrite-gold	+	Lineament Fault zone	Marias oral comm. 1994
Baia Sprie, Baia-Nistru (Baia-Mare region, Romania)	Epith. Au-Ag, Base metal	Quartz-py.-hbl.-biotite dacite, Basaltic andesite, dacite. Quartz and porphyry diorite	Adularia, sericite, argillite	0.5 my Younger than the last volcanic event galena-sphalerite	+	Lineament Fault zone	Borcós and Vlad 1994
Rosia Montana (Apuseni Mts., Romania)	Epith. Au-Ag, Base metal Porph.-Cu	Dacite, Diorite	Sericite, argillite, silicic rocks	13 my pyrite-galena-sphalerite-chalcopyrite-gold	+	Fault zone	Borcós and Vlad 1994

very significant in the studied areas, their ore reserves are not comparable with those of Banska Stiavnica (Stiavnica Mts. Slovakia), Baia Mare (Oas-Gutin Mts., Romania) or Rosia Poeni (Apuseni Mts., Romania) (Table 2).

Until now, exploration has been carried out only in the central part of both mountains. However, the marginal part of the Börzsöny and the southeastern part of the Mátra Mts. seem to be worthy of further exploration. The intrusions and their contact with carbonate sediments can hide porphyry copper or skarn types of mineralization. On the basis of the deposit models it may be expected that faults and shear zones formed in the neighbourhood of the subvolcanic intrusions may also contain new deposits.

5. REFERENCES

- BORCÓS, M.-VLAD, S. 1994: Plate Tectonics and Metallogeny in the East Carpathians and Apuseni Mts. — Guide book, Bucharest: 1-33.
- COX, D. P.-SINGER, D. A. 1986: Mineral Deposit Models. — US Geological Survey Bulletin 1693. Washington US Department of the Interior.
- CSILLAGNÉ-TEPLÁNSZKY, E.-CSONGRÁDI, J.-KORPÁS, L.-PENTELENYI, L.-VETŐ-ÁKOS, É. 1983: A Börzsöny hegység központi területének földtani felépítése és ércesedése. (Geology and mineralization in the central area of the Börzsöny Mts.) — Magyar Állami Földtani Intézet Évi Jelentése 1981: 77-127. (In Hungarian with English abstract).
- CSONGRÁDI, J. 1984: Epi-telettermális Hg-Sb indikáció az Asztagkö-Üstökfő környékén. (An epi-telettermal Hg-Sb indication in the region Asztagkö-Üstökfő). — Magyar Állami Földtani Intézet Évi Jelentése 1982: 119-136.
- DREW, L. J.-BERGER, B. R.-BAWIEC, W. J.-SUTHPIN, D. M.-CSIRIK, GY.-KORPÁS, L.-VETŐ-ÁKOS, É.-ÓDOR, L.-KISS, J. 1998: Mineral-resource assessment of the Mátra and Börzsöny-Visegrád Mountains, North Hungary. — *Geologica Hungarica Series Geologica* 24: 79-96.
- FÖLDESSY, J. 1993: Relationship of Volcanic Features and Ore Genesis in the Recsk Ore Complex. — (Manuscript)
- FÖLDESSY, J. 1996: Lahóca Epithermal Gold Deposit, Recsk-Hungary. — Plate Tectonic Aspects of the Alpine Metallogeny in the Carpatho-Balkan Region UNESCO IGCP Project No 356 Proceedings of the Annual Meeting-Sofia, Vol 2: 67-74.

- FÜGEDI, U.–MOYZES, A.–ÓDOR, L.–VETŐ-ÁKOS, É. 1995: Case studies on Mercury Related Environmental Problems in Hungary. — *in*: BAEYENS–EBINGHAUS–VASILIEV (eds.): Global and Regional Mercury Cycles: Sources, Fluxes and Mass Balances, Kluwer Academic Publishers, Novosibirsk, Russia.
- KÁZMÉR, M.–KOVÁCS, S. 1985: Permian-Paleogene paleogeography along the eastern part of the Insubric-Periadriatic lineament system: Evidence for continental escape of the Bakony-Drauzung unit. — *Acta Geologica Hungarica*, 28(2): 69–82.
- KISS, J.–SIKHEGYI, F.–VETŐ-ÁKOS, É.–ZELENKA, T. 1996: Volcanic structures, Alpine Metallogeny and Tectonics in the south-eastern-Mátra Mts. NE-Hungary. — Plate Tectonic Aspects of the Alpine Metallogeny in the Carpatho-Balkan Region UNESCO IGCP Project No 356 Proceedings of the Annual Meeting-Sofia, Vol. 2: 145–156.
- KORPÁS, L.–LANG, B. 1991: K-Ar geochronology of the volcanism and associated metallogenesis in the Börzsöny Mountains Hungary. — Report of the Hungarian Geological Survey and Geological Survey of Israel Jerusalem.
- KORPÁS, L.–LANG, B. 1993: Timing of volcanism and metallogenesis in the Börzsöny Mountains, Northern Hungary. — *Ore Geology Reviews*, 8: 477–501.
- KUN, B. 1989: 25 éves az Országos Érc és Ásványbányák. (25 years old the National Ore and Mineral Company). — (In Hungarian).
- MÁRTON, E. 1997: Plate Tectonic Aspects of Paleomagnetism in the Carpatho-Pannonian Region. — *Mineralia Deposita* 32: 441–445.
- NAGY, B. 1983: Arany-, ezüst- és bizmuttelluridok a parádfürdői ércesedés ásványparagenezisében. (Gold, silver and bismuth tellurides in the mineral paragenesis of the Parádfürdő mineralization. — *Magyar Állami Földtani Intézet Évi Jelentése 1983*: 321–357. (In Hungarian).
- NAGYMAROSY, A. 1990: Paleogeographical and Paleotectonical Outlines of some Intracarpethian Paleogene Basins. — *Geologický Zborník–Geologica Carpathica*, 41(3): 259–274.
- ÓDOR, L.–WANTY, R. B.–HORVÁTH, I.–FÜGEDI, U. 1999: Environmental signatures of mineral deposits and areas of regional hydrothermal alteration in northeastern Hungary. — *Geologica Hungarica Series Geologica* 24: 107–129.
- PÉCSKAY, Z.–EDELSTEIN, O.–SEGHEDI, I.–SZAKÁCS, A.–KOVACS, M.–CRIHAN, M.–BERNAD, A. 1996: K-Ar datings of Neogene–Quaternary calc-alkaline volcanic rocks in Romania. — *Acta Volcanologica*, 7(2): 53–61.
- STOHL, J.–LEXA, J.–KALICIAK, M.–BACSÓ, Z. 1994: Metalogénéza zilnickovich polymetallickych mineralizácii v neovulkanitoch Západnych Karpát — *Mineralia Slovaca* 26: 75–117.
- VETŐNÉ-ÁKOS, É. 1982: Folyadék-gáz zárványok és az ércesedés kapcsolata a Börzsöny hegység központi részén. (Relationship between fluid-gas inclusions in hydrothermal calcite quartz veins and mineralizations in the central Börzsöny Mountains, N-Hungary). — *Magyar Állami Földtani Intézet Évi Jelentése 1980*: 59–76. (In Hungarian with English abstract).
- VETŐ, É. 1988: Conditions of Pb-Zn ore formation in the Carpathian Neogene volcanic arc: Evidence from Gyöngyösorszi mine, N-Hungary. — Proceedings of the Seventh Quadrennial IAGOD Symposium, E. Schweitzerbart'sche Verlagsbuchhandlung, 245–252.
- VETŐ-ÁKOS, É.–ITAMAR, A. 1991: Volcanic cycles, Hydrothermal alteration and sulfide mineralization: Evidence from the Gys.-5 borehole, Mátra Mts., Northern Hungary. — Unpublished report.
- VETŐ-ÁKOS, É. 1994: Genetic Model of the Middle Mátra base metal mineralization. — Unpublished report in Hungarian.
- VETŐ-ÁKOS, É. 1996a: Descriptive genetic models: Börzsöny Mountains. 1. Epithermal, vein-type, precious and base metal mineralizations. 2. "Weak" copper porphyry mineralization., 3. Metasomatic Pb-Zn (Ag-Au) mineralization. — Unpublished report in Hungarian.
- VETŐ-ÁKOS, É. 1996b: Descriptive genetic model of the Gyöngyösorszi base metal mineralization. — Unpublished report in Hungarian.
- VETŐ-ÁKOS, É. 1997: Alpine Metallogeny and Plate Tectonics in the Carpatho-Balkan Region: Cenozoic Mineralization in Hungary. — AGM of Mineral Deposits Studies Group and IGCP 356. Programme with Abstracts
- VETŐ-ÁKOS, É.–ZELENKA, T. 1998: Alpine deposit models in Hungary — Unpublished report.
- ZELENKA, T. 1994: The Geological Bild-up of the Mátra Mts. — Unpublished report.

MINERAL-RESOURCE ASSESSMENT OF THE MÁTRA AND BÖRZSÖNY-VISEGRÁD MOUNTAINS, NORTH HUNGARY

LAWRENCE J. DREW¹, BYRON R. BERGER², WALTER J. BAWIEC¹, DAVID M. SUTPHIN¹,
GYÖRGY CSIRIK³, LÁSZLÓ KORPÁS³, ÉVA VETŐ-ÁKOS³, LÁSZLÓ ÓDOR³, and JÁNOS KISS⁴

¹ US Geological Survey, 12201 Sunrise Valley Drive, Reston, VA 20142, USA

² US Geological Survey, P. O. Box 25046, Denver, CO 80225, USA

³ Geological Institute of Hungary, H-1143 Budapest, Stefánia út 14., Hungary

⁴ Eötvös Loránd Geophysical Institute, H-1145 Budapest, Kolumbusz utca 17–23., Hungary

ABSTRACT

A pilot mineral-resource assessment for a study area in the Mátra and Börzsöny–Visegrád Mountains, North Hungary was used to transfer the assessment method developed during the past 25 years at the US Geological Survey to the Geological Institute of Hungary. A wide range of geological, geochemical, geophysical, drill core, and mining data were used in this assessment. These data were acquired from field observation and satellite images, as well as the large body of recent literature on the geology, tectonics, and magmatic activity associated with the formation of the Pannonian Basin. The results of the assessment confirm that the Middle Miocene volcanic complexes in the study area are permissive for the occurrence of mineral deposits that belong to the porphyry copper/polymetallic vein kin-deposit system. The estimated undiscovered resources for each volcanic complex, the expected number of undiscovered deposits by type, and the aggregated metal tonnages across all deposit types are reported.

1. INTRODUCTION

Mineral-resource assessment is a field of research and application of economic geology that has developed rapidly during the past 25 years (SINGER 1993). The goal of this field is to produce information about the occurrence of undiscovered resources for minerals exploration and land-use planning. The region chosen for the pilot mineral-resource assessment was the Mátra and Börzsöny–Visegrád Mountains, North Hungary (Fig. 1). For the assessment, geologic information on the occurrence of metallic mineral deposits was collected, reconnaissance field trips to Slovakia (1995) and Romania (1997) were made to examine mineral deposits of the types known to occur in the study area, and estimates were made of the numbers of undiscovered mineral deposits of these types in the study area.

2. MINERAL-DEPOSIT MODELS

The Mátra and the Börzsöny Mountains have been prospected for base metal mineral deposits during the past several decades. A large polymetallic vein deposit type (BLISS and COX 1986, COX 1986) was discovered and mined until 1986 at Gyöngyösoroszi in the southern Mátra Mountains (Fig. 2; VARGA et al. 1975, BARTÓK and NAGY 1992) and a similar but much smaller deposit was mined until 1954 near Nagyborzsöny at Rózsa-bánya in the Börzsöny Mountains (Fig. 2; CSILLAGNÉ–TEPLÁNSZKY et al. 1983, KORPÁS and LANG 1993, KORPÁS et al. 1998). The Gyöngyösoroszi deposit has proven reserves of 4.8 million tonnes (t) of lead, zinc, and silver ores, whereas the Nagyborzsöny deposit has 40,000 t of reserves of similar ores. In addition to the Nagyborzsöny polymetallic vein deposit, three small low-grade porphyry copper deposits were discovered and evaluated (CSILLAGNÉ–TEPLÁNSZKY et al. 1983, KORPÁS et al. 1998). Collectively, the porphyry copper deposits contain approximately 100 million t of material with a grade of 0.1 percent copper. Magnetite-, sphalerite-, and chalcopyrite-bearing xenolites of skarn deposits ($\text{Fe}_2\text{O}_3 + \text{FeO}$: 63.4–67.7 percent; Zn: 4,000–6,000 ppm, Cu: 100–400

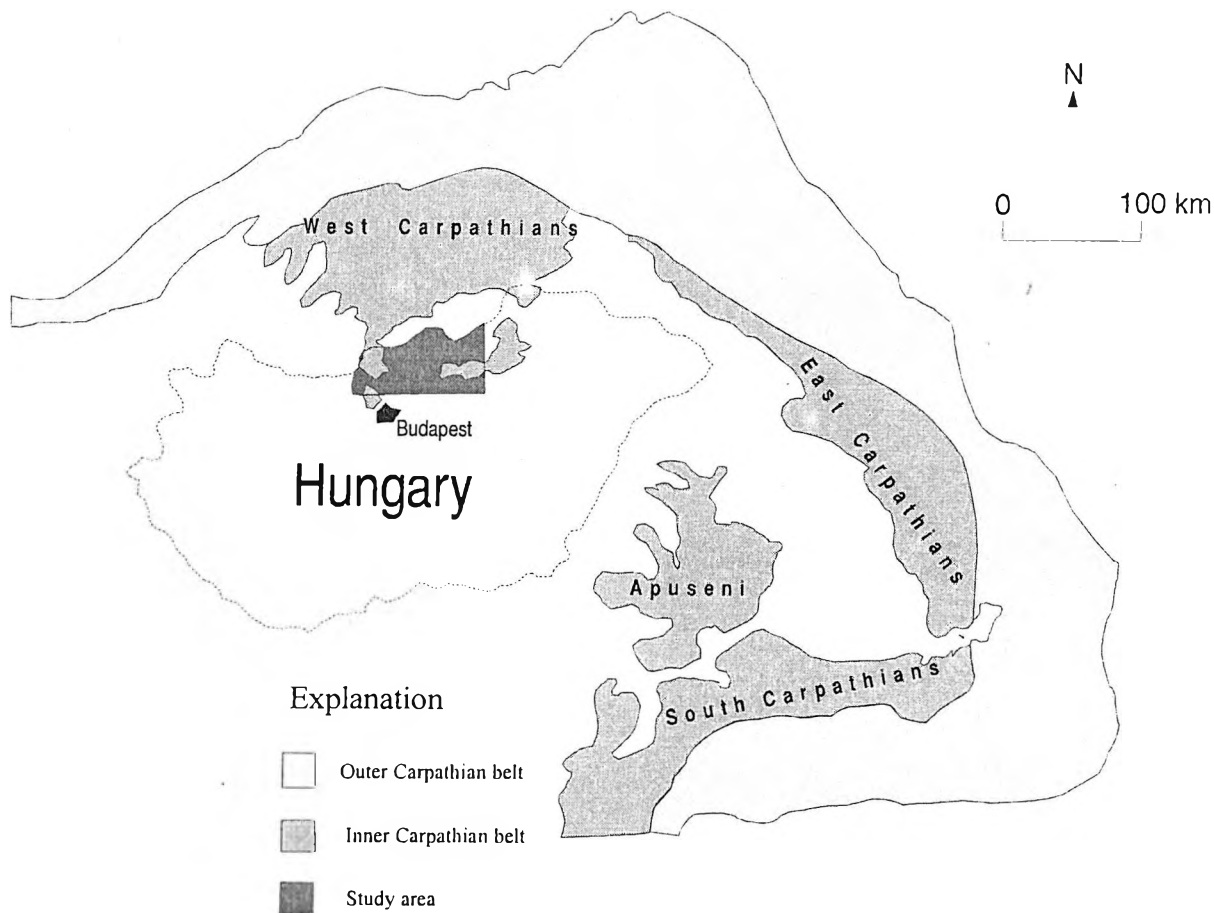


Fig. 1: Map showing the location of the study area in North Hungary and the inner and outer Carpathian regions Modified from CSONTOS et al. (1992)

ppm) were described by CSILLAGNÉ-TEPLÁNSZKY and KÖRPÁS (1982) from the basal horizon of the Börzsöny–Visegrád Andesite at Dunabogdány. The primary skarn deposit, hosted in Middle to Late Triassic dolomites and limestones of the pre-Tertiary basement, is located at a depth between 1500 to 2500 m.

In addition to being permissive for the occurrence of porphyry copper and polymetallic vein deposits, calc-alkaline volcanic complexes, such as those in the Börzsöny–Visegrád and the Mátra Mountains, are generally permissive for the occurrence of skarn deposits (COX 1986, SAWKINS 1990). No assessment for skarn deposits was performed for the Börzsöny and the Visegrád Mountains because of the deep position of the possible skarn deposits. An assessment for these deposits was initially considered for one small area where limestone occurs in the Mátra Mountains, but too little field data for this area were available to execute a quantitative assessment for this deposit type.

The determination that certain packages of rocks are permissive for the occurrence of particular types of mineral deposits (for example, polymetallic veins and porphyry copper deposits) implies that there is at least a specific probability for the occurrence for these type of deposits. SINGER (1993) defined a package of rocks as permissive if the probability of occurrence of an economic deposit is 1 to 10,000 or greater. In application, the concept of permissiveness is based on the fact that particular types of deposits usually occur in association with particular packages of rocks in various parts of the world. Further, given the permissiveness, the probability of occurrence is usually assumed to increase with the size of the permissive rock volume. The probability estimate, however, must be determined from the available data on the land tract under consideration. Further, in such highly explored regions as the study area, the probability that most (perhaps all) of the mineral resources have already been discovered must be considered.

The Mátra Andesite and the Börzsöny–Visegrád Andesite Formation are each about 600 km² in areal extent. These areas are only small parts of the much larger inner Carpathian magmatic arc (Fig. 1) in which about 50 sig-

EXPLANATION

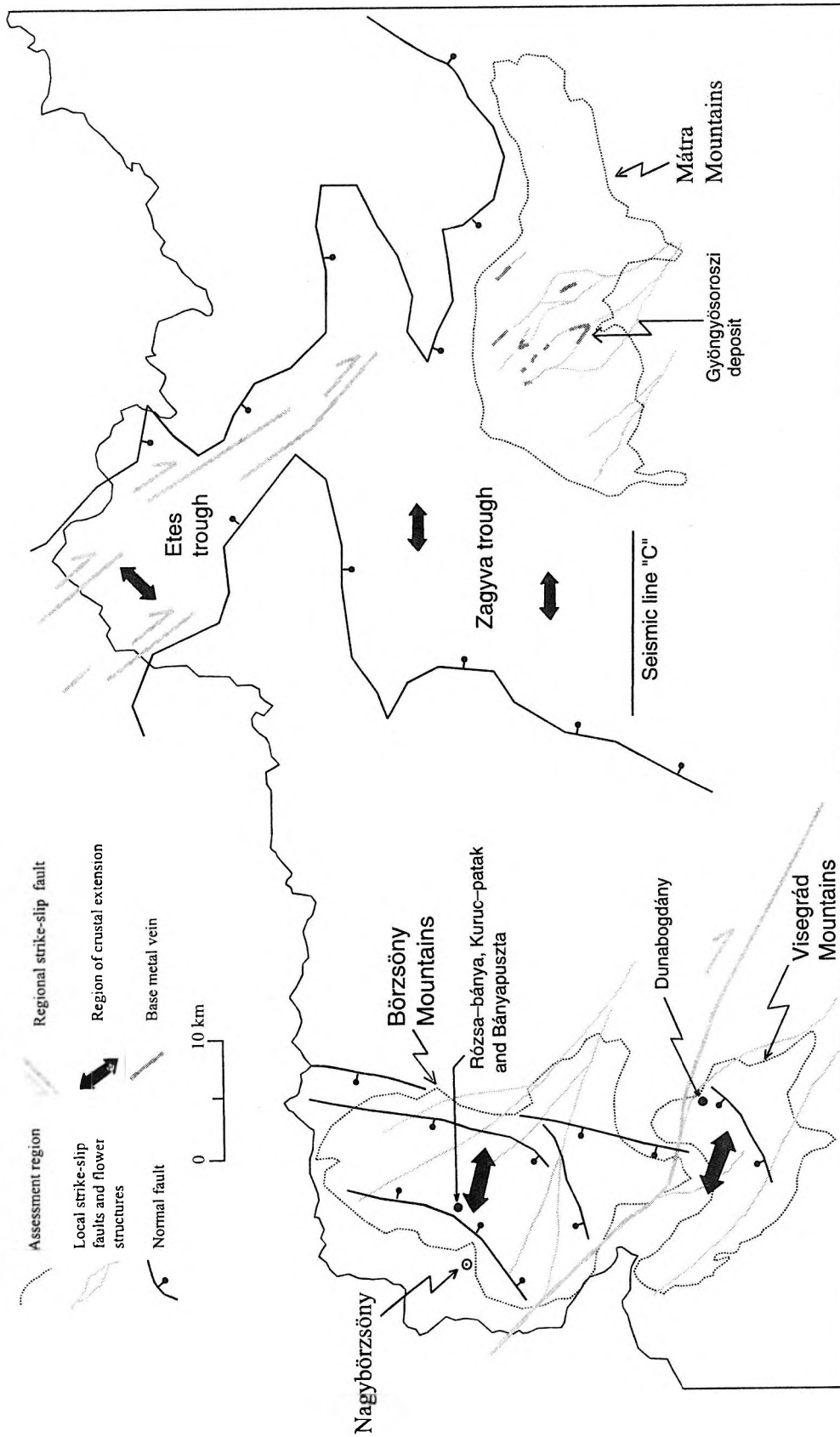


Fig. 2: Map showing the location of the study area in the Börzsöny and Visegrád and the Mátra Mountains. The Mátra Mountains, which are located in a Middle Miocene right-lateral strike-slip fault system, are probably within a right-stepping extensional duplex. As the extension began to dominate in the Middle to Late Miocene, the strike-slip faults became connecting transfer structures among the developing sedimentary basins, one of which is the Zagyva trough. The volcanic complex in the Börzsöny and the Visegrád Mountains is probably located in a similar pull-apart basin. Compiled from TARI et al. (1992), KORPÁS and LANG (1993), MÁRTON and FODOR (1995), and KORPÁS et al. (1998)

nificant polymetallic vein districts and several porphyry deposits have been discovered in Slovakia (Western Carpathians) and Romania (Apuseni Mountains and East Carpathians; BORCOS 1994). Therefore, solely from the ratio of the areal size of the study area to the areal size of the inner Carpathian magmatic arc, we might expect that a small number of polymetallic vein districts and porphyry deposits occur in the study area.

3. TECTONIC MODEL OF PORPHYRY COPPER/POLYMETALLIC VEIN KIN-DEPOSIT SYSTEM

A tectonic model for the porphyry copper/polymetallic vein kin-deposit system is developed from empirical descriptive models from field data (COX and SINGER 1986), model and theoretical studies of the behavior of strike-slip fault systems (SEGALL and POLLARD 1980), and studies of heat dissipation and mechanics associated with intrusive rocks (NORTON 1982, SONDER and ENGLAND 1989). The kernel of this model is derived from the observation that these kin deposits occur in close spatial and temporal associations in the strike-slip fault systems and, in particular, in duplexes.

The members of this system of kin deposits range from those formed in an initial magmatic phase to those that are derived from mixed meteoric/magmatic inputs; that is, from porphyry copper deposits to polymetallic veins. The initial phase begins when far-field stress in the crustal plate is released in the principal deformation zones (PDZ) of strike-slip fault systems. As stress is propagated, it is transferred from one master fault tip to another, and, depending on the direction of transfer, either extensional or compressional duplexes are formed (SEGALL and POLLARD 1980). Extensional duplexes form at the releasing bends, whereas compressional duplexes form at the constraining bends. Extensional duplexes are easily recognized by the sedimentary basins that form and are readily preserved. Compressional duplexes are formed less frequently and, as structural high features, are eroded easily and, therefore, are less well preserved. Within both of these duplex structures, zones of crustal extension develop that provide channelways for magma to rise to shallow levels in the crust. The zones of extension, however, are smaller in the compressional duplexes. These duplexes may also hold a shallowly intruded stock in place for the necessary length of time so that hydrothermal fluid can be focused into small rock volumes where the necessary mesothermal reactions (carapace development, hydrofracturing, and brittle intrusive fracturing) can occur to create a porphyry copper deposit.

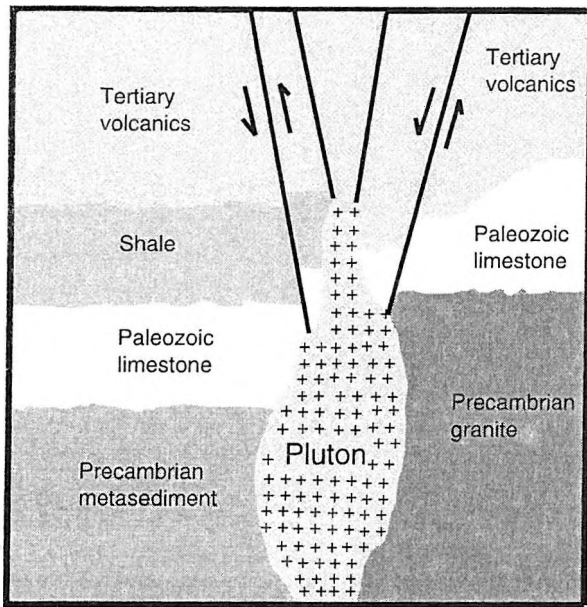
During this process, the intruding igneous stock elevates the temperature of the encapsulating host rocks (Fig. 3; NORTON 1982) enough to nullify the effect of the far-field stress (σ_1 and σ_3 are made nearly equal; that is, $\Delta\sigma$ is near zero). In this structural environment, ductile behavior can occur at a shallow level in the Earth's crust. With high temperature and low differential stress, the rocks fracture when the hydraulic pressure under the carapace exceeds the confining pressure. Additional brittle fractures are formed by the mechanical/hydraulic processes associated with emplacement of magma and hydrothermal convection. With repeated sealing through mineral precipitation and fracturing, an interconnected stockwork of veins is developed. Silica, potassium feldspar, and copper sulfide minerals precipitate in the low-pressure environment that exists after a fracturing event.

When new batches of magma are no longer emplaced into the magma chamber and heat dissipates in the stock and surrounding wallrock, the likelihood of throughgoing brittle fracturing increases as the far-field stress regains structural dominance over the rock volume (σ_1 again dominates, or $\Delta\sigma \gg 0$); that is, as the thermal environment becomes retrograde, the effect of the stress in the far field is reestablished, and throughgoing straight brittle fracturing dominates.

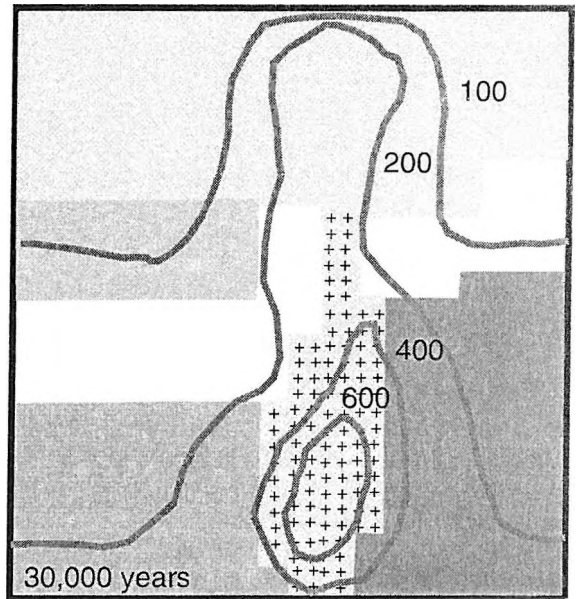
The polymetallic veins that often crosscut and (or) are intimately associated with porphyry copper deposits are deposited in the brittle fractures that develop after strain is partitioned and accommodated within the large volume of rock that surrounds the porphyry. The polymetallic nature of these veins is attributed to the introduction of meteoric water into the igneous hydrothermal system. When the porphyry system is arrested owing to strain partitioning, the hydrothermal system is then opened to nonmagmatic sources of zinc, lead, and other components that have been leached from the rocks that surround the intrusive complex by the incoming meteoric waters. The Mátra Andesite and the Zagyva trough tectonic system is interpreted as an example of this type of tectonic evolution.

Polymetallic veins often occur in positive flower structures (Fig. 4A). These structures break upward toward a free surface and are compressive. The converse structure [the negative flower structure (Fig. 4B)], which also forms in the same fault system, breaks upward along expansion fractures. The negative flower structure is then open to the surface, and the hydrothermal system often leaks out at the surface. The configurations shown in Fig. 4 are the end members often observed in a PDZ of a strike-fault system.

Because the movement of the masses of rock in a PDZ of a major strike-slip fault system can be rather heterogeneous, and the general model has to be modified on a case-by-case basis to allow for the progressive nature of

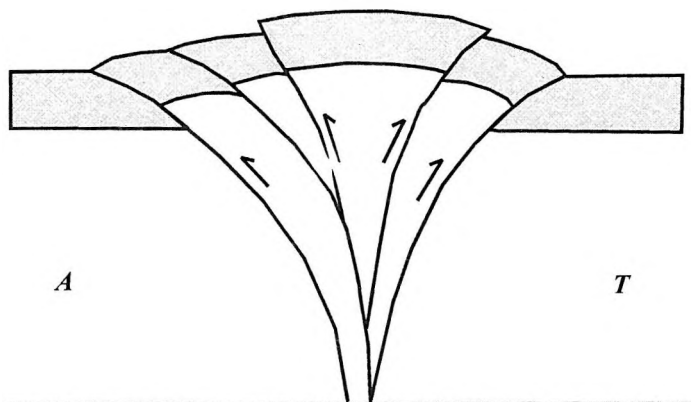


Geological cross section

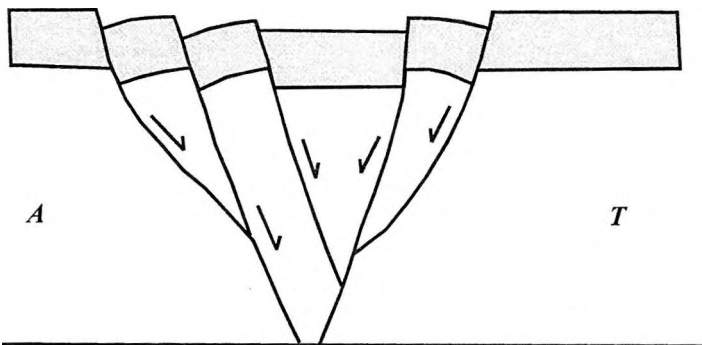


Model isotherms, °C

Fig. 3: Diagram showing the model of the distribution of magmatic heat associated with a plutonic stock and isotherms for temperatures after 30,000 years of heat dissipation (NORTON 1982)



A



B

Fig. 4: Diagrams showing cross sections through flower structures
A, positive; B, negative; A, tectonic movement is away from viewer; T, tectonic movement is toward viewer

simple shear. In this progression, individual horses may record different histories of internal strain (domains) as the local stress fields reorientate to accommodate rotation and locking and unlocking of horse blocks. When horse blocks unlock, previously developed faults may be reactivated, and other structures (bedding planes and foliations) may be activated. Consequently, the permeability that controls fluid flow can vary in direction over time, and the deposition of mineralization in negative and positive flower structures can occur (WILLIS and TOSDAL 1992).

The positive flower structure is, by virtue of its compressional nature, a fluid-flow-constraining reaction-containing (self-sealing) structure; that is, locally along a positive flower structure, there will be regions where σ_1 is equal or nearly equal to σ_3 . These compressional structures are frequently found in the field as readily mappable antiforms. Before the flower structures were formally identified and named by R. F. GREGORY in 1970 (HARDING and LOWELL 1979), many examples were known. A summary diagram has been widely used to express the idea that such structures are compressional and that they are created in transpressive sections (constraining bends) of strike-slip fault systems (Fig. 5; LOWELL 1972).

Well-documented examples of the porphyry copper/polymetallic vein kin-deposit system that illustrate the initial phase of porphyry development followed by the development of polymetallic veins are found within the inner Carpathian magmatic arc in the Apuseni Mountains, Romania (BORCOS 1994, BERBELEAC et al. 1995a, b, MITCHELL 1996). For example, in the Zlatna region (Fig. 6), where low-grade porphyry copper deposits have been emplaced, these deposits are often cut by polymetallic veins that have grades in the range of 5 to 7 percent combined zinc and lead (I. BERBELEAC, P. S. A., oral commun., May 1997). Also in the same region, the economic polymetallic veins that occur in the Hanes deposits (Fig. 6 and Fig. 7) are in the footwall (more-compressive) section of complex positive flower structures. Interpretation of the evolution of this structure is ambiguous because of the intruding andesite. This complexity is probably associated with large vertical and horizontal displacements on the main fault with considerable left-oblique movement. The intruding andesite completely filled the hanging-wall segment (northeastern side) of this flower structure, and the footwall (southwestern side) is interleaved with horses of marl beds that were thrust upward from lower in the stratigraphic section.

At Hanes, then, the intimate relation between the strain features created by the strike-slip faults (flower structure) and the intruding andesite is obvious—the andesite body takes the form of the flower structure with a dikelike root and a dome-shaped top (Fig. 5). Subsequent to intrusion of the andesite along the fault system, throughgoing brittle fracturing occurred in the andesite, and polymetallic veins were deposited in the southwestern side of the flower structure. Northwestward along the fault system, however, compression increased across the whole structure. Consequently, the polymetallic veins are more broadly distributed across the flower structure.

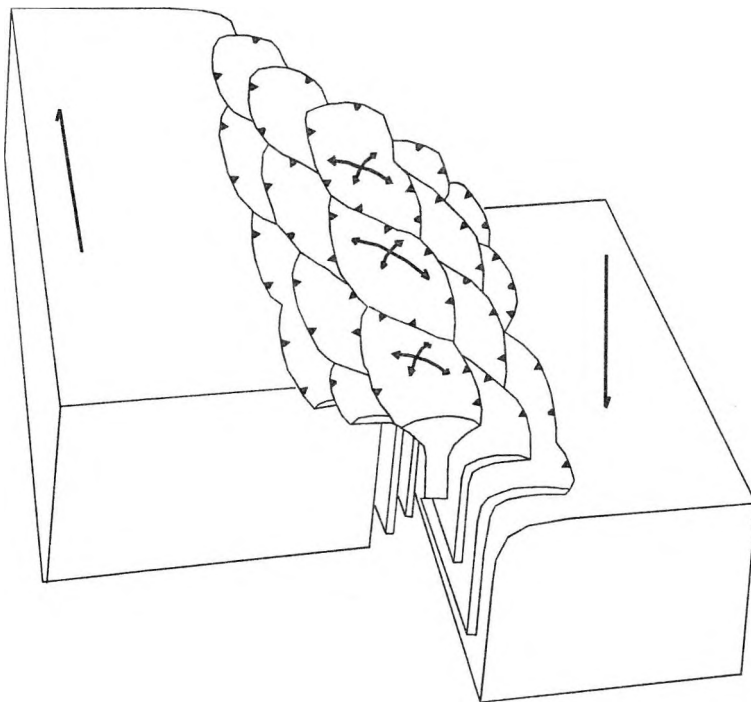


Fig. 5: Diagram showing a positive flower structure as a self-sealing reaction-containing structure (LOWELL 1972)

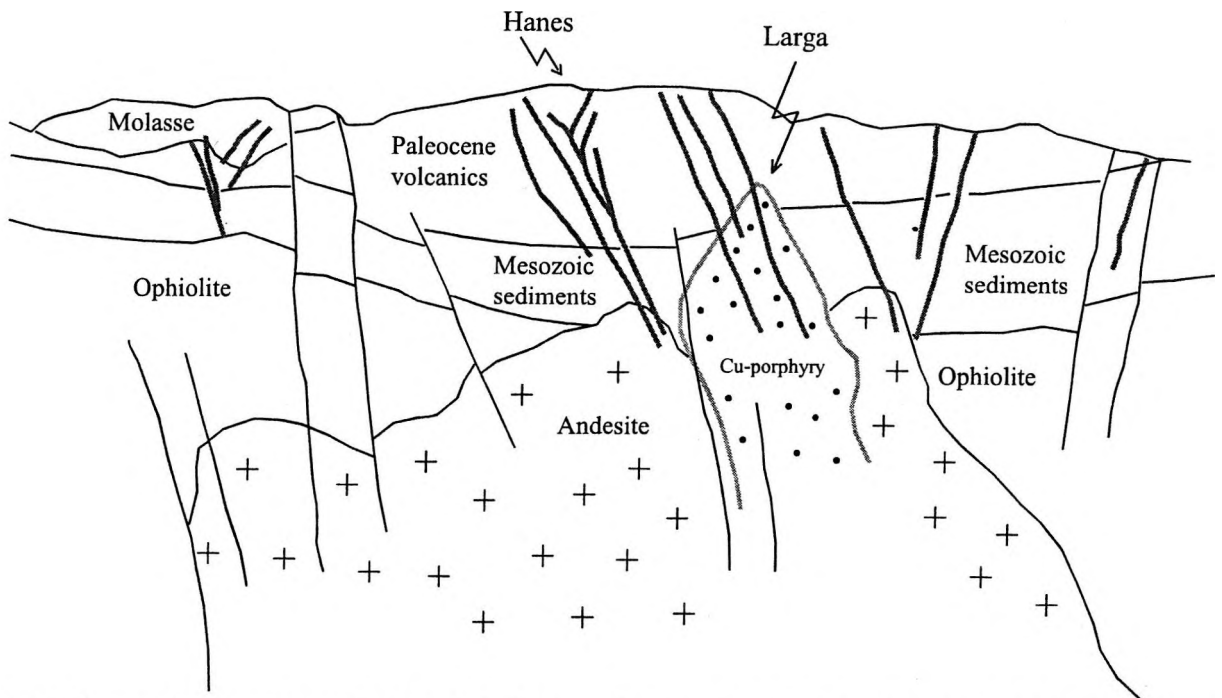


Fig. 6: Diagram showing a cross section through the Larga porphyry copper and the Hanes polymetallic vein deposits, Zlatna district, Romania (BORCOS 1994)

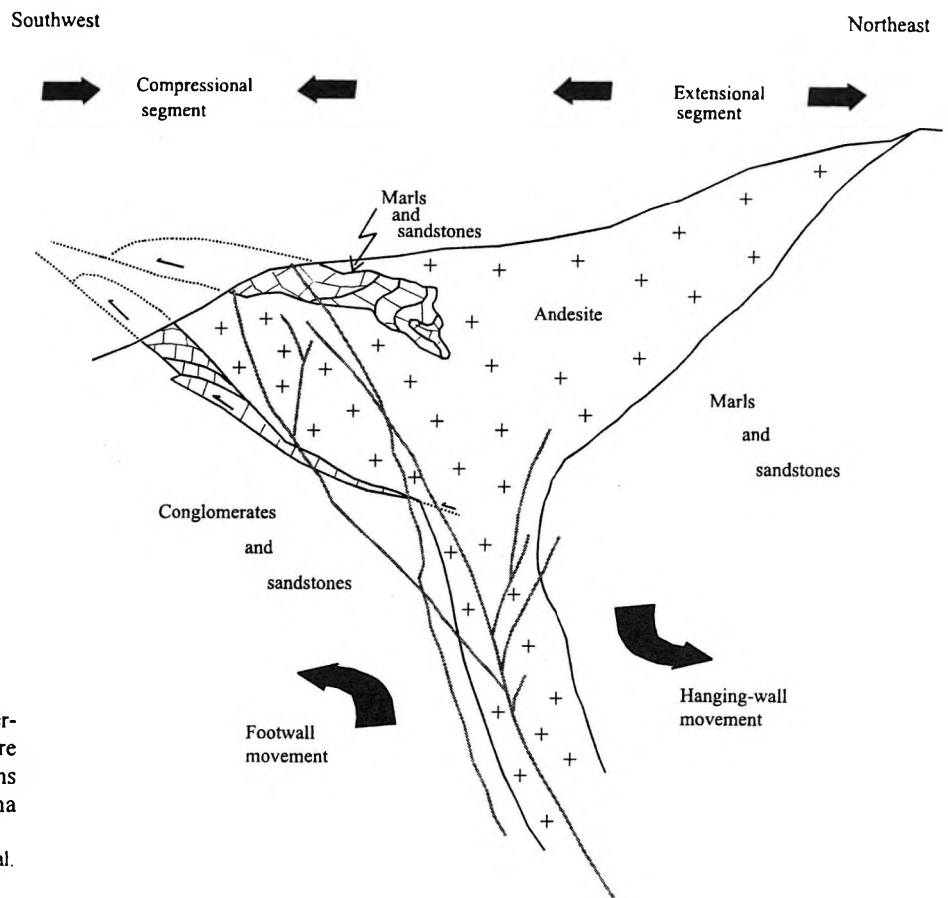


Fig. 7: Diagram showing interpretation of the flower structure that hosts the polymetallic veins in the Hanes deposit, Zlatna district, Romania
Based on data from BORCOS et al. (1962)

4. GEOLOGICAL SETTING AND TECTONIC HISTORY OF THE STUDY AREA

The study area is located in the West Carpathians within the inner volcanic arc of the Carpathian-Pannonian region (Fig. 1, ROYDEN et al. 1982, SANDULESCU 1988, CSONTOS et al. 1992). The pilot mineral-resource assessment for this area was confined to volcanic complexes [the Börzsöny–Visegrád and the Mátra Mountains (Fig. 2)] permissive for selected mineral-deposit types. These volcanic complexes are Middle Miocene and localized in zones of crustal extension within a continental plate that overrode the subducting plate in a continent-to-continent collision (ROYDEN et al. 1983).

The zones of extension in which these volcanic/plutonic complexes evolved (Fig. 2) are interpreted as strain features that resulted from the release of stress that was built up during the continent-to-continent collision of the Pannonian and the European plates. WOODCOCK (1986) described the mechanism that produced these strain features as "indent-linked strike-slip fault systems" (Fig. 8). An additional condition was the development of a large escape structure to the east (ROYDEN et al. 1983). Many small basins were formed in the region as this escape structure fragmented along a series of northeast- to southwest-trending strike-slip faults. Individual basins and pop-up structures vary greatly in configuration because the various fragments escaped at differential rates during the Miocene. The Börzsöny–Visegrád and the Mátra Mountains were formed during the evolution of this structurally dynamic system. The volcanic rocks in these complexes are of calc-alkaline affinity and are principally andesitic in composition with some dacites and rhyolites (SZABÓ et al. 1992, KÖRPÁS et al. 1998).

PÓKA (1988) placed the main period of volcanic activity in the Börzsöny Mountains between 19 and 16.5 Ma and somewhat later in the Mátra Mountains (18 to 14.5 Ma). SZABÓ et al. (1992) reported ages of 16.5 to 15.5 Ma for the volcanics in the Börzsöny Mountains and 16.5 to 14 Ma for the Mátra Mountains. PÉCSKAY et al. (1995) have summarized the chronology of the Neogene to Quaternary volcanism of the Carpatho-Pannonian region. They estimated similar age intervals for the Börzsöny–Visegrád Mountains (16.5 to 13.5 Ma) and the Mátra Mountains (16.0 to 13.7 Ma). KARÁTSÓN (1995) estimated the same age (16.0 to 13.7 Ma) for the Börzsöny volcanism. KÖRPÁS and LANG (1993) and KÖRPÁS et al. (1998) reported a much tighter and younger age (15.2 to 14.5 Ma) for the volcanic activity of the Börzsöny–Visegrád Mountains.

WOODCOCK (1986) discussed, in general terms, how stress is released through the development of strain features in the continental crust above the subducting plate in a continent-to-continent collision (Fig. 8). Consequently, indent-linked strike-slip faults then become the far-field strain features caused by such collisions [thus, the maximum principal stress (σ_1) is in the plane of the Earth's surface]. Within the PDZ of these fault systems, extensional and compressional strain features develop that can localize magmas at shallow crustal levels. The flow of hydrothermal fluids is similarly controlled by the same stress field and localized in the resulting strain features (SIBSON 1986). Simultaneously with this focusing of magma and fluids in the crust, sedimentary basins (strain features) are created as surface expressions of dissipated stress in the same PDZ (SYLVESTER 1988).

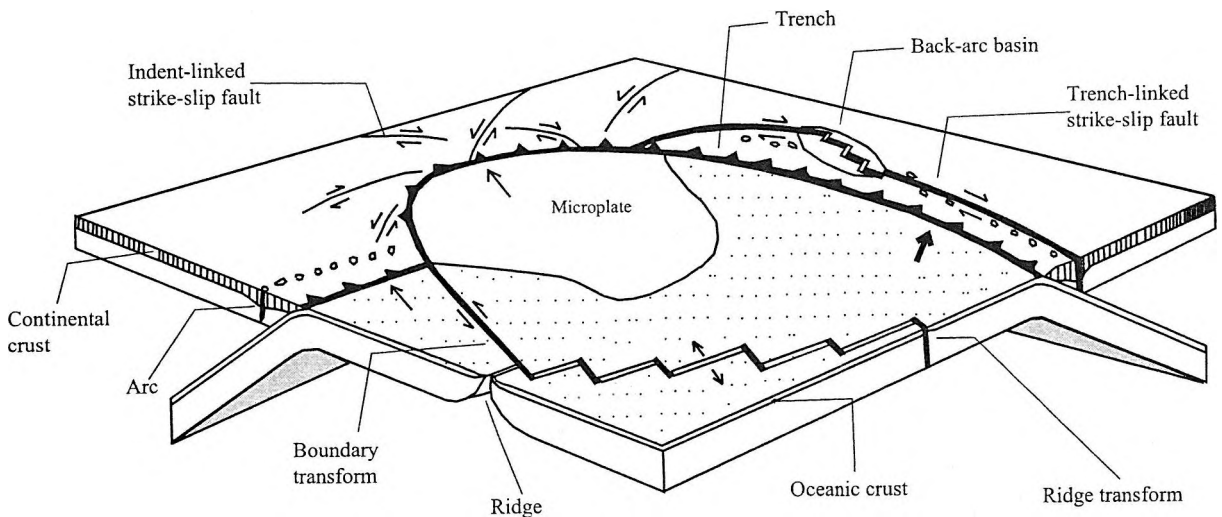


Fig. 8: Diagram showing the plate tectonic setting of the major classes of strike-slip faults (WOODCOCK 1986)

In the vicinity of the study area, the direction of σ_1 during the Early and Middle Miocene has been established as having been north-south through detailed analysis of kinematic indicator data (PERESSON and DECKER 1997), whereas the Late Miocene was characterized by a transient east-west compression. PERESSON and DECKER (1997) argued that the inversion of motion on Early and Middle Miocene structures indicates that east-west tension switched to east-west compression during the Late Miocene. They suggest that the Late Miocene soft collision in the East Carpathians transmitted east-west compression from the East Carpathian plate boundary westward through the previously extended upper plate and into the eastern Alps; that is, the effect of this collision was transmitted for more than 1,000 kilometers behind the subduction zone. FODOR (1995) presented a similar analysis for the Vienna Basin and the East Alpine-Western Carpathian junction where the Oligocene through Miocene period is characterized within the same context of having evolved from transpression to transtension and identified four different stress fields.

The strain features developed in the study area as a result of the dissipation of stress during the Middle Miocene (Fig. 2) are shown in detail in Fig. 9 (Mátra Mountains) and Fig. 10 and Fig. 11 (Börzsöny and Visegrád Mountains). The Mátra Andesite ascended to the surface in a zone of extension clearly identifiable on the geologic sketch map presented by MÁRTON and FODOR (1995). Elements of this map were used to compile the tectonic map shown in Fig. 2 where the northern boundary of the Mátra Andesite is located at the top of a right-lateral right-stepping strike-fault system. The GyöngyöSOROSZI polymetallic vein mining district is hosted in a flower structure with the same northwest orientation as the master fault system (Fig. 2 and Fig. 4). The age of the mineralization is about 14 Ma (PÉCSKAY et al. 1995). As the right-lateral strike-slip fault system continued to evolve, sedimentary basins developed marginal to the Mátra Andesite like the Zagyva trough to the west, and other minor basins to the east and south (Fig. 2 and Fig. 9). A seismic section through the Zagyva trough (Fig. 2) has been interpreted by TARI et al. (1992) as a half-graben structure in a transfer fault system. This interpretation is consistent with the idea that the Mátra Andesite and the volcanosedimentary complex of the Zagyva trough was created in an extensional duplex between two master faults. One of these faults is located in the Etes trough (expressed as a negative flower structure at the surface?), and the other has to lie mostly buried to the south (Fig. 2). This second master fault is clearly identified on tectonic maps by CSONTOS et al. (1991) and MÁRTON and FODOR (1995). The southern master fault is also identified in the Börzsöny–Visegrád Mountains as a regional strike-slip fault (Fig. 2) and as a collection of faults forming a PDZ in Fig. 10. The movements of the strike-slip faults controlling the porphyry copper and polymetallic vein mineralization in the area (Fig. 2, Fig. 9 and Fig. 10) are discussed below.

5. ASSESSMENT OF THE UNDISCOVERED DEPOSITS IN THE STUDY AREA

In the study area, both members of the porphyry copper/polymetallic vein kin-deposit system have been discovered. In the Mátra Mountains, however, only polymetallic vein deposits have been discovered, whereas in the Börzsöny Mountains, small porphyry copper deposits have been discovered. The three deposits discovered to date near NagyBörzsöny have a total of 100 million t of material with an average grade of 0.1 percent copper. The associated polymetallic vein deposits discovered in the same area (Fig. 2, Fig. 10 and Fig. 11) are also small (40,000 t) and have low grades (combined lead and zinc grade of 2.4 percent, 0.85 ppm gold, and 45 ppm silver; BARTÓK and NAGY 1992).

The polymetallic veins discovered at GyöngyöSOROSZI in the Mátra Mountains are large (4.8 million t) and of higher grade (4.8 percent combined lead and zinc; BARTÓK and NAGY 1992). No associated porphyry copper deposits, however, have been found. The porphyry copper deposit located nearby at Recsk, on the northern edge of the Mátra Mountains, has an Eocene age (approximately 35 Ma; BAKSA 1984) and is in an exotic tectonic block. This deposit may have been emplaced during the formation of the western Alps and carried eastward along strike-slip faults associated with the development of the Carpathian/Pannonian escape structure (KÁZMÉR and KOVÁCS 1985).

5.1. Previous exploration data

In April 1995, the assessment team examined several kilometers of drill core from the NagyBörzsöny porphyry copper deposits (Börzsöny Mountains) and one core from the area in the vicinity of the GyöngyöSOROSZI deposit (Mátra Mountains). The cores from the NagyBörzsöny area contained sparse vertical fractures filled with quartz and occasional chalcopyrite, pyrite, magnetite, pyrrhotite, sphalerite, and galena. Little connective fracturing was evident, although sections of the cores were silicified. The assessment team also examined maps of the

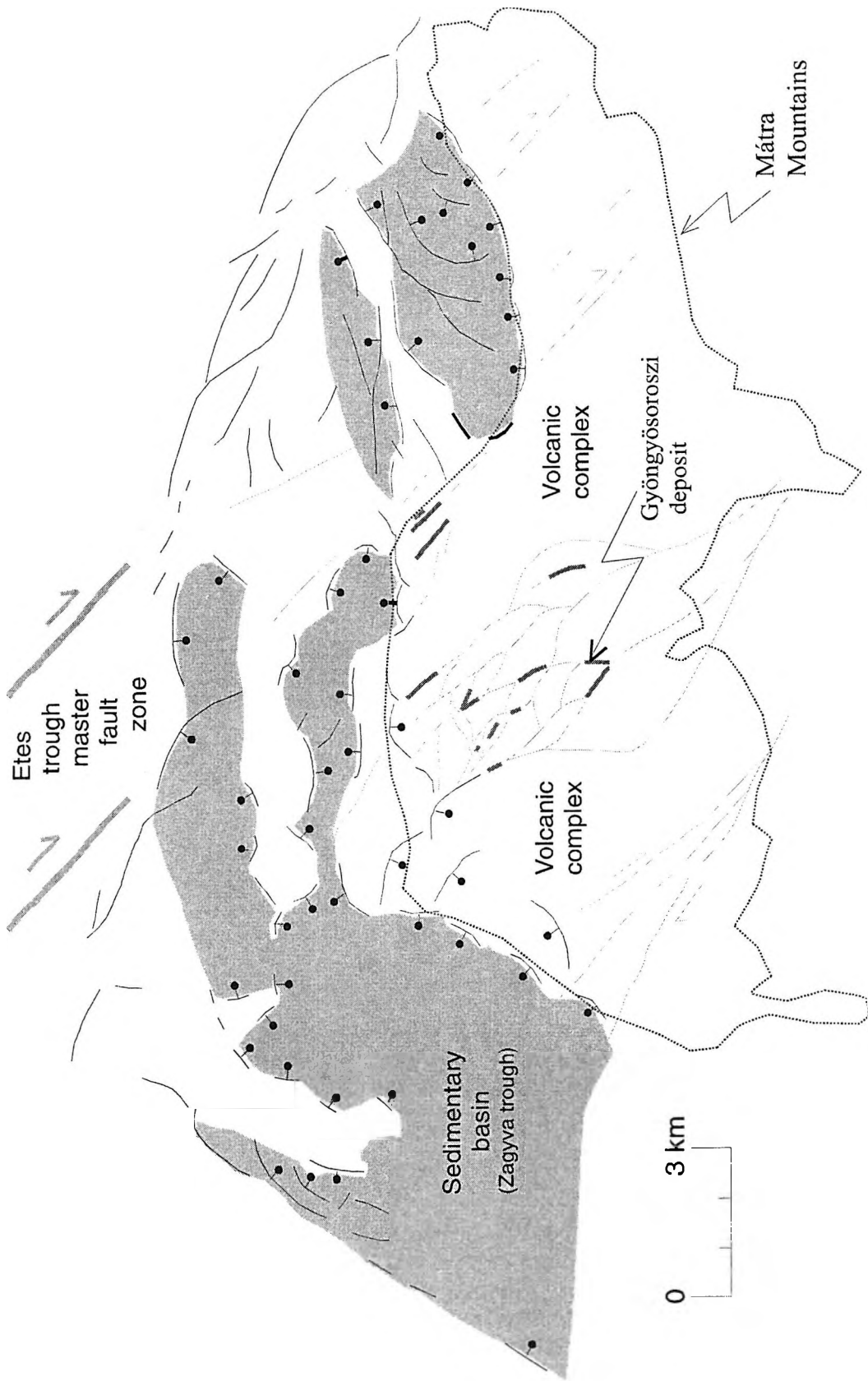
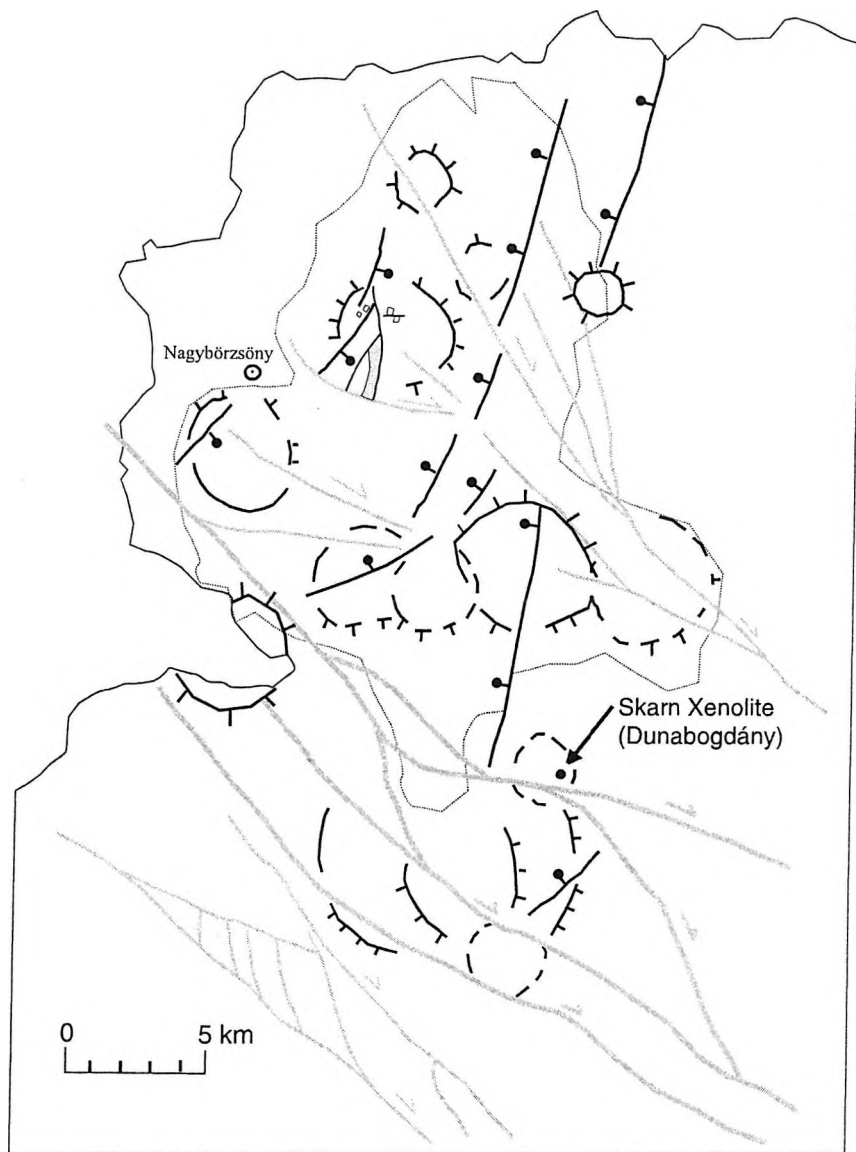


Fig. 9: Map showing locations of strike-slip faults, mineralized faults, and sedimentary basins in the Mátra Mountains. See Fig. 2 for the location of the study area and the description of symbols.



EXPLANATION



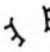
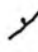


- | | | | |
|---|----------------------------|---|---|
|  | Assessment area |  | Local strike-slip faults |
|  | Volcano |  | Normal fault |
|  | Regional strike-slip fault |  | Location of porphyry copper mineralization (Rózsa-bánya, Kuruc-patak, Bánya-pusztá) |

Fig. 10: Map showing locations of volcanoes, faults, and mineralization in the Börzsöny–Visegrád Mountains

Börzsöny and the Mátra Mountains that showed a dense pattern of drilling, as well as many cross sections that had been constructed by using the data in these drill holes. Many chemical analyses of vein material and wallrock were studied (VARGA et al. 1975, CSILLAGNÉ–TEPLÁNSZKY et al. 1983, KÖRÖSI et al. 1998). From these data, as well as supporting geochemical and geophysical investigations and associated literature (CSILLAGNÉ–TEPLÁNSZKY and KÖRÖSI 1982, VETŐ 1988, ÓDOR et al. 1997, KÖRÖSI et al. 1998), the team concluded that the volcanic complexes in the Börzsöny–Visegrád and the Mátra Mountains had been extensively explored for porphyry copper and polymetallic vein deposits. This conclusion was the basis for the prediction that only a small number of deposits remain to be discovered in the study area.

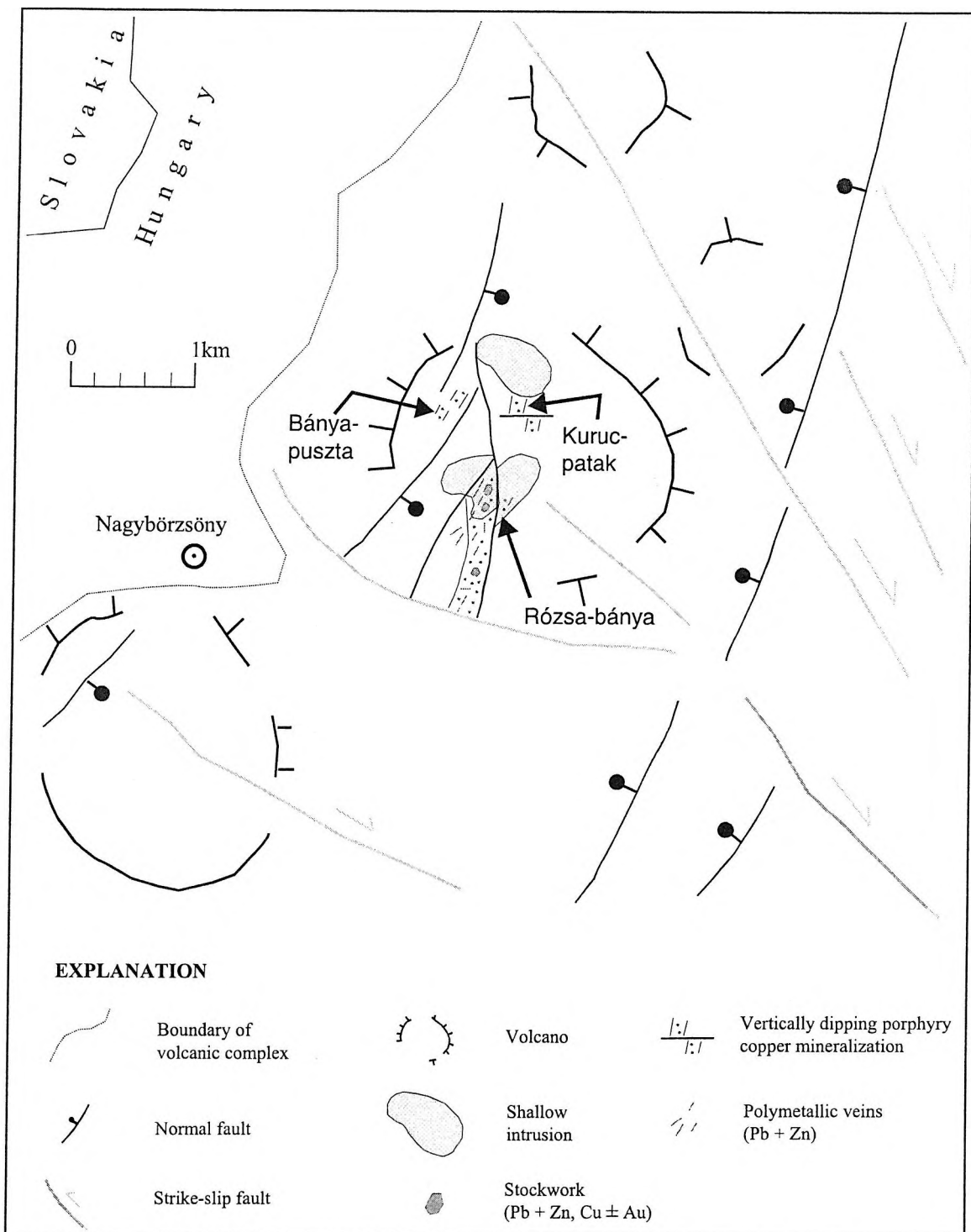


Fig. 11: Map showing geological and mineralization features near Nagybörzsöny in the Börzsöny Mountains

5.2. Assessment of the Mátra Mountains

The Mátra Andesite was supplied by at least six volcanic centers (KISS et al. 1996, ZELENKA oral commun., 1998). The assessment area is shown by a dotted line in Fig. 9. Within the approximately 100 km² area, a collection of strike-slip faults that host the polymetallic veins occurs. The collection of northwest-to southeast-trending faults that cut across these mountains were located by combining data from a detailed map (VARGA et al. 1975)

and photolinear analysis of a satellite image of the area. Although fieldwork would be required to measure the kinematic indicators essential to establish fault movement, it can be argued from the surface expression of these faults, that the central group (faults near the Gyöngyösoroszi deposit) are a complex flower structure with compressional segments (right-lateral and left-stepping), as well as extensional segments (right-lateral and right stepping); that is, a cross section from southwest to northeast would show a mixture of positive and negative flower structure features (Fig. 4). Such mixed flower structures host the gold-bearing quartz vein in the Mesquite mining district of southeastern California (WILLIS and TOSDAL 1992). Again, this structural interpretation of these faults must be to be considered preliminary because field work is required to ensure proper structural analysis.

During the assessment of the Mátra Mountains, the following data were considered to be most relevant for predicting the occurrence of undiscovered polymetallic vein deposits – the basic geology is permissive (six or more volcanic centers), hydrothermal alteration is widely distributed, one major producing polymetallic vein district (Gyöngyösoroszi) has been discovered, and the inner Carpathian arc hosts many polymetallic veins nearby in Slovakia and Romania. The consensus estimate for the inventory of undiscovered polymetallic veins in the Mátra Mountains is a 90 percent probability of 4 deposits, a 50 percent probability of 5 deposits, a 10 percent probability of 6 deposits, and a 1 percent probability of 10 deposits. On the basis of this distribution, the expected number of undiscovered deposits is 5.08 deposits, which was estimated by using the method in which the solution is determined by weighing the individual probabilities associated with the regions of the probability among each number of deposits (ROOT et al. 1992).

This estimate of 5.08 deposits is for the occurrence of deposits distributed in size as shown in Fig. 12. Inspection of this figure reveals that the Gyöngyösoroszi deposit is an exceptionally large polymetallic vein deposit with proven reserves of 4.8 million t of ore (BARTÓK and NAGY 1992). This tonnage is at the upper end of the observed range of sizes for this type of deposit. The mean size of these deposits is 111,000 t, which is 43 times smaller than that of the Gyöngyösoroszi deposit. The assessment of an expected 5.08 deposits remaining to be discovered is associated with this mean, the distribution of which is shown in Fig. 12. Therefore, the assessment team's conclusion for ore grade material "at the mean" is equal to $5.08 \times 111,000 = 560,000$ t. This expectation is also a small fraction of the amount of ore produced from the Gyöngyösoroszi deposit.

In addition to an assessment for polymetallic vein deposits, the assessment team concluded that the probability of porphyry copper deposits remaining to be discovered in the Mátra Andesite is nontrivial. The general basis for

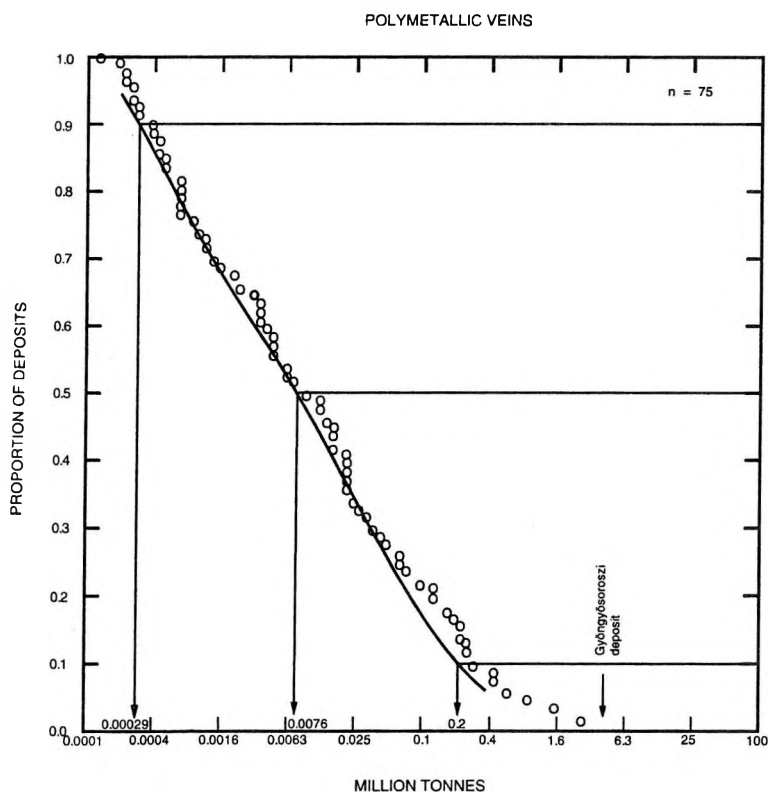


Fig. 12: Graph showing cumulative distribution for the size of polymetallic veins Modified from BLISS and COX (1986)

this determination was that although no porphyry copper deposits have been discovered, three silicified areas have been mapped, and polymetallic vein deposits have been discovered. The observed silicification could be a manifestation of a porphyry copper system and (or) the occurrence of polymetallic vein deposits. After considering the field data and exploration history, the assessment team reached a consensus that no porphyry copper deposits occur in the Mátra Mountains at the 90 and 50 percent probability levels, that one would occur at the 10 percent level, and that two would occur at the 1 percent level. The expected number of undiscovered porphyry copper deposits was computed to be 0.38 deposit (ROOT et al. 1992).

Finally, because no limestone or dolomite beds are known in the basement of the Mátra Andesite, the assessment team assigned a zero probability for the occurrence of undiscovered lead-zinc skarn deposits.

5.3. Assessment of the Börzsöny and the Visegrád Mountains

The assessment for undiscovered deposits in the porphyry copper/polymetallic vein kin-deposit system and associated lead-zinc skarn deposits in the Börzsöny and the Visegrád Mountains was less favorable than that for the Mátra Mountains. The assessment team concluded that there is no chance for the occurrence of a porphyry copper deposit of the size and grade described in the grade and tonnage model (SINGER et al. 1986). The porphyry copper deposits that have been discovered and drilled (Fig. 10 and Fig. 11) proved to be very small and of low grade, little more than occurrences. After discussion of the field data, the team concluded that insufficient data exist to continue with this assessment; thus, no assessment for undiscovered porphyry copper deposits was reported. A primary determinant in this decision was that the necessary rock-alteration patterns associated with this deposit type are not present. No assessment is reported for lead-zinc skarn deposits because of the deep level of the only occurrence described to date.

As postulated by the assessment team, the lack of porphyry copper deposits is probably related to the structural history of the Börzsöny and the Visegrád Mountains. The pattern of faulting in the vicinity of the volcanoes is predominately extensional (Fig. 10), which is shown clearly in the north-northeast-to-south-southwest cross section constructed by KORPÁS and LANG (1993, Fig. 8). In the middle of this area of extension, a domal feature (north-south-trending antiform) with a crestal fault is shown on Fig. 10; this fault is also shown on a map in CSILLAGNÉ-TEPLÁNSZKY et al. (1983, Fig. 14). The porphyry copper and polymetallic vein mineralization is directly adjacent to and almost entirely to the west of this fault (Fig. 11). The porphyry copper mineralization is confined on the east by this crestal fault and is mapped as a steeply dipping jumble of five small and adjacent fault blocks, each with lengths and widths that range from about 100 to 200 meters (CSILLAGNÉ-TEPLÁNSZKY et al. 1983).

As a consequence of extensional fault mechanics in the Middle and Late Miocene, the Börzsöny and the Visegrád Mountains are not favorable for the occurrence of high-grade and high-tonnage mineralization because the fault system was open (that is, the difference between σ_1 and σ_3 was large) and fluid flow was not sufficiently focused to result in large tonnages of high grade ore. Within this zone of general extension, however, it is not uncommon to find local compression features, such as the central anticline. In such a region of compression, fluid flow is contained (focused), thus allowing for the conditions that result in ore formation. As shown in Fig. 11, the location of the strike-slip faults relative to the volcano, shallow intrusions, and mineralization are consistent with the notion that in an even smaller area (less than 1 km²) the stress field was equant (σ_1 equal to σ_3).

Although the assessment team concluded that no undiscovered porphyry copper and lead-zinc skarn deposits remain to be discovered in the Börzsöny and the Visegrád Mountains, it did reach a consensus that the region was permissive for polymetallic veins whose tonnages are described by the cumulative frequency distribution in Fig. 12. The range of opinion within the team was vast—one member was almost certain that the probability that these deposits occur is nearly zero, and another member was sure that as many as 10 such deposits occur in the volcanic complexes of these mountains.

The consensus was that there is a 90 percent probability of one polymetallic vein deposit occurring, a 50 percent probability of two occurring, a 10 percent probability of three occurring, and a 1 percent probability of four occurring. The mean of a distribution with these probabilities is two deposits (ROOT et al. 1992). Thus, the assessment team concluded that in the approximately 600 km² Börzsöny–Visegrád Mountains assessment area, the statistical expectation is that two polymetallic vein deposits remain to be discovered.

6. AGGREGATE RESOURCE ESTIMATES

The Mark3 simulation software (ROOT et al. 1992) was used to estimate the inventory of undiscovered mineral resources contained in porphyry copper and polymetallic veins deposits in the study area (Table 1). The num-

ber of these deposits expected to occur in the study area is shown in Table 2. The estimates of aggregate metal and ore tonnages were computed as probability distributions (Fig. 13 and Table 3). The three quantiles and the mean of each of these aggregate metal distributions are shown in Table 3. These distributions are bimodal for copper and ore tonnage because the probability masses for contained metal and ore tonnages in porphyry copper deposits are much larger than those for polymetallic vein deposits (Fig. 13). This bimodality is clearly shown by the leftward breaks in the cumulative distributions for copper and ore tonnage at about the 35 percent probability level, which is the estimated marginal probability for the occurrence of this type of deposit. This result is based on the assessment team's consensus estimate that there is only a 35 percent probability that a porphyry deposit remains to be discovered anywhere in the study area.

Mineral-deposit models considered in the assessment of the undiscovered mineral resources in the study area
(pct, percent; g/t grams per tonne)

Table 1

	Median tonnage	Median grades				
		Copper (pct)	Lead (pct)	Zinc (pct)	Gold (g/t)	Silver (g/t)
Polymetallic veins	7,600	–	9.0	2.1	0.13	820
Porphyry copper	99x10 ⁶	0.51	–	–	0.38	–
Zinc-lead skarns	1.4x10 ⁶	–	2.8	5.9	–	–

Summary of the expected number of undiscovered mineral deposits determined by the USGS/GIH assessment team in the study area

Table 2

Area	Porphyry copper	Polymetallic veins	Lead-zinc skarns
Mátra Mountains	0.38	5.08	–
Börzsöny and Visegrád Mountains	–	2.0	–

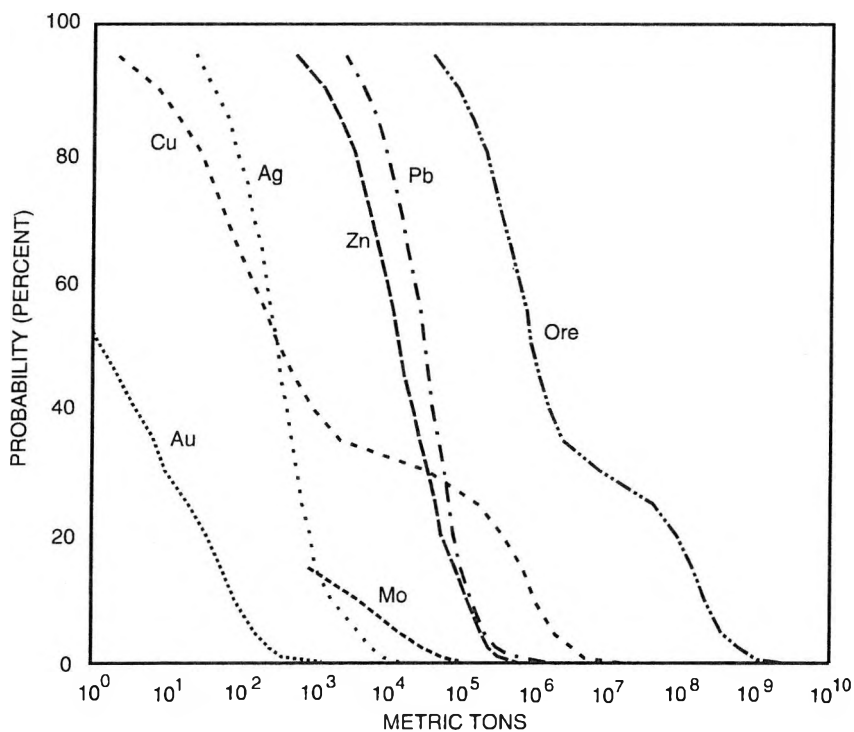


Fig. 13: Graph showing the cumulative distributions of the aggregate metal and ore tonnages contained in the undiscovered porphyry copper and polymetallic vein deposits in the study area.

Metal or ore	Tonnage			
	90 percent	50 percent	10 percent	Mean
Copper	7.4	310	1.0x10 ⁶	350,000
Silver	41	300	1,600	800
Zinc	1,300	13,000	110,000	39,000
Lead	4,400	30,000	130,000	58,000
Gold	0.024	1.1	83	28
Molybdenum	0.0	0.0	3,700	2,300
Ore material	85,000	890,000	2.1x10 ⁸	68x10 ⁶

Once such marginal probabilities for each type of deposit were considered, the Mark3 simulator produced the following summations for the mean undiscovered tonnages listed in the fifth column of Table 3. The mean tonnage of ore material from both deposit types is estimated to be 68 million t. The individual mean-aggregate metal tonnages are estimated to be 350,000 t of copper, 800 t of silver, 39,000 t of zinc, 58,000 t of lead, 28 t of gold, and 2,300 t of molybdenum. The table also lists the companion tonnages for each metal at three probability levels in the aggregate metal distributions shown in Fig. 13.

7. CONCLUSIONS

The methods developed at the USGS during the past 25 years for mineral-resource assessment were successfully transferred by performing an assessment on a study area in Mátra and the Börzsöny–Visegrád Mountains, North Hungary, from 1994 to 1997. A wide variety of field evidence, which included descriptions of the known deposits, geologic maps, geophysical information, inspections of drill core, and data from the literature, were used in the assessment of the undiscovered resources of the study area. The tectonic history of the Mátra and the Börzsöny–Visegrád Mountains was a principal determinate in constructing a geologic framework for the assessment. The volcanic mountains are situated in extensional duplexes associated with northwest- to southeast-trending master strike-slip faults. The assessment team determined that these areas are permissive for the occurrence of deposits that belong to the porphyry copper/polymetallic vein kin-deposit system. The broadly extensional tectonics that prevailed during the Middle Miocene, however, did not create many sites where conditions were favorable for the formation of economic mineral deposits. Therefore, the resulting assessment of the undiscovered metallic resources in the study area, although not insignificant, was low.

8. REFERENCES

- BAKSA, Cs. 1984: A recski ércesedés genetikai vázlata. (Genetic aspects of the Recsk mineralized complex). — *Földtani Közlöny* 114: 335–348. (In Hungarian with English abstract).
- BARTÓK, A.–NAGY, I. 1992: Magyarország érchordozó ásványi nyersanyagai, színes és feketefémérc vagyona. (Ore deposits of Hungary. Reserves of polymetallic and iron–manganese ores). — *Központi Földtani Hivatal, Budapest*: 70 p. (in Hungarian).
- BERBELEAC, I.–ILIESCU, D.–ANDREI, J.–CIUCULESCU, O.–CIUCULESCU, R. 1995a: Relationships between alterations, porphyry copper–gold and base metal–gold hydrothermal vein mineralizations in tertiary intrusions, Talagiu area, Zarland Mountains, Romania. — *Journal of Mineral Deposits*, 76: 31–39.
- BERBELEAC, I.–POPA, T.–MARIAN, I.–ILIESCU, D.–COSTEA, CR. 1995b: Neogene porphyry copper–gold, gold, and gold bearing epithermal deposits in the South Apuseni Mountains, Romania, 1995. — 15th Congress of the Carpathian–Balcan Geological Association, Proceedings: 665–670.
- BLISS, J. D.–COX, D. P. 1986: Grade and tonnage model for polymetallic veins. — *in* COX, D. P.–SINGER, D. A. (eds.): *Mineral deposit models: US Geological Survey Bulletin* 1693: 125–129.

- BORCOS, M. 1994: Volcanicity/metallogeny in the south Apuseni Mts (Metalliferi Mts). — *in* BORCOS, M.–VLAD, S. (eds.): Plate tectonics and metallogeny in the east Carpathians and Apuseni Mts. June 7–19, 1994, Field trip guide: Geological Institute of Romania, IGCP Project No. 356: 32–38.
- BORCOS, M.–GHEORGHITA, I.–BOSTINESCU, S.–MATIES, P. 1962: Consideratii asupra unor manifestari magmatice Neogene cu caracter linear in Muntii Metaliferi si sasupra structurii aparatului vulvanic Hanes. — *Dari de Seama ale Sedintelor*, 99: 19–30.
- COX, D. P. 1986: Descriptive model for porphyry Cu. — *in* COX D. P.–SINGER D. A. (eds.): Mineral deposit models: U.S. Geological Survey Bulletin 1693: 76. p.
- COX, D. P.–SINGER, D. A. eds. 1986: Mineral deposits models. — US Geological Survey Bulletin 1693: 379 p.
- CSILLAGNÉ–TEPLÁNSZKY, E.–CSONGRÁDI, J.–KORPÁS, L.–PENTELENYI, L.–VETÖNÉ–ÁKOS, É. 1983: A Börzsöny hegység központi területének földtani felépítése és ércesedése. (Geology and mineralization of the central area in the Börzsöny Mountains). — *A Magyar Állami Földtani Intézet Évi Jelentése 1981*: 125–153. (In Hungarian with English abstract).
- CSILLAGNÉ–TEPLÁNSZKY, E.–KORPÁS, L. 1982: Magyarázó a Börzsöny–Dunazug hegység földtani térképeihez. (Explanations to the geological maps of the Börzsöny Dunazug Mountains). — *Magyar Geológiai Szolgálat Országos Földtani és Geofizikai Adattára, Kézirat* (Unpublished report in Hungarian).
- CSONTOS, L.–NAGYMAROSY, A.–HORVÁTH, F.–KOVAC, M. 1992: Tertiary evolution of the Intra–Carpathian area. A model. — *Tectonophysics*, 208: 221–241.
- CSONTOS, L.–TARI, G.–BERGERAT, F.–FODOR, L. 1991: Evolution of the stress fields in the Carpatho–Pannonian area during the Neogene. — *Tectonophysics*, 199: 73–91.
- FODOR, L. 1995: From transpression to transtension. Oligocene–Miocene structural evolution of the Vienna basin and the East Alpine–Western Carpathian junction. — *Tectonophysics*, 242: 151–182.
- HARDING, T. P.–LOWELL, J. D. 1979: Structural styles, their plate–tectonic habitats, and hydrocarbon traps in petroleum provinces. — *American Association of Petroleum Geologists Bulletin*, 63. (7): 1016–1058.
- KARÁTSÓN, D. 1995: Ignimbrite formation, resurgent doming and dome collapse activity in the Miocene Borzsony Mountains, North Hungary. — *in* DOWNES, H.–VASELLI, D. (eds.): Neogene and related magmatism in the Carpatho–Pannonian Region. *Acta Vulcanologica*, 7(2): 107–117.
- KÁZMÉR, M.–KOVÁCS, S. 1985: Permian Palaeogene palaeogeography along the eastern part of the Insubric–Periadriatic lineament system. Evidence for continental escape of the Bakony–Drauzug unit. — *Acta Geologica Hungarica*, 28: 71–84.
- KISS, J.–SÍKHEGYI, F.–VETŐ–ÁKOS, É.–ZELENKA, T. 1996: Structure, alpine metallogeny and tectonics in the south–eastern Mátra Mountains, North–East Hungary. — *Proceedings of the Annual Meeting of the Plate Tectonic Aspects of the Alpine Metallogeny in the Carpatho–Balkan Region, 1996, Sofia 2*: 145–155.
- KORPÁS, L.–LANG, B. 1993: Timing of volcanism and metallogenesis in the Börzsöny Mountains, Northern Hungary. — *Ore Geology Reviews*, 8: 477–501.
- KORPÁS, L.–CSILLAGNÉ–TEPLÁNSZKY, E.–HÁMOR, G.–ÓDOR, L.–HORVÁTH, I.–FÜGEDI, U.–HARANGI, SZ. 1998: Magyarázó a Börzsöny és a Visegrádi-hegység földtani térképéhez. M=1:50 000 (Explanations to the geological map of the Börzsöny and Visegrád Mountains. Scale 1:50 000. — *Magyar Állami Földtani Intézet, Budapest*: 216 p. (In Hungarian with English abstract).
- LOWELL, J. D. 1972: Spitsbergen Tertiary Orogenic Belt and the Spitsbergen fracture zone. — *Geological Society of America Bulletin*, 83: 3091–3102.
- MÁRTON, E.–FODOR, L. 1995: Combination of paleomagnetic and stress data. A case study from North Hungary. — *Tectonophysics*, 242: 99–114.
- MITCHELL, A. H. G. 1996: Distribution and genesis of some epizonal Zn–Pb and Au provinces in the Carpathian–Balkan region. — *Transaction of the Institution of Mining and Metallurgy, Section B, Applied Earth Science*, 105: 127–138.
- NORTON, D. L. 1982: Fluid and heat transport phenomena typical of copper–bearing pluton environments — *in* TITLEY, S. R. ed.: *Advances in the geology of the porphyry copper deposits, Southwestern North America: Tucson, University of Arizona Press*: 59–72.
- ÓDOR, L.–HORVÁTH, I.–FÜGEDI, U. 1997: Észak–Magyarország nemesfém perspektívái a patakfordalékok geokémiai felvétele alapján. (Precious metal perspectives of northern Hungary based on stream sediment surveys). — *Földtani Kutatás*, 34: 9–12.
- PERESSON, H.–DECKER, K. 1997: Far–field effects of Late Miocene subduction in the Eastern Carpathians – E–W compression and inversion of structures in the Alpine–Carpathian–Pannonian region. — *Tectonics*, 16(1): 38–56.

- PÉCSKAY, Z.–LEXA, J.–SZAKÁCS, A.–BALOGH, KAD.–SEGHEDI, I.–KONECNY, V.–KOVÁCS, M.–MÁRTON, E.–KALICIAK, M.–SZÉKY–FUX, V.–PÓKA, T.–GYARMATI, P.–EDELSTEIN, O.–ROSU, E.–ZEV, B. 1995: Space and time distribution of Neogene–Quaternary volcanism in the Carpatho–Pannonian Region. — *in* DOWNES, H.–VASELLI, D. (eds.): Neogene and related magmatism in the Carpatho–Balcanian Region. *Acta Vulcanologica*, 7(2): 15–28.
- PÓKA, T. 1988: Neogene and Quaternary volcanism of the Carpathian–Pannonian region. Changes in chemical composition and its relationship to basin formation. — *in* ROYDEN, L. H.–HORVÁTH, F. (eds.): *The Pannonian Basin. – A study of basin evolution: American Association of Petroleum Geologists Memoir 45: 257–277.*
- ROOT, D. H.–MENZIE, W. D.–SCOTT, W. A. JR. 1992: Computer Monte Carlo simulation in quantitative resource estimation. — *Nonrenewable Resources*, 1(2): 125–138.
- ROYDEN, L. H.–HORVÁTH, F.–BURCHFIEL, B. C. 1982: Transform faulting, extension, and subduction in the Carpathian Pannonian region. — *Geological Society of America Bulletin*, 93: 717–725.
- ROYDEN, L. H.–HORVÁTH, F.–RUMPLER, J. 1983: Evolution of the Pannonian Basin system. — *Tectonics*, 2(1): 63–90.
- RUMPLER, J.–HORVÁTH, F. 1988: Some representative seismic reflection lines for the Pannonian basin and their structural interpretation. — *in* ROYDEN, L. H.–HORVÁTH, F. (eds.): *The Pannonian Basin. – A study of basin evolution: American Association of Petroleum Geologists Memoir 45: 153–170.*
- SANDULESCU, M. 1988: Cenozoic tectonic history of the Carpathians. — *in* ROYDEN, L. H.–HORVÁTH, F. (eds.): *The Pannonian Basin. – A study of basin evolution: American Association of Petroleum Geologists Memoir 45: 17–26.*
- SAWKINS, F. J. 1990: *Metal deposits in relation to plate tectonics.* — Berlin, Springer–Verlag: 461 p.
- SEGALL, P.–POLLARD, D. D. 1980: Mechanics of discontinuous faults. — *Journal of Geophysical Research*, 86. B8: 4337–4350.
- SIBSON, R. H. 1986: Earthquakes and lineament infrastructure. — *Transactions of the Royal Philosophical Society of London A–317: 63–79.*
- SINGER, D. A. 1993: Basic concepts in three–part quantitative assessments of undiscovered mineral resources. — *Nonrenewable Resources*, 2. (2): 69–81.
- SINGER, D. A.–MOSIER, D. L.–COX, D. P. 1986: Grade and tonnage model for porphyry Cu. — *in* COX, D. P.–SINGER, D. A. (eds.): *Mineral deposit models: U.S. Geological Survey Bulletin 1693: 77–81.*
- SONDER, L. J.–ENGLAND, P. C. 1989: Effects of temperature–dependent rheology on large–scale continental extension. — *Journal of Geophysical Research*, 94. B6: 7603–7619.
- SYLVESTER, A. G. 1988: Strike–slip faults. — *Geological Society of America Bulletin*, 100: 1666–1703.
- SZABÓ, CS.–HARANGI, SZ.–CSONTOS, L. 1992: Review of Neogene and Quaternary volcanism of the Carpathian–Pannonian region. — *Tectonophysics*, 208: 243–256.
- TARI, G.–HORVÁTH, F.–RUMPLER, J. 1992: Styles of extension in the Pannonian Basin. — *Tectonophysics*, 208: 203–219.
- VARGA, GY.–CSILLAGNÉ–TEPLÁNSZKY, E.–FÉLEGYHÁZI, ZS. 1975: A Mátra hegység földtana. (Geology of the Mátra Mountains). — *Magyar Állami Földtani Intézet Évkönyve*, 57: 575 p. (In Hungarian with English abstract).
- VETŐ, É. 1988: Conditions of Pb–Zn ore formation in the Carpathian Neogene volcanic arc: Evidence from Gyöngyösoroszi mine, North–Hungary. — *Proceedings of the Seventh Quaderannel IAGOD Symposium*, E. Schweitzerbartische Verlagbuchhandlung: 245–252.
- WILLIS, G. F.–TOSDAL, R. M. 1992: Formation of gold veins and breccias during dextral strike–slip faulting in the Mesquite mining district, Southeastern California. — *Economic Geology*, 87: 2002–2022.
- WOODCOCK, N. H. 1986: The role of strike–slip faults systems at plate boundaries. — *Transactions of the Royal Philosophical Society of London A–317: 13–29.*

ENVIRONMENTAL MODELS OF MINERAL DEPOSITS A STATE OF THE ART

RICHARD B. WANTY, BYRON R. BERGER, and GEOFFREY S. PLUMLEE

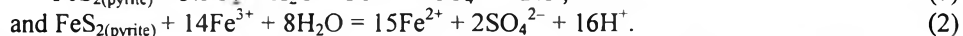
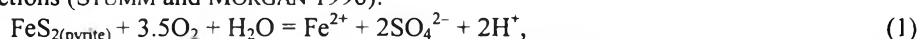
US Geological Survey, P. O. Box 25046 Denver, Colorado 80225, USA

ABSTRACT

Although mineral deposits have been classified by their geologic and mineralogical characteristics for decades, the recognition that mineral deposits also could be classified by their environmental characteristics is relatively new. In the past 5 years, numerous advancements have been made in this subject area, building on the earlier work of economic geologists who classified geologic characteristics. Several different approaches to understanding the environmental behavior of mineral deposits and associated altered areas have been taken, ranging from wholesale assessments of large areas (millions of km²) to detailed assessments of individual watersheds or individual mines. While these first attempts have succeeded in describing some of the environmental characteristics of ore deposits in a number of ways, many important “environmental variables” are not included in present descriptive models. For example, the models should be expanded in scope to include a more thorough treatment of climatic and ecoregional effects—embodying such physical environmental characteristics as precipitation, evaporation, temperature, and ground water-surface water interactions. More complete model descriptions will have applications to the determination of baselines and natural backgrounds in mined and unmined areas, as well as possible anticipated effects of new mining in a given area, and mitigation and remediation strategies. The challenge to geologists and geochemists is to incorporate a widely disparate set of physical and chemical characteristics of mineralized and altered zones at scales ranging from microscopic (sub-millimeter) to macroscopic (10’s to 100’s of kilometers). This paper presents an overview of the development of mineral deposit environmental models, the current state of the art, an evaluation of needed improvements, and expected advancements in this field.

1. WHAT IS THE PROBLEM?

It has long been recognized that weathering of sulfide minerals may have deleterious effects on the environment. This is particularly true for mineral deposits which, when exposed to the weathering environment, can produce acidic, sulfate-rich waters capable of transporting harmful concentrations of various heavy metals. The most important mineral in terms of acid generation is pyrite, which reacts with oxygen from the atmosphere according to the following overall reactions (STUMM and MORGAN 1996):



The latter reaction consumes dissolved ferric iron rather than oxygen, so to maintain the reaction, an adequate supply of ferric ions must be present in the system. Lacking a mineral source for Fe³⁺ such as oxidized biotites or chlorites, the ferrous product in reaction 2 must be reoxidized so that reaction 2 can continue to proceed. The oxidation of ferrous iron can be written as:



Adding reactions 2 and 3 produces reaction 1, so the net reaction of pyrite oxidation follows reaction 1 in either case. Similar reactions can be written for the oxidation of other sulfide-bearing minerals, but pyrite oxidation is generally the predominant acid-generating reaction because pyrite is usually the most common sulfide mineral in a mineralized zone. Other sulfides such as pyrrhotite, chalcopyrite, arsenopyrite, galena, and sphalerite also

may generate acid as they oxidize. Because of their generally lower abundance in a body of mineralized rock, the amount of protons produced by the oxidation of the other sulfide-bearing minerals is subordinate to that from pyrite oxidation. When pyrite is oxidized, the acidic waters generated, if not neutralized by reaction with other minerals such as carbonates, may lead to increased mobility of metals such as Fe, As, Cu, Zn, Cd, Cr, Pb, etc. These metals may be present as trace elements in the pyrite (esp. As), or they may be mobilized from other mineral sites.

Oxidation of pyrite and other sulfide-bearing minerals may take place any time these sulfides are exposed to oxygen in the presence of water, whether at the surface or in the shallow subsurface. The rates of the oxidation reactions are enhanced by the action of bacteria (GOULD et al. 1994), which in turn require a moist environment to facilitate their existence. The moisture becomes acidic as the oxidation reaction proceeds, leading to the phenomenon of acidic drainage. The basic requirements for rapid sulfide oxidation, then, are the presence of sulfide, a supply of water and oxygen or ferric iron, and bacteria and their required nutrients.

Acidic drainage may be generated as a natural process or it may result from mining activities. In nature, a deposit exposed at the surface will generate acidic drainage in some amount. The concentration of the acid (measured as pH) is enhanced by increased rates of oxidation, increased rates and amounts of exposure of sulfide-bearing minerals to air, increased bacterial activity (i.e., warmer temperatures, presence of organic material), and, to some extent, decreased water fluxes through the zone of oxidation. The latter is true because if a greater quantity of water flows through the oxidation zone, then the acid will be diluted. In systems with a smaller flux of water, stronger acid concentrations accumulate, resulting in pH's typically in the range of 2-4, but perhaps lower (FICKLIN et al. 1992, NORDSTROM et al. 1979, NORDSTROM 1982, NORDSTROM et al. 1991, PLUMLEE et al. 1992). The rate and amount of exposure of sulfide-bearing minerals to the air may be controlled by the relative rates of mechanical versus chemical weathering (MILLER and MCHUGH in press). Mechanical weathering (erosion) rates are greatest in areas with steep slopes, well-developed fracture networks, and intense freeze/thaw action. In areas where mechanical weathering rates are greatest, fresh sulfide minerals are continually brought to the surface and oxidized, this increased availability of sulfides leads to greater rates of acid production.

1.1. Enhancement of weathering rates by mining

Mining activities may enhance the rate and extent of sulfide oxidation through several mechanisms: fresh sulfide-bearing minerals are continuously brought to the surface and exposed to air; the rock is crushed and ground in the mining and milling processes, thus increasing the surface area of exposed sulfides; and the mine workings themselves may serve as conduits for flow of ground-water and air, thus enhancing the exposure of sulfides still in the ground to oxygenated water. Each of these three activities leads to a slightly different effect on the weathering process. The exposure of fresh (unoxidized) sulfide minerals to air results in an increased mass of sulfide available for oxidation. If left undisturbed in the ground, these sulfides might remain stable until natural processes of uplift or erosion brought them to the surface. Crushing and grinding of rock increases the available reactive surface area, and thus increases the rate at which the sulfides oxidize. For example, the surface area for a given mass of pyrite in the form of cubic crystals increases with the square of decreasing cube dimension, so that the smaller the average crystal size, the greater the surface area available for reaction with oxygen. Because the oxidation rate depends on exposed surface area, the rate increases with decreasing particle size. Lastly, mine workings themselves may become conduits for ground-water flow. Transmissivity of fractures is roughly proportional to the cube of fracture dilation, so more open fractures transmit exponentially greater volumes of water. In this context, mine workings represent almost infinitely transmissive features, especially when compared to the available water supply in most mines. By increasing the rates of ground-water flow, mine workings may increase the rate of delivery of oxygenated water to sulfide minerals still in the ground, thus increasing the rate at which those sulfides oxidize. Conversely, it is possible that the mine workings may speed up the flow rate of ground water to the point that the sulfide oxidation reaction is slow relative to the rate of ground-water flow and smaller masses of sulfides are oxidized. However, in most documented literature cases, the flow from mine tunnels is acidic and metal rich, indicating that the mine workings have the effect of increasing acidity and metal loads to surface-water supplies. Some mine tunnels are specifically designed to lower the local water table and thus to drain mine workings, such as the Reynolds tunnel at Summitville, Colorado, the Argo tunnel at Idaho Springs, Colorado, and numerous other locations. These drainage tunnels are usually driven at the lowest possible elevation to dewater large areas of mine workings. In addition to serving as effective drainage pathways, they speed the delivery of metal loads from the ground water to streams.

The pre-mining condition of the environment depends on the exposure of the deposit to air, as described above. If the deposit is exposed at the surface, the pre-mining condition may include surface waters with low pH and high concentrations of dissolved metals, unfit for most aquatic life other than microbes. Examples of such

conditions have been studied in a few places, such as the Red Dog zinc deposit in northwest Alaska (GRAY et al. 1996, KELLEY 1997), Bald Mountain in Maine (SEAL and WANDLESS 1997), Geneva Creek in central Colorado (BASSETT et al. 1992), and Bitter, Iron, and Alum Creeks near Summitville in southwestern Colorado (GRAY and COOLBAUGH 1994, GRAY et al. 1994, KING 1995, MILLER et al. in press), etc. It is perhaps a bit difficult to find such examples today, because many deposits exposed near the surface have already been mined, so it is difficult to establish the pre-mining condition. Useful analogs may be found by examining weakly mineralized altered areas in areas which are geologically and climatically similar to the areas of interest. Also, the proportion of deposits which are actually exposed at the surface may be small. Nevertheless, methods are being developed to estimate the pre-mining concentrations of metals; these will be described later in this paper.

1.2. Natural and manmade contamination of the environment

The quality of surface waters may be poor as a result of the oxidation of sulfide minerals. Numerous case studies (JAMBOR and BLOWES 1994, NELSON et al. 1997) have shown that the primary environmental concerns associated with mineralization, alteration, and mining are the acidity and dissolved or suspended metal loads, and the effect(s) of these additions on aquatic life or potential use of the water resource. Attenuation of the metal loads may occur as a result of dilution or mixing with water of better quality, reaction with country rock or bed material, adsorption or ion exchange, precipitation or coprecipitation, or some combination of these. In most cases, the dissolved metal loads are somehow transferred to the bed load or bed material, through precipitation and settling, or adsorption onto iron oxides that coat the streambed, etc. Thus, the processes that lead to degradation of water quality also may lead to degradation of sediment quality. Sediment quality also may be affected in mined areas by the direct transport of mine-waste material by surface runoff. In many cases, dumps from abandoned mines are in or near active drainages and the dump material may be transported downstream during high stream stages.

When material from a sulfide-bearing deposit is oxidized, the low pH waters that result effectively dissolve many heavy metals. These include: Fe, Mn, Al, Zn, Cu, Cr, Ni, Co, and many of the rare earth elements and actinides. In general, these metals are present in acidic solutions as hydrated cations or weakly hydrolyzed ions. As pH increases, these elements are more strongly hydrolyzed and may precipitate by themselves (esp. Fe, Al, and Mn) as oxyhydroxide solids, or may be adsorbed on the Fe, Al, and Mn oxyhydroxides which precipitate. Metals other than Fe, Al, and Mn are rarely concentrated enough to exceed solubility limits, so adsorption or ion exchange are the most potent attenuation processes for these other elements. Detailed discussions of the mobility of metals in acidic drainages is beyond the scope of this paper, but reviews can be found in JAMBOR (1994), LANGMUIR (1997), NELSON et al. (1997).

2. HOW HAVE WE TRIED TO SOLVE IT IN THE PAST?

2.1. Acid-base accounting

The protocol of acid-base accounting (ABA) was developed, in part, to predict the environmental consequences of developing a mineral deposit. The method is deceptively simple- by conducting a series of analyses of rock samples from a deposit, analyze for minerals which produce acid on weathering (mainly sulfides) and for those which consume acid (mainly carbonates such as calcite; (MORIN 1990). A number of assumptions are implicit in the method. All sulfides are assumed to behave the same as pyrite, effectively, the assumption is made that pyrite is the only sulfide mineral in the sample. Similarly, all acid-neutralizing minerals in the sample are assumed to be equivalent to CaCO_3 . The ABA method assumes that the total abundance of these minerals is available for reaction, and that no minerals are shielded from the solution either by other mineral grains or by mineral overgrowths. Because this is a total accounting technique, kinetics are ignored. The "static" nature of this test means that it ignores flow rates, water chemistry, and hydrology. Each of these (and other) assumptions limits the degree to which the ABA method describes reality. Therefore, the ABA method, though simple and relatively inexpensive, is severely limited in its application and interpretation. For more information on the ABA method and its limitations, the reader is referred to MORIN (1990) and MILLS (1997).

2.2. Geoenvironmental maps

Environmental impacts of natural mineralized areas and mined areas may be efficiently organized and portrayed within the framework of a Geographic Information System (GIS). In a GIS approach, different layers of in-

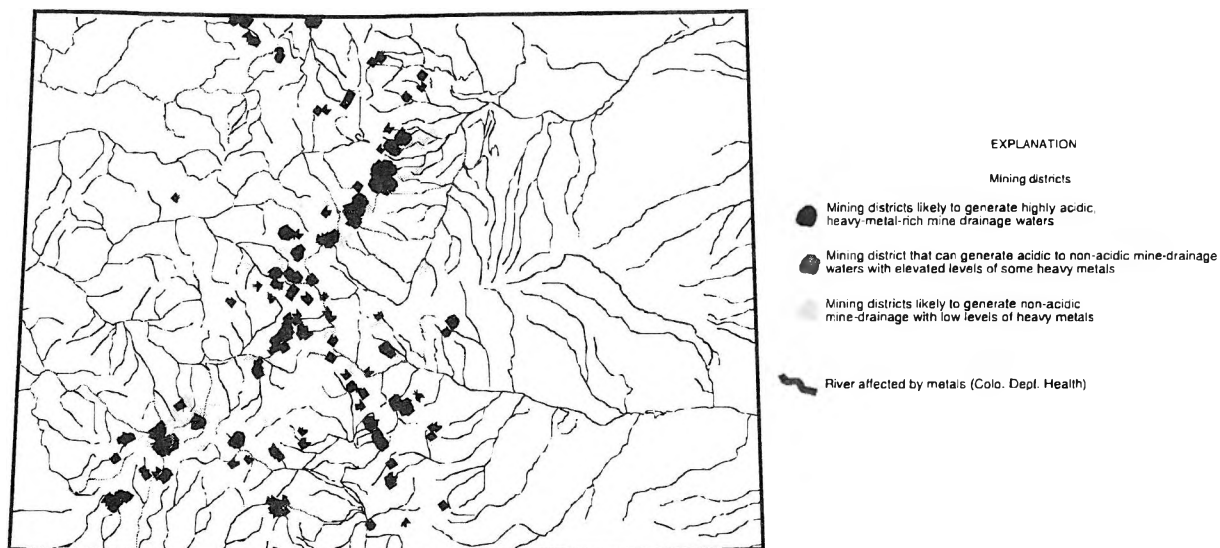


Fig. 1: Map showing potential metal-mine drainage hazards in Colorado, based on mineral-deposit geology (modified from PLUMLEE et al. 1995)

formation can be displayed on a map base, and criteria can be selected for highlighting the display of the data based on specific attributes of the data. Such an approach was taken by PLUMLEE et al. (1995) to evaluate the state of Colorado, USA, for mine-drainage hazard potential (Fig. 1). This geoenvironmental map was the first effort undertaken by USGS to portray a major mineralized region, the Colorado Mineral Belt, in the context of known or expected environmental conditions.

The Colorado map is an highly interpretive product with objective and subjective data layers. Objective data layers include: land ownership (important from the perspective of responsible management of government-owned land); major surface-water divides and drainages; precipitation (for those regions with $>50 \text{ cm a}^{-1}$); and locations of major mining districts. The subjective data layers on the map include: drainages which have degraded water quality due to mineralization or mining; and a color-coded portrayal of the major mining districts based on their presumed propensity to cause adverse environmental impacts. This latter ranking derives from an analysis of mineralogic and geochemical investigations of representative ore-deposit types and their known or expected environmental impacts.

The various ore-deposit types were ranked on the basis of the nature and extent of alteration, mineral assemblages, metals present in the assemblage, and the presence of acid-generating minerals like pyrite versus the remnant or natural acid-consuming capacity of the host rocks. In this ranking, deposits which are rich in pyrite and metals and poor in acid-consuming minerals are ranked as most likely to cause environmental problems, pyrite-poor deposits the least. In some ways, this analysis resembles that of the ABA method described above, so there is a need to improve the overall evaluation method. For example, mineral deposits with quartz-alunite and advanced argillic alteration were ranked as most likely to cause deleterious metal impacts because whatever natural acid-neutralizing capacity the host rocks may have had prior to mineralization was consumed by the intensely acidic mineralizing/altering fluids. Thus, during present-day weathering of such deposits, the acid which is generated by sulfide oxidation is not neutralized by reaction with the host rocks. Waters flowing downgradient from such deposits (either in the ground or on the surface) are likely to have extremely low pH (usually <3) and high metals concentrations (usually in the ppm range or greater for metals such as Cu, Zn, As, Cr, Ni, Pb, Co, U and Th). Examples of such deposits in Colorado include Summitville and Red Mountain near Lake City. European deposits in this ranking may include Lahóca, near Recsk, Hungary, and Talagiu, Romania. To effectively remediate the drainage waters from these deposits, the acid must be neutralized and metals removed from the drainage waters. In comparison, drainage waters in contact with carbonate-hosted deposits may be expected to have higher pH's, although concentrations of some metals, especially Zn with minor Pb, Cu, and As, may still be great enough to cause adverse impacts to aquatic life. For these deposits, the greatest remediation concern is to remove the metals dissolved in the water. Examples of this deposit type include parts of the Leadville district, Colorado, and Banska Stiavnica, Slovakia.

The geoenvironmental map of Colorado was an early attempt to classify deposits in a regional and geologic framework. As such, it has the advantage of showing a wide range of deposit types on a single map. This format offers the intuitive ease that comes from assimilating a relatively large amount of information into a spatial, color-coded display. There are also some drawbacks to this approach, which offers the possibility to improve the approach for various applications and end users. For example, the data layers are displayed, but are not queryable. Thus, interpretations can only be derived from the map upon intense inspection and reading of ancillary materials. Because the map is published on paper, it is difficult to add new layers of information, which the user may need in order to customize the map for their particular application. Depending on the specific interests of the end user, it may be desirable to add any of a number of additional data layers to suit a specific need.

The final issue to be raised concerning the Colorado map is that of scale. The map is published at a scale of 1:750,000. This scale is appropriate for the type and specificity of information displayed, and permits display of the map on a conveniently handled piece of paper, approximately 1 meter by 1.2 meter. It is inevitable, however, that the end-users of the map will direct their scrutiny to a specific part of the map and attempt to extract more information than can be reasonably accomplished. The printed map format guards against such abuse because the detailed information is not forthcoming. At the same time, although it leaves the end user with a general regional knowledge and perspective, the lack of specific information may be construed by some as a drawback. The ideal product may be one, which is available in a digital format with scale-appropriate layers of information. More discussion of scale issues will be found in the succeeding section of this paper.

2.3. Geoenvironmental models

Incorporation of environmental considerations into the mineral deposit models was first attempted by the US Geological Survey and summarized in a report by DU BRAY (1995). The format of this effort was designed to be an add-on to the mineral deposit model scheme developed by COX and SINGER (1986) and BLISS (1992). As such, it includes individually authored chapters for major mineral deposit types, cross-referenced to COX and SINGER (1986). Each chapter can be thought of as being an individual geoenvironmental model for the given deposit type. Within the format of this report, major headings exist for overview information for the deposit type, specific geologic and mineralogical factors which influence the environmental behavior of the deposit type, and environmental signatures. Each of these major headings may contain general information about the deposit type, and each may also contain specific information obtained from case studies.

In a published form, DU BRAY (1995) represents the state of the art of geoenvironmental modeling. In particular, the first chapter PLUMLEE and NASH (1995) presents a description of the philosophical approach used in the remainder of the volume and represents what may still be legitimately considered as the state of the art of geoenvironmental modeling. Perhaps the most important observation in PLUMLEE and NASH (1995) is the fact that the environmental effects of ore deposits and mineralized/altered areas extends beyond the boundaries of the alteration because of transport of elements by surface or ground water. Thus, although it would be desirable to develop geoenvironmental models in the same framework as resource models, it may not be practical because the two applications have a different focus and the sphere considered in the resource model is a subset of that considered for the geoenvironmental model. Still, there must be considerable overlap between the two model types because the mineral deposit is the primary source of environmental contaminants in most cases. The altered rock surrounding the mineralized core may be volumetrically important, but in many cases, the concentration of sulfide minerals in the rocks decreases radially outward from the mineralized core so that the altered rocks contain a lesser mass of sulfide than the ore deposit they surround.

Ongoing efforts at the USGS center mainly around refining geoenvironmental models for specific deposits. More work is needed to characterize deposit types in more detail, and to add additional deposit types. For example, placer gold deposits are mentioned only as a highly-eroded extension of low-sulfide Au-quartz vein deposits GOLDFARB et al. (1995). Little or no mention is made of certain deposit types, for example, Ni-laterites. In addition to adding to the environmental databases for specific deposit types, new research at USGS is being directed at watershed-based approaches which may include a number of ore deposits of various types.

While it is important to add to the existing databases, a broader unifying framework is needed within which new deposit environmental models can be developed, and which can be used to conduct environmental assessments of regions containing one or more deposit types. The remainder of this paper is devoted to descriptions of various existing methods by which environmental impacts can be anticipated, and to descriptions of other physical and chemical properties of mineral deposits and the environments in which they occur, which may contribute to the formulation of geoenvironmental models.

3. USES FOR GEOENVIRONMENTAL MODELS

Once a framework for geoenvironmental models is established, their potential uses and applications are numerous. They fall under two categories: as a framework for environmental or ecosystem classification; and as an evaluation tool for mineral deposits and altered areas and the expected environmental impact of these areas, whether mined or not. The framework for ecosystem classification may be established by observing that the rocks, soils and water in an ecosystem comprise the substrate for all biological activity. Thus, a detailed understanding of the geologic and hydrologic properties of an ecosystem is a logical first step towards understanding the ecosystem as a whole. As an evaluation tool for the environmental impacts of mineral deposits, geoenvironmental models should characterize the nature and extent of acid generation versus consumption, and mobilities of certain metals and other elements.

Geoenvironmental models have applications to the "life-cycle" treatment of mineral deposits. The life-cycle concept examines all aspects of a mineral deposit from the time of its formation through the post-mining reclamation. Because each step in the life cycle is fundamentally a geologic or hydrologic process, the geoenvironmental models should be able to address expected or known environmental issues associated with each step in the life cycle as well. As a subset of the life-cycle, the geoenvironmental models may be one component of a pre-mining economic analysis for an as yet undeveloped deposit.

Other issues specifically related to mining may be addressed by the geoenvironmental models. These include: determination of pre-mining background concentrations of acidity and metals in mined and unmined areas; anticipating the environmental impacts of new mining developments prior to mining; and resolving the relative contributions of different deposit types in a watershed to the overall loads of metals and acidity. These issues are of keen interest to regulatory authorities who must decide whether a mine has caused environmental impacts which exceed those caused by natural weathering and erosion processes. Therefore, in addition to qualitative descriptions of mineral deposits and altered areas, the geoenvironmental models should contain quantitative information which may relate to acid and metal loads in the environment.

4. NEW DIRECTIONS

Having developed the existing framework of environmental models and their uses, the remainder of this paper is devoted to describing some types of information that may be included in geoenvironmental models, as well as some proposed approaches to geoenvironmental modeling in a regional context. The data layers required and the approach taken to formulating the models must be sufficient to address the intended uses, and for the sake of completeness, the format in which the models are presented should be able to accommodate new data layers, which the end user may see fit to add. Depending on the application, these additional data layers may address climatic and biological effects, scale-dependent phenomena such as mineralogic and geologic variability, and other physical and chemical properties of mineralized rocks.

New research at USGS is aimed at developing a unifying framework for geoenvironmental models. At this writing, the concept which seems to offer the most promise is to describe the environmental characteristics of mineralized areas in the context of ecoregions. Ecoregions, broadly defined, are geographic divisions of land masses which are distinguished from one another on the basis of landform, climate, soils, vegetation, and other characteristics. BAILEY (1995) presents a thorough description of ecoregions for the United States, based on the original ecoregion concept proposed by KÖPPEN (1931). The same physical characteristics which cause a region to lie within a particular ecoregion also affect the environmental behavior of mineralized areas, and so may represent a useful scheme by which environmental impacts of mineralized areas can be classified. The ecoregion map for the conterminous US (excluding Hawaii and Alaska) is shown in Fig. 2. The domains shown on the map represent the broadest level of classification of ecoregions. On the original map BAILEY (1995), there are numerous divisions within each domain, based strongly on latitude and its attendant climatic effects. On Fig. 2, stippled regions represent generally warmer, wetter climates with well-developed soils and vegetation. Striped areas represent mountainous regions with climates, soils, and vegetation, which vary greatly with altitude. Areas with gray shading represent generally drier climates with less extensive soil development and decreased density of vegetation.

Undoubtedly there will be a dramatic difference in the environmental behavior of a mineralized area in one ecoregion from another. For all the factors mentioned above—temperature, moisture, biological productivity, etc.—there is an attendant effect on the rate and extent of sulfide weathering which in turn dictates the environmental signature of a mineralized area. This concept is the basis for new research at USGS and several projects

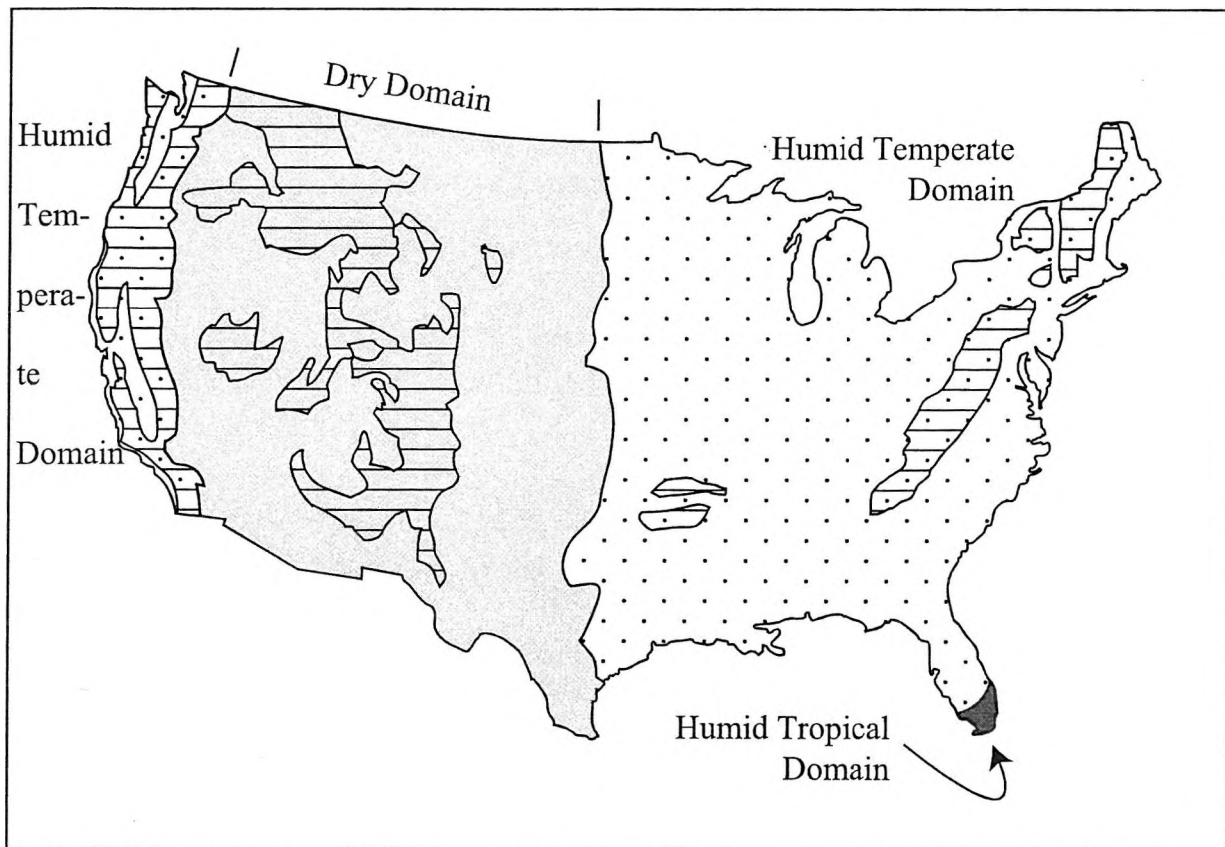


Fig. 2: Map of the conterminous United States showing major ecoregion domains (modified from BAILEY 1995)

are examining the comparative environmental signatures of geologically similar mineral deposits in different climatic or ecoregional settings. The results of this research should help refine many of the concepts discussed in this paper.

It is possible that the combined ecosystem/watershed approach to understanding water/rock interactions will have applications to other environmental problems, such as understanding regional geochemistry and baselines, evaluating ecosystem conditions within regions subject to dramatic fluxes of human population or to changing climate, etc. Full discussion of these topics is beyond the scope of this paper, but more information can be obtained in HUGGETT (1995), BAILEY (1998), and SHUGART (1998)

5. HOW ARE THESE MODELS GENERATED?

Given the rather broad scope of geoenvironmental models, some fundamental questions remain:

- What types of data should be gathered in field investigations?
- How will the models be constructed?
- Who are the primary end users of these models, and what data layers are most critical for their uses?
- How will the models be presented or published; on paper, electronic media, etc.?

These four questions lead to a fundamental question which geoscientists must now answer, namely: How should a research program be designed to gather all the data and interpretations necessary to construct a geoenvironmental model? At this writing, the question remains unanswered, largely because the market of end users has not been developed. Therefore, an evolutionary period has now begun within which geoenvironmental models will continue to change as new uses and applications are discovered by land-use managers and planners, environ-

mental regulators, the public, etc. In this volume, ÓDOR et al. (1999) present a geoenvironmental assessment for northeastern Hungary which is based on a regional sampling of sediments in floodplain and overbank deposits. These samples were collected from near-surface (0-10 cm depth) and deeper (50-60 cm depth) horizons, and are thought to represent the present and the pre-anthropogenic conditions. Based on statistical analyses of the sediment chemistry, anomalies are plotted as ranked scores on a base map of the area under investigation. This relatively new approach demonstrates the potentially widespread environmental effects associated with mineralized or mined areas. It has the advantage of showing a relatively small region (tens of thousands of square kilometers) in great detail through a rigorous sampling program. Because of the great sample density, it is possible to resolve the environmental signatures of individual mines or districts on the maps presented by ÓDOR et al. (1999). On the other hand, many of the long-range framework items discussed in this report (ecoregion, climate, etc.) cannot be addressed by ÓDOR et al. (1999) because the area they studied does not have great climatic or ecoregion variability. Thus scale dependence is seen once again as an fundamental parameter in geoenvironmental models.

6. CONCLUSIONS

Development of geoenvironmental models represents a new direction in the environmental geosciences as it incorporates regional syntheses of climatic and ecological variables with a geologic and geochemical framework to describe environmental signatures associated with mineralized and altered areas. Uses of geoenvironmental models include land-use management and planning, and environmental regulation. Properly and completely constructed, these models should aid land-management decisions such as whether a region would be expected to be severely impacted by new mine development, whether observed high metal loads in an area can be attributed to natural or anthropogenic processes, and the regional environmental impact attributable to mineralization, alteration, or mining. The art of the geoenvironmental model is relatively young and a great degree of evolutionary development is to be expected. The forces driving and guiding this evolution include technological developments and end-user applications. The former will control the amount of information which can be reasonably presented in a single package and the mode of presentation; the latter will control the content of the models. As the end-user market is more fully developed, the desired or required content will likely change, and it is expected that geoenvironmental models will not follow a standard template. That is, depending on specific local or regional issues, the various data layers which may be incorporated into the geoenvironmental models are expected to change in priority.

7. REFERENCES

- BAILEY, R. G. 1995: Descriptions of Ecoregions of the United States. — U.S. Forest Service Miscellaneous Publication 1391: Washington, D.C., U.S. Government Printing Office: 108 p.
- BAILEY, R. G. 1998: Ecoregions: The Ecosystem Geography of the Oceans and Continents. — New York, Springer, 176 p.
- BASSETT, R. L.—MILLER, W. R.—MCHUGH, J. B.—CATTS, J. G. 1992: Simulation of natural acid sulfate weathering in an alpine watershed. — *Water Resources Research*, v. 28, no. 9: 2197–2209.
- BLISS, J. D. 1992: Developments in Mineral Deposit Modeling. — US Geological Survey Bulletin 2004: Washington, D.C., U.S. Government Printing Office: 168 p.
- COX, D. P.—SINGER, D. A. 1986: Mineral deposit models. — US Geological Survey Bulletin 1693: Washington, D.C., U.S. Government Printing Office: 379 p.
- DU BRAY, E. A. 1995: Preliminary compilation of descriptive geoenvironmental mineral deposit models. — US Geological Survey Open-File Report 95-831: Washington, D.C., US Government Printing Office: 272 p.
- FICKLIN, W. H.—PLUMLEE, G. S.—SMITH, K. S.—MCHUGH, J. B. 1992: Geochemical classification of mine drainages and natural drainages in mineralized areas. — *in* KHARAKA, Y. K.—MAEST, A. S. (eds.): *Water-Rock Interaction: Water-Rock Interaction. Proceedings of the Seventh International Symposium on Water-Rock Interaction*: Rotterdam, A.A. Balkema: 381–384.
- GOLDFARB, R. J.—BERGER, B. R.—KLEIN, T. L.—PICKTHORN, W. J.—KLEIN, D. P. 1995: Low sulfide Au quartz veins. — *in* DU BRAY E. A. (ed.): *Preliminary compilation of descriptive geoenvironmental mineral deposit models*: Denver, Colorado, US Government Printing Office: 261–267.
- GOULD, W. D.—BÉCHARD, G.—LORTIE, L. 1994: The nature and role of microorganisms in the tailings environment. — *in* JAMBOR, J. L.—BLOWES, D. W. (eds.): *Mineralogical Association of Canada: Short Course Hand-*

- book on Environmental Geochemistry of Sulfide Mine Wastes: Nepean, Ontario, Mineralogical Association of Canada: 185–199.
- GRAY, J. E.–COOLBAUGH, M. F. 1994: Geology and geochemistry of Summitville, Colorado: an epithermal acid sulfate deposit in a volcanic dome. — *Econ Geol Bull Soc Econ Geol*, 89(8): 1906–1923.
- GRAY, J. E.–COOLBAUGH, M. F.–PLUMLEE, G. S.–ATKINSON, W. W. 1994: Environmental geology of the Summitville Mine, Colorado.— *Econ Geol Bull Soc Econ Geol*, 89(8): 2006–2014.
- GRAY, J. E.–SANZOLONE, R. F.–BAILEY, E. A.–FOLGER, H. W.–GOLDFARB, R. J.–GOUGH, L. P.–KELLEY, K. D.–MUELLER, K. A.–NELSON, S. W.–OTTON, J. K.–PHILPOTTS, J. A.–SNYDER, C. E.–TAYLOR, C. D.–THEODORAKOS, P. M. 1996: Environmental studies of mineral deposits in Alaska. — *US Geological Survey Bulletin* 2156: 40. p.
- HUGGETT, R. J. 1995: *Geocology: An Evolutionary approach*. — New York, Routledge: 320 p.
- JAMBOR, J. L. 1994: Mineralogy of sulfide-rich tailings and their oxidation products. — *in* JAMBOR, J. L.–BLOWES, D. W. (eds.): *Mineralogical Association of Canada: Short Course Handbook on Environmental Geochemistry of Sulfide Mine Wastes: Nepean, Ontario, Mineralogical Association of Canada*: 59–102.
- JAMBOR, J. L.–BLOWES, D. W. eds. 1994: *Mineralogical Association of Canada Short Course Handbook on Environmental Geochemistry of Sulfide Mine Wastes: Nepean, Ontario*. — Mineralogical Association of Canada, v. 22: 438 p.
- KELLEY, K. D. 1997: Natural acid drainage associated with shale-hosted Ag-Pb-Zn massive sulfide deposits in the Brooks Range, Northern Alaska, USA. — *in* WANTY, R. B.–MARSH, S. P.–GOUGH, L. P. (eds.): *4th International Symposium on Environmental Geochemistry Proceedings: US Geological Survey Open-File Report OF97-496: Washington, D.C., US Government Printing Office*: 44. p.
- KING, T. V. V. ed. 1995: *Environmental considerations of active and abandoned mine lands: Lessons from Summitville, Colorado*. — *US Geological Survey Bulletin* 2220: Washington, D.C., U.S. Government Printing Office: 38 p.
- KÖPPEN, W. 1931: *Grundriss der Klimakunde*. — Berlin, Walter deGruyter Co.: 388 p.
- LANGMUIR, D. 1997: *Aqueous Environmental Geochemistry*. — Englewood Cliffs, NJ, Prentice Hall: 600 p.
- MILLER, W. R.–MCHUGH, J. B. in press: Calculations of geochemical baselines of stream waters in the vicinity of Summitville, Colorado, before historic underground mining and prior to open-pit mining. — *in* PLUMLEE, G. S.–LOGSDON, M. (eds.): *Reviews in Economic Geology: El Paso, Texas, Economic Geology Publishing Company*.
- MILLS, C. 1997: Acid-Base Accounting. — on the internet at: <http://www.enviromine.com/ard/acidbase/abadiscussion.htm>.
- MORIN, K. A. 1990: Problems and proposed solutions in predicting acid drainage with acid-base accounting, in *Geological Association of Canada, Mineralogical Association of Canada, Joint Meeting, Vancouver, B.C., Geological Association of Canada*: 91. p.
- NELSON, J. D.–CINCILLA, W. A.–FORD, R. C.–HINSHAW, L. L.–KEITH, D. C.–MEDLOCK, R. L.–MILLER, D. J.–MULLER, S. C.–SHACKELFORD, C. D.–VAN LIEW, W. P.–VAN ZYL, D. J. A. eds. 1997: *Tailings and Mine Waste '97*. — Rotterdam, A.A. Balkema: 788 p.
- NORDSTROM, D. K.–JENNE, E. A.–BALL, J. W. 1979: Redox equilibria of iron in acid mine waters. — *in* JENNE, E. A. ed.: *Chemical Modeling in Aqueous Systems: Washington, D.C., American Chemical Society*: 51–79.
- NORDSTROM, D. K. 1982: Aqueous pyrite oxidation and the consequent formation of secondary iron minerals. — *in* KITTRICK, J. A. ed.: *Acid Sulfate Weathering, Soil Science Society of America Special Publication* Number 10: 37–56.
- NORDSTROM, D. K.–ALPERS, C. N.–BALL, J. W. 1991: Measurement of negative pH values and high metal concentrations in extremely acidic mine waters from Iron Mountain, California. — *Geol. Soc. Am. Abs. Prog.*, 23 (5): p. A383.
- ÓDOR, L.–WANTY, R. B.–HORVÁTH, I.–FÜGEDI, U. 1999: Environmental signatures of mineral deposits and areas of regional hydrothermal alteration in Northeastern Hungary. — *Geologica Hungarica Series Geologica* 24: 107–129.
- PLUMLEE, G. S.–SMITH, K. S.–FICKLIN, W. H.–BRIGGS, P. H. 1992: Geological and geochemical controls on the composition of mine drainages and natural drainages in mineralized areas. — *in* KHARAKA, Y. K.–MAEST, A. S. (eds.): *Water-Rock Interaction: Water-Rock Interaction: Proceedings of the Seventh International Symposium on Water-Rock Interaction: Rotterdam, A.A. Balkema*: 419–422.
- PLUMLEE, G. S.–NASH, J. T. 1995a: Geoenvironmental models of mineral deposits. — *Fundamentals and applications*. — *in* DU BRAY, E. A. ed.: *Preliminary compilation of descriptive geoenvironmental mineral deposit models: US Geological Survey Open-File Report 95-831: Washington, D.C., US Government Printing Office*: 1-9.

- PLUMLEE, G. S.—STREUFERT, R. K.—SMITH, K. S.—SMITH, S. M.—WALLACE, A. R.—TOTH, M. I.—NASH, J. T.—ROBINSON, R.—FICKLIN, W. H.—LEE, G. K. 1995: Map showing potential metal-mine drainage hazards in Colorado, based on mineral-deposit geology.— US Geological Survey Open-File Report: 95-26.
- SEAL, R. R.—WANDLESS, G. A. 1997: Stable isotope characteristics of waters draining massive sulfide deposits in the eastern United States. — *in* WANTY, R. B.—MARSH, S. P.—GOUGH, L. P. (eds): 4th International Symposium on Environmental Geochemistry Proceedings: US Geological Survey Open-File Report OF97-496: Washington, D.C., US Government Printing Office: 82 p.
- SHUGART, H. H. 1998: Terrestrial Ecosystems in Changing Environments. — New York, Cambridge University Press: 537 p.
- STUMM, W.—MORGAN, J. J. 1996: Aquatic Chemistry, 3rd ed. (Third ed.). — New York, John Wiley and Sons: 1022 p.

ENVIRONMENTAL SIGNATURES OF MINERAL DEPOSITS AND AREAS OF REGIONAL HYDROTHERMAL ALTERATION IN NORTHEASTERN HUNGARY

LÁSZLÓ ÓDOR¹, RICHARD B. WANTY², ISTVÁN HORVÁTH¹, and UBUL FÜGEDI¹

¹Geological Institute of Hungary, H-1143 Budapest, Stefánia út 14., Hungary

²U.S. Geological Survey, P. O. Box 25046 Denver, CO 80225, USA

ABSTRACT

Mineral deposits of northeastern Hungary are classified according to the well-known models of COX and SINGER (1986). These deposits and prospects in three mountainous regions (Zemplén, Mátra and Börzsöny Mts.) are all associated with Miocene andesitic volcanism. These regions have been mined intermittently since the Middle Ages. Environmental effects of old and recent mining activities are investigated through an examination of the minor element compositions of flood-plain and stream sediment deposits. Geochemical signatures of ore deposits are used and compared to the element associations observed in reconnaissance stream-sediment surveys. Stream-sediment geochemical data are used to outline areas with elevated concentrations of potentially toxic elements derived from the ore deposits and associated hydrothermal alteration using additive geochemical indices. These indices are derived from a statistical analysis of regional geochemical data. The suites and concentrations of elements typical of the environmental signatures or surface features of the known deposits and mineralized regions was also determined. Geoenvironmental mineral deposit models also were used to evaluate possible environmental behavior of ore deposits in Hungary. The actual environmental effects of development of the studied mineral deposits can be used to infer the potential impact of development of mines in the future. The list of elements analysed during our geochemical survey was limited compared to the list of elements given by the models. Prediction of the possible future appearance of a few elements in the environment was done this way. One mining site with a polluted flood plain below a base metal deposit was investigated in detail and the main results are summarized.

1. INTRODUCTION

Among the objectives of Joint Fund Project No. 415 (“Deposit Modeling, Assessment of Mineral Resources, and Mining Induced Environmental Risks.”), the major aim was to exchange information on deposit types, methodology of mineral resources and environmental risk assessments between Hungarian and US scientists. Some results related to the 3rd component of this project (Mining Induced Environmental Risks) will be shown here.

Broad geological and geochemical investigations of ore deposits related to Miocene andesitic volcanism in north-eastern Hungary have been carried out in the last few decades. These studies permit comparisons to the Hungarian deposits so that the deposits can be classified in a developing scheme of geoenvironmental deposit modeling. These generalizations use geological information to anticipate possible environmental effects of development of new mines. With the accumulated knowledge of the geology and metallogeny of Hungary and through the use of geochemical data, potentially toxic element enrichments of natural and anthropogenic origin will be outlined.

Based mainly on US deposit modeling and assessment studies (COX and SINGER 1986, MCCAMMON et al. 1995, DREW 1997, BERGER et al. 1999) and new developments in environmental modeling (DU BRAY E. A. 1995, WANTY et al. 1999) a survey of mineral deposit types found in northern Hungary and related to Miocene volcanism can be conducted. The environmental signatures or behaviour of these mineral deposit types relate, in turn, to expected natural background and mining-related contributions in certain regions. The geology and geochemistry of these deposits (ÓDOR et al. 1992) can be interpreted in the context of the results of a low-density geochemical survey based on flood-plain sediments to characterise the actual regional natural background. In addition, surface

geochemical anomalies can be attributed to economic and non-economic mineralizations or to regional rock alteration processes. This paper describes the use of a conventional stream sediment survey to find possible geochemical anomalies indicating ore mineralization and intensive alteration processes; to delineate areas with elevated geochemical baselines, to give additional data to the assessment method, and to summarize the main environmental concerns related to geology, that is, to outline areas in which high background concentrations may be related to geologic factors. Using this approach, an attempt also can be made to resolve pre-mining baseline conditions from mining related drainage signatures.

2. GENERAL DEFINITIONS

“Geoenvironmental models” (DU BRAY 1995, PLUMLEE and NASH 1995, WANTY et al. 1999) have been developed to complement mineral deposit models (COX and SINGER 1986, BLISS 1992). For a given deposit type the geoenvironmental model is: “A compilation of geologic, geochemical, geophysical, hydrologic, and engineering information pertaining to the environmental behavior of geologically similar mineral deposits (a) prior to mining, and (b) resulting from mining, mineral processing, and smelting.” Starting from the ore-deposit models established for the deposits of the Mátra and Börzsöny Mountains (VETŐ-ÁKOS 1999) some aspects of these geoenvironmental models, especially those related to the “environmental signatures” of mineralizations, will be dealt with below. The term: “environmental signatures” (PLUMLEE and NASH 1995) is defined as: “the suites, concentrations, residences, and availabilities of chemical elements in soil, sediment, airborne particulates, and water at a site that result from the natural weathering of mineral deposits and from mining, mineral processing, and smelting.” These terms will be used here in a larger sense, as not only mineral deposits, but surface geochemical anomalies will be included in the study. For lack of the necessary data only certain aspects of the environmental signatures of these Hungarian deposits will be dealt with in detail.

3. METHODS AND AREA DESCRIPTION

Achievements in deposit modeling in Hungary will be considered, emphasising geoenvironmental aspects of the existing data. Former investigations will be re-evaluated and deposit types of COX and SINGER (1986) will be assigned to the deposits in Hungary. Geochemical data for this work will be provided by two surveys.

1. Low-density survey based on flood-plain deposits. This survey was carried out in 1991–1995 in Hungary. In regions with well-developed drainage systems 196 catchment basins of approx. 400 km² were delineated and flood-plain deposits were sampled at their outlets. The samples were taken from 0–10 cm and from 50–60 cm depths. The Geochemical Atlas of Hungary is in preparation and it will show the distribution of 25 elements in the two sampled layers. Maps for the deeper layer are thought to represent regional geochemical baseline values, prior to significant anthropogenic influence.

2. Conventional stream sediment survey with 1 sample/4 km² sampling density. Hidden ore mineralizations and potentially toxic enrichments of natural origin may be expected on hilly and mountainous areas in Hungary. The aims of the stream sediment survey were twofold: to prospect for precious metal deposits and to evaluate the environmental state of the surface. The analytical data is available for the Zemplén, Mátra and Börzsöny Mts. and it is possible now to evaluate the geochemical data of these three volcanic terranes. Aqua regia dissolution was applied and ICP-OES, ICP hydride and AAS techniques were used for the analysis. The elements (and components) analysed included: Mo, Cr, Zn, Pb, Co, Cd, Ni, Ba, Mn, Cu, Sr, Li, K₂O, Hg, As, Sb, Au and Ag.

Geological setting and location of known mineral deposits are shown by Fig. 1.

4. GEOCHEMICAL BACKGROUND BASED ON A LOW-DENSITY SURVEY

The geochemical database containing the results of the low-density survey (ÓDOR et al. 1996, 1997c) for the 196 catchment basins has been an important contribution to the establishment of guidance values for soils in Hungary. Using the database, safe concentration levels were established for As, Cd, Cr, Cu, Hg, Pb and Zn. This kind of survey has the advantage of providing regional surface background geochemical data for more than 20 elements and for the whole country. Because of regional geologic differences, the northern part of Hungary can be treated separately; baseline values and other parameters are given below for the northern part of Hungary (Table 1), based on 38 catchment basins in this region.

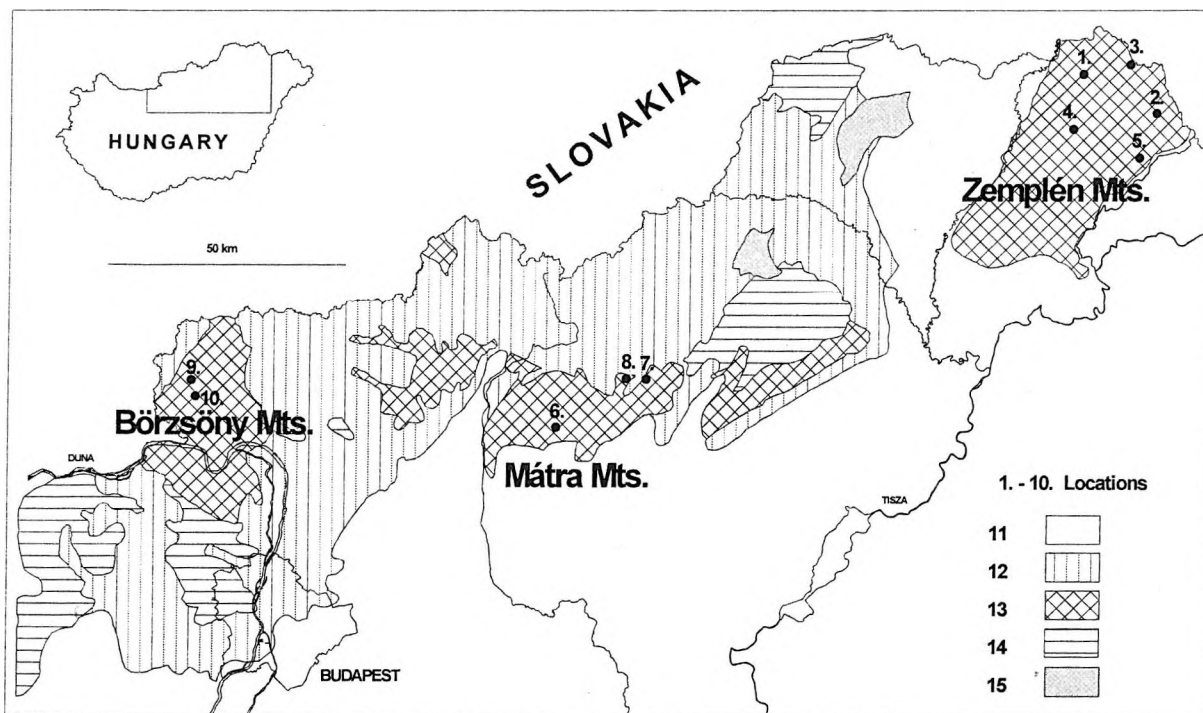


Fig. 1: Geological setting of the area

Location of mineral deposits and prospects: Zemplén Mountains: 1. Telkibánya, 2. Rudabányáscka, 3. Füzérradvány, 4. Regéc, 5. Sárospatak; Mátra Mountains: 6. Gyöngyösoroszi, 7. Lahóca, 8. Recsk; Börzsöny Mountains: 9. Nagybörzsöny, 10. Nagyirtáspuszta. Geology: 11. Holocene and Pleistocene sediments, 12. Miocene–Palaeogene sediments, 13. Tertiary volcanic rocks, 14. Mesozoic sedimentary rocks, 15. Paleozoic sedimentary rocks

Geochemical background values for northern Hungary based on flood-plain sediments (g/t, unless otherwise noted, N = 38)

Table 1

Element	Upper layer (0–10 cm)				Lower layer (50–60 cm)			
	Background			Anomalous values	Background			Anomalous values
	minimum	median	maximum		minimum	median	maximum	
As	< 2.5	7.3	27	58	< 2.5	5.5	18	140
Ba	39	107.5	209		39	111.5	184	
Cd	< 0.5	< 0.5	1.5	12.8; 4.0	< 0.5	< 0.5	1	6.8; 3.5
Cr	10	17.5	40	470	10	18.6	31	310; 47
Cu	11	15.8	31	400; 100; 66; 42	6.5	14.2	30	216; 52; 39
Hg (mg/t)	40	80	140	430; 340; 330; 230; 200; 200; 200	<20	80	260	400
Pb	10	17.3	28	80; 66; 49; 44	< 5	13.5	24	48; 47; 46
Zn	44	57.7	100	1260; 205; 190; 166	28	52.2	105	701; 176

The low-density survey has its limitations, but it helps to outline areas of possible surface contamination or anomalies (Based on the results of factor analysis, element associations have been distinguished: Ag-Au-Cd-Hg-Pb-(Cu-Zn) was found to be very characteristic, showing the elements of low to medium temperature hydrothermal ore processes. The samples collected from the flood-plains of the north-eastern rivers contain both traces of ore material coming from Slovakia and the pollution products of heavy industry from within the region.)

5. ENVIRONMENTAL SIGNATURES OF MINERAL DEPOSITS USING STREAM SEDIMENT SURVEYS FOR NORTHERN HUNGARY

Results are presented below for each region, from the Zemplén Mts. through the Mátra Mts. to the Börzsöny Mts. in order. Results of prospecting and mining activities carried out earlier and related to the characterization of deposits are our starting point. The next step is to use the established international and existing domestic models. A survey of the deposit models and their geochemical characterization will follow which correspond to the deposit types found in northeastern Hungary (Table 2).

Deposits will be surveyed on the basis of COX and SINGER (1986) and generalized geochemical features will be given. From the above approach the assignment of deposit types and classification numbers to our deposits in the three regions will result. Then the data of our stream sediment survey will be processed, element associations established and the results will be compared to those of the models. Finally delineation of additive geochemical anomalies based on the stream sediment survey and determination of the suites and concentrations of elements typical of the environmental signatures or surface features of these actual deposits and mineralized regions will be done. The actual and possible environmental effects of the studied mineral deposits, of potential future mines will also be given.

5.1. Zemplén Mountains

5.1.1. Polymetallic veins, hot-spring precious metal and Hg mineralizations

Geological setting, results of earlier investigations

The main volcanic sequences in the Zemplén Mountains are characterised by rhyodacite tuffs, welded rhyolite tuffs, redeposited rhyolite tuffs, rhyolites and pyroxene-hornblende dacites of Miocene age. Clayey and sandy shales appear in the lower part of the sequence, whereas pyroxene andesites cover extensive areas in the upper part.

A summary is given below of the main results of the geologic and geochemical investigations (VETŐ 1971, GYARMATI 1981, HARTIKAINEN et al. 1992, 1993, HORVÁTH et al. 1993, ÓDOR et al. 1997a,b). In the rhyolitic tuffs, quartzites and andesites, common ore minerals include pyrite, marcasite, native gold, native silver, chalcocopyrite, galena, sphalerite, antimonite, argentite, cinnabar and barite. At Telkibánya (ZELENKA 1997a,b), in addition to vein type mineralization, the ore is also found in brecciated silicified and argillised bodies. In this environment, the predominant ore minerals are: pyrite, sphalerite, galena, chalcocopyrite, argentite, tetrahedrite, pirargirite, native gold and antimonite. The characteristic gangue minerals are: chlorite, adularia, sericite, quartz, siderite, ankerite, dolomite, calcite, gypsum, alunite, illite, kaolinite and montmorillonite. Gold is associated with pyrite. The epithermal Au-Ag mineralization is related to alteration of the andesitic-rhyolitic succession of the Late Miocene, resulting in assemblages including quartz, alunite, kaolinite, montmorillonite, illite, adularia, carbonate propylitic types.

Deposit models

The models given by COX and SINGER (1986) and the studies of BERGER (1985), CSONGRÁDI and ZELENKA (1995), ZELENKA and CSONGRÁDI (1995), ZELENKA (1997b), MOLNÁR (1997) indicate that the polymetallic vein ("22c"), the hot-spring Au-Ag model ("25a") and the hot-spring Hg model ("27a") describe the ore mineralization processes taking place in the Zemplén Mountains (Table 2).

In ZELENKA and CSONGRÁDI (1995), a summary is given for three occurrences in the Zemplén Mts.: the Telkibánya vein type, the Mád epithermal and hot-spring type and the Füzérvány-Koromhegy hot-spring type Au-Ag mineralizations. The generalized model (COX and SINGER 1986) is characterized by the following mineralogy: native gold + pyrite + stibnite + realgar; or arsenopyrite ± sphalerite ± chalcocopyrite ± fluorite; or native gold + Ag-selenides or tellurides + pyrite. At deeper levels (more than 1 km below the present-day land surface) the sulfide minerals of Cu, Pb and Zn can also appear. The geochemical signature is given by the following elements:

Deposits and prospects in northeastern Hungary			Corresponding deposit models of COX and SINGER (1986)		Geochemical signatures derived from the deposit models
Locality	Category	Commodities resources	Descriptive deposit models	Model No.	
Zemplén Mountains					
Telkibánya (1)*, Rudabányáska (2)	Deposit	Au, Ag	Polymetallic veins	22c	Zn, Cu, Pb, As, Au, Ag, Mn, Ba
Füzérradvány,-Füzérkajata (3)	Deposit	Au, Ag	Hot-spring Au-Ag	25a	Au, As, Sb, Hg, (Tl) higher in system, increasing Ag with depth; locally (W)
Regéc (4), Sárospatak (5)	Prospect	Hg	Hot-spring Hg	27a	Hg, As, Sb±Au
Mátra Mountains					
Gyöngyösoroszi (6)	Deposit	Zn, Pb, Cu, Ag, Au	Polymetallic veins	22c	Zn, Cu, Pb, As, Au, Ag, Mn, Ba
Lahóca (Recsk) (7)	Deposit	Cu, Au, Ag	Volcanic-hosted Cu-As-Sb	22a	As, Sb, Cu, Zn, Ag, Au, (Sn, W)
Recsk (deep level) (8)	Deposit	Cu, Mo	Porphyry Cu	17	Cu+Mo+Au+Ag+(W)+(B)+Sr (center); Pb, Zn, Au, As, Co, Ba, (Se, Te, Rb) (outer zone), locally (Bi, Sn)
Recsk (deep level) (8)	Deposit	Cu, Zn	Cu skarn	18b	Cu+Au+Ag (inner zone), Pb-Zn-Ag (outer zone); no Co, As, Sb, (Bi) anomalies
Recsk (deep level) (8)	Deposit	Zn, Pb	Zn-Pb skarn	18c	Zn, Pb, Cu, Co, Au, Ag, As, Mn, (W, Sn, F), possibly (Be)
Börzsöny Mountains					
Nagybörzsöny (Kurucpatak, Bányapuszta, Rózsahegy) (9)	Prospect	Cu, Zn, Pb	Polymetallic veins	22c	Zn, Cu, Pb, As, Au, Ag, Mn, Ba
Nagyirtápuszta (10)	Prospect	Pb, Zn	Polymetallic replacement	19a	Cu, Pb, Ag, Zn, Mn; locally Au, As, Sb (Bi); high Ba in jasperoids

Remarks: (1)* = see localities on Fig. 1; Elements in parentheses were not analysed during the geochemical surveys.

higher in the system Au + As + Sb + Hg + Tl, increasing Ag and decreasing As + Sb + Tl + Hg with depth (BERGER 1985). The hot-spring Hg mineralization ("27a") is associated with these types of deposits. In the Zemplén Mts. this deposit type is represented by the presence of cinnabar, pyrite and marcasite and by the element association Hg + As + Sb + Au. All the hydrothermal systems of the Zemplén Mts. belong to the low sulfidation types (MOLNÁR 1997).

5.1.2. Stream sediment survey of the Zemplén Mountains

The survey was conducted between 1989 and 1991. At that time the majority of elements was determined by semiquantitative OES (Optical Emission Spectrometry). Only a few elements (Au, As, Sb and Hg) were analysed by quantitative AAS and ICP techniques. That is why this survey has its limitations in outlining characteristic suites of elements and establishing geochemical signatures of the ore mineralizations and alterations occurring in the Zemplén Mountains. On the other hand, four different geologic media were simultaneously sampled at that time (heavy mineral concentrate and fine fraction of stream sediment, composite soil and composite rock fragments) and their results helped to more reliably outline distribution patterns of elements.

The geochemical anomalies (Fig. 3) occurring in the Zemplén Mts. are characterized by Au, Ag, As, Sb and Hg (HARTIKAINEN et al. 1992). Anomalies and shows of Hg occur throughout the area (about 30 sites are known). Mercury is one of the elements giving the geochemical signature of one type of deposit (independent mercury mineralization) found in the Zemplén Mts. as shown by the fact that according to stream sediment data, gold has good and significant correlations only with As, Sb and Ag, but not with Hg. Elements having good correlations with each other are used to calculate additive anomalies. Anomaly scores are plotted to get a reliable distribution pattern.

A few words about the procedure follow. The underlying principle of the method lies in the observation that the frequency distributions of ore forming elements and their followers are never normal. From a background characterized by low concentrations of non correlating elements in certain areas, groups of elements can be found with high concentrations and good correlation. On the frequency distribution of elements enriched during ore forming processes there are distinct maxima. So certain concentration ranges can be attributed to certain frequency peaks and these peaks can be numbered. The boundaries of these ranges were chosen to be at frequency minima or at their apparent breaking places (Fig. 2; compare with data in Tables 3, 6 and 8). The additive index is then the sum of the numbers characterising given concentration ranges of different elements. Elements belonging to an association and having significant, positive correlation can only be used for the calculation of this index. It is not always the target element of a mineralization which has the highest score in this index, pathfinder elements like Ag and As are sometimes more useful to outline dispersion areas. In the Börzsöny Mts. +2 was added to the additive index of an element having more weight in the element association when its concentration was above the background range. This way it was possible to include those elements (Mn and Hg) with less weight into the additive index which were left out in the other two regions (Zemplén and Mátra Mts.), either because their role in the ore forming processes was insignificant (Mn) or because they also participated in the formation of other types of ores (Hg). There are of course many other ways to generate an additive index (different units can be used depending on the communality within the factor and in cases of element distributions close to lognormal geometric progressions can also be used).

In order to characterise the overall geochemical signatures, parameters of gold and its pathfinder elements are given in Table 3 for the fine fraction of stream sediments, together with how to calculate additive indices for the Zemplén Mts.

Figure 3 shows the distribution of additive indices and of anomalies for the four elements shown in Table 3. Favorability of a catchment area for mineralization will be evaluated on the basis of additive indices of elements. Spatial zonality of minor elements characterising these deposits (upper level and outside: Ba, Hg; below these: Sb, Au and Ag; then Pb and Zn; with downwardly increasing Cu) did not become visible here because of the scale of the survey.

5.1.3. Environmental considerations

It appears that sub-areas on Fig. 3 outline places of alterations and mineralizations with high concentrations of potentially toxic elements like As and Sb. Parts of these additive anomalies belong to known mineralizations (Telkibánya and Rudabányácska), giving evidence of the usefulness of our approach, while others suggest new targets for exploration around Füzérkajata–Füzérradvány and at the southern rim of the region (in the vicinity of Mád and Tállya. See Fig 3 for localities.). Füzérradvány can now be considered the site of possible future exploitation.

Environmental effects

On areas indicated by the anomaly maps, element associations characteristic for the deposit types can always be found. For As, Sb and Hg, the concentrations are much higher than guideline values for soil contaminants. These values are not due to pollution but to natural variation. They indicate that some local damage to certain species of plants or animals might be expected in limited areas with high toxic element content. In other areas, centuries old mining has left many dumps at the surface, especially at the upper courses of creeks in the Telkibánya region. These, in certain cases, have an influence on the geochemical signatures of the catchment basins, because the anomalies are not entirely generated by the natural outcrops of the ore mineralizations (see for example the anomalous area of cell No. 23 in Table 4).

On Fig.1 locations of mineral deposits and mining activities are shown for the Zemplén Mts. Drainage basins of the reconnaissance and stream sediment surveys including the area of these deposits were selected to show their possible environmental effects. Table 4 shows the data for several elements in the upper (0–10 cm) and lower (50–60 cm) sampling levels of these flood-plain sediments. Also shown in Table 4 are the relevant stream sediments' catchment areas lying within the larger flood-plain drainage basins and including sites of old mines.

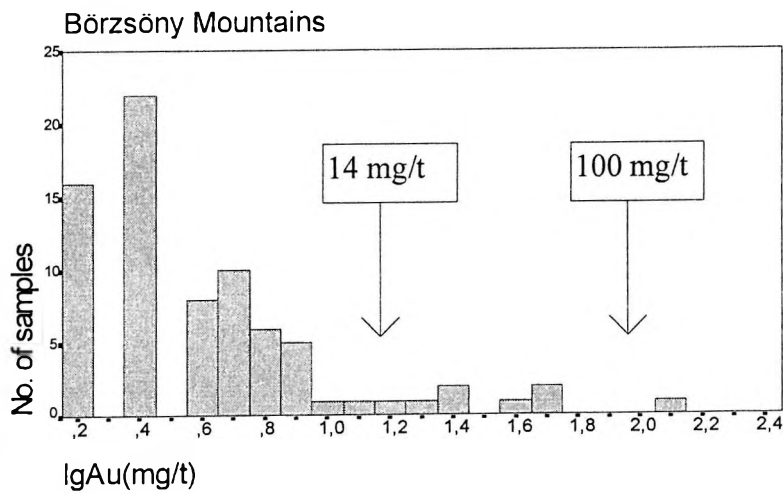
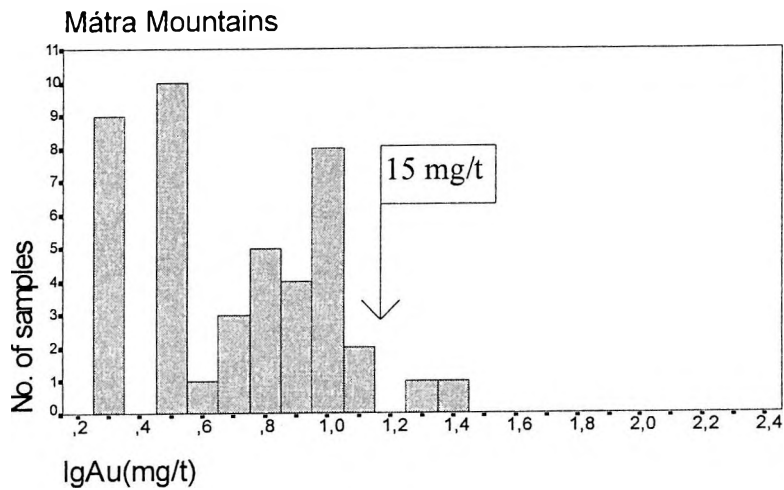
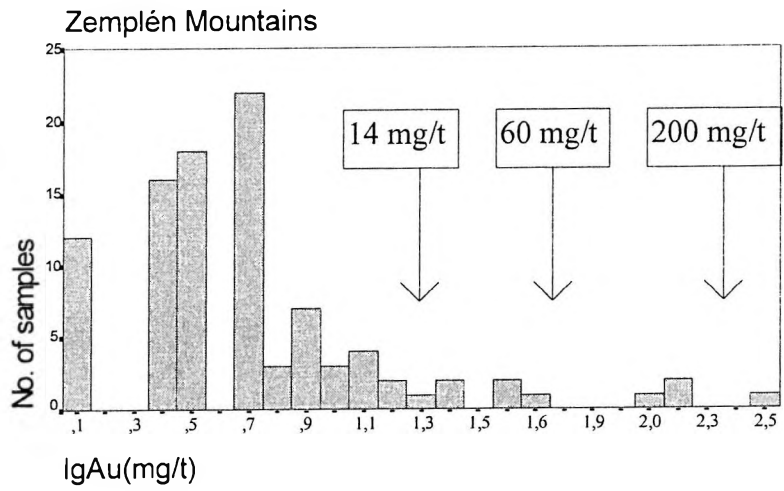


Fig. 2: Calculation of additive indices using frequency distributions of elements: Example of gold (See also Tables 3, 6 and 8 for concentration intervals and corresponding additive indices.)

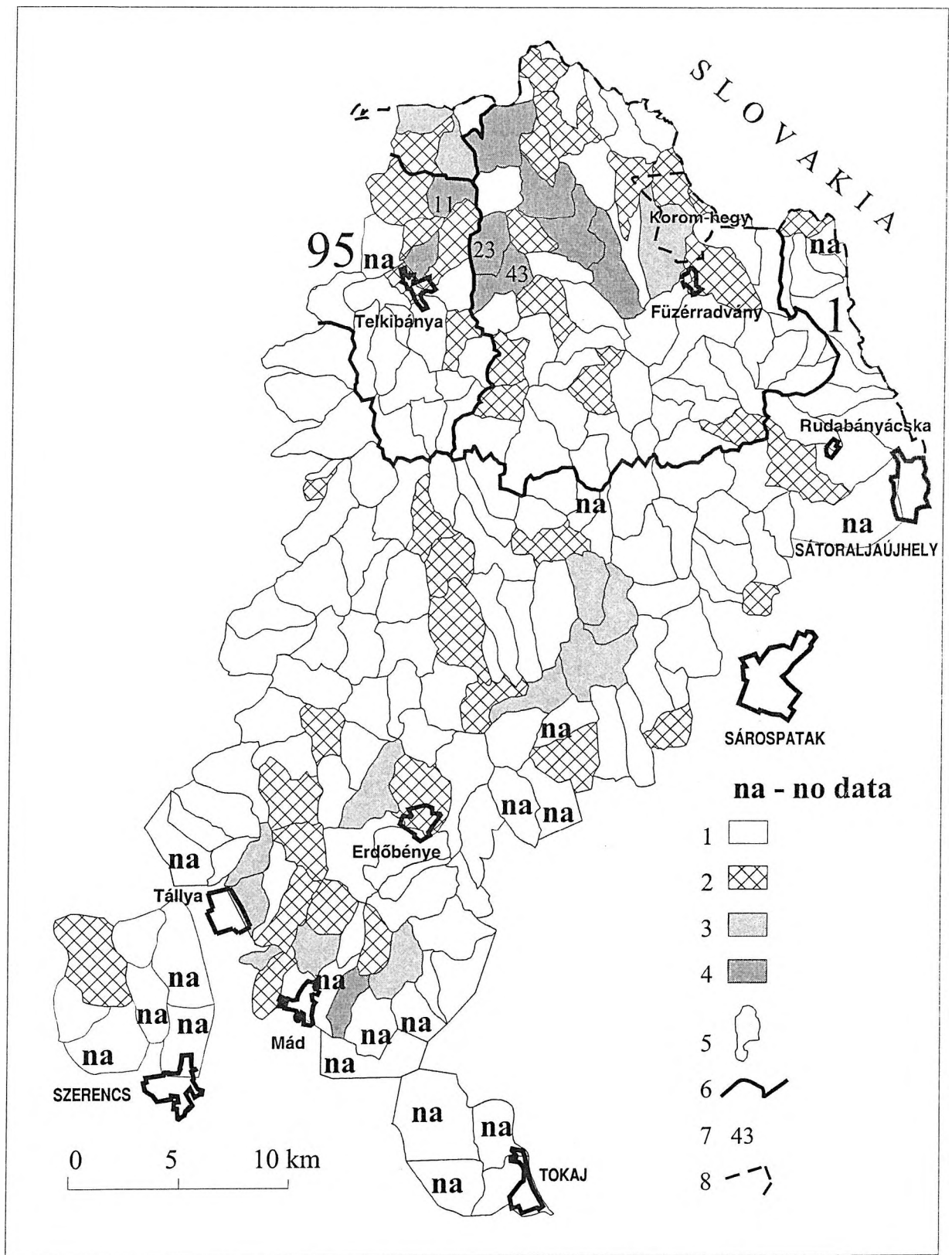


Fig. 3: Aggregated anomaly map of the Zemplén Mts. based on the stream sediment survey
 Values of the additive indices: 1: 0-1; 2: 2-3; 3: 4-5; 4: 6-14; 5: Sampled catchment areas; 6: Drainage basins (Nos. 1. and 95) of the low-density survey (floodplain sampling) comprising old mining sites; 7: Catchment areas of the stream sediment survey comprising old mining sites (No. of cells), 8: Location of the follow-up soil survey near Füzérradvány

Geochemical parameters of elements in the fine fraction of stream sediments.
Calculation of additive indices. Zemplén Mts.
 (g/t, unless otherwise noted, N=187)

Table 3

Element	Geochemical parameters				To calculate additive indices			
	Min.	Median	Threshold of anomaly	Max.	Index value +1	Index value +2	Index value +3	Index value +4
Au mg/t	< 1	1	50	257	10-13	15-45	100-160	257
Ag	< 0.4	< 0.4	15	46	0.4-8		46	
As	< 1	5	60	311	10-20	20-50	70-150	>280
Sb	< 1	< 1	12	22	1-7	8-10	14-15	18-22
Hg	<0.05	0.28	1.1	1.34	*			
Ba	160	1,000	-	1,600	*			
Cr	10	60	-	160	*			
Pb	< 6	40	-	250	*			
Zn	< 100	< 100	150	250	*			

Remark: * = elements not used for the calculation of additive anomalies.

Composition of the flood-plain deposits of large drainage basins
 (low density survey) and that of the stream sediments within them covering
 areas of known mineral deposits and mining sites in the Zemplén Mts. (g/t)

Table 4

Region	Zemplén Mountains, flood-plain deposits				Zemplén Mountains, stream sediments		
	No. 1*		No. 95*		23*	43*	11*
Level	upper	lower	upper	lower	-	-	-
Ag	< 0.2	0.5	0.3	< 0.2	34	12	2.5
As	12.0	7.2	9.2	5.1	253	101	147
Ba	154	128	88	70	112	180	102
Cd	<0.5	<0.5	<0.5	<0.5	8	1	1
Cu	31	13	14	9	51	36	27
Hg	0.04	0.1	0.09	0.05	0.26	0.10	0.23
Pb	20	15	16	12	296	119	45
Zn	74	45	51	34	276	142	134

* = See position of the cells on Fig. 3.

The large flood-plain drainage basins show small concentrations for the above elements compared to the medians of the background (see Table 1). This might mean that the environmental effects of these deposits are insignificant either because of their distances from the sources of pollution or because many centuries had passed after the medieval mining activities. As to the stream sediments' catchment areas in the immediate surroundings of these old deposits, the difference in the concentrations of all the elements analysed is striking.

In the evaluation of environmental effects we have to consider the following facts. In the Zemplén Mts. Telkibánya was a significant mining region for gold and silver in medieval times. Quartz veins were mined in surface pits then in underground drifts. Ore crushers were in use from the 15th century on. Contamination of the environment became more and more intense after the 17th century, because of the new technology introduced into the mining industry. In the Telkibánya area water reservoirs and crushers were built in the valleys and waste dumps of the processed ore had also been deposited there. The dams erected in the Middle Ages, the crusher stones and the waste dumps can be still recognized at the site (ZELENKA 1997a). Geochemical signatures prior to mining would be important to be given, but the only suitable medium to sample would be the deep level horizon of flood-plain deposits, close to the site. Stream sediment signatures after the development of mining are shown on Tables 3 and 4.

Investigations conducted on the anomalies of the reconnaissance stream sediment survey (Fig. 3), revealed significant concentrations in the soil around Füzérradvány, an area with no prior mining activities. Consequently the stream sediments contained only the natural weathering products of the outcropping rocks. A follow-up soil survey using a 200 m x 40 m grid helped to outline areas of high heavy metal contents in soils originated by natural weathering processes (Fig. 4). These concentrations are compared with the concentration ranges of stream sediments transported from the same area and with tolerable values in soils (Table 5).

Concentrations of one or more heavy metals are much higher for the major part of the detailed soil survey (Fig. 4B) than tolerable values in soils. On the other hand catchment areas having the same or higher additive indices than these Füzérradvány cells, cover large surface areas on the aggregated anomaly map (Fig. 3) of the Zemplén Mts. So one can infer from this fact, that natural environmental loads of the extent of many km² can be taken for granted in the whole Zemplén Mountains for the heavy metals and associated elements.

Potential environmental considerations

The activities of foreign companies interested in ore exploration in Hungary have recently been intensified. In some concession areas detailed investigations are going on and production will probably start in the near future. The most important effects to be expected of possible future mining are the following: 1. Modern open-pit mining

Environmental loads revealed by the follow-up soil survey in a mineralized area in the Zemplén Mountains. (g/t)

Table 5

Element	As	Sb	Pb	Hg
Concentration range in the stream sediments *	16-94	2-22	10-40	0.11-0.58
Background (median) for the area of the follow-up soil survey	10	3.6	57	0.16
Max. concentration in the soil	2,810	395	160	29.4
Tolerable values in soils **	30	--	100	1

* = Based on catchment areas Nos. 19, 27, 29, and 199, which include the area of the follow-up survey.

** = Values taken from the environmental quality criteria prepared by the Ministry of the Environment in 1995, as a draft of a new law. The values are limits for very sensitive areas.

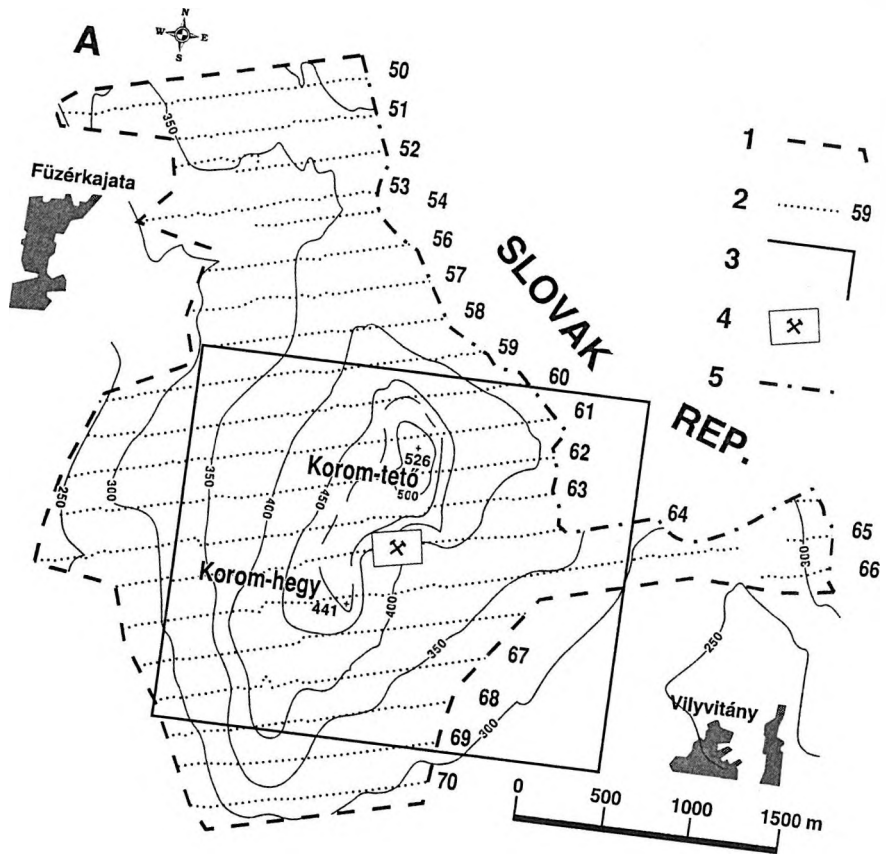
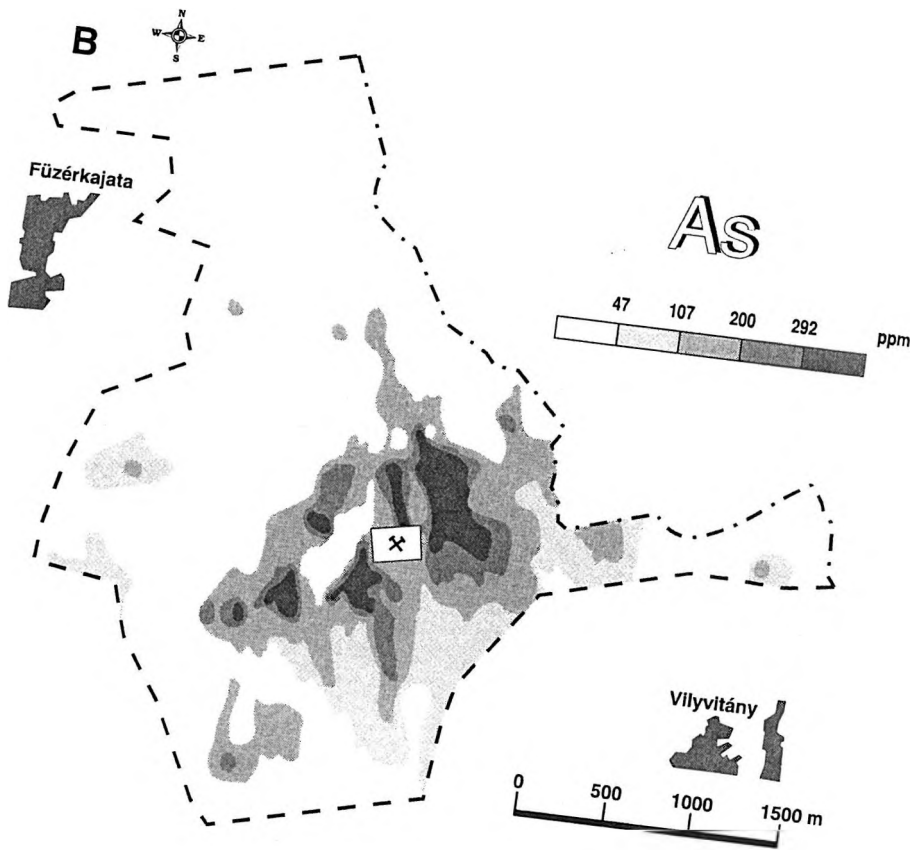


Fig. 4: A. Sampling sites for the follow-up soil study in the Füzérradvány (Korom) Zemplén Mts. 1. The area of the follow-up study, 2. Soil sampling sites, 3. Area of detailed soil profile, 4. Area of physical investigations, 5. State boundary. B. Distribution of As in soil



methods are to be expected. These produce great volumes of untreated waste rock. Increased traffic, noise and dust generation is also expected. This poses quality of life problems. 2. Disposal of tailings by erosion processes will cause sedimentation problems in stream valleys. 3. The possible future mine (or mines) will probably produce gold from low-grade ore, using cyanide heap-leach techniques. The cyanide used for gold extraction will be a potential additional contaminant in waste water discharge downstream in the valleys if mining operations are not carefully constructed. 4. The sulfide minerals (pyrite, marcasite, chalcopyrite, galena, sphalerite etc.) contained in the mine tailings will be oxidised and potentially hazardous components (As, Sb, Cd, Hg, methylated species, etc.) may be released and carried into the water in moderate amounts. 5. Acid mine drainage will not cause serious problems, because of the low sulfide and high carbonate contents of this type of ore.

According to environmental deposit models, in addition to the elements analysed the appearance of Tl is also to be expected in the ores of Füzérradvány, in the alteration zones and erosion products of the hot-spring type Au-Ag mineralization.

5.2. Mátra Mountains

5.2.1. Polymetallic veins, volcanic-hosted Cu, porphyry copper and Cu-Zn-Pb skarn mineralizations

Geological setting, main results of earlier investigations

The rocks of the andesitic stratovolcanic sequence of Middle Miocene age comprise the bulk of the Mátra Mts. Andesitic volcanism of Eocene age is restricted to an area of a few km² in the Recsk-Parádfürdő area. In a clastic sedimentary sequence with diversified composition deposited in the Oligocene to Lower Miocene there are many intercalations of dacitic tuffs. Mesozoic sedimentary formations are observed only in boreholes and adits of the Recsk deposit.

The history of mining in the Mátra Mts. (NAGY B. 1997a) probably goes back to the Middle Ages. The Lahóca copper mine was discovered in 1852. The base metal mining at Gyöngyösoroszi was in its prime from 1950–1970. In the 1960's the important deep-level copper-zinc deposit of Recsk was discovered.

All known ore occurrences are the products of postvolcanic geologic activities. At Recsk, copper porphyry ores can be found in the upper part of diorite porphyry bodies lying below Eocene andesites. Cu-Zn skarns are found in the contact zone between the diorite and Mesozoic carbonate rocks, while in the upper part of the sedimentary sequence and in the stratovolcanic series metasomatic mineralizations are characteristic (these are all related to the Recsk deep level mineralization). At and around the centers of geyser and hot-spring activities gray copper ores with precious metals were mined at Lahóca. In the Miocene andesites of the Mátra Mountains polymetallic vein-type mineralization is found. Our stream sediment survey did not cover the area near Lahóca, so the only area that can be analysed in detail is the surface geochemical features of the Gyöngyösoroszi polymetallic mineralization. These results will be applied to understanding possible environmental effects of the ores, as well as for other types of mineralization, which are developed in this region. (An epi-telethermal Hg-Sb indication has been known in the region of Asztagkő, (CSONGRÁDI 1984).

Deposit models

At the Gyöngyösoroszi deposit, the ore mineralization is of polymetallic vein type, locally in stockwork form; there are 15 to 20 veins of ore. Carbonate alteration is the strongest and youngest process but siliceous, sericitic and chloritic alteration is also frequent along the veins and in the host rocks. (VETŐ É. 1988, VETŐ-ÁKOS 1994, VETŐNÉ ÁKOS É. 1996, NAGY 1997a and VETŐ-ÁKOS 1999). This alteration assemblage corresponds to model "22c" of COX and SINGER (1986). According to this model the ore mineralization can be geochemically characterized by the element association: Zn, Cu, Pb, As, Au, Ag, Mn, Ba (Table 2). The epithermal gold-Cu mineralization of Eocene age at Lahóca (FÖLDESSY 1997, GATTER 1997) is associated with intrusion, tectonic, hydrothermal and explosion breccias. The ore bearing breccia contains a considerable amount of sulfides (mainly pyrite, less enargite, luzonite and tetrahedrite). The gold is concentrated in the sulfides. On the basis of COX and SINGER (1986) this corresponds to volcanic hosted Cu-As-Sb ("22a") deposits. Model Nos. "17", "18b" and "18c" can be assigned to the deep level deposits at Recsk (see Table 2). The stream sediment geochemical survey did not cover the Lahóca region, so the geochemical signatures of this deposit are not considered in this survey.

5.2.2. Stream sediment survey of the Mátra Mountains

The surface geochemical features in the Mátra Mountains are basically determined by the characteristics of the known ore mineralization at Gyöngyösoroszi. In the fine fraction of the stream sediments gold, in accordance with the polymetallic nature of the mineralization, shows positive significant correlation with Ag, As, Cu, Pb and

Zn (ÓDOR et al. 1997b). These elements have been used for the calculation of additive anomalies for the Mátra Mts. The statistical parameters and the calculation of additive indices used to outline additive anomalies are summarised in Table 6.

The additive indices are plotted on Fig. 5. The mineralization situated in the Western Mátra Mts. has been known and mined for a long time. It gives elevated values towards northwest and strong anomalies towards Gyöngyösoroszi in the distribution pattern. Another area, south of Parádsasvár, is also well outlined: this is the Middle Mátra region, also formerly mined. The dispersion fans can be traced for long distances along the creeks. There are two other additive geochemical anomalies in the eastern part of the mountains partly known from previous investigations. Among the elements in Table 6 not used for the calculation of additive anomalies Hg and Ba are enriched in and around a mercury mineralization of lesser importance.

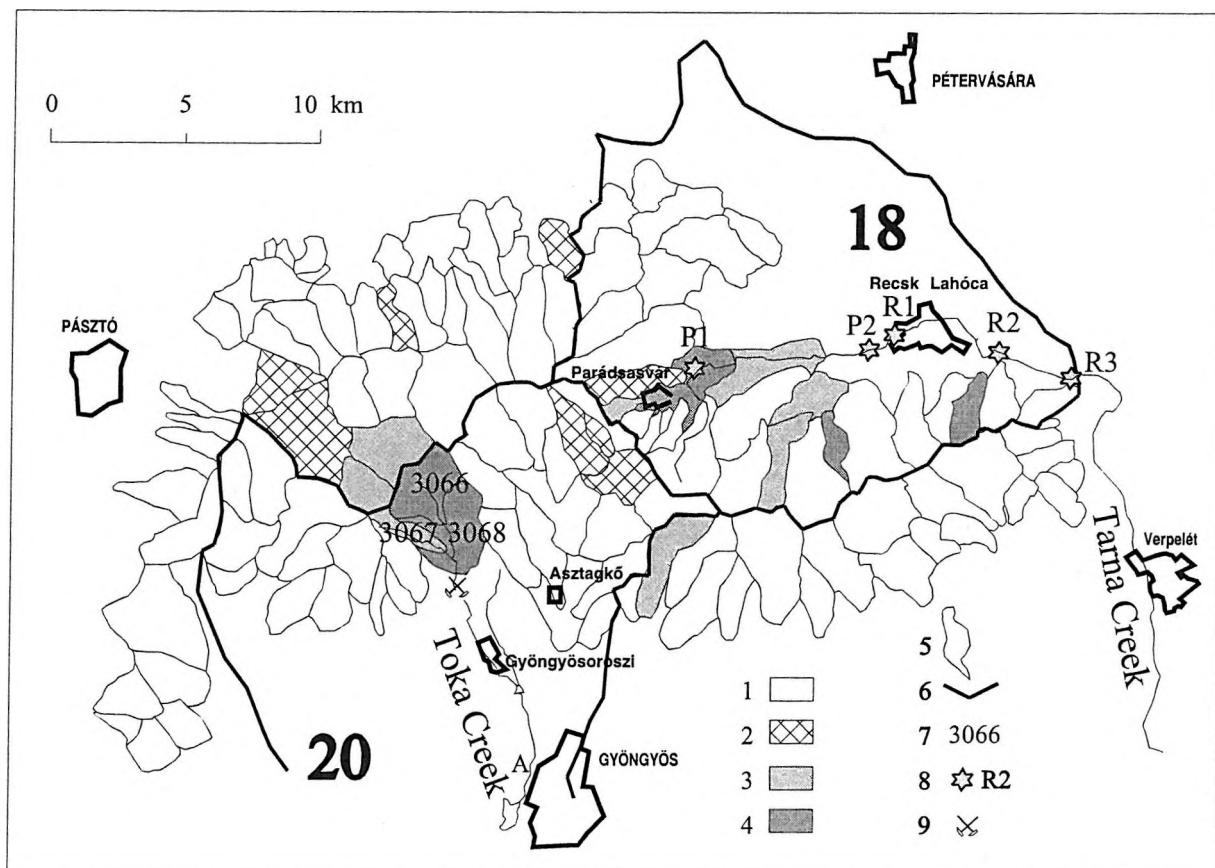
5.2.3. Environmental considerations

On Fig. 1 locations of mineral deposits and mining activities are shown for the Mátra Mts. Environmental considerations are mainly based on COX et al. 1995; KING, 1995; PLUMLEE and NASH 1995, PLUMLEE et al. 1993, 1995a,b,c., WANTY et al. 1999.

Environmental effects

Drainage basins which include these deposit sites were selected to show their possible environmental effects in the composition of flood-plain deposits and stream sediments. Table 7 shows the data for several elements in the upper (0–10 cm) and lower (50–60 cm) sampling levels of these flood-plain sediments together with the minor element composition of the stream sediments covering areas of known mineralization.

Fig. 5: Aggregated anomaly map of the Mátra Mts. based on the stream sediment survey
 Values of the additive indices: 1: 0–1; 2: 2–3; 3: 4–5; 4: 6–11; 5: Sampled catchment areas; 6: Drainage basins (Nos. 18. and 20.) of the low-density survey (floodplain sampling) comprising old and recent mining sites; 7. Catchment areas of the stream sediment survey comprising old mining sites (No. of cells), 8. Sampling sites upstream and downstream of Recsk, 9: The Gyöngyösoroszi base metal mine and polluted flood-plain below



Geochemical parameters of elements in the fine fraction of stream sediments. Calculation of additive indices. Mátra Mountains (g/t, unless otherwise noted, N = 104)

Table 6

Element	Geochemical parameters				To calculate additive indices			
	Min.	Median	Threshold of anomaly	Max.	Index value + 1	Index value + 2	Index value + 3	Index value + 4
Au mg/t	< 2	< 2	16	24	6.5-12	> 20		
Ag	< 0.4	< 0.4	—	0.4	=> 0.2			
As	1.7	5.7	50	163	12-22	39-44	> 60	
Cu	2	14	50	153	30-45	> 100		
Pb	7	18.5	50	288	40-45	55-110	> 190	
Zn	34	65	280	12 200	100-250	300-700	900-2,000	> 10,000
Ba	41	123	280	320	*			
Cd	< 1	< 1	4	47	*			
Cr	3	11	-	23	*			
Hg mg/t	< 20	140	600	2560	*			

Remark: * = elements not used for the calculation of additive anomalies.

Composition of the flood-plain deposits of large drainage basins (low density survey) and that of the stream sediments within them covering areas of known mineral deposits and mining sites in the Mátra Mts. (g/t)

Table 7

Region	Mátra Mountains, flood-plain deposits				Mátra Mts., stream sediments		
	No. 18*		No. 20*		3066*	3067*	3068*
Level	upper	lower	upper	lower	-	-	-
Ag	0.4	0.2	0.3	0.2	0.3	0.2	0.3
As	54.8	7.3	14.6	16.2	18.1	17.7	163
Ba	158	118	177	184	41	85	73
Cd	1.47	<0.5	0.68	0.68	2.6	1	47
Cu	100	30	42	30	41	29	153
Hg	0.3	0.2	0.33	0.4	0.5	1.28	0.44
Pb	21	17	49	47	95	59	241
Zn	71	77	191	176	382	185	12 200

* = see position of the cells on Fig. 5

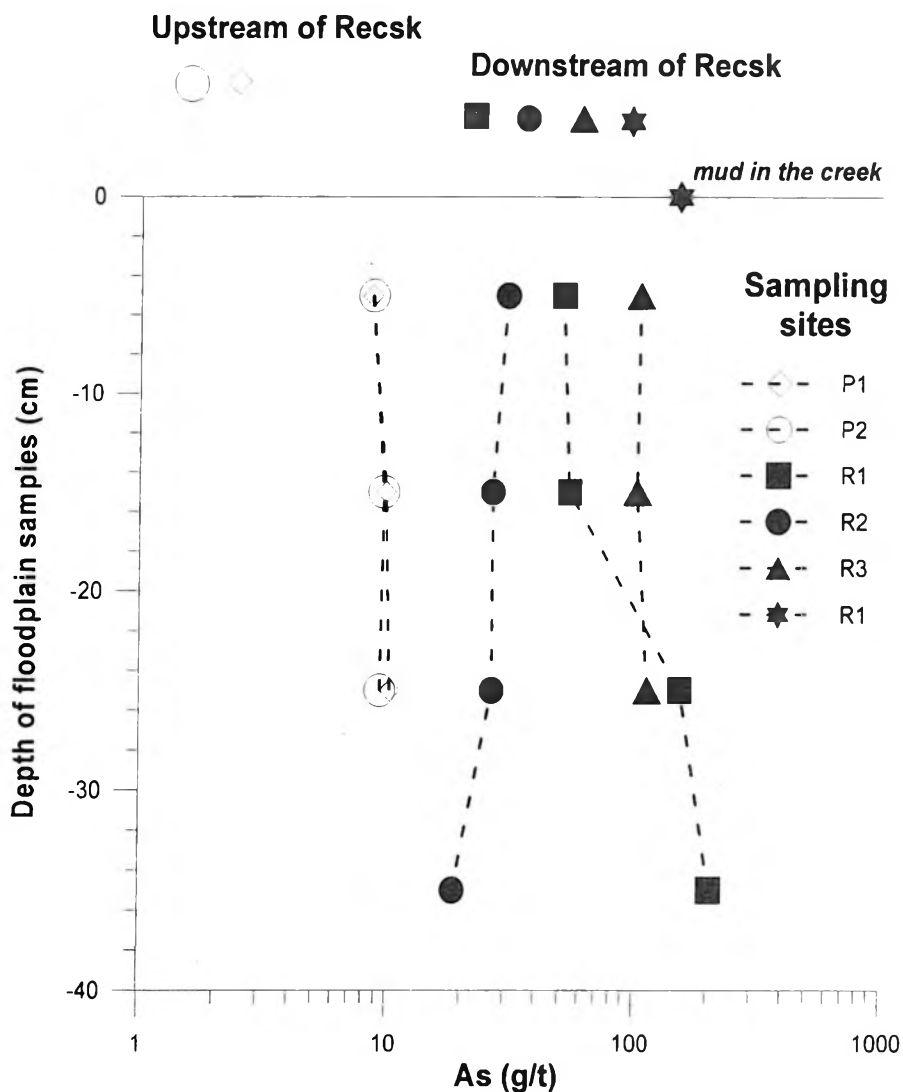


Fig. 6: Arsenic contents of the floodplain deposits upstream and downstream of Recsk (For sampling sites see Fig. 5.) Description of the sampled profiles: at P1, P2, R1 = predominantly silt with small pebbles; at R2, R3 = clayey fine sand; R1 mud = mud in the creek collected at site R1

Elevated concentrations of a few elements are observed in cell No. 18 of the low-density survey (see on Fig. 5), which covers part of the Mátra Mountains, the other drainage basin shows small concentrations for the above elements compared to the medians of the background (see in Table 1). This might mean that the environmental effects of the near-surface deposits are insignificant in such distances from the mineralized centers. (Cell No. 18 might show the recent contaminating effects of the ore and waste material originating from the Lahóca deposit. A new sampling was conducted in 1997 upstream and downstream of the Recsk (and Lahóca) mining sites (Fig. 6) to show the effects on the environment of the ore and waste dumps being eroded. Floodplain (overbank) sediments were sampled from 0 to 40 cm at 5 sites and analysed for 18 elements. Differences in the element contents of Ba, Cu, Sr, Hg, As, Sb and Au of the floodplain sediments in the valley above and below Recsk are significant and can be illustrated by the distribution of arsenic (Fig. 6). The arsenic contents of floodplain sediments downstream of Recsk (Lahóca deposit) are increased by an order of magnitude compared to the unpolluted sediments higher up in the valley of the Tarna Creek above Recsk. This contamination of the floodplain sediments was probably caused by the Lahóca deposit (WANTY et al. 1999) and related mining activities.

The deep level Recsk deposit will probably be mined in the future. The main commodities will be: Zn, Cu, Ag (Au). The geochemical investigation of the skarn mineralization of this deposit was carried out by U. FÜGEDI at the Geochemistry Department in 1985–90 using OES semiquantitative data. It can be assumed that the concentration of Zn, Cu and Cd will be much higher in the flotation waste after the processing of ore than the allowable limits for soil. So these elements will be the main contaminants to be released to the environment if the dumps are eroded. Lead will not be an important factor in this respect.

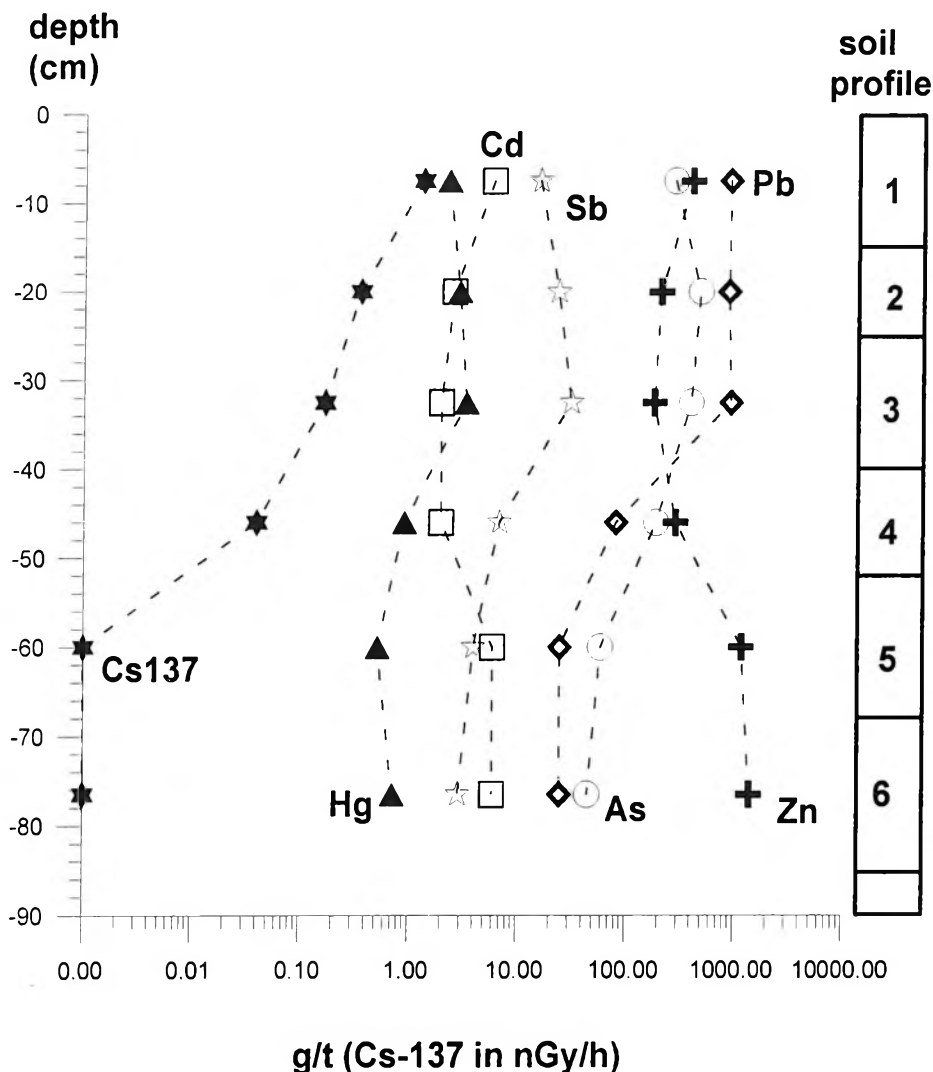


Fig. 7: Gyöngyösoroszi: Geochemical profile at site A on the flood-plain (see location on Fig. 5.)
Description of the profile: 1. Brown silty sand, 2. Greyish yellow clayey sand, 3. Yellow clayey sand, 4. Dark brown sand, 5. and 6. Brown clayey sand

In the stream sediment catchment areas near the Gyöngyösoroszi deposit, concentrations of As, Cd, Hg, Pb and especially Zn are high and anomalous. The environmental effects of the Gyöngyösoroszi mine were studied in detail and their description is based mainly on Ódor et al. (1997d). The waste material of the Gyöngyösoroszi base metal mine, the mine water, the ore-dressing, the washed away concentrate and the flotation waste dump (cleaner tailings) are all sources of contamination along Toka Creek and its flood sediments (for location see Fig. 5). During floods the mud of high metal content which had accumulated in the reservoirs was also carried away and spread out. The sand fraction was deposited near the bed as long and narrow sand bars ("yellow sand") and the finer fractions accumulated elsewhere on the flood-plain. By studying the petrologic composition, toxic element and Cs-137 contents of soil profiles on the flood-plain, thickness of recent sediments deposited in the last 40–50 years can be established. The majority of the sedimentary material comprising this recent upper layer (30–50 cm thick) is composed of the flotation waste (Fig. 7). So mining has contributed a huge quantity of fine-grained material of anthropogenic origin to the natural processes. The extent of the contamination on the surface and at depth has roughly been delineated. The area of the land used for agriculture and affected by floods is marked or indicated. Detailed studies on the toxic element content of different plants and vegetables were also conducted in the Toka Creek valley (unpublished data of Peter Marth, Soil Information Monitoring System at the Budapest Plant Health and Soil Protection Station, Hungary). These results can be compared to uptake ratios of elements by plants established by JOHN and LEVENTHAL (1995) and suggestions can be made for the most appropriate edible garden plants which can be safely grown on these contaminated soils.

The main problem to be solved in this area is not caused by the polluted mine water. Attenuation of metals in stream water is taking place within a relatively short distance. The most important problem is the presence of pol-

luted soils on the flood-plain. Floods had carried and will probably carry the flotation material to great distances (> 10 km) from its source and there is no significant attenuation of metal contents of this material downstream (ÓDOR et al. 1997d).

Potential environmental considerations

Toxic elements enriched in the upper layers of soils situated on the flood-plain in the GyöngyöSOROSZI area are the main sources of future pollution. The flotation waste is a long-term source of metals and acid, and is impossible to remediate. Both the material deposited in the reservoirs along the Creek and the so called "yellow sand" and their toxic metal content can be continuously remobilised, horizontally and vertically by new floods and under hypogene conditions, respectively. According to geoenvironmental deposit models, the elements analysed and shown on Table 2 are the ones to be expected in the flood-plain and stream sediment deposits below the GyöngyöSOROSZI base metal mine.

The environmental effects enumerated above for possible mining in the Zemplén Mts. apply as well to the Láhóca area. The elements indicated by the geoenvironmental deposit models for the deep level Recsk deposit should also be taken into consideration in case of future mining when evaluating potential effects of the ores. The porphyry copper and the skarn deposits, in addition to the elements analysed by our Laboratory, would give the following elements as possible future contaminants: Se, Te, Bi, Be.

5.3. Börzsöny Mountains

5.3.1. Polymetallic veins and replacement mineralizations

Geological setting, main results of earlier investigations

Two volcanic units have been delineated in the Börzsöny Mts. In the lower unit products of explosive-extrusive activities are mainly found, resulting in the accumulation of a thick stratovolcanic complex of andesites and dacites. Both lavas and pyroclastics are characterized by great mineralogical variations (CSILLAGNÉ-TEPLÁNSZKY et al. 1983, KÖRPÁS and LANG 1991). In the upper volcanic event a large stratovolcanic structure was formed. The maximum thickness of this andesitic stratovolcanic complex is 450 m. This late complex shows no signs of hyd-rothermal alteration.

The main features of the mineralization developed in the central part of the Börzsöny Mountains are based on CSILLAGNÉ-TEPLÁNSZKY et al. (1983), KÖRPÁS and LANG (1993), NAGY B. (1983, 1990, 1997b). The mineralization (and alteration) took place at the end of the first phase of the Börzsöny volcanic activity. Clear zonation can be seen at the different occurrences. Copper mineralization is associated with a central biotitic zone, which is surrounded by either barren or polymetallic zones. Three main zones with typical hydrothermal mineral assemblages can be distinguished vertically. In the upper zone the argillite-carbonate-pyrite facies is accompanied by polymetallic mine-ralization which comprises the following mineralogy: pyrite, marcasite, pyrrhotite, sphalerite, galena, chalcopyrite, argentite, Bi- and Ag minerals, quartz, calcite, siderite and clay minerals. In the middle or transitional zone the facies described above is accompanied by a biotite-bearing chalcopyrite ore mineralization in its center and by a polymetallic mineralization at the margins. In the lower zone the biotite-bearing chalcopyrite facies is found with a copper ore mineralization: pyrite, pyrrhotite, magnetite, chalcopyrite, sphalerite, phlogopite, chlorite, and quartz.

Deposit models

Genetic models of the Börzsöny mineralizations were described by CSILLAGNÉ-TEPLÁNSZKY et al. 1983, VETÖNÉ-ÁKOS 1996 and VETÖ-ÁKOS 1999). In the central part of the mountain there are three well-defined base metal mineral occurrences: 1. The environs of Kuruc-patak; 2. Bányapuszta and 3. Rózsa-hegy (Table 2). Near the surface there are vein type, epithermal precious and base metal occurrences (COX and SINGER: type "22c"), at deeper level metasomatic type Pb-Zn (Ag, Au) ore mineralization is known (NAGY B. 1990, 1997). This corresponds to model "19a", which, at places, can be found near the surface too. The weak and unimportant porphyry copper mineralization had originally been formed below the metasomatic type of mineralization (according to recent views this type of mineralization does not exist in the region, see VETÖ-ÁKOS 1999). Thus the near-surface precious and base metal mineralizations are characterised by the appearance of Zn, Cu, Pb, As, Au, Ag, Mn, and Ba; these elements are found also in the Mátra Mts. The copper enriched central part of the metasomatic mineralizations at deeper level is surrounded by a broad, Pb-Ag enriched zone, while Zn and Mn are enriched at the fringes. The mineralization in the central part is characterised by Cu + Mo + Ag (\pm W \pm B \pm Sr), while Pb, Zn, Au, As, Sb, Co, and Ba are found in the outer zone.

5.3.2. Stream sediment survey of the Börzsöny Mountains

In the Börzsöny Mts. the correlations of the gold contents of the fine fraction of stream sediment are more extensive and include more elements than in the other two regions studied (ÓDOR et al. 1997b, 1998). The reason for that might be that there is only one ore-generating event in the Börzsöny Mts. Geochemical parameters of gold and pathfinder elements, as well as the calculation of additive indices are shown in Table 8.

On the favorability map of the Börzsöny Mts. (Fig. 8) the Middle Börzsöny is spectacularly highlighted by the aggregated anomalies giving the area of old mining activities and recent prospecting. This anomaly is surrounded by a broad dispersion halo. There are two other anomalous regions worth mentioning. 1. The anomalous cell, situated northwest of Szokolya lies at the northern edge of a collapsed caldera, there are hematite and limonite indications here. 2. North of Szob the anomalies outline the center of a stratovolcano. These two isolated anomalies are not significant with respect to economic ore mineralization.

5.3.3. Environmental considerations

Environmental effects

On Fig. 1 locations of mineral deposits and mining activities are shown for the Börzsöny Mts. Drainage basins which include the area of these deposits were selected to show their possible environmental effects (Fig. 8). Table 9 shows the data for several elements in the upper (0–10 cm) and lower (50–60 cm) sampling levels of the flood-plain sediments.

The drainage basin of the low-density survey incorporating the old mines and mining-related activities of a few decades ago shows only small concentrations for the above elements compared to the medians of the background (see in Table 1). This might mean that the environmental effects of these deposits are insignificant in such distances from the mines. In the small catchment areas in the immediate surroundings of these deposits, the concentrations of the following elements are high in the fine fraction of stream sediments: Ag, As, Pb and Zn.

Geochemical parameters of elements in the fine fraction of stream sediments. Calculation of additive indices. Börzsöny Mountains (g/t, unless otherwise noted, N = 91)

Table 8

Element	Geochemical parameters				To calculate additive indices				
	Min.	Median	Threshold of anomaly	Max.	Index value + 1	Index Value + 2	Index value + 3	Index value + 4	Index value + 5
Au mg/t	< 2	< 2	15	123			2–13	15–100	> 100
Ag	< 0.3	0.4	—	1.6			0.8–1	1–1.5	>1.5
As	0.5	2.6	10	22.5	> 10				
Cu	3	6.6	25	64		12–21	30	64	
Hg mg/t	< 20	< 20	100	284	40–45	50–80	> 284		
Mn	170	640	1,600	3,194	1,600–2,000	3,194			
Pb	4	9.5	20	187			30–50	60–110	187
Zn	19	44.5	100	583			54–120	250–400	583
Ba	38	93	170	2,468	*				
Cr	5	13.3	40	73	*				
Sb	< 0.2	< 0.2	1	1.2	*				

Remark: * = elements not used for the calculation of additive anomalies.

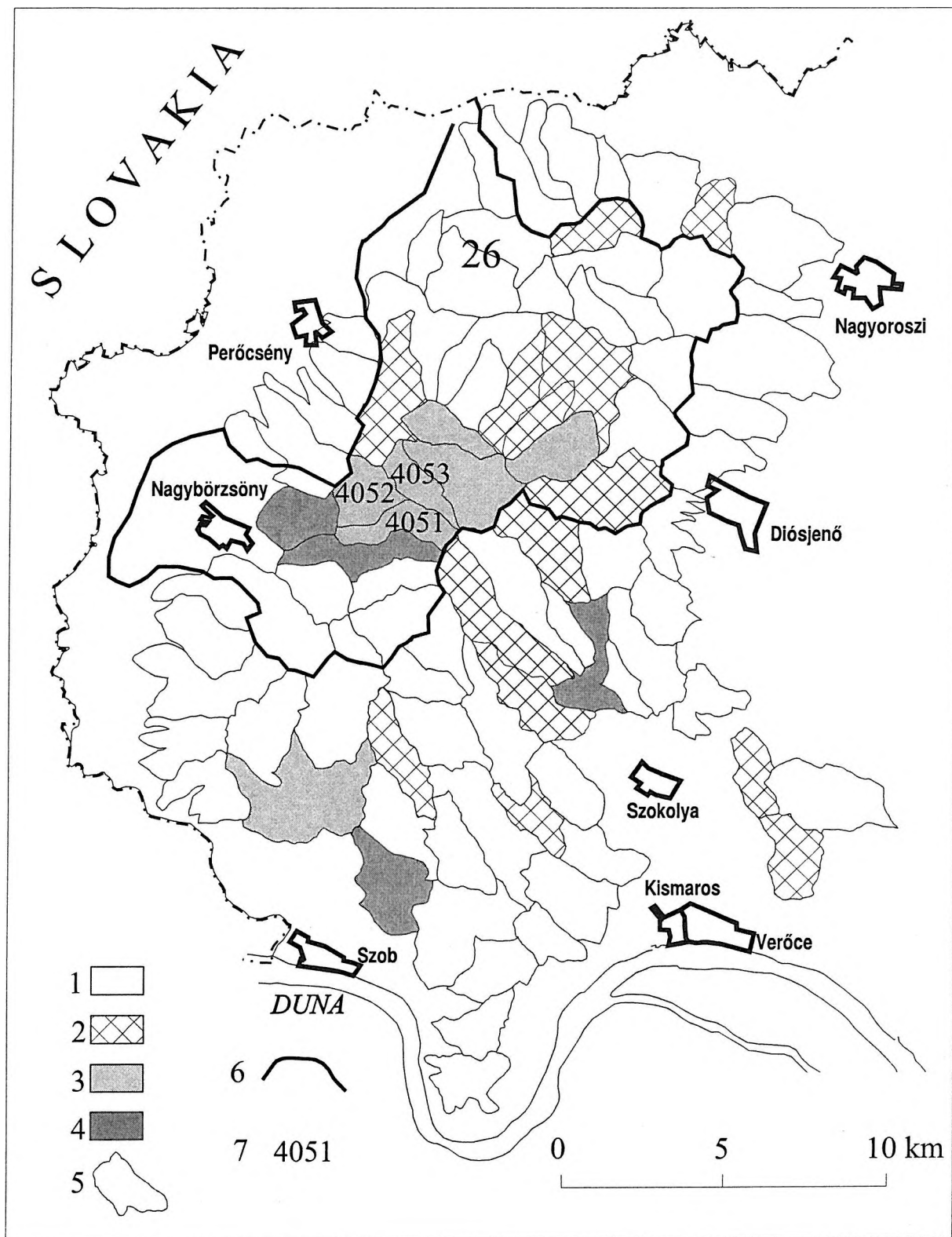


Fig. 8: Aggregated anomaly map of the Börzsöny Mts. based on the stream sediment survey
 Values of the additive indices: 1: 0–3; 2: 4–7; 3: 9–11; 4: 14–19; 5: Sampled catchment areas; 6: Drainage basin (No. 26) of the low-density survey (floodplain sampling) comprising old mining sites; 7: Catchment areas of the stream sediment survey comprising old mining sites (No. of cells)

Composition of the flood-plain deposits of large drainage basins (low density survey) and that of the stream sediments within them covering areas of known mineral deposits and mining sites in the Börzsöny Mts. (g/t values)

Table 9

Region	Börzsöny Mts., flood-plain deposits		Börzsöny Mts., stream sediments		
	No. 26*		4051*	4052*	4053*
Level	upper	lower	–	–	–
Ag	0.2	0.2	0.7	0.9	0.7
As	<2.5	<2.5	22.5	3.8	3.2
Ba	98	85	82	96	90
Cd	<0.5	<0.5	< 1	< 1	< 1
Cu	13	12	21	30	15
Hg	0.05	0.04	0.05	0.06	0.029
Pb	24	24	107	32	30
Zn	76	61	376	103	92

* = see position of the cells on Fig. 8

Mining at Nagybörzsöny goes back to the middle of the 13th century (BENKE 1994). It flourished in the 15th century, when at least 100 miners worked here (there are old adits and hollows along the veins over a length of approximately 1 km). The second boom was in the 18th century (crushers, mills and furnaces had been built). Mining activities in the 1950's (an adit of 1800 m long had been made) brought great quantities of ore and waste material to the surface.

Potential environmental considerations

According to the deposit models (COX and SINGER 1986, COX et al. 1995), in addition to the elements analysed, the appearance of minor elements like Se, Te and Bi is also to be expected in the ores, in the alteration zones and weathering products of mineralized rocks in the Börzsöny Mountains.

6. CONCLUSIONS

The lithogeochemical zonality derived from the deposit models cannot be revealed with certainty by the use of a sampling density of 4–5 km²/catchment area.

Comparing the geochemical features of the volcanic regions in northern Hungary, based on the stream sediment survey, it can be stated that the background values of andesitic areas are very similar for most of the elements analyzed. Arsenic is the only element accompanying the gold-silver couple which can be used for geochemical purposes in every mountain unit. Comparing the medians of the elements for the three different mountain regions, Hg and Ba have significantly higher values in the Zemplén Mts. than in the other regions. These units are characterized, one by one, by the following element associations: Zemplén Mts.: Au, Ag, As, Sb and an independent Hg, (Ba) suite; Mátra Mts.: Au, Ag, As, Cu, Pb, Zn and independent Hg; Börzsöny Mts.: Au, Ag, As, Cu, Hg, Pb and Zn. The dispersion haloes are toxic heavy metal anomalies of natural origin, as far as environmental aspects are concerned. Follow-up soil investigations have only been carried out in a small anomalous area in the Zemplén Mts. Exact data for the environmental loads of heavy metals in soils in a mineralized area can

only be given for this location. For the major part of the Zemplén Mts. and for the two other regions (Mátra and Börzsöny Mts.) detailed soil data are not available and only the patterns derived from the additive geochemical anomalies of the stream sediment survey refer to the existence of actual environmental loads in the soils.

An important remark must be made here. We have to consider the list of minor elements analysed in the Laboratory of GIH, and compare them to the list given by the generalized deposit type and geoenvironmental mineral deposit models. There will be quite a few elements not yet detected in these three volcanic regions of Hungary. So geochemical signatures of the Hungarian deposits can only be predicted on the basis of international models but cannot be completely covered or established by the use of our analytical data. Improved analytical data may be obtained in the future, but the current data set provides a useful synthesis of the environmental conditions in the mineralized areas of northern Hungary.

7. REFERENCES

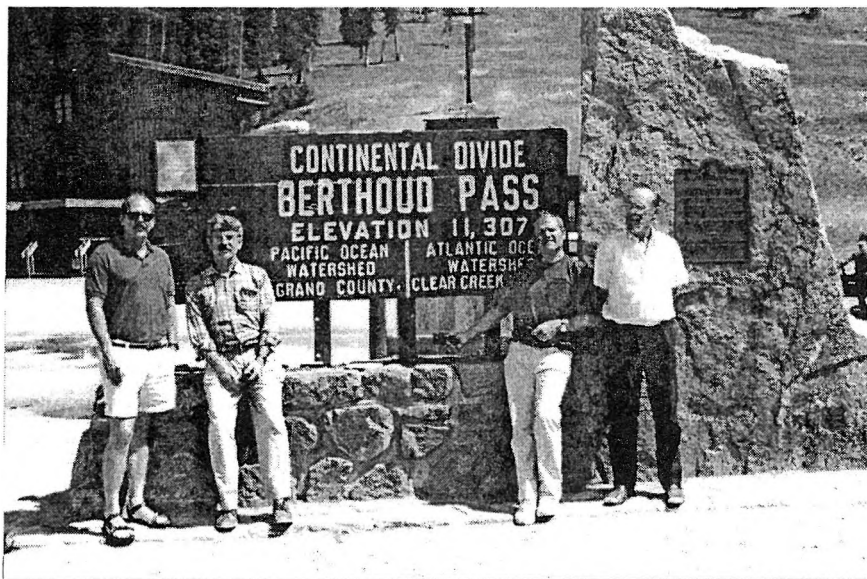
- BENKE, I. 1994: A nagybörzsönyi ércbányászat története (The History of Mining at Nagybörzsöny). — Miskolc. 102 p. (In Hungarian).
- BERGER, B. R. 1985: Geologic-geochemical features of hot-spring precious-metal deposits. — US Geological Survey Bulletin 1646: 47–53.
- BERGER, B. R.–DREW, L. J.–SINGER, D. A. 1999: Quantifying mineral-deposit models for resource assessment: future possibilities. — *Geologica Hungarica Series Geologica* 24: 41–54.
- BLISS, J. D. 1992: Developments in mineral deposit modeling. — US Geological Survey Bulletin 2004: 168 p.
- COX, D. P.–SINGER, D. A. 1986: Mineral deposit models. US Geological Survey Bulletin 1693: 379 p.
- COX, L. J.–CHAFFEE, M. A.–COX, D. P.–KLEIN, D. P. 1995: Porphyry Cu deposits, — *in* DU BRAY, E. A. ed.: Preliminary compilation of descriptive geoenvironmental mineral deposit models. US Department of the Interior, US Geological Survey, Open File Report 95-831: 75–90
- CSILLAGNÉ TEPLÁNSZKY, E.–CSONGRÁDI, J.–KORPÁS, L.–PENTELENYI, L.–VETÖNÉ ÁKOS, É. 1983: A Börzsöny hegység Központi területének földtani felépítése és ércesedése. (Geology and mineralization in the central area of the Börzsöny Mts.). — Magyar Állami Földtani Intézet Évi Jelentése 1981: 77–127. (In Hungarian with English abstract).
- CSONGRÁDI, J. 1984: Epi-telettermális Hg-Sb indikáció az Asztag-kő-Üstök-fő környékén. (An epi-telettermal Hg-Sb indication in the region Asztagkő-Üstökfő). — Magyar Állami Földtani Intézet Évi Jelentése 1982: 119–136. (In Hungarian with English abstract).
- CSONGRÁDI, J.–ZELENKA, T. 1995: Hot-spring type gold-silver mineralizations in the Tokaj Mts. (Northeastern Hungary). — Geological Society of Greece Special Publication No. 4/2., XV. Congress of the Carpatho-Balkan Geological Association, September 17–20, 1995, Athens, Greece: 689–693.
- DREW, L. J. 1997: Undiscovered Petroleum and Mineral Resources. Assessment and Controversy. — Plenum Press. New York and London: 210 p.
- DU BRAY, E. A. ed. 1995: Preliminary compilation of descriptive geoenvironmental mineral deposit models. — US Department of the Interior, US Geological Survey, Open File Report: 95–831
- FÖLDESSY, J. 1997: A recski Lahóca aranyérc előfordulás (The occurrence of gold mineralization at Lahóca of Recsk). — *Földtani Kutatás*, 34(2): 12–16. (In Hungarian).
- GATTER, I. 1997: A Recsk-parádfürdői “kovás sapka” aranyérc perspektívái a fluid zárvány vizsgálatok tükrében. (The perspectives of gold mineralization in the “silicon hat” at Recsk-Parádfürdő in the light of fluid-inclusion studies). — *Földtani Kutatás*, 34(2): 16–20. (In Hungarian).
- GYARMATI, P. 1981: A Tokaji hegység alunit és ércprognózisa. (Alunite and ore prognosis for the Tokaj Mountains). — Magyar Geológiai Szolgálat Országos Földtani és Geofizikai Adattára, Kézirat (Unpublished report in Hungarian).
- HARTIKAINEN, A.–HORVÁTH, I.–ÓDOR, L.–Ó. KOVÁCS, L.–CSONGRÁDI, J. 1992: Regional multimedia geochemical exploration for Au in the Tokaj Mountains, northeast Hungary. — *Applied Geochemistry*, 7: 533–547.
- HARTIKAINEN, A.–ÓDOR, L.–HORVÁTH, I.–Ó. KOVÁCS, L.–FÜGEDI, U. 1993: Regional geochemical survey of the Tokaj Mountains, Northeast Hungary. — *Geologian Tutkimuskeskus, Tutkimusraportti* 120, Geological Survey of Finland, Espoo. Report of Investigation 120: 29 p.
- HORVÁTH, I.–ÓDOR, L.–FÜGEDI, U.–HARTIKAINEN, A. 1993: Aranyindikációk a Tokaji-hegységi geokémiai érc-kutatásban. (Gold indications in the regional-scale geochemical survey of the Tokaj Mts. (Hungary), — *Földtani Közlöny* 123(4): 363–378. (In Hungarian with English abstract).

- JOHN, D. A.–LEVENTHAL, J. S. 1995: Bioavailability of metals, — *in* DU BRAY, E. A. (ed.): Preliminary compilation of descriptive geoenvironmental mineral deposit models. US Department of the Interior, US Geological Survey, Open File Report: 95–831: 10–19
- KING, T. V. V. ed. 1995: Environmental considerations of active and abandoned mine lands: lessons from Summitville, Colorado. — US Geological Survey Bulletin 2220: 38 p.
- KORPÁS, L.–LANG, B. 1991: K–Ar geochronology of the volcanism and associated metallogenesis in the Börzsöny Mountains, Hungary. — Unpublished report, Geological Survey of Israel, 36/91.
- KORPÁS, L.–LANG, B. 1993: Timing of volcanism and metallogenesis in the Börzsöny Mountains, Northern Hungary. — *Ore Geology Reviews* 8: 457–501.
- MCCAMMON, R. B.–LUDINGTON, S.–COX, L. J. (National Editors) 1995: Data Base for a National Mineral-Resource Assessment of Undiscovered Deposits of Gold, Silver, Copper, Lead, and Zinc in the Conterminous United States. — US Geological Survey Minerals Team, Presented on CD-ROM.
- MOLNÁR, F. 1997: Epitermás aranyércesedések kialakulásának modellezése ásványtani genetikai vizsgálatok alapján: példák a Tokaji-hegységből. (Modelling of the formation of epithermal gold deposits on the basis of mineralogic-genetic studies, examples from the Tokaj Mountains.) — *Földtani Kutatás*, 34(1): 8–13. (In Hungarian).
- NAGY, B. 1983: Adatok a nagybörzsönyi Rózsabánya ércesedésének genetikai ismereteihez. (Contribution to the genesis of the Rózsabánya ore mineralization in Nagybörzsöny.) — *A Magyar Állami Földtani Intézet Évi Jelentése 1981*: 129–154. (In Hungarian with English abstract).
- NAGY, B. 1990: A nagyirtáspusztai ércesedés. (The Nagyirtáspusztá ore mineralization, Börzsöny Mountains) — *A Magyar Állami Földtani Intézet Évi Jelentése 1988*: 277–325. (In Hungarian with English abstract).
- NAGY, B. 1997a: A Gyöngyösoroszi nemesfém ércesedés perspektívái. (The perspectives of noble metal occurrence in Gyöngyösoroszi). *Földtani Kutatás*, 34(2): 7–9. (In Hungarian).
- NAGY, B. 1997b: Az 1990-es évek Börzsöny-hegységi aranyérc kutatási munkálatok eredményei. (Research activities for gold mineralizations of Börzsöny Mts. in the 1990's.) — *Földtani Kutatás*, 34(4): 9–11. (In Hungarian with English abstract).
- ÓDOR, L.–CSALAGOVITS, I.–HORVÁTH, I. 1992. The relationship between geological setting and toxic element enrichments of natural origin in Hungary. — *International Symposium on Environmental Contamination in Central and Eastern Europe. Symposium Proceedings. Budapest '92, October 12–16, 1992, Budapest, Hungary*: 51–53.
- ÓDOR, L.–HORVÁTH, I.–FÜGEDI, U. 1996: Low-density Geochemical Survey of Hungary. — *Volume of Abstracts, Environmental Geochemical Baseline Mapping in Europe Conference, May 21–24, 1996, Spisska Nova Ves, Slovakia*: 53–57.
- ÓDOR, L.–HORVÁTH, I.–FÜGEDI, U. 1997a: Az arany és ezüst geokémiai háttérértékei az ártéri üledékek alapján. (The geochemical background values of gold and silver on the basis of flood-plain deposits.) — *Földtani Kutatás*, 34(1): 13–17. (In Hungarian).
- ÓDOR, L.–HORVÁTH, I.–FÜGEDI, U. 1997b: Észak-Magyarország nemesfém perspektívái a patakfordalékok geokémiai felvétele alapján. (Precious metal perspectives of northern Hungary based on stream sediment survey.) — *Földtani Kutatás*, 34(2): 9–12. (In Hungarian).
- ÓDOR, L.–HORVÁTH, I.–FÜGEDI, U. 1997c: Low-density geochemical mapping in Hungary. — *Journal of Geochemical Exploration* 60: 55–66.
- ÓDOR, L.–WANTY, R. B.–HORVÁTH, I.–FÜGEDI, U. 1997d: Mobilization and attenuation of metals downstream from a base-metal mining site in the Mátra Mountains, northeastern Hungary. — *Journal of Geochemical Exploration* 65: 47–60.
- ÓDOR, L.–HORVÁTH, I.–FÜGEDI, U. 1998: Geokémiai felvételek. (Geochemical survey). — *in* KORPÁS, L.–CSILLAGNÉ TEPLÁNSZKY, E.–HÁMOR, G.–ÓDOR, L.–HORVÁTH, I.–FÜGEDI, U.–HARANGI, SZ.: *Magyarázó a Börzsöny és a Visegrádi-hegység földtani térképéhez 1: 50 000*. (Explanation to the geological map of the Börzsöny and Visegrád Mountains, scale: 1: 50 000), Budapest.
- PLUMLEE, G. S.–SMITH, S. M.–TOTH, M. I.–MARSH, S. P. 1993: Integrated Mineral-Resource and Mineral-Environmental Assessments of Public Lands: Applications for Land Management and Resource Planning, — US Geological Survey, Open File Report: 93–571.
- PLUMLEE, G. S.–NASH, J. T. 1995: Geoenvironmental models—fundamentals and applications., — *in* DU BRAY, E. A. (ed.): Preliminary compilation of descriptive geoenvironmental mineral deposit models. US Department of the Interior, US Geological Survey, Open File Report: 95–831: 1–10.
- PLUMLEE, G. S.–MONTOUR, M.–TAYLOR, C. D.–WALLACE, A. R.–KLEIN, D. P. 1995a: Polymetallic vein and replacement deposits, — *in* DU BRAY, E. A. (ed.): Preliminary compilation of descriptive geoenvironmental mineral deposit models. US Department of the Interior, US Geological Survey, Open File Report: 95–831: 121–130.

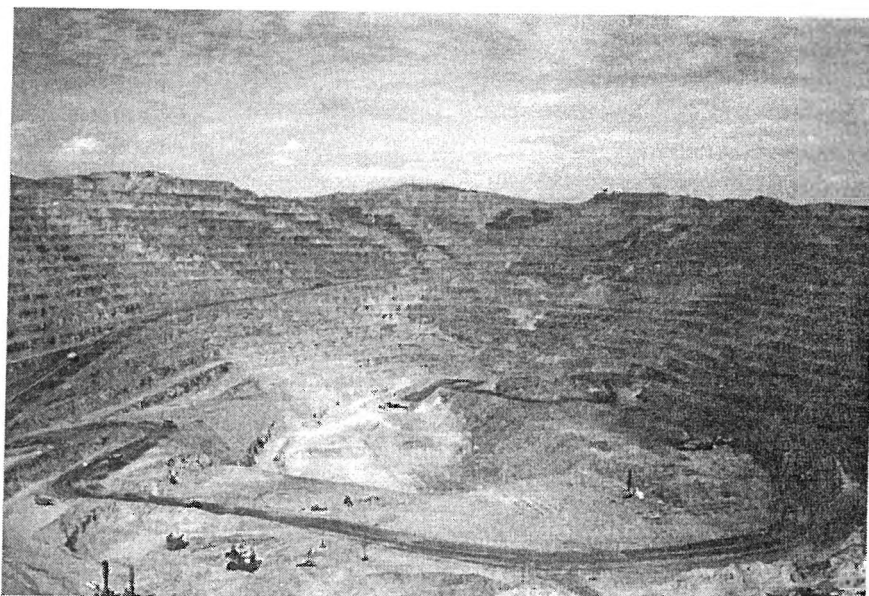
- PLUMLEE, G. S.—SMITH, K. S.—BERGER, B. R.—FOLEY—AYUSO, N.—KLEIN, D. P. 1995b: Creede, Comstock and Sado epithermal vein deposits, — *in* DU BRAY, E. A. (ed.): Preliminary compilation of descriptive geoenvironmental mineral deposit models. US Department of the Interior, US Geological Survey, Open File Report: 95–831: 152–162.
- PLUMLEE, G. S.—STREUFERT, R. K.—SMITH, K. S.—SMITH, S. M.—WALLACE, A. R.—TOTH, M. I.—NASH, T.—ROBINSON, R.—FICKLIN, W. H.—LEE, G. K. 1995c: Map showing potential metal-mine drainage hazards in Colorado, based on mineral-deposit geology. — US Department of the Interior, US Geological Survey, Open File Report: 95–26.
- VETŐ, I. 1971: A Tokaji-hegység szarmata hévforrástavi képződményeinek ritkalelem indikációi. (Rare element indications in the hydrothermal-lacustrine formations of the Tokaj Mountains). — Magyar Állami Földtani Intézet Évi Jelentése 1969: 477–484. (In Hungarian with English abstract).
- VETŐ, É. 1988: Conditions of Pb-Zn ore formation in the Carpathian Neogene volcanic arc: Evidence from Gyöngyösorszi mine, N-Hungary. — Proceedings of the Seventh Quadrennial IAGOD Symposium, E. Schweitzerbart'sche Verlagsbuchhandlung.
- VETŐ-ÁKOS, É. 1994: A Közép-Mátrai szinesércesedés genetikai modellje. (Genetic model of the Middle Mátra base metal mineralization.) — Magyar Geológiai Szolgálat Országos Földtani és Geofizikai Adattára, Kézirat (Unpublished report in Hungarian).
- VETŐNÉ-ÁKOS, É. 1996: Leíró genetikai modellek: A. Börzsöny hegység. 1. Epitermális-telérés, nemes- és szinesércesedés; 2. "Gyenge" porfirós rézércesedés; 3. metasomatikus Pb-Zn (Ag, Au) ércesedés; B. A Gyöngyösorszi szinesércesedés leíró genetikai modellje. (Descriptive genetic models: A. Börzsöny Mountains. 1. Epithermal, vein-type, precious and base metal mineralizations., 2. "Weak" copper porphyry mineralization., 3. Metasomatic Pb-Zn (Ag, Au) mineralization; B. The Gyöngyösorszi base metal mineralization.) — Magyar Geológiai Szolgálat Országos Földtani és Geofizikai Adattára, Kézirat (Unpublished report in Hungarian).
- VETŐ-ÁKOS, É. 1999: Alpine deposit models for the Mátra and Börzsöny Mountains, northern Hungary. — *Geologica Hungarica Series Geologica* 24: 63–77.
- WANTY, R. B.—BERGER, B. R.—PLUMLEE, G. S. 1999: Environmental models of mineral deposits — a state of the art. — *Geologica Hungarica Series Geologica* 24: 97–106.
- ZELENKA, T.—CSONGRÁDI, J. 1995: Genetic model of gold mineralization in the Tokaj Mts. (NE-Hungary), — Volume of Abstracts, XV. Congress of the Carpatho-Balkan Geological Association, September 17–20, Athens, Greece.
- ZELENKA, T. 1997a: A nemesfémek kutatásának története a Kárpát-medencében. (Precious metal ore exploration in the Carpathian Basin — a historic review.) — *Földtani Kutatás*, 34(1): 4–8. (In Hungarian).
- ZELENKA, T. 1997b: Nemesfém ércesedési modellek összehasonlítása Tokaj-hegységi példákon. (A comparison of noble metal mineralization models: Case studies of Tokaj Mts.) — *Földtani Kutatás*, 34(4): 15–20. (In Hungarian).

LÁSZLÓ KÖRPÁS and ALBERT H. HOFSTRA editors:

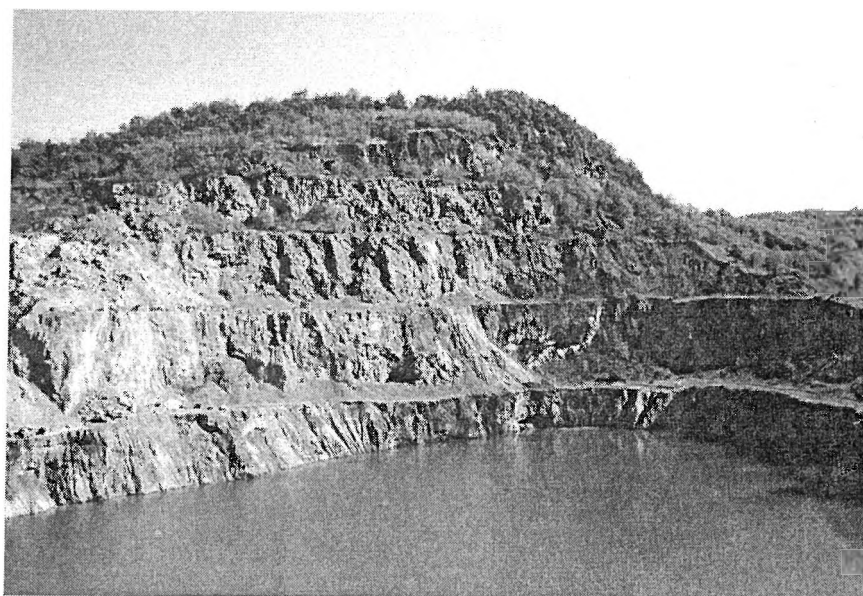
CARLIN GOLD IN HUNGARY



Participants of the project
(from left to right: ALBERT H. HOFSTRA, JOEL S. LEVENTHAL, JÁNOS HAAS and ISTVÁN HORVÁTH)
(L. KÖRPÁS, 1995)



Betze Post gold deposit in Nevada, central part of the open pit
(L. KÖRPÁS, 1995)



Rudabánya iron ore deposit in Hungary, Vilmos open pit
(L. KÖRPÁS, 1995)

POTENTIAL FOR CARLIN-TYPE GOLD DEPOSIT IN HUNGARY

LÁSZLÓ KORPÁS¹ and ALBERT H. HOFSTRA²

¹Geological Institute of Hungary, H-1143 Budapest, Stefánia út 14., Hungary

²US Geological Survey, P. O. Box 25046, Denver, CO 80225, USA

ABSTRACT

The project No. 435 of the US-Hungarian Science and Technology Joint Fund, entitled “Potential for Carlin-type gold deposit in Hungary” was carried out between 1995 and 1998 by the researchers of the Geological Institute of Hungary and the US Geological Survey. It aimed at the estimation of the Carlin gold potential of Hungary. The results of the project were published in this special issue and are described in the papers cited below.

1. MODEL OF CARLIN-TYPE GOLD DEPOSITS

Discovery, increasing exploration and exploitation of the large Carlin-type gold deposits during the last 30 years in many countries of the world resulted in even more detailed understanding and modeling of ore forming processes. The paper of HOFSTRA gives an excellent overview about sizes, mineralizations, ore grade, and reserves of these gold deposits. On examples of the type-localities Carlin Trend and Battle Mountain–Eureka Trend, Nevada were described by him the general features of large scale and long term geologic-tectonic processes, controlling the mineralization. Analysis of the mineral association and transfer-processes has led to the reconstruction and modeling of huge hydrothermal fluid systems operating in deep crustal levels. The paper includes a brief summary concerning rational geochemical and geophysical methods of exploration and is completed by an extense and upto date source of references.

2. THE DEVELOPMENT OF THE CARLIN GOLD PROJECT IN HUNGARY

Hungary's last project on ore exploration of the century was aimed at the estimation of the Carlin gold potential of the country. Since this type of gold mineralization was unknown earlier the paper of KORPÁS, HOFSTRA, ÓDOR, HORVÁTH, HAAS and LEVENTHAL offers a good overlook about data and scientific base, from where started the geochemical exploration in 1995. A preliminary screening resulted in selection of 97 formations was followed by their systematic rock chip sampling representing almost 1400 samples from 604 sample sites. This sampling was completed by a complimentary stream sediment survey. Both type of samples were analyzed for Carlin suite elements (Au, Ag, As, Sb, Hg and Tl) at the Laboratory of the Geological Institute of Hungary.

The paper of BERTALAN and BARTHA presents the good analytical background for both geochemical methods in gold prospection. They describe the applied techniques (AAS, ICP-MS, ICP-OES) including instruments, processes and methods of digestion and analysis, precision and detection levels of the elements. Comparison on sensibility and precision of different analytical methods have given good results.

3. GEOLOGICAL AND TECTONIC MODELS

Success of an exploration could be strongly influenced by the concept and reality of the applied geological and tectonic models. From this point of view Hungary is a rather well studied country because of its high grade of

geological exploration. Large scale geologic and tectonic processes play an important role in the formation of Carlin gold deposits. Consequently the goal of the paper of HAAS, HÁMOR and KORPÁS is to reconstruct the main stages of evolution and paleotectonic settings which were permissive for the occurrence of massive disseminated gold deposits. Paleozoic and Mesozoic rifting, subduction and collision overprinted by a Paleogene subduction and collision are considered favorable situations.

4. THE CARLIN GOLD POTENTIAL OF HUNGARY

The final results of Carlin gold exploration are discussed in details by the paper of KORPÁS, HOFSTRA, ÓDOR, HORVÁTH, HAAS and ZELENKA. The systematic evaluation of the prospected areas and formations led to the estimation of a rather modest Carlin gold potential for Hungary. This potential is hosted mainly in Paleozoic, Early Mesozoic subordinately in Young Mesozoic and Paleogene formations. The anomalous and subanomalous groups of formation are located in favorable geologic and tectonic settings of rifting, subduction and collision and in related master faults and shear zones. From almost hundred formations 18 show subanomalous (10-100 ppb Au) and anomalous (> 100 ppb Au) gold values. Ten predictive areas of 3 to 190 km² were recommended by them for further explorations. Two of them in the Velence Hills and in the Rudabánya Mountains is considered promising.

To this latter one has contributed the study of HOFSTRA, KORPÁS, CSALAGOVITS, JOHNSON and CHRISTIANSEN presenting new isotopic data and genetic model of the Rudabánya Iron Ore. The ore deposit formed during the Middle Triassic rifting in the mixing zone of ascending acidic, basinal brines rich in Fe, base metals and sulfate and of the descending indigenous ground waters rich in Ba and H₂S.

5. CONCLUSIONS

The main result of our work lies in that we have confirmed the previous expectations done in the project description: "a.....proposal will be prepared for further study of the selected 2-5 zones" (KORPÁS and HOFSTRA 1994). Although Hungary's Carlin gold-potential is rather modest, still we have recommended ten areas for further explorations and two of them seems to promise good perspectives.

The value of the research includes some more aspects: 1) The successful collaboration of researchers from the Geological Institute of Hungary and the United States Geological Survey has been resulted not only in exchange of knowledges and experiences but in common publication of these volume. 2) The issue, the first one in the 10 year long history of the US-Hungarian Science and Technology Joint Fund should be considered as a reference-work for all participating institutions and noted in the international field of geosciences too. 3) The common work has contributed to the better understanding of style of working and thinking of researchers from different continents and to the creation of new friendships.

6. ACKNOWLEDGEMENTS

We would like to express our gratitude to Dr. Dóra GROÓ, manager director of the US-Hungarian Science and Technology Joint Fund in Hungary for her help in realisation of the project and in edition of this special issue.

7. REFERENCES

- BERTALAN, É.–BARTHA, A. 1999: Analytical background of Carlin-type gold prospection in Hungary. — *Geologica Hungarica Series Geologica* 24: 169–178.
- HAAS, J.–HÁMOR, G.–KORPÁS, L. 1999: Geological setting and tectonic evolution of Hungary. — *Geologica Hungarica Series Geologica* 24: 179–196.
- HOFSTRA, A. H. 1999: Descriptive model of Carlin-type gold deposit. — *Geologica Hungarica Series Geologica* 24: 137–150.
- HOFSTRA, A. H.–KORPÁS, L.–CSALAGOVITS, I.–JOHNSON C. A.–CHRISTIANSEN, W. D. 1999: Stable isotopic study of the Rudabánya iron mine. A carbonate-hosted siderite, barite, base-metal sulfide replacement deposit. — *Geologica Hungarica Series Geologica* 24: 295–302.
- KORPÁS, L.–HOFSTRA, A. 1994: Potential for Carlin-type gold deposits in Hungary. Carlin gold in Hungary. — Project JFNo 435. US–Hungarian Joint Fund, Budapest.

- KORPÁS, L.–HOFSTRA, A. H.–ÓDOR, L.–HORVÁTH, I.–HAAS, J.–LEVENTHAL, J. 1999: The Carlin gold project in Hungary (1995-1998). — *Geologica Hungarica Series Geologica* 24: 151–167.
- KORPÁS, L.–HOFSTRA, A. H.–ÓDOR, L.–HORVÁTH, I.–HAAS, J.–ZELENKA, T. 1999: Evaluation of the prospected areas and formations. — *Geologica Hungarica Series Geologica* 24: 197–293.

DESCRIPTIVE MODEL OF CARLIN-TYPE GOLD DEPOSITS

ALBERT H. HOFSTRA

US Geological Survey, P. O. Box 25046, Denver, CO 80225, USA

1. INTRODUCTION

The goal of this study is to provide a list of the physical and chemical attributes of Carlin-type gold deposits useful for prospect evaluations and mineral resource assessments. The information is compiled from the literature and my own research. Although some of the information is controversial, most is generally accepted.

2. OVERVIEW

Carlin-type deposits are epigenetic, disseminated, gold deposits that are typically hosted in calcareous sedimentary rocks. The deposits are known mainly in northern Nevada and northwestern Utah where they are arranged in clusters and belts (Fig. 1). The deposits in this region are estimated to contain about 5000 tons of gold, more than half of which resides in the Carlin Trend (~3100 tons). Approximately 1500 tons of gold has been produced. Carlin-type deposits are frequently called as sediment-hosted disseminated gold, sediment-hosted micron gold or invisible gold as synonyms.

They are spatially associated with syngenetic barite deposits and related base-metal occurrences, porphyry Cu-Mo-Au deposits, volcanic-hosted precious-metal deposits, or epithermal mercury, stibnite, or barite vein occurrences. Temporally associated deposit types include porphyry Cu-Mo-Au deposits and volcanic-hosted epithermal Au-Ag deposits.

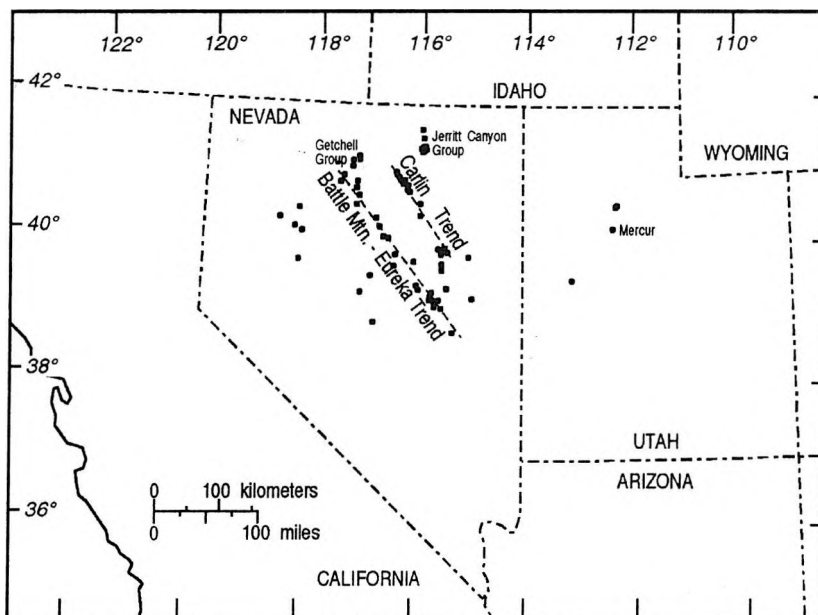


Fig. 1: Location map

Two ore types, the refractory ore and the oxide ore are exploited. Most of the gold in refractory ore occurs in arsenian pyrite, arsenian marcasite, or arsenopyrite. The sulfides are oxidized in the mill so that gold can be recovered by cyanide carbon in leach methods. Some of the ore is refractory because it contains organic carbon that can rob gold from cyanide solutions in which case the carbon must be deactivated before entering the carbon in leach circuit in the mill. Natural weathering and oxidation of refractory ores results in the formation of oxide ores with low sulfide and organic carbon contents that are suitable for gold recovery by cyanide heap leach methods.

Average ore grades in individual deposits range from 0.6 to 22 g/t. The lowest grades are in open pit mines that exploit oxide ore. Underground mines have higher average grades because of the higher costs associated with development of underground workings and processing of refractory ores. The ore tonnage of discrete deposits may range over 200,000,000 t or less than 100,000 t, and may contain as much as 1000 t of gold or less than 1 t of gold. Most of the deposits contains between 10 and 100 t of gold.

The host rocks of the deposits are Cambrian to Triassic in age, although more than half of the deposits is in Devonian sediments. Most of the deposits are in platform margin or intraplatform calcareous sediments, but some are hosted in oceanic deep marine siliciclastic sequences. Ore locally occurs in Jurassic to Mid-Tertiary igneous rocks and contact metamorphic rocks. Fig. 2 shows the distribution of gold ore through the stratigraphic sequence in the Carlin Trend.

The age of the deposits is very difficult to estimate because they contain few datable minerals, cogenetic with the gold. The age constraints are mainly of two types, those provided by cross cutting relationships with dated igneous rocks, and those provided by isotopic dates on sericite. Sericite separated from mineralized sedimentary and igneous rock yields a wide range of old dates that at best place an older limit on gold mineralization. These dates are not very meaningful because they are from incompletely reset pre-ore micas or from mixtures of pre-ore and ore-stage mica. The isotopic dates from igneous rocks constrain the age of several deposits to between 42 and 32 Ma. Hydrothermal adularia from one deposit has been dated at 42.0 Ma. Supergene alunite is 30 Ma or younger. The deposits are therefore Mid-Tertiary in age (42-30 Ma).

Concerning the tectonic setting of the deposits regional scale tectonic and magmatic processes were required to drive these systems. The deposits are located in the backarc of the North American Cordillera; a region that in the Mid-Tertiary was characterized by high regional heat flow, widespread calcalkaline magmatism, and crustal extension. However, there is not a one-to-one spatial correspondence between the deposits and volcanic centers or epizonal plutons which has made it difficult to determine the relation between the deposits and magmatism.

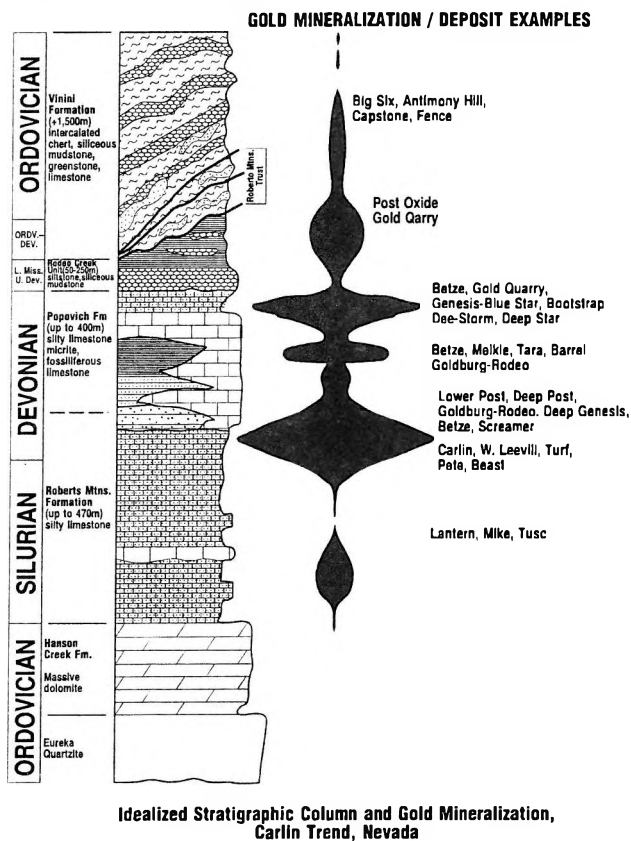


Fig. 2: Idealized stratigraphic column and gold mineralization, Carlin Trend Nevada (TEAL and JACKSON 1997)

3. ORIGIN OF THE CARLIN TREND AND BATTLE MOUNTAIN-EUREKA TREND

The NNW striking Carlin Trend is 60 km long and is defined by more than 40 gold deposits. The Battle Mountain-Eureka Trend also strikes NNW is more than 80 km long and is defined by over 20 gold deposits. At the surface, the trends are manifest by a complex array of faults, folds, and igneous intrusions suggesting that they are zones of weakness in the crust. Gravity gradients and Sr and Pb isotopic variations of granitic intrusions in the region indicate that the trends developed along major crustal discontinuities. Magnetotelluric surveys across the trends show that they are underlain by deep penetrating fault zones. These faults may have originated as normal faults during late Proterozoic rifting of the continental margin and appear to have influenced subsequent patterns of sedimentation, deformation, magmatism, and hydrothermal activity. Most of the deposits in the Carlin Trend, Battle Mountain-Eureka Trend, and Jerritt Canyon district are in the lower plate of the Roberts Mountains thrust that placed oceanic deep marine siliciclastic rocks on top of silty carbonate rocks of the platform margin. The deposits are exposed in tectonic windows through the allochthon. The windows commonly reflect antiformal structures or tilted fault blocks. Recent discoveries adjacent to the windows have been found by drilling through the allochthon.

The ore deposits are preferentially localized in permeable and reactive rocks that focused fluid flow. The primary permeability controls are faults and fault intersections that were feeders for ascending hydrothermal fluids. Secondary permeability controls influenced flow away from feeders and include permeable strata, breccias, thrust faults, joint sets, anticlines, and igneous intrusions. Breccia types include sedimentary debris flows and breccias, solution collapse breccias, and fault breccias. The deposits are commonly overlain by less permeable rocks that acted as a caprock (e.g. Roberts Mountains allochthon). Chemically favorable host rocks are those that contain carbonate and iron-bearing minerals. Dissolution of carbonate increases permeability allowing continued influx of ore fluids. Sulfidation of reactive iron-bearing minerals consumes H_2S causing gold to precipitate. Many deposits are localized along faults where ascending ore fluids encountered less permeable caprocks and were forced to move laterally through permeable and reactive rocks below the cap rock. Fig. 3 shows the distribution of ore deposits in the northern Carlin Trend relative to major faults and Jurassic intrusions. Ore controls for several deposits in the Carlin Trend are illustrated on Figs. 4–10; Fig. 11 summarizes the relative importance of various ore controls on deposits in the Carlin Trend.

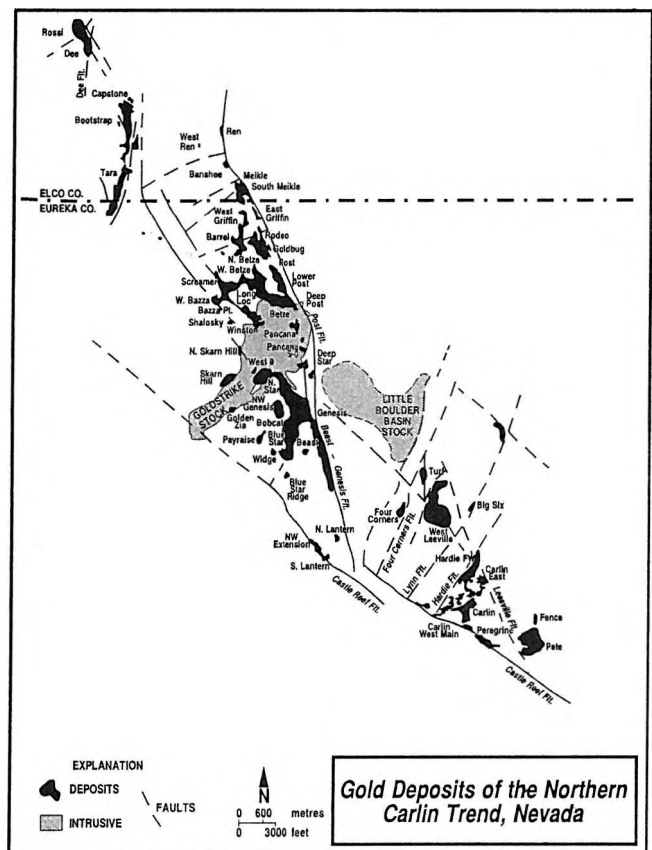


Fig. 3: Gold deposits of the Northern Carlin trend (TEAL and JACKSON 1997)

The geometry of the ore deposit varies as a function of the predominant ore controls (e.g. stratigraphy=tabular and stratiform, fault=tabular discordant, breccia pipe =carrot shaped, joint sets=irregular stockwork)

4. MINERAL ASSOCIATION AND TRANSFER

The hydrothermal mineral assemblage of the ores consists of ore minerals (arsenian pyrite, arsenian marcasite, arsenopyrite, realgar, orpiment, stibnite, cinnabar and thallium sulfides with native gold and arsenic), accompanied by silicates (quartz, kaolinite, illite-smectite, montmorillonite, rare adularia), carbonates (calcite, dolomite, ± ankerite, ± siderite), phosphates (rare apatite), sulfates (barite), oxides (rutil, leucoxene) and some halides (fluorite).

The supergene ore minerals are composed of goethite, hematite, pyrolusite, scorodite, stibiconite and native gold in association with silicates (halloysite and other clay minerals), phosphates (variscite, wawellite and others), sulfates (alunite, jarosite, gypsum and melanterite).

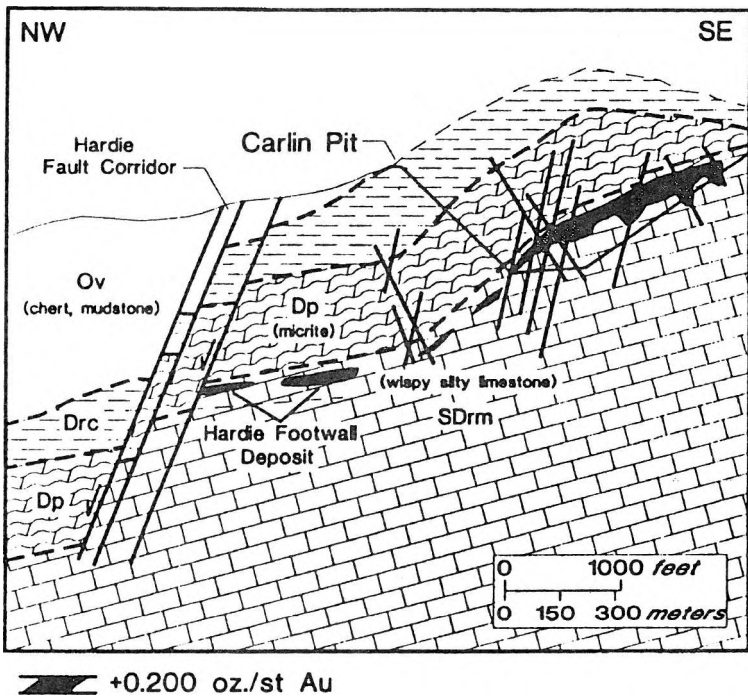
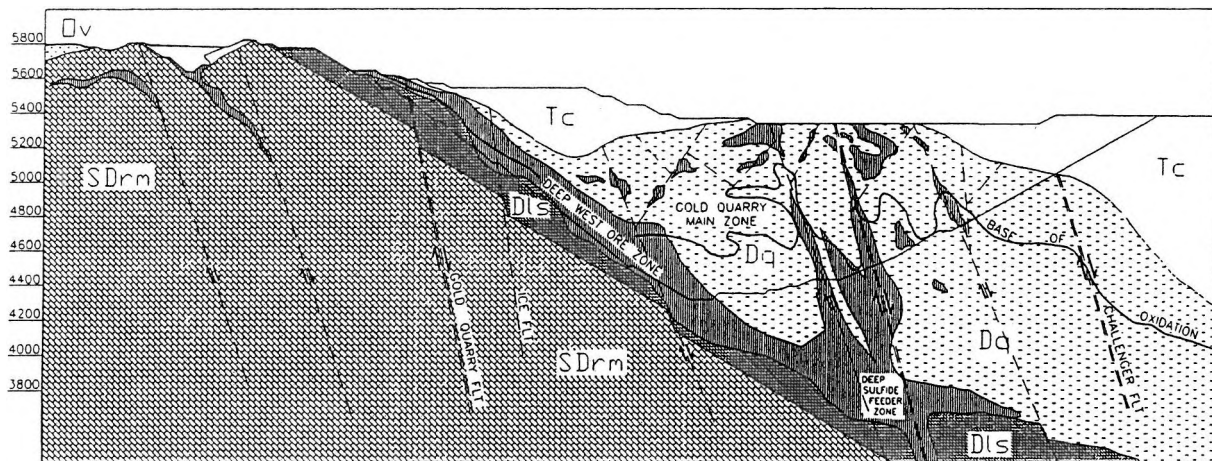


Fig. 4: Cross section of the Carlin and Hardie Footwall deposit (TEAL and JACKSON 1997)
Tc=Tertiary cover; Ov=Vinini Formation; Dp=Popovich Formation; Drc=Rodeo Creek Formation; SDrm=Roberts Mountains Formation

Fig. 5: Cross section of the Gold Quarry deposit (TEAL and JACKSON 1997)
(Legend see on Fig. 4)



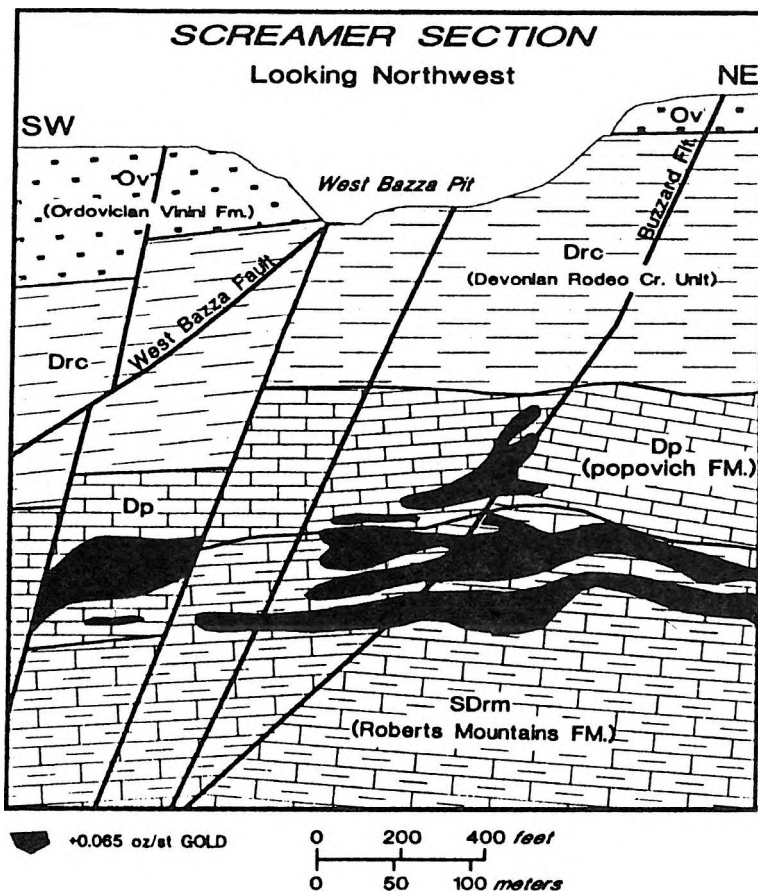


Fig. 6: Cross section of the Screamer deposit (TEAL and JACKSON 1997)

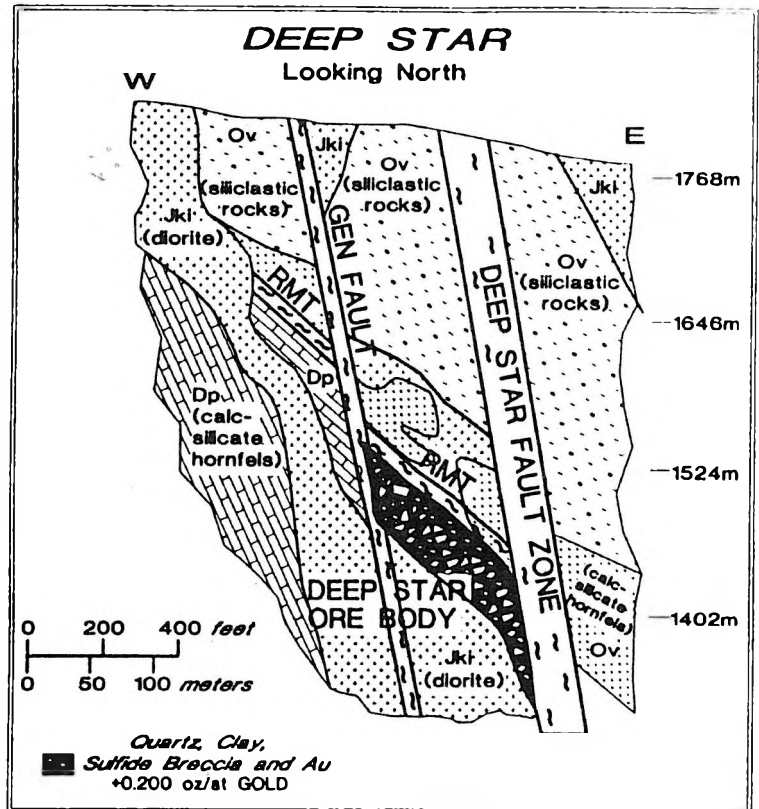


Fig. 7: Cross section of the Turf deposit (TEAL and JACKSON 1997) (Legend see on Fig. 4)

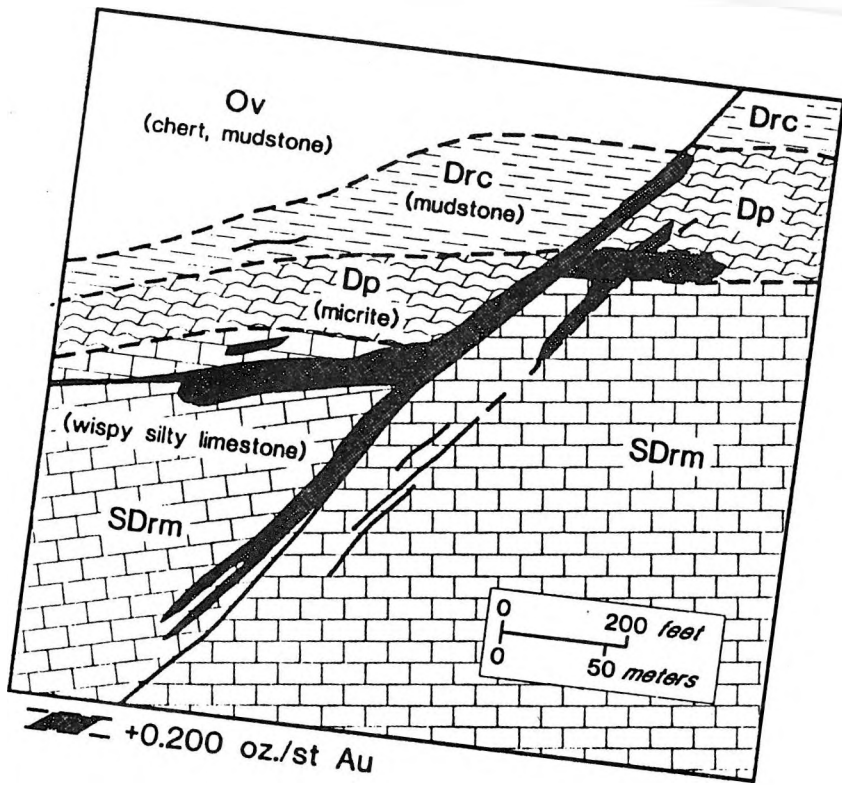


Fig. 8: Cross section of the
(TEAL and JACKSON 1997)
(Legend see on Fig. 4)

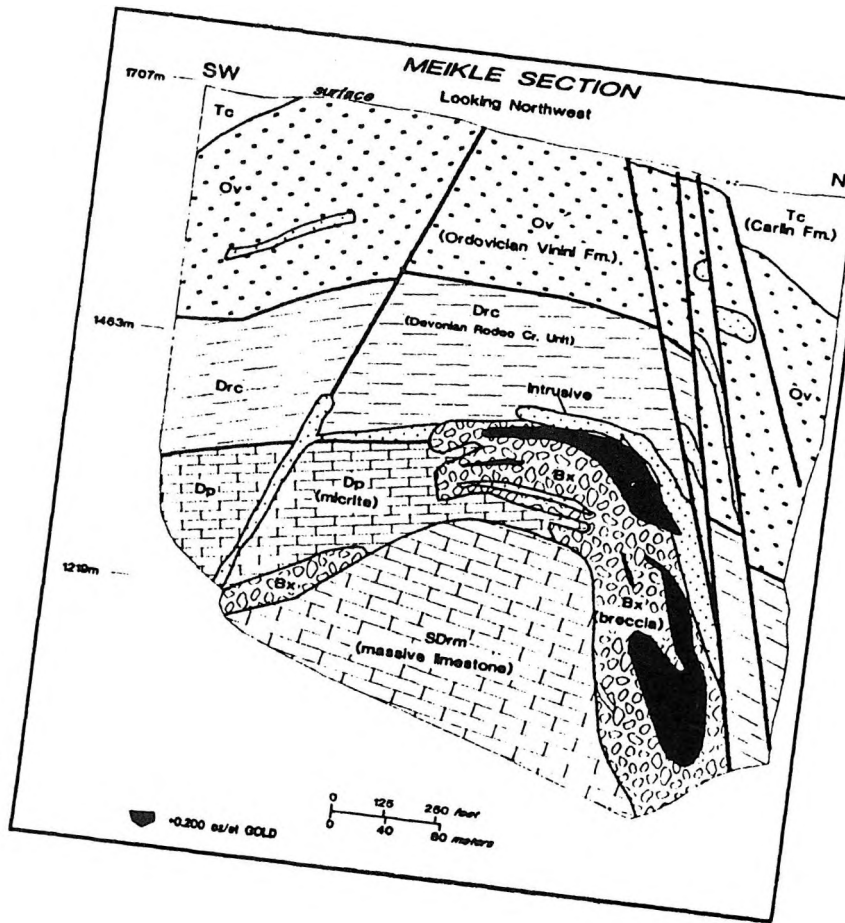
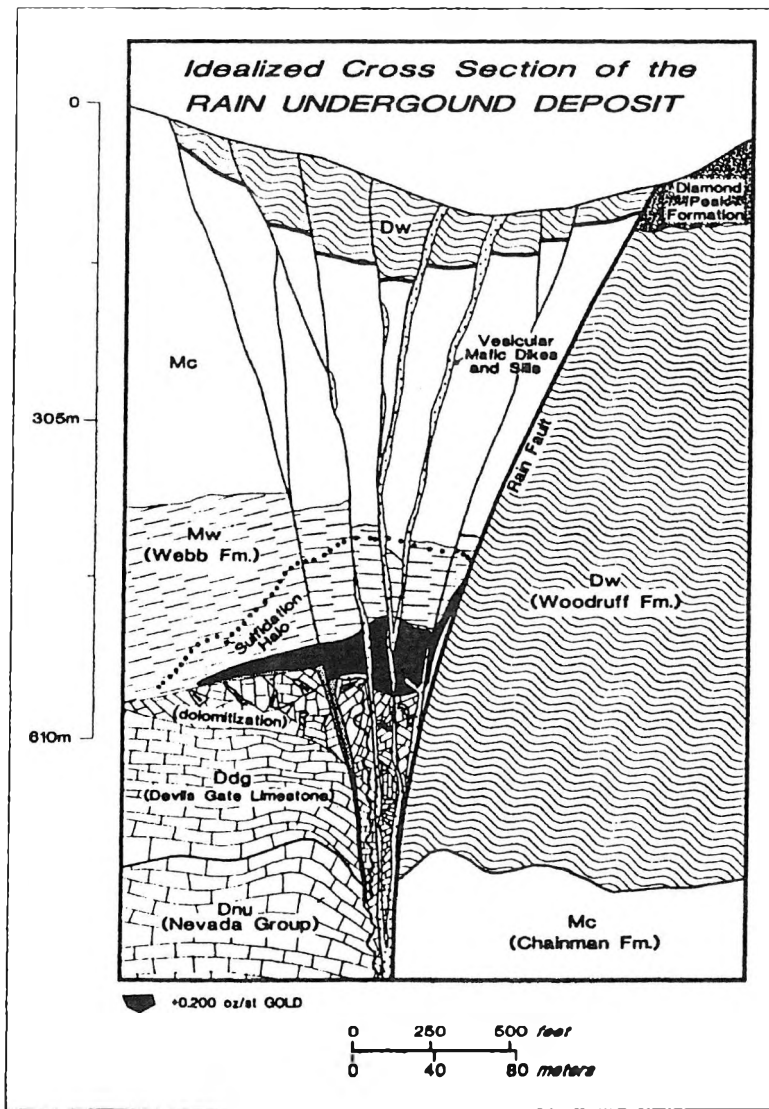


Fig. 9: Cross section of the Deep Star de-
posit (TEAL and JACKSON 1997)
(Legend see on Fig. 4)

Fig. 10: Cross section of the Rain deposit (TEAL and JACKSON 1997)



The mineral texture is represented by ore stage pyrite, marcasite, and arsenopyrite which in the deposits usually occur as small 1 mm to 1 micron disseminations or overgrowths on preexisting diagenetic pyrite. Orpiment, realgar, stibnite, cinnabar, calcite, and barite generally fill open spaces in fractures and breccias. Late botryoidal pyrite and marcasite line open spaces in fractures and breccias.

The gold is invisible and occurs primarily in arsenian pyrite as submicron sized grains of native gold and as Au⁺ in the pyrite lattice. Arsenian pyrite also contains elevated concentrations of thallium, antimony, and mercury. Gold and trace elements occur in a similar fashion in arsenian marcasite and arsenopyrite. The ores contain 0.5 to 10% pyrite (marcasite or arsenopyrite) with gold concentrations of 200 to 5,000 ppm. Gold has also been observed in quartz, dolomite, clays, organic carbon, cinnabar, and barite. In oxidized ores native gold is larger and usually occurs as 1 micron to 1 mm sized grains in limonite.

The host rocks of the deposits locally contain several percent organic carbon. The carbon is either indigenous to the host rock or was introduced as liquid petroleum. In some deposits, the organic carbon was metamorphosed into cryptocrystalline graphite with 30-150 angstrom crystal domains prior to gold mineralization. Both types of carbon are concentrated by dissolution of the carbonate host rocks. In rocks that contain immature organic matter, the thermal maturity of organic carbon increases in ore zones. In rocks that contain thermally mature carbon, the thermal maturity of organic carbon is the same within and outside the deposit. There is no consistent relationship between the amount of carbon in the host rocks and gold grades. Organic carbon does not appear to have played a major role in mineral precipitation.

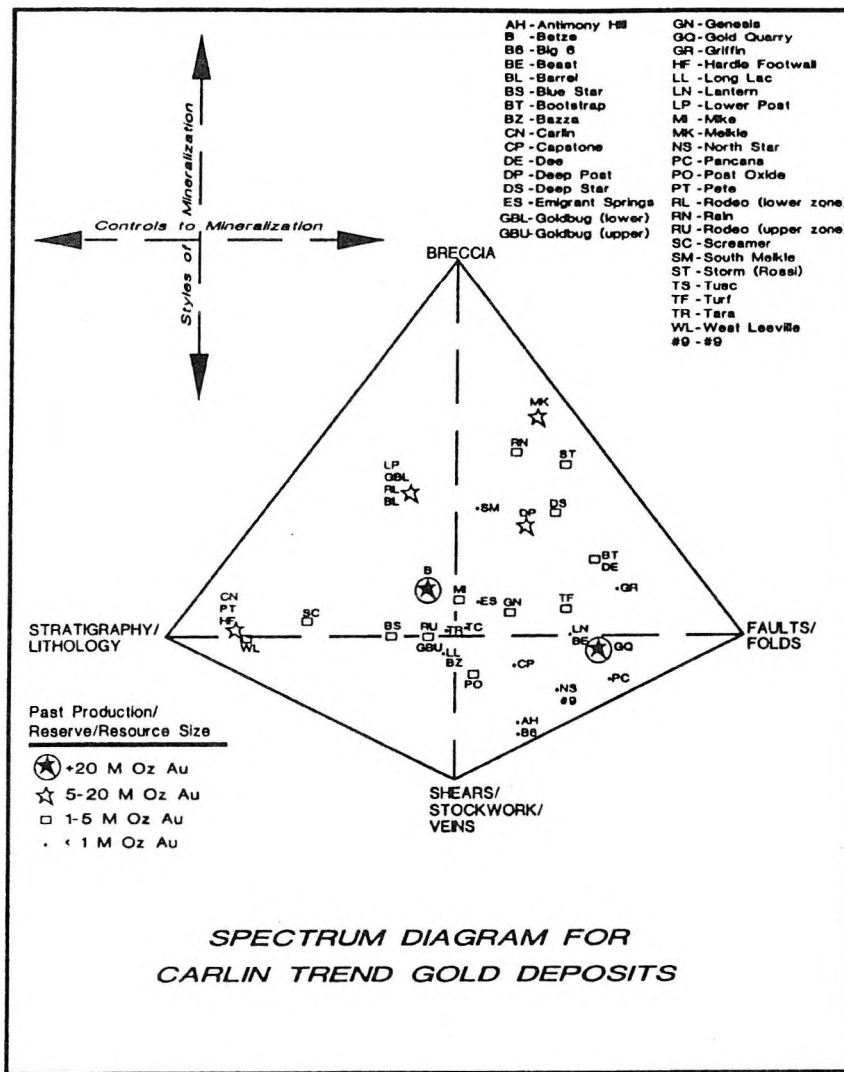


Fig. 11: Factors of ore control, Carlin Trend gold, Nevada (TEAL et al. 1997 in TEAL and JACKSON 1997)

The main alteration types are silicification, argillization, carbonate dissolution and sulfidization of iron-bearing minerals. Sometimes K-metasomatism of silicates also may occur. The silicification of carbonates is common, but its spatial correlation to mineralization is erratic. In some deposits silicification is best developed in feeder zones while in others it can occur above, below, beside, in, or away from ore zones. Igneous rocks are less often silicified. Argillization of silicates is best developed in igneous rocks, hornfels, skarn, and sedimentary rocks containing detrital feldspar. Preexisting illite in the host rocks is relatively resistant to argillization and often persists when other silicate minerals are argillized. The carbonate dissolution is very common resulting in increased porosity, volume loss, concentration of insoluble minerals, and formation of solution collapse breccias. The sulfidization of iron-bearing minerals is very important and results in the formation of disseminated arsenian pyrite, arsenian marcasite, or arsenopyrite which contain the bulk of the gold in the deposits. Ferroan calcite and dolomite are probably the principle iron-bearing minerals in the host rocks although iron bearing clays, phosphates, and oxides may also be sulfidized. The K-metasomatism of silicates is rare and was manifested by the presence of adularia only in one single district.

The minerals are distributed in proximal to distal zoning which is reflected in the following (proximal → distal). Carbonates: carbonate absent → dolomite → calcite±siderite±ankerite. Silicates: dickite or kaolinite → illite/smectite, ±illite → montmorillonite → feldspars, amphibole, biotite, pyroxene. Organic matter: mature → immature. Sulfides: arsenian pyrite or marcasite → arsenopyrite → iron bearing carbonates, silicates, phosphates, oxides, and pyrrhotite. Sulfates: preexisting barite is relatively unaffected by ore fluids. Phosphates: diagenetic apatite is dissolved in proximal ore zones, igneous apatite is resistant to ore fluids. Oxides: leucoxene → preexisting ilmenite and Ti-bearing silicates.

The introduced elements of the mass transfer are represented by $\pm\text{Si}$, S, Au, As, Sb, Hg, Tl, Ag, Ba, $\pm\text{Te}$, $\pm\text{Se}$ and $\pm\text{W}$, while CO_3 , Ca, Sr, Na, $\pm\text{Mg}$, $\pm\text{K}$ are considered to be depleted. Among the immobile elements (Al, Ti, $\pm\text{Fe}$, $\pm\text{Si}$, $\pm\text{K}$) plays the Fe an important role in the setting of introduced Au, As, and sulfur. This indicates that the disseminated iron sulfides formed by sulfidation of host rock iron. Sulfidation decreases the H_2S concentration of the ore fluids causing gold to precipitate.

5. METHODS OF EXPLORATION

Geochemical assaying is generally applied as first step on exploration. Beside the main elements of Au and Ag, pathfinder elements like As, Sb, and Hg are ubiquitous, with $\pm\text{Tl}$, $\pm\text{W}$. Reconnaissance stream sediment sampling is used to discriminate between areas of high and low potential. In stream sediments, As, Sb, and Hg are usually more widespread than Au. The major districts and trends are readily outlined by As anomalies in stream sediments. Rock chip and soil surveys are used to define surface mineralization and detect mineralized structures and stratigraphy. In soil and rocks chips, As, Sb, and Hg usually form broader higher contrast anomalies than Au. Ground water in the vicinity of the deposits has elevated concentrations of As, and other trace elements.

Geophysical methods can be used in delineation of the trends and ore districts. Regional gravity data indicates that the Battle Mountain–Eureka trend lies along a major crustal discontinuity. Magnetotelluric surveys across the Carlin Trend and Battle Mountain–Eureka Trend indicate that both trends are underlain by deep penetrating structures. These structures served to localize intrusions of Jurassic, Cretaceous, and Tertiary age; some of which are apparent on regional aeromagnetic maps. Geophysical methods generally cannot be used to directly detect gold ores. However, satellite and airborne multispectral data are helpful in defining major lithologic boundaries, structural zones, and areas of hydrothermal alteration (e.g. silicification). Ground magnetic and various electromagnetic methods may be used to map high or low angle faults, fractures, and highly permeable altered zones that may have served as conduits for ore fluids. Electrical resistivity methods are able to delineate hydrothermal alteration and fault zones as a resistivity low and silicification as a high. Electrical and seismic methods can be employed to determine the depth to bedrock or the location of permeable and impermeable beds. The organic carbon in the host rocks is the dominant source of anomalies observed by electrical methods. The induced polarization method can be used to estimate the percent sulfide in the ores if the carbon content is low. It can also be used to locate the boundary between oxide and refractory ores due to the lack of organic carbon and sulfide in the oxide ores.

6. GENESIS AND MODEL OF THE DEPOSITS

Fluid inclusions data indicate temperatures from 150° to 250 °C of the ore fluids, having a salinity 0 to 6 eq. wt. % NaCl. Among the gas phases CO_2 is predominant (1-10 mole %), H_2S minor but ubiquitous (10^{-2} to 10^{-1} molal), with $\pm\text{N}_2$ and $\pm\text{CH}_4$ in minor quantity. Estimated pressure ranges between 1 to 3 kbars, corresponding to a depth of 1 to 5 km.

Moderately acidic pH (4.0 to 5.5) of ore fluids is indicated by the presence of marcasite and kaolinite and by the dissolution of dolomite. High H_2S -concentrations ($\log f\text{H}_2\text{S} = -1$ to -2) in ore fluids are shown by the common occurrence of high sulfidation state minerals such as orpiment and realgar. Mass transfer studies prove that sulfur was one of the most abundant elements introduced by the hydrothermal fluids, while gas analyses of fluid inclusions indicate that the fluids contained 10^{-1} to 10^{-2} m H_2S . Low $f\text{O}_2$ ($\log f\text{O}_2 = -39$ to -43) is indicated by the predominance of CO_2 over CH_4 , the presence of graphitic carbon, the absence of magnetite and hematite, the narrow $f\text{O}_2$ for realgar and orpiment at the given $f\text{H}_2\text{S}$, and the low SO_4 content of ore stage fluids.

Stable isotope studies on fluid inclusions and clay minerals show that Mid-Tertiary meteoric water in this region had δD values between -160 and -120‰ and $\delta^{18}\text{O}$ values of -21 to -16‰ . In most deposits, hypogene kaolinite and water extracted from fluid inclusions have δD values between -160 and -110‰ and $\delta^{18}\text{O}$ values of -20 to 10‰ . The low δD and variable $\delta^{18}\text{O}$ values are consistent with a meteoric origin for the water. However, the deposits in the Getchell district have an enormous range of δD values between -155 and -40‰ and $\delta^{18}\text{O}$ values of -20 to $+15\text{‰}$. The high δD and $\delta^{18}\text{O}$ values require the presence of a deep sourced magmatic or metamorphic fluid. *Quartz* – The $\delta^{18}\text{O}$ compositions of ore stage jasperoid and quartz veins range from 1 to 26‰. The broad range of values requires mixing between a high $\delta^{18}\text{O}$ fluid and low $\delta^{18}\text{O}$ unexchanged meteoric water. Gold was transported by the high $\delta^{18}\text{O}$ fluid. Fluid mixing was probably common in these systems and took place where as-

ascending ore fluids displaced indigenous ground waters in the host rocks. *Organic matter* – The organic carbon in the host rocks has low $\delta^{13}\text{C}$ values of -34 to -21‰ that are typical of sedimentary organic matter. Bitumen has $\delta^{13}\text{C}$ values a few permil less than the indigenous organic matter in the rocks. *Calcite and dolomite* – Calcite and dolomite in unaltered host rocks have a broad range of $\delta^{13}\text{C}$ and $\delta^{18}\text{O}$ compositions between about -8 to 3‰ and 22 to 28‰ respectively. The $\delta^{13}\text{C}$ and $\delta^{18}\text{O}$ values of calcite and dolomite in strongly altered rocks are restricted to a much narrower range between -4 to 2‰ and 7 to 13‰ respectively. Ore stage calcite veins have $\delta^{13}\text{C}$ values of -5 to 3‰ and extend to $\delta^{18}\text{O}$ values as low as 1‰ . The high $\delta^{13}\text{C}$ values of ore related carbonates indicate that only a very small proportion of the CO_2 in ore fluids could have been derived from oxidation of organic matter or hydrocarbons. The data permit that the ore fluid consisted of isotopically evolved meteoric water but cannot exclude other possibilities. *Barite* – The $\delta^{34}\text{S}$ and $\delta^{18}\text{O}$ values for barite cover a huge range from 5 to 40‰ and -7 to 15‰ . The large range requires more than one source of sulfate. The sulfate in the isotopically heavy barites was probably derived from dissolution of the sedimentary barite in the rocks. The lower $\delta^{18}\text{O}$ values are indicative of meteoric water. The lower $\delta^{34}\text{S}$ values suggest that some of the sulfate was derived from either the oxidation of H_2S in ore fluids or from the oxidation of preexisting sedimentary or hydrothermal sulfides. Many samples have intermediate $\delta^{34}\text{S}$ values and probably contain mixtures of sulfate derived from each end member. *Sulfides* – The $\delta^{34}\text{S}$ composition of ore stage pyrite, marcasite, and arsenopyrite is mainly between 0 and 24‰ . Orpiment, realgar, and stibnite are mainly between -3 and $+17\text{‰}$. The calculated isotopic composition of H_2S in the ore fluids using a temperature of 225 °C is between 0 and 20‰ with a mode at 10‰ . This range is within that of sedimentary pyrite and organosulfur sources in lower Paleozoic sedimentary rocks. The highest $\delta^{34}\text{S}$ values suggest that some H_2S came from thermochemical or inorganic reduction of sedimentary sulfate; barite being the most abundant and likely source of sulfate in the rocks. The entire range of $\delta^{34}\text{S}$ values from the deposits is consistent with derivation of H_2S from sedimentary or metasedimentary sources. The lowest $\delta^{34}\text{S}$ values allow (but do not require) that some H_2S came from magmatic fluids or from preexisting magmatic sulfides. The source of H_2S is very important because gold was transported as a bisulfide complex.

Processes and model of ore formation will be outlined in the following. Ascending ore fluids were apparently impeded by impermeable caprocks at depths of 1 km or more where they moved laterally away from feeder zones and were dispersed into local ground water. Increased interactions between the acidic CO_2 - and H_2S -rich ore fluids and the host rocks in these zones resulted in carbonate dissolution, volume loss, increased porosity, argillization of silicate minerals, sulfidation of host rock iron to form arsenian pyrite, arsenian marcasite, or arsenopyrite, and precipitation of gold. Cooling of fluids resulted in silicification of carbonates and precipitation of orpiment and realgar in open spaces. Mixing with indigenous ground waters with elevated iron content may also have contributed to gold precipitation. The CO_2 liberated by dissolution of carbonate may have lead to transient fluid over pressures, boiling, and precipitation of calcite in open spaces. Precipitation of gold may also have been promoted by boiling.

To concentrate $\sim 5,000$ tons of gold from the background levels in the crust requires the development of large hydrothermal systems. The energy required to drive these systems is also large. Regional scale tectonic and magmatic processes were probably required. The large number of similarities among Carlin-type deposits suggests they have common origins and formed in response to a single event. The most reliable isotopic dates constrain the age of many deposits to between 42 and 30 Ma . The deposits probably formed over a period of about 10 Ma soon after the onset of extension and magmatism in northern Nevada and NW Utah. The increased permeability and high heat flow in this setting may have provided the drive for deep circulation of meteoric water and development of Carlin-type deposits in fracture systems that focused fluid flow. If these structures penetrated to mid-crustal levels, they may also have tapped metamorphic fluids generated in the middle crust or magmatic fluids released from deep intrusions or batholiths. However, if extensional faulting and regional magmatism were all that was required to produce Carlin-type deposits they should be present in similar tectonic settings to the north and south. As yet, none have been recognized. Apparently additional factors were critical to the formation of Carlin-type deposits. Current research is directed towards improving constraints on the age of the deposits and identifying the critical factors that led to their formation.

7. BIBLIOGRAPHY

- ALBINO, G. V. 1994: Geology and litho-geochemistry of the Ren gold prospect, Elko County, Nevada – the role of rock sampling in exploration for deep Carlin-type deposits. — *Journal of Geochemical Exploration*, 51: 37–58.

- AREHART, G. B. 1996: Characteristics and origin of sediment-hosted disseminated gold deposits: a review. — *Ore Geology Reviews*, 11: 383–403.
- AREHART, G. B.—ELDRIDGE, C. S.—CHRYSSOULIS, S. L.—KESLER, S. E. 1993a: Ion microprobe determination of sulfur isotope variations in iron sulfides from the Post/Betze sediment-hosted disseminated gold deposit, Nevada, USA. — *Geochimica et Cosmochimica Acta*, 57: 1505–1519.
- AREHART, G. B.—FOLAND, K. A.—NAESER, C. W.—KESLER, S. E. 1993b: $^{40}\text{Ar}/^{39}\text{Ar}$, K/Ar, and fission track geochronology of sediment-hosted disseminated gold deposits at Post/Betze, Carlin Trend, northeastern Nevada. — *Economic Geology*, 88: 622–646.
- AREHART, G. B.—KESLER, S. E.—O'NEIL, J. R.—FOLAND, K. A. 1992: Evidence for the supergene origin of alunite in sediment-hosted micron gold deposits, Nevada. — *Economic Geology*, 87: 263–270.
- BAGBY, W. C.—BERGER, B. R. 1985: Chapter 8, Geologic characteristics of sediment-hosted, disseminated precious metal deposits in the western United States. — *Reviews in Economic Geology*, 2: 169–202.
- BAKKEN, B. M.—HOCELLA, M. F. JR.—MARSHALL, A. F.—TURNER, A. M. 1989: High-resolution microscopy of gold in unoxidized ore from the Carlin mine, Nevada. — *Economic Geology*, 84: 171–179.
- BAKKEN, B. M.—EINAUDI, M. T. 1986: Spatial and temporal relations between wall rock alteration and gold mineralization, main pit, Carlin gold mine, Nevada, USA. — in MACDONALD, A. J. (ed.): *Proceedings of Gold '86, an International Symposium on the Geology of Gold: Toronto, Canada*: 388–403.
- BERGER, B. R.—BAGBY, W. C. 1990: The geology and origin of Carlin-type gold deposits. — in FOSTER, R. P. (ed.): *Gold Metallogeny and Exploration*, Blackie and Son Ltd, Glasgow, Scotland.
- BIRAK, D. J.—HAWKINS, R. J. 1985: The geology of the Enfield Bell mine and Jerritt Canyon district, Elko County, Nevada. — *US Geological Survey Bulletin* 1646: 95–105.
- BIRAK, D. J. 1986: Exploration and geologic development of the Jerritt Canyon gold deposits, Elko County, Nevada, USA. — in MACDONALD, A. J. (ed.): *Proceedings of Gold '86, an International Symposium on the Geology of Gold: Toronto, Canada*: 488–496.
- BIRAK, D. J.—DOE T. C.—STEVENS D. L. 1992: North Generator Hill gold deposit, Jerritt Canyon district, Nevada. — in HARTMAN H. L. (ed.): *SME Mining Engineering Handbook, 2nd Edition*: Society for Mining, Metallurgy, and Exploration, Inc., Littleton, Colorado, 1: 366–377.
- BLAKELY, R. J.—JACHENS, R. C. 1991: Regional study of mineral resources in Nevada: Insights from three-dimensional analysis of gravity and magnetic anomalies. — *Geological Society of America Bulletin*, 103: 795–803.
- BROOKS, R. A.—BERGER, B. R. 1978: Relationship of soil mercury values to soil type and disseminated gold mineralization, Getchell mine area, Humboldt County, Nevada. — *Journal of Geochemical Exploration*, 9: 183–194.
- CHRISTENSEN, O. (ed.) 1993: *Gold Deposits of the Carlin Trend, Nevada*. — SEG Guidebook Series, 18: 105 p.
- COYNER, A. R.—FAHEY, P. L. (eds.) 1996: *Geology and Ore Deposits of the American Cordillera, Symposium Proceedings*. — Geological Society of Nevada, Reno, Nevada: 1747 p.
- CUNNINGHAM, C. G.—ASHLEY, R. P.—CHOU, I.—ZUSHU, H.—CHAOYUAN, W.—WENKANG, L. 1988: Newly discovered sedimentary rock-hosted disseminated gold deposits in the People's Republic of China. — *Economic Geology*, 83: 1462–1467.
- DONGSHENG, L.—YUNJIN, T.—JIANYE, W.—LUANLING, L. 1991: Carlin-type gold deposits in China. — *Brazil Gold '91*, E.A. Ladeira, ed., Balkema, Rotterdam: 80–93.
- DREWES—ARMITAGE, S. P.—ROMBERGER, S. B.—WHITNEY, C. G. 1996: Clay alteration and gold deposition in the Genesis and Blue Star deposits, Eureka County, Nevada. — *Economic Geology*, 91: 1383–1393.
- ERICKSON, R. L.—MARRANZINO, A. P.—ODA, U.—JANES, W. W. 1964: Geochemical Exploration near the Getchell mine, Humboldt, county, Nevada. — *US Geological Survey Bulletin* 1198-A: 26 p., 2 pl.
- ERICKSON, R. L.—VAN SICKLE, G. H.—NAKAGAWA, H. M.—MCCARTHY, J. H. JR.—LEONG, K. W. 1966: Gold geochemical anomaly in the Cortez district Nevada. — *US Geological Survey Circular* 534.
- FLEET, M. E.—MUMIN, A. H. 1997: Gold-bearing arsenian pyrite and marcasite and arsenopyrite from Carlin Trend gold deposits and laboratory synthesis. — *American Mineralogist*, 82: 182–193.
- GRANEY, J. R.—KESLER, S. E.—JONES, H. D. 1991: Application of gas analysis of jasperoid inclusion fluids to exploration for micron gold deposits. — *Journal of Geochemical Exploration*, 42: 91–106.
- GRAUCH, V. J. S.—JACHENS, R. C.—BLAKELY, R. J. 1995: Evidence for a basement feature related to the Cortez disseminated gold trend and implication for regional exploration in Nevada. — *Economic Geology*, 90: 203–207.
- GRIMES, D. J.—FICKLIN, W. H.—MEIER, A. L.—MCHUGH, J. B. 1995: Anomalous gold antimony, arsenic, and tungsten in ground water and alluvium around disseminated gold deposits along the Getchell Trend, Humboldt County, Nevada. — *Journal of Geochemical Exploration*, 52: 351–371.

- GROFF, J. A.—HEIZLER, M. T.—MCINTOSH, W. C.—NORMAN, D. I. 1997: $^{40}\text{Ar}/^{39}\text{Ar}$ dating and mineral paragenesis for the Carlin-type gold deposits along the Getchell Trend, Nevada: Evidence for Cretaceous and Tertiary Gold mineralization. — *Economic Geology*, 92: 601–622.
- HAUSEN, D. M.—PARK, W. C. 1986: Observations on the association of gold mineralization with organic matter in Carlin-type ores. — in DEAN, W. C. (ed.): *Organics and Ore Deposits*, proceedings of the Denver Region Exploration Geologists Society: 119–136.
- HAUSEN, D. M.—KERR, P. F. 1968: Fine gold occurrence at Carlin, Nevada. — in RIDGE, J. D. (ed.): *Ore Deposits of the United States, 1933–1967*, v. 1, New York, AIME: 908–940.
- HERAN, W. D.—MCCAFFERTY, A. M. 1986: Geophysical surveys in the vicinity of Pinson and Getchell mines, Humboldt County, Nevada. — US Geological Survey Open-File Report 86–432.
- HERAN, W. D.—SMITH, B. D. 1984: Geophysical surveys at the Getchell and Preble disseminated gold deposits, Humboldt County, Nevada. — US Geological Survey Open-File Report 84–795.
- HOEKSTRA, P.—HILD, J.—BLOHM, M. 1989: Geophysical surveys for precious metals exploration in the Basin-and Range, Nevada. — in BHAPPO, R. B.—HARDEN, R. J. (eds.): *Gold Forum on Technology and Practices – World Gold '89: Society of Mining Engineering, Proceedings*: 69–75.
- HOFSTRA, A. H.—LEVENTHAL, J. S.—NORTHROP, H. R.—LANDIS, G. P.—RYE, R. O.—BIRAK, D. J.—DAHL, A. R. 1991: Genesis of sediment-hosted disseminated gold deposits by fluid mixing and sulfidization: Chemical-reaction-path modeling of ore-depositional processes documented in the Jerritt Canyon district, Nevada. — *Geology*, 19: 36–40.
- HOFSTRA, A. H.—DALY, W. E.—BIRAK, D. J.—DOE T. C. 1992: Geologic framework and genesis of Carlin-type gold deposits in the Jerritt Canyon district, Nevada, USA. — in LADEIRA, E. A. (ed.): *Brazil Gold '91*, Rotterdam, A.A. Balkema: 77–87.
- HOFSTRA, A. H.—SNEE, L. W.—RYE, R. O.—FOLGER, H. W.—PHINISEY, J. D.—NAESER, C. W.—STEIN, H. J.—LORANGER, R. J.—DAHL, A. R.—LEWCHUK, M. in press: Age constraints on Jerritt Canyon and other Carlin-type gold deposits in the western United States. – Relation to mid-Tertiary extension and magmatism. — *Economic Geology*.
- HOLLAND, P. T.—BEATY, D. W.—SNOW, G. G. 1988: Comparative elemental and oxygen isotope geochemistry of jasperoid in the northern Great Basin; evidence for distinctive fluid evolution in gold-producing hydrothermal systems. — *Economic Geology*, 83: 1401–1423.
- HOOVER, D. B.—PIERCE, H. A.—MERKEL, D. C. in 1986: Telluric traverse and self potential data release in the vicinity of the Pinson mine, Humboldt County, Nevada. — US Geological Survey Open-File Report 86–341.
- ILCHIK, R. P.—BARTON, M. D. 1997: An amagmatic origin of Carlin-type gold deposits. — *Economic Geology*, 92: 269–288.
- ILCHIK, R. P. 1990: Geology and geochemistry of the Vantage gold deposits, Alligator Ridge–Bald Mountain mining district, Nevada. — *Economic Geology*, 85: 50–75.
- ILCHIK, R. P.—BRIMHALL, G. H.—SCHULL, H. W. 1986: Hydrothermal maturation of indigenous organic matter at the Alligator Ridge gold deposits, Nevada. — *Economic Geology*, 81: 113–130.
- JEWELL, P. W.—PARRY, W. T. 1987: Geology and hydrothermal alteration of the Mercur gold deposit, Utah. — *Economic Geology*, 82: 1958–1966.
- JEWELL, P. W.—PARRY, W. T. 1988: Geochemistry of the Mercur gold deposit, Utah, USA. — *Chemical Geology*, v. 69: 245–265.
- JORALEMAN, P. 1951: The occurrence of gold at the Getchell mine, Nevada. — *Economic Geology*, 46: 276–310.
- KUEHN, C. A.—ROSE, A. R. 1992: Geology and geochemistry of wall-rock alteration at the Carlin gold deposit, Nevada. — *Economic Geology*, 87: 1697–1721.
- KUEHN, C. A.—ROSE, A. R. 1995: Carlin gold deposits, Nevada: Origin in a deep zone of mixing between normally pressured and over pressured fluids. — *Economic Geology*, 90: 17–36.
- LANDIS, G. P.—HOFSTRA, A. H. 1991: Fluid inclusion gas chemistry as a potential minerals exploration tool: Case studies from Creede, CO, Jerritt Canyon, NV, Coeur d'Alene district, ID and MT, southern Alaska mesothermal veins, and mid-continent MVT's. — *Journal of Geochemical Exploration*, 42: 25–59.
- LEVENTHAL, J.—HOFSTRA, A. 1990: Characterization of carbon in sediment-hosted disseminated gold deposits, north central Nevada. — in HAUSEN, D. M.—HALBE, D. N.—PETERSEN, E. U.—TAFURI, W. J. (eds.): *Gold '90, Proceedings of the Gold '90 Symposium*, Salt Lake City, Utah, Society for Mining, Metallurgy, and Exploration, Inc., Littleton, CO: 365–368.
- LOVERING, T. G. 1972: Jasperoid in the United States—Its characteristics, origin, and economic significance. — U.S. Geol. Survey Prof. Paper 710: 164 p.

- MAHER, B. J.—BROWNE, Q. J.—MCKEE, E. H. 1993: Constraints on the age of gold mineralization and metallogenesis in the Battle Mountain–Eureka mineral belt, Nevada. — *Economic Geology*, 88: 469–478.
- MAO, S. H. 1991: Occurrence and distribution of invisible gold in a Carlin-type gold deposit in China. — *American Mineralogist*, 76: 1964–1972.
- NELSON, C. E.: Comparative geochemistry of jasperoids from Carlin-type gold deposits of the western United States. — *Journal of Geochemical Exploration*, 36: 171–195.
- ONEIL, J. R.—BAILEY, G. B.: Stable isotope investigation of gold-bearing jasperoid in the central Drum Mountains, Utah. — *Economic Geology*, 74: 852–859.
- RADTKE, A. S.—SCHEINER, B. J. 1970: Studies of hydrothermal gold deposition (I). Carlin gold deposit, Nevada: The role of carbonaceous materials in gold deposition. — *Economic Geology*, 65: 87–102.
- RADTKE, A. S.—RYE, R. O.—DICKSON, F. W. 1980: Geology and stable isotope studies of the Carlin gold deposit, Nevada. — *Economic Geology*, 75: 641–672.
- RADTKE, A. S. 1985: Geology of the Carlin gold deposit, Nevada. — US Geological Survey Professional Paper 1267: 124 p.
- RAINES, G. L.—LISLE, R. E.—SCHAFER, R. W.—WILKINSON, W. H. (eds.) 1991: Geology and Ore Deposits of the Great Basin. — Symposium Proceedings, Geological Society of Nevada, Reno, Nevada: 1251 p.
- ROBERTS, R. J. 1960: Alinement of mining districts in north-central Nevada. — US Geological Survey Professional Paper 400-B: B17–B19.
- ROBERTS, R. J.—RADTKE, A. S.—COATS, R. R.—SILBERMAN, M. L.—MCKEE, E. H. 1971: Gold-bearing deposits in north-central Nevada and southwestern Idaho, with a section on periods of plutonism in north-central Nevada. — *Economic Geology*, 66: 14–33.
- ROMBERGER, S. B. 1986: Ore deposits #9. Disseminated gold deposits. — *Geoscience Canada*, 13: 23–31.
- RYE, R. O. 1985: A model for the formation of carbonate-hosted disseminated gold deposits based on geologic, fluid inclusion, geochemical, and stable isotope studies of the Carlin and Cortez deposits, Nevada. — *in* TOOKER, E. W. (ed.): *Geologic Characteristics of Sediment- and Volcanic-Hosted Disseminated Gold deposits—Search for an Occurrence Model*, US Geological Survey Bulletin 1646: 35–42.
- RYTUBA, J. J. 1985: Geochemistry of hydrothermal transport and deposition of gold and sulfide minerals in Carlin-type systems. — US Geological Survey Bulletin 1646: 27–34.
- SCHAFER, R. W.—COOPER, J. J.—VIKRE, P. G. (eds.) 1988: Bulk Mineable Precious Metal Deposits of the Western United States. — Symposium Proceedings, The Geological Society of Nevada, Reno, Nevada: 755 p.
- SILBERMAN, M. L.—BERGER, B. R.—KOSKI, R. A. 1974: K-Ar age relations of granodiorite emplacement and W and Au mineralization near the Getchell mine, Humboldt County, Nevada. — *Economic Geology*, 69: 646–656.
- SILLITOE, R. H.—BONHAM, H. F. 1990: Sediment-hosted gold deposits: Distal products of magmatic-hydrothermal systems. — *Geology*, 18: 157–161.
- TEAL, L.—JACKSON, M. 1997: Geologic overview of the Carlin Trend gold deposits and descriptions of recent discoveries. — *SEG Newsletter*, 31: 1 and 13–25.
- THORMAN, C. H.—CHRISTIANSEN, O. D. 1991: Geologic settings of gold deposits in the Great Basin, western United States. — *in* LADEIRA, E. A. (ed.): *Brazil Gold'91*, Balkema, Rotterdam.
- TINGLEY, J. V.—BONHAM, H. F. eds. 1986: *Sediment-Hosted Precious-Metal Deposits of Northern Nevada*. — Nevada Bureau of Mines and Geology Report 40: 103 p.
- TOOKER, E. W. ed. 1985: *Geologic Characteristics of Sediment- and Volcanic-Hosted Disseminated Gold deposits. — Search for an Occurrence Model*. — US Geological Survey Bulletin 1646.
- TURNER, S. J.—FLINDELL, P. A.—HENDRI, D.—HARDJANA, I.—LAURICELLA, P. F.—LINDSAY, R. P.—MARPAUNG, B.—WHITE, G. P. 1994: Sediment-hosted gold mineralization in the Raratotok district, North Sulawesi, Indonesia. — *Journal of Geochemical Exploration*, 50: 317–336.
- VIKRE, P.—THOMPSON, T. B.—BETTLES, K.—CHRISTENSEN, O.—PARRATT, R. eds. 1997: *Carlin-Type Gold Deposits Field Conference* — SEG Guidebook Series, 28: 287 p.
- WANG, K.—ZHOU, Y. 1994: Mineralogy of the Carlin-type Dongbeizhai and Jinya gold deposits, southwestern China. — *International Geology Review*, 36: 194–202.
- WELLS, J. D.—MULLINS, T. E. 1973: Gold-bearing arsenian pyrite determined by microprobe analysis, Cortez and Carlin gold mines, Nevada. — *Economic Geology*, v. 68: 187–201.
- WELLS, J. D.—STOISER, L. R.—ELLIOTT, J. E. 1969: Geology and geochemistry of the Cortez gold deposit, Nevada. — *Economic Geology*, 64: 526–537.
- WILLIAMS, C. 1993: Northeastern Nevada breccia bodies. — Symposium proceedings, Elko Chapter-Geological Society of Nevada.

- WILSON, P. N.–PARRY, W. T. 1990: Mesozoic hydrothermal alteration associated with gold mineralization in the Mercur district, Utah. — *Geology*, 18: 866–869.
- WILSON, P. N.–PARRY, W. T. 1995: Characterization and dating of argillic alteration in the Mercur gold district, Utah. — *Economic Geology*, 90: 1197–1216.
- WRUCKE, C. T.–ARMBRUSTMACHER, T. J. 1975: Geochemical and geologic relations of gold and other elements of the Gold Acres open pit mine, Lander County, Nevada. — US Geological Survey Professional Paper 860: 27 p.

THE CARLIN GOLD PROJECT IN HUNGARY (1995–1998)

LÁSZLÓ KORPÁS¹, ALBERT H. HOFSTRA², LÁSZLÓ ÓDOR¹, ISTVÁN HORVÁTH¹,
JÁNOS HAAS³, and JOEL S. LEVENTHAL²

¹Geological Institute of Hungary, H-1143, Budapest, Stefánia út 14., Hungary

²US Geological Survey, P. O. Box 25046, Denver, CO 80225 USA

³Hungarian Academy of Sciences–Eötvös Loránd University, Geological Research Group,
H-1088, Budapest, Múzeum krt. 4a., Hungary

ABSTRACT

The economic success of exploration and mining companies exploiting Carlin-type gold deposits in Nevada has generated a new wave of gold exploration around the world. Since this type of gold mineralization was unknown in Hungary and because research to discover it had never been initiated, a research proposal was elaborated in 1994 to evaluate the potential for Carlin-type gold mineralization in Hungary. This proposal was accepted and financially supported by the US-Hungarian Joint Fund between 1995 and 1998. The resource assessment was performed by the Geological Institute of Hungary (GIH) with participation of László KORPÁS project leader, László ÓDOR, István HORVÁTH, János HAAS and György CSIRIK and by the US Geological Survey (USGS) with Albert HOFSTRA co-leader, and Joel LEVENTHAL. Important stages in the development of the project are summarized below.

First, a preliminary screening was made on the basis of the geological and geochemical characteristics of about 400 pre-Quaternary formations. This screening resulted in the selection of 36 Paleozoic, Mesozoic, and subordinately Paleogene Formations for further study and sampling. Systematic rock chip sampling of these formations was carried out between 1995 and 1998. The selected formations were sampled at their type localities and at other outcrops, drill cores, or mining tunnels. Altogether, 1398 samples were taken from 604 sample sites and analyzed for Au, Ag, As, Sb, Tl and Hg. Complimentary stream sediment surveys were conducted in selected areas. After studying Carlin-type gold deposits in Nevada, the mineral potential of the selected formations was re-evaluated in 1995 and the number of formations sampled increased to 97. Visit of the USGS experts to Hungary in 1996 resulted in a preliminary evaluation of the potential for Carlin-type gold deposits, and in the selection of seven areas and formations for further exploration. Most of these areas and formations are located in the Darnó Zone, a major NE-striking fault system, and near Late Eocene–Early Oligocene igneous rocks. Preparation of publications that summarize the results of the project started in 1997.

1. INTRODUCTION

Discovery of Carlin-type gold deposits in the Great Basin in 1962, based in part on previous USGS studies, has opened a new chapter in the history of gold exploration and production of the world. By the 90's more than 100 ore deposits of this type, located mainly in Nevada and subordinately in Utah, have accounted for 60% of the USA's gold production (CRAIG and RIMSTIDT 1998) and about 10% of the world's gold production. Exploration for these deposits has led to the discovery of similar gold deposits in many places around the world (e. g. Canada, Mexico, Peru, China, Spain, Uzbekhistan, Philippines, Turkey, Albania, Greece and Slovakia).

Over the past fifteen years understanding of Carlin-type gold deposits in the United States has progressed considerably, enabling elaboration of an updated deposit model (HOFSTRA 1999). Carlin-type deposits are large tonnage, low grade, epigenetic, sedimentary rock hosted, disseminated gold deposits. They are hosted in complexly deformed carbonate and siliciclastic sedimentary sequences accumulated in extensional platform margins and intraplateau basins. The gold deposits are broadly contemporaneous with mid-Tertiary extensional tectonism and calc-alkaline magmatism and were deposited from moderate temperature (c.a. 200 °C), moderately acidic, CO₂-

and H₂S-rich hydrothermal fluids. The disseminated auriferous pyrite in the ores formed by sulfidation of host-rock iron.

Carlin-type gold mineralization was unknown in Hungary and initiatives to prospect for it had never been made previously, despite the fact that certain abandoned base metal and iron ore districts (Szabadbattyán, Veleence Hills and Rudabánya) were known to contain gold in low concentrations (less than 2.0 g/t).

These facts inspired us to elaborate a research proposal in 1994 to evaluate the potential for Carlin-type gold deposits in Hungary (KORPÁS and HOFSTRA 1994). This proposal was accepted and financially supported by the US-Hungarian Joint Fund, between 1995 and 1998. Participants of the Joint Fund project No. 435., entitled "Carlin gold in Hungary", were as follows. László KORPÁS project leader, László ÓDOR, István HORVÁTH, János HAAŠ and György CSIRIK from the GIH, Albert HOFSTRA co-leader and Joel LEVENTHAL from the USGS. The project started in 1995 and important stages of its development are summarized and discussed below.

2. PRELIMINARY EVALUATION—GEOLOGICAL AND GEOCHEMICAL CRITERIA

Since this type of gold mineralization was unknown and had never been explored for in Hungary, a preliminary evaluation of prospective formations was made based on existing geological descriptions and geochemical data.

It was evident from the beginning of the project that the level of geological and geochemical knowledge of the mountainous areas in Hungary needed to be improved to adequately rank the gold potential of prospective formations. For example, regional rare element research, carried out by the Geological Institute of Hungary in the late 60's, was based on a systematic, densely spaced, and representative rock sampling program. Although this research yielded a great number of multielement geochemical data (FÖLDVÁRINÉ VOGL 1970), the analytical methods used at that time were incapable of detecting low, ppb level, gold anomalies. Similar soil and rock geochemical data with poor detection limits for gold were generated in the early 70's during assessments of some of the mid-mountainous regions of Hungary (Bükk Mts., Aggtelek and Rudabánya Mts., and Szendrő Mts.). This geochemical data permitted us to evaluate mineral resource potential in the Rudabánya Iron Ore District (CSALAGOVITS 1973), the Kőszeg Mts. (NAGY 1972) and the Recsk deep level porphyry copper deposit (CSILLAG 1975), but is inadequate to assess the potential for gold. Therefore, stream sediment surveys of the mountainous areas in Hungary started in 1991 with analytical techniques capable of detecting ppb level gold anomalies. Results of the still ongoing stream sediment project (ÓDOR et al. 1994 and 1997) were successfully used to assess the potential for Carlin-type gold mineralization in the Mecsek Mts., the Buda and Pilis Mts., the Bükk and Uppony Mts. and the Aggtelek–Rudabánya and Szendrő Mts.

Due to an insufficient amount of relevant geochemical data, geological criteria played a crucial role in a preliminary estimation of the potential for Carlin-type gold mineralization in Hungary (KORPÁS and HOFSTRA, 1994). Since a great part of the geological criteria of the Carlin model (HOFSTRA 1999) was applicable in the screening of the potentially ore bearing formations, we used them for evaluation and delineation of the prospective formations and areas. The areal distribution, age, lithology, thickness, facies, content of organic matter and pyrite in each formation were systematically documented. In addition, evidence of hydrothermal alteration such as silicification, argillization, and dolomitization were taken in account. Presence of ore related minerals like gold and silver bearing sulfides, Cu–Pb–Zn sulfides, stibnite and cinnabar were recorded. Special indicator rocks like grey jasper and supergene minerals such as jarosite and phosphates were also noted. In some cases, available geochemical data made it possible to delineate Au and Ag anomalies in the ppm range or anomalies of pathfinder elements like As, Sb, Hg, Tl, Ba, Cu, Pb and Zn. An attempt was made to incorporate information on the location and timing of extensional and compressional tectonism and estimation of maximum temperatures of metamorphism.

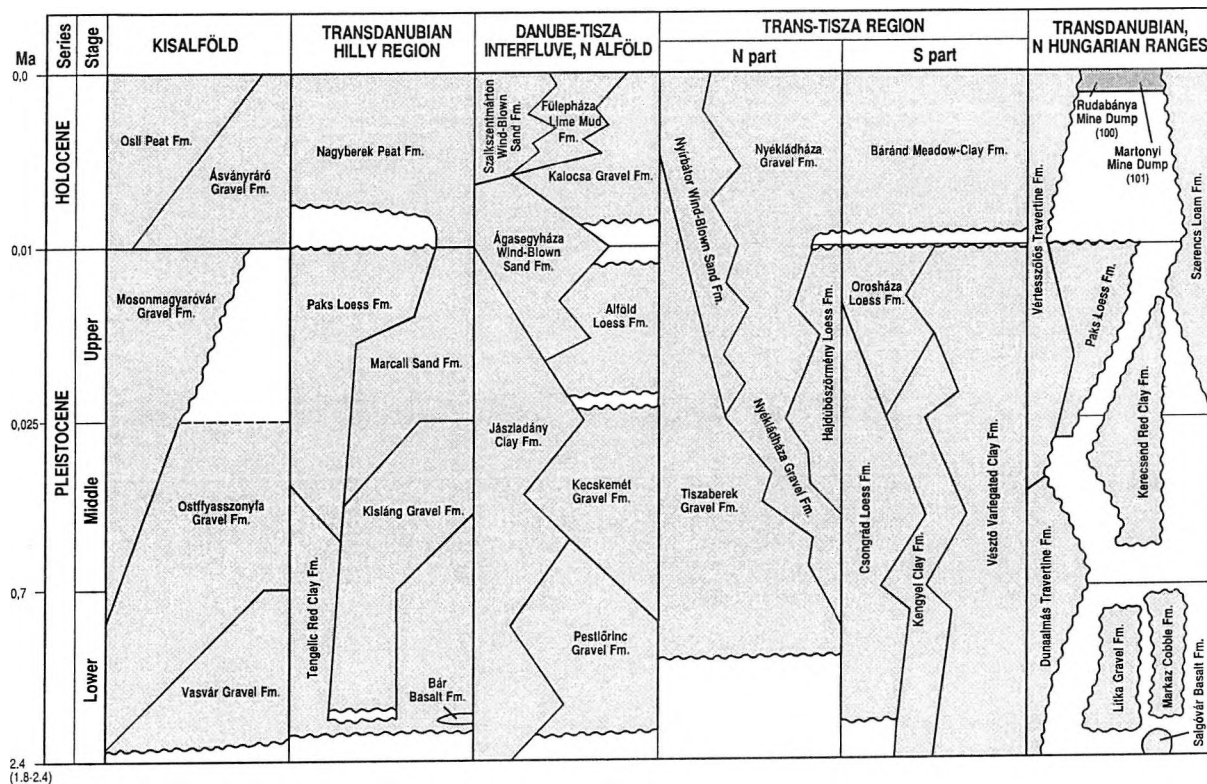
After screening of about 400 pre-Quaternary formations only 36 remained for further exploration. Fig. 1 shows the stratigraphic setting of the selected formations while their most important data are summarized in Table 1. The areal distribution of these formations is displayed on Fig. 2.

The main criteria used to assess the potential of Carlin-type gold mineralization in Hungary were as follows:

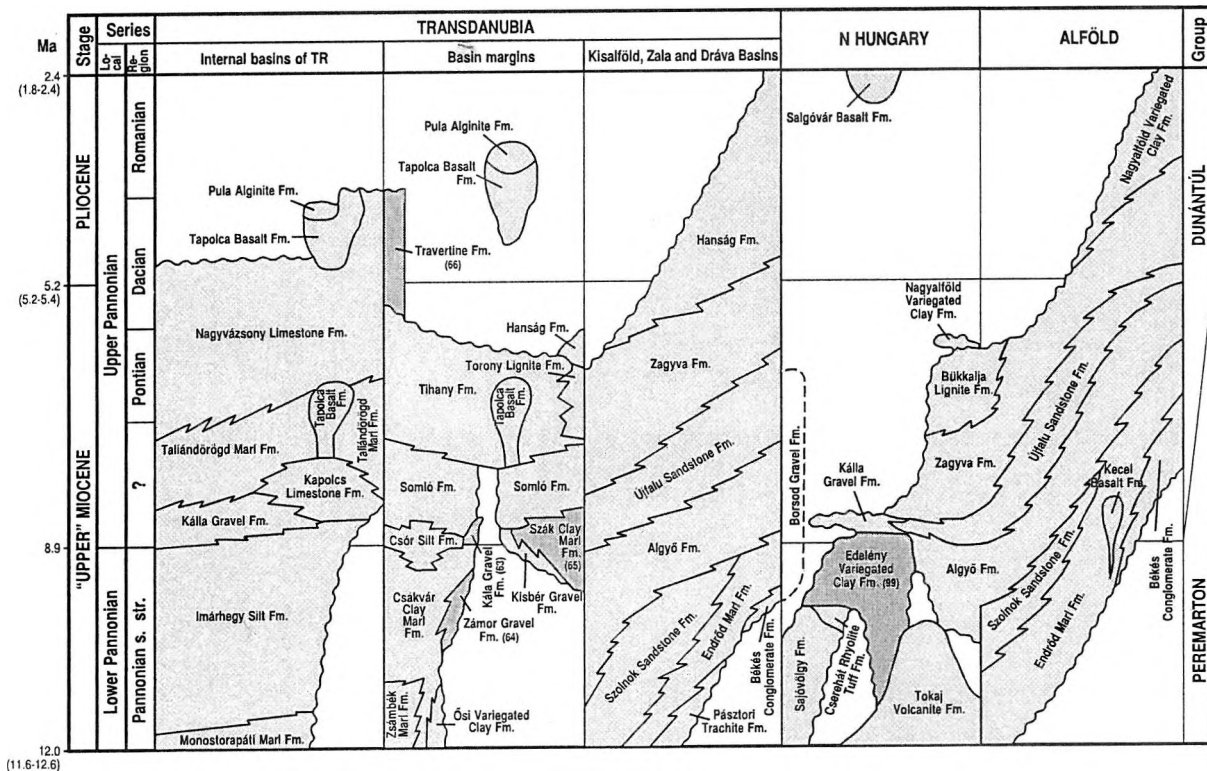
- Triassic–Early Jurassic, Silurian–Devonian–Permian, and Eocene–Oligocene formations accumulated at platform margins or in intraplateau basins.
- Areas where gold potential was never evaluated previously or where available data are of limited use.
- Based on the preliminary evaluation (KORPÁS and HOFSTRA 1994), the prospective formations were ranked as follows:

Fig. 1: Stratigraphic chart showing the position of prospective formations (after Császár 1997)
 Quaternary, Pannonian s. l., Miocene, Oligocene, Paleocene-Eocene, Cretaceous, Jurassic, Triassic, Permian, Paleozoic I.
 (shaded formations = sampled formations)

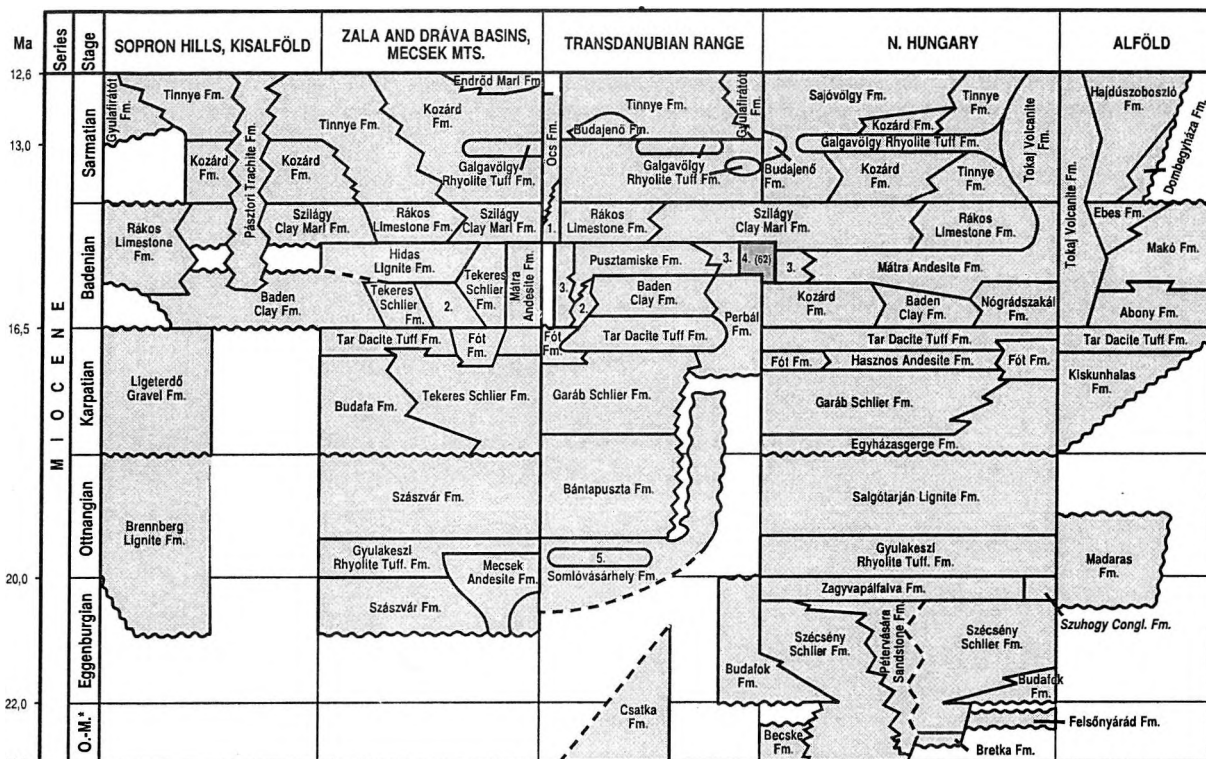
QUATERNARY



PANNONIAN S. L.

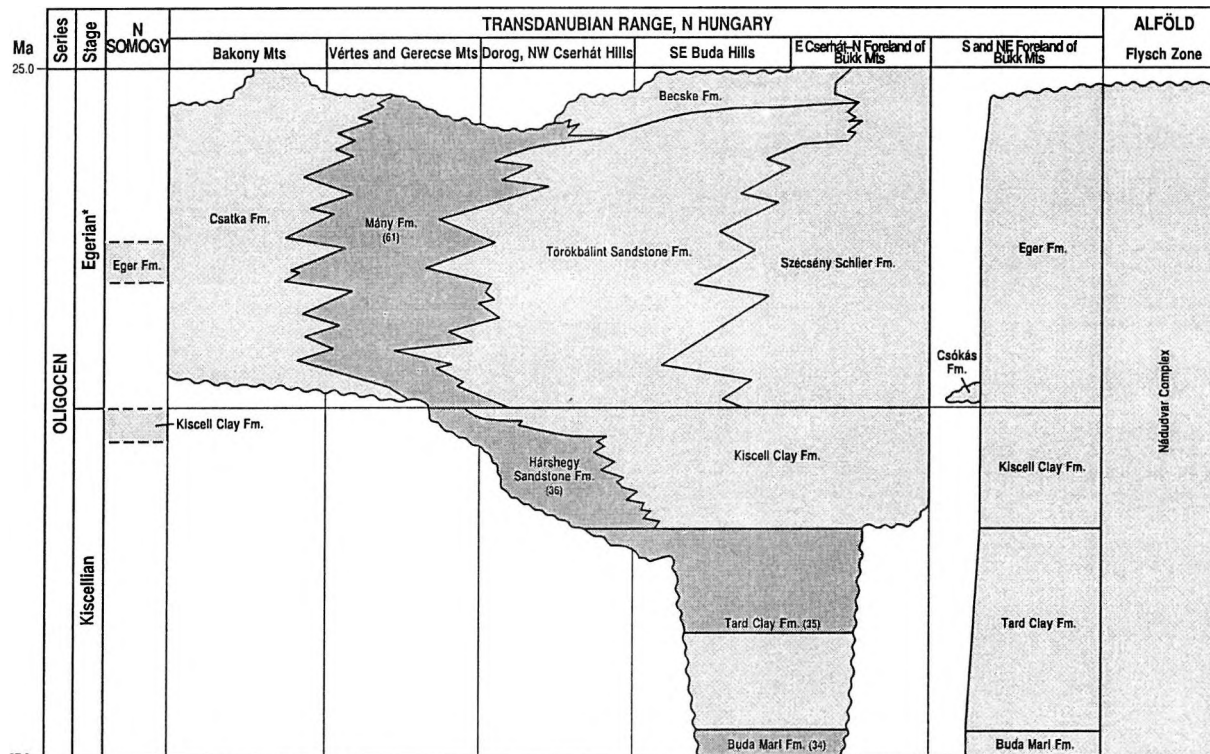


MIOCENE



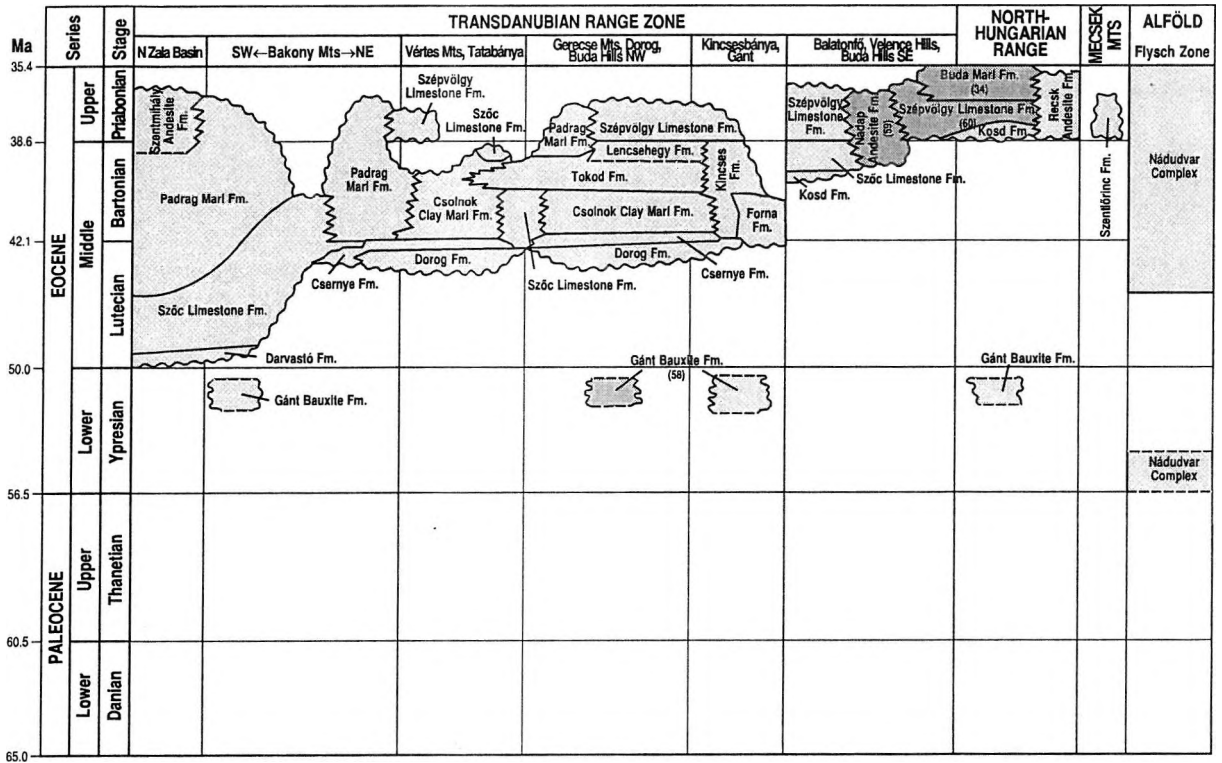
*Oligocene - Miocene 1. Vöröstó Fm., 2. Pécszabolcs Limestone Fm., 3. Hidas Lignite Fm., 4. Mátra Andesite Fm. (62) Börzsöny and Visegrád Andesite, 5. Gyulakeszi Rhyolite Tuff. Fm.

OLIGOCENE

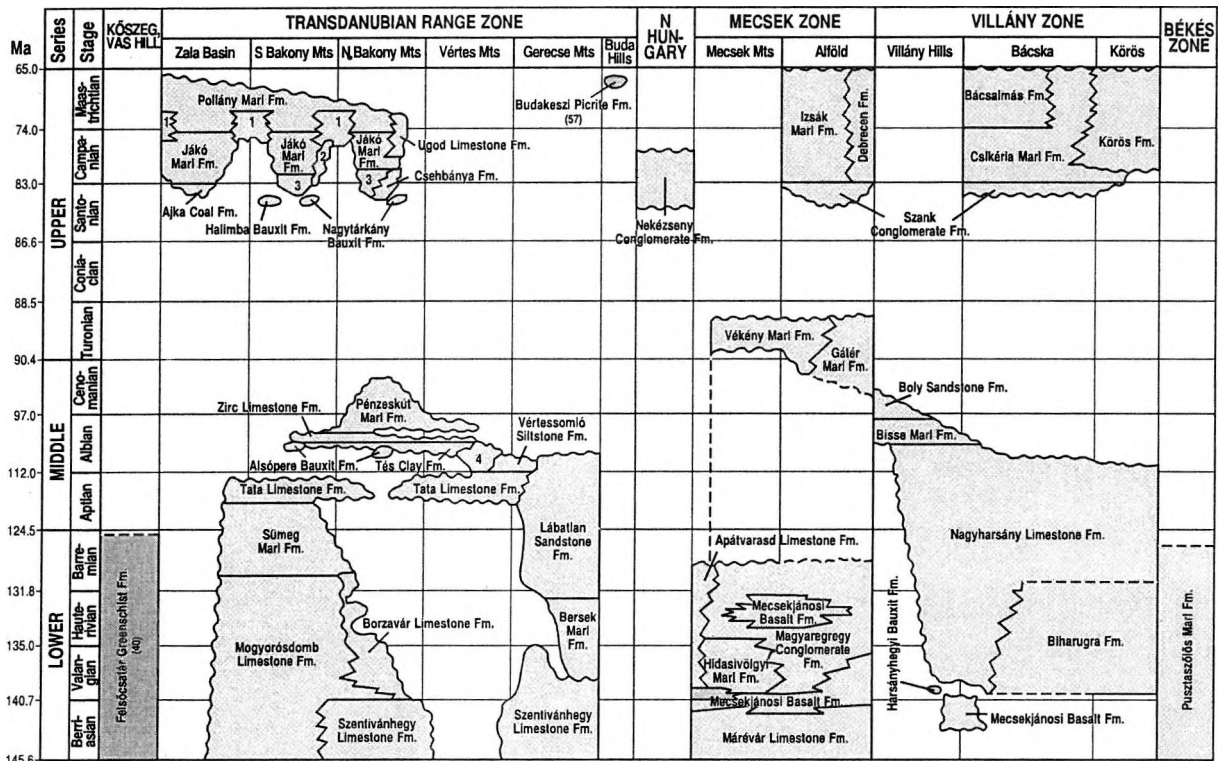


* Lower Egerian substage sensu Báldi-Seneš 1975

PALEOCENE-EOCENE

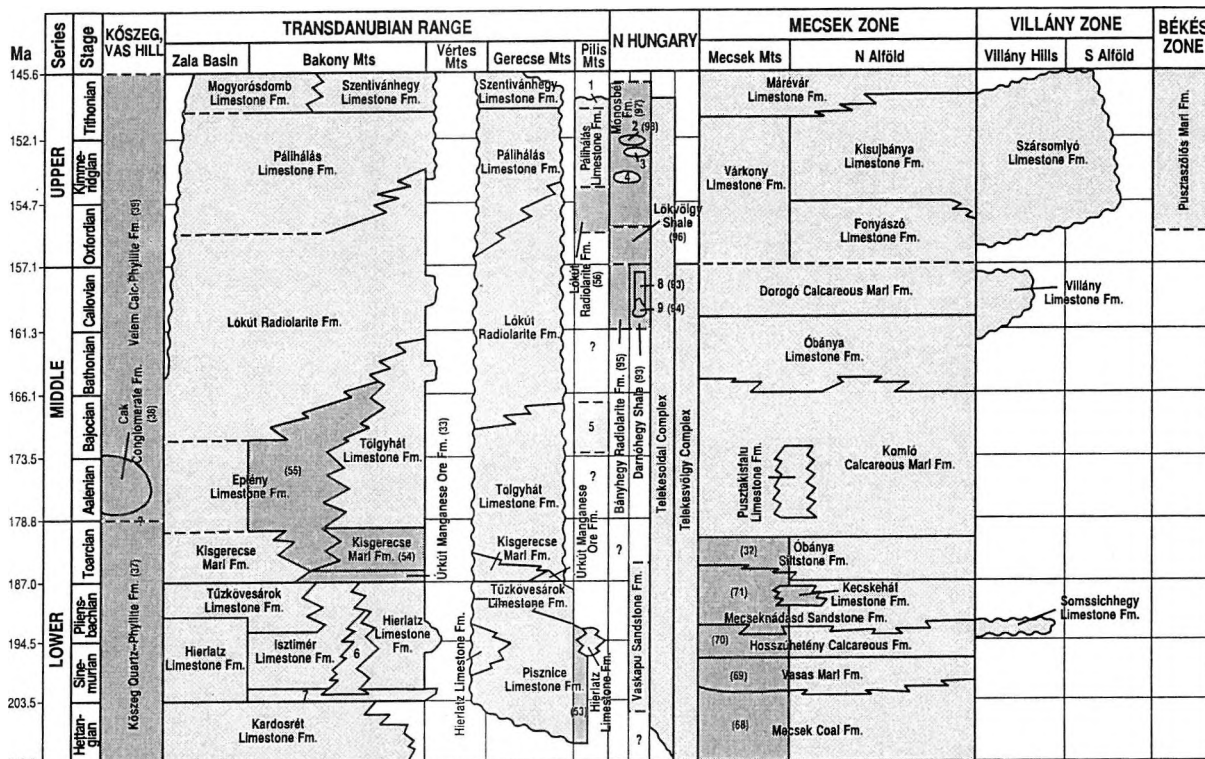


CRETACEOUS



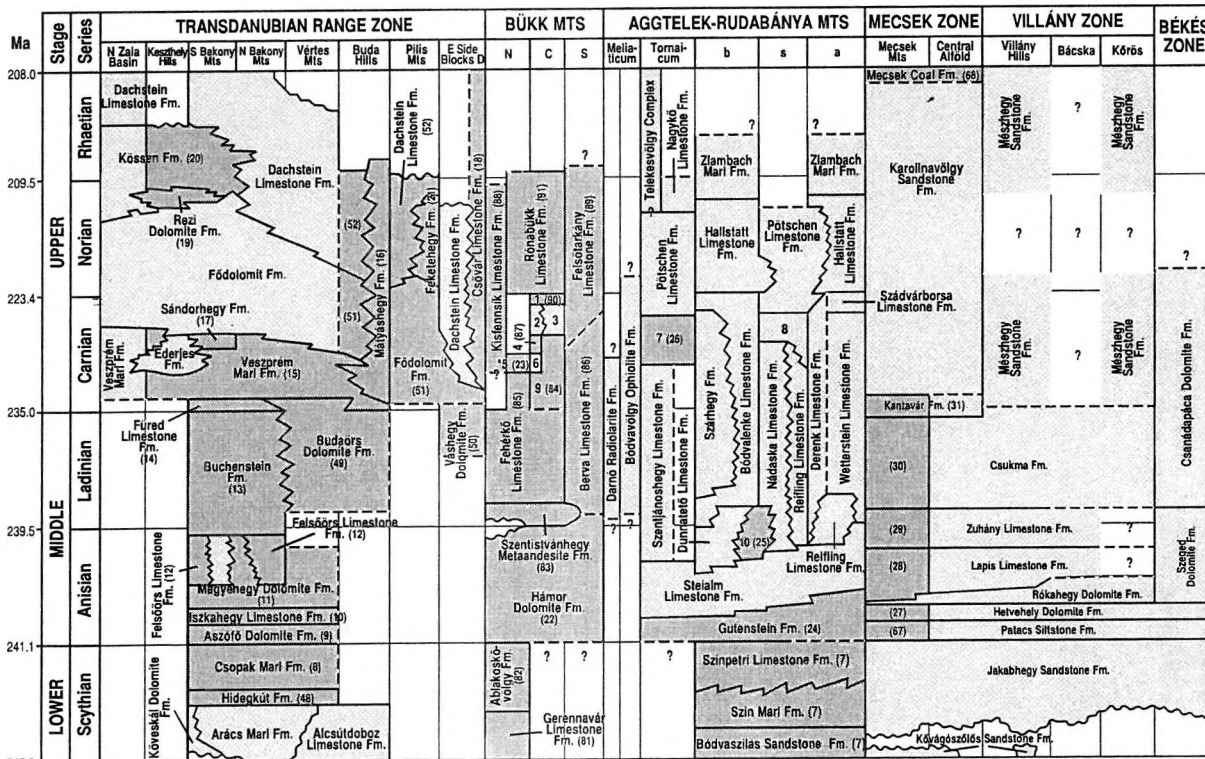
1. Ugod Limestone Fm., 2. Kozmatag Fm., 3. Ajka Coal Fm., 4. Környe Limestone Fm.

JURASSIC



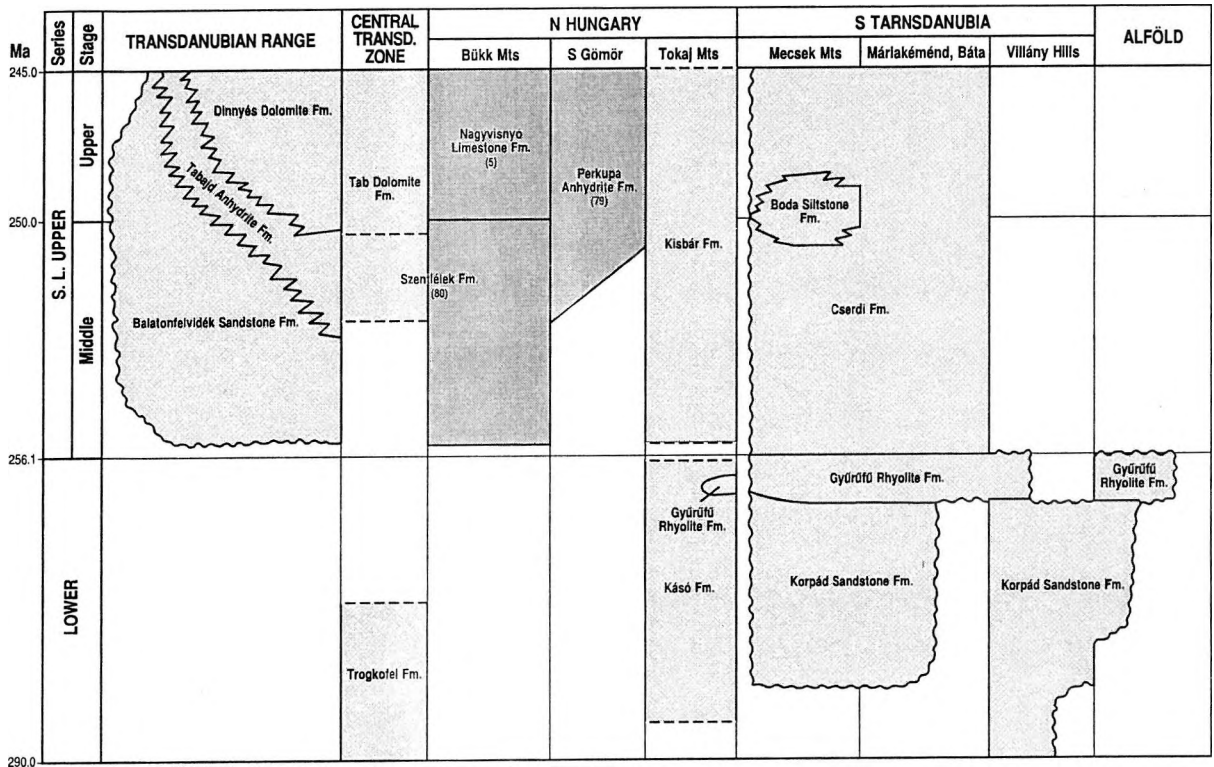
1. Szentiványi Limestone Fm., 2. Oldalvölgy Fm., 3. Bükkszérc Fm., 4. Cspikéztető Radiolarite Fm. 5. Tölgyhát Limestone Fm. 6. Kishát Limestone Fm., 7. Pisznice Limestone Fm., 8. Darnó Radiolarite Fm., 9. Szarvaskő Basalt Fm.

TRIASSIC

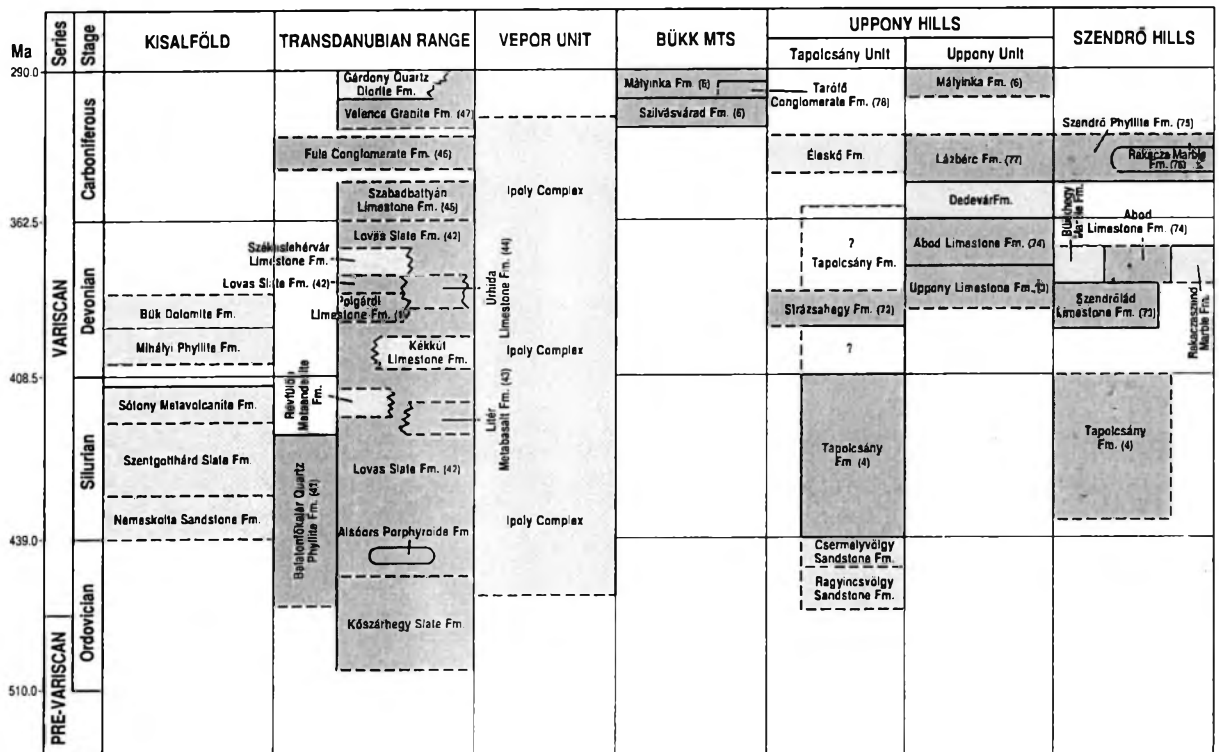


1. Répáshuta Limestone Fm., 2. Hollóstető Limestone Fm., 3. Bükkszéncs Limestone Fm., 4. Szinva Metabasalt Fm. 5. Vesszős Fm., 6. Hegyestető Fm., 7. Tornaszentandrás Shale Fm., 8. Szőlőszárdó Marl Fm., 9. Parad Limestone Fm., 10. Bódvárakó Fm. * Létras Metabasalt Fm.

PERMIAN



PALEOZOIC I



THE LIST OF PERSPECTIVE FORMATIONS FOR CARLIN-TYPE GOLD MINERALIZATION IN HUNGARY (1994)

No	AGE	NAME, LITHOLOGY AND THICKNESS OF THE FORMATION	FACIES	ORGANIC MATTER	PYRITE	EXTENSIONAL TECTONICS	COMPR. TECTONICS	THERMAL EFFECTS	ALTERATION	MINERALIZATION AND ORE SHOWS	ROCK GEOCHEMISTRY (ppm)
1	DEVONIAN	TRANSDANUBIAN RANGE: POLGÁRDI LIMESTONE: grey, massive, bituminous limestone with shales (100)	platform, peritidal	0.05%	+	?	+	+	silicification, ankerite, siderite,	galena, malachite, ankerite,	Pb(13%), Ag(1-50), Au(0.4-2.0) **
2	DEVONIAN	SZENDRŐ MOUNTAINS: SZENDRŐLAD LIMESTONE: grey, massive, metamorphosed limestone with graphitic shale (250-300 m)	platform and intraplatform basin	1.0%	+	?	+	no data	silicification	hematite and jarosite	Ag(0.04-0.06), Ba(316-461), Cu(51-101), Mo(<2), Pb(5-13), Sb(2.5-16), Zn(5-83)
3	DEVONIAN	UPPONY MOUNTAINS: UPPONY LIMESTONE: grey, crystalline limestone with shales and tuffs	platform and intraplatform basin	no data	no data	?	?	no data	no data	no data	no data
4	CARBONIFEROUS	TAPOLCSÁNY FORMATION: grey sericite-shales with chert and tuffs	intraplatform basin	+	+	?	?	no data	no data	iron and manganese ore shows	Ag(0.06-0.15), Ba(243-692), Cu(44-93), Mo(<2-18), Pb(7-27), Zn(74-203)
5	CARBONIFEROUS	NAGYVÍSNYÓ LIMESTONE: grey bituminous limestone (250 m)	ramp-lagoon	0.5%	no data	?	?	no data	no data	no data	Ag(0.03-0.11), Ba(330), Cu(60-73), Mo(3), Pb(5-12), Zn(43-174)
6	CARBONIFEROUS	BÜKK MOUNTAINS: SZILVÁSARAD and MÁLYINKA FORMATION: grey sericite-shales with sandstone and limestone	intraplatform basin	no data	no data	?	+	no data	no data	no data	Ag(0.06-0.24), Ba(244-381), Cu(55-327), Pb(10), Zn(6-1047)
7	LOWER TRIASSIC	RUDABÁNYA MOUNTAINS: RUDABÁNYA IRON ORE FORMATION: evaporites, sandstone, marls, limestones and dolomites (300-500 m)	evaporite, lagoon, intraplatform basin	+	+	+	+	+	argillite, siderite, limonite, silicification	barite, anhydrite, chalcopyrite, galena, cinnabar, gold	siderite(25-30%), limonite(50-55%), Ag(2.7), Cu(358), Pb(331), Sb(25), Hg(16), Cd(0.7), As(7), Te(?), Au(traces)
8	LOWER TRIASSIC	TRANSDANUBIAN RANGE: CSOPAK MARL: grey and red marls, siltstones, limestone and dolomite (200 m)	platform, peritidal, lagoon	0.1-2.5%	no data	?	+	+	no data	chalcopyrite, galena, sphalerite	Cu(<0.25%), Pb(<0.1%), Zn(<0.2%)
9	MIDDLE TRIASSIC	ASZÓFÓ DOLOMITE: grey, bituminous dolomite and dolosilt (100-200 m)	platform, lagoon	0.08%	no data	+	+	+	no data	no data	Ag(0.15-0.8), As(102-421), Ba(451-473), Cu(38-62), Mo(<2.5), Pb(12-25), Sb(<16-21), Tl(<1), Zn(102-272)
10	MIDDLE TRIASSIC	ISZKAHEGY LIMESTONE: grey, bituminous, crystalline limestone and marl (100-150 m)	intraplatform restricted lagoon	+	+	+	+	+	no data	no data	Ag(0.15-0.3), As(102-421), Ba(451-473), Cu(38-62), Mo(<2.5), Pb(12-25), Sb(<16-21), Tl(<1), Zn(102-272)
11	MIDDLE TRIASSIC	MEGYEHEGY DOLOMITE: grey, yellow, massive dolomite (30-280 m)	platform	+	+	+	+	+	no data	no data	Ag(0.4), As(<10), Ba(62), Cu(29), Mo(1.3), Pb(60), Tl(<1), Zn(43)
12	MIDDLE TRIASSIC	FELSŐÓRS LIMESTONE: grey, brown, cherty, bituminous limestone (0-180 m)	intraplatform basin	+	+	+	+	+	no data	no data	Ag(0.4), As(<10), Ba(62), Cu(29), Mo(1.3), Pb(60), Tl(<1), Zn(43)
13	MIDDLE TRIASSIC	BÜCHENSTEIN FORMATION: grey, red, green, cherty limestone with volcanoclastites (50-80 m)	intraplatform basin	+	no data	+	+	+	slight silicification	no data	Ag(0.4), As(<10), Ba(62), Cu(29), Mo(1.3), Pb(60), Tl(<1), Zn(43)
14	UPPER TRIASSIC	FÜRED LIMESTONE: grey, cherty, bituminous limestone with marl (10-60 m)	intraplatform basin	+	no data	+	+	no data	no data	no data	no data
15	UPPER TRIASSIC	VESZPRÉM MARL: grey, silty marl with limestone, dolomite intercalations (500-1000 m)	intraplatform restricted basin	0.15-0.60%	+	+	+	max. T 432 °C	no data	no data	Ag(0.01), As(16), Ba(254), Cu(47), Mo(5), Pb(7), Sb(<16), Tl(<1), Zn(35)
16	UPPER TRIASSIC	MÁTYÁSHEGY FORMATION: grey, bituminous, cherty limestone and dolomite with marl (250 m)	intraplatform restricted basin	0.1-0.6%	+	+	+	max. T 430 °C	no data	no data	Ag(<2.5), Cu(<160), Mo(<160), Sb(<60), Pb(<160), As(<600), Au(1-12 ppb)
17	UPPER TRIASSIC	SANDORHEGY LIMESTONE: grey, bituminous limestone, marl and dolomite (100-200 m)	intraplatform restricted basin	0.11-2.73%	+	+	+	max. T 410 °C	no data	no data	no data
18	UPPER TRIASSIC LOWER JURASSIC	CSÓVÁR LIMESTONE: grey, bituminous, cherty limestone and dolomite	intraplatform restricted basin	+	+	+	+	+	no data	no data	no data

N _o	AGE	NAME, LITHOLOGY AND THICKNESS OF THE FORMATION	FACIES	ORGANIC MATTER	PYRITE	EXTENSIO- NAL TECTONICS	COMPR. TECTONICS	THERMAL EFFECTS	ALTERATION	MINERALI- ZATION AND ORE SHOWS	ROCK GEOCHEMISTRY (ppm)
19	UPPER TRIASSIC	REZI DOLOMITE: grey, bituminous, dolomite, cherty dolomite (150-300)	intraplatform restricted basin	0.1-0.2%	+	+	+	max T 437 °C	no data	no data	no data
20	UPPER TRIASSIC	KÖSSEN FORMATION: grey, bituminous marl, dolomite and limestone with oilshale (20-400 m)	intraplatform euxine basin	1-2%	1%	+	+	no data	no data	no data	Ag(<0.4), Cu(16-100), Pb(<16), Sb(<60), Zn(<100)
21	UPPER TRIASSIC	FEKETEHEGY FORMATION: grey, bituminous limestone and dolomite with oilshaws (300 m)	intraplatform restricted basin	+	+	+	+	+	no data	cinnabar and phosphorite	no data
22	MIDDLE TRIASSIC	BÜKK MOUNTAINS HAMOR DOLOMIT grey, massive dolomite (250-450 m)	intraplatform lagoon	no data	+	+	+	+	no data	no data	Ag(2.4), As(16), Bz(170), Cu(47), Mo (<2.5), Pb(280), Sb(62.7), Tl(<1), Zn(403)
23	UPPER TRIASSIC	VESSZÓS SHALE: black, sericite-shale with bituminous limestone, silt and volcanomict sandstone (150-200 m)	intraplatform restricted basin	+	+	+	+	+	no data	chalcocopyrite	Cu(0.3%)
24	MIDDLE TRIASSIC	RUDABÁNYA MOUNTAINS GÜTENSTEIN FORMATION: black, bituminous, massive dolomite and limestone with marl (250 m)	intraplatform euxine lagoon	+	+	+	+	+	no data	no data	Ag(1.7), As(<10), Ba(3566), Cu(857), Mo (3.1), Pb(230), Sb(99.7), Tl(<1), Zn(117)
25	MIDDLE TRIASSIC	BODVÁRAKÓ FORMATION: black, cherty limestone, dolomite with shales and tufts (40 m)	intraplatform restricted basin	+	+	+	+	+	no data	no data	no data
26	MIDDLE TRIASSIC	TORNASZENTANDRÁS SHALE: black shale with marl and cherty limestone (50-100 m)	intraplatform restricted basin	+	+	+	+	+	no data	no data	no data
27	MIDDLE TRIASSIC	MECSEK MOUNTAINS HETVEHELY DOLOMITE: grey dolomite, dolomarl with bituminous limestone and gypsum, anhydrite (100-200 m)	intraplatform hypersaline lagoon	0.1-0.3%	+	+	+	+	no data	no data	Ag(<0.01), As(<10), Ba(455), Cu(30), Mo (<2.5), Pb(17), Sb(<16), Tl(<1), Zn(105)
28	MIDDLE TRIASSIC	MISINA GROUP/ LAPIS LIMESTONE: grey, bituminous limestone, dolomite with coal lenses (200-300 m)	shallow ramp	+	+	+	+	+	no data	no data	Ag(<0.01), As(<10), Ba(201), Cu(57), Mo (<2.5), Pb(15), Sb(<16), Tl(<1), Zn(100)
29	MIDDLE TRIASSIC	MISINA GROUP/ ZUHANYA LIMESTONE: grey, nodular, argillaceous, bituminous limestone, dolomite with shale (50-200 m)	deeper ramp	+	no data	+	+	+	no data	no data	Ag(<0.01), As(<10), Ba(201), Cu(57), Mo (<2.5), Pb(15), Sb(<16), Tl(<1), Zn(100)
30	MIDDLE TRIASSIC	MISINA GROUP/ CSUKMA FORMATION: grey, massive limestone, dolomite (100-370 m)	shallow ramp	+	no data	+	+	max T 270 °C*	no data	azurite, malac- hite	no data
31	MIDDLE TRIASSIC	KANTAVAR FORMATION: black, bituminous limestone with shale and coal interlayers (50-100 m)	brackish lagoon	0.2-3.1%	0.6-2.5 %	+	+	+	no data	no data	Ag(0.2), Mo(55), Cu(30)
32	LOWER JURASSIC	OBANYA SILT FORMATION: black shales with sandstone and limestone (10 m)	anoxic basin	0.2-4.1%	+	+	+	max T 430 °C	no data	pyrite, limonite	Cu(160), Pb(60), Ba(1600), Mn(2500)
33	LOWER JURASSIC	TRANS-DANUBIAN RANGE: URKÚT MANGANESE ORE FORMATION: grey-green, manganese carbonate and oxide ores with black, bituminous shales and radiolites (100 m)	restricted basin	1-2%	1-5 %	+	+	about 100 °C	silicification	rodrosicrite, psilomelan, siderite, phosphorite	MnCO ₃ (20-30%), MnO ₂ (20-30%), FeCO ₃ (5%), P(1.5%)
34	LOWER OLIGOCENE	BUDA MARL: grey, partly bituminous marl, sandstone with limestone and volcanomict layers (60-120 m)	platform, open shelf basin	1%	+	+	+	max T 300 °C	silicification argillite, limonite	cinnabar, native Hg, calcite, barite, fluonite	Ag(<0.4), As(<600), Sb(<60), Hg(0.21- 0.95***)
35	LOWER OLIGOCENE	TARD CLAY: grey, black bituminous shales with sandstones and volcanomict layers (100-120 m)	intraplatform, euxine basin	1-2.6%	1-2.4 %	+	+	+	silicification	no data	no data
36	LOWER OLIGOCENE	HARSHEGY SANDSTONE: grey, silicified, arcotic, quartz sandstone (30 m)	ramp, near shore	+	+	+	+	max T 300 °C	silicification, argillite, limonite	no data	no data

Explanation * max T values based on fluid inclusion data; ** metal concentrations in ore; *** values for stream sediment samples

(1) Polgárdi Limestone (D₂), (2) Szendrőlád Limestone (D_{2,3}), (3) Uppony Limestone (D_{2,3}), (4) Tapolcsány Formation (S-C₁), (5) Nagyvisnyó Limestone (P₂), (6) Szilvásvárad Formation and Mályinka Formation (C₂), (7) Rudabánya Iron Ore (T_{1,2}, Rudabánya, Martonyi, Esztramos), (8) Csopak Marl (T₁), (9) Aszófő Dolomite (T₂), (10) Iszkahegy Limestone (T₂), (11) Megyehegy Dolomite (T₂), (12) Felsőörs Limestone (T₂), (13) Buchenstein Formation (T₂), (14) Füred Limestone (T₃), (15) Veszprém Marl (T₃), (16) Mátyáshegy Formation (T₃), (17) Sándorhegy Formation (T₃), (18) Csövár Limestone (T₃-J₁), (19) Rezi Dolomite (T₃), (20) Kössen Formation (T₃), (21) Feketehegy Formation (T₃), (22) Hámor Dolomite (T₂), (23) Vesszős Shale (T₃), (24) Gutenstein Dolomite (T₂), (25) Bodvarákó Formation (T₂), (26) Tornaszentandrás Shale (T₃), (27) Hetvehely Dolomite (T₂), (28) Lapis Limestone (T₂), (29) Zuhánya Limestone (T₂), (30) Csukma Formation / Kozár Limestone (T₂), (31) Kantavár Formation (T_{2,3}), (32) Óbánya Silt (J₁), (33) Úrkút Manganese Ore (J₁), (34) Buda Marl (E₃-O₁), (35) Tard Clay (O₁), (36) Hárshegy Sandstone (O₁), (37) Kőszeg Quartz Phyllite (J₁), (38) Cák Conglomerate (J₂), (39) Velem Calc Phyllite (J_{2,3}), (40) Felsőcsatár Greenschist (K₁), (41) Balatonfőkajár Quartz Phyllite (O-S), (42) Lovas Slate (O-D), (43) Litér Metabasalt (S), (44) Úrhida Limestone (D_{1,2}), (45) Szabadbattyán Limestone (C₁), (46) Füle Conglomerate (C₂), (47) Velence Granite (C₂), (48) Hidegkút Formation (T₁), (49) Budaörs Dolomite (T₂), (50) Vashegy Dolomit (T₂), (51) Fődolomit Formation (T₃), (52) Dachstein Limestone (T₃) (53) Pisznice Limestone (J₁), (54) Kisgerecse Marl (J₁), (55) Eplény Limestone (J_{1,2}), (56) Lókút Radiolarite (J_{2,3}), (57) Budakeszi Picrite (K₃), (58) Bauxite Formation (K₃-E₁) (59) Nadap Andesite (E_{2,3}), (60) Szépvölgy Limestone (E₃), (61) Mány Formation (O₂) (62) Börzsöny and Visegrád Andesite (M₂), (63) Källa Gravel (M₃), (64) Zámor Gravel (M₃), (65) Szák Marl (M₃), (66) Travertine Formation (P-Q₁), (67) Patacs Siltstone (T₂), (68) Mecsek Coal (T₃-J₁), (69) Vasas Marl (J₁), (70) Hosszúhetény Marl (J₁), (71) Mecseknádasd Sandstone (J₁), (72) Strázsahely Formation (D₂), (73) Irota Formation (D₂), (74) Abod Limestone (D₃), (75) Szendrő Phyllite (C), (76) Rakaca Marble (C), (77) Lázberc Formation (C), (78) Tarófi Conglomerate (C₂), (79) Perkupa Anhydrite (P₂), (80) Szentlélek Formation (P₂), (81) Gerennavár Limestone (T₁), (82) Ablakoskövölgy Limestone (T₁), (83) Szentistvánhegy Metaandesite (T₂), (84) Parád Complex, (T_{2,3}), (85) Fehérkő Limestone (T_{2,3}), (86) Berva Limestone (T_{2,3}), (87) Szinva Metabasalt (T₃), (88) Kisfennsík Limestone (T₃), (89) Felsőtárkány Limestone (T₃), (90) Répáshuta Limestone (T₃), (91) Rónabükk Limestone (T₃), (92) Darnóhegy Shale (J₂), (93) Darnó Radiolarite (J₂), (94) Szarvaskő Basalt (J₂), (95) Bányahely Radiolarite (J₂), (96) Lök völgy Shale (J_{2,3}), (97) Mónosbél Formation (J₃), (98) Oldalvölgy Formation (J₃), (99) Edelény Clay (M₃), (100) Rudabánya Mine Dump (H), (101) Martonyi Mine Dump (H)

Fig. 2

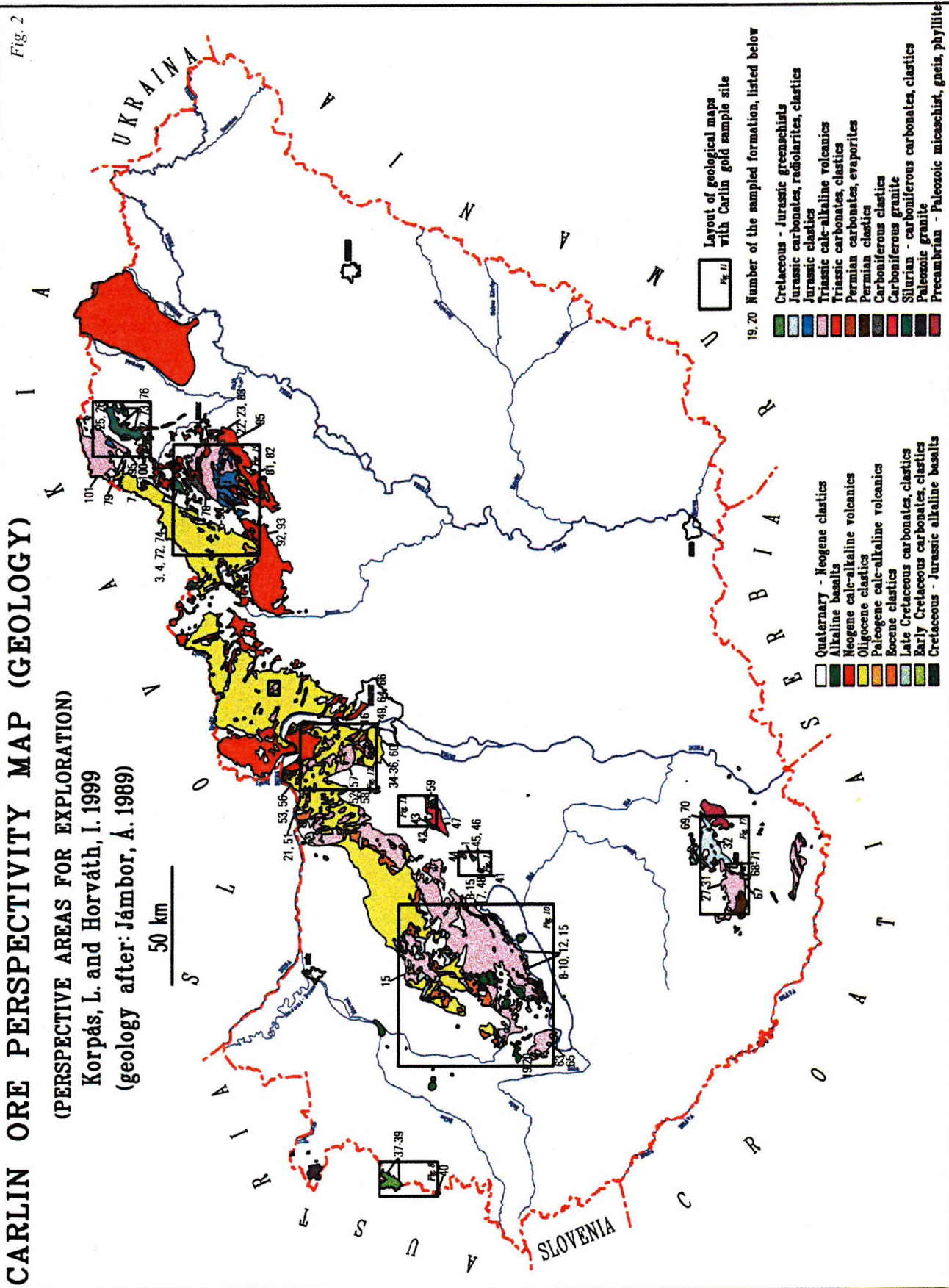
CARLIN ORE PERSPECTIVITY MAP (GEOLOGY)

(PERSPECTIVE AREAS FOR EXPLORATION)

Korpás, L. and Horváth, I. 1999

(geology after: Jámboor, A. 1989)

50 km



Layout of geological maps with Carlin gold sample site

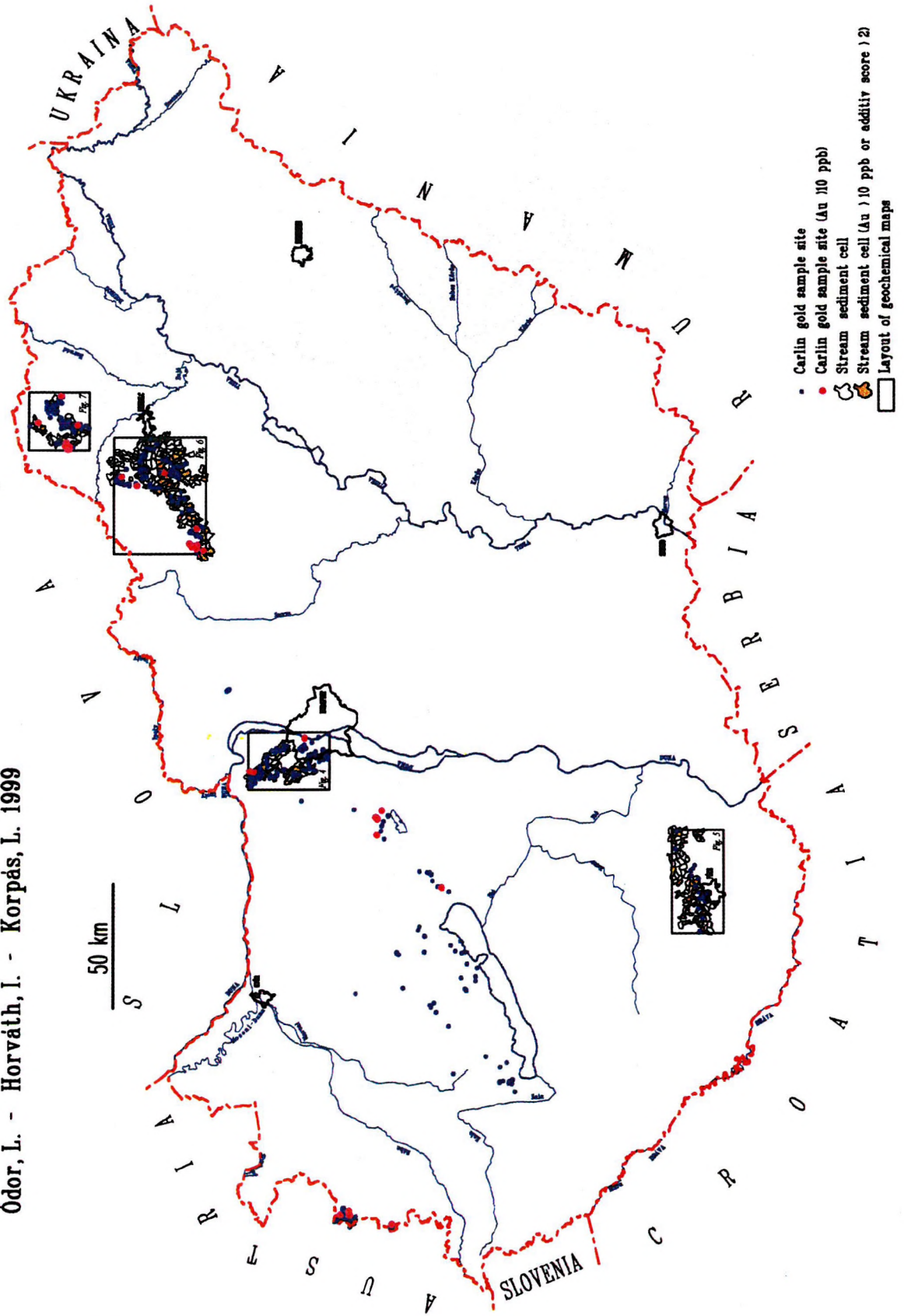
19, 20 Number of the sampled formation, listed below

- | | | | |
|--|---------------------------------------|--|---|
| | Quaternary - Neogene clastics | | Cretaceous - Jurassic greenschists |
| | Alkaline basalts | | Jurassic carbonates, radiolarites, clastics |
| | Neogene calc-alkaline volcanics | | Jurassic clastics |
| | Oligocene clastics | | Triassic calc-alkaline volcanics |
| | Paleogene calc-alkaline volcanics | | Triassic carbonates, clastics |
| | Eocene clastics | | Permian carbonates, evaporites |
| | Late Cretaceous carbonates, clastics | | Carboniferous clastics |
| | Early Cretaceous carbonates, clastics | | Carboniferous granite |
| | Jurassic alkaline basalts | | Silurian - carboniferous carbonates, clastics |
| | | | Paleozoic granite |
| | | | Precambrian - Paleozoic micaceous, gneiss, phyllite |

CARLIN ORE PERSPECTIVITY MAP (GEOCHEMISTRY) I

Ódor, L. - Horváth, I. - Korpás, L. 1999

Fig. 3



- A) Formations with high potential: Rudabánya Iron Ore Formation (7), Polgárdi Limestone (1), Úrkút Manganese Ore Formation (33)
- B) Formations with medium potential: Csupak Marl (8), Aszófő Dolomite (9), Iszkahegy Limestone (10), Megyehegy Dolomite (11), Felsőörs Limestone (12), Buchenstein Formation (13), Veszprém Marl (15), Mátyáshegy Formation (16), Sándorhegy Limestone (17), Csővár Limestone (18), Rezi Dolomite (19), Kössen Formation (20), Feketehegy Limestone (21), Vesszős Shale (23), Gutenstein Formation (24), Hetvehely Dolomite (27), Misina Formation Group (28-30), Kantavár Formation (31), Óbánya Silt (32), Buda Marl (34), Tard Clay (35), Hárshegy Sandstone (36)
- C) Formations with low potential: Szendrőlád Limestone (2), Uppony Limestone (3), Tapolcsány Formation (4), Nagyvisnyó Limestone (5), Szilvásvár and Mályinka Formation (6), Füred Limestone (14), Hámor Dolomite (22), Bódvarákó Formation (25), Tornaszentandrás Shale (26)

The original project proposal (KORPÁS and HOFSTRA 1994) suggested that existing geological information and geochemical data be used to select and delineate 2 to 5 formations or areas with the highest potential for more detailed study.

3. PROJECT DEVELOPMENTS

Systematic rock chip sampling began in 1995. The 36 prospective formations were sampled mainly in their type sections or in other outcrops. In some cases, where the prospective formations were poorly exposed, samples of float were collected. The rock chip samples consist of 0.5 to 1.0 kg of the most altered rock types present at a given sample site (silicified, argillized, or limonitic). At sites where the formation was homogeneous, a single rock sample was collected, but at sites where the formation was heterogeneous, a composite sample representing the total variability of rock types present was collected. The sample sites were marked on Gauss–Krüger topographic map sheets (1 : 25,000 scale).

Core samples were obtained from regional core libraries (Szépvízér, Rákóczi telep and Vasas) of the Geological Institute of Hungary. Drill cores were selected for sampling based on the results of previous regional evaluations (Mecsek Mts.: NAGY and KORPÁS 1995, Balatonfő: ÓDOR and LAJTOS 1995, Rudabánya: KALÓ and HERNYÁK 1995-1996, Transdanubian Range: KNAUER 1996, Bükk Mts. and Uppony Mts.: PELIKÁN 1996, Reck and Darnó Hill: ZELENKA 1996) or because the cores are of prospective formations. Where previous geochemical data was available, cores containing more than 1 ppm Au, 1 ppm Ag, 600 ppm As, or 100 ppm Pb, Zn or Cu were sampled. Prospective formations were sampled at intervals of 20 to 50 meters.

In the case of the Buda and Pilis Mts., the results of the previous stream sediment survey (ÓDOR et al. 1994) were used to choose anomalous cells for additional sampling. In the Mecsek Mts., Bükk and Uppony Mts., the Aggtelek–Rudabánya Mts. and Szendrő Mts. rock chip sampling of prospective formations and stream sediment sampling were conducted simultaneously. The total number of sample sites on surface, in cores, and mining tunnels was 604 and chemical analyses of 1398 samples from these sites were carried out (Fig. 3, Appendix 1). Analytical results from both the rock chip samples and stream sediment surveys were used in the final evaluation (KORPÁS et al. 1999).

More than 90% of the samples were analyzed in the Laboratory of the Geological Institute of Hungary for Au, Ag, As, Hg, Sb and Tl. Rock chip samples were prepared and analyzed as follows. A 0.15–0.20 kg split of each sample was crushed to an average diameter of 5 mm and then ground in a ball-mill to a final grain size of 0.63 mm. After sieving and homogenization, 20 g of the powdered sample was digested in aqua regia. The concentration of Ag, As, Sb and Tl were determined from solution by ICP-OES and ICP-MS. Mercury and gold were extracted from the samples in high pressure bombs and analyzed by AAS. Detection limits were as follows: Au - 2 ppb, Ag - 0.02 ppm, As - 2.5 ppm, Sb - 0.02 ppm, Hg - 0.02 ppm, Tl - 0.02 ppm (BERTALAN and BARTHA 1999). For statistical evaluations and plotting, the analytical results were compiled in a geochemical database by Sándor LAJTOS.

Field studies of Carlin-type gold deposits in Nevada in 1995 resulted in conceptual changes that affected our assessments of gold potential. Taking into consideration analogies in structure and geology between the Carlin Trend and the Darnó Zone, we changed the ranking of prospective formations (KORPÁS and HOFSTRA 1996). For example, the Szendrőlád Limestone, Uppony Limestone, Tapolcsány Formation, Nagyvisnyó Limestone, Szilvásvár Formation, Mályinka Formation and Hámor Dolomite entered the medium potential group, while all previously selected formations of the Mecsek Mts. (Hetvehely Dolomite, Misina Formation Group, Kantavár Formation and Óbánya Silt) were excluded from the group of prospective formations. Since most of the gold deposits in Nevada are hosted in very common rock types, we sampled an expanded list of potentially ore-bearing formations. Follow-up rock chip sampling in the anomalous cells of the ongoing stream sediment survey also increased the number of prospective units. In total, 97 formations including two mine dumps were sampled (Fig. 2).

Field studies conducted by the USGS experts in Hungary in 1996 resulted in a preliminary evaluation of the potential for Carlin-type gold in Hungary (KORPÁS et al. 1997) and delineation of ten prospective areas and formations that were recommended for further evaluation (KORPÁS et al. 1999). Most of these areas and formations are located at the master faults and related shear zones of Hungary and overprinted by multiphase magmatic events.

Preparation of publications that summarize the results of the project started in 1997.

4. REFERENCES

- BARTHA, A. 1996: A Carlin típusú ércesedés néhány elemének analitikai kémiai vizsgálata. (About analytical methods of some elements of Carlin type mineralization). — Magyar Geológiai Szolgálat Országos Földtani és Geofizikai Adattára, Kézirat (Unpublished report in Hungarian).
- BERTALAN, É.–BARTHA, A. 1999: Analytical background of Carlin-type gold prospecting in Hungary. — *Geologica Hungarica Series Geologica* 24: 169–178.
- CRAIG, J. R.–RIMSTIDT, J. D. 1998: Gold production history of the United States. — *Ore Geology Reviews* 13: 407–464.
- CSALAGOVITS, I. 1973: A Rudabánya környéki triász összlet geokémiai és ércgenetikai vizsgálatának eredményei. (Results of geochemical and ore genetic investigations of a Triassic sequence in the vicinity of Rudabánya). — *A Magyar Állami Földtani Intézet Évi Jelentése 1971*: 61–90. (In Hungarian with English abstract)
- CSÁSZÁR, G. 1997: Basic Lithostratigraphic Units of Hungary. Charts and short descriptions. — Geological Institute of Hungary, Budapest: 114 p.
- CSILLAG, J. 1975: A recski terület magmás hatásra átalakult képződményei. (Rocks transformed upon magmatic effect in the Recsk area, Hungary). — *Földtani Közlöny* 105: 646–671. (In Hungarian with English abstract).
- FÖLDVÁRINÉ VOGL, M. 1970: Összefoglaló értékelő jelentés a területi ritkaelemkutatás tájékoztató jellegű kutatási fázisának eredményeiről. (Summary report about results of the regional orientative rare element research). — *Magyar Állami Földtani Intézet, Budapest*: 95 p. (In Hungarian).
- HOFSTRA, A. 1999: Descriptive model of Carlin-type gold deposits. — *Geologica Hungarica Series Geologica* 24: 137–150.
- JÁMBOR, Á. 1989: Magyarország földtani térképe. M=1:1 000 000. (Geological map of Hungary. Scale: 1:1 000 000). — *Magyar Állami Földtani Intézet*
- KNAUER, J. 1996: A Dunántúli–középhegység DNY-i és középső része Carlin aranyérc potenciáljának értékelése irodalmi és adattári források alapján. (Evaluation of Carlin gold potential of SW and Central Transdanubian Range, based on published and unpublished data). — *Magyar Geológiai Szolgálat Országos Földtani és Geofizikai Adattára, Kézirat* (Unpublished report in Hungarian).
- KALÓ, J.–HERNYÁK, G. 1995–1996: Rudabányai ércelemzések, arany és ezüst. (Analytical data from Rudabánya, gold and silver). — *Magyar Geológiai Szolgálat Országos Földtani és Geofizikai Adattára, Kézirat* (Unpublished report in Hungarian).
- KORPÁS, L.–HOFSTRA, A. 1994: Potential for Carlin-type gold deposits in Hungary. Carlin gold in Hungary. — Project JFNo 435. US–Hungarian Joint Fund, Budapest
- KORPÁS, L.–HOFSTRA, A. 1996: Potential for Carlin-type gold deposits in Hungary. — 30th International Geological Congress, Beijing, Abstracts, CD.
- KORPÁS, L.–ÓDOR, L.–HORVÁTH, I.–CSIRIK, GY.–HAAS, J.–HOFSTRA, A.–LEVENTHAL, J. 1997: Carlin arany Magyarországon (Carlin gold in Hungary). — *Földtani Kutatás*. 34(4): 3–9. (In Hungarian).
- KORPÁS, L.–HOFSTRA, A.–ÓDOR, L.–HORVÁTH, I.–HAAS, J.–ZELENKA T. 1999: Evaluation of the prospected areas and formations. — *Geologica Hungarica Series Geologica* 24: 197–293.
- NAGY, E. 1972: Vizsgálataink a Kőszegi-hegységben. (Investigations in the Kőszeg Mountains). — *Magyar Állami Földtani Intézet Évi Jelentése 1970*: 197–207. (In Hungarian with German abstract).
- NAGY, E.–KORPÁS, L. 1995: Carlin arany Magyarországon. A mecseki terület értékelése. (Carlin gold in Hungary. Evaluation of the Mecsek area). — *Magyar Geológiai Szolgálat Országos Földtani és Geofizikai Adattára, Kézirat* (Unpublished report in Hungarian).
- ÓDOR, L.–HORVÁTH, I.–FÜGEDI, U. 1994: A Börzsöny–Dunazug–Pilis–Budai-hegység geokémiai felvétele. (Geochemical survey of the Börzsöny–Dunazug–Pilis–Buda Hills region). — *Magyar Geológiai Szolgálat Országos Földtani és Geofizikai Adattára, Kézirat* (Unpublished report in Hungarian).

- ÓDOR, L.–LAJTOS, S. 1995: A szabadbattyáni terület felszíni és fúrásmintáinak nyomelem adatai (Ag, As, Pb ppm). (Rare element data of surface and drillhole samples of the Szabadbattyán area, Ag, As, Pb ppm). — Magyar Geológiai Szolgálat Országos Földtani és Geofizikai Adattára, Kézirat (Unpublished report in Hungarian).
- ÓDOR, L.–HORVÁTH, I.–FÜGEDI, U. 1997: Észak-Magyarország nemesfém perspektívái a patakhordalékok geokémiai felvétele alapján. (Precious metal perspectives of northern Hungary based on stream sediment survey). — Földtani Kutatás. 34(2): 9–12. (In Hungarian with English abstract).
- PELIKÁN, P. 1996: Geokémiai és földtani adatok a Bükk-hegységi Carlin aranyérc potenciál felméréséhez. (Geochemical and geological data for estimation of Carlin gold ore potential in the Bükk Mountains). — Magyar Geológiai Szolgálat Országos Földtani és Geofizikai Adattára, Kézirat (Unpublished report in Hungarian).
- ZELENKÁ, T. 1996: Carlin-típusú aranyércesedés lehetőségei Recskén. (Possibility of Carlin-type gold mineralization in Recsk). — Magyar Geológiai Szolgálat Országos Földtani és Geofizikai Adattára, Kézirat (Unpublished report in Hungarian).

ANALYTICAL BACKGROUND OF CARLIN-TYPE GOLD PROSPECTION IN HUNGARY

ÉVA BERTALAN and ANDRÁS BARTHA

Geological Institute of Hungary, H-1143 Budapest, Stefánia út 14., Hungary

ABSTRACT

Analytical methods used for the purposes of the project J.F. No. 435 "Potential for Carlin-type gold deposit in Hungary" are described in this paper. Ag, As, Au, Sb and Tl were determined from the samples after aqua regia decomposition and Hg directly from the solid sample (by AMA 254 instrument, dedicated to mercury determination). Determination of gold was performed by electrothermal (graphite furnace) atomization atomic absorption spectrometry (GF-AAS), after separation and preconcentration by extraction with isobutylmethylketon. Other elements were determined by inductively coupled plasma mass spectrometry (ICP-MS). Results of the ongoing "Geochemical mapping project" at the Geological Institute of Hungary including the stream sediment survey of the hilly areas in Hungary were also involved into interpretation of the Carlin gold project. In this project, a considerably wider range of elements (18 elements) was determined. In this case, determination of mercury and gold was carried out in the same way as it was done during the Carlin gold project. Determination of arsenic and antimony was performed by hydride generation atomic absorption spectrometry (HG-AAS) and silver was analyzed by flame atomization atomic absorption spectrometry (Flame-AAS). Further elements were determined by inductively coupled plasma optical emission spectrometry (ICP-OES). Analytical methods used were checked by comparison with different analytical methods. Results show pretty good agreement.

1. INTRODUCTION

Chemical analysis of the samples collected in the frameworks of the Carlin gold project was performed in the laboratory of the Geological Institute of Hungary. Analytical background of the research can be summarized as follows.

Determination of the aqua regia leachable elements was carried out. Elements to be determined were going into solution probably in 100 per cent or close to this ratio, because of their chemical characteristics.

Chemical analyses were carried out for the elements as Au, Ag, As, Sb, Hg and Tl.

Determination of gold and mercury was done by atomic absorption spectrometry and the other elements were determined by inductively coupled plasma mass spectrometry technique.

We used this analytical scheme because: it was an important point of view of convenience to use multi-elemental method if possible. That is why the use of ICP-MS is practical (JARVIS et al. 1992, HALL 1992, BRENNER and ZANDER 1996). For the gold and mercury, however, despite of their high atomic mass and freedom from spectral interferences, we could not obtain proper sensitivity by ICP-MS technique.

Gold will be ionized only in 51% in the plasma. Despite of that, the limit of detection seems favorable, it can be calculated to be about 10-20 ppb. This value, however, is much higher than the average abundance of gold (which is about 2 ppb). That is why we had to choose the atomic absorption method with preconcentration and separation. The latter method does not have any competitor in this field.

For the mercury, it was not the case. In fact, mercury will be ionized only in 38% in the plasma. Detection limits are still sufficient to fulfil the requirements of this research. Mercury, however, produces very strong memory effect. Aspirating mercury solution into the plasma, the wash-up time is very long even at very low concentra-

tions (e.g. using 10 µg/l solution). So, we could not obtain reliable results after aspirating a calibration solution or a sample solution with higher mercury concentration. That is why determination of mercury by ICP-MS is generally avoided. Fortunately, a very simple and reliable analytical method i.e. cold vapour atomic absorption spectrometry (directly from solids) is available (BARTHA et al. 1996).

Results of the stream sediment survey were also utilized. During this project, a wide range of elements was determined from the samples, namely: Ag, As, Au, Ba, Cd, Co, Cr, Cu, Hg, K, Li, Mn, Mo, Ni, Pb, Sb, Sr and Zn. Determinations were performed mostly by inductively coupled optical emission spectrometry (ICP-OES), utilizing multi-elemental characteristic of the method (JARVIS and JARVIS 1992, BRENNER and ZANDER 1996). Detection limits were generally low enough to fulfil the requirements of the survey but for some elements, atomic absorption spectrometry (AAS) was applied, using different atomization methods: electrothermal (graphite furnace) atomization (for gold, after preconcentration by MIBK extraction), hydride generation (for arsenic and antimony), cold vapour technique (for mercury) and flame atomization (for silver). Interpreting results for the purposes of Carlin research, only analysis results for Ag, As, Au, Ba, Hg and Sb were utilized (KORPÁS et al. 1999).

2. INSTRUMENTATION

In the laboratory of the Geological Institute of Hungary a considerable technical infrastructure is available.

ICP-MS measurements were performed on a commercial quadrupole system (VGE PlasmaQuad II STE, VG Elemental, Winsford, Cheshire, UK). Ion optics was optimized for indium, a medium-mass element.

Determination of gold was performed by a SpectrAA-10BQ atomic absorption spectrometer (Varian, Melbourne, Victoria, Australia), equipped with a Varian GTA-95 Graphite Furnace Unit. Sample introduction was done automatically, using a PSD Programmable Sample Dispenser. A commercial Varian uncoded hollow cathode lamp and the 242.8 nm resonance line was used. Background correction was made by deuterium lamp method. Partitioned coated graphite tubes were used (Varian Part. No.: 63-100012-00).

Mercury was determined by cold vapour atomic absorption spectrometry, directly from the solid sample. AMA 254 instrument (Advanced Mercury Analyzer) was used (made by Altech, Czech Republic, distributed by LECO). Sample was placed into sampling boat and introduced into a decomposition tube. Sample was there first dried and then thermally decomposed (or even burned) in oxygen flow, by controlled heating of the decomposition furnace. Oxidation was finalized in a catalytic furnace and some of combustion products were trapped here. Mercury vapours were selectively trapped by a gold-containing amalgamator. In a second stage, mercury was released by heating of amalgamator and transferred into the measuring cells where measurement of absorbance was carried out. In case of low mercury concentrations, determinations were carried out directly from the solid sample. Samples containing higher concentrations of mercury were decomposed and solution was analyzed.

ICP-OES determinations were performed by a combined instrument (sequential instrument also equipped with a 20-channel polychromator) (JY70, Jobin Yvon, Longjumeau, France).

During the stream sediment survey, several elements were determined by atomic absorption spectrometry, using different atomization methods. Instrument used was a SpectrAA-10BQ atomic absorption spectrometer (Varian, Melbourne, Victoria, Australia). For flame atomization, a commercial 10 cm burner head (Mark VI) was used. For the determination of hydride forming elements, instrument was equipped with a continuous hydride generation unit, made by Labtech (Brno, Czech Republic). Determination of gold and mercury was performed as written above.

3. CHEMICALS AND REAGENTS

Distilled water (glass distillation unit, made by SIMAX, former Czechoslovakia) was used throughout the work. In ICP-MS work (for dilution of samples and preparation of calibration standards), ultrapure water, with a resistivity of 18 MΩcm, was used, obtained from a Purite HP Still Plus system (Purite Ltd., Thame, Oxfordshire, UK). Hydrochloric acid 36% and nitric acid 70% used for decomposition were BDH (Poole, Dorset, UK) products, "Spectrosol" quality. For preparation of ICP-MS calibration standards, nitric acid 65% of "Suprapur" quality (Merck, Darmstadt, Germany) was used. "Procedure blank" was prepared by each batch of samples.

Stock solutions for ICP-MS calibration standards were mono-elemental solutions (1 g/l each) and were from BDH, "Spectrosol" grade (Ag, As and Sb) and from SPEX Industries, Inc. (Edison, NJ, USA) (TI, SPEX Plasma Standard solution, PLTL2-2Y). These solutions were diluted to give concentration of 10 mg/l. Calibration standard solutions were made up by mixing and dilution of these latter solutions. Final acid concentration was 1% of

nitric acid. (Nitric acid 65% used throughout ICP-MS work was Merck product, "Suprapur" quality). Stock solution for indium internal standard was a mono-elemental solution (1 g/l) and was from BDH, "SpectrosoL" grade. This solution was diluted to give a concentration of 1 mg/l. The latter solution was added to the sample solutions to give a final In concentration of 10 µg/l.

Gold stock solution for GF-AAS calibration standards was mono-elemental solution (1 g/l) and was from BDH, "SpectrosoL" grade. Calibration standard solutions were made up by stepwise dilution of this stock solution. Final acid concentration was about 1.2 mol/l of hydrochloric acid. Isobutylmethylketone used for gold extraction was from BDH, "AnalaR" grade.

4. ANALYTICAL METHODS

4.1. Sample decomposition methods

Decomposition is a key question in course of the chemical analysis. In geological and geochemical research it is especially difficult to decide which decomposition method would be the most suitable one for the task in question. Using methods providing "complete" decomposition, several problems will be faced (increased total dissolved solids content, use of hydrofluoric acid etc.). Analyzing chalcophile elements, however, some of these problems can be diminished. In this case, dissolution of the samples by some acidic mixture (mostly aqua regia) is completely sufficient (CHAO and SANZOLONE 1992, TOTLAND et al. 1992, BERTALAN et al. 1999)

Two different dissolution techniques were applied. One of them is decomposition in closed, high-pressure bomb which allows also the volatile mercury to be determined. (PTFE bomb vessels in stainless steel housing by Parr Instruments, Moline, Illinois, USA, were used.) Another decomposition is open vessel dissolution by aqua regia which is suitable to handle also large sample portions.

For the open vessel decomposition, it was advisable to roast the samples previously. Roasting was necessary because of the weak solubility of the possible arsenopyrite content of the sample. Roasting was performed in electric furnace, held the sample at 700 °C for 2 hours. Relatively weakly soluble sulfides were oxidized during roasting. Sample weight was 5 g. After finishing roasting, samples were transferred into glass beakers, 12.5 ml of concentrated hydrochloric acid and 5 ml of concentrated nitric acid were added and samples were evaporated to dryness on waterbath. Residues were dissolved by 10 ml of 1:1 diluted hydrochloric acid and solutions were made up to 50 ml. Final sample concentration was 100 g/l. Determination of gold was carried out from an aliquot of this solution by graphite furnace atomic absorption spectrometry (GF-AAS) after preconcentration and separation by organic extraction. Determination of arsenic, antimony, silver and thallium was performed by ICP-MS technique after proper dilution of sample solution. ICP-OES and AAS determinations were performed from this solution as well, also after proper dilution of sample solution.

Performing high pressure decomposition, 0.5 g of sample was weighed into PTFE vessel of the bomb. Weighed samples were suspended with some drops of distilled water, 2 ml of concentrated hydrochloric acid and 2 ml of concentrated nitric acid were added, bombs were closed and held at 150 °C for 1 hour in drying oven. After cooling down, sample solutions were made up to 100 ml. Sample concentration was 5 g/l. These solutions served for the determination of higher mercury concentrations (much higher than 10 ppm) by cold vapour technique atomic absorption spectrometry. In this case, determination of mercury could not be carried out directly from the solid sample because mercury vapours could be condensed in the catalytic furnace of the instrument and could not be removed from there any more.

Determination of mercury (below 10 ppm) was made directly from solid sample.

4.2. ICP-MS determinations

Elements as As, Ag, Sb, Tl were determined by ICP-MS method. Analyses were performed by a VG Plasma-Quad II STE ICP-MS instrument. Sample solution of 100 g/l sample concentration was diluted 100-fold, obtaining solution of 1 g/l sample concentration to measure. 10 µg/l In was added as internal standard into this solution. Detection limit of the measurements was 0.2 ppm for arsenic and 0.02 ppm for the other elements. Instrument operating parameters are listed in Table 1.

In the ICP-MS determinations, only arsenic could be considered as critical element as it can be subjected to spectral interferences. Arsenic has got only one natural isotope ⁷⁵As and a polyatomic ion, with a mass number of 75, formed from argon and chlorine atoms, will cause an overlap, a spectral interference. In our case the system contained chloride ions because during the open vessel decomposition, evaporation residue was dissolved by hy-

Instrument	VG Elemental PlasmaQuad II STE
Plasma	all argon
Forward power	1350 W
Reflected power	<5 W
Coolant gas flow	13.5 l/min
Auxiliary gas flow	1.4 l/min
Nebuliser gas flow	0.928 l/min
Peristaltic pump	Gilson Minipuls 3
Uptake rate	about 1 ml/min
Nebuliser	V-groove
Spray chamber	double-pass, water-cooled (10 °C)
Sampling cone type	Ni, 1 mm orifice
Skimmer	Ni, VG design
Acquisition mode	scan
Detector mode	PC
Channel/amu	20
Dwell time	320 μ s
Acquisition time	60 s
Scanned regions	71.6 - 79.4 amu
	103.6 - 125.4 amu
	199.6 - 206.4 amu
Internal standard	^{115}In (10 $\mu\text{g/l}$)

drochloric acid. For the ICP-MS determination, however, this solution was diluted 100-fold, so the final concentration of hydrochloric acid was about 0.01 mol/l. According to our experiences, this concentration did not cause serious problem and could be corrected properly by mathematical methods, using peak with mass number of 77. It was proven by comparison with another independent analytical methods (see Section 5). Results obtained by hydride generation AAS or ICP-OES showed very good agreement with the ICP-MS results.

4.3. Analysis of gold

Gold content of samples was determined from the solution obtained by open vessel decomposition (final sample concentration of 100 g/l), after preconcentration by isobutylmethylketon, by electrothermal (graphite furnace) atomization atomic absorption spectrometry (GF-AAS). Analyses were performed by a Varian SpectrAA-10BQ instrument. Graphite furnace operating parameters are listed in Table 2.

10 ml of sample solution was extracted by 2 ml of isobutylmethylketon for 2 minutes and the phases left to be separated. Aliquots of the organic phases were transferred into the autosampler vials. 10 μl of the organic phase was injected into the graphite furnace and analyzed. In case of high gold concentrations, sample solution was diluted by a proper dilution factor and extracted again. Detection limit of the method was 2 ppb Au.

4.4. Analysis of mercury

Mercury was determined by cold vapour atomic absorption spectrometry (CV-AAS). AMA 254 instrument was used. In case of low mercury concentrations, determinations were carried out directly from the solid sample. Sample weight was 100 mg. Instrument operating parameters are listed in Table 3. Detection limit was 0.1 ppb Hg.

Graphite furnace operating parameters*Table 2*

Step No.	Temperature (°C)	Time (s)	Gas flow (l/min)	Gas type	Read command
1.	95	5.0	3.0	Normal	No
2.	120	5.0	3.0	Normal	No
3.	150	10.0	3.0	Normal	No
4.	300	5.0	3.0	Normal	No
5.	700	30.0	3.0	Normal	No
6.	1000	2.0	0.0	Normal	No
7.	2600	1.0	0.0	Normal	Yes
8.	2600	2.0	0.0	Normal	Yes
9.	2600	2.0	3.0	Normal	No

Mercury analyzer operating parameters*Table 3*

Stage	Temperature (°C)	Time (s)
Drying	120	60
Pyrolysis	850	150
Waiting	120	40
Measurement	Release: 950 Reading: 120	45

Operating parameters of the ICP-OES instrument*Table 4*

RF power	1000 W
Reflected power	<10 W
Plasma gas flow rate	12 l/min
Sheath gas flow rate	0.2 l/min
Nebuliser type	cross-flow
Nebuliser flow rate	0.4 l/min
Nebuliser pressure	2.7 bar
Observation height	15 mm (above load coil)
Integration time	0.5 s (poly) to 5 s (mono)

Integration time depends on using polychromator or monochromator and depends on the element in question (relative intensity of the selected line, wavelength, quality of background etc.).

Samples containing higher concentrations of mercury were decomposed and solution was analyzed. 100 µl of sample solution was measured onto an amount of ignited sample. This served to avoid splashing of sample and damage of sample boat by the acidic solution. After this, analysis cycle was started. Detection limit was 20 ppb Hg, calculated for solid sample.

Element	Wavelength (nm)	Background (nm)	Calibration concentration (mg/l)	Calibration conc. in rock (ppm)	Det. lim. in rock (3 σ) (ppm)
Cr	205.552 p	+0.0635	1.0	200	2
Zn	213.856 p	+0.0635	1.0	200	1
Co	228.616 p	-0.0635	1.0	200	2
Ni	231.604 p	+0.0635	1.0	200	2
Ba	233.527 p	+0.0635	1.0	200	0.5
Cu	324.754 p	-0.0635	1.0	200	0.5
Sr	407.771 p	+0.0635	1.0	200	1
Mn	257.610 p	+0.1143	1.0	200	0.2
Mo	202.030 m	-0.0295	1.0	200	1
Pb	220.353 m	+0.0206 -0.0235	1.0	200	5
Cd	228.802 m	+0.0586	1.0	200	1
Li	670.784 m	-0.0595	1.0	200	0.5
K	769.896 m	-0.0447	100	2.408% (K ₂ O)	20

m=using monochromator
p=using polychromator

Wavelengths used in atomic absorption spectrometry and detection limits obtained

Table 6

Element	Wavelength (nm)	Det. lim. in rock (ppm)
As	197.26	0.5
Sb	206.83	0.5

4.5. ICP-OES determinations

Analyses were performed by a Jobin Yvon JY70 instrument. Sample solution of 100 g/l sample concentration was diluted 20-fold, obtaining solution of 5 g/l sample concentration to measure. Internal standard was not used. Instrument operating parameters are listed in Table 4.

Spectral lines chosen for the determinations and detection limits are listed in Table 5.

4.6. Analysis of arsenic and antimony

Arsenic and antimony content of samples was determined by hydride generation AAS. Varian SpectrAA-10BQ instrument equipped with a hydride generation unit (Labtech, Brno, Czech Republic) was used. Sample solution of 100 g/l sample concentration was diluted 10-fold, obtaining solution of 10 g/l sample concentration to measure. To bring the analytes into proper valence state, pre-reduction of the sample was carried out by potassium iodide. Spectral lines chosen for the determinations and detection limits are listed in Table 6.

4.7. Analysis of silver

Silver content of samples was determined by flame atomization AAS. Varian SpectrAA-10BQ instrument was used. Sample solution of 100 g/l sample concentration was diluted 2-fold, obtaining solution of 50 g/l sample concentration to measure. Wavelength used was 328.10 nm. Detection limit (3 σ) is 0.3 ppm, calculated for the original rock sample.

5. COMPARISONS WITH DIFFERENT ANALYTICAL METHODS

Analytical methods used in the course of the project were checked for some elements by analyzing a number of samples by independent analytical methods and by comparison of results. During this study, results obtained by inductively coupled plasma mass spectrometry (ICP-MS) were compared with data produced by electrothermal (graphite furnace) atomization atomic absorption spectrometry (GF-AAS, in case of silver), flame atomization atomic absorption spectrometry (Flame-AAS, also for silver), hydride generation atomic absorption spectrometry (HG-AAS, in case of arsenic and antimony) and inductively coupled plasma optical emission spectrometry (ICP-OES, also for arsenic).

Firstly, comparison of silver results is shown as follows (Figs. 1, 2 and 3). More than 50 selected samples were analyzed both by inductively coupled plasma mass spectrometry (ICP-MS) and by electrothermal (graphite furnace) atomization atomic absorption spectrometry. Analytical results are plotted (Fig 1). Plain line is the ideal case: if results were identical. Lower concentration values are shown in a separate graph (Fig. 2).

Agreement is rather good or at least acceptable.

Flame atomization atomic absorption spectrometry is suitable to measure also higher concentration values. Fig. 3. shows comparison of analytical results of about 80 samples, obtained by ICP-MS and Flame-AAS methods.

Agreement is pretty good except for the higher concentration values where some deviation can be seen – ICP-MS values are a bit higher. It is very common in the ICP-MS technique to get some positive error analyzing much higher concentrations than the highest calibration solution. In this case, proper dilution of the sample solutions can completely eliminate this source of error.

As it was mentioned above (Section 4.2.), ICP-MS determination of arsenic is prone to chloride interferences. This problem, however, can be eliminated using mathematical corrections. To check the applicability of these correction methods and the correctness of the ICP-MS analyses, about 150 selected samples were analyzed both by inductively coupled plasma mass spectrometry (ICP-MS) and by inductively coupled plasma optical emission spectrometry (ICP-OES). For the comparison, results were plotted (Fig. 4).

Results show pretty good agreement. Lower concentration values are plotted also in separate graphs (Figs. 5 and 6).

It can be seen very well, that the agreement between the results is extremely good even for the low concentrations. This agreement is also a good proof of the fact that none of these analytical methods are influenced by the possible interference sources (chloride interference in ICP-MS and interference by iron in ICP-OES).

ICP-MS analysis results were also checked by analyzing some selected samples by hydride generation atomic absorption spectrometry (HG-AAS). In the latter, also a separation of the analyte from the matrix is done, so possible interference effects will be significantly diminished. Plot of the results is shown in Fig. 7.

Results are in very good agreement also in this case.

HG-AAS analysis of antimony from some selected samples was also carried out. Plot of the results is shown in Fig. 8.

Results show good agreement again.

Determination of mercury was also involved in this study. Analysis results for mercury, obtained by cold vapour atomic absorption spectrometry (CV-AAS) directly from the solids and from a solution of decomposed sample, respectively, were also compared. Plot of results of about 100 samples is shown in Fig. 9.

Agreement is good. That means, occurrence of the mercury in the sample is rather homogeneous, so small sample weight used in the direct solids analysis will not cause significant problem.

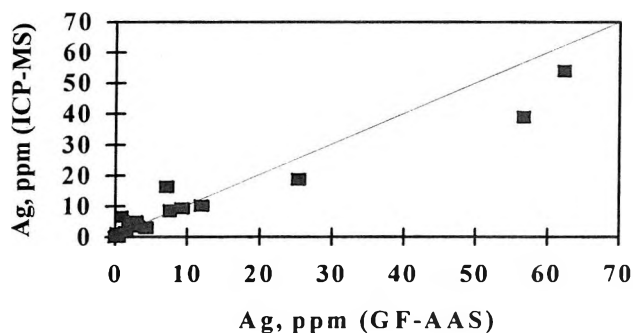


Fig. 1: Determination of silver from rock samples: comparison of ICP-MS and GF-AAS methods

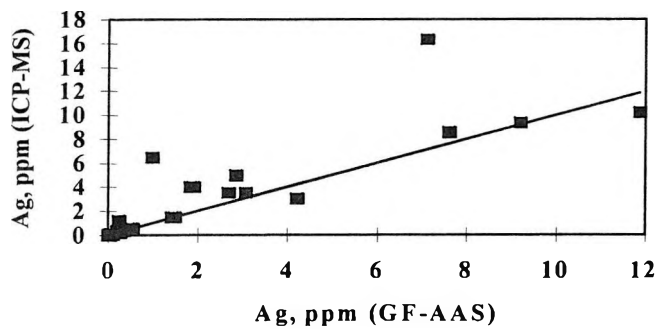


Fig. 2: Determination of silver from rock samples: comparison of ICP-MS and GF-AAS methods (lower concentration values only)

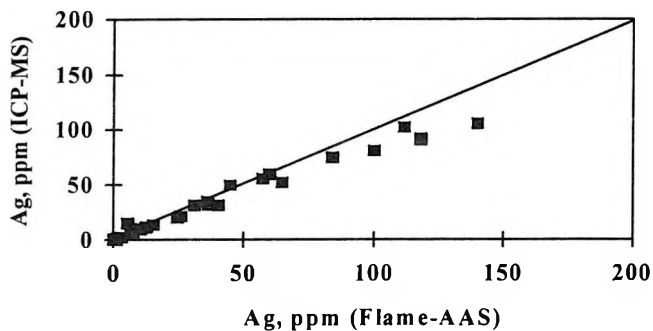


Fig. 3: Determination of silver from rock samples: comparison of ICP-MS and Flame-AAS methods

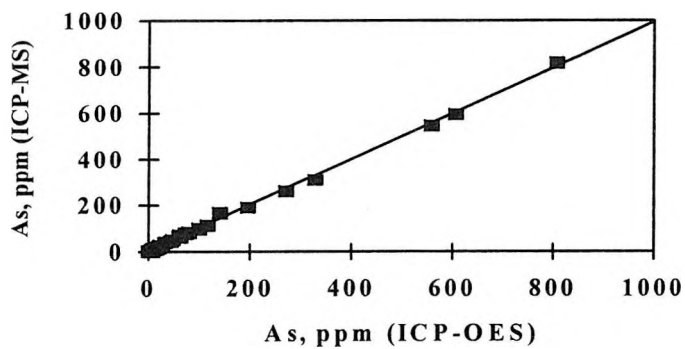


Fig. 4: Determination of arsenic from rock samples: comparison of ICP-MS and ICP-OES methods

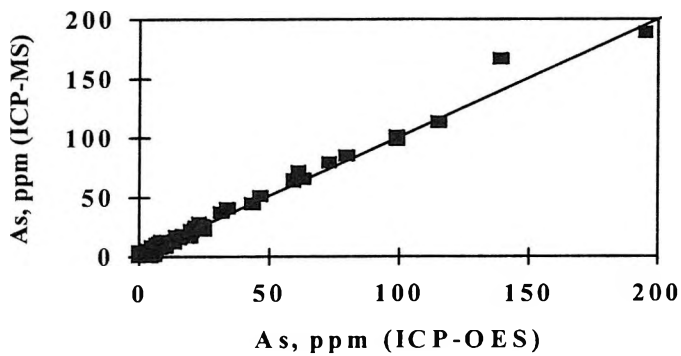


Fig. 5: Determination of arsenic from rock samples: comparison of ICP-MS and ICP-OES methods (lower concentration values only)

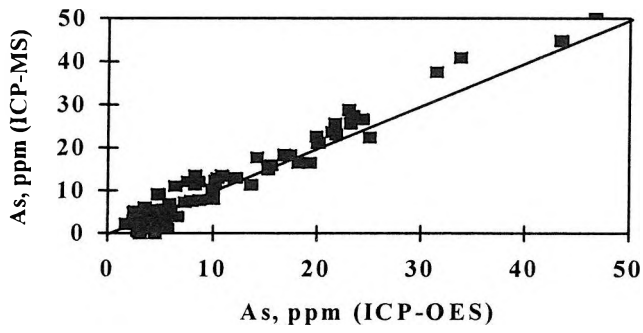


Fig. 6: Determination of arsenic from rock samples: comparison of ICP-MS and ICP-OES methods (concentration values below 50 ppm only)

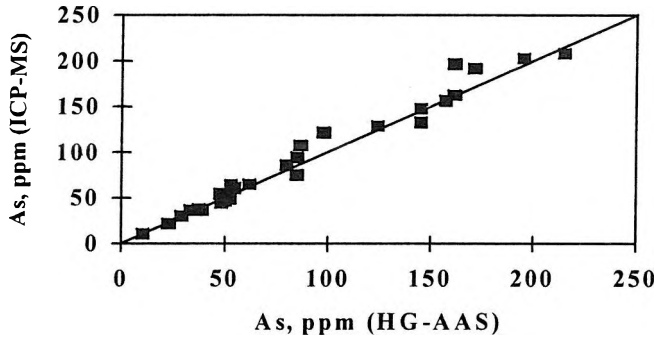


Fig. 7: Determination of arsenic from rock samples: comparison of ICP-MS and HG-AAS methods

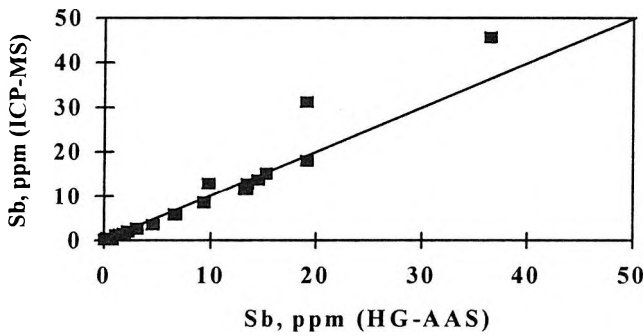


Fig. 8: Determination of antimony from rock samples: comparison of ICP-MS and HG-AAS methods

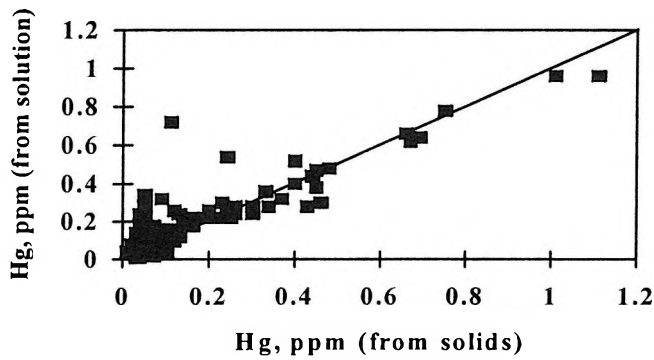


Fig. 9: AAS determination of mercury from rock samples: comparison of analysis directly from the solids and analysis from solutions of decomposed samples

6. CONCLUSION

Analytical methods used in the course of the Carlin gold project are suitable to solve emerging analytical tasks. Comparison of results with results of different independent analytical methods shows good agreement.

7. REFERENCES

- BARTHA, A.–VARGA–BARNA, ZS.–MARTH, P.–HORVÁTH, I.–ÓDOR, L.–FÜGEDI U. 1996: Ártéri üledékek higany-tartalmának meghatározása AMA-254 készülékkel. (Determination of mercury content of overbank sediment samples by AMA-254 – Advanced Mercury Analyzer). — Proc. of the 39th Hungarian Annual Conference on Spectrochemistry, Mosonmagyaróvár, Abstracts, 131. (In Hungarian).
- BERTALAN, É.–BARTHA, A.–BALLÓK, M.–VARGA–BARNA, ZS. 1999: Laboratóriumi módszerek harmonizációjának szükségessége talaj- és üledékminták kioldható elemtartalmának meghatározásánál. (Necessity of harmonization of analytical methods at the determination of acid soluble content of soil and stream sediment samples). — Proc. of the 42nd Hungarian Annual Conference on Spectrochemistry, Veszprém, Abstracts, 125–128. (In Hungarian).
- BRENNER, I. B.–ZANDER, A. 1996: Geoanalysis using plasma spectrochemistry– milestones and future prospects. — *Fresenius Journal of Analytical Chemistry*, 355: 559–570.
- CHAO, T. T.–SANZOLONE, R. F. 1992: Decomposition techniques. — *Journal of Geochemical Exploration*, 44: 65–106.
- HALL, G. E. M. 1992: Inductively coupled plasma mass spectrometry in geoanalysis — *Journal of Geochemical Exploration*, 44: 201–249.
- JARVIS, K. E.–GRAY, A. L.–HOUK, R. S. 1992: *Handbook of Inductively Coupled Plasma Mass Spectrometry*. — Blackie, Glasgow and London, 256 p.
- JARVIS, I.–JARVIS, K. E. 1992: Inductively coupled plasma-atomic emission spectrometry in exploration geochemistry. — *Journal of Geochemical Exploration*, 44: 139–200.
- KORPÁS, L.–HOFSTRA, A. H.–ÓDOR, L.–HORVÁTH, I.–HAAS, J.–ZELENKA, T. 1999: Evaluation of the prospected areas and formations. — *Geologica Hungarica Series Geologica* 24: 197–293.
- TOTLAND, M.–JARVIS, I.–JARVIS, K. E. 1992: An assessment of dissolution techniques for the analysis of geological samples by plasma spectrometry. — *Chemical Geology*, 95: 35–62.

GEOLOGICAL SETTING AND TECTONIC EVOLUTION OF HUNGARY

JÁNOS HAAS¹, GÉZA HÁMOR² and LÁSZLÓ KORPÁS³

¹ Hungarian Academy of Sciences–Eötvös Loránd University, Geological Research Group,
H–1088 Budapest, Múzeum krt. 4a., Hungary

² Eötvös Loránd University, Department of Regional Geology, H–1143 Budapest, Stefánia út 14., Hungary

³ Geological Institute of Hungary, H–1143 Budapest, Stefánia út 14., Hungary

ABSTRACT

Hungary is located in the central part of the Pannonian Basin filled up with a thick clastic sedimentary cover Neogene to Quaternary in age. Its basement is made up by Paleozoic to Early Tertiary formations representing the Austroalpine–Tatro-Veporic, the Pelso and the Tisza Megaunits, which are separated by major lineaments from each another.

At the end of the Variscan cycle the polymetamorphic complexes of the Tisza Megaunit belonged to the Variscan Foldbelt forming the southern margin of the European plate. Metamorphic formations of the Pelso Megaunit and the Austroalpine nappes may have formed in the Prototethys existed between the Eurasian and African plates. Closure of the Prototethys in the Middle Carboniferous led to accretion of the Variscan Foldbelt. Middle Carboniferous flysch and Late Carboniferous to Middle Permian continental molasse deposits indicate stages of this process. Low to high level gold anomalies were detected in some of the pre–Alpine formations of the Pelso Megaunit.

The Alpine evolution may be characterized by multiphase opening (Permian to Jurassic), closure of the Tethys (Cretaceous to Paleogene) and which was followed by the formation and filling up of the Pannonian Basin (Neogene to Quaternary).

Early rifting stage during Middle Triassic resulted in the disintegration of the ramp system and in opening of the Neotethys (Vardar-Meliata) oceanic basin between the European and African plate. The Tisza Megaunit together with the Aggtelek Unit belonged that time to the European plate margin, whereas dispersed blocks of the later Pelso Megaunit belonged to the African margin. Stabilisation of these passive margins led to the formation of extended carbonate platforms during Late Triassic. Low to high level gold anomalies may be bounded to rifting and passive margin formations in the realm of the Pelso Megaunit.

Continuation of ocean opening in the Tethys system in the Early to Middle Jurassic led to a segmentation of the passive margins and to the opening of a new oceanic branch (Ligurian-Penninic ocean). Ophiolites and related deep sea sediments of the Penninic unit in the Kőszeg Mts., and of the Szarvaskő Nappe which belonged to Neotethys (Vardar-Meliata) oceanic basin show low to high level gold anomalies, forming target for further explorations. The Jurassic continental margin formations of the Pelso and Tisza Megaunits are free of gold.

The closure of the Tethys started gradually by early subduction and collision during Late Jurassic to Upper Cretaceous and completed by late subduction and collision in the course of the Eocene and Oligocene, resulting in the formation of the Paratethys basins. Sedimentary formations of these stages of evolution are unfavorable for Carlin-type gold mineralization, in spite the fact, that the volcano-plutonic formations of the Paleogene Island Arc can be considered generators of gold mineralization in the areas of the Velence Hills and Recsk.

Evolution of the Pannonian Basin (Miocene to Quaternary) was controlled mainly by the formation of the early Inner Carpathian and the late East Carpathian volcanic arcs and back arc rifting. These processes led to the uplift of the Alp–Carpathian Chain and to the collapse of the Pannonian Basin. This stage in evolution was not favorable for Carlin-type gold mineralization, although some sedimentary formations exhibit sporadic gold anomalies near to detection level.

1. INTRODUCTION

Present-day geological setting of the Pannonian Basin, and within it Hungary, is the final result of a complicated and multiple evolutionary history. Complexity of the evolution is the consequence of the peculiar setting of the Pannonian region: it is located in the buffer zone of the European and the African continental plates where a series of ocean openings and continent collisions took place resulting in disruption of the lithosphere. Microplates, lithosphere chunks were formed. During the Alpine tectogenic stage, folding and nappe formation were followed by sizeable displacement of microplates leading to accretion of the mosaic-like basement of the Pannonian Basin. Formation of half-grabens, smaller basins and also the intense magmatic activity can be bound to Miocene orogeny of the Carpathians. In the same time, formation of a rift-type graben system of NW–SE direction (Vardar Graben, HÁMOR 1999) appears to be also of crucial importance. Attenuation of the crust (mantle diapir formation) led to generation of large basins of the Pannonian Basin System which primarily determine the present-day tectonic setting. The Carlin gold potential of Hungary was controlled by this multiphase evolution.

2. TECTONIC SETTING AND MAIN STAGES OF EVOLUTION

Hungary is located in the central part of the Pannonian Basin, thus sedimentary successions filling the young, deep Neogene depressions play a crucial role in the geology of the country (Fig. 1). Basement of the basins is made up by Paleozoic to Early Tertiary formations. Three major tectonic units (megaunits, composite terranes) separated by major faults or fracture zones (lineaments) constitute the pre-Middle Miocene basement of the Hungarian part of the Pannonian Basin (Fig. 2). These are as follows:

- the Austroalpine–Tatro–Veporic Megaunit bounded by the Piennini Klippen Belt on the north and the Rába–Diósjenő–Lubenic–Margecany Line on the south. The Penninic Unit, and above it some parts of the Austroalpine nappe complex, extend over western Hungary, whereas crystalline complexes of the Veporic Unit extend over northern Hungary;
- the Pelso Megaunit (Pelsonia Composite Terrane – Kovács et al. 1996-97) is located south to the above-mentioned megaunit and bounded by the Mid-Hungarian Line on the south. It consists of the Transdanubian Range, the Zagreb–Mid-Transdanubian, the Bükk and the Aggtelek Units, showing Alpine–Dinaridic facies affinity;
- the Tisza Megaunit (Tisia Terrane – KOVÁCS et al. 1996-97) is situated south of the Pelso Megaunit and limited by the Dinaridic Ophiolite Complex on the south and southwest and the Mures Ophiolite Belt on the east. Variscan tectogenesis led to accretion of the Tisia Terrane by the Late Permian. Paleozoic to Middle Jurassic sequences show definite European facies affinity. Differentiation of definite facies zones initiated in the Late Triassic leading to the formation of three facies units: Mecsek, Villány–Bihar and Békés–Kodru Zones, respectively. These are bounded by Alpine thrust sheets.

The Austroalpine–Tatro–Veporic Megaunit moved together with the Pelso Megaunit from the Late Oligocene. The large composite unit, which came into existence on this way, was named as Alcapa Megaunit (Csontos et al. 1992). The Alcapa got into juxtaposition with the Tisza Megaunit in the Early Miocene creating the Pannonian Megaunit, i.e. the basement of the Pannonian Basin.

2.1. Pre–Alpine evolution

Due to polymetamorphic transformation of a significant part of the pre-Variscan formations and lack of fossils in many other cases, paleogeographic reconstruction for the Early Paleozoic interval is particularly difficult.

Polymetamorphic complexes of the Tisza Megaunit suffered their first metamorphism perhaps in the Cadomian or the Caledonian or the Early Variscan tectogenic phase, however, their meso- to ultrametamorphic transformation occurred certainly during the Variscan phase. According to petrographic and geochemical features of the granitoids of the crystalline complexes, they show affinity to those of the Moldanubicum Zone of the Variscan Orogenic Belt (BUDA 1996). It means that the Tisza Megaunit may have belonged to the Variscan Foldbelt which was formed along the southern margin of the European plate during the Middle Carboniferous.

Lower Paleozoic rocks of the Pelso Megaunit and the Austroalpine nappes, which suffered metamorphism of various grades, may have formed in the Prototethys realm, in the foreground of the African plate. First metamorphic transformation of the Lower Paleozoic sedimentary and magmatic rocks of the Lower Austroalpine nappes might have taken place in the Caledonian, or more likely in the Variscan phase. Lower Paleozoic very low- to low-grade metamorphic series in the Upper Austroalpine nappes in the basement of the Little Plain and in the

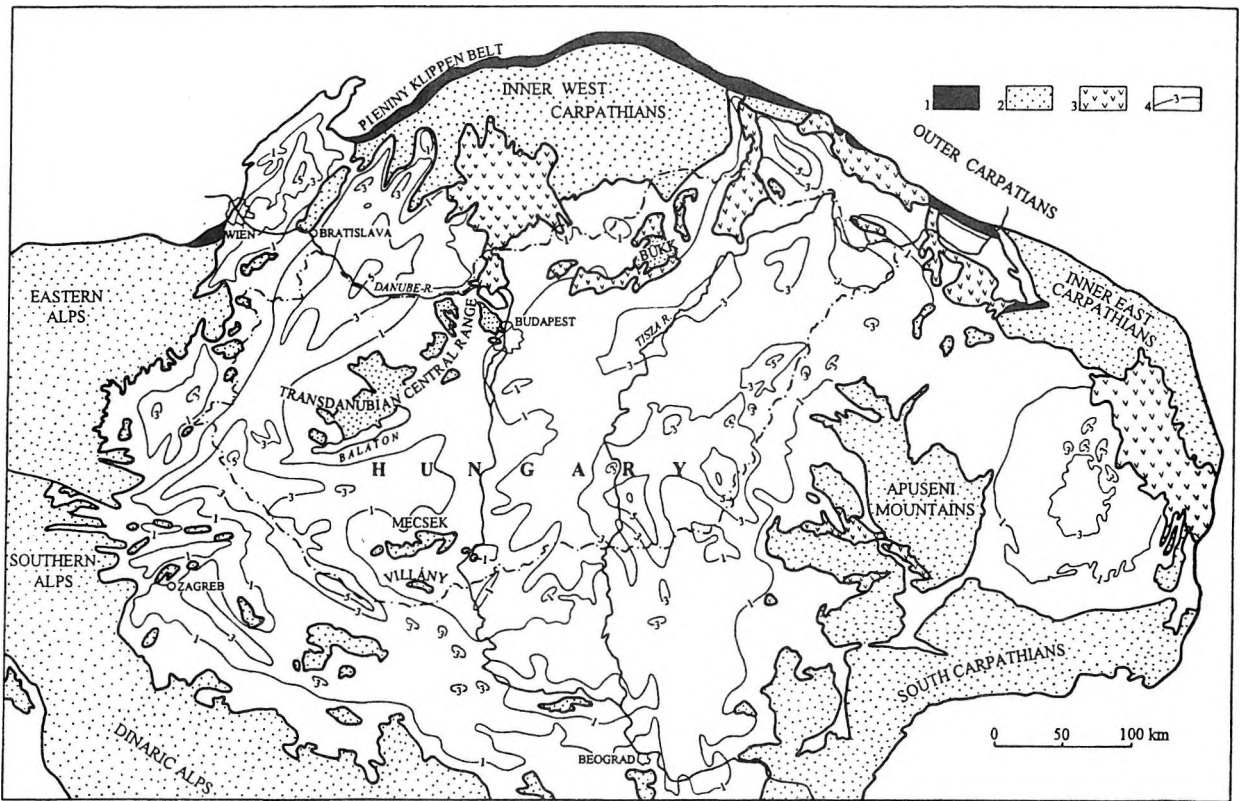


Fig. 1: Geological sketch of the Pannonian Basin (after ROYDEN and SANDULESCU 1988)
 1. Pieniny Klippen Belt, 2. Pre-Neogene basement, 3. Neogene volcanics, 4. Clastic basin infilling with thickness in km

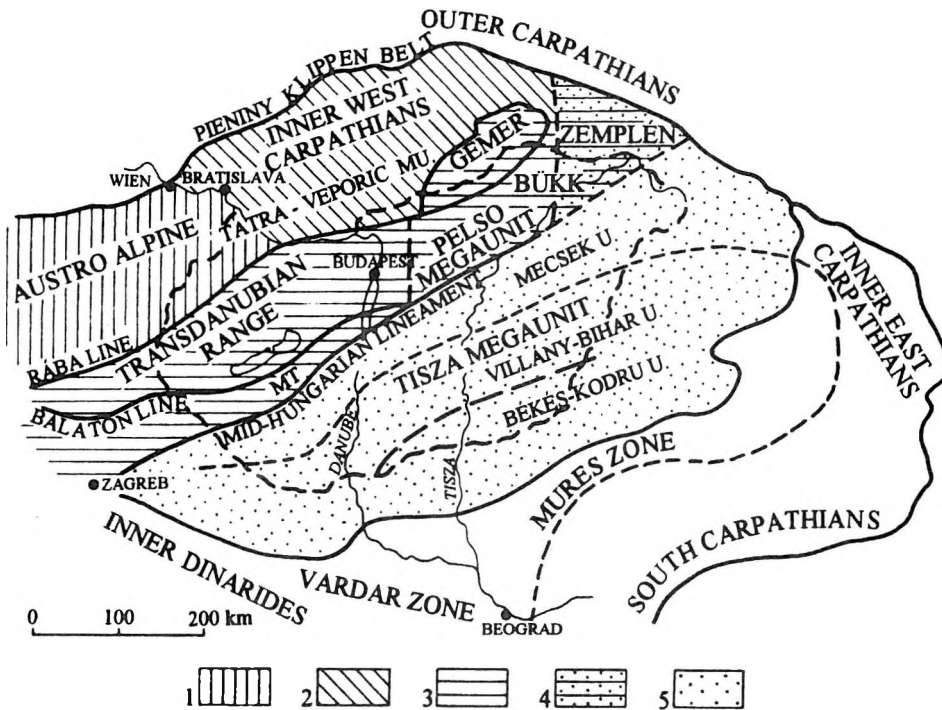


Fig. 2: Tectonic scheme of the pre-Tertiary basement of the Pannonian Basin (after HAAS et al. 1995)
 1. Austro alpine Megaunit, 2. Inner West Carpathians (Tatra-Veporic) Megaunit, 3. Pelso Megaunit, 4. Zemplén Unit, 5. Tisza Megaunit
 Abbreviation: MT=Mid-Transdanubia

MIDDLE CARBONIFEROUS ~325 Ma

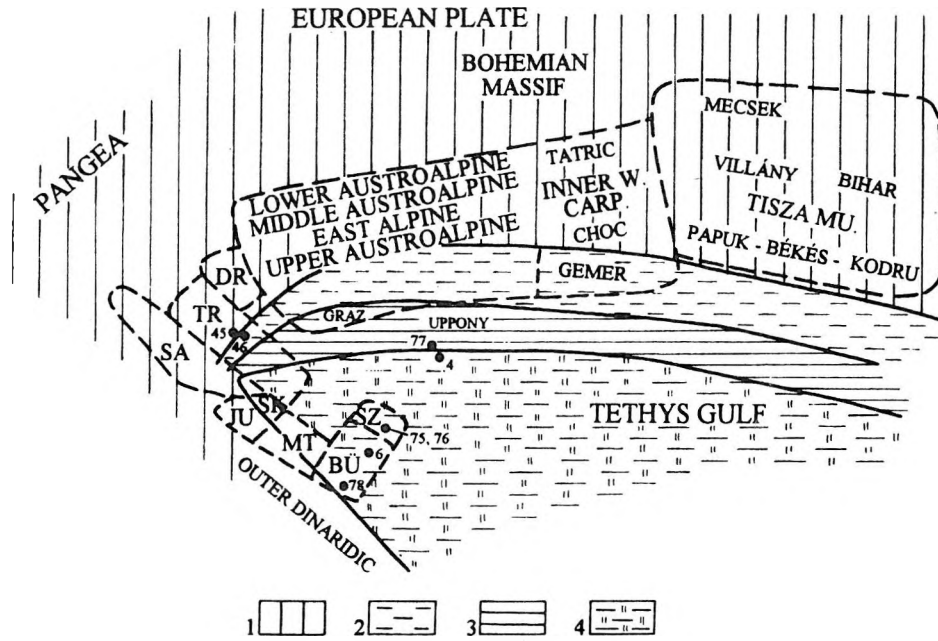


Fig. 3: Middle Carboniferous (~ 325 Ma) reconstruction (after EBNER et al. 1991)

1. Exposed land, 2. Shallow marine shale, 3. Shallow marine carbonates, 4. Flysch. Abbreviations: DR=Drauzug, TR=Transdanubian Range, SA=Southern Alps, JU=Julian Alps, SK=Southern Karavanks, MT=Mid-Transdanubia, BÜ=Bükk, SZ=Szendrő. • Sampled formations, 4=Tapolcsány Formation, 6=Szilvásvárad and Mályinka Formation, 45=Szabadbattyán Limestone, 46=Füle Conglomerate, 75=Szendrő Phyllite, 76=Rakaca Marble, 77=Lázberc Formation, 78=Tarótfő Conglomerate

LATE PERMIAN ~255 Ma

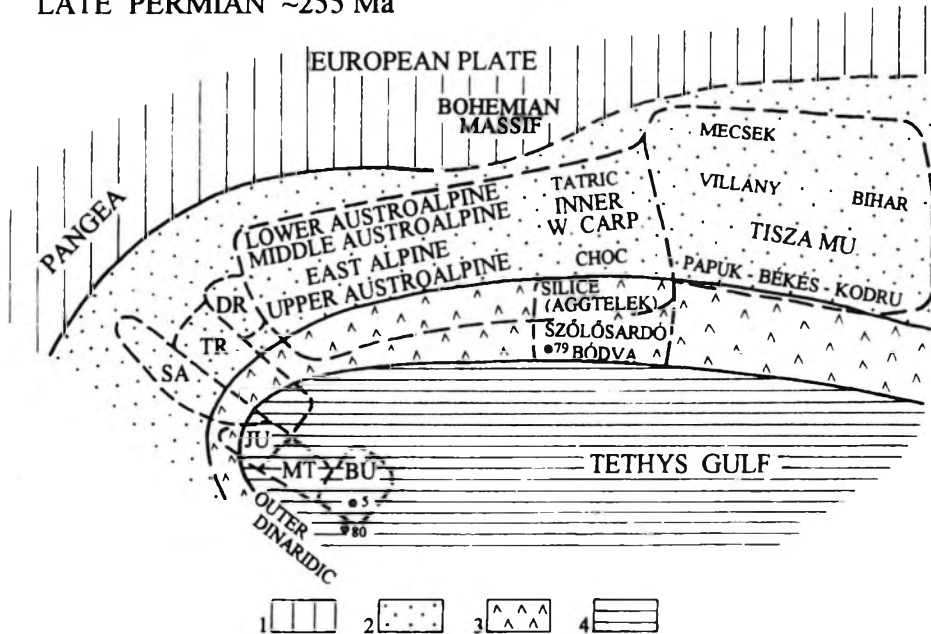


Fig. 4: Late Permian (~255 Ma) reconstruction (after HAAS et al. 1995)

1. Exposed land, 2. Continental clastics, 3. Sabkha, 4. Shallow marine carbonates. Abbreviations: DR=Drauzug, TR=Transdanubian Range, SA=Southern Alps, JU=Julian Alps, MT=Mid-Transdanubia, BÜ=Bükk. • Sampled formations, 5=Nagyvisnyó Limestone, 79=Perkupa Anhydrite, 80=Szentlélek Formation

Transdanubian Range Unit were transformed in the Variscan phase, whereas series of similar age and metamorphic grade in the Bükk Unit only in the Alpine phase (LELKESNÉ FELVÁRI et al. 1984, ÁRKAI 1983).

Closure of the Prototethys in the Middle Carboniferous led to accretion of the Pangea supercontinent and consolidation of the Variscan Foldbelt (Meso-Europe – STILLE 1924). However, in a relatively narrow zone, the marine sedimentation remained practically continuous from the Early to the Late Paleozoic. The Bükk, Szendrő and Uppony Units belonged to this zone which was not affected by significant tectonic deformations and metamorphism (Fig. 3).

In the Szendrő Unit, carbonate platforms, foreslope and siliciclastic flysch basin formed coevally in the Early Carboniferous. It was exchanged by overall flysch deposition in the Middle Carboniferous. In the Bükk, the flysch sequence is overlain by a Late Carboniferous shallow marine carbonatic–siliciclastic series. In the Uppony Unit, the Lower to Middle Carboniferous is represented by basin facies, whereas the Upper Carboniferous sandstones and conglomerates are post-tectonic molasse deposits. Upper Carboniferous siliciclastic sequences, occurring in the Transdanubian Range, are typical continental molasse deposits. Siliciclastic, coal-bearing series of similar age are known also in the Slavonian–Drava Unit of the Tisza Megaunit and in the Zemplén Unit which may have formed in a continental foreland basin of the Variscan Foldbelt (EBNER et al. 1991).

In Early to Middle Permian, in the Tisza Megaunit, belonging still to the southern margin of the European plate, continental sedimentation continued in the previously formed molasse basins and initiated in the newly formed rift troughs. Deposition of continental red-beds was punctuated by an intense acidic magmatic activity at the end of the Early Permian, roughly coeval with a significant extension of the area of the continental depositional basins. Similar continental rift system and related sedimentary and magmatic series were formed on the African margin, i.e. in the Southern Alps, and although less pronounced, in the southwestern part of the Transdanubian Range, too. In the Bükk, belonging formerly to the inner zone of the Prototethys, subsequent to a short gap the Alpine evolutionary cycle appears to initiate as early as the base of the Middle Permian with continental – peritidal–shallow marine siliciclastic and dolomitic–evaporitic series. Here, the Upper Permian (Fig. 4) is represented by shallow marine facies akin to that in the Carnic Alps, Southern Karavanks and the northeastern segment of the Transdanubian Range which belonged to the same facies belt.

Geological background for Carlin-type gold mineralization of this stage can be outlined after KÖRPÁS et al. (1999) as follows. Ordovician to Late Permian evaporites, platform carbonates, foreslope carbonatic and siliciclastic sediments, molasse and flysch sequences with volcanics were checked in the Transdanubian Range, Bükk, Uppony, Szendrő and Bódva Unit (Figs. 3 and 4). Low level gold anomalies (up to 27 ppb Au) were found in pyrite and organic matter rich sediments of the Tapolcsány and Irota Formations of the Uppony and Szendrő Unit. Low to high level gold anomalies (from some to 2090 ppb Au) were detected in the platform carbonates (Úrhida Limestone, Polgárdi Limestone, Szabadbattyán Limestone) and metamorphosed flyschoid sequences (Balatonfőkajár Quartz Phyllite, Lovas Slate) in the Balatonfő–Velece Hills area of the Transdanubian Range. The latter ones are considered as targets of further explorations.

2.2. Alpine evolution

The Alpine history may be subdivided into the following main stages:

1. Multiphase opening of the Mesozoic Tethys ocean by rifting (Permian–Jurassic);
2. Multiphase closure of the Tethys by subduction and collision resulting in orogenesis, large-scale displacement of the lithosphere blocks between the European and African plates (Cretaceous–Paleogene);
3. Formation and development of the Pannonian Basin (Neogene–Quaternary).

Based on polarity and fitting of the Upper Permian–Triassic facies belts in the various tectonic units, setting of these units prior to the major orogenic dislocations could be reconstructed. Main starting points of the reconstruction are as follows:

- the Transdanubian Range Unit was located between the Southern Alps and the Northern Calcareous Alps (Upper Austroalpine Megaunit);
- the Zagreb–Mid–Transdanubian and the Bükk Units may have situated between the Dinaridic and the Southern Alpine realms;
- position of the Tisza Megaunit can be determined at the margin of the European plate, east to the Tatroveporic Megaunit. Within the Tisza Megaunit, the Mecsek Zone was located in the most external position.

Facies pattern, which came into being subsequent to the Late Permian transgression, sufficiently proves the above described setting (Fig. 4). Shallow marine deposits, formed in the inner belt of the Paleotethys Gulf, are known in the Bükk Mts. Marginal evaporitic sabkha–salina facies appear in the Aggtelek Mts. and also in the NE part of the Transdanubian Range. Continental red-beds characterize the developments of the SW part of the Transdanubian Range and the Mecsek and Villány Mts. Main stages of the evolution are summarized below.

2.2.1. Pre-rifting stage (P_3 – T_2)

It is characterized by continuous, moderate but differentiated subsidence. Based on sedimentological features, the following substages can be distinguished:

- continental to shallow marine siliciclastic-carbonatic ramp deposition (P_3 – T_1);
- shallow carbonate ramp–carbonate platform evolution (T_2 Anisian).

Features of sequences belonging to this stage are fairly similar to each other as they were formed on the weekly articulated ramp of the Paleotethys Gulf not very far to each other in a tectonically tranquil period (Figs. 4 and 5).

The Carlin gold potential of this stage is considered by KÖRPÁS et al. (1999) extremely low. Twenty one formations including Late Permian evaporites, Early Triassic siliciclastic-carbonatic and Middle Triassic carbonate ramp deposits in the Transdanubian Range, Mecsek, Bükk and Bodva Unit were checked. Two of them, the Szentlélek Sandstone (up to 234 ppb Au) in the Bükk Unit and the Rudabánya Iron Ore Formation (with some tens to 630 ppb Au) in the Bódva Unit show anomalous gold values. The Rudabánya Iron Ore was considered as a perspective target for further and more detailed explorations.

2.2.2. Rifting stage (T_2)

Rifting is manifested in the disintegration of the carbonate ramps and opening of an oceanic basement (Fig. 5). Consequences of the ocean opening significantly differ depending on the paleo-position of the individual units.

Tholeiitic basic-ultrabasic rocks of oceanic crust occur in some nappes of the Aggtelek Unit together with deep-sea shales and radiolarites. Slope sediments of the Szőlösárdó Unit and pelagic basin deposits of the Bódva and Torna Units are known in the Aggtelek Mts. (KOVÁCS et al. 1989). The Silice nappe of the Aggtelek Mts. was probably formed on the European shelf of the Tethys, whereas the Bükk Unit may have formed on the African (Apulian) shelf where, as a consequence of rifting, intense volcanism initiated and intraplateau basins came into existence. Similar intermediate to acidic volcanic activity and extensional basin formation characterise also the South Alpine evolution. Although geochemical characteristics of these volcanites show similarities with those of island-arc magmatites, the tectonic evolution suggests rift-related volcanism (HARANGI et al. 1996). In the Transdanubian Range, the extensional tectonics are manifested in facies differentiation and synchronous volcanic activity.

Since the area of the Tisza Megaunit belonged to the external zones of the European shelf far from the oceanic basins, evolution of this region was not disturbed by the rifting. Thus, carbonate deposition on ramps and platforms continued in the Tisza Megaunit.

The Ladinian–Lower Carnian Berva Limestone in the Bükk Unit exhibit sporadic low level gold anomalies (less than 25 ppb Au). The volcanic and volcano-sedimentary formations belonging to this stage do not show any sign of gold, consequently they appear to be unfavorable for Carlin-type gold mineralization (KÖRPÁS et al. 1999).

2.2.3. Stabilisation of the passive margins (T_3)

In the Late Triassic (Fig. 6), cessation of rifting led to filling up of the intraplateau basins. Widely extended carbonate platforms evolved keeping place with the thermal subsidence. Climatically controlled enhanced siliciclastic input characterizes the western Neotethys realm in the Carnian. Initiation of terrigenous siliciclastic input is very conspicuous in the external belt of the European shelf which is represented by the Mecsek Zone where deposition of siliciclastics continued also in the Jurassic.

Increased terrigenous input led to upfilling of the intraplateau basins of the Transdanubian Range, the Aggtelek Mts. and the Bükk Unit.

By the Late Carnian, a levelled topography came into existence on the shelves giving rise to formation of large carbonate platforms, which continued as long as the end of the Triassic or even in the earliest Jurassic (HAAS 1988).

A major part of the nineteen checked formations, including platform carbonates and siliciclastics, slope and intraplateau basin deposits were free of gold. The Veszprém Marl, Mátyáshegy Formation, Hauptdolomite and Dachstein Limestone in the Transdanubian Range (less than 25 ppb Au). Gold anomalies ranging between some to 84 ppb Au were detected in the Parád Complex of the Recsk porphyry copper deposit in the Bükk Unit (KÖRPÁS et al. 1999). This later one is considered target of further, more detailed explorations.

MIDDLE TRIASSIC ~230 Ma

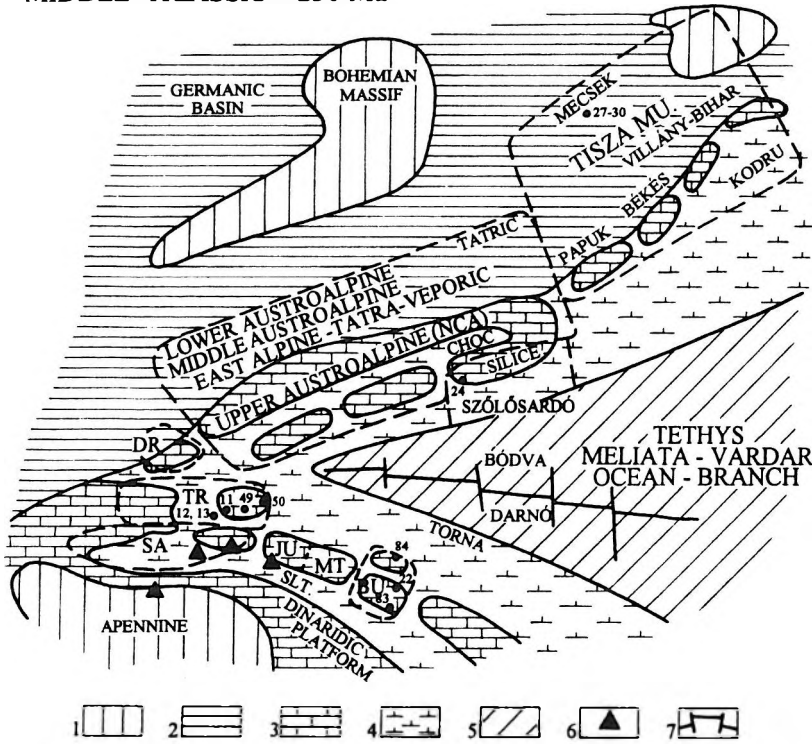


Fig. 5: Middle Triassic (~230 Ma) reconstruction (after HAAS et al. 1995)

1. Exposed land, 2. Shallow marine carbonates, 3. Shallow marine carbonate platforms, 4. Pelagic carbonates, 5. Oceanic basement, 6. Andesitic island arc volcanoes, 7. Rift zone. Abbreviations: NCA=Northern Calcareous Alps, DR=Drauzug, TR=Transdanubian Range, SA=Southern Alps, JU=Julian Alps, SLT=Slovenian Trough, MT=Mid-Transdanubia, BÜ=Bükk. • Sampled formations, 11=Megyehely Dolomite, 12=Felsőörs Limestone, 13=Buchenstein Formation, 22=Hámor Dolomite, 24=Gutenstein Dolomite, 27=Hetvehely Dolomite, 28=Lapis Limestone, 29=Zuhánya Limestone, 30=Csukma Formation/Kozár Limestone, 49=Budaörs Dolomite, 50=Vashegy Dolomite, 83=Szentistvánhegy Metaandesite, 84=Parád Complex

LATE TRIASSIC ~215 Ma

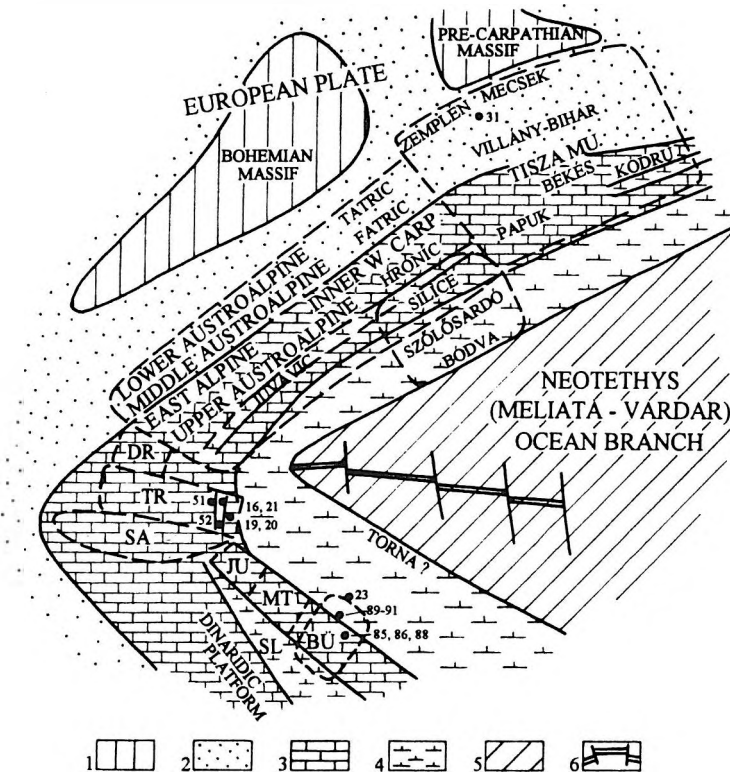


Fig. 6: Late Triassic (~215 Ma) reconstruction (after HAAS et al. 1995)

1. Exposed land, 2. Continental clastics, 3. Shallow marine carbonate platform, 4. Pelagic carbonates, 5. Oceanic basement, 6. Rift zone. Abbreviations: DR=Drauzug, TR=Transdanubian Range, SA=Southern Alps, JU=Julian Alps, SL=Slovenian Basin, MT=Mid-Transdanubia, BÜ=Bükk. • Sampled formations, 16=Mátyáshegy Formation, 19=Rezi Dolomite, 20=Kössen Formation, 23=Vesszős Shale, 51=Födömit Formation, 52=Dachstein Limestone

2.2.4 Late rifting stage (J₁₋₂)

In the early Jurassic, in connection with the Atlantic opening, a new ocean branch (Ligurian–Penninic ocean) began forming in the region (Fig. 7). Meanwhile, opening of Neotethys still continued. This intense multiple rifting resulted in the disruption and drowning of the former carbonate platforms.

The process began in the Liassic leading to segmentation of the platforms. Highs and grabens came into being in the Transdanubian Range, in the Silice Nappe and the Bükk Unit similar to those in the Southern Alps and in the area of the Austroalpine and Tatro–Veporic Megaunit.

Jurassic ophiolites in the Szarvaskő Nappe of the Bükk Unit can be bound to the opening of the Neotethys (HARANGI et al. 1996) whereas redeposited sediments in the Bükk and Aggtelek Mts. may have accumulated at the toe of the continental slope.

Ophiolites of the Penninic Unit in West–Hungary, formed the basement of the Penninic ocean (KUBOVICS et al. 1990).

In the Transdanubian Range, drowning of the Triassic–earliest Jurassic carbonate platforms, formation of uplifted blocks and grabens refer to rifting (GALÁ CZ 1988, VÖRÖS and GALÁ CZ 1998). From the Late Liassic to the end of the Jurassic, pelagic deep-sea sedimentation prevailed which continued also in the Early Cretaceous in the SW part of the unit. In contrast, generation of a flysch basin initiated, in the Gerecse area, in the NE part of the unit (Fig. 8), indicating the closure of the Neotethys ocean (HAAS et al. 1990). In the same time, appearance of ophiolitic rock fragments and heavy minerals in the siliciclastic sediments refers to the obduction of the oceanic basement not far from the sedimentary basin (ÁRGYELÁN 1996).

A significant change in the setting of the Tisza Megaunit took place during the Jurassic. As a result of eastward propagation of the Penninic ocean, it began to separate from the southern margin of the European plate in the Middle Jurassic and this process continued also in the Early Cretaceous (HAAS et al. 1990).

Lower Jurassic siliciclastic and coal bearing sequences of the most external Mecsek Zone clearly indicate the vicinity of the continental source areas at the southern margin of the European plate. The rifting may have initiated in the Dogger by opening of pelagic basins with coeval submarine volcanism. This process continued in the Early Cretaceous when large amount of alkali mafic magmatites were formed mainly in the Mecsek Zone (KUBOVICS et al. 1990, HARANGI et al. 1996). The rift-related volcanic activity came into an end in the middle part of the Cretaceous when the whole region was affected by compression.

Estimation of Carlin gold potential of this stage is based on evaluation of 22 formations (KORPÁS et al. 1999). All investigated siliciclastic, coal bearing and basin formations of the Mecsek Unit were free of gold. Among the pelagic basin and slope deposits showed only the Úrkút Manganese Ore, the Kisgercse Marl, the Lókút Radiolarite (Transdanubian Range) and the Bányahegy Radiolarite (Bükk Unit) low gold values, ranging between 2 and 7 ppb Au, slightly above detection level. Ophiolites and related deep sea sediments of the Penninic Unit (Köszeg Quartz Phyllite, Cák Conglomerate, Velem Calc Phyllite and Felsőcsatár Greenschist) and of the Szarvaskő Nappe in the Bükk Unit (Darnóhegy Shale, Darnó Radiolarite and Szarvaskő Basalt) exhibit low gold values (up to 19 ppb Au) with two extremely high values in the Felsőcsatár Greenschist (300 ppb Au) and in the Darnóhegy Shale (334 ppb Au). Consequently, formations of the Penninic Unit and the Szarvaskő Nappe will be subjected to further explorations.

2.2.5. Early Tethys subduction and collision stage (J₃–Cr)

The step-by-step closure of the Tethys started in the latest Jurassic and continued during the Cretaceous in several stages. It resulted in nappe formation, tectonic deformations, metamorphism as well as disruption and dislocation of lithosphere blocks.

According to classic concepts for tectonics of the Alps, formation of nappe systems and Alpine metamorphism of the lower nappes commenced at the end of the Early Cretaceous (Austrian phase) in connection with closure of the South Penninic ocean (TOLLMANN 1987). Metamorphism of the young Mesozoic formations of the Penninic Unit in West Hungary can be bound to this event (Fig. 8).

The peculiar nappe structure of the Transdanubian Range (ÁDÁM et al. 1985, RUMPLER and HORVÁTH 1988) with its central megasyncline was formed also by the Austrian tectogenesis, during the Aptian. This compressional phase was followed by a transgression-regression cycle in the Albian–Early Cenomanian. Orogenic collapse subsequent to the Pre-Gosau tectogenic phase led to formation of extensional basins and a new transgression-regression cycle during the Senonian (HAAS and CSÁSZÁR 1987).

Collision at the end of Cretaceous (Fig. 9) is marked by regional uplift and slight deformation (Laramian phase). Uppermost Cretaceous alkali basic and ultrabasic dikes in the NE part of the Transdanubian Range may be bound to extensional zones perpendicular to the collision front (KUBOVICS et al. 1990).

MIDDLE JURASSIC ~170 Ma

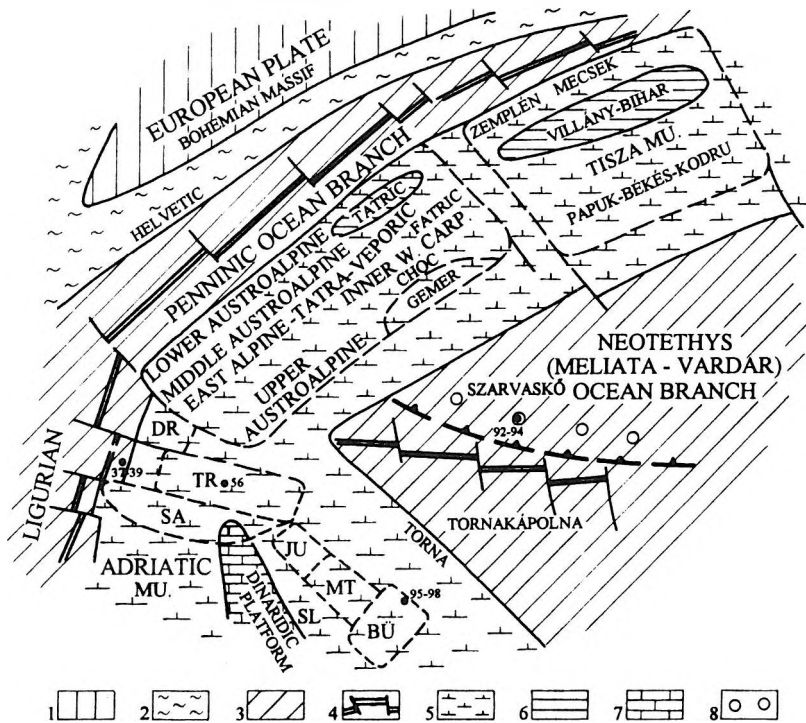


Fig. 7: Middle Jurassic (~170 Ma) reconstruction (after HAAS et al. 1990)
 1. Exposed land, 2. Neritic to deep marine marls and clastics, 3. Oceanic basement, 4. Rift zone, 5. Pelagic carbonates, 6. Shallow marine carbonates, 7. Shallow marine carbonate platform, 8. Oceanic basalt island arc volcanoes. Abbreviations: DR=Drauzug, TR=Transdanubian Range, SA=Southern Alps, JU=Julian Alps, SL=Slovenian Basin, MT=Mid-Transdanubia, BÜ=Bükk. • Sampled formations, 37=Kőszeg Quartz Phyllite, 38=Cák Conglomerate, 39=Velem Calc Phyllite, 56=Lőkút Radiolarite, 92=Darnóhegy Shale, 93=Darnó Radiolarite, 94=Szarvaskő Basalt, 95=Bányahegy Radiolarite, 96=Lökvölgy Shale, 97=Mónosbél Formation, 98=Oldalvölgy Formation

EARLY CRETACEOUS ~120 Ma

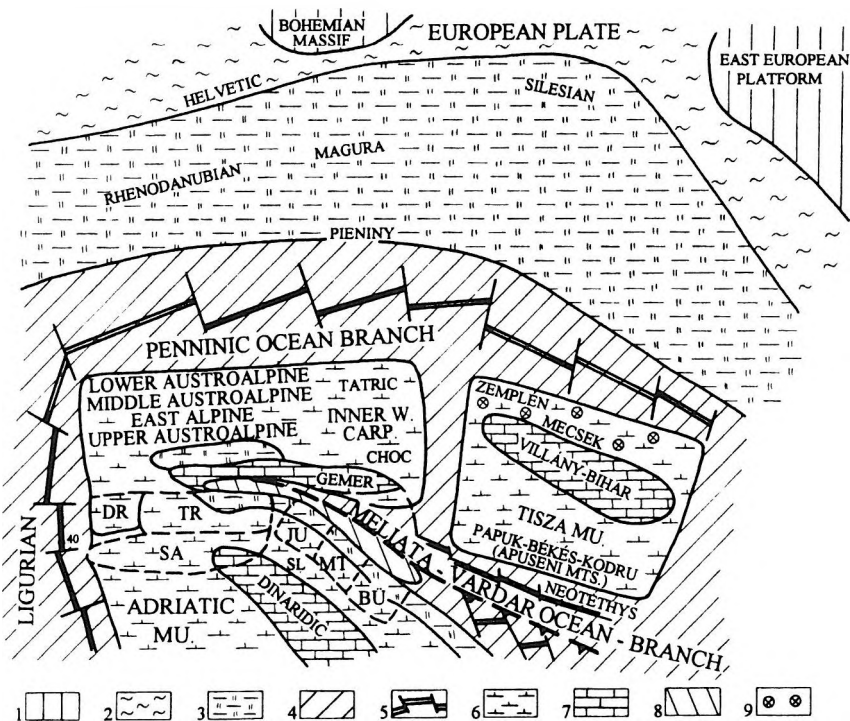


Fig. 8: Early Cretaceous (~120 Ma) reconstruction (after HAAS et al. 1990)
 1. Exposed land, 2. Neritic to deep marine marls and clastics, 3. Flysch, 4. Oceanic basement, 5. Rift zone, 6. Pelagic carbonates, 7. Shallow marine carbonate platform, 8. Obducted oceanic basement, 9. Rift basalt volcanoes. Abbreviations: DR=Drauzug, TR=Transdanubian Range, SA=Southern Alps, JU=Julian Alps, SL=Slovenian Basin, MT=Mid-Transdanubia, BÜ=Bükk. • Sampled formation, 40=Felsőcsatár Greenschist

The main nappe formation in the Bükk Unit took place also probably prior to the Late Cretaceous. However, Upper Cretaceous formations, resting unconformably on the Paleozoic of the Uppony Unit, are folded.

As a consequence of the closure of the Tethys during Late Jurassic–Early Cretaceous (Figs. 7 and 8) the Bükk Unit, which was located on the southern (Dinaridic) shelf, may have approached the Tatro–Veporic Megaunit belonging to the northern (European) shelf. Collision led to obduction and nappe formation.

In the Tisza Megaunit, the first Alpine compression occurred at the end of the Early Cretaceous (Fig. 9). It is indicated by folding and cessation of basalt volcanism too. In the Villány–Bihar Zone, flysch-type sedimentation refers to initiation of nappe forming in the Albian. In the Apuseni Mts., main phase of nappe forming was at the beginning of the Senonian (pre-Gosau phase–IANOVICI et al. 1976). End of Cretaceous tectogenesis is marked by regional uplift which affected even the deep-sea basins.

This stage was considered unfavorable for Carlin type mineralization. The Felsőcsatár Greenschist of the Peninic Unit was evaluated earlier, while some bauxites and alkali ultrabasites in NE Transdanubian Range proved to be empty (KORPÁS et al. 1999).

2.2.6. Late Tethys subduction and collision stage, formation of the Paratethys basins (E–O)

Process of closure of the Tethys system continued in the Early Eocene and finished at the Eocene/Oligocene boundary. Subduction and subsequent collision of the Adriatic (Apulian) microplate and the European plate resulted in the emergence of the Alpine and Dinaridic ranges. Juxtaposition of Transdanubian Range, Mid-Transdanubian and Bükk Units took place probably during the Eocene (Fig. 10) when, moving eastward, the Transdanubian Range reached, and dragged blocks of the Mid-Transdanubian Unit and pushed forward the Bükk Unit on its front. Calc-alkaline island arc volcanism in the afore-mentioned units mark the relationship of these units in the Late Eocene and Early Oligocene. At this time, they were located along the northern margin of the southern (Slovenian–Bosnian) flysch basin.

A series of basins belonging to the Paratethys, i.e. a remnant basin of the former Tethys ocean came into existence in the Early Oligocene (NAGYMAROSY 1990). These basins include also the Hungarian Paleogene Basin (Fig. 11) which were formed as a consequence of large scale eastward motions of the Pelso Megaunit (ROYDEN and BÁLDI 1988). The fact, that the North Hungarian Paleogene Basin oversteps the Pelso Unit and continues in the Tatro–Veporic Megaunit (BÁLDI and BÁLDINÉ–BEKE 1985), indicates that the two units had come into juxtaposition by this time and moved further eastward together. In the Mecsek Unit of the Tisza Megaunit (“Flysch Belt of the Szolnok Subunit”), marine deposition continued till the end of Oligocene.

Although the carbonate platform formations and its slope deposits, furthermore the siliciclastic delta and pro-delta, restricted basin sediments of the Transdanubian Range were affected by hydrothermal overprints in this period, they do not show any sign of gold mineralization. The volcano-plutonic formations of the Paleogene Island Arc, represented by the Nadap Andesite in the Velence Hills of the Transdanubian Range, and Recks Andesite in the Bükk Unit, can be considered as generators of Carlin-type gold mineralization (KORPÁS et al. 1999).

2.2.7. Pannonian Basin stage (M–Q)

Miocene tectogenesis of the Pannonian Basin was controlled by post-collision effects of the African (Adriatic) and European plates and elastic deformation of the collisional fronts. The Neogene deep basins are located and formed approximately above the “collisional sutures” (HÁMOR 1983, 1984). The cause of rejuvenation is the weakening of stresses which led to formation of a network of tensional troughs and subsequently basins at the crossing of the troughs, as a rule.

Three aspects make this simple model complicated:

- existence and rotation of small fragmented microplates between the large continental plates,
- volcanic masses of “Neogene and superimposed island-arcs” generated by subduction,
- effects of vertical movements of the NW–SE Vardar system during the Miocene.

Evolution of the Pannonian basin took place in four cycles with alternating changes of compressional and tensional intervals and stress fields.

The Savian cycle (26–19 Ma) is characterized by an intense NE-ward piling up of the Alpine systems and uplifting of the Vardar zone of NW–SE strike, parallel to the collision front (Fig. 12) In this period, displacement and rotation of plate fragments were still probable. Generation of great alluvial depositional systems in W, SW and SE Hungary, graben structures of the Late Egerian–Ottományian marine sedimentary basins in the NE and outflow of fracture-controlled ignimbrites (“lower rhyolite tuff”) in the NE and SW may be attributed to this tensional cycle.

LATE CRETACEOUS ~65 Ma

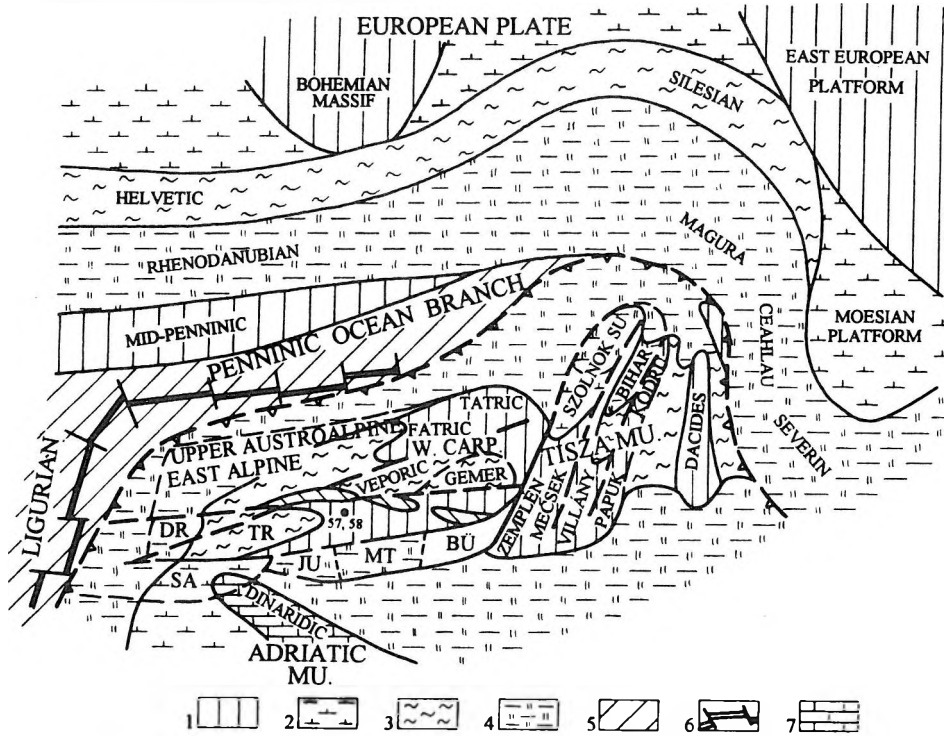


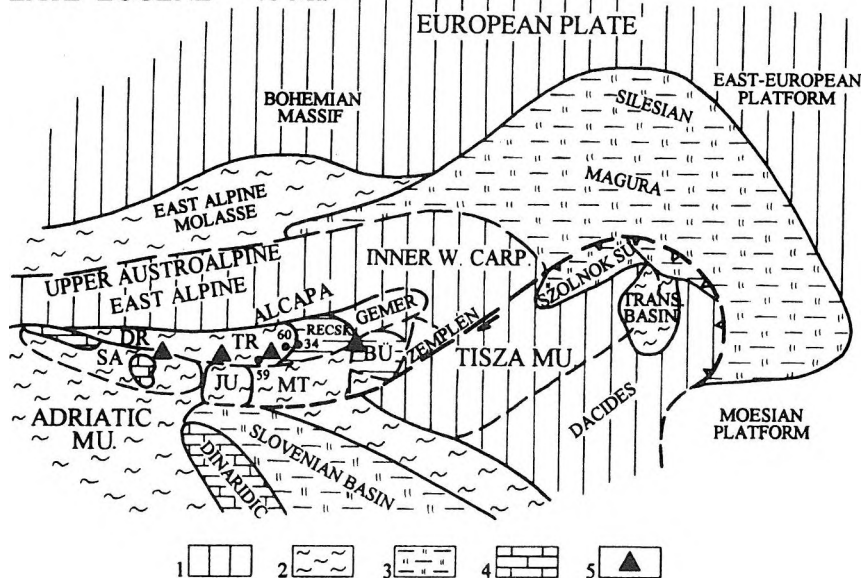
Fig. 9: Late Cretaceous (~65 Ma) reconstruction (after HAAS et al. 1990)

1. Exposed land, 2. Pelagic carbonates, 3. Neritic to deep marine marls and clastics, 4. Flysch, 5. Oceanic basement, 6. Rift zone, 7. Shallow marine carbonate platform. Abbreviations: DR=Drauzug, TR=Transdanubian Range, SA=Southern Alps, JU=Julian Alps, MT=Mid-Transdanubia, BÜ=Bükk, TRANS=Transylvanian. • Sampled formations, 57=Budakeszi Picrite, 58=Bauxite Formation

Fig. 10: Late Eocene (~40 Ma) reconstruction (after CSONTOS et al. 1992)

1. Exposed land, 2. Neritic to deep marine marls and clastics, 3. Flysch, 4. Shallow marine carbonate platform, 5. Andesitic island arc volcanoes. Abbreviations: ALCAPA=Alp-Carpathian-Pannonian megaunit, DR=Drauzug, TR=Transdanubian Range, SA=Southern Alps, JU=Julian Alps, MT=Mid-Transdanubia, BÜ=Bükk. • Sampled formations, 34=Buda Marl, 59=Nadap Andesite, 60=Szépvolgy Limestone

LATE EOCENE ~40 Ma



LATE OLIGOCENE ~25 Ma

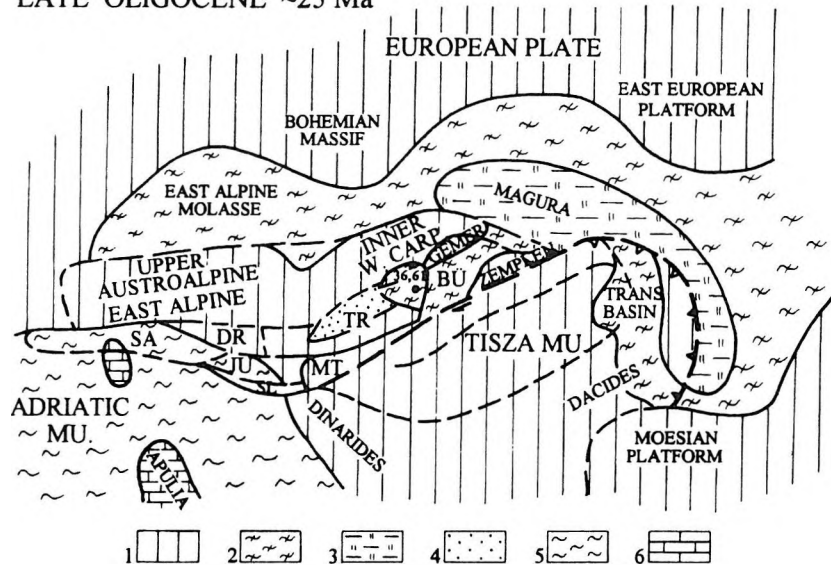


Fig. 11: Late Oligocene (~25 Ma) reconstruction (after CSONTOS et al. 1992)

1. Exposed land, 2. Shallow marine clastics, 3. Flysch, 4. Continental clastics, 5. Neritic to deep marine marls and clastics, 6. Shallow marine carbonate platform. Abbreviations: DR=Drauzug, TR=Transdanubian Range, SA=Southern Alps, JU=Julian Alps, SL=Slovenian Basin, MT=Mid-Transdanubia, BÜ=Bükk. • Sampled formations, 36=Hárshegy Sandstone, 61=Mány Formation

Main result of the Styrian cycle (19–15 Ma) was the uplift of the Alps and Carpathians, generation of the southern foredeep of the Alps and collapse of the Dinarides (Fig. 13). At that time the Pelso and Tisza Megaunits already got into juxtaposition and, along dislocation zones of their units the NE–SW oriented Karpatian and Early Badenian pull apart basins came into existence. The compressive forearc basin of the to NE directed subduction-front is marked by explosion maximums of the “middle rhyolite tuff” and by the intermediate andesitic volcanism along the early Inner Carpathian Arc.

In the Leithan cycle (HÁMOR, 1978), during the Late Badenian–Sarmatian–Pannonian s.s. (15–6 Ma), took place the last nappe generation in the Alpine–Carpathian–Dinaridic system and general uplift of this realm. In the same time, tension in the inner part of the system excepting the isolated midmountainous ranges led to collapse of the Pannonian Basin (Fig. 14). On the completely consolidated basement, incipient elements of the present-day orography, i.e. large depressions and isolated mountains came into being at this time. Characteristic tectonic elements are extensional faults shifting in time towards the margin of the basin. Unconformities and onlap geometry are common. The deep basins (1–5 km) came into existence in the Transisza area, Drava basin and Little Plain (Kisalföld). Uplifting of the Vardar system continued also in this period. Traces of basalt volcanism were encountered on the uplifting range. The late acidic–intermediate volcanism of the East Carpathian Arc migrating to NE and E started in the Late Badenian, reached its paroxysm during Sarmatian and practically finished at the end of the Late Pannonian.

In the course of the Rhodanian cycle (6–2.4 Ma), uplifting of the Alpine–Carpathian chain continued, whereas compression characterized the inner regions. Forcing effects from NW and SE enhanced the NW–SE transverse faults causing small displacements and minor folds.

Upfilling of the Pannonian Basin (Fig. 15) took place by continuous progradation of delta systems from the margins towards the centre. At the margin of the isolated mountains, in the inner part of the basin, onlap of the younger formation is usual. Marine connection to SE might have existed through the Al-Duna or Timok trough. Volcanic activity was completed by rifting generated basalts on the Balaton Highland, in the Little Plain, in N Hungary and in the Great Plain during Late Miocene to Quaternary.

Evaluation of Carlin gold potential of this stage is based on geochemical signatures of eight formations (KORPÁS et al. 1999). The Early Badenian Börzsöny and Visegrád Andesite can be considered as the generator of the low-level gold anomalies in the Hauptdolomite and Dachstein Limestone in NE Transdanubian Range. Traces of gold (some ppb Au) were detected in the pyrite and limonite rich basal horizons of some Late Pannonian to Quaternary formations (Transdanubian Range), furthermore in the residual dump deposits of the Rudabánya Iron Ore in the North Hungarian Range.

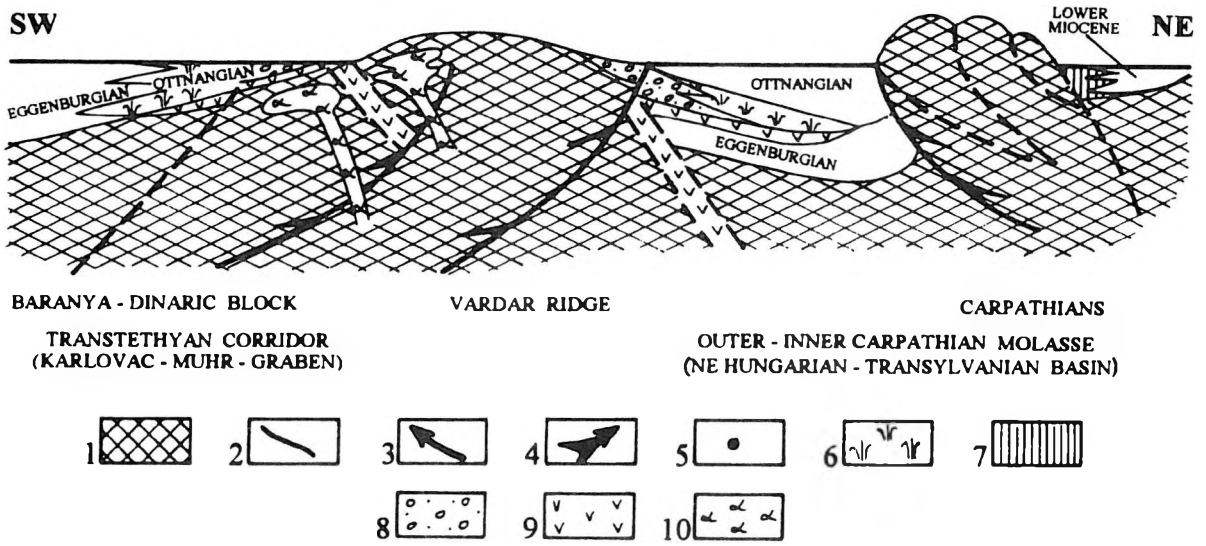
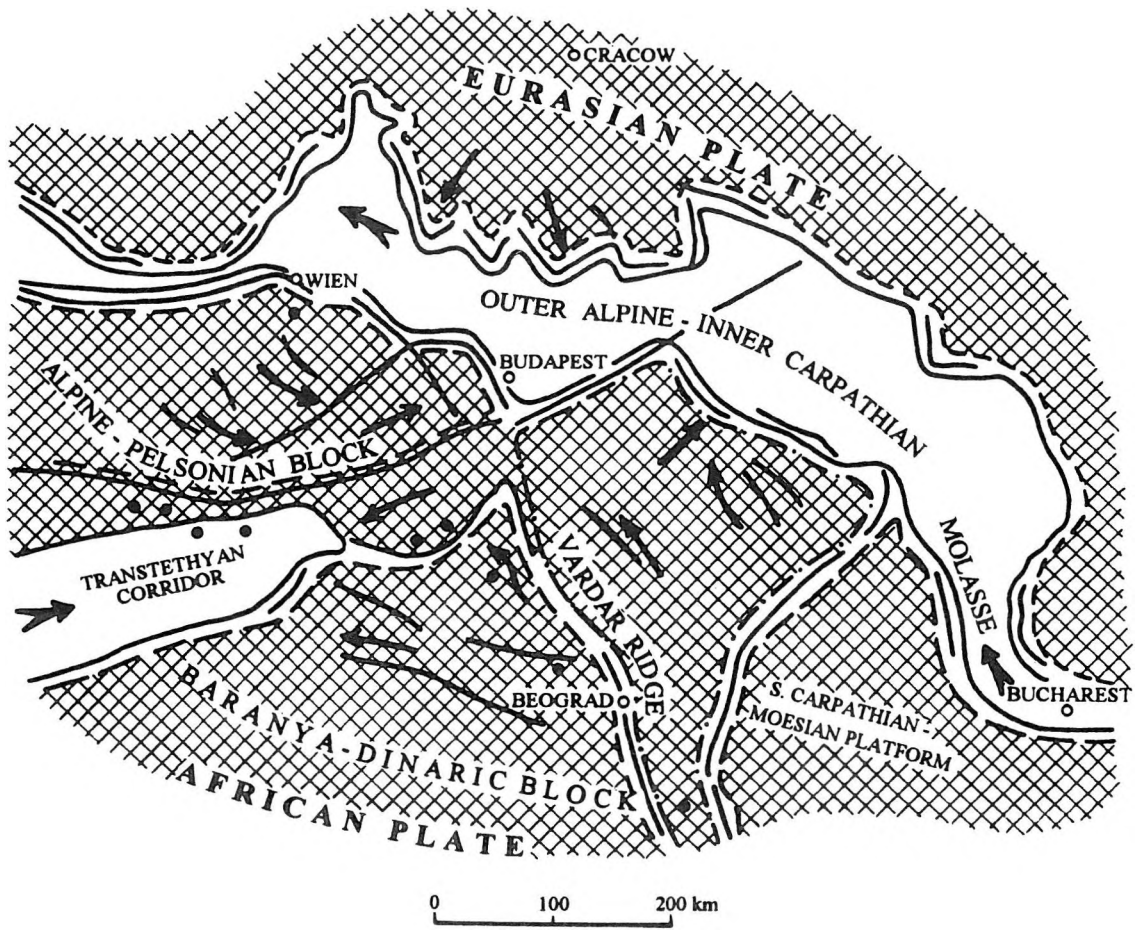


Fig. 12: Early Miocene (22–20 Ma) reconstruction (HAMOR 1995)

1. Exposed land, 2. Master faults, 3. Direction of continental source, 4. Direction of transgression, 5. Early Miocene volcanic centres, 6. Fresh water and paralic coal marshes, 7. Evaporites, 8. Alluvial fans, 9. Pyroclastics, 10. Andesite

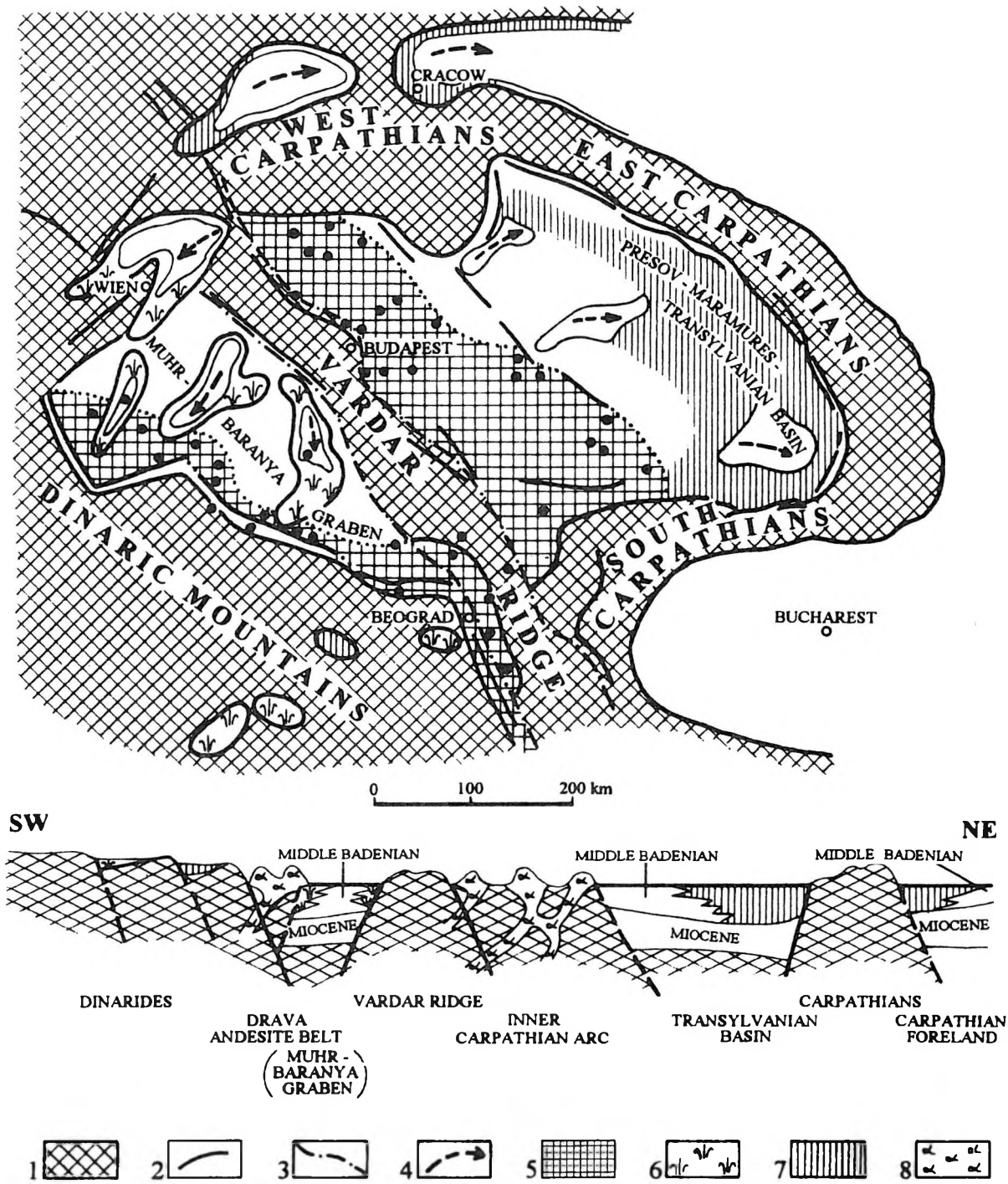


Fig. 13: End of the Middle Miocene (15.5–14.4 Ma) reconstruction (HÁMOR 1995)
 1. Exposed land, 2. Master faults, 3. Presumed master faults, 4. Direction of regression, 5. Volcanic centres of the Middle Miocene Early Inner Carpathian Arc, 6. Fresh water and paralic coal marshes, 7. Evaporites, 8. Andesite

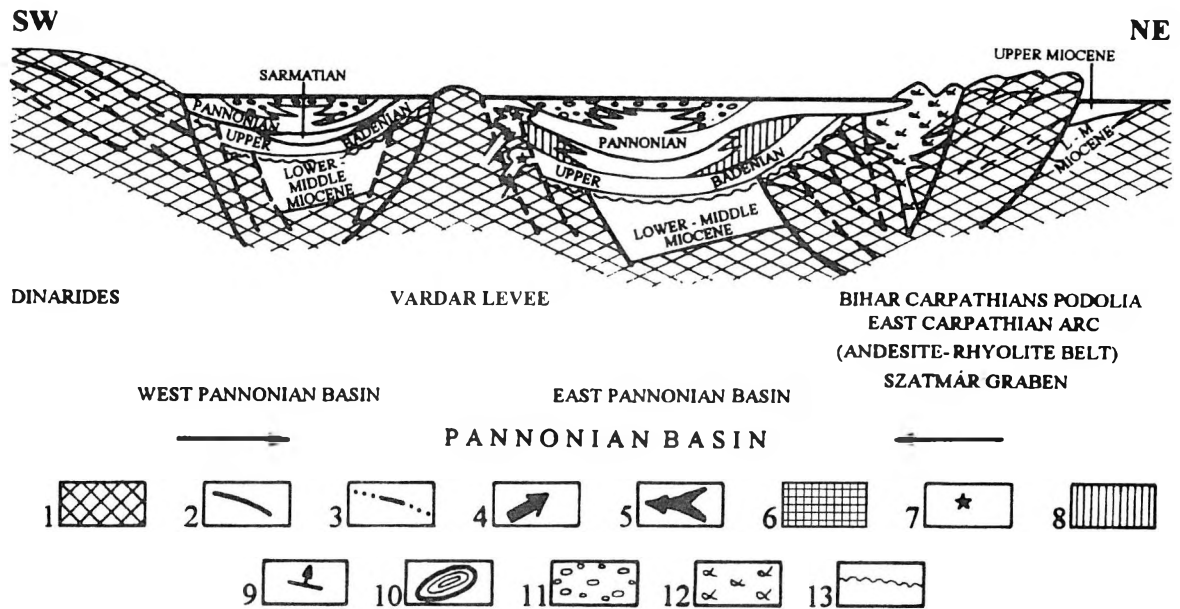
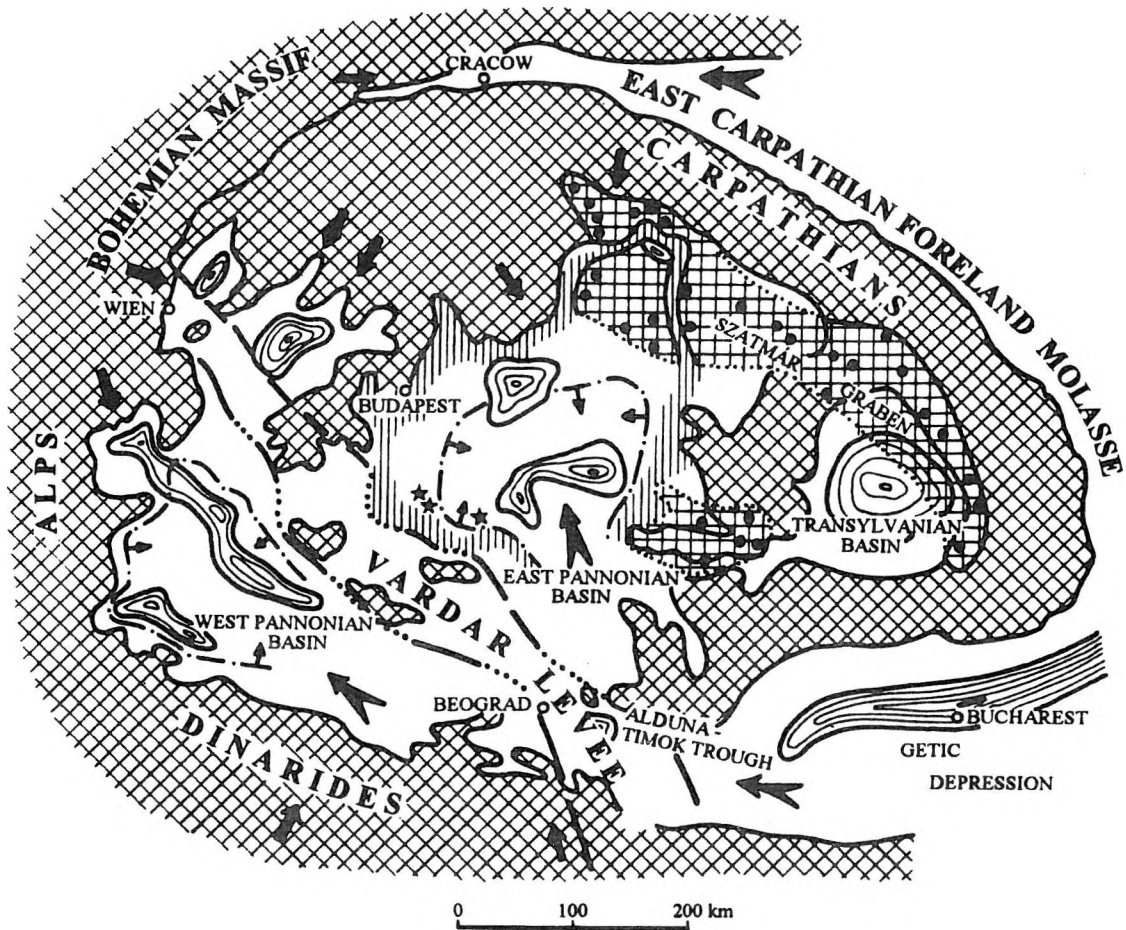


Fig. 14: Late Miocene (14.0–10.0 Ma) reconstruction (HÁMOR 1995)

1. Exposed land, 2. Master faults, 3. Presumed master faults, 4. Direction of continental source, 5. Direction of transgression, 6. Volcanic centres of the Late Miocene East Carpathian Arc, 7. Volcanic centres of the back arc rift-basalts, 8. Evaporites, 9. Direction of delta progradation, 10. Depocentres, 11. Alluvial fans, 12. Andesite, 13. Unconformity

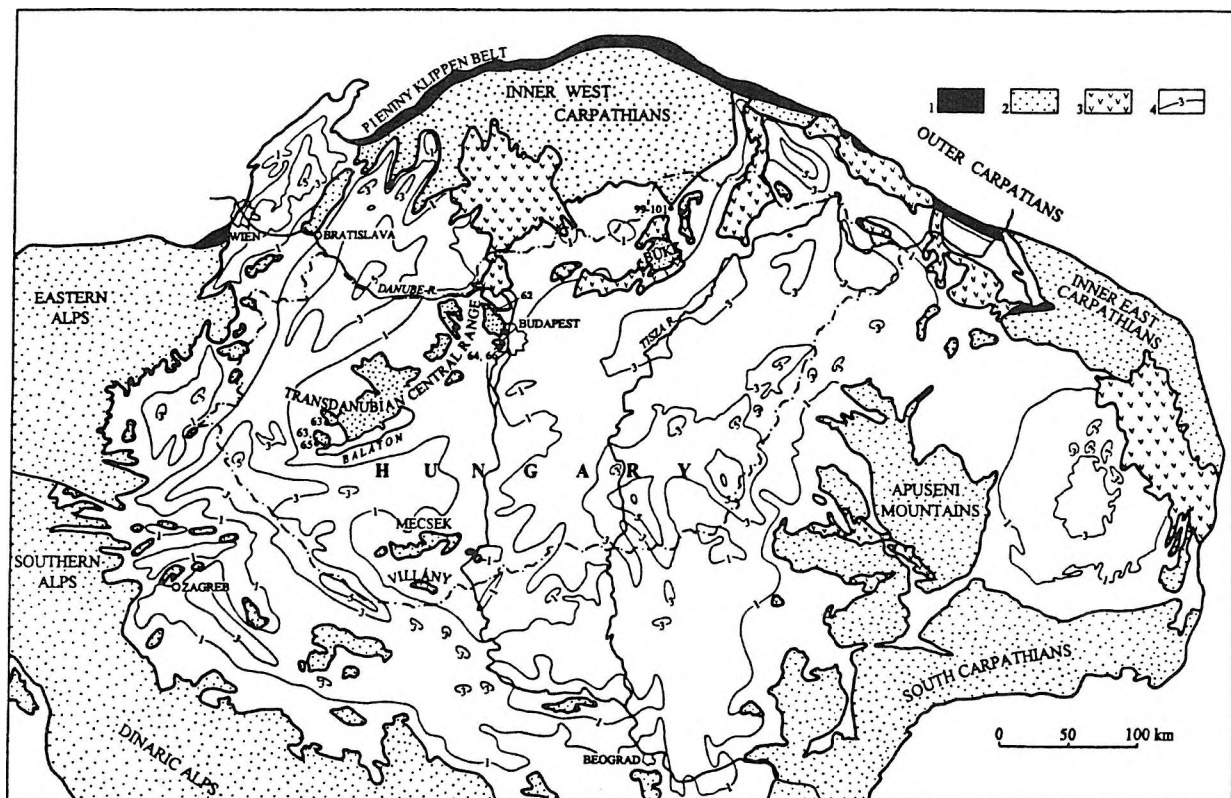


Fig. 15: Late Miocene to Quaternary Pannonian Basin (after ROYDEN and SANDULESCU 1988)

1. Pieniny Klippen Belt, 2. Pre-Neogene basement, 3. Neogene volcanics, 4. Clastic basin infilling with thickness in km. • Sampled formations. 62=Börsöny and Visegrád Andesite, 63=Källa Gravel, 64=Zámor Gravel, 65=Szák Marl, 66=Travertine Formation, 99=Edelény Clay, 100=Rudabánya Mine Dump, 101=Martonyi Mine Dump

3. CONCLUSIONS

The Carlin gold potential of Hungary has been evaluated in the frame of multiphase geologic evolution of the region. Our most important considerations will be summarised in the following:

1. Major stages of structure evolution related both to Paleozoic (Variscan) and Mesozoic (Alpine) rifting or subduction may be favorable phases for gold mineralization.
2. Among them the pre-Alpine stages may have of special importance, manifesting in perspective formations which were formed along the paleomargins of the Pelso Unit.
3. Early and late rifting as well as subduction stages of the Alpine cycle may have yielded favorable host formations both in the shelf (Pelso Unit) and oceanic domains (Penninic Unit, Meliata Unit) during Triassic to Middle Jurassic.
4. Subsequent subduction and collision stages during Cretaceous and Paleogene, and the stage of formation of the Pannonian Basin during Neogene to Quaternary are not considered as favorable for Carlin type gold mineralization.

4. REFERENCES

- ÁDÁM, O.-RÁNER, G.-HAAS, J. 1985: Az MK-1/82. Geofizikai alapvonal Dabrony-Devecser közti szakaszának földtani értelmezése. (Geological interpretation of the Dabrony-Devecser sketch of the geophysical traverse MK-1/82.). — Magyar Állami Földtani Intézet Évi Jelentése 1983: 117–119. (In Hungarian with English abstract).
- ÁRGYELÁN, B. G. 1996: Geochemical investigations of detrital chrome spinels as a tool to detect an ophiolitic source area (Gerecse Mountains, Hungary). — Acta Geologica Hungarica, 39(4): 341–368.

- ÁRKAI, P. 1983 Very low- and low-grade Alpine regional metamorphism of the Paleozoic and Mesozoic formations of the Bükkium, NE Hungary. — *Acta Geologica Hungarica* 26: 83–101.
- BALOGH, K.–JÁMBOR, Á.–PARTÉNYI, Z.–RAVASZNÉ–BARANYAI, L.–SOLTI, G. 1982: A dunántúli bazaltok K/Ar radiometrikus kora. (K/Ar dating of basaltic rocks in Transdanubia, Hungary). — *Magyar Állami Földtani Intézet Évi Jelentése* 1980: 243–260. (In Hungarian with English abstract).
- BALDI, T.–BÁLDI–BEKE, M. 1985: The evolution of the Hungarian Paleogene Basins. — *Acta Geologica Hungarica* 28(1–2): 5–28.
- BUDA, GY. 1996: Correlation of Variscan granitoids occurring in Central Europe. — *Acta Mineralogica Petrographica* 37: Supplementum, 24. p.
- CSONTOS, L.–NAGYMAROSY, A.–HORVÁTH, F.–KOVÁCS, M. 1992: Tertiary evolution of the Intracarpathian area: a model. — *Tectonophysics* 208: 221–241.
- EBNER, F.–KOVÁCS, S.–SCHÖNLAUB, H. P. 1991: Das klassische Karbon in Österreich und Ungarn – ein Vergleich der sedimentären fossilführenden Vorkommen. — *Jubiläumsschrift 20 Jahre Geologische Zusammenarbeit Österreich–Ungarn. – Teil 1*: 263–294.
- GALÁCZ, A. 1988: Tectonically controlled sedimentation in the Jurassic of the Bakony Mountains (Transdanubian Central Range, Hungary). — *Acta Geologica Hungarica* 31(3–4): 313–328.
- HAAS, J. 1988: Upper Triassic carbonate platform evolution in the Transdanubian Mid-Mountains. — *Acta Geologica Hungarica* 31(3–4): 299–312.
- HAAS, J.–CSÁSZÁR, G. 1987: Cretaceous of Hungary: Paleogeographic implication. — *Rendiconti della Società Geologica Italiana* 9: 203–208.
- HAAS, J.–CSÁSZÁR, G.–KOVÁCS, S.–VÖRÖS, A. 1990: Evolution of the western part of the Tethys as reflected by the geological formations of Hungary. — *Acta Geodaetica Geophysica et Montanistica Hungarica* 25: 325–344.
- HAAS, J.–KOVÁCS, S.–KRYSZYN, L.–LEIN, R. 1995: Significance of Late Permian–Triassic facies zones in terrane reconstructions in the Alpine–North Pannonian domain. — *Tectonophysics* 242: 19–40.
- HÁMOR, G. 1978: Die Orogenphasen des Badenien. Chronostratigraphie und Neostatotypen. — *M4-Badenien, VEDA, Bratislava*, 109 p.
- HÁMOR, G. 1983: The quantitative methods of palaeogeographical reconstruction. — *Magyar Állami Földtani Intézet, Special Papers* 2: 3–70.
- HÁMOR, G. 1984: Palaeogeographic reconstruction of Neogene plate movements in the Paratethyan realm. — *Acta Geologica Hungarica* 27(1–2): 5–21.
- HÁMOR, G. 1995a: Miocene palaeogeographic and facies map of the Carpathian Basin I.-II.-III. — *in Geological Atlas of Hungary. No. 19. Hungarian Geological Institute, Budapest*
- HÁMOR, G. 1995b: Neogene evolutionary, palaeogeographic and facies model of the Pannonian Basin, with lithostratigraphic units. — *in Geological Atlas of Hungary. No. 19. Hungarian Geological Institute, Budapest*
- HÁMOR, G. 1999: Megatectonic and palaeogeographic significance of Vardar system. — *Acta Geologica Hungarica*, in press
- HÁMOR, G.–RAVASZ–BARANYAI, L.–HALMAI, J.–BALOGH, K.–ÁRVA–SÓOS, E. 1987: Dating of Miocene acid and intermediate volcanic activity of Hungary. — *Magyar Állami Földtani Intézet Évkönyve*, 62: 149–154.
- HARANGI, SZ.–SZABÓ, CS.–JÓZSA, S.–SZOLDÁN, ZS.–ÁRVA–SÓOS, E.–BALLA, M.–KUBOVICS, I. 1996: Mesozoic igneous suites in Hungary: Implications for genesis and tectonic setting in the northwestern part of Tethys. — *International Geology Review* 38: 336–360.
- IANOVICI, V.–BORCOS, M.–PATRULIUS, D.–LUPU–DIMITRESCU, R.–SAVU, H. 1976: *Geologia Muntilor Apuseni*. — R.S.R., Bucuresti, 631 p.
- KOVÁCS, S.–LESS, GY.–PIROS, O.–RÉTI, ZS.–RÓTH, L. 1989: Triassic formations of the Aggtelek–Rudabánya Mountains (Northeastern Hungary). — *Acta Geologica Hungarica* 32(1–2): 31–63.
- KOVÁCS, S.–SZEDERKÉNYI, T.–ÁRKAI, P.–BUDA, GY.–LELKES–FELVÁRI, GY.–NAGYMAROSY, A. 1996–97: Explanation to the terrane map of Hungary. — *in: PAPANIKOLAOU, D. (ed): Annales Géologiques des Pays Helléniques* 37: 271–330.
- KORPÁS, L.–HOFSTRA, A.–ÓDOR, L.–HORVÁTH, I.–HAAS, J.–ZELENKA, T. 1999: Evaluation of the prospected areas and formations. — *Geologica Hungarica Series Geologica* 24: 197–293.
- KUBOVICS, I.–SZABÓ, CS.–HARANGI, SZ.–JÓZSA, S. 1990: Petrology and petrochemistry of mesozoic magmatic suites in Hungary and adjacent areas – an overview. — *Acta Geodaetica Geophysica et Montanistica Hungarica* 25(3–4): 345–371.
- LELKES–FELVÁRI, GY.–KOVÁCS, S.–MAJOROS, GY. 1984: Alsó-devon pelágikus mészkő a Kékkút-4 sz. fúrásban. (Lower Devonian pelagic limestone in borehole Kékkút-4, Bakony Mts.). — *Magyar Állami Földtani Intézet Évi Jelentése* 1982: 289–315. (In Hungarian with English abstract).

- NAGYMAROSY, A. 1990: From Tethys to Paratethys, a way of survival. — *Acta Geodaetica Geophysica et Montanistica Hungarica* 25(3–4): 373–385.
- ROYDEN, L. H.–BÁLDI, T. 1988: Early Cenozoic tectonics and paleogeography of the Pannonian and surrounding regions. — *in* ROYDEN, L. H.–HORVÁTH, F. (eds.): *The Pannonian Basin. A study in basin evolution*. AAPG Memoir 45: 1–16.
- ROYDEN, L.–SANDULESCU M. 1988: The Carpathian-Pannonian region with Outer Carpathian units. — *in* ROYDEN, L. H.–HORVÁTH, F. (eds.): *The Pannonian Basin. A study in basin evolution*. AAPG Memoir 45: map 2.
- RUMPLER, J.–HORVÁTH, F. 1988: Some representative seismic reflection lines from the Pannonian Basin and their structural interpretation. — *in* ROYDEN, L. H.–HORVÁTH, F. (eds.): *The Pannonian Basin. A study in basin evolution*. AAPG Memoir 45: 153–171.
- STILLE, H. 1924: *Grundfragen der vergleichenden Tektonik*. — Berlin, Borntraeger 443 p.
- TOLLMAN, A. 1987: Neue Wege in der Ostalpengeologie und die Beziehungen zum Ostmediterrän. — *Österreichische Geologische Gesellschaft, Mitteilungen*, 80: 47–113.
- VÖRÖS, A.–GALÁ CZ, A. 1998: Jurassic palaeogeography of the Transdanubian Central Range. — *Rivista Italiana di Paleontologia e Stratigrafia* 104(1): 69–83.

EVALUATION OF THE PROSPECTED AREAS AND FORMATIONS

LÁSZLÓ KÖRPÁS¹, ALBERT H. HOFSTRA², LÁSZLÓ ÓDOR⁴, ISTVÁN HORVÁTH¹, JÁNOS HAAS³ and TIBOR ZELENKA⁴

¹ Geological Institute of Hungary, H-1143, Budapest, Stefánia út 14., Hungary

² US Geological Survey, P.O. Box 25046, Denver, CO 80225, USA

³ Hungarian Academy of Sciences, — Eötvös Loránd University, Geological Research Group, H-1088 Budapest, Múzeum krt. 4a., Hungary

⁴ Hungarian Geological Survey, H-1143, Budapest, Stefánia út 14., Hungary

ABSTRACT

A systematic geochemical study by applying stream sediment survey and rock chip sampling was carried out between 1995 and 1998 at the Geological Institute of Hungary to evaluate the potential of Carlin-type gold mineralization in Hungary. Main results of the geochemical explorations will be summarized in the following:

Investigation of 97 formations represented by 1398 samples of 604 sample sites resulted in the estimation of a rather modest Carlin gold potential of Hungary. This potential is hosted mainly in Paleozoic, Early Mesozoic subordinately in Late Mesozoic and Paleogene formations. The anomalous and subanomalous groups of formation are located in favourable geologic and tectonic settings of rifting, subduction and collision and in related master faults and shear zones.

Using threshold values for subanomalous (10–100 ppb Au) and anomalous (>100 ppb Au) groups 18 formations contain gold in subanomalous or anomalous concentrations. Anomalous gold values were detected in the following seven formations: the Paleozoic (1) Lovas Slate (max. 4770 ppb Au), (2) Velence Granite (max. 2090 ppb Au) and (3) Szentlélek Formation (max. 234 ppb Au), the Triassic (4) Rudabánya Iron Ore (max. 630 ppb Au), the Jurassic (5) Darnóhegy Shale (max. 340 ppb Au), the Cretaceous (6) Felsőcsatár Greenschist (max. 300 ppb Au) and the Eocene (7) Nadap Andesite (max. 1000 ppb Au).

Ten predictive areas of 2 to 190 km² below were recommended for further explorations: (1) the Velence Hills (190 km²) and (2) Balatonfő (150 km²) in the Transdanubian Range, (3) the Rudabánya Mountains (35 km²), (4) Reck area (80 km²), (5) Uppony Mountains (60 km²) and (6) Szendrő Mountains (40 km²) in the Northeastern Range, the (7) the Vas-hegy (3 km²) and (8) Kőszeg Mountains (42 km²) in Western Transdanubia, (9) the Pilis Mountains (80 km²) in the Transdanubian Range, and (10) the Mecsek Mountains (2 km²) in South Transdanubia. Two of them in the Velence Hills and in the Rudabánya Mountains exhibit promising Carlin gold potential.

1. INTRODUCTION

The evaluation of the prospected areas and formations is based on systematic study and sampling of 97 formations, mainly pre-Tertiary in age (Fig. 1). The Carlin ore perspective map (geology) of the Fig. 2 illustrates the areal distribution of these formations. Analytical data of 1398 samples representing altogether 604 sample sites are recorded in Appendix 1 Their areal distribution completed with the cells of the stream sediment survey is demonstrated on the Carlin ore geochemistry map (Fig. 3).

2. MAIN FEATURES OF OUR GEOCHEMICAL TREATMENT

Geochemical methods have always been important in gold exploration of the Carlin Trend in the USA. (WAKEFIELD 1993, PAUL et al. 1993, DOYLE-KUNKEL 1993 and ROTA 1993). During the investigations going on for many years on geochemical patterns related to gold mineralization, a very important discovery was the recognition of element associations. Detailed geochemical investigation of Carlin ore samples revealed the close association of gold with As, Sb and Hg. These elements have become known as the "Carlin Suite". Some other analy-

ses have shown that Tl has also given anomalous concentrations in some deposits. But Au, As, Sb and Hg are still thought to be the consistent indicator elements of Carlin-type gold mineralization.

In our survey of the potential for Carlin-type gold mineralization in Hungary we have closely followed and used the methods recommended by the USGS geologists and geochemists. In the USA, stream sediment, soil and rock-chips geochemistry have been used in the detailed investigations for Carlin-type gold.

The main sampling media during our reconnaissance survey was the rock-chip sampling or litho-geochemistry. Outcrops, roadcuts and drillcores of many boreholes have been sampled. Geological formations have been the main units to be characterized. Sampling was very uneven and sometimes scarce. Our aim was to collect samples from as many geologic formations as possible—using a previous geologic screening and consideration as to the possible worth of a given formation for this type of mineralization. This means that alterations which are considered to be spatially associated with gold mineralization (like silicification, argillization and sulfidation) have always been preferred when taking the samples for our survey. So it is basically a biased sampling to show the best possible conditions. It happens that there are formations with only 1 or 2 samples and other formations with dozens of samples to help geochemical characterization. The geologic formations themselves are not always uniform and they consist of many different rock-types. One has to take all these into consideration when evaluating the results.

Parallel with this research another geochemical survey was also conducted at the Geological Institute of Hungary—a reconnaissance stream sediment survey of the hilly and mountainous parts of the country (Fig. 3), with the aims of outlining possible hidden mineralizations and giving surface geochemical data to evaluate the state of the environment.

2.1. Processing of the data

Six elements have been analyzed: Au, Ag, As, Hg, Sb and Tl. Analytical methods are described by BERTALAN and BARTHA (1999). Analytical results of earlier investigations (mainly data for Au and Ag) have also been incorporated and used in the survey (see Appendix 1). We have had the possibility to check the quality of our data by using outside control.

We have the analytical data of altogether 1398 samples for our disposal to make the geochemical evaluation. These data are in Dbase files and are given in Appendix 1. SPSS PC+software package was used to calculate the main geochemical parameters, to study the distribution of the concentrations of elements, to decide as to the threshold of anomalies and to investigate the possible correlations of elements.

So at the general geochemical description of the different formations sample numbers (Nos.) are enumerated first according to Appendix 1, in order to help the reader to see the detailed analytical results. Then the lithology of the samples is given, followed by the main parameters (minimum value, maximum value and the median) for the elements analysed. The lithology of the samples showing the highest concentrations within the formation is also indicated.

Because the investigated samples or populations are not normally distributed and some include outliers, Spearman's rank correlation method was used to calculate correlation coefficients (rs). The calculation of these coefficients was one of the main steps in the examination of our geochemical data-sets. Correlation coefficients (rs's) were taken only into consideration above which the correlation was considered statistically significant at the 1% level for a given number of degrees of freedom. (That is there is a 99% chance that the relationship observed in the sample also applies to the population.)

When the number of samples available for the given formation made it possible we have examined the histograms, boxplot diagrams and frequencies of elements to find out distribution characteristics and threshold values for anomalies.

Detailed description of the prospected areas and formations will be given in the following, according to the layouts of the above maps.

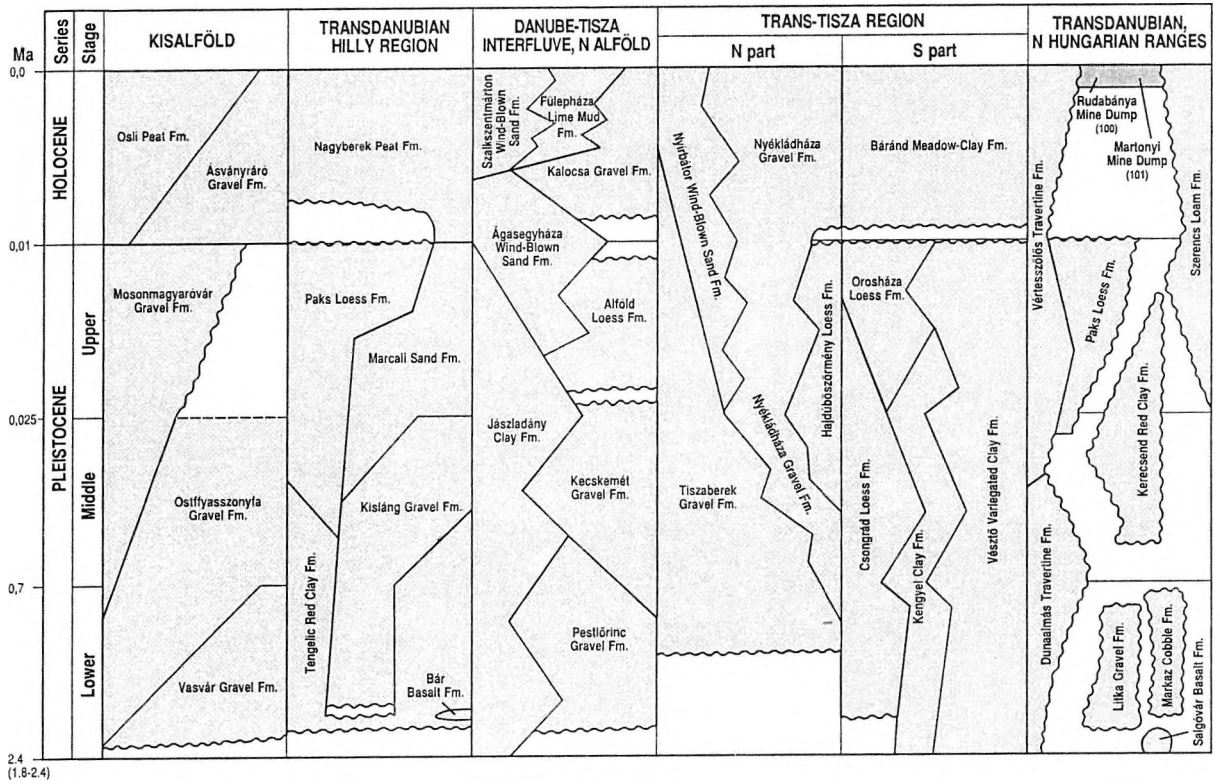
2.2. Anomaly patterns of the stream sediment surveys

A stream sediment survey was launched in the previous years to cover the hilly and mountainous parts of Hungary with 1 sample/4 km² density. The fine fraction of stream sediments was analysed for 16 elements. The data of these detailed surveys were mainly used to outline surface geochemical anomalies and environmental signatures of ore deposits and alteration zones in the regions (HORVÁTH et al. 1999, ÓDOR et al. 1999). Out of the 6 Carlin suite elements, 5 elements (Au, As, Ag, Hg and Sb) had also been included in the element list of the stream sediment survey. So it is quite obvious to use the relevant stream sediment data and anomaly maps as further information and an independent control for our present Carlin survey.

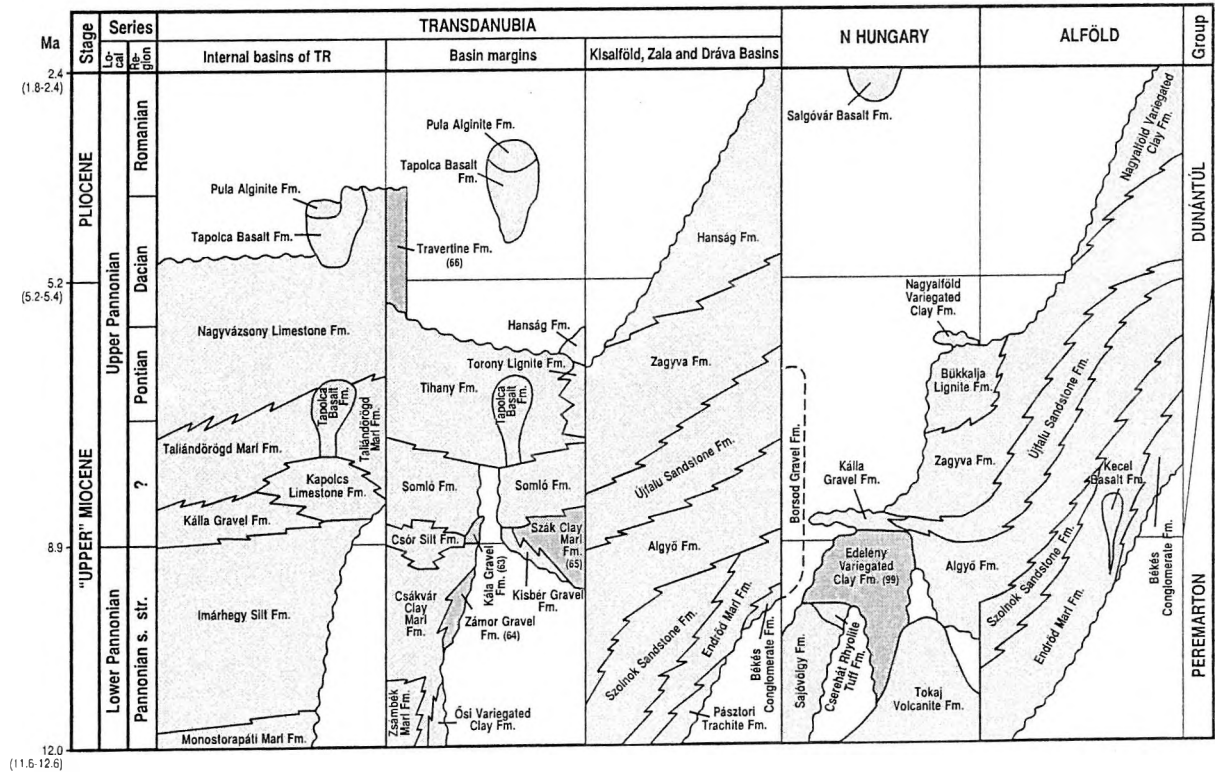
All the processing of the stream sediment data was restricted to the areas or regions outlined by the sampling and anomaly maps (Figs. 4, 5, 6 and 7) areas outside these boundaries were left out of the calculations.

Fig. 1: Stratigraphic chart showing the position of prospective formations (after CSÁSZÁR 1997)
 Quaternary, Pannonian s. l., Miocene, Oligocene, Paleocene-Eocene, Cretaceous, Jurassic, Triassic, Permian, Paleozoic I.
 (shaded formations = sampled formations)

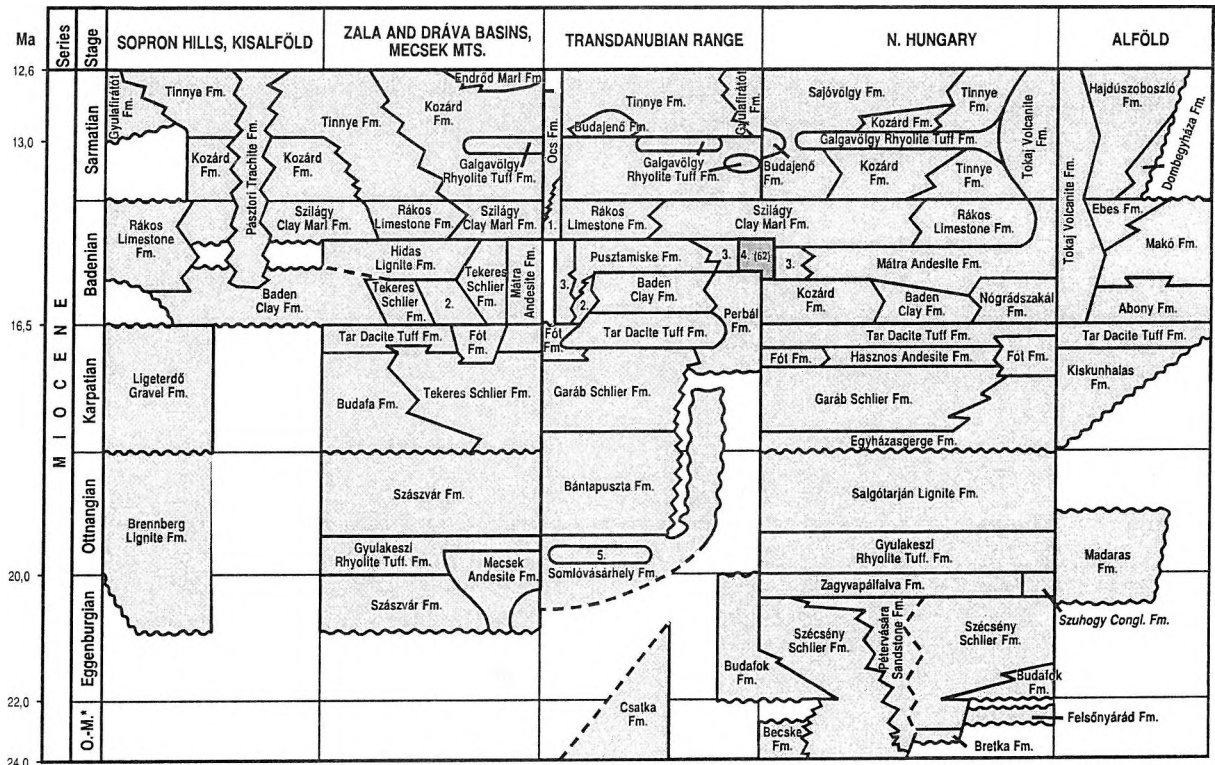
QUATERNARY



PANNONIAN S. L.



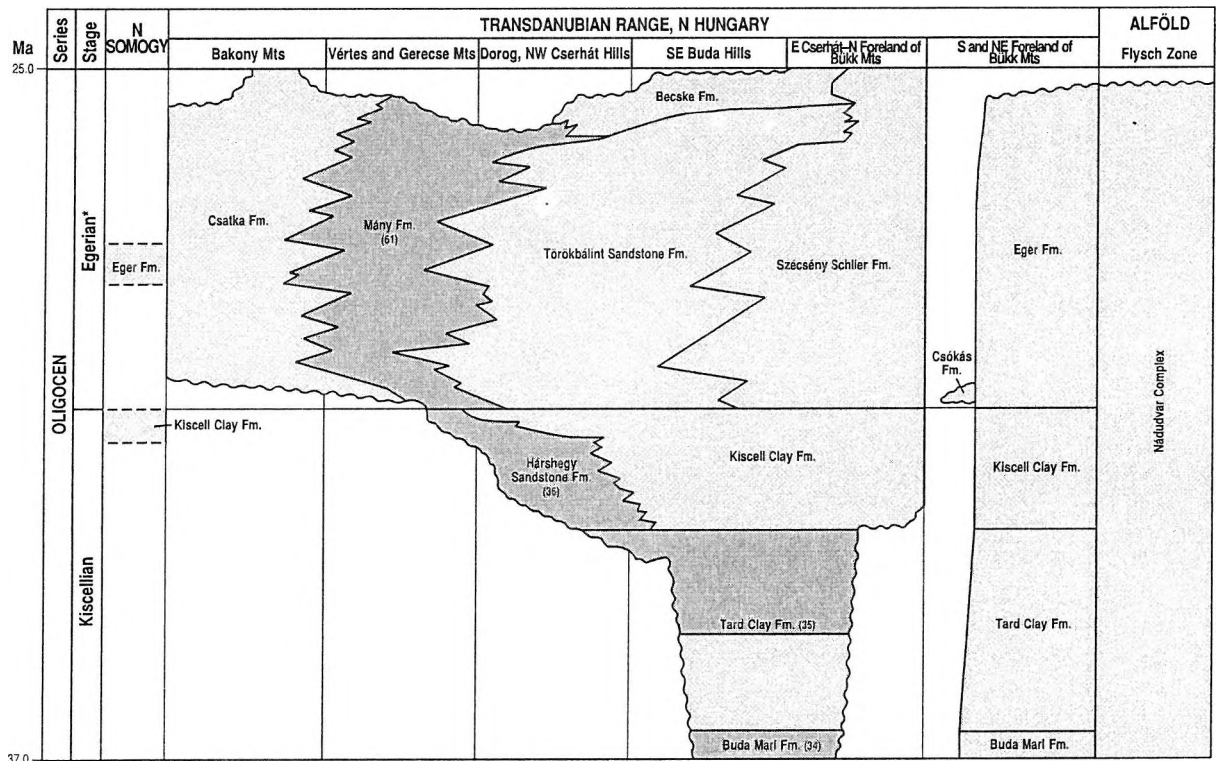
MIOCENE



*Oligocene - Miocene

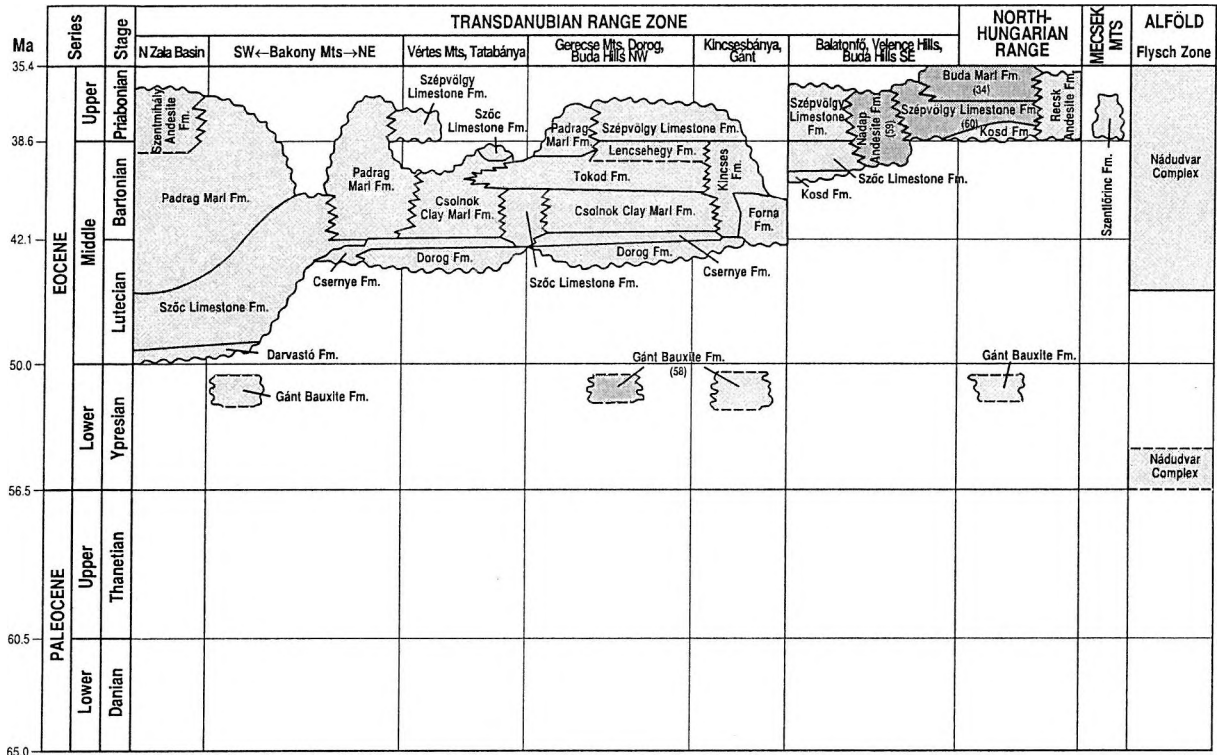
1. Vöröstó Fm., 2. Péccsabolcs Limestone Fm., 3. Hidas Lignite Fm., 4. Mátra Andesite Fm., (62) Börzsöny and Visegrád Andesite, 5. Gyulakeszi Rhyolite Tuff Fm.

OLIGOCENE

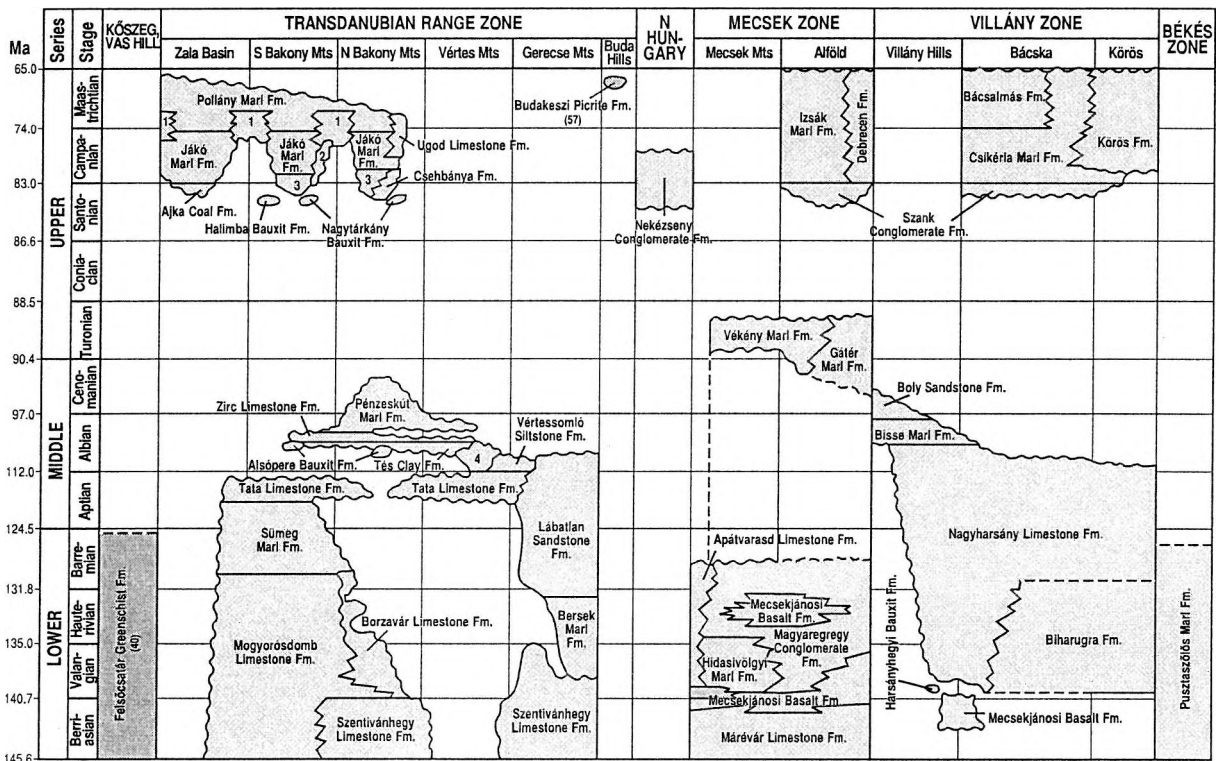


* Lower Egerian substage sensu Báldi-Seneš 1975

PALEOCENE-EOCENE

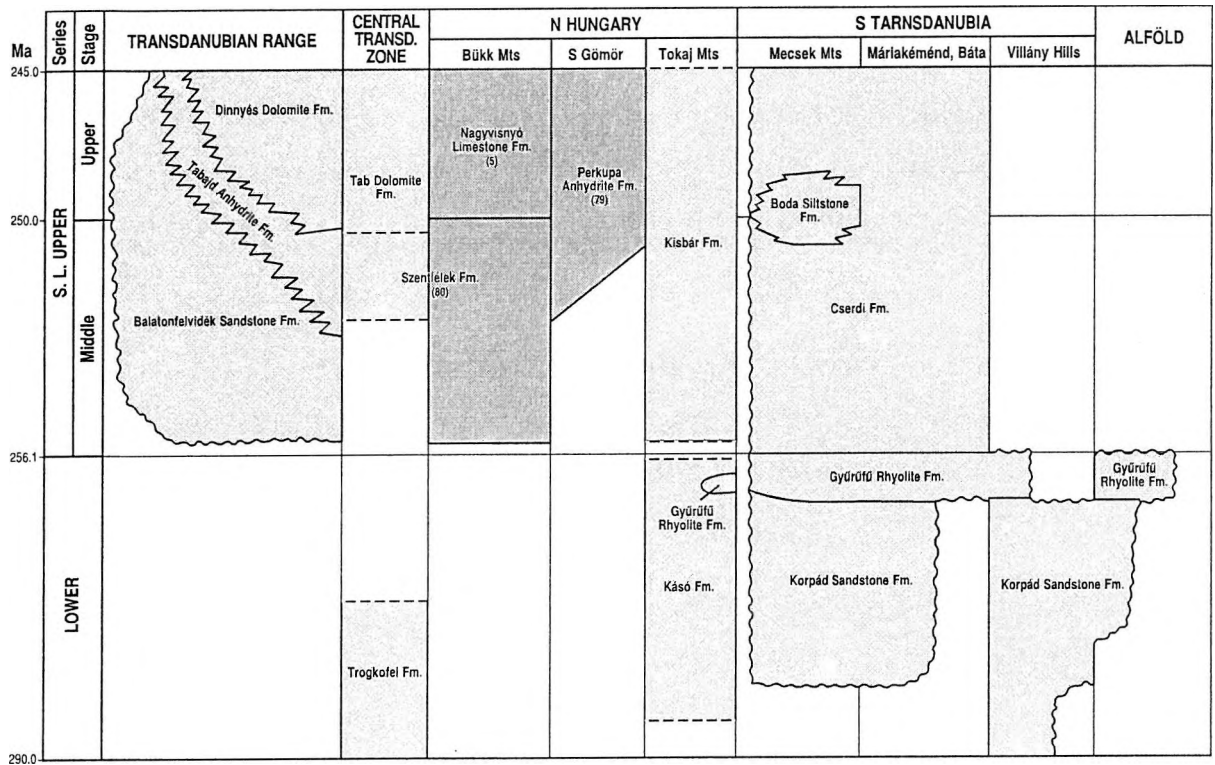


CRETACEOUS

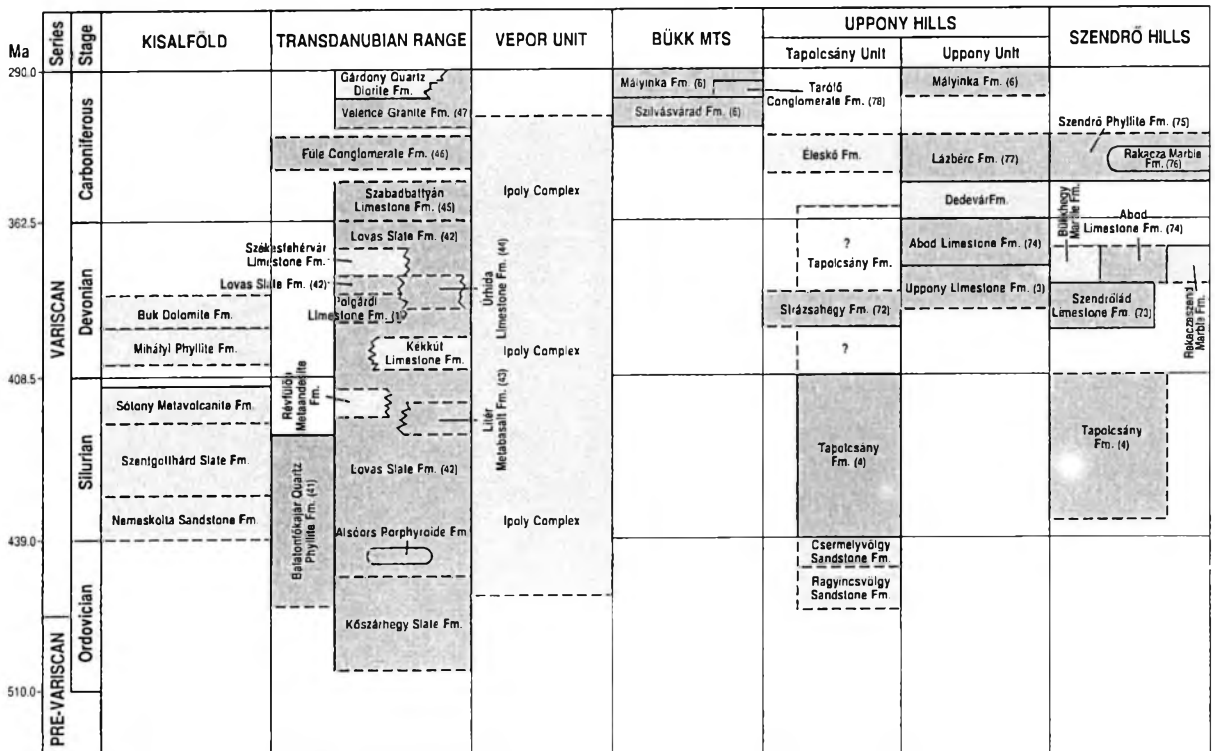


1. Ugod Limestone Fm., 2. Kozmatag Fm., 3. Ajka Coal Fm., 4. Környe Limestone Fm.

PERMIAN



PALEOZOIC I



(1) Polgárdi Limestone (D₂), (2) Szendrőlád Limestone (D_{2,3}), (3) Uppony Limestone (D_{2,3}), (4) Tapolcsány Formation (S-C₁), (5) Nagyvisnyó Limestone (P₂), (6) Szilvásvár Formation and Mályinka Formation (C₂), (7) Rudabánya Iron Ore (T_{1,2}, Rudabánya, Martonyi, Eszteramos), (8) Csapok Marl (T₁), (9) Aszófő Dolomite (T₂), (10) Iszkahegy Limestone (T₂), (11) Megyehegy Dolomite (T₂), (12) Felsőörs Limestone (T₂), (13) Buchenstein Formation (T₂), (14) Füred Limestone (T₃), (15) Veszprém Marl (T₃), (16) Mátyáshegy Formation (T₃), (17) Sándorhegy Formation (T₃), (18) Csövár Limestone (T₃-J₁), (19) Rezi Dolomite (T₃), (20) Kössen Formation (T₃), (21) Feketehegy Formation (T₃), (22) Hámor Dolomite (T₂), (23) Vesszős Shale (T₃), (24) Gutenstein Dolomite (T₂), (25) Bodvarákó Formation (T₂), (26) Tomaszent-
 andrás Shale (T₃), (27) Hetvehely Dolomite (T₂), (28) Lapis Limestone (T₂), (29) Zuhánya Limestone (T₂), (30) Csukma Formation / Kozár Limestone (T₂), (31) Kantavár Formation (T_{2,3}), (32) Óbánya Silt (J₁), (33) Úrkút Manganese Ore (J₁), (34) Buda Marl (E₃-O₁), (35) Tard Clay (O₁), (36) Hárshégy Sandstone (O₁), (37) Kőszeg Quartz Phyllite (J₁), (38) Cák Conglomerate (J₂), (39) Velem Calc Phyllite (J_{2,3}), (40) Felsőcsatár Greenschist (K₁), (41) Balatonfőkajár Quartz Phyllite (O-S), (42) Lovas Slate (O-D), (43) Litér Metabasalt (S), (44) Úrhida Limestone (D_{1,2}), (45) Szabadbattyán Limestone (C₁), (46) Füle Conglomerate (C₂), (47) Velence Granite (C₂), (48) Hidegkút Formation (T₁), (49) Budaörs Dolomite (T₂), (50) Vashegy Dolomit (T₂), (51) Földolomit Formation (T₃), (52) Dachstein Limestone (T₃) (53) Pisznice Limestone (J₁), (54) Kisgerecse Marl (J₁), (55) Eplény Limestone (J_{1,2}), (56) Lókút Radiolarite (J_{2,3}), (57) Budakeszi Picrite (K₃), (58) Bauxite Formation (K₃-E₁) (59) Nadap Andesite (E_{2,3}), (60) Szépvölgy Limestone (E₃), (61) Mány Formation (O₂) (62) Börzsöny and Visegrád Andesite (M₂), (63) Kálla Gravel (M₃), (64) Zámor Gravel (M₃), (65) Szák Marl (M₃), (66) Travertine Formation (P-Q₁), (67) Patacs Siltstone (T₂), (68) Mecsek Coal (T₃-J₁), (69) Vasas Marl (J₁), (70) Hosszúhetény Marl (J₁), (71) Mecseknádasd Sandstone (J₁), (72) Strázsahegy Formation (D₂), (73) Irota Formation (D₂), (74) Abod Limestone (D₃), (75) Szendrő Phyllite (C), (76) Rakaca Marble (C), (77) Lázberc Formation (C), (78) Tarófi Conglomerate (C₂), (79) Perkupa Anhydrite (P₂), (80) Szentlélek Formation (P₂), (81) Gerennavár Limestone (T₁), (82) Ablakoskövölgy Limestone (T₁), (83) Szentistvánhegy Metaandesite (T₂), (84) Parad Complex, (T_{2,3}), (85) Fehérvő Limestone (T_{2,3}), (86) Berva Limestone (T_{2,3}), (87) Szinva Metabasalt (T₃), (88) Kisfennsík Limestone (T₃), (89) Felsőtárkány Limestone (T₃), (90) Répáshuta Limestone (T₃), (91) Rónabükk Limestone (T₃), (92) Darnóhegy Shale (J₂), (93) Darnó Radiolarite (J₂), (94) Szarvaskő Basalt (J₂), (95) Bányahegy Radiolarite (J₂), (96) Lök völgy Shale (J_{2,3}), (97) Mónosbél Formation (J₃), (98) Oldalvölgy Formation (J₃), (99) Edelény Clay (M₃), (100) Rudabánya Mine Dump (H), (101) Martonyi Mine Dump (H)

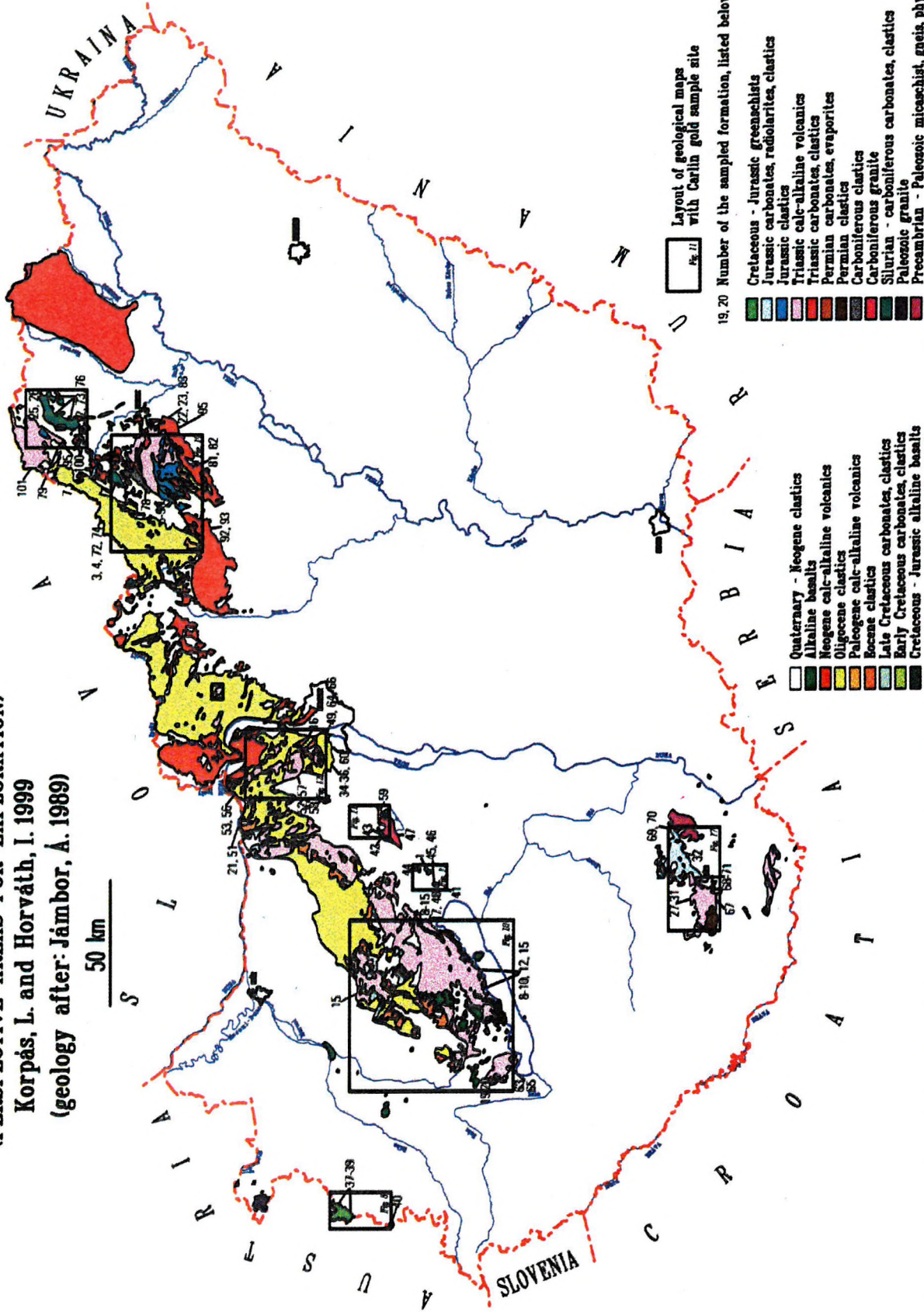
Fig. 2

CARLIN ORE PERSPECTIVITY MAP (GEOLOGY)

(PERSPECTIVE AREAS FOR EXPLORATION)

Korpás, L. and Horváth, I. 1999
(geology after: Jámbo, A. 1989)

50 km



Layout of geological maps with Carlin gold sample site

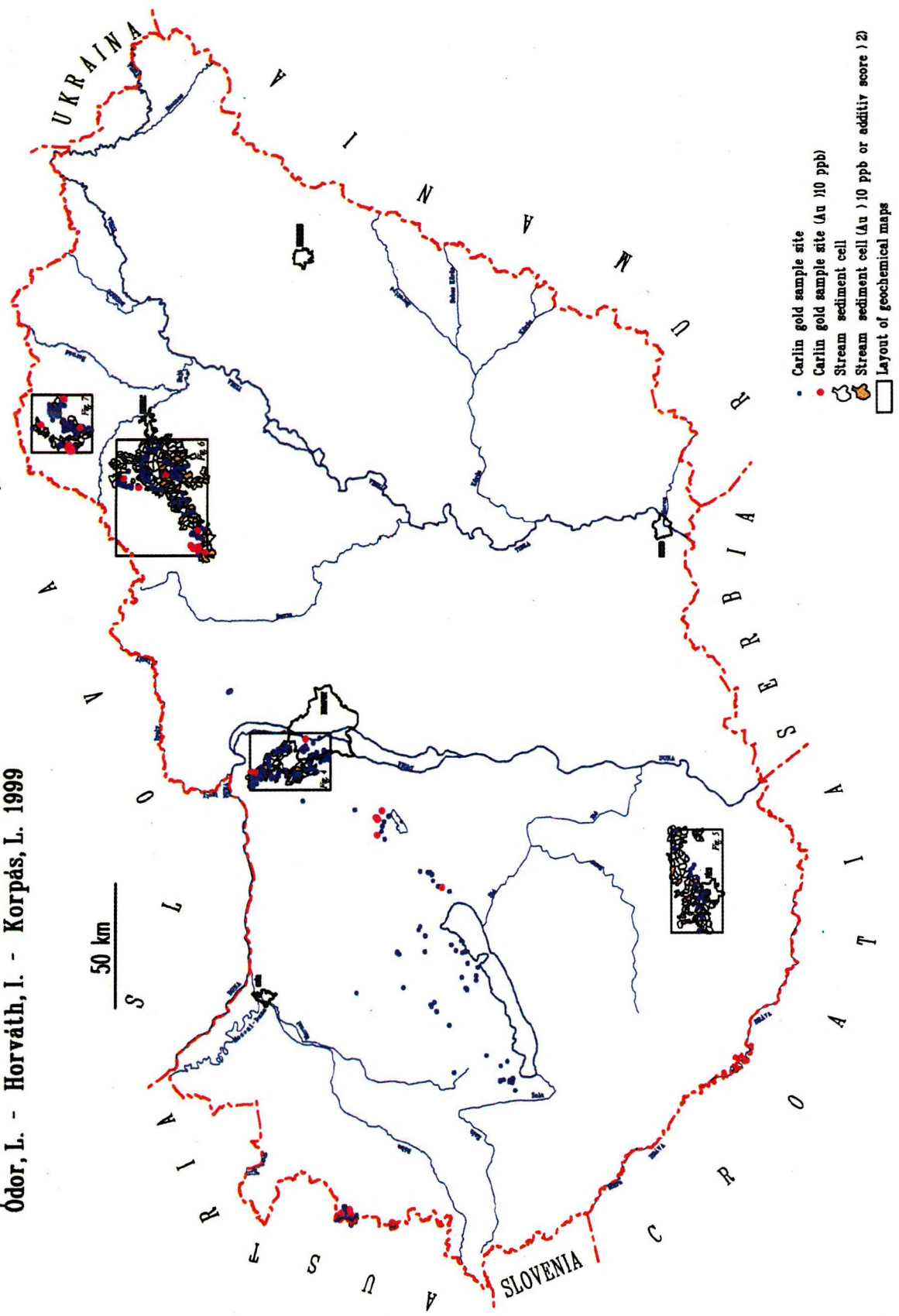
19, 20 Number of the sampled formation, listed below

- | | | | |
|--|--|--|--|
| | Cretaceous - Jurassic greenachists | | Quaternary - Neogene clastics |
| | Jurassic carbonates, radiolarites, clastics | | Alkaline basalts |
| | Jurassic clastics | | Neogene calc-alkaline volcanics |
| | Triassic calc-alkaline volcanics | | Oligocene clastics |
| | Triassic carbonates, clastics | | Paleogene calc-alkaline volcanics |
| | Permian carbonates, evaporites | | Eocene clastics |
| | Permian clastics | | Late Cretaceous carbonates, clastics |
| | Carboniferous clastics | | Early Cretaceous carbonates, clastics |
| | Carboniferous granite | | Cretaceous - Jurassic alkaline basalts |
| | Silurian - carboniferous carbonates, clastics | | |
| | Paleozoic granitoids | | |
| | PreCambrian - Paleozoic micaschist, gneiss, phyllite | | |

CARLIN ORE PERSPECTIVITY MAP (GEOCHEMISTRY) I

Ódor, L. - Horváth, I. - Korpás, L. 1999

Fig. 3



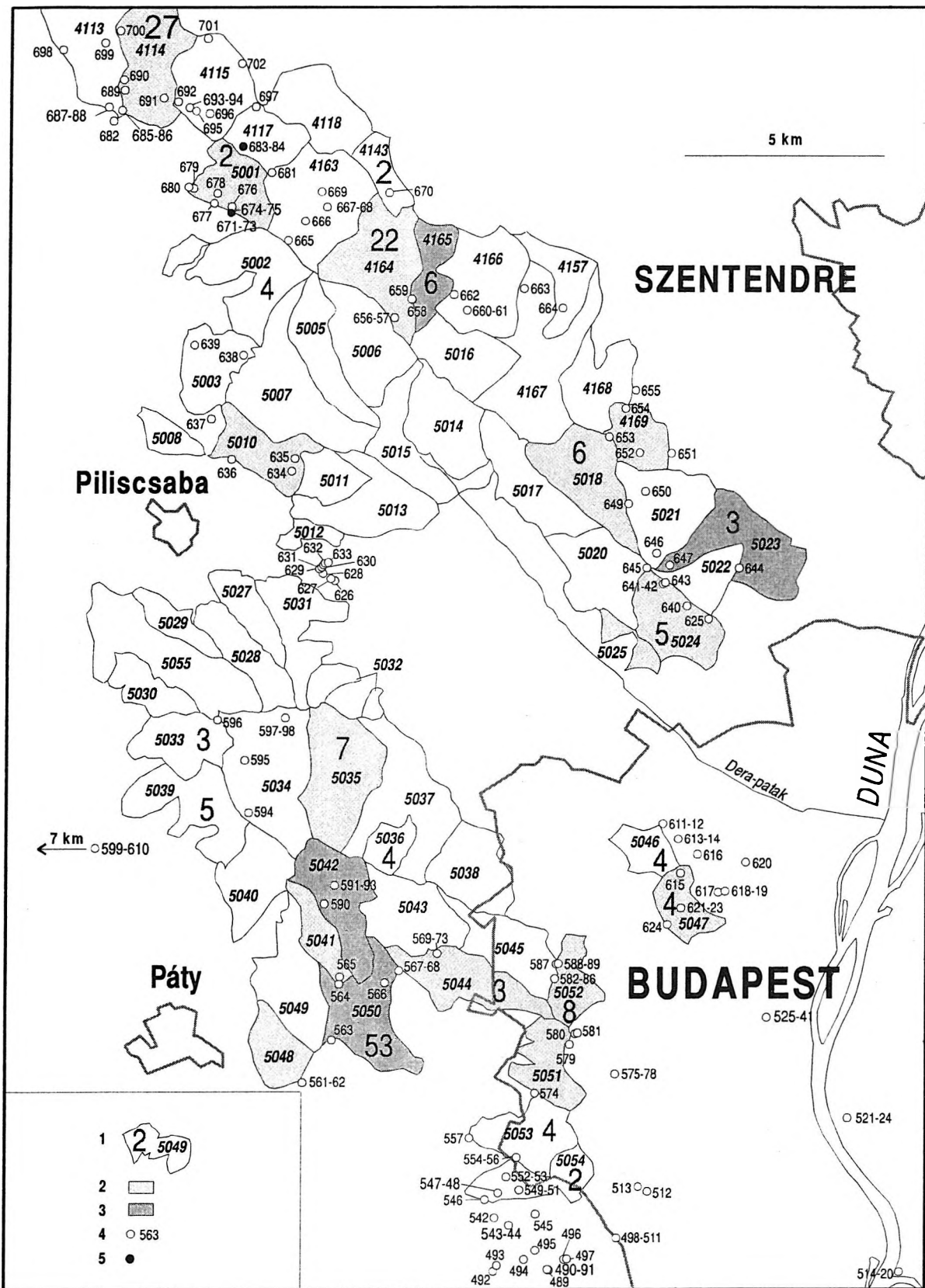


Fig. 4: Stream sediment map of the Buda-Pilis and Visegrád Mountains with Carlin gold sample sites
 1) Number (5049) and gold value (2) of stream sediment cells, 2) Additive anomaly score 3-4 of stream sediment cells, 3) Additive anomaly score 5-6 of stream of sediment cells, 4) Carlin gold sample site, 5) Carlin gold sample site with subanomalous (10-100 ppb Au) value

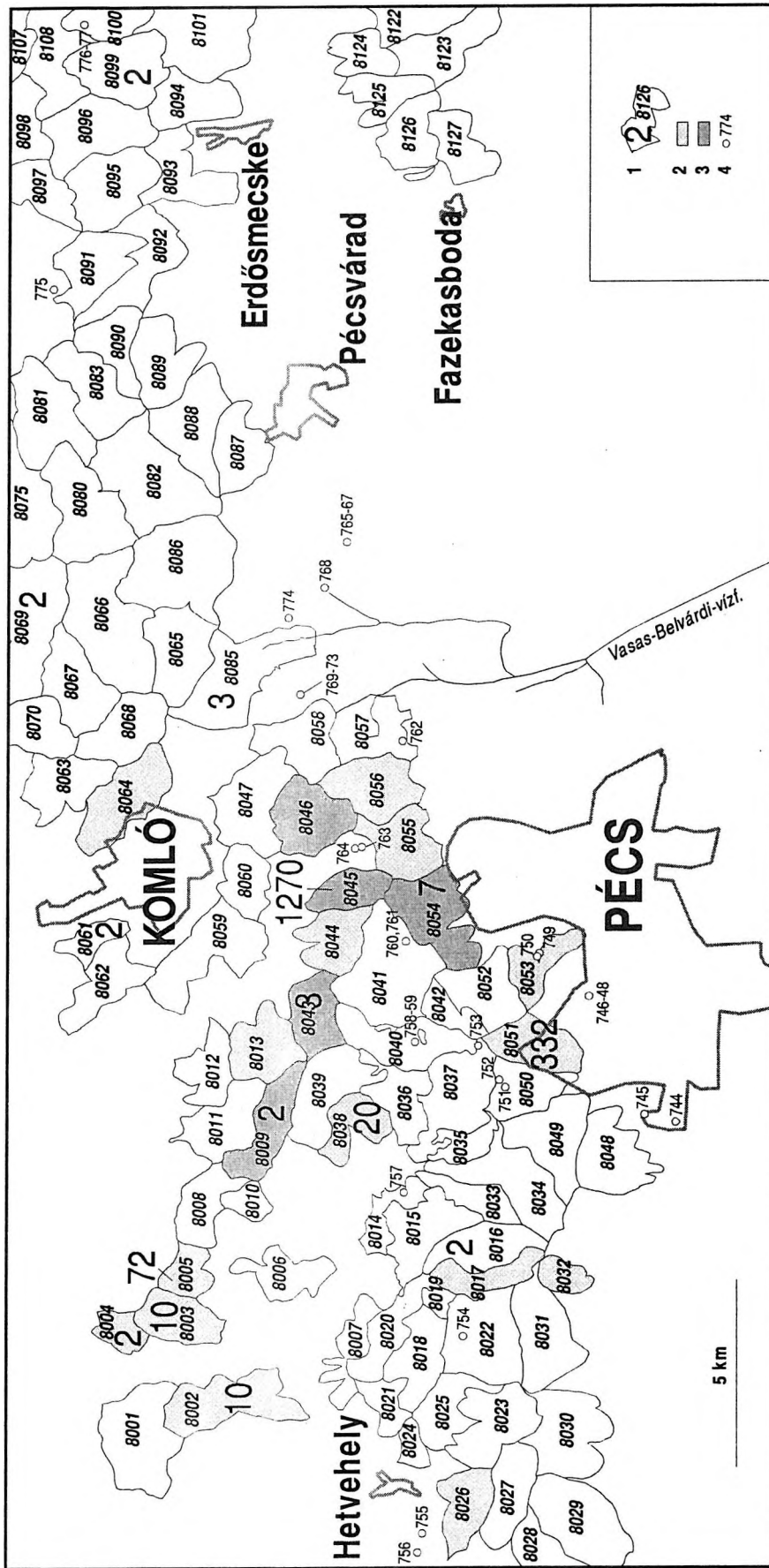


Fig. 5: Stream sediment map of the Mecsek Mountains with Carlin gold sample sites
 1) Number (8126) and gold value (2) of stream sediment cells, 2) Additive anomaly score 2-3 of stream sediment cells, 3) Additive anomaly score 4-7 of stream of sediment cells, 4) Carlin gold sample site

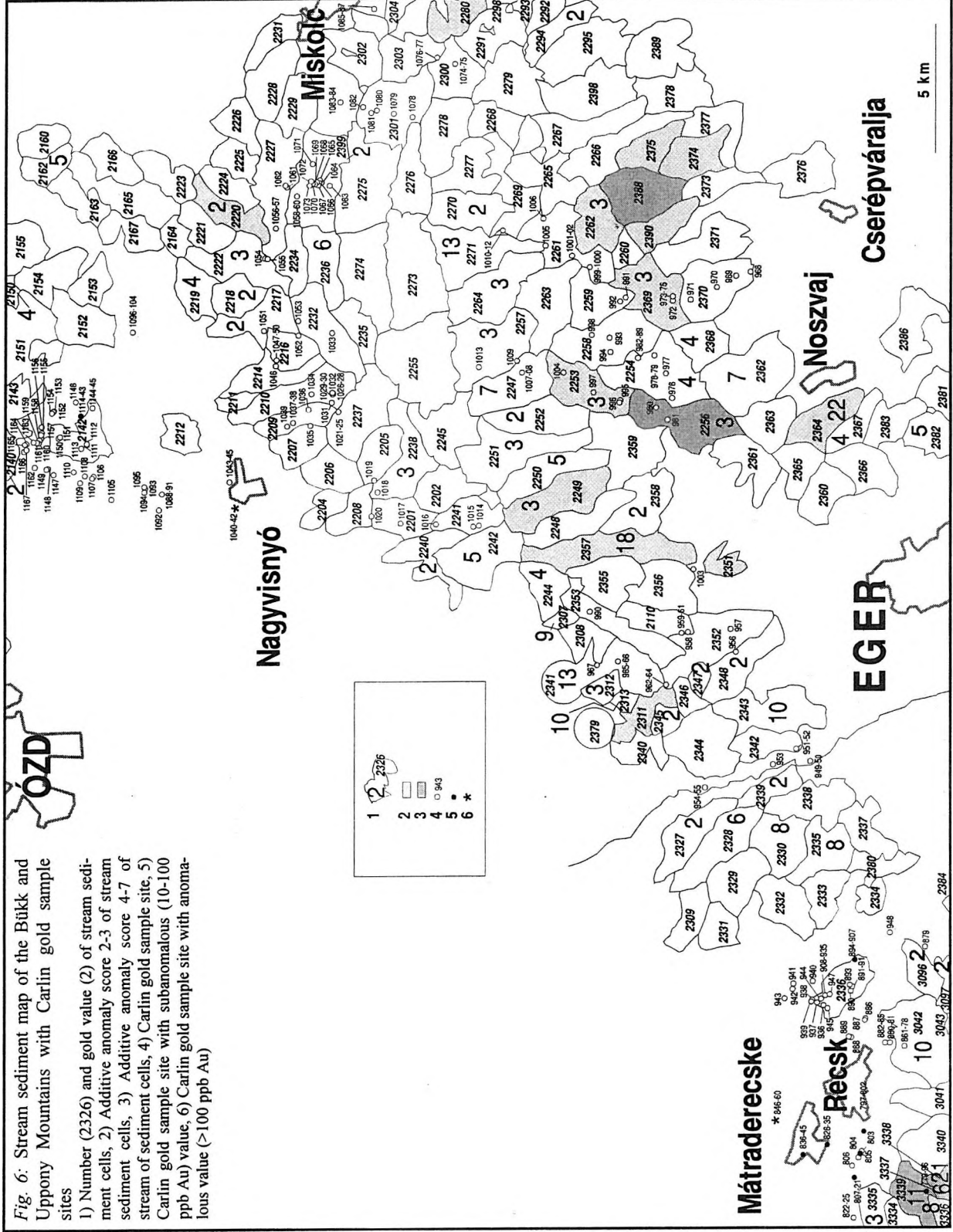


Fig. 6: Stream sediment map of the Bükk and Uppony Mountains with Carlin gold sample sites

- 1) Number (2326) and gold value (2) of stream sediment cells, 2) Additive anomaly score 2-3 of stream sediment cells, 3) Additive anomaly score 4-7 of stream of sediment cells, 4) Carlin gold sample site, 5) Carlin gold sample site with subnormal (10-100 ppb Au) value, 6) Carlin gold sample site with anomalous value (>100 ppb Au)

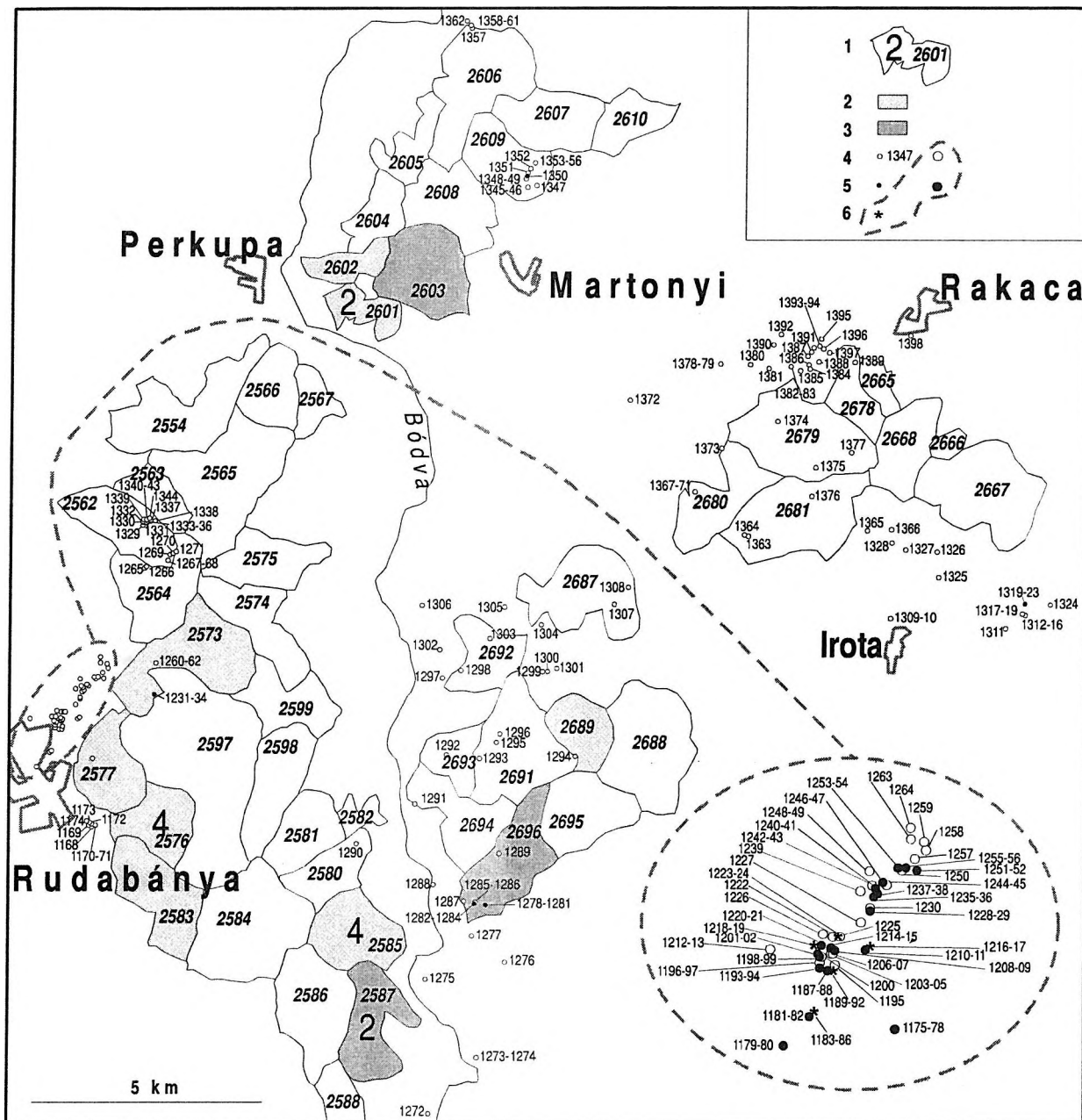


Fig. 7: Stream sediment map of the Rudabánya and Szendrő Mountains with Carlin gold sample sites

1) Number (2601) and gold value (2) of stream sediment cells, 2) Additive anomaly score 2 of stream sediment cells, 3) Additive anomaly score 3-7 of stream of sediment cells, 4) Carlin gold sample site, 5) Carlin gold sample site with subanomalous (10-100 ppb Au) value, 6) Carlin gold sample site with anomalous (>100 ppb) value

Geochemical parameters of the stream sediment surveys in different regions of Hungary
(Minimum, maximum and median values for Au, As, Ag, Hg, Sb and Ba)

Table 1

Element	Minimum	Maximum	Median	N
Mecsek Mountains				97
Au (ppb)	<2	1270	<2	
As (ppm)	1.53	42.6	5.72	
Ag (ppm)	<0.3	<0.3		
Hg (ppm)	<0.02	0.1	0.02	
Sb (ppm)	0.12	6.83	0.39	
Ba (ppm)	39.4	281	85.3	
Buda and Pilis Mountains				64
Au (ppb)	<2	53	<2	
As (ppm)	3.1	34.0	9.1	
Ag (ppm)	<0.3	3.9	0.6	
Hg (ppm)	<0.02	0.95	0.06	
Sb (ppm)	<0.2	9.1	<0.2	
Ba (ppm)	19.0	511	131	
Bükk and Uppony Mountains				172
Au (ppb)	<2	22	<2	
As (ppm)	3.0	82.6	7.9	
Ag (ppm)	<0.2	11.0	<0.2	
Hg (ppm)	0.02	2.22	0.08	
Sb (ppm)	<0.1	2.5	0.5	
Ba (ppm)	49.2	481	107	
Rudabánya and Szendrő Mountains				43
Au (ppb)	<2	4	<2	
As (ppm)	3.9	37.4	9.2	
Ag (ppm)	<0.2	0.7	<0.2	
Hg (ppm)	0.02	10.7	0.09	
Sb (ppm)	<0.1	4.7	0.6	
Ba (ppm)	24.7	315	161	

There are four regions covered by the stream sediment surveys (Figs. 4, 5, 6 and 7) where their data together with geochemical parameters for Ba Table 1 can supplement our Carlin-studies.

Maximum values of gold in the Mecsek Mountains (No. 8045–1270 ppb and 8051–332 ppb), in the Buda Hills (No 5050–53 ppb), Pilis Mountains (No. 4114–27 ppb, 4164–22 ppb), and in the Bükk Mountains (No. 2364–22 ppb) are worth mentioning. Otherwise there are no striking differences in the median or maximum concentrations of elements in these four regions.

In each region element associations were first studied by Spearman's rank correlation method in order to see which elements can be used to construct an additive geochemical anomaly map. Pairs of elements which show significant correlations (at significance level of 0.01) are:

Mecsek Mountains: Hg–As; Sb–As and Hg–Sb.

Buda–Pilis and Visegrád Mountains: none (at significance level 0.05: Sb–Ag; Sb–As; Hg–As; Hg–Sb)

Bükk Mountains: Au–Ag; Hg–As; Sb–As; Hg–Au and Hg–Sb.

Rudabánya and Szendrő Mountains: Hg–As; Sb–As; and Sb–Hg.

So it was possible to use all 5 elements in the computation of additive anomalies. Histograms for each element, together with frequency tables and boxplot diagrams were used to understand the distribution features of the elements. Table 2 might help to understand the procedure. Each element in every sample was given a score

Stream sediment surveys in different regions of Hungary
Summary of how the additive indices were calculated according to the concentration ranges of elements

Table 2

Element	The increase of the additive value according to concentration			N
	+1	+2	+3	
Mecsek Mountains				97
Au (ppb)	>=2-10	>=10-100	>=100	
As (ppm)	>=8-12	>=12-19	>=19	
Ag (ppm)	-	-	-	
Hg (ppm)	-	-	-	
Sb (ppm)	>=0.8-1.2	>=1.2		
Buda and Pilis Mountains				64
Au (ppb)	>=2-10	>=10		
As (ppm)	>=8-15	>16-25	>=25	
Ag (ppm)	>=1			
Hg (ppm)	>=0.1-0.24	>=0.24		
Sb (ppm)	>=0.9			
Bükk and Uppony Mountains				172
Au (ppb)	>=2-14	>15		
As (ppm)	16-24	>=24-30	>=30	
Ag (ppm)	0.2-6	>=6		
Hg (ppm)	0.2-0.5	>0.5		
Sb (ppm)	>=1.2			
Rudabánya and Szendrő Mountains				43
Au (ppb)	>=2			
As (ppm)	<15	16-30	>30	
Ag (ppm)	>0.2			
Hg (ppm)	>=0.3-10		>10	
Sb (ppm)	>3			

according to its concentration. These scores were then added up to get the final scores for each sample, that is for each catchment basin of the stream sediment survey. Additive anomalies were plotted according to the values of these final scores (see geochemical maps: Figs. 4, 5, 6 and 7).

3. DESCRIPTION OF THE PROSPECTED AREAS AND FORMATIONS

3.1. Kőszeg Mountains

3.1.1. Mesozoic

3.1.1.1. Jurassic

Kőszeg Quartz Phyllite (37)

This 300 to 400 m thick formation (Fig. 8) is a typical graywacke and consists of metaquartzite, quartz phyllite and phyllite (FÖLDVÁRI et al. 1948). Veins and boudinage like lenses of quartzite are frequent and traces of graphite were described by DEÁK (1981). The mineralogical composition includes quartz, muscovite, paragonite, chlorite, few albite, graphite, turmaline, zircon, apatite, titanite and ore minerals (LELKES-FELVÁRI 1998a). Estimated age is Lower Jurassic (IVANCSICS in CSÁSZÁR 1997).

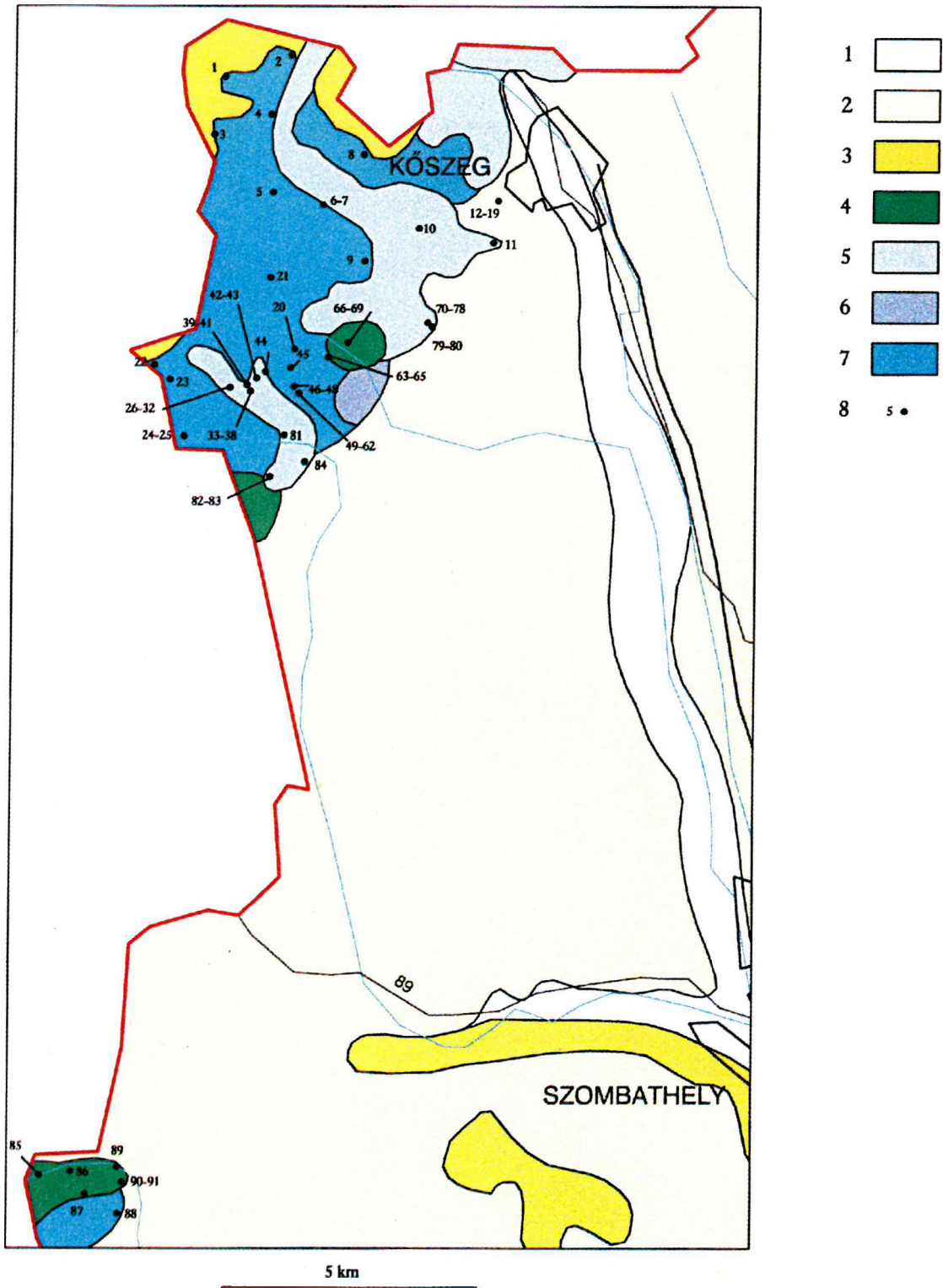


Fig. 8: Geological map of the Kőszeg Mountains with Carlin gold sample sites
 1. Holocene alluvial sediments, 2. Quaternary sediments, 3. Late Miocene sediments, 4. Felsőcsatár Greenschist, 5. Velem Calc Phyllite, 6. Cák Conglomerate, 7. Kőszeg Quartz Phyllite, 8. •72 Carlin gold sample site

Geochemistry :

The geochemical features of this formation are represented by 20 samples (Nos. 1–20 of Appendix 1). Phyllites, quartzites, micaschists have been sampled. Ranges and medians are given below:

Au (<2–13),	<2 ppb	As (0.4–286.0),	3.51 ppm
Ag (<0.05–0.21),	0.05 ppm	Hg (<0.02–0.21),	0.021 ppm
Sb (<0.01–119.0),	1.17 ppm	Tl (<0.02–0.3),	0.13 ppm

Relatively high concentration of elements (Au, As and Ag) are found in a quartzite breccia. Low level anomalies of As and Sb were detected with anomaly thresholds of 20 ppm for As and 10 ppm for Sb. Significant correlation have only been found for Sb–Tl.

Cák Conglomerate (38)

This is a clast supported monomictic, upward fining metaconglomerate. It forms lenslike bodies in the Velem Calc Phyllite, and was generated by slumping (IVANCSICS in CSÁSZÁR 1997). Its thickness changes between 1 and 15 m and the pebbles are composed of mainly oolitic dolomite, chalky dolomite, less limestone and marl, with subordinated gneis, micaschist and phyllite with a diameter ranging between 2 mm and 30 cm (NAGY 1972, LELKES–FELVÁRI 1998a). Few quartzite cement and a dense network of quartzite-veins is giving its cellular structure. Rare benthic fossils (ostracods, foraminifera, algae and fragments of molluscs, bryozoan and echinoids were mentioned from the pebbles (NAGY 1972, DEÁK 1981). Presence of graphite, pyrite, limonite and manganese crust was documented by FÖLDVÁRI et al. (1948). The presumed age is Middle Jurassic after CSÁSZÁR (1997).

Geochemistry:

There are only one quartzite and one conglomerate samples (Nos. 79–80 of Appendix 1) to represent the formation. The higher values are in the quartzite sample.

Au (<2–13) ppb	As (4.2–245.0) ppm
Ag (<0.05–0.65) ppm	Hg (0.0057–0.707) ppm
Sb (1.84–6.27) ppm	Tl (<0.05–0.53) ppm

The quartzite sample exhibits subanomalous Au and anomalous As contents.

Velem Calc Phyllite (39)

The 400–600 m thick formation is Middle to Late Jurassic in age (CSÁSZÁR 1997) and consists of mainly calc phyllite, calc mica schist, graphitic phyllite, with intercalations of bedded crystalline limestone, dolomite and some quartz phyllites and metaquartzites. Partly mined oreshows of stibnite, chalkopyrite-azurite, manganese, siderite and pyrite on the Velem Szent Vid-hegy were mentioned by BENDA (1932) and FÖLDVÁRI et al. (1948). They were confirmed by later geochemical studies presenting anomalies of Cr, Ni, V, Cu, Pb, Zn and Ag (BÖJTÖSNÉ–VARRÓK 1965, FÖLDVÁRINÉ–VOGL 1970) and completed with the results of geophysical and drill hole ore prospections outlined after NAGY (1972) in the following. Nine drill holes located above SP (spontaneous potential) anomalies have discovered a disseminated mineralization of pyrite and marcasite (1–12%) with traces of magnetite, chalkopyrite, stibnite, native gold, galena and sphalerite. Six samples of the drill hole Velem 5 have given the next analytical results: Cu: 0.0–0.05%, Fe: 1.83–12.12%, Au: 0.0–0.20 ppm, Ag: 0.70–2.1 ppm. Average organic carbon content of the rocks composed of semianthracite-anthracite-graphite is about 4%, while their sulfur content bounded to pyrite and marcasite amounts to 6%.

Geochemistry :

62 samples have been taken from this formation (Nos. 21–78, 81–84 of Appendix 1). Phyllite, graphite shales, slates and quartzites have been sampled. Ranges and medians are given below:

Au (<2–19)	<2 ppb	As (0.4–34.9)	4.9 ppm
Ag (<0.05–0.38)	0.09 ppm	Hg (0.0037–0.18)	0.0199 ppm
Sb (0.05–10.7)	0.40 ppm	Tl (<0.05–0.35)	0.16 ppm

The higher concentration values were found in graphite slate and phyllite. Insignificant, low value anomaly thresholds were detected for Sb and Au, 2 ppm and 7 ppb respectively. Correlation coefficients are significant for the following pairs of elements: Hg–Ag, Tl–As, Hg–Au and Tl–Sb.

3.1.1.2. Cretaceous

Felsőcsatár Greenschist (40)

The 100 m thick formation consists of basic metatuffs (greenschists), chlorite-actinolite-tremolite schists with bodies of foliated and massive serpentinites, gabbros and related talc deposits. Its typical mineral assemblage is represented by klnozoisite, epidote, tremolite-actinolite, chlorite, few titanite, biotite, muscovite, albite and

Kőszeg Mountains
Summary of geochemical parameters—median and maximum values

Table 3

Form-code	Au (ppb)		Ag (ppm)		As (ppm)		Hg (ppm)		Sb (ppm)		Tl (ppm)		N
	Med.	Max.	Med.	Max.	Med.	Max.	Med.	Max.	Med.	Max.	Med.	Max.	
37	<2	13	0.05	0.21	3.51	286.0	0.021	0.21	1.17	119.0	0.13	0.30	20
38	<2	13	.02m	0.65	4.2m	245	.01m	0.707	1.8m	6.27	.02m	0.53	2
39	<2	19	0.09	0.38	4.9	34.9	0.02	0.18	0.40	10.7	0.16	0.35	62
40	2	310	<.05	0.76	3.76	71.3	0.003	0.027	0.87	6.49	<.05	0.1	7

Remarks:

Formcode = the code number of the Formation:

37=Kőszeg Quartz Phyllite, 38=Cák Conglomerate, 39=Velem Calc-Phyllite, 40=Felsőcsatár Greenschist

Med.=median value; Max.=maximum value; m=minimum values.

quartz in the greenschist, and by amphibole, chlorite, biotite, klnozoisite-epidote, titanite in the metagabbro (LELKES-FELVÁRI 1998a). Its presumed age is Early Cretaceous (CSÁSZÁR 1997).

Geochemistry :

7 samples have been taken from the formation (Nos. 85–91. of Appendix 1). The sampled lithology is a mixed one: greenschists, phyllites, diabase, serpentinite. Ranges and medians are given below:

Au (<2–310)	2 ppb	As (1.7–71.3)	3.76 ppm
Ag (<0.05–0.76)	<0.05 ppm	Hg (0.0015–0.027)	0.003 ppm
Sb (0.38–6.49)	0.87 ppm	Tl (<0.05–0.1)	<0.05 ppm

Gold values are near detection level, the 310 ppb gold is in the diabase. No significant correlation was found between pairs of elements.

Summary for the Kőszeg Mountains:

Main features for the four formations of Kőszeg Mountains are summarized in Table 3 and illustrated on Fig. 9. Formations represented by less than three samples are not plotted. Reference lines at 10 ppb and 100 ppb are given to indicate subanomalous and anomalous threshold values of gold. There are some As and Sb anomalies (>100 ppm) with week subanomalous gold concentrations and a noticeable gold value in the Felsőcsatár Greenschist Formation without the enrichment of Carlin suite elements. This last formation is recommended for further detailed exploration. All the other formations can be classed to the subanomalous group and considered less favorable for this type of mineralization.

3.2. Transdanubian Range

The prospected areas and formations of the Transdanubian Range will be evaluated using the regional geological map series of Figs. 10–13 and the regional geochemical map of the stream sediment survey (Fig. 4).

3.2.1. Paleozoic

3.2.1.1. Ordovician–Silurian–Devonian

Balatonfőkajár Quartz Phyllite (41)

The formation (Fig. 11) is several hundred meter thick and consists of grey, greenish grey or black quartz-phyllite, sericite phyllite, sericite quartzite and chlorite-muscovite phyllite accompanied by carbonate-quartz-phyllite, albite-gneiss and graphitic phyllite. Scarce intercalations of acidic volcanoclastites and veins of quartzite are typical. The mineralogical composition is represented by quartz, albite, muscovite, chlorite, carbonate (calcite, siderite and traces of dolomite), biotite, epidote, garnet. Siltstones, claystones and sandstones poor in carbonates and organic matter with few intercalations of rhyolitic or dacitic volcanoclastites are considered as protolithes. The grade of metamorphism corresponds to the lower-middle part of greenschist facies (FÜLÖP 1990, LELKES-FELVÁRI 1998b). K/Ar ages measured on muscovite (from 320 to 343 Ma) and fission track ages on zircon (247±39 and 270±45 Ma) indicate a pre-Alpine variscan metamorphism (LELKES-FELVÁRI 1998b). The presumed age is Late Ordovician to Silurian (CSÁSZÁR 1997).

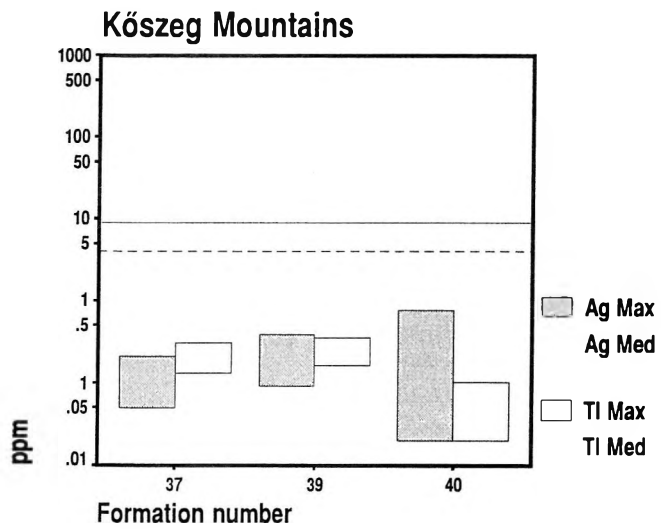
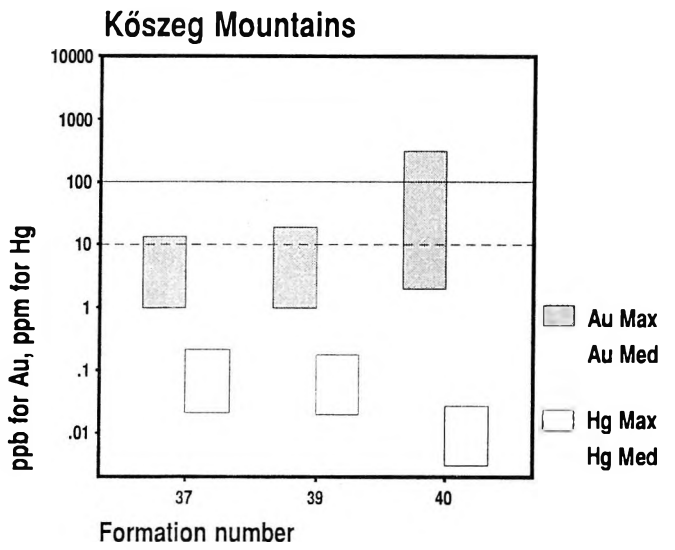
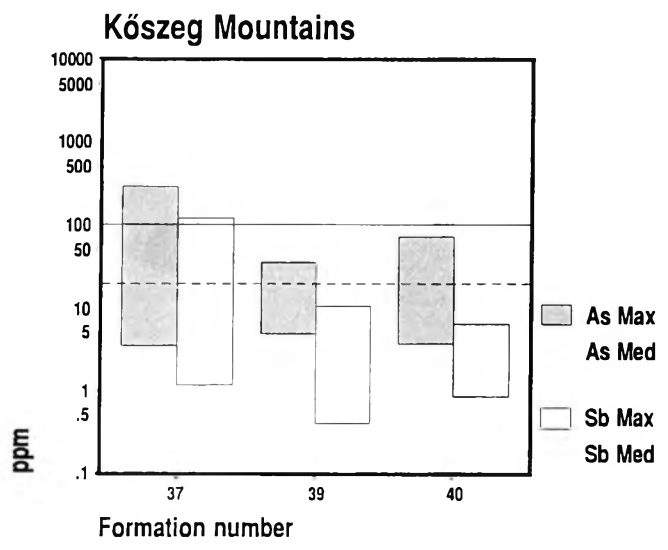


Fig. 9: The median (Med)-maximum (Max) concentration ranges of Au-Hg, As-Sb and Ag-Tl. Kőszeg Mountains



Geochemistry:

The data of 9 samples represent this formation (Nos. 283–291 of Appendix 1). Quartz phyllites and phyllites were sampled. Ranges and medians are given below:

Au (<2–27)	<2 ppb	As (0.4–13.8)	3.3 ppm
Ag (<0.02–0.52)	0.07 ppm	Hg (0.0048–0.30)	0.20 ppm
Sb (0.2–4.40)	0.86 ppm	Tl (0.05–0.33)	0.12 ppm

There are only two positive values for gold. For four out of the 6 elements analysed high concentrations values are in a phyllite sample. Correlation coefficients are significant for Sb–Ag and Sb–As.

Lovas Slate (42)

The folded formation (Figs. 10 and 11) is 400 to 1050 m thick and consists of grey, greenish grey slate, metasiltstone and metasandstone with intercalations of metavolcanoclastites, porphyroides and metabasalts. Laminated metaanthracite bearing grey and black jasper (lidite) horizons up to some metres also occur. As protoliths are considered Late Ordovician–Devonian flysch like sediments deposited in an inner shelf basin and suffered an anchizone metamorphism of pumpellyit-prehnite-quartz facies. The mineralogical composition is represented by sericite, chlorite, quartz, feldspar, muscovite, biotite, zircon, tourmaline, rutil and apatite (FÜLÖP 1990). Estimated metamorphic ages (LELKES–FELVÁRI 1998b) are the followings: 316±22 Ma (by Rb/Sr method), 311–327 Ma (by K/Ar method), 252–253 Ma and 288 Ma (by fission track method). At the contact with the intrusion of the Velence Granite has formed a wide actinolite, andalusite and tourmaline bearing hornfels horizon (HORVÁTH et al. in press)

Hydrothermal alterations and related polymetallic oreshows with gold and silver in the Lovas Slate are known for a long time (FÖLDVÁRI 1947, JANTSKY 1957, KUBOVICS 1958, BÖJTÖSNÉ–VARRÓK 1967). Among the polymetallic geochemical anomalies main elements of the Carlin suite, like Au, Ag, As, Sb, Hg and Tl (+Cd) were also detected (JANTSKY 1957, KUBOVICS 1958, BÖJTÖSNÉ–VARRÓK 1967, FÖLDVÁRI–VOGL 1970). Native gold up to 8.5 ppm and silver up to 363.5 and 11,000 ppm was reported by KUBOVICS (1958) in the Meleghegy quartzite at the contact zone with Velence Granite. Systematic metallometry of soil and rock sampling resulted in discovery of anomalies of Ag (soil: >0.36 ppm, rock: >0.79 ppm), As (rock: >194 ppm), Cu and Ba (soil: >1340 ppm, rock: >1677 ppm) in the Meleghegy and Bencehegy area (ÓDOR et al. 1982) and anomalies of gold (up to 2 ppm), silver, antimony and mercury were detected in rock chip samples of borehole-cores (Nadap Nt-1 and 2, Sukoró St-4 and S-3) too (HORVÁTH et al. 1990).

The polyphase hydrothermal mineralization can be related both to the Late Carboniferous Velence Granite and Late Eocene Nadap Andesite (JANTSKY 1957, KUBOVICS 1958, BÖJTÖSNÉ–VARRÓK 1967, HORVÁTH et al. 1989 and MOLNÁR 1998). MOLNÁR (1998) postulates that hydrothermal mineralization was generated by the Velence Granite at temperatures about 300 °C, at a pressure of 1.0–2.4 kbars and took place in the mixing zone of two different, CO₂ rich fluids.

Geochemistry :

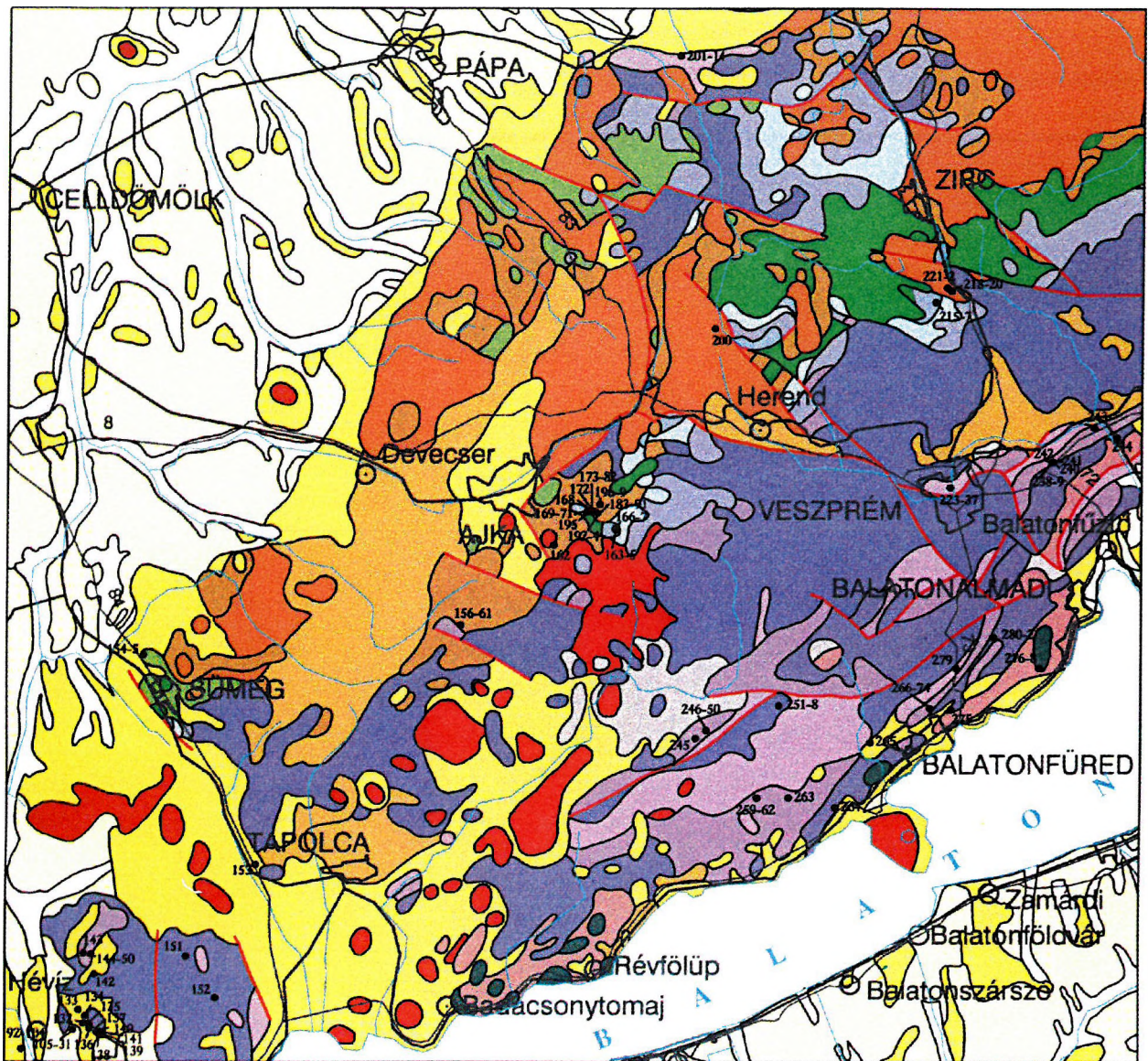
74 samples were analysed representing this formation (Nos. 276–278, 316, 332–340, 349–357, 359–361, 363–364, 370–372, 374, 376, 378, 380, 382, 384, 386, 388–389, 391, 393, 395, 397, 399, 401, 402, 404, 406, 408, 410–413, 415, 416, 418, 420, 422, 424, 426, 428, 430, 432, 434, 436, 438, 440, 442, 444, 455, 456, 458, 459, 487. of Appendix 1). Slates, limonitic slates, contact slates, contact slate breccias, quartzites and quartzite breccias were sampled. We have the data of 74 samples for Au and Ag and of 31 samples for As, Sb, Tl and Hg. Ranges and medians are given below:

Au (<2–4770)	<2 ppb	As (1.17–1255)	26.8 ppm
Ag (<0.02–140)	0.095 ppm	Hg (<0.02–0.966)	0.0253 ppm
Sb (0.07–791.0)	1.16 ppm	Tl (<0.05–1.06)	0.16 ppm

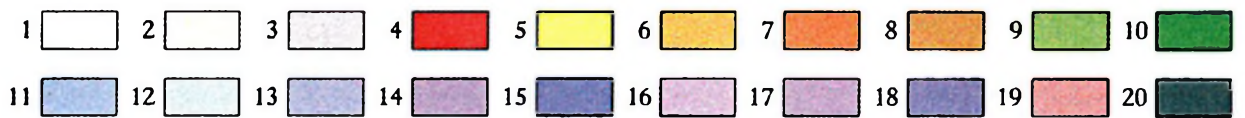
A limonitic quartzite breccia contains the highest values for almost every element analysed. Gold is in the vuggy silica of quartzite breccias and in the contact slate. Thresholds for anomalies were detected for the following elements (number of anomalous values above thresholds are in paranthesis): 100 ppb for Au (5); 5 ppm for Ag (5); 100 ppm for As (10) and 5 ppm for Sb (7). All elements are significantly correlated with each other, except Tl–Ag, Tl–Hg and Tl–Sb.

Litér Metabasalt (43)

According to LELKES–FELVÁRI (in CSÁSZÁR 1997) the formation consists of “greyish green, schistose rocks of porphyric texture with plagioclase and monocline pyroxene phenocrystals recrystallised to albite, actinolite, epidote and chlorite. Fine-grained metagabbro, haematite carbonate schist and albitic schist can also be identified. The grade of metamorphism corresponds to higher anchizone and the lower greenschist facies. Thickness: over 100 m. The age is unknown.”



5 km



152.

Fig. 10: Geological map of the Keszthely Mountains, Balatonfelvidék and Bakony with Carlin gold sample sites

1. Holocene alluvial sediments, 2. Quaternary sediments, 3. Late Miocene travertine, 4. Late Miocene basalts, 5. Källa Gravel and Szák Marl, 6. Middle-Late Miocene sediments, 7. Oligocene-Early Miocene sediments, 8. Middle-Late Eocene sediments, 9. Senonian sediments, 10. Albian-Cenomanian sediments, 11. Lókút Radiolarite and Pisznice Limestone, 12. Úrkút Manganese Ore, Kisgerecse Marl and Eplény Limestone, 13. Dachstein Limestone, 14. Kössen Formation, 15. Födölovit Formation and Rezi Dolomite, 16. Veszprém Marl and Sándorhegy Limestone, 17. Megyehegy Dolomite, Buchenstein Formation and Felsőörs Limestone, 18. Hidegkút Formation, Csopak Marl, Aszfő Dolomite and Iszkahegy Limestone, 19. Late Permian sediments, 20. Lovas Slate, 21. •89 Carlin gold sample site

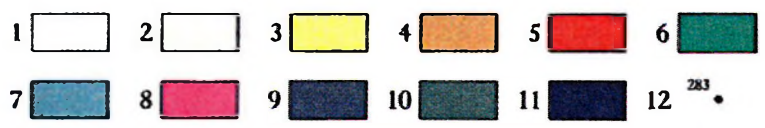
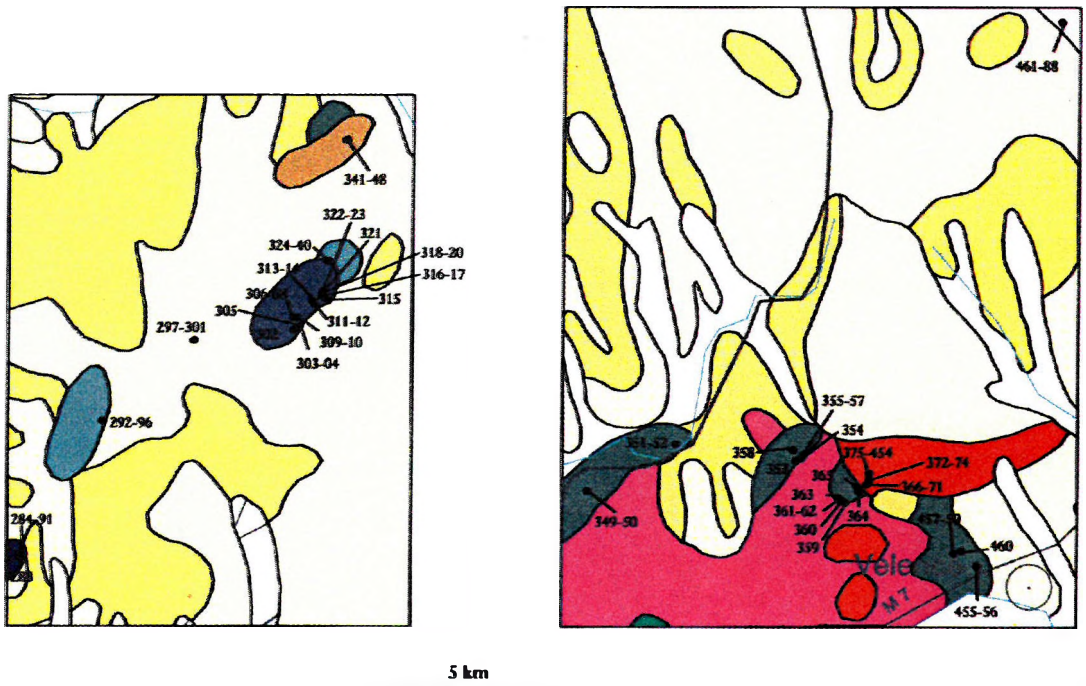


Fig. 11: Geological map of the Balatonfő–Velence Hill with Carlin gold sample sites
 1. Holocene alluvial sediments, 2. Quaternary sediments, 3. Late Miocene sediments, 4. Middle–Late Eocene sediments, 5. Nadap Andesite, 6. Budakeszi Picrite, 7. Füle Conglomerate, 8. Velence Granite, 9. Polgárdi Limestone, 10. Lovas Slate, 11. Balatonfőkajár Quartz Phyllite, 12. •352 Carlin gold sample site

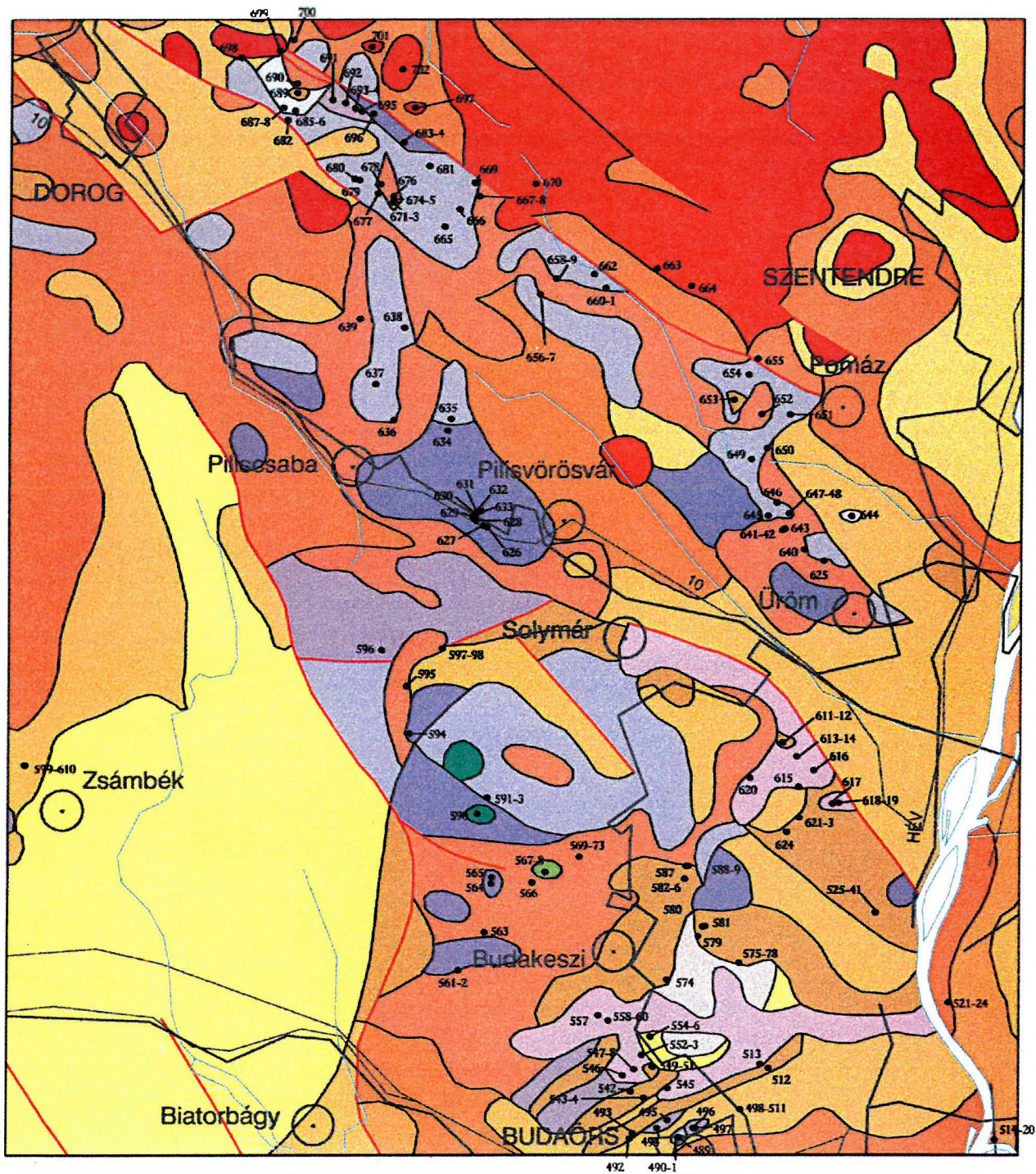


Fig. 12: Geological map of the Buda-Pilis and Visegrád Mountains with Carlin gold sample sites

1. Travertine Formation, 2. Zámor Gravel, 3. Late Miocene sediments, 4. Late Miocene limestone, 5. Middle Miocene sediments, 6. Börzsony and Visegrád Andesite, 7. Early-Middle Miocene sediments, 8. Late Oligocene sediments, 9. Kiscell Clay and Mátyás Formation, 10. Hárshégy Sandstone, 11. Buda Marl and Szépvölgy Limestone, 12. Bauxite Formation, 13. Budakeszi Picrite, 14. Pisznice Limestone and Lókút Radiolarite, 15. Dachstein Limestone, 16. Feketehegy Formation, 17. Földolomit Formation, 18. Mátyáshegy Formation, 19. Budaörs Dolomite, 20. • 672 Carlin gold sample site

Geochemistry:

We have only two samples analysed for gold and silver and one sample for the other elements (Nos. 460, 488 of Appendix 1).

Au <2 ppb	As 1 ppm
Ag (<0.02–0.07) ppm	Hg 0.055 ppm
Sb 0.08 ppm	Tl 0.18 ppm

Úrhida Limestone (44)

The 220 m thick formation, exposed by its type-section of the borehole Úrhida 4 consists of white, light grey, thin bedded, stylolitic, nodular, limestone with flaser structures and some intercalations of dolomites, shales and black lidite (jasper). This is a pelagic limestone with few slope debris composed of thin horizon of calcareous turbidites and authigenic breccias. Estimated age is Early to Middle Devonian (FÜLÖP 1990)

Geochemistry:

8 limestone samples of the borehole Úrhida 4 represent the formation (Nos. 341–348 of Appendix 1). Ranges and medians are given below:

Au (<2–5)	<2 ppb	As (1.06–13.70)	3.72 ppm
Ag (0.03–1.35)	0.065 ppm	Hg (0.04–0.51)	0.08 ppm
Sb (0.16–4.23)	1.14 ppm	Tl (<0.02–0.29)	0.055 ppm

Significant correlations were found for the following pairs of elements: Sb–Hg, Tl–As, Tl–Hg and Tl–Sb.

Polgárdi Limestone (1)

One of the former candidate of perspective formations during previous screening (KORPÁS and HOFSTRA 1994) It is described below after LELKES–FELVÁRI (1978), HORVÁTH and ÓDOR (1989) and FÜLÖP (1990). The folded crystalline limestone is composed of cyclic Lofér facies, overprinted by equigranular xenomorphic-hypidiomorphic textures metamorphic in origin. The original depositional and diagenetic features, like loferites, mud cracks, fenestrae and early dolomitization are frequently preserved despite recrystallisation. The Middle Devonian limestone is poor in fossils, some individual corals and alga-horizons, including weakly developed stromatolites have been mentioned by FÜLÖP (1990) from the Kőszár-hegy quarry. The depositional system is interpreted by him as a shallow peritidal carbonate bank. Its long term and multiphase paleokarst evolution including hydrothermal events too was outlined recently by KORPÁS (1998).

The limestone is cut by the narrow dikes of Late Carboniferous granite-porphyrites and by the shallow intrusive bodies of Middle Triassic porphyritic andesites (HORVÁTH and ÓDOR 1989). Beside the diagenetic features mentioned above, hydrothermal and metasomatic alteration can be observed, such as skarns related contact metamorphism and metasomatism. The products of this alteration are: silicification, iron metasomatism with manganese, surface and subsurface galena mineralization (KISS 1951, FÜLÖP 1990), formation of marble, brucite-serpentinite mineral assemblages and skarns of vesuvianite-diopside-garnet type (HORVÁTH and ÓDOR 1989).

A minor underground MVT type (?) ore deposit at Szababattyán was mined between 1941 and 1954, producing about 9,000 t galena (10–13% Pb) with high content of silver (150 ppm) and traces of gold (0.4–2 ppm Au) too (KISS 1951, FÜLÖP 1990).

Geochemistry:

27 samples represent the formation (Nos. 297–305, 308, 310–315, 317–319, 321–328. of Appendix 1). Lithology of the samples: limestones, limonitic, ankeritic limestones, limonitic infillings, calcite, Mn-rich infilling, limonitic limestone breccia, clay. Ranges and medians are given below:

Au (<2–8)	<2 ppb	As (2.09–596.0)	11.1 ppm
Ag (0.014–1.22)	0.11 ppm	Hg (0.016–2.76)	0.26 ppm
Sb (0.18–23.1)	1.04 ppm	Tl (<0.02–6.56)	0.13 ppm

Mn-rich infillings and limonitic infillings contain the anomalous and elevated concentrations for most of the elements. Threshold values of anomalies have been determined for the following elements (number of anomalous values above thresholds are in paranthesis): 100 ppm for As (4), 10 ppm for Sb (3), and 1 ppm for Tl (2). Correlation coefficients are significantly high for pairs of elements: Hg–Au, Sb–As, Tl–As, Tl–Hg and Tl–Sb.

3.2.1.2. Carboniferous

Szababattyán Limestone (45)

The 90 m thick formation consists of black massive, stylolitic bituminous and pyritic limestone with intercalations of light green dolomarl, meta-sandstone, siliceous schist and slate. It is rich in benthic fossils (algae, foraminifera, corals, bivalves, brachiopods and echinoids) indicating a shallow marine patch reef of Viseian age (FÜLÖP 1990).

Geochemistry:

3 samples have only been collected from this formation (Nos. 329–331. of Appendix 1). They were limestones and a limonitic shale. Ranges and medians are given below:

Au (<2–2)	<2 ppb	As (2.57–99.7)	17.7 ppm
Ag (0.03–0.16)	0.03 ppm	Hg (0.0158–0.136)	0.128 ppm
Sb (0.15–5.28)	1.16 ppm	Tl (<0.02–0.23)	0.10 ppm

Füle Conglomerate (46)

A rock body consisting of terrestrial-fluvial, grey or variegated conglomerate, fanglomerate, sandstone, siltstone and mudstone cycles. At some places it also contains coal seams. Thickness: over 600 m. (LELKES–FELVÁRI in CSASZÁR 1997)

The cyclic alluvial formation comprises of grey and variegated matrix supported massive breccias and conglomerates, subarcose sandstones, siltstones and mudstones with few intercalations of coal seams. The coarse grained clasts and pebbles are represented mainly by quartzites, quartz phyllites, with some slates and black jasper (lidite) with scarce meta-rhyolite and garnet-micaschist. The rich flora consists of fragments of carbonised plant remains and tree-trunks, sporomorphs and pollens. Depositional system: alluvial fan deposited in intramountainous molasse basin. The estimated age is Late Carboniferous (FÜLÖP 1990, MAJOROS 1998).

Geochemistry:

Sandstones and shales have been sampled (5 samples altogether) from the formation (Nos. 292–296. of Appendix 1). Ranges and medians are given below:

Au <2 ppb		As (0.57–5.54)	1.46 ppm
Ag (0.04–0.15)	0.05 ppm	Hg (0.0242–0.0596)	0.0372 ppm
Sb (0.18–0.62)	0.22 ppm	Tl (0.11–0.48)	0.22 ppm

Gold is below detection limit in all samples, concentrations of other elements are insignificant.

Velence Granite (47)

This formation consists of calc-alkaline, post-collisional, S type, nearly eutectic biotitic orthoclase granite intruded at a hypabyssal (4–5 km) depth (BUDA 1985). It includes some small lenses of pegmatites, aplites (some m × some 100 m), minor intrusions of microgranite (200 × 300 m), two types of granite-porphry dikes (5–25 m × up to 2 km) and few kersantites. Based on radiometric dating, its age is 280 to 320 Ma. (HORVÁTH in FÜLÖP 1990 and HORVÁTH et al. in press).

Well developed phenomena of pneumatolitic and hydrothermal alterations are the followings: tourmalinisation with fluorite and molibdenite; epidotisation and chloritisation; silicification, sericitisation, kaolinitisation with pyrite and beresitisation. The few hydrothermal quartz-veins are some metres wide and up to km long. They frequently contain sphalerite, galena, chalcopyrite, stibnite and fluorite. A small sphalerite and galena deposit (with 1.23% Pb and 4.81% Zn) was mined at Pátka–Körakás-hegy between 1964 and 1972 producing 146,000 t ore. The estimated proven reserves are about 180,000 t. Small fluorite-veins up to 1,2 m width and 100 m longitud (with 5–95% CaF₂) were mined at Pákozd between 1951 and 1961 producing about 8,000 t of fluorite (Fülöp 1990). The Szűzvár underground mine, operating till 1967 on a 40–60 cm thick and 500 m long fluorite-vein has given about 58,000 t of fluorite and 11,300 t of basemetals /Pb: 2,21%, Zn: 1,62%/ as by-product (DARIDA TICHY in HORVÁTH et al. in press). Some thin cm to dm wide and <50 m long barite-veins were explored at Sukoró (FÜLÖP 1990).

Au, Ag, As, Sb, Hg and Tl (+Cd, Se and Te) were detected from the Carlin suite elements mainly by semiquantitative analytical methods (JANTSKY 1957, KUBOVITS 1958 BÖJTÖSNÉ–VARRÓK 1967 and FÖLDVÁRINÉ–VOGL 1970). Systematic metallometric survey of soil and rock sampling in 1979–80 resulted in discovery of anomalies of Ag (soil >0.28 ppm, rock >2.2 ppm) As (soil >95 ppm, rock >330 ppm) and Sb (rock >35 ppm) in the Meleg-hegy and Bence-hegy area (ÓDOR et al. 1982). Rock chip sampling of the boreholes Nadap Nt 2, Sukoró St-4, and S-3 has given anomalies of Au (0.03–1.6 ppm), Ag (5–142 ppm), Sb (120–250 ppm) and Hg: 0.22–2 ppm (HORVÁTH 1990).

Geochemistry:

14 samples were analysed for Au and Ag and 4 samples for the other elements (Nos. 306–307, 309, 358, 362, 365, 387, 443, 445, 447, 449, 450, 453, 454. of Appendix 1). Granite, granite porphyry, microgranite, quartzite and limonitic quartzite were sampled. Ranges and medians are given below:

Au (<2–2090)	<2 ppb	As (2.95–38.5)	10.76 ppm
Ag (<0.05–18.0)	0.04 ppm	Hg (0.0097–0.24)	0.13 ppm
Sb (0.22–2.72)	0.375 ppm	Tl (0.16–0.19)	0.17 ppm

There are only 3 positive values for gold. Limonitic quartzite, microgranite and quartzite contain these Au concentrations. Threshold for Au is >10 ppb and it is 1 ppm for Ag (with 4 anomalous values above threshold). Significant correlation coefficient was found only for Au–Ag.

3.2.2. Mesozoic

3.2.2.1. Triassic

Lithological description of the Triassic formations will be given after HAAS et al. (1993) in the followings:

Hidegkút Formation (48)

Lithology: the formation consists of thin bedded to laminated red siltstones and sandstones with thin intercalations of dolomites and limestones. Cross stratification, wave ripples and worm tracks are very common. Its lower member comprises the Hidegkút Sandstone while the upper one is represented by the Hidegkút Dolomite.

Facies: both members were formed at a wide and flat shelf zone. The sandstone represents a shallow marine subtidal environment, while the dolomites deposited mainly in peritidal sometimes evaporitic lagoons.

Age: Lower Triassic.

Thickness: 80–100 m on the Balaton Highland

Geochemistry:

The geochemical characteristics are illustrated by the data of 7 samples (Nos. 275, 481–486. of Appendix 1). Sandstones, siltstone and predominantly dolomite were sampled. Ranges and medians are given below:

Au <2 ppb		As (1.52–23.80)	11.0 ppm
Ag (0.04–0.21)	0.09 ppm	Hg (0.0007–0.0189)	0.0043 ppm
Sb (0.08–3.14)	0.39 ppm	Tl (0.02–0.30)	0.13 ppm

Gold is below detection limit in all samples. Neither anomalous values of other elements nor correlation at significance level of 0.01 have been found.

Csopak Marl (8)

Lithology: it is built up in the lower part by grey marls and marly limestones, followed by red calcareous siltstones and capped at the top by greenish grey marls and sandy marls. The thin bedded formation is characterised by well developed bioclastic horizons represented by wackestones and grainstones furthermore by bioturbation and worm tracks. This horizons are rich in bituminous organic matter (0.1–2.5%, VETŐ 1988).

Oreshows of chalcopyrite (malachite, azurite) galena and sphalerite (Cu <0.25%, Pb <0.1% and Zn <0.2%) were reported in the Balatonfüred (SZENTES et al. 1972) and Litér area (RAINCSÁK 1984, KÖRPÁS and HOFSTRA 1994).

Facies: normal marine open shelf subtidal environment with storm horizons represented by the bioclastic limestones.

Age: Lower Triassic, Schythian

Thickness: about 200 m

Geochemistry:

14 samples represent this formation (Nos. 244, 470–480, 510, 511. of Appendix 1). Limestone, dolomite, sandstone and siltstone were sampled. Ranges and medians are given below:

Au <2 ppb		As (2.19–41.50)	5.29 ppm
Ag (0.03–0.12)	0.06 ppm	Hg (0.0017–0.040)	0.0034 ppm
Sb (0.11–0.70)	0.225 ppm	Tl 0.02–0.34)	0.14 ppm

Gold is below detection limit in all 14 samples. The other elements were analysed only in 12 samples. There are no anomalous values and no significant correlation of any pairs of elements.

Aszófő Dolomite (9)

Lithology: it consists of grey, yellowish grey and white, saccharoidal and porous “cellular” laminated and bedded somewhere bituminous dolomites, with few intercalations of laminated silty dolomites and dolomarls. Mud-cracks and shrinkage structures are very common. Typical microfacies are represented by ooidic-oncoidal grainstones and mikrites, pelmicrites.

Facies: flat peritidal, periodically evaporitic lagoon.

Age: Lower–Middle Triassic, Schythian to Lower Anisian

Thickness: 100 to 200 m

Previous data of hard rock geochemistry (KÖRPÁS and HOFSTRA 1994): Ag (0.15–0.8 ppm), As (102–421 ppm), Ba (451–473 ppm), Cu (58–62 ppm), Mo (<2.5 ppm), Pb (12–25 ppm), Sb (<16–21 ppm), Tl (<1 ppm), Zn (102–272 ppm)

Geochemistry:

One dolomite sample was analysed from this formation (No. 264. of Appendix 1). Gold is below detection limit (<2 ppb) and the other element are present in very low concentration (As 1.12; Ag 0.14; Hg 0.0035 and Sb 0.25 ppm).

Iszkahegy Limestone (10)

Lithology: Based on its lithological and structural features two parts may be distinguished within the formation. The lower part of the succession is made up by dark grey, platy or laminitic bituminous, argillaceous limestones. Worm tracks are common on the bedding planes. 1–10 cm thick intrabreccia interlayers also occur.

The upper part of the formation is characterised by dark grey, locally yellowish, medium bedded micritic limestones. The 10–30 cm thick beds are generally covered by thin clayey coatings.

Facies: Platy, microlaminated structure, poor fossil assemblage, relatively high organic content in the lower part of the formation refer to oxygen depleted conditions at the bottom of the basin, indicating restricted basin environment, most probably under humid climate. Bioturbated thicker beds of the upper interval may have formed under disaerobic conditions i.e. restriction of the basin decreased.

Age: Lower–Middle Anisian

Thickness: 100–150 m on the Balaton Highland

Previous data of hard rock geochemistry (KORPÁS and HOFSTRA 1994): Ag (0.15–0.8 ppm), As (102–421 ppm), Ba (451–473 ppm), Cu (58–62 ppm), Mo (<2.5 ppm), Pb (12–25 ppm), Sb (<16–21 ppm), Tl (<1 ppm), Zn (102–272 ppm)

This formation was deleted from the list of predictive formations and was not sampled after studying the Carlin gold deposits in Nevada, in 1995.

Megyehegy Dolomite (11)

Lithology: It is made up by light grey, yellowish grey thick-bedded dolomites. The bedding plains are smooth. The texture is typically sparitic (saccharoidal), the original textural elements are generally unrecognisable due to the dolomitization. However, in a few cases, the oncoidal or ooidic texture is recognisable. Due to tectonic effects the dolomites are often strongly fractured, brecciated.

Facies: It was formed on a shallow ramp of sluggish water circulation, under arid climatic condition. Based on microfossils, slightly enhanced salinity can be assumed. In certain areas it progresses into a platform facies (Tagyon Formation) which was also effected by dolomitization and used to be considered to belong to the Megyehegy Formation.

Age: Middle Anisian

Thickness: 30–250 m (it is also included the dolomitized platform facies which was not separated from the Megyehegy Formation earlier).

Previous data of hard rock geochemistry (KORPÁS and HOFSTRA 1994): Ag (0.4 ppm), As (<10 ppm), Ba (62 ppm), Cu (29 ppm), Mo (1.3 ppm), Pb (60 ppm), Sb (<16–21 ppm), Tl (<1 ppm), Zn (43 ppm)

Geochemistry:

Seven samples of dolomite and dolomite breccias were taken (Nos. 238–243, 282. of Appendix 1). Ranges and medians are given below:

Au <2 ppb		As (0.57–31.50)	5.85 ppm
Ag (0.011–0.035)	0.021 ppm	Hg (<0.02–0.20)	0.02 ppm
Sb (0.07–3.54)	0.50 ppm	Tl (0.01–0.19)	0.04 ppm

Au is below detection limit in all samples. There are no anomalous concentrations in this formation. Correlation coefficients are significant for Sb–As, Hg–As and Hg–Sb.

Budaörs Dolomite (49)

Lithology: dolomites. It is made up by medium, rarely dark grey, thin to medium-bedded dolomites. Cyclic facies stacking is characteristic: a few dm thick algal mat beds alternate with beds of similar thickness containing Dasycladacean algae or they are poor in fossils. The Dasycladacean beds are generally packed with tubular pores of dissolved algae. The texture is predominantly or totally recrystallized xenotopic dolosparite. The original texture elements are scarcely recognisable or completely destroyed.

Facies: carbonate platform deposit. The Dasycladacean dolomites were formed in the internal part of the platform under normal salinity conditions in the euphotic, shallow subtidal zone. The algal mat facies represent the tidal flat environment. High frequency alternation of these facies reflect sea-level oscillation.

Age: Ladinian–lowermost Carnian.

Thickness: Extension of the Budaörs Dolomite is limited to the NE part of the Transdanubian Range (Buda Mts., Gerecse, Vértes and eastern part of the Southern Bakony). 1000–1200 m thickness can be assumed.

Geochemistry:

28 samples have been analysed (Nos. 461–469, 493–509, 596, 598. of Appendix 1). We have 28 values for gold and 16 data for the other elements. Breccias, infillings and predominantly dolomites were sampled. Ranges and medians are given below:

Au (<2–5)	<2 ppb	As (0.69–706.0)	16.35 ppm
Ag (0.01–0.56)	0.0835 ppm	Hg (0.0019–10.70)	0.0083 ppm
Sb (0.1–18.10)	0.305 ppm	Tl (<0.02–2.63)	0.11 ppm

There are only 5 gold values above detection limit, the highest concentration (but it is only 5 ppb) is in a limonitic infilling. Limonitic breccia contains the high values of Sb, Hg and As within the formation. In a dolomite sample As is of high concentration (706 ppm) together with high Tl value. A few elements are considered anomalous. Thresholds are in the low concentration ranges. Arsenic is anomalous above 50 ppm (5 samples belong to this population). There are perhaps anomalous concentrations of Ag (1 sample above the 0.5 ppm threshold), Hg (5 samples above the 1 ppm threshold), Sb (5 samples above 2 ppm) and Tl (1 sample above 2 ppm). Coefficients of correlation are significant for As–Sb, Tl–As and Sb–Hg.

Vashegy Dolomite (50)

The areal distribution of the formation is illustrated by the Fig. 13.

Lithology: dolomites. It is made up by white, medium, rarely dark grey, thin to medium-bedded dolomites. Cyclic facies stacking is characteristic: a few dm thick algae bearing beds alternate with massive and brecciated dolomites. The texture is predominantly or totally recrystallized xenotopic dolosparite. The original texture elements are scarcely recognisable or completely destroyed. In the outcrops on the Vas–hegy the dolomites are cut by Late Eocene hydrothermal calcite veins.

Facies: carbonate platform deposit.

Age: Ladinian (?)

Thickness: more than 500 m

Geochemistry:

3 samples (dolomites and calcite vein) were sampled (Nos. 741–743. of Appendix 1). Ranges and medians are given below:

Au (<2–3)	<2 ppb	As (<2.5–9.40)	3.50 ppm
Ag (<0.3–0.40)	<0.3 ppm	Hg (0.06–1.66)	0.30 ppm
Sb (0.23–0.54)	0.53 ppm	Tl (<0.02–0.36)	0.22 ppm

The vein of calcite contains the relative high value for Hg.

Felsőörs Limestone (12)

Lithology: Brownish grey generally clayey limestone. In some places it can be subdivided into well definable members. They are as follows: thin-bedded bituminous argillaceous calcareous dolomites; bedded, cherty limestones; crinoidal–brachiopodal limestones; thin-bedded platy bituminous pyritic limestones; nodular cherty limestones with tuffaceous interlayers and phosphate (6.3–27.2%) bearing horizons. Characteristic microfacies of the bedded cherty limestone is biomicrite with sponge spicules, whereas the bituminous platy limestone is filament-bearing as a rule.

Facies: The cherty limestones were deposited in a relatively deep pelagic basin. The crinoidal-brachiopodal member was formed in a shallower, agitated environment, the upper, platy bituminous limestones were deposited in a deep but restricted basin. Ostracode assemblage refer also to deep marine oxygen-depleted environment.

Age: Middle–Upper Anisian

Thickness: Extension of the formation is limits to the Balaton Highland. Its thickness significantly changes laterally between 20–180 m.

Previous data of hard rock geochemistry (KORPÁS and HOFSTRA 1994): Ag (0.4 ppm), As (<10 ppm), Ba (62 ppm), Cu (29 ppm), Mo (1.3 ppm), Pb (60 ppm), Sb (<16–21 ppm), Tl (<1 ppm), Zn (43 ppm)

Geochemistry:

The two samples are limestone and bituminous limestone (Nos. 245, 280. of Appendix 1).

Au <2 ppb	As (2.36–3.13)
Ag (0.09–0.12)	Hg (0.0103–0.0534)
Sb (0.24–0.64)	Tl (0.09–0.43)

The concentrations are insignificant.

Buchenstein Formation (13)

Lithology: It is made up by nodular, generally cherty or siliceous limestones and tuff with thin limestone or dolomite interlayers. Share of tuffs and carbonates is highly variable, consequently the formation is characterised by high lithological variability. It can be subdivided into members. The lower member (Vászoly Member) consists mainly of light brownish grey bedded limestone with tuffaceous interlayers of various thickness. The middle

member (Nemesvámos Member) is made up by bedded nodular limestones, typically with flaser bedding and chert nodules. The most characteristic rock-type is the reddish or light brown limestone with dark red chert nodules, another typical rock-type is light greenish grey limestone with brownish grey cherts and dark grey tuffaceous marl interlayers. Locally a third upper member also occurs (Keresztfatető Member). It consists of thin-bedded limestones with coquinas of thin-shelled bivalves and siliceous tuffs.

Facies: Condensed pelagic basin facies. The carbonate deposition was punctuated by deposition of tuffaceous material partly of primary origin but partly reworked.

Age: Upper Anisian to Ladinian

Thickness: The formation is known in the Balaton Highland area and also explored in the Northern Bakony. Its maximum thickness is 80 m in the depocenter of the Middle Triassic basins whereas above the Anisian platform it is thinner, about 50 m.

Previous data of hard rock geochemistry (KORPÁS and HOFSTRA 1994): Ag (0.4 ppm), As (<10 ppm), Ba (62 ppm), Cu (29 ppm), Mo (1.3 ppm), Pb (60 ppm), Sb (<16–21 ppm), Tl (<1 ppm), Zn (43 ppm)

Geochemistry:

The formation is represented by 12 samples (Nos. 246–250, 259–263, 281, 320. of Appendix 1). Limestone, marl, andesite and tuff were sampled. Ranges and medians are given below:

Au <2 ppb		As (0.31–22.7)	1.95 ppm
Ag (0.009–0.21)	0.085 ppm	Hg (0.0016–0.10)	0.0076 ppm
Sb (0.07–1.16)	0.17 ppm	Tl (0.02–0.27)	0.12 ppm

Gold is below detection limit in all samples. Marls and andesite contain the relative high values within the formation. There are no anomalous values for any of the elements. Correlation coefficients are significant for Sb–As and Sb–Hg.

Füred Limestone (14)

Lithology: light grey, typically with brownish patches bedded slightly bituminous limestone. Upsection it shows continuous transition with marl interlayers into the overlying Veszprém Formation. Its most typical microfacies are the following: filament biomicrite, pelmicrosparite, biomicrosparite.

Facies: pelagic basin facies which reflected its fossil assemblage

Age: Based on ammonites, conodont and radiolarians it is lowermost Carnian, however the Foraminifera association indicate topmost Ladinian in the lower part of the formation

Thickness: The formation is known in the southern belt of the Balaton Highland region. Its maximum thickness is 60 m.

Geochemistry:

1 sample was only taken from this formation (No. 265. of Appendix 1). Gold was below detection limit and no important concentrations of other elements were found.

Veszprém Marl (15)

Lithology: grey argillaceous marl, marl, silty marl with carbonate interlayers. In its type locality on the Balaton Highland it can be subdivided into three consecutive members. The lower member (Mencshely Marl) is made up predominantly by clay marl and marl. It is dark grey, grey. Graded allodapic limestone and calcareous marl interlayers, slump structures occur, locally. Bioturbation is common and contains bituminous organic matter (0.15–0.60%). The middle member (Nosztor Limestone) consists of light grey thin-bedded, nodular limestones with uneven bedding planes and various amount of chert lenses. Lithoclastic layers and brachiopod coquina beds are also typical. The upper member (Csicsó Marl) is made up of grey marl, calcareous marl and subordinately clay marl. Mudstone, wackestone and packstone texture are typical in the marl layers with radiolarians, sponge spicules and filaments. In the carbonate interlayers ooidic-encrinal, bioclastic and intraclastic textures are characteristic.

Presence of Cu (≤ 160 ppm), Pb (≤ 30 ppm) and Ag (≤ 8 ppm) was described by BOHN (1979) from the Keszthely Mountains.

Facies: It was formed in relatively deep, more or less restricted basins which were separated by elevated carbonate banks. Majority of the deposited sediments is fine terrigenous material whereas the carbonate content of the rocks is derived partly from the ambient platforms partly from the test of pelagic organisms. The sediment deposition took place in unagitated, normal salinity basins, generally under oxygen-depleted conditions. Subordinate proportion of platform derived carbonates in the lower and upper members refer to inner basin conditions, while lithoclastic development of the Nosztor Limestone indicate toe-of-slope environment i.e. progradation of the foreslopes.

Age: Carnian

Thickness: It is known in many parts of the Transdanubian Range, though its thickness extremely variable. It

is thin in the Buda Mts., it may exceed 300 m. in the southern foreland of the Gerecse, but further to the southwest it decreases again and does not exceed 40–80 m. In the Balaton Highland region it is about 600 m, whereas 1000 m in the Northern Bakony. It is also encountered in the basement of the Small Plain and the Zala Basin.

Previous data of hard rock geochemistry (KORPÁS and HOFSTRA 1994): Ag (0.01 ppm), As (16 ppm), Ba (254 ppm), Cu (47 ppm), Mo (5 ppm), Pb (7 ppm), Sb (≤ 16 ppm), Tl (≤ 1 ppm), Zn (35 ppm)

Geochemistry:

71 samples represent the formation (Nos. 92–104, 201–214, 223–237, 251–258, 266–274, 599–610. of Appendix 1). Dolomite, limestones, dolomarl, clay and predominantly marls were sampled. Ranges and medians are given below:

Au (<2–4)	<2 ppb	As (0.8–27.5)	5.10 ppm
Ag (<0.02–0.48)	0.06 ppm	Hg (<0.02–0.42)	0.0116 ppm
Sb (<0.1–0.99)	0.22 ppm	Tl (<0.02–0.86)	0.15 ppm

Marls, clays and dolomitic limestones have the elevated values. It is interesting to note that the behaviour of Ag is slightly different than that of other elements. Its correlation coefficients are negative, while the coefficients of Hg–Sb, Tl–As, Hg–Tl and Tl–Sb are positive and they show a significant correlation. No anomalous values were detected in this formation.

Mátyáshegy Formation (16)

Lithology: thin-bedded bituminous, slightly pyritic limestones and dolomites punctuated by marl interlayers. Chert lenses and nodules are characteristic both in the limestones and dolomites, but intervals free of chert also occur. The limestones are thin-bedded, commonly argillaceous and dolomitic, locally. They are of yellowish brown, brownish grey in colour. The chert nodules are of darker shade, brownish or greyish. Wackestones with sponge spicules, ostracodes and filaments and peloids are typical. The dolomites are well bedded, and grey as a rule. Their texture do not differ significantly from that of the limestones where the original texture elements are recognisable, but they generally strongly recrystallized transforming to dolosparite or dolomicrosparite.

Content of organic matter has a range between 0.1 and 0.6%. Slight anomalies of Ag (≤ 2.5 ppm), Cu (≤ 160 ppm), Mo (≤ 160 ppm), Sb (≤ 60 ppm), Pb (≤ 160 ppm) and As (≤ 600 ppm) were detected from the chip samples of the borehole Vérhalom 1.

Facies: It was formed in a more or less restricted basin. The poor macrofossil and foraminifera assemblage refer to restriction of the basin. However, massive occurrence of fragments of thin shelled pelagic bivalves (filaments) suggest open marine connections.

Age: According to the poor biostratigraphic data, deposition of the formation may have initiated in the Buda Mts. in the Carnian and continued in the Norian–Rhaetian.

Thickness: not known exactly, several hundred meters can be estimated in the Buda Mts.

Geochemistry:

There are 44 data for gold and 27 data for the other elements (Nos. 513, 516–520, 525–541, 543, 546–548, 552–560, 578, 613–619. of Appendix 1). The lithology sampled is the following: dolomite, cherty dolomite, dolomite breccia (infilling), dolomarl, marl, limestone, cherty limestone and siliciclastic sandstone infilling. Ranges and medians are given below:

Au (<2–12)	<2 ppb	As (0.86–463.0)	12.7 ppm
Ag (<0.02–0.39)	0.05 ppm	Hg (0.002–111.37)	0.74 ppm
Sb (0.16–1760.0)	1.7 ppm	Tl (<0.02–33.7)	0.09 ppm

A dolomite sample contains the max. gold value, limonitic dolomite and limonitic infilling contain the anomalous values for Hg, Sb and Tl.

Sándorhegy Formation (17)

Lithology: It is highly variable unit containing limestones, dolomites and shales. The following members can be distinguished. The lower member (Pécsely Mb.) begins with dark grey thick-bedded limestones. It is usually followed by laminitic, bituminous limestones (organic matter of 0.11–2.73%) with slump structures and intraclastic layers. They are overlain by calcareous marls and marls. Some parts of the member are dolomitic. Locally a dolomite member (Henyé Mb.) appears between the lower and the upper members. It is light brownish grey and massive, as a rule. Pelmicrosparite or recrystallized dolosparite textures are typical. The upper member (Nosztor Mb.) begins with light grey, greyish brown bedded, oncoidal, cherty limestones. The clay content shows an upward increasing trend. Calcareous marls rich in bioclasts make up the upper part of the member.

Facies: It represents the final stage of the upfilling of the Ladinian–Carnian basins. Bituminous limestones of the lower member were deposited in an oxygen-depleted restricted basin. The dolomite member is an intercalated, dolomitized platform carbonate unit. The marl intercalations may have formed under deeper water conditions

when the sea-level rise made possible the input of terrigenous fines into the basin. Above a marl interval the upper member were formed in a shallowing basin which was supplied by carbonate mud from the surrounding platforms but it was not restricted from the fine terrigenous material, too.

Age: Upper Carnian

Thickness: The formation is developed in the Balaton Highland area, in a thickness of 100–200 m.

Geochemistry:

One sample, a bituminous limestone was analysed (No. 279. of Appendix 1). Its gold content is less than 2 ppb. The concentration of other elements is not important.

Födolomit Formation (51)

Lithology: It consists of dolomites of various facies. Meter scale cyclicity is common. The cycles are made up generally by two members: subtidal Megalodont-bearing and algal-laminated (loferitic) beds. The rock are light colour, yellowish, brownish, greyish, as a rule. Darker, organic rich developments also occur, locally, mainly in the western part of the Transdanubian Range. In a lot of cases, secondary processes i. e. tectonic fracturation and weathering led to deterioration of the original structure. Due to the early pervasive dolomitization the original textural characters also usually destroyed although their traces are recognisable, locally. Sedimentary breccias of various origin are common.

Facies: It was formed in the inner part of a large peri-continental carbonate platform, influenced by high frequency sea-level oscillations. In the high sea-level periods carbonate mud deposited in the subtidal lagoon while in the low sea-level intervals the tidal flat prograded onto the lagoon and the lime mud pervasively dolomitized.

Age: Upper Carnian–Middle Norian

Thickness: It extends over the whole territory of the Transdanubian Range Unit in a thickness of 800–1500 m.

Geochemistry:

We have got 21 data for gold and 16 data for the other elements (Nos. 161, 561, 565, 569–573, 581, 594, 626–633, 683–684, 696. of Appendix 1). Dolomites and brecciated dolomites were sampled and analysed. Ranges and medians are given below:

Au (<2–25)	<2 ppb	As (0.63–401.0)	3.37 ppm
Ag (<0.02–0.28)	<0.02 ppm	Hg (<0.02–1.76)	0.055 ppm
Sb (<0.02–11.3)	1.05 ppm	Tl (<0.02–0.415)	0.023 ppm

Brecciated dolomite infilling contains the high values of Au, As and Sb. Thresholds and number of anomalous values above them (in paranthesis) are as follows. Au ≥ 20 ppb (1); As ≥ 10 ppm (2); Hg ≥ 1 ppm (1) and finally Sb ≥ 4 ppm (2). No significant correlations were detected.

Rezi Dolomite (19)

Lithology: grey, thin-bedded, platy, laminated bituminous (0.1–0.2% organic matter), pyrite bearing dolomites, cherty dolomites, with intercalations of thick-bedded, porous, saccharoidal dolomites. Its lower member consists of platy, bituminous, cherty dolomites. The middle member is made up by thick-bedded dolomites with remnants or moldic pores of dasycladacean algae and also contains thin interlayers of the platy dolomites. The upper member is platy dolomitic mudstone with mollusc coquina lenses.

Facies: The lower and the upper member was formed in an oxygen-depleted, restricted basin, whereas the middle one in a well oxygenated lagoon.

Age: Upper Norian

Thickness: Outcrops of the formation occur in the Keszthely Mts. and the westernmost part of the Southern Bakony. Its thickness here about 300 m. It may also occur in the basement of the Zala Basin.

Geochemistry:

11 samples represent the formation (Nos. 131, 143–152. of Appendix 1). Dolomites, bituminous dolomite, dolomarl have been sampled. Ranges and medians are given below:

Au <2 ppb		As (<1.0–2.65)	0.9 ppm
Ag (<0.05–0.23)	0.07 ppm	Hg (0.0044–0.0159)	0.0093 ppm
Sb (<0.1–1.48)	0.36 ppm	Tl (<0.05–0.09)	0.03 ppm

Marls and bituminous dolomites contain the insignificant elevated concentrations within the formation. Neither anomalous values nor correlation of the elements was found.

Kössen Formation (20)

Lithology: dark grey, organic rich, pyritic, argillaceous marl, marl, calcareous marl, silty marl with dolomite or limestone intercalations in the transitional intervals. Within its extension area, lithology of the formation markedly changes depending on the paleogeographic setting of the given area. In the western part of the Transdanu-

bian Range Unit (in the Keszthely Mts. and northward to it) i. e. in the inner part of the basin monotonous dark grey shales (locally oilshales with 1–2% of organic matter and about 1% of sulfur) were formed with lithoclastic and bioclastic toe-of-slope facies in its basal part in the Keszthely Mts. In the western part of the Southern Bakony argillaceous dolomite and limestone interbeds appear within the shales and the shales pinch out further northeastward i.e. towards the coeval carbonate platform.

Facies: It was formed in a restricted basin behind a large carbonate platform (“Dachstein platform”). In the inner part of the basin, stagnant, oxygen depleted conditions came into being near to the bottom. The gentle slope between the basin and the ambient platform was populated by a rich epibenthic mollusc fauna. Fragments of mollusc shells redeposited at the toe of the slope together with lithoclasts. The upper slope may have reached the euphotic zone.

Age: Upper Norian to Rhaetian

Thickness: Its maximum thickness exceeds 500 m in the basement of the Zala Basin. It is about 300 m in the sector of the Keszthely Mts. It pinches out from the western end of the Bakony northeastward.

Previous data of hard rock geochemistry (KORPÁS and HOFSTRA 1994): Ag (<0.4 ppm), Cu (16–100 ppm), Pb (<16 ppm), Sb (<60 ppm), Zn (<100 ppm)

Geochemistry:

9 limestone, limonitic limestone, dolomite and marl samples were analysed (Nos. 142, 154–160, 200. of Appendix 1). Gold was below detection limit in all samples. Ranges and medians are given below:

Au (<2 ppb)		As (< 1.0–10.2)	1.9 ppm
Ag (< 0.05–0.16)	0.05 ppm	Hg (< 0.02–0.08)	0.0063 ppm
Sb (< 0.1–3.34)	0.2 ppm	Tl (0.05–0.53)	0.15 ppm

There is no anomalous value, slightly elevated concentrations are in limonitic limestones. Only the Sb–As correlation is significant at 0.01 level.

Feketehegy Formation (21)

Lithology: It is made up by thin-bedded, platy, bituminous limestones and dolomites. The lower dolomitic member is characterised by a thin-bedded structure. The bituminous rock-types are laminated, as a rule. They are of greyish brown, dark grey colour. The limestone member is also thin-bedded with meter thick cross-bedded bivalve coquina and graded calcarenite interbeds. They are light grey in colour. Mudstone, wackestone with pebbles, ostracodes and sponge spicules are the most characteristic microfacies.

Facies: A more or less restricted intraplatform basin was the site of deposition. The lower member was formed in an oxygen-depleted lagoon. The limestone member may have formed in a deeper basin receiving large amount of bioclasts, oncoids and lithoclasts from the ambient platforms. The cross-bedded coquinas were formed in a high energy current-agitated environment.

Age: Middle–Upper Norian

Thickness: Its extension is restricted to the Pilis Mts. where a thickness of 300 m can be estimated.

Geochemistry:

5 limestone and dolomite samples were analysed (Nos. 691–695. of Appendix 1). Ranges and medians are given below:

Au (<2–3)	<2 ppb	As (2.9–31.9)	5.36 ppm
Ag (0.02–0.08)	0.05 ppm	Hg (0.0484–0.1552)	0.1435 ppm
Sb (0.15–4.58)	0.94 ppm	Tl (< 0.02–0.28)	0.03 ppm

There are no remarkable anomalies in this formation.

Dachstein Limestone (52)

Lithology: it consists predominantly of white, light grey, rarely darker grey limestones. It shows definite cyclicity, as a rule. The ideal cycle begins with reddish or greenish argillaceous limestones or clays with intraclasts (generally black pebbles). It is overlain by algal laminated or fenestral laminoid, peloidal limestones or generally dolomitic limestones. It is followed by thick-bedded wackestones, ooidic-oncoidal packstones or grainstones with characteristic *Megalodont* bivalves. The cycle is ended by another algal laminated layer. The cycles are frequently incomplete or truncated, they are separated by unconformity surfaces as a rule.

Facies: The formation is formed in various facies belts of a carbonate platform under periodically alternating sea-level. In the high sea-level periods a predominant part of the carbonate platform was covered by shallow sea. On the outer platform ooid and oncoid shoals came into being whereas in the inner part of the platform carbonate mud settled. During the sea-level lowering tidal flats prograded onto the former inner shelf and early diagenetic and soil-forming processes took place.

Age: Norian–Rhaetian

Thickness: It extends over a large part of the Transdanubian Range Unit. Coeval deeper water basin facies are known in the Csővár Block, in the Buda Hills, some parts of the Pilis Mts. and in the southwestern part of the unit. Its thickness is 700–1000 m as a rule, except of the southwestern area, where overlying the Kössen Formation it is only about 100 m.

Geochemistry:

28 samples have been analysed (Nos. 567, 580, 583, 585, 586, 592, 593, 635–638, 641, 645, 647, 650, 651, 658, 660, 662, 665, 666, 669, 671, 676, 677, 681, 682, 690. of Appendix 1). The main rock types collected are: dolomite, dolomitic limestone, limestone, limestone breccia, limonitic breccia infilling, sandstone. Ranges and medians are given below:

Au (<2–11)	<2 ppb	As (0.22–198.0)	3.39 ppm
Ag (<0.02–0.15)	<0.02 ppm	Hg (<0.02–2.90)	0.0717 ppm
Sb (<0.02–6.92)	0.50 ppm	Tl (<0.02–0.95)	0.0335 ppm

The high concentrations are in limestone and limonitic limestone. There are good correlations for the following pairs of elements: As–Hg, As–Sb, As–Tl and Sb–Hg. Threshold values are established for: As (10 ppm, 6 samples above), Hg (1 ppm, 3 samples above) and Sb (2 ppm, 7 samples above).

3.2.2.2. Triassic–Jurassic

Csővár Limestone (18)

The areal distribution of the formation is shown on Fig. 13.

Lithology: brownish grey, medium to dark grey, predominantly thin-bedded slightly bituminous limestones, dolomitic limestones, dolomites with siliceous patches, chert lenses and nodules. The burial dolomitization affected the lower segment of the succession. The upper, predominant part of the formation is made up by limestones. Laminitic layers of distal turbidite origin, alternate with allodapic calcarenites of proximal turbidite origin. Slump beds and lithoclastic intercalations are common mainly in the upper part of the formation. Below the ruins of the fortress on the top of Vár-hegy, the limestones are cut by Late Eocene calcite veins.

Facies: it was formed in a more or less restricted basin and in the toe-of-slope belt of a carbonate platform. The lithoclasts and bioclasts of platform origin were accumulated at the base of the slope, whereas the turbiditic layers were deposited in the distal part of the slope apron or in the basin. The radiolarian and filament microfacies types represent the basin facies.

Age: Carnian to Hettangian (Sinemurian?)

Thickness: This formation is known only in the area of the Csővár horst. The lower part of the formation was penetrated by a borehole in a thickness of 600 m. A more than 100 m thick succession crops out on the slope of the Vár-hegy in Csővár, representing the Jurassic part of the sequence.

Geochemistry:

35 data are available for gold and 10 data for the other elements (Nos. 706–740. of Appendix 1). Limestone, marl, dolomite and cherty limestone were sampled. Ranges and medians are given below:

Au (<2–4)	<2 ppb	As (1.25–17.3)	3.40 ppm
Ag (<0.3–1.0)	0.35 ppm	Hg (0.06–0.7)	0.18 ppm
Sb (<0.02–1.10)	0.47 ppm	Tl (<0.02–0.38)	0.065 ppm

Elevated concentrations are found in limonitic infillings and cherty limestones. Neither anomalies nor correlations were encountered at the accepted significance level.

3.2.2.3. Jurassic

Pisznice Limestone (53)

The formation consists of “intraclastic, generally well-stratified, bedded limestone with stylolitic bed surfaces. Bioclastic material forms a minor fraction in variable amounts. The colour is generally light, ranging from greyish violet, through violet-grey, pale pink, red, and flesh-colored to cream” (KNAUER in CSÁSZÁR 1997). Thickness varies between 10 and 20 m.

Geochemistry:

Two samples (limestone and limestone breccia) were only analysed (Nos. 685–686. of Appendix 1). Ranges are given below:

Au <2 ppb	As (1.05–4.62)
Ag (<0.02–0.03)	Hg (<0.02–0.09)
Sb (0.3–0.5)	Tl (<0.02–0.252)

These concentrations are insignificant.

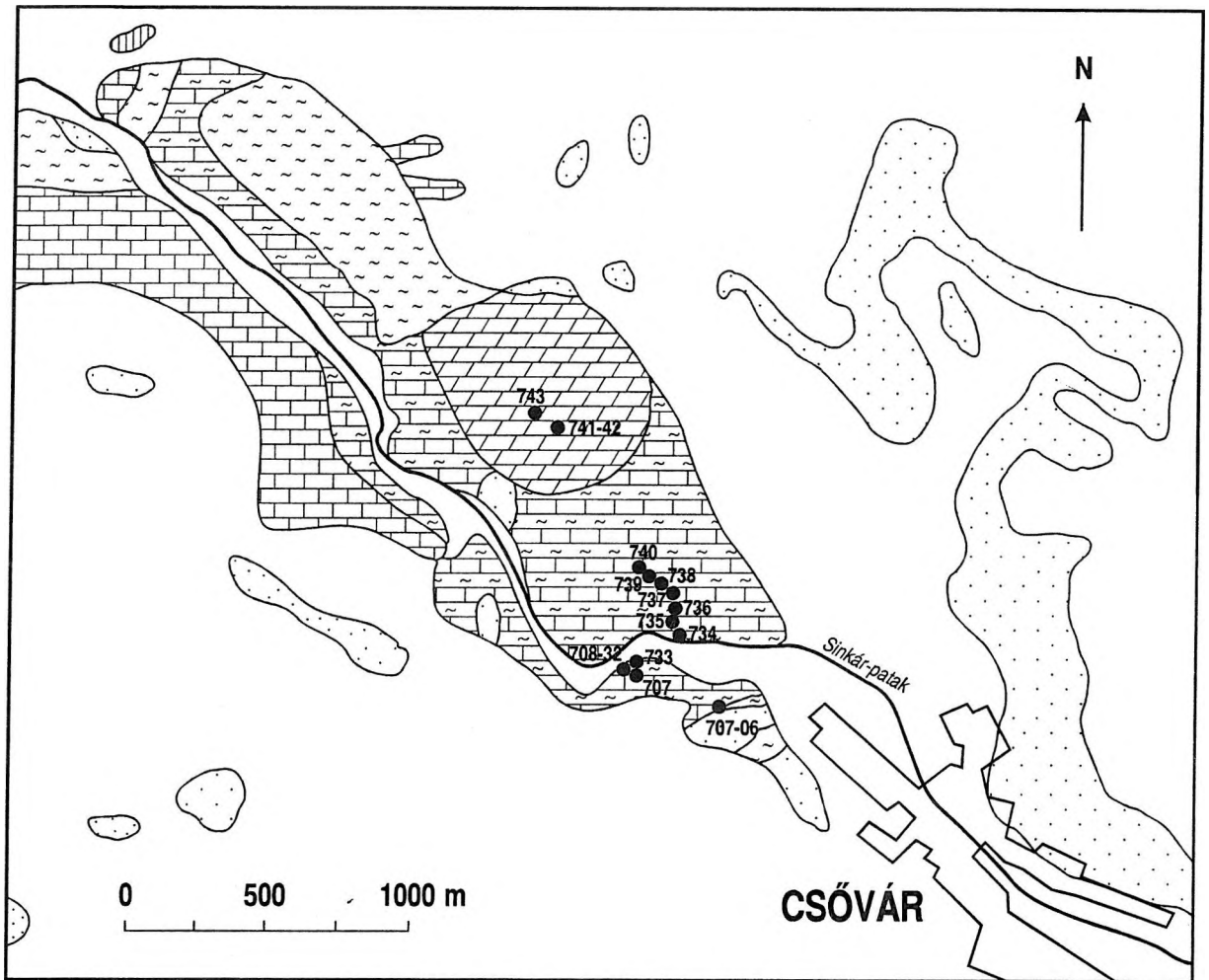


Fig. 13: Geological map of the Csővár horst and its surroundings with Carlin gold sample sites (Detail of the geological map-sheet 4862/4–Vác, Unified Stereographic Geological Map Serie)

1) Holocene to Quaternary alluvial and eolian sediments, 2) Oligocene clastics, 3) Late Eocene to Early Oligocene Buda Marl, 4) Cretaceous to Eocene Bauxite Formation, 5) Late Triassic to Early Jurassic Csővár Limestone, 6) Late Triassic Dachstein Limestone, 7) Middle Triassic Vashegy Dolomite, 8) Carlin gold sample site

Úrkút Manganese Ore (33)

It was one of the former candidates of perspective formations in the previous screening (KORPÁS and HOFSTRA 1994). The lithology consists of dark brown, greenish manganese carbonates, oxidic manganese ores of variable appearance and laminated black shales or organic rich black clay overlain by marls or crinoidal, locally glauconitic limestones.

Facies: Restricted basin facies which was formed during the early Toarcian anoxic event (VETŐ et al. 1997) preferentially in the western current-shadow of paleohighs. Thus the manganese deposit may have formed in oxygen-depleted, stagnant sub-basins.

The formation contains organic matter (1–2%) and sulfides (1–5%) with some phosphorites ($P < 1.5\%$). The Mn ore of the operating underground mine is composed partly of primary ore of rodocrosite (20–30%) and partly of secondary ore of psilomelan, pirolusite and manganite (40–50%) accompanying with siderite (5%) (SZABÓ et al. 1981). Traces of Ag were detected by POLGÁRI (1993).

Age: Lower Toarcian

Thickness: It is extremely variable. In some part of the Bakony (Úrkút Basin) it may reach as much as 50 m, but generally much less, a few metre or in the Gerecse Mts. a few decimetre only.

Geochemistry:

Predominantly Mn ores and marls were sampled in the Úrkút mine (Nos. 168–172, 182–188, 192–195, 218–220. of Appendix 1). Ranges and medians are given below:

Au (<2–5)	<2 ppb	As (1.66–59.1)	13.8 ppm
Ag (0.05–1.08)	0.29 ppm	Hg (0.0053–1.671)	0.1249 ppm
Sb (0.14–1.14)	0.59 ppm	Tl (0.04–0.7)	0.16 ppm

Elevated concentrations are detected mostly in marls. Threshold values are in the low concentration ranges: Ag (1 ppm, 1 sample above) and Hg (1 ppm, 1 sample above). Coefficients of correlation are significant only for Tl–Ag.

Kisgercese Marl (54)

Lithology: Red marls with limestone nodules, locally. It forms a clayey interbed within the Ammonitico Rosso type pelagic carbonate sequences as a rule.

Facies: pelagic, deep sea facies which may have formed in a well oxygenated environment. In contrast to the significant amount of benthic microfossils in the underlying formations, predominantly pelagic fossil assemblage of the Kisgercese Marl indicates a fast deepening.

Age: Lower Toarcian

Thickness: a few metre

Geochemistry:

12 samples (all radiolarian marls) were analysed (Nos. 173–181, 189–191. of Appendix 1). Ranges and medians are given below:

Au (<2–7)	3 ppb	As (9.41–147.0)	23.9 ppm
Ag (0.24–0.9)	0.435 ppm	Hg (0.06–0.66)	0.28 ppm
Sb (0.27–2.63)	1.38 ppm	Tl (0.12–0.97)	0.275 ppm

There are only two anomalous As values above the 100 ppm threshold. The correlation coefficient is significant for Sb–Ag.

Eplény Limestone (55)

Lithology: yellowish brown, light grey, thin-bedded or laminated limestones argillaceous limestones, calcareous marls with marl intercalations or red, brownish or greenish nodular limestones. Siliceous or cherty in a lot of cases. The most typical microfacies is the bositra packstone but radiolarian varieties (bositra-radiolaria packstone) are also common.

Facies: pelagic basin facies, formed in deep sea above the calcite compensation depth, deeper than the coeval Ammonitico Rosso limestones but shallower than the radiolarites (Lókút Formation). Interfingering relationship of the Eplény Formation with the above mentioned ones marks its intermediate paleo-environmental setting.

Age: Toarcian–Callovian

Thickness: 40–70 m.

Geochemistry:

6 limestone samples were analysed for this formation (Nos. 162, 215–217, 221–222. of Appendix 1). Ranges and medians are given below:

Au (<2–5)	<2 ppb	As (0.5–24.5)	1.26 ppm
Ag (0.04–0.42)	0.16 ppm	Hg (0.0038–0.4492)	0.0348 ppm
Sb (0.05–1.23)	0.12 ppm	Tl (0.06–0.58)	0.115 ppm

There are no anomalous values. Correlation is significant between Hg–As.

Lókút Radiolarite (56)

Lithology: yellowish grey, thin-bedded, laminated radiolarite with chert stripes, lenses and nodules, brown or black chert interbeds and siliceous limestones. In some localities red or yellowish radiolarian clays occur at the base of the formation. In the Gerecse area it is represented by two red chert members separated by limestones.

Facies: deep-sea deposits. They were formed in nutrient-rich pelagic basins. The bottom of the basins may have reached the calcite compensation depth. The radiolarian ooze was accumulated first in the deepest basins, the highs reached the critical depth later whereas on the highest seamounts the radiolarites are completely missing.

Age: Bathonian–Oxfordian or even Lower Kimmeridgian in the Gerecse Mts.

Thickness: More than 100 m in the Zala Basin and in the westernmost part of the Bakony, tens of metres in the Bakony and a few metres in the Gerecse Mts.

Geochemistry:

Two samples (radiolarite and radiolarite breccia) were analysed (Nos. 687–688. of Appendix 1). Ranges are given below:

Au (<2–5)	As (126–152)
Ag (0.04–0.08)	Hg (1.35–1.43)
Sb (3.5–4.7)	Tl (0.15–0.404)

Relatively high As and Hg values are worth mentioning.

3.2.2.4. Cretaceous

Budakeszi Picrite (57)

The formation consists of “igneous rock bodies of alkaline basic (spessartite, picrite, microgabbro, basalt) and ultramafic (monchiquite, beforite, silico-carbonatite) composition appearing as small, subvolcanic bodies, dikes. Based on radiometric dating, the age is 77 Ma” (HORVÁTH in CSÁSZÁR 1997).

Geochemistry:

The 1 sample (a microgabbro) is far from being enough to characterise the formation and the alterations related to it (No. 590. of Appendix 1). This sample gave insignificant concentrations for all elements analysed.

3.2.3. Cenozoic

3.2.3.1. Cretaceous–Eocene

Bauxite Formation (58)

The formation corresponds to the Gánt Bauxite and comprises of “bauxite, bauxitic clay, kaoline clay, bauxite with extraclasts and intraclasts lenses. A bauxite sequence with Eocene overburden. Most likely age: (Paleocene to) Early Eocene” (BERNHARDT in CSÁSZÁR 1997).

Geochemistry:

Clay and bauxitic clays were sampled (4 samples altogether) from this formation (Nos. 568, 591, 672 and 674. of Appendix 1). Ranges and medians are given below:

Au (<2–6)	<2 ppb	As (5.42–28.4)	16.65 ppm
Ag (0.02–0.15)	0.06 ppm	Hg (<0.02–0.3294)	0.0509 ppm
Sb (0.22–5.2)	0.9 ppm	Tl (0.026–1.59)	0.2785 ppm

Higher concentrations are in the bauxitic clay.

3.2.3.2. Eocene

Nadap Andesite (59)

“Product of multiple cycles of stratovolcanic activity, comprising lava, pyroclastite, subvolcanic and metasomatic rock bodies. The formation consists of volcanites (biotite-amphibole-andesite, biotite-agglomerate, tuff, tuffite, pyroxene-andesite, and dacite which form the Sorompóvölgy Andesite Member), intrusives (diorite, diorite-porphyrite, the Cseplekhegy Diorite Member), and altered rocks (quartzite with clay minerals, alunite” +pyrophyllite, “topaz and pyrites, the Pázmánd Metasomatite Member). Within the stratovolcanic sequence there are sediment layers with Middle to Late Eocene fossils. The volcanics are over 1000 m thick, the subvolcanic body over 900 m. Based on radiometric dating the age is 29 to 44 Ma” (ZELENKA and DARIDA–TICHY in CSÁSZÁR 1997).

Hydrothermal alterations and metasomatism in the core zone of the East Velence paleovolcano (DUDKO 1988, DUDKO et al. 1989) were described in detail by DARIDA–TICHY et al. (1984). Composite and multiphase metasomatites and intrusive breccias widely developed in the area between the Templom-hegy and Cseplek-hegy–Zsidó-hegy have resulted Ag, As and Sb anomalies detected by soil and rock sampling of the systematic metallogenic survey. The estimated threshold values of anomalies for the elements above are the followings: Ag / soil: 0.5 ppm, rock: 1.3 ppm. As / soil: 141 ppm, rock: 458 ppm, Sb / rock: 26 ppm (ÓDOR et al. 1982, HORVÁTH et al. 1990). Gold and silver shows up to 1000 ppm and 142 ppm were detected in the boreholes of Nadap Nt 2 and 4 (HORVÁTH et al. 1990).

Geochemistry:

The data of 40 samples were available to characterise the gold and silver contents and only of two samples to show the concentrations of other elements (Nos. 366–369, 373, 375, 377, 379, 381, 383, 385, 390, 392, 394, 396, 398, 400, 403, 405, 407, 409, 414, 417, 419, 421, 423, 425, 427, 429, 431, 433, 435, 437, 439, 441, 446, 448,

451, 452, 457. of Appendix 1). Mainly intrusive breccia, silicified intrusive breccia and andesite were sampled. Ranges and medians are given below:

Au (<2–1000)	<2 ppb	As (80.4–173.0)
Ag (<0.02–142.0)	0.3 ppm	Hg (0.0162–0.0188)
Sb (1.35–2.20)		Tl (0.044–1.37)

Data are only reliable for Au and Ag. There are three gold values above the 100 ppb threshold and 5 anomalous values for silver above the 3 ppm threshold. In 6 samples out of the 40 gold is above the detection limit. These two elements are significantly correlated. Intrusive breccias and silicified intrusive breccias contain the high concentrations of these elements. Data are insufficient as to the behaviour of the other elements.

Szépölggy Limestone (60)

The formation will be described after KÖRPÁS (1998). It is 50–80 m thick, well bedded and composed of bioclasts. The lower corallgal unit is 5–20m thick, while the upper one with thickness of 30–50m contains Nummulites, Discocyclina and Lepidocyclina in mass quantity. The main components of sand size are benthic foraminiferas (Nummulites, Discocyclina), corallinacean algae, bryozoans, echinoids, some fragments of corals, bivalves and decapods. Planktonic fossils, such as globigerinids and radiolaria are subordinate. Few extraclasts of Triassic limestone, dolomite, chert, further of altered volcanites and quartzites are accumulated in horizons of some centimetres to decimetres in thickness. Dominant microfacies types are the following: corallinacea-foraminifera-echinodermata-bryozoa packstone; foraminifera floatstone-rudstone; bryozoa-corallinacea-foraminifera packstone; coral boundstone; echinodermata grainstone-packstone. Its age is based on biostratigraphic and on magnetostratigraphic evidences (KÖRPÁS et al. 1999) are the following: nannoplankton zones of NP 18–19/20; chrons C15r and C15n. Estimated age of its formation is 35.3–34.6 Ma, according to the timescale of CANDE and KENT (1992). The following sedimentological, early diagenetic and/or hydrothermal features are to mention: signs of mass movement and redeposition; presence of submarine, partly subaerial discontinuity surfaces; phreatic-marine primary intergranular and mouldic porosity with few vadose influence; early stylolites; slight dolomitization and silicification; well developed system of hydrothermal veins and veinlets of calcite, quartz, barite, fluorite, pyrite and cinnabar; high temperature hydrothermal heating of <110–220 °C, confirmed by fluid and gas inclusion studies; elevated mean vitrinite-reflectance values of 0.30–0.55 R%. The depositional system of the Szépölggy Limestone is considered as a carbonate bank, located on a mobile dissected shelf. It represents a deepening upward sequence, interrupted by two low stand events before being drowned definitively at 34.9 Ma.

Geochemistry:

9 samples have been analysed (only 8 for Sb and Tl), these were limestones, basal breccia and a hydrothermal calcite vein with cinnabar (Nos. 514, 574, 621–622, 624, 653, 689, 778–779. of Appendix 1). Ranges and medians are given below:

Au (<2–4)	<2 ppb	As (<2.5–64.3)	5.53 ppm
Ag (<0.02–0.16)	<0.02 ppm	Hg (0.0098–58.2)	0.1094 ppm
Sb (0.25–5.4)	0.63 ppm	Tl (<0.02–0.87)	0.024 ppm

Calcite vein, limestone and basal breccia contain the elevated and anomalous values. The low threshold for arsenic is 30 ppm (2 samples show higher concentration than this), for mercury is 4 ppm (2 samples above) and for Sb is 2 ppm (1 sample with higher value). Au–Ag are well correlated, no other relationship was found.

3.2.3.3. Eocene–Oligocene

Buda Marl (34)

The 60 to 120 m thick formation will be outlined after KÖRPÁS (1998). It consists of flaser-bedded and laminated layers with a variable amount of clay (10–30%) and of carbonate (70–90%). The upper horizons frequently include strata of calcareous or siliciclastic sandstones. The entire profile comprises of redeposited volcanomictic layers of andesite-sand. Bioclastic calcareous turbidites and allodapic limestones are very common in the basal horizons. The disperse organic matter amounts to about 1%, accumulated on the surface of the bedding plains, consists of carbonized fragments of plants. The formation is rich in fossils, composed of mainly planktonic foraminifera, coccoliths, sporomorphs and pollens as well as, benthic forms (a few molluscs, large foraminifera, ostracods, algae, echinoids, bryozoans) redeposited and accumulated in turbiditic layers. Dominant microfacies are bryozoan packstone-floatstone in the lower portion of the formation and globigerina wackestone in its upper part. Estimated age based on nannoplankton, on planktonic foraminifers, respectively on sporomorphs and pollen is Late Eocene to Early Oligocene: NP zones 19/20–21. Magnetostratigraphic data (KÖRPÁS et al. 1999) suggest chron 13r, with an age of 34.6–33.5 Ma for its deposition. Among the sedimentological, early diagenetic and/or

hydrothermal phenomena the following will be outlined: sharp lower and gradational upper contacts of the strata; gradation; autoclastic breccias; synsedimentary slump structures; presence of allodapic limestones; synsedimentary, sometimes overturned folds; early diagenetic pyrite; early solutional and fracture porosity; well developed fracture system with hydrothermal calcite; high mean values of vitrinite reflectance; hydrothermal silicification and argillitization. The depositional system should be considered a narrow, mobile pelagic shelf margin, deep outer shelf and slope with dissected morphology.

Previous data of hard rock geochemistry: Ag (<0.4 ppm), As (<600 ppm), Sb (<60 ppm), and 0.21–0.95 ppm of Hg from stream sediment sampling (KORPÁS and HOFSTRA 1994).

Geochemistry:

Limestone, marl, limonitic marl, silicified marl, sandstone and dolomite (16 samples altogether) have been analysed (Nos. 489–492, 522–524, 542, 544, 579, 611, 612, 623, 703–705. of Appendix 1). Ranges and medians are given below:

Au (<2–5)	<2 ppb	As (<2.5–1296.0)	5.49 ppm
Ag (0.016–0.4)	0.0935 ppm	Hg (0.0253–66.80)	2.55 ppm
Sb (0.33–46.70)	0.93 ppm	Tl (<0.02–4.42)	0.13 ppm

The high concentrations and anomalies are in the limonitic marl and in the limonitic silicified marl. There are only 3 positive values for gold. Thresholds have been established for As (50 ppm, 6 samples above), Hg (1 ppm, 8 samples above), Sb (2 ppm, 7 samples above) and Tl (2 ppm, 3 samples above). Correlations are significant for the following pairs of elements: (Hg, Sb, Tl)–As, Hg–Tl, Hg–Sb and Sb–Tl. There are no correlations of Au and Ag with the other elements.

3.2.3.4. Oligocene

Tard Clay (35)

The formation characterised after KORPÁS (1998) is 100–120 m thick and comprises of rhythmic, laminated layers free or poor in carbonate (<10%). Its basal horizons frequently contain beds of bioclastic and allodapic limestones or redeposited siliciclastic layers. The entire section consists of volcanoclastic intercalations, andesitic in composition and produced by coeval volcanism. The formation is rich in bitumen with a content of 1.0–2.6% in TOC and with extractable bitumen of 380–1450 ppm. Content of total S oscillates between 0.98–2.37%, with pyrite bounded sulfur of 0.17–1.66%. The source of immature kerogene is the terrestrial vegetation. This is confirmed by assemblages of sporomorphs and pollens, respectively by fragments of resin and pines. The formation is rich in planktonic fossils, first of all in coccoliths, with a few pteropods, while the scarce benthic elements (bivalves, foraminifera, algae) are mainly redeposited. The uppermost levels contain well preserved, carbonized plant debris and reprints of fishes in mass quantity. Age constraints based on nanoplankton, on radiometric K–Ar measurements and fission track analysis, further on magnetostratigraphic studies are the following: nanoplankton of NP–(21)–22–23 zones; K–Ar ages of 32.25±0.9 Ma; fission track age of 32.45±0.54 Ma; chrons C13n, C12r, C12n and C11r representing a depositional record of 33.5–30.0 Ma (KORPÁS et al. 1999). Among the sedimentological, early diagenetic and hydrothermal features the following are to mention: frequent synsedimentary slumps and folds; gradation and redeposition; presence of early diagenetic bacterial pyrite; hydrothermal silicification; partly open fracture system infilled by white calcite and crystalline pyrite. The depositional system is considered an anoxic, isolated bathyal basin with periodic oceanic connections.

Geochemistry:

Clay and marl samples (5 altogether) were sampled and analysed (Nos. 514, 521, 575–577. of Appendix 1). Ranges and medians are given below:

Au <2 ppb		As (2.48–52.9)	13.8 ppm
Ag (0.08–0.23)	0.16 ppm	Hg (0.0271–0.2019)	0.0905 ppm
Sb (0.37–14.5)	1.17 ppm	Tl (0.13–1.83)	0.43 ppm

A clay sample contains the anomalous concentration of Sb (threshold. 2 ppm, 1 sample above it) and the max. concentration of all other elements.

Hárshegy Sandstone (36)

The limonite (pyrite) rich formation “is a deposit of marine, littoral or shallow sublittoral, and at its lower part brackish lagoon facies. It consists of dominantly of coarse-grained sandstone, locally fine-grained sandstone, with intercalations of conglomerate and fire-clay, possibly coal seams (Esztergom Coal Member) and, in the lower part, kaolinite sandstone. The cement is silica, chalcedony, and less frequently, barite, formed in response to a

post-hydrothermal impact. The top part includes some kaolinitic sandstone. Thickness: 20 to 200 m” (NAGYMAROSY in CSÁSZÁR 1997).

Geochemistry:

Mainly sandstones and limonitic sandstones (N=30) have been sampled and analysed (Nos. 562–564, 566, 582, 584, 587–589, 595, 597, 620, 625, 634, 640, 642, 643, 646, 648, 649, 652, 656, 657, 659, 661, 667, 673, 675, 678, 680. of Appendix 1). Ranges and medians are given below:

Au (<2–2)	<2 ppb	As (1.13–1065.0)	42.8 ppm
Ag (<0.02–0.22)	0.04 ppm	Hg (<0.02–11.54)	0.525 ppm
Sb (<0.02–176.0)	2.95 ppm	Tl (<0.02–8.86)	0.166 ppm

Thresholds and the number of samples above them are the following: As (100 ppm, 11 samples), Hg (>5 ppm, 2 samples), Sb (20 ppm, 4 samples) and Tl (>4 ppm, 2 samples). Both sandstones and limonitic sandstones contain the high and anomalous values of the elements. The following pairs of elements show good, significant correlations: Hg–As, Sb–As and Sb–Hg. Ag and Tl has no correlation with any other elements.

Mány Formation (61)

“Alternation of calcareous silt, argillaceous silt, sand and sandstone, with conglomerate, coal stringers and varegated clay intercalations. It is mainly of brackish, shallow lagoon facies, rarely with limnic and matine intercalations.”... “Limnic, paralic lignite beds (Vértessomló Member) are also included at the bottom of the formation. Thickness: 200 to 600 m” (NAGYMAROSY and GYALOG in CSÁSZÁR 1997).

Geochemistry:

Because of the location within an anomalous stream sediment cell a single sand sample was taken (No. 639. of Appendix 1) and analysed. The sample did not show any important concentrations of the six elements analysed.

3.2.3.5. Miocene

Börzsöny and Visegrád Andesite (62)

The formation comprising two units will be described after KÖRÖSI et al. (1998). “The Lower Unit (15.2–14.8 My) of the volcanics represented by dacites and andesites developed as individual volcanic cones of 2 to 10 km in diameter. This early phase is characterised by products of explosive activity”. Extrusions and lava domes furthermore “... dikes and shallow intrusive bodies are frequent, but lava flows are fairly rare. Products of explosive volcanism include coarse- to fine grained pyroclastic falls, pyroclastic flows, pyroclastic surge deposits and related epiclastics. These deposits and the lava bodies from the phreato-magmatic eruptions filled the....” eastern part of the Danube-Ipoly “...basin rapidly and almost completely resulting in a thick stratovolcanic complex made up of andesites and dacites. Extrusive domes and breccias as well as shallow cylindrical subvolcanic intrusions accompanied the extrusive activity. The subvolcanic intrusions took place preferentially during the end of the early volcanic phase. The lavas and pyroclastics are characterised by large mineralogical variations. The diagnostic accessory mineral is biotite (±garnet) and the main mafic phases are hornblende, augite and/or hyperstene.” Slight hydrothermal alteration and mineralization with ore shows is related to this volcanic phase in the Central Börzsöny area.

“The Upper Unit (14.8–14.5 My) is represented by large stratovolcanoes”...“ about 10 to 12 km in diameter and 1100–1200 m high....” and by small parasitic cones of 2.5 km. “The subaerial volcanics are of andesitic composition, and mainly consist of coarse grained pyroclastics. interbedded with five to seven lava flows on the Magas–Börzsöny cone. The maximum thickness of this stratovolcanic complex is 450 m. The diagnostic minerals are hyperstene and basaltic amphibole. Associated shallow intrusive bodies and dikes show a similar mineral composition. Hornblende-bearing, leucocratic andesite dikes representing the final products of the volcanic activity, cut the Magas–Börzsöny stratovolcanic complex. The products of the Upper Unit discordantly overlie the Lower Unit and do not show any signs of hydrothermal alteration and/or mineralization. The entire volcanism took place within the Badenian stage”,....“ between 15.2 and 14.5 My”.

Geochemistry:

Volcanics of the Lower Unit in the contact zone with the Mesozoic carbonate-mass of the Pilis Mountains and representing andesites, dacites and pyroclastics (13 samples in anomalous stream sediment cells) were sampled and analysed (Nos. 654, 655, 663, 664, 668, 670, 679, 697–702. of Appendix 1). Ranges and medians are given below:

Au <2 ppb		As (0.43–4.7)	1.18 ppm
Ag (<0.02–0.3)	0.02 ppm	Hg (<0.02–0.04)	0.014 ppm
Sb (<0.02–0.4)	0.1 ppm	Tl (0.046–0.20)	0.08 ppm

The elevated concentrations are found in andesite breccia and in biotite dacite. There are no anomalous values and no correlations of any pairs of elements.

Kálla Gravel (63)

The formation consists of “yellow, limonitic and white quartz-sand beds formed in a shoreline zone of an inland sea, subjected to swell of the sea, as well as gravel (pearl gravel) bed consisting of fine-grained, well rounded and polished grains, rarely comprising siliceous sandstone-quartzite lenses, and locally polymict bodies of coarse (10 to 50 cm) pebbles. It has a thickness ranging from 5 to 10 m” (JÁMBOR in CSÁSZÁR 1997). From the pyrite and marcasite bearing (quartzite) horizons near Cserseztomaj and Rezi (Keszthely Mountains) of this formation reported SZENTES (1948 p. 92) traces of gold (Au: 0.60 ppm) and silver (Ag: 23.00 ppm). Our sampling aimed at the checking of these data.

Geochemistry:

21 samples for gold and mercury and 20 samples for the other elements were analysed (Nos. 112–130, 133, 153. of Appendix 1). Sand, pyritic sand, limonitic sand and silicified sandstone were sampled. Ranges and medians are given below:

Au (<2–7)	<2 ppb	As (1.59–37.9)	8.47 ppm
Ag (<0.05–0.4)	0.09 ppm	Hg (0.0262–0.3593)	0.1392 ppm
Sb (0.11–5.48)	0.39 ppm	Tl (0.04–2.18)	0.455 ppm

Pyritic sand and silicified sandstone contain the elevated values. A slight anomaly of Sb (at 1.5 ppm threshold with 2 samples above it) is established. Well correlated pairs of elements are: Hg–As and Tl–As.

Zámor Gravel (64)

The formation comprises of “grey, well rounded, mainly quartz or quartzite bearing sand and pebbly sand (“pearl gravel” facies), with and arched cross bedding. An inland shore deposit representing mainly a basal rock, less frequently an intercalation in the Csákvár and Algyó Formations. Thickness: 10 to 30 m” (JÁMBOR in CSÁSZÁR 1997).

Geochemistry:

Two limonitic sand samples (Nos. 512, 545. of Appendix 1) have been analysed. Ranges are given below:

Au <2 ppb	As (152.0–1810.0)
Ag (0.06–0.11)	Hg (0.05–25.63)
Sb (3.9–48.4)	Tl (0.071–0.525)

There are high concentrations of As, Hg and Sb, but due to the small number of samples the formation cannot be reliably evaluated.

Szák Marl (65)

“Almost always grey, shallow, sublittoral calcareous argillaceous silt with, molluscs and ostracods, rarely with thin silt and fine grained sandstone intercalations. Thickness: 50 to 200 m” according to JÁMBOR in CSÁSZÁR (1997). Samples were taken near to the Cserseztomaj pyrite-marcasite bearing horizon.

Geochemistry:

Mainly marls and sandstones were sampled (16 altogether, Nos. 106–111, 132, 134–141. of Appendix 1). Ranges and medians are given below:

Au (<2–3)	<2 ppb	As (1.18–21.6)	4.62 ppm
Ag (0.04–0.23)	0.09 ppm	Hg (0.0129–0.0939)	0.0373 ppm
Sb (0.18–2.11)	0.305 ppm	Tl (0.12–3.41)	0.27 ppm

There is only one positive value for gold. The marl and the palaeosol samples contain the maximum values within the formation. Correlations are significant for: Hg–As, Sb–As, Tl–As and Sb–Hg.

3.2.3.6. Pliocene–Pleistocene

Travertine Formation (66)

The 20 m thick formation of the Buda Hills will be outlined after KORPÁS (1998). Its yellow to brown basal clastic strata of 3–5 m in thickness consist of fining upward alluvial gravels and sands. The matrix supported, slightly cemented gravels are derived from local angular to subangular clasts. They are overlain by lenses of friable, limonitic, badly sorted, medium to coarse grained sands. The transition to the overlying laminated travertine is represented by laminated silts and sandy clays. The greyish white laminated, sometimes muddy travertine is 2–5 m thick and consists alternating laminae of soft or altered muddy algal limestones, rich in dispersed organic matter. This laminated unit is dissected by synsedimentary normal microfaults and capped by a subaerial unconformity surface reflecting a significant depositional break and internal erosion. It is the richest in fossils and consists of both terrestrial and freshwater molluscs, vertebrata, arthropods, algae, red grasses, charophytes, bryophytes, prints and detritus of plants. Dominant microfacies is considered pelmicrosparites, pelmicrites with less stromatolite-like types and phytoclastic calcarenites. The top of the laminated travertine is covered by an

unconformity related paleosol horizon (15–50 cm), consisting of smectite-type soft clays, bearing angular clasts derived from the footwall laminites. The main level of the massive, friable, clastic and grainy paleosol includes the horizon “A”, dark reddish in colour and the brown carbonate rich “B” horizon. Both are rich in fossils, represented mainly by terrestrial gastropods and vertebrates. Above this paleosol horizon lies the white massive, crystalline, sometimes cavernous travertine in a thickness of 8–10 m. The poor fossil ensemble consists of moulds and recrystallized shells of terrestrial and fresh water gastropods and some fragments of plants. The depositional environment is interpreted as a very shallow flat pool fed by coeval thermal springs.

Geochemistry:

Bituminous and limonitic travertines (N=4) were sampled (Nos. 549–551, 644. of Appendix 1). Ranges and medians are given below:

Au <2 ppb		As (2.87–500.0)	20.93 ppm
Ag (<0.02–0.06)	0.025 ppm	Hg (0.04–12.24)	0.185 ppm
Sb (<0.02–48.4)	0.4 ppm	Tl (<0.02–4.88)	0.106 ppm

Gold is below detection limit in all samples. Thresholds cannot be established but elevated concentrations of As, Hg, Sb and Tl are interesting. A limonitic travertine contains all the high values, especially for As, Sb and Hg.

Summary for the Transdanubian Range:

Main features of the formations of Transdanubian Range are summarized in Table 4 and illustrated on Figs. 14, 15 and 16. Formations characterised by less than three samples are not plotted.

Reference lines at 10 ppb and 100 ppb are given to indicate subanomalous and anomalous threshold values of gold. Comparison of the gold values of Paleozoic, Mesozoic and Cenozoic formations is illustrated on Fig. 14. Anomalous gold values (Au>100 ppb) can only be found in the Paleozoic and Cenozoic [Lovas Slate (42), Velence Granite (47) and Nadap Andesite (59) respectively]. Slight subanomalous gold (Au>10 ppb) exhibit the Paleozoic Balatonfőkajár Quartz Phyllite (41) and some Late Triassic formations like the Mátyáshegy Formation (16), Földolomit Formation (51) and Dachstein Limestone (52). Mercury anomalies higher or around the threshold (10 ppm) are found in the Budaörs Dolomite (49), in the Mátyáshegy Formation (16), in the Szépvölgy Limestone (60), in the Buda Marl (34), in the Hárshegy Sandstone (36) and in the Travertine Formation (66) of the Buda Hills.

Fig. 15 also helps overviewing the anomalies of other elements appearing in the studied formations. There are a lot of formations (Paleozoic, Mesozoic and Cenozoic as well) with As maximum values higher than 100 ppm, which is considered the threshold value for anomalies: Lovas Slate (42), Polgárdi Limestone (1), Budaörs Dolomite (49), Mátyáshegy Formation (16), Földolomit Formation (51), Dachstein Limestone (52), Kisgerecse Marl (54), Buda Marl (34), Hárshegy Sandstone (36) and the Travertine Formation (66). Formations with Sb maximum values higher than 20 ppm are the following: Lovas Slate (42), Polgárdi Limestone (1), Mátyáshegy Formation (16), Buda Marl (34), Hárshegy Sandstone (36) and the Travertine Formation (66).

The following formations are characterised by silver values above the threshold: Lovas Slate (42), Velence Granite (47) and Nadap Andesite (59). Anomalous Tl values are only found in the following formations: Mátyáshegy Formation (16) and Hárshegy Sandstone (36) (Fig. 16).

Results and interpretations of stream sediment survey of the Buda–Pilis and Visegrád Mountains (Fig. 4) will be summarized in the following. Two subanomalous areas can be outlined: the Pilis fault zone and the Buda Hills.

The Pilis fault zone is accompanied by slight additive anomalies and demonstrated with the following cells, from NW to SE: No. 4114, 5001, 4164, 4165, 4169, 5018, 5023, 5024 and 5010 respectively. Low level gold anomalies ranging between 3 and 27 ppb Au were detected in the cells No. 4114 (27 ppb), 5002 (4 ppb), 4164 (22 ppb), 4165, 5018 (6 ppb), 5023 (3 ppb) and 5024 (5 ppb). Gold values above detection level of the chip sampling (Appendix No. 1) within the cells are related to the Földolomit Formation (Ns. 683–684: 5, 25 ppb), the Feketehegy Formation (Ns. 693–694: 3 ppb), the Dachstein Limestone (No. 671: 11 ppb), the Lókút Radiolarite (No. 687: 5ppb) and the Bauxite Formation (No. 674: 6 ppb). All other Tertiary formations are free of gold.

The situation in the Buda Hills is similar to the afore mentioned. Slight additive anomalies exhibit the cells below: No. 5035, 5042, 5041, 5050, 5048, 5044, 5052, 5051 and 5047. Low level gold anomalies of 3 to 53 ppb were discovered in the cells of 5033 (3 ppb), 5035 (7 ppb), 5036 (4 ppb), 5039 (5 ppb), 5044 (3 ppb), 5050 (53 ppb), 5052 (8 ppb), 5053 (4 ppb), 5046 (4 ppb) and 5047 (4 ppb). Surface chip sampling has given gold values near to the detection level in the following formations (Appendix No. 1): Budaörs Dolomite (No. 499: 5 ppb), Földolomit Formation (No. 569: 4 ppb), Szépvölgy Limestone (No. 624: 3 ppb) and Buda Marl (No. 490: 5 ppb).

The slight gold anomalies of the Pilis Mountains and the Buda Hills can be related mainly to Middle and Late Triassic carbonates and connected bauxites.

Anomalies and subanomalies of gold detected by both chip sampling and stream sediment survey appear in the Balatonfő and Velence Hills area, in the Pilis fault zone and in the Buda Hills. The gold anomalies of the Velence

Transdanubian Range
Summary of geochemical parameters – median and maximum values.

Table 4

Form-code	Au (ppb)		Ag (ppm)		As (ppm)		Hg (ppm)		Sb (ppm)		Tl (ppm)		N
	Med.	Max.	Med.	Max.	Med.	Max.	Med.	Max.	Med.	Max.	Med.	Max.	
41	<2	27	0.07	0.52	3.3	13.8	0.20	0.30	0.86	4.40	0.12	0.33	9
42	<2*	4770	.095*	140	26.8	1255	0.025	0.966	1.16	791	0.16	1.06	74*31
44	<2	5	0.065	1.35	3.72	13.70	0.08	0.51	1.14	4.23	0.055	0.29	8
1	<2	8	0.11	1.22	11.1	596.0	0.26	2.76	1.04	23.10	0.13	6.56	27
45	<2	2	0.03	0.16	17.7	99.7	0.128	0.136	1.16	5.28	0.10	0.23	3
46		<2	0.05	0.15	1.46	5.54	0.037	0.060	0.22	0.62	0.22	0.48	5
47	<2*	2090	0.04*	18.0	10.76	38.5	0.13	0.24	0.375	2.72	0.17	0.19	14*4
48		<2	0.09	0.21	11.0	23.80	0.004	0.019	0.39	3.14	0.13	0.30	7
8		<2	0.06	0.12	5.29	41.5	0.003	0.04	0.225	0.70	0.14	0.34	14
11		<2	0.021	0.035	5.85	31.50	0.02	0.20	0.50	3.54	0.04	0.19	7
49	<2	5	0.084	0.56	16.35	706.0	0.008	10.70	0.305	18.1	0.11	2.63	28
50	<2	3	<0.3	0.4	3.50	9.40	0.30	1.66	0.53	0.54	0.22	0.36	3
12		<2	0.09m	0.12	2.36m	3.13	0.01m	0.053	0.24m	0.64	0.09m	0.43	2
13		<2	0.085	0.21	1.95	22.7	0.008	0.10	0.17	1.16	0.12	0.27	12
15	<2	4	0.06	0.48	5.10	27.5	0.012	0.42	0.22	0.99	0.15	0.86	71
16	<2	12	0.05	0.39	12.7	463.0	0.74	111.4	1.70	1760	0.09	33.7	44
51	<2	25	<0.02	0.28	3.37	401.0	0.055	1.76	1.05	11.3	0.023	0.415	21
19		<2	0.07	0.23	0.9	2.65	0.009	0.016	0.36	1.48	0.03	0.09	11
20		<2	0.05	0.16	1.9	10.2	0.006	0.08	0.2	3.34	0.15	0.53	9
21	<2	3	0.05	0.08	5.36	31.9	0.144	0.155	0.94	4.58	0.03	0.28	5
52	<2	11	<0.02	0.15	3.39	198.0	0.072	2.90	0.50	6.92	0.034	0.95	28
18	<2	4	0.35	1.0	3.40	17.30	0.18	0.70	0.47	1.10	0.065	0.38	35
53		<2	<0.02	0.03	1.05m	4.62	0.02m	0.09	0.3m	0.5	<0.02	0.252	2
33	<2	5	0.29	1.08	13.8	59.1	0.125	1.671	0.59	1.14	0.16	0.70	19
54	<2	8	0.31	0.90	24.3	147.0	0.28	0.66	1.06	2.63	0.38	3.18	21
55	<2	5	0.16	0.42	1.26	24.8	0.035	0.449	0.12	1.23	0.115	0.58	6
56	<2	5	0.04m	0.08	126m	152	1.35m	1.43	3.5m	4.7	0.15m	0.404	2
58	<2	6	0.06	0.15	16.65	28.40	0.051	0.329	0.90	5.20	0.279	1.59	4
59	<2*	1000	0.3*	142	80.4m	173	.016m	0.019	1.35m	2.20	0.44m	1.37	40*2
60	<2	4	<0.02	0.16	5.53	64.3	0.109	58.2	0.63	5.4	0.024	0.87	9
34	<2	5	0.094	0.40	5.49	1296	2.55	66.80	0.93	46.70	0.13	4.42	16
35		<2	0.16	0.23	13.8	52.9	0.091	0.202	1.17	14.5	0.43	1.83	5
36	<2	2	0.04	0.22	42.8	1065	0.525	11.54	2.95	176.0	0.166	8.86	30
62		<2	0.02	0.30	1.18	4.70	0.014	0.04	0.10	0.40	0.08	0.20	13
63	<2	7	0.09	0.40	8.47	37.9	0.139	0.359	0.39	5.48	0.455	2.18	21
64		<2	0.06m	0.11	152m	1810	0.05m	25.63	3.9m	48.4	0.07m	0.525	2
65	<2	3	0.09	0.23	4.62	21.6	0.037	0.094	0.305	2.11	0.27	3.41	16
66		<2	0.025	0.06	20.93	500.0	0.185	12.24	0.40	48.40	0.106	4.88	4

Remarks:

Formcode = the code number of the Formation:

41=Balatonfőkajár Quartz Phyllite, 42=Lovas Slate, 44=Úrhida Limestone, 1=Polgárdi Limestone, 45=Szabadbattyán Limestone, 46=Füle Conglomerate, 47=Velence Granite, 48=Hidegkút Fm., 8=Csopek Marl, 11=Megyehégy Dolomite, 49=Budaörs Dolomite, 50=Vashegy Dolomite, 12=Felsőörs Limestone, 13=Buchenstein Fm., 15=Veszprém Marl, 16=Mátyáshegy Fm., 51=Földolomite Fm., 19=Rezi Dolomite, 20=Kössen Fm., 21=Feketehegy Fm., 52=Dachstein Limestone, 18=Csovár Limestone, 53=Pisznice Limestone, 33=Úrkút Manganese Ore, 54=Kisgercese Marl, 55=Eplény Limestone, 56=Lökút Radiolarite, 58=Bauxite Fm., 59=Nadap Andesite, 60=Szép völgy Limestone, 34=Buda Marl, 35=Tard Clay, 36=Hárshegy Sandstone, 62=Börzsöny and Visegrád Andesite, 63=Kálla Gravel, 64=Zámor Gravel, 65=Szák Clay Marl, 66=Travertine Fm.

Med.=median value; Max.=maximum value; m=minimum value;

74*31=number of analyzed samples for the components marked by *, number of samples for the other elements analyzed.

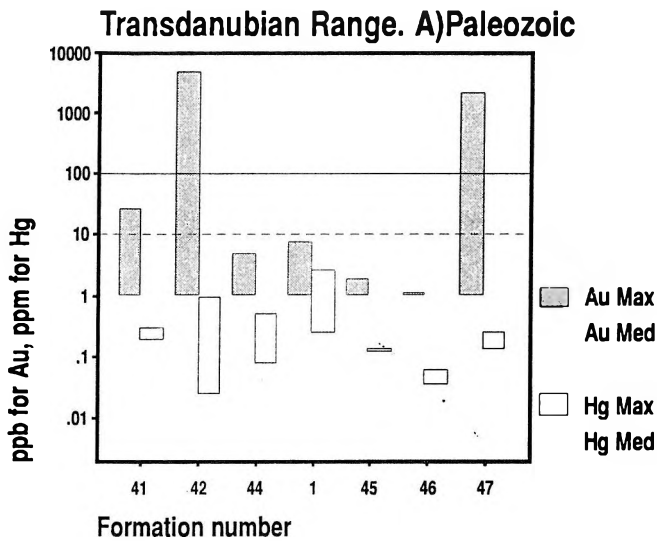
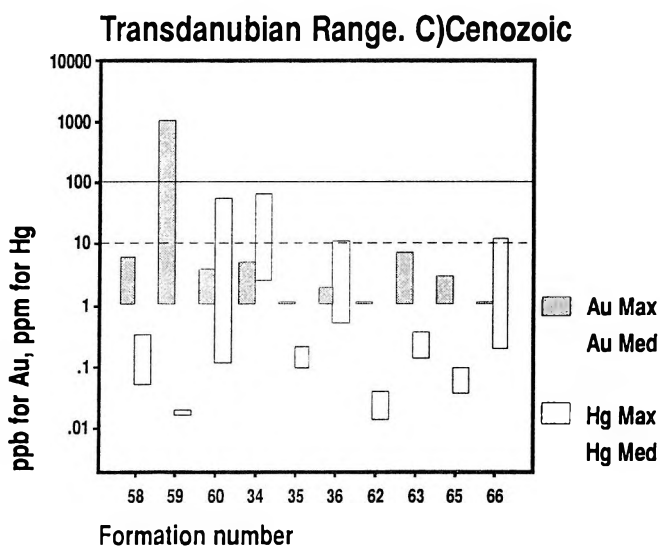
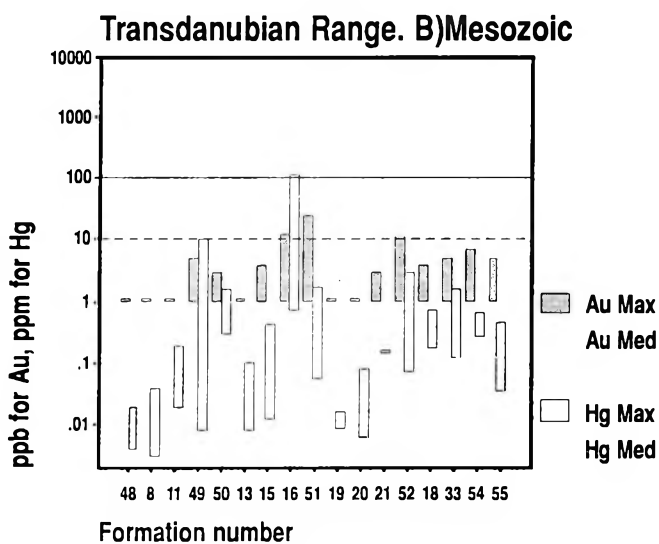


Fig. 14: The median (Med)–maximum (Max) concentration ranges of Au–Hg, Transdanubian Range A/ Paleozoic formations, B/ Mesozoic formations and C/ Cenozoic formations



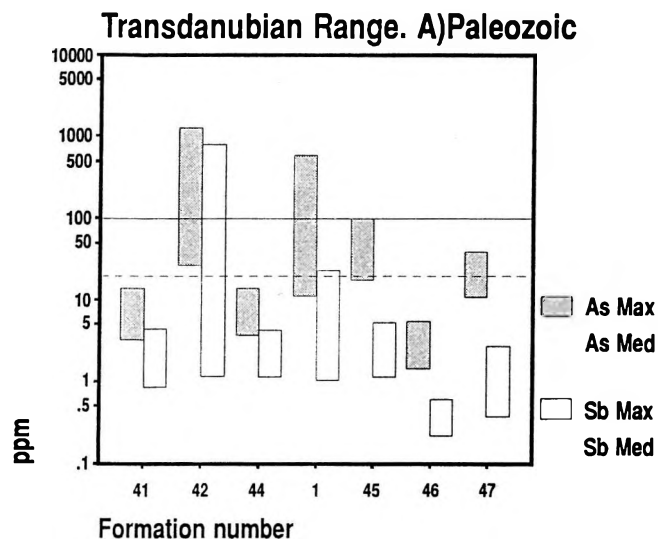
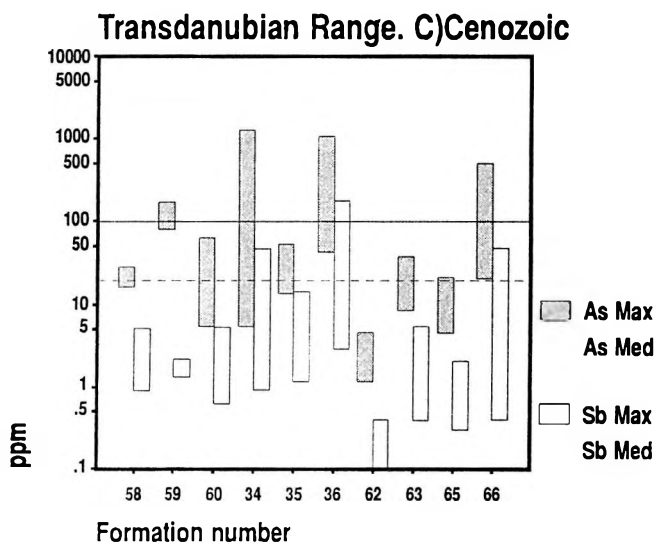
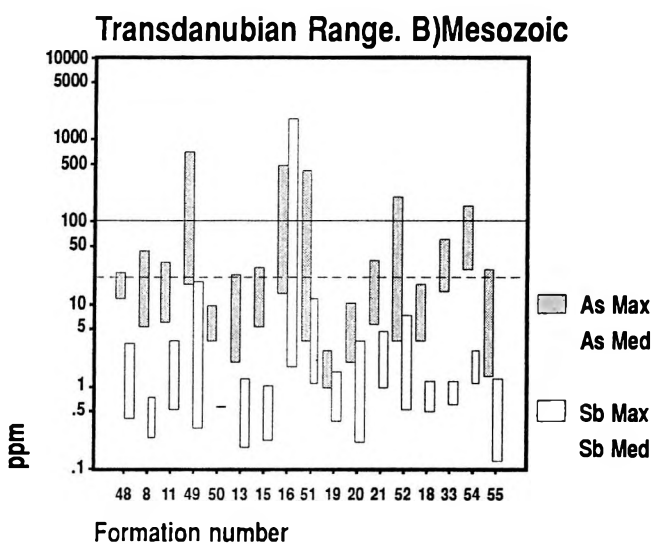


Fig. 15: The median (Med)–maximum (Max) concentration ranges of As–Sb, Transdanubian Range A/ Paleozoic formations, B/ Mesozoic formations and C/ Cenozoic formations



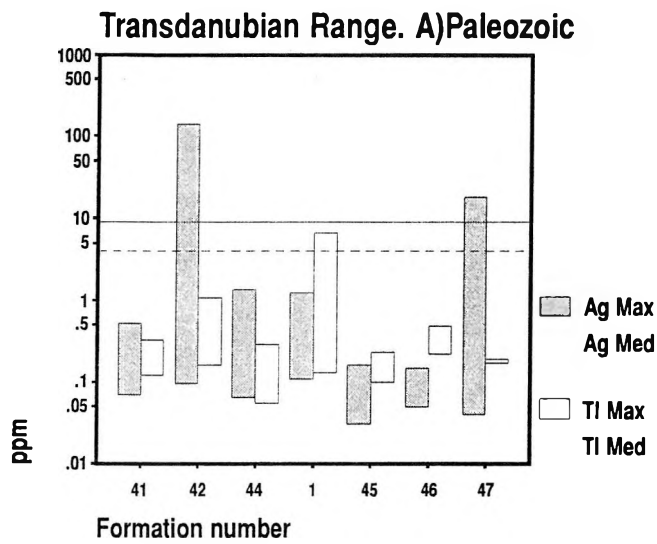
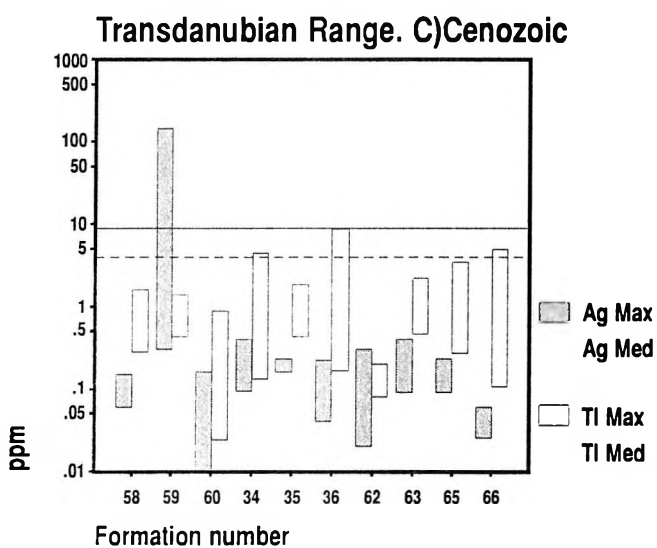
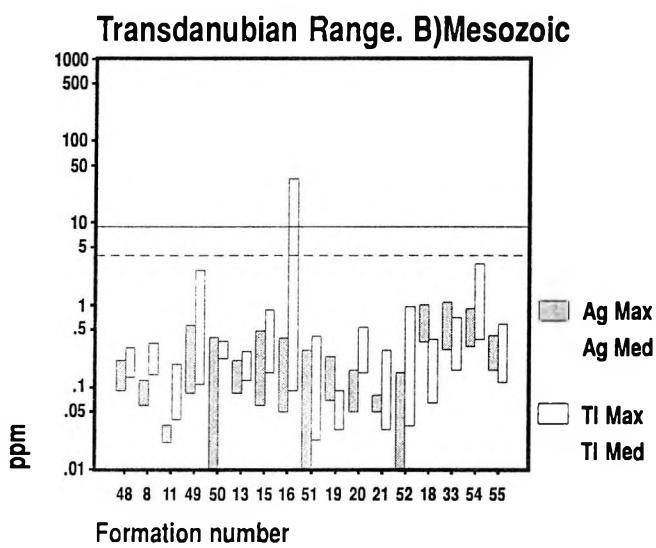


Fig. 16: The median (Med)–maximum (Max) concentration ranges of Ag–TI, Transdanubian Range A/ Paleozoic formations, B/ Mesozoic formations and C/ Cenozoic formations



Hills are accompanied by arsenic and silver anomalies too. Arsenic and mercury anomalies are concentrated in the formations of the Buda Hills and the Pilis Mountains, especially in the Triassic and Paleogene.

The Paleozoic metamorphites and granites overprinted by the Late Eocene volcanic-plutonic complexes of the Balatonfő–Velence Hills area are considered targets of further, more detailed explorations. The Triassic carbonates of the Pilis fault zone with slight subanomalous gold are related to the second group in perspective while, all other areas and formations are considered unfavorable for gold prospection.

3.3. Mecsek Mountains

3.3.1. Mesozoic

3.3.1.1. Triassic

The prospected areas and formations of the Mecsek Mountains will be evaluated using the geological map in Fig. 17.

Patacs Siltstone (67)

The formation (Fig. 17) is made up by alternation of red siltstones and fine-grained sandstones and green claystones. In its lower part intercalations of calcareous, ferroan, manganese-oxide rich siltstones are common. In its upper part dolomitic marl interlayers occur. Thick bedded as a rule, but microlamination or crossbedding within the layers scarcely occurs. On the bedding plains of the sandstone layers ripple marks are common.

Copper ore shows of azurite and malachite (Cu: 0.15–1.10%) near to Magyarürög were described by VÁR-SZEGI (1965) in a sandstone bed of the formation.

Facies: Tidal-flat to shallow marine subtidal ramp–lagoon facies. The manganese rich layers may represent an oxygen-depleted bog facies.

Age: Lower Anisian

Thickness: It is 100–150 m thick in the Mecsek and 10–35 m in the Villány Mts.

Geochemistry:

The 4 samples taken consist of claystone, marl and sandstone (Nos. 744,745, 766, 767. of Appendix 1). Ranges and medians are given below:

Au (<2–3)	<2 ppb	As (1.81–19.2)	2.32 ppm
Ag (0.08–0.91)	0.285 ppm	Hg (0.04–0.08)	0.05 ppm
Sb (0.07–0.13)	0.125 ppm	Tl (0.16–1.09)	0.205 ppm

A silty marl sample shows the elevated concentrations, but the whole formation is characterised by very low values of all elements analysed.

Hetvehely Dolomite (27)

Lithology: grey carbonates with evaporites and shales. In the Mecsek Mts. it can be subdivided into two members. The lower member (Magyarürög Anhydrite) is made up of dolomites, dolomitic marls and claystones with anhydrite and gypsum deposits, and intraformational breccias. This series is overlain by clayed dolomites, dolomites, claystones, magnesian dolomitic marls and yellowish grey dolomitic marl. The upper member (Viganvár Limestone) consists of grey, dark grey thin-bedded commonly bituminous (TOC: 0.1–0.3%), limestones with marl or claystone interlayers. Dolomitic rock types are scarce. In the Villány Mts. the formation is made up by dolomites, dolomitic marls, clay-marls, siltstones and rarely limestones. In the lower third of the succession fine-grained sandstone and anhydrite–gypsum intercalations also occur.

Facies: Evaporites in the basal part of the succession refer to a restricted lagoon environment, with hypersaline condition near to the bottom. The dolomites may have formed also in a restricted lagoon. Disappearance of evaporites and prevalence of limestones in the upper part of the sequence indicate the opening of the basin, establishment of a ramp of open circulation.

Age: Lower Anisian

Thickness: 100–200 m in the Mecsek and less than 80 m in the Villány Mts.

Previous data of hard rock geochemistry (KORPÁS and HOFSTRA 1994): Ag (<0.01 ppm), As (<10 ppm), Ba (455 ppm), Cu (30 ppm), Mo (<2.5 ppm), Pb (17 ppm), Sb (<16 ppm), Tl (<1 ppm), Zn (105 ppm)

Geochemistry:

4 samples were collected (dolomites, limestone and marl, Nos. 752, 754–756. of Appendix 1). Ranges and medians are given below:

Au (<2–3)	<2 ppb	As (0.7–4.47)	0.96 ppm
Ag (0.03–4.39)	0.05 ppm	Hg (<0.02–0.06)	0.03 ppm
Sb (0.05–0.14)	0.085 ppm	Tl (0.06–0.2)	0.08 ppm

The only thing worth mentioning is the relatively high max. concentration of silver.

Lapis Limestone (28)

Lithology: grey, dark grey nodular, bioturbated locally bituminous limestones with mollusc coquina and crinoidal interlayers. In the lower part of the formation dolomite interlayers are common. Dolomitic intercalations are more characteristic in the Villány Mts. The most typical microfacies type is bioclastic wackestone.

Facies: It was formed on a shallow ramp of open water-circulation as a rule, becoming restricted, occasionally. The bioclastic coquina layers are storm deposits.

Age: Lower–Middle Anisian

Thickness: Its thickness is between 200–300 m in the Mecsek Mts., more than 200 m in the northern foreland of the Villány Mts., but within the Villány Mts. not more than 80–120 m.

Previous data of hard rock geochemistry (KORPÁS and HOFSTRA 1994): Ag (<0.01 ppm), As (<10 ppm), Ba (201 ppm), Cu (57 ppm), Mo (<2.5 ppm), Pb (15 ppm), Sb (<16 ppm), Tl (<1 ppm), Zn (100 ppm)

Geochemistry:

7 limestone samples were analysed (Nos. 749–751, 753, 757, 759, 765. of Appendix 1). Ranges and medians are given below:

Au (<2–3)	<2 ppb	As (1.32–38.5)	3.03 ppm
Ag (0.07–0.62)	0.15 ppm	Hg (0.02–0.08)	0.06 ppm
Sb (0.09–0.21)	0.11 ppm	Tl (0.07–0.45)	0.12 ppm

There are no anomalous values and there is no correlation between any pairs of elements.

Zuhány Limestone (29)

Lithology: grey, patchy, locally variegated nodular limestones. In the Mecsek Mountains two members can be distinguished. The Bertalanhegy Member is made up of calcareous marl and nodular limestone beds with intercalations of brachiopod–crinoid coquinas. The Dömörkapu Member consists of dark grey almost black bituminous limestones with irregular lilac or yellowish red patches. The relationship of the two members is ambiguous, the Bertalanhegy Member is probably intercalated into the Dömörkapu Member. In the Villány Mts. thin-bedded nodular, patchy limestones are the most typical. However, thick-bedded greyish limestones with lilac or brownish patches are also known, locally. Texture of the rocks is very variable: mudstone, intraclastic, bioclastic grainstone, ooidic grainstone. Burial dolomitization is common.

Facies: open, relatively deep ramp facies. Conodonts and ammonites in the Bertalanhegy Member indicate a direct communication with the pelagic environments. The coquina beds are storm deposits.

Age: Middle–Upper Anisian

Thickness: It varies between 40–250 m.

Previous data of hard rock geochemistry (KORPÁS and HOFSTRA 1994): Ag (\leq 0.01 ppm), As (\leq 10 ppm), Ba (201 ppm), Cu (57 ppm), Mo (\leq 2.5 ppm), Pb (15 ppm), Sb (\leq 16 ppm), Tl (\leq 1 ppm), Zn (100 ppm)

This formation was canceled from the list of the predictive formations and not sampled after studying the Carlin gold deposits in Nevada, in 1995.

Csukma Formation / Kozár Limestone (30)

Lithology: It is made up by shallow marine dolomites and limestones. Two members can be distinguished in the Mecsek Mts. The lower that is Kozár Member consists of grey thick-bedded limestones with ooidic and crinoidal intercalations. In the upper part of the member gastropod-rich layers occur which are overlain by layers consisting of large oncoids, bivalves and small gastropods. Patchy dolomitization is common. The upper that is Kán Member is grey, brownish, yellowish, thin-bedded, sucrosic dolomite with limestone enclaves. In its upper part laminitic dolomites with ooidic interlayers also occur, locally. In the Villány Mts. the lower part of the formation consists of brownish grey, greyish brown, yellowish thin and thick-bedded rarely platy dolomites. Limy layers, limestone enclaves also occur, locally. The upper part of the formation is made up by yellowish grey, white thick-bedded to platy dolomites, calcareous dolomites, dolomitic limestones, dolomitic marls (Templomhegy Dolomite Member). The clay content shows an upward increasing trend.

Copper ore shows of azurite and malachite in the Kozár quarry were described by TOKODY (1952) in the paleokarstic infilling breccia of the formation.

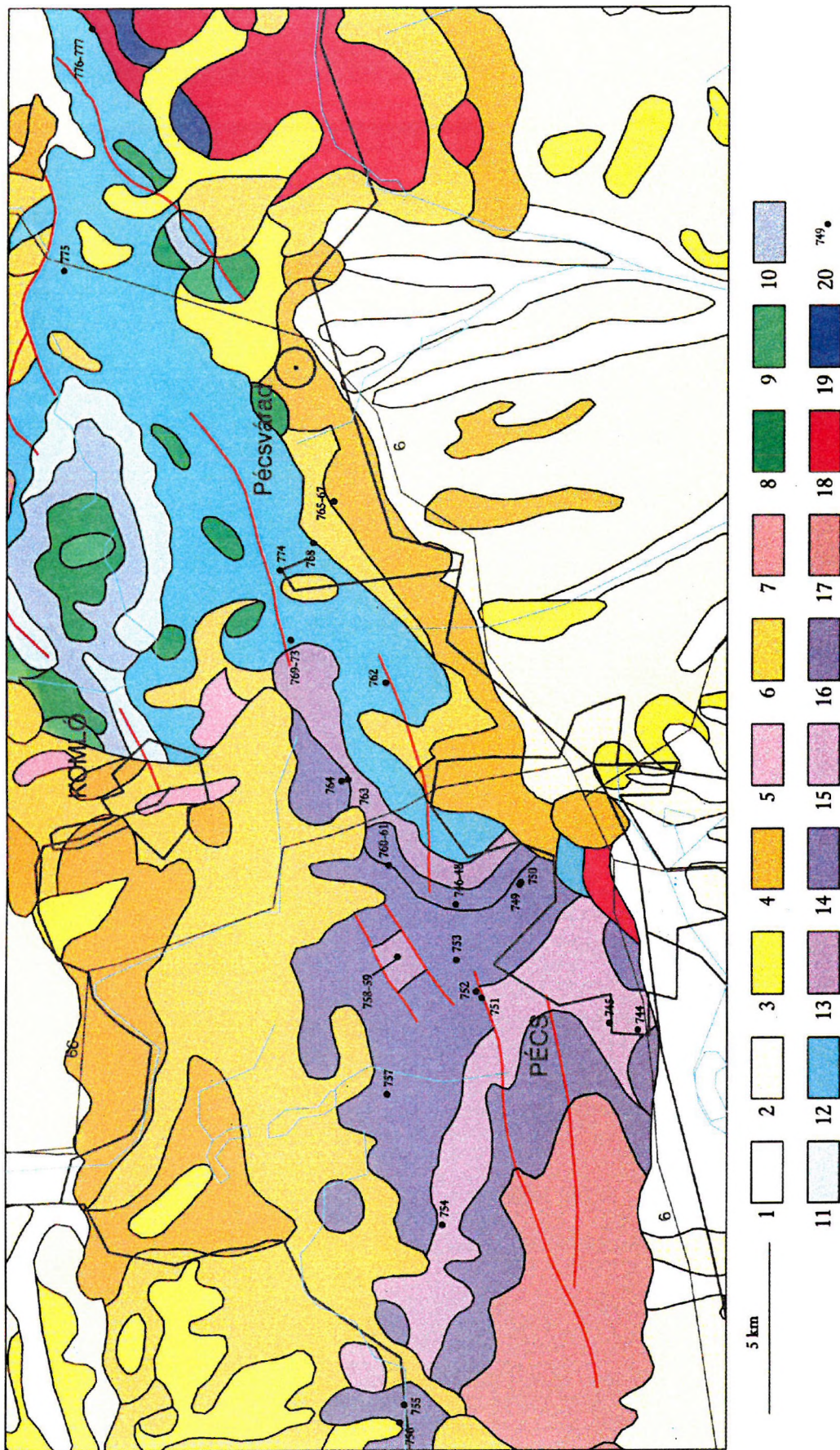


Fig. 17: Geological map of the Mecsek Mountains with Carlin gold sample sites

1. Holocene alluvial sediments, 2. Quaternary sediments, 3. Late Miocene sediments, 4. Middle-Late Miocene sediments, 5. Middle rhyolite tuff, 6. Early-Middle Miocene sediments, 7. Lower rhyolite tuff, 8. Early Cretaceous volcanics, 9. Early Cretaceous sediments, 10. Late Jurassic sediments, 11. Middle Jurassic sediments, 12. Óbánya Silt, Mecsekátság Sandstone, Hosszúhetény Marl, Vass Mar, Mecsek Coal, 13. Kantavár Formation/Kozár Limestone, Lapis Limestone, 14. Czukma Formation/Kozár Limestone, Zuhány Limestone, 15. Hetvehely Dolomite, Patacs Siltstone, 16. Early Triassic sediments, 17. Permian sediments, 18. Mórágó Granite, 19. Precambrian metamorphites, 20. •745 Carlin gold sample site

Facies: The successions of the formation show an upward shoaling trend. The lower part is formed in an open ramp environment, deeper in the Mecsek and somewhat shallower in the Villány Mts. The oncoidal layers may have formed in the shallow subtidal zone. The Templomhegy Dolomite was formed in the shallow subtidal to peritidal zones.

Age: Due to lack of age-diagnostic fossils the age of the formation is ambiguous, most probably Ladinian.

Thickness: The thickness of the formation is between 100 and 350 m, it is thinner in the Mecsek and thicker in the Villány Mts.

Geochemistry:

2 samples (limestone and limestone breccia) were collected (Nos. 760, 761. of Appendix 1). Ranges are given below:

Au <2 ppb	As (7.99–264.0)
Ag (1.03–5.1)	Hg (<0.02–2.1)
Sb (0.22–15.3)	Tl (0.1–0.17)

The high concentrations bound to the limestone breccia (containing the Kozár azurite shows). Because of the limited number of samples, the high concentrations cannot be considered as reliable for the whole formation.

Kantavár Formation (31)

Lithology: Dark grey, black platy, laminated argillaceous limestone (biomicrite–wackestone). On the bedding planes of the limestone layers prints of ostracodes are common and the thin marl interlayers are packed with ostracodes as a rule. In the uppermost part of the formation the claystone and sandstone intercalations are more and more frequent. At the base of the formation locally the Mánfa Siderite Member occurs. It is made up by poorly bedded, sideritic, kaolinitic claystone and altered tuffite.

Facies: It shows a regressive trend from a restricted and slightly brackish water basin to a strongly diluted and to a lacustrine environment. The Mánfa Member consists of strongly altered tuff mixed with sediments. The mollusc and monospecific ostracode fauna indicate brackish to freshwater environment.

NAGY and RAVASZNÉ-BARANYAI (1968) reported relatively high organic content (0.2–3.1%), and pyrite (0.6–2.5%) with Ag (<0.2 ppm), Mo (≤55 ppm) and Cu (≤30 ppm) from the Mánfa Siderite Member.

Three bituminous limestone samples from the Kantavár quarry which were analysed by the Laboratories of the Recsk Ore Mine Company in 1983 yielded the following results: Cu: 0.01–0.16%, Pb: 0.00–0.04%, Zn: 0.01–0.04%, Fe: 0.65–0.70%, S: 0.00%, Mo: 0.00%, Au: 0.00 ppm, Ag: 0.00–6.00 ppm (NAGY B. 1996, pers. comm.).

Age: age-indicator fossils are missing. According to its stratigraphic position it is presumably uppermost Ladinian–lowermost Carnian.

Thickness: 50–100 m

Geochemistry:

Limestone, claystone and bituminous marl samples (5 samples) were taken from this formation (746–748, 763, 764. of Appendix 1). Ranges and medians are given below:

Au <2 ppb	As (1.23–6.5)	4.64 ppm	
Ag (0.02–0.05)	0.04 ppm	Hg (0.02–0.1)	0.06 ppm
Sb (0.04–0.12)	0.05 ppm	Tl (0.09–0.16)	0.15 ppm

Limestone and pyritic bituminous marl samples yielded relative high values but no anomalies were encountered.

3.3.1.2. Triassic–Jurassic

Mecsek Coal (68)

Lithology: It consists of cyclic alternation of grey arkosic sandstone, dark grey shale, claystone and coal layers. Number of coal seams (thicker than 0.5 m) is 10–38. The formation may be subdivided into 3 members (seam groups). Within the formation a few meter thick rhyolitic tuff and tuffite intercalations occur.

Facies: The lowermost part of the formation (it is partly Triassic) was formed in a lacustrine as well as lacustrine-delta environment. Its middle part (Hettangian) is essentially alluvial (channel, flood plain, and swamp facies) however, brackish interlayers show growing frequency upsection. The upper part of the formation was deposited in a supratidal marsh environment.

Age: Upper Rhaetian–Lower Sinemurian

Thickness: 150–300 m in general in the Mecsek Zone and also in the northern part of the Mecsek Mts. but in the southern part of the Mecsek Mts. it shows a significant thickening (1200 m). This thickness pattern can be explain by a half-graben structure which may have begun forming in the latest Triassic.

Geochemistry:

The sampled lithology is a mixed one: coal, pyritic coal, trachydolerite dike and tuff (6 samples, Nos. 762, 769–773. of Appendix 1). Ranges and medians are given below:

Au (<2–7)	<2 ppb	As (3.52–29.2)	13.7 ppm
Ag (0.05–0.39)	0.07 ppm	Hg (0.08–0.3)	0.14 ppm
Sb (0.15–1.79)	0.56 ppm	Tl (0.15–0.93)	0.245 ppm

Pyritic coal carries the high values for Sb, Hg and Tl. No significant correlations were found.

3.3.1.3. Jurassic

Vasas Marl (69)

Lithology: It is made up by fine grained siliceous sandstone in the lower part of the formation. It is followed by sphaerosideritic clay marls with Gryphaea sandstone interlayers and above them shales with calcareous marl intercalations and in the topmost part calcareous marls. The upper members contain rich mollusc, echinoderm, brachiopod and foraminifera assemblage.

Facies: It shows a wide spectrum from the shallow sublittoral in the lower part of the formation to deeper neritic, open shelf facies in the upper one. The fauna in the upper part of the formation refers to normal salinity marine conditions. The whole succession shows a deepening upward trend.

Age: Sinemurian

Thickness: 300–700 m, showing marked thickening southward in the Mecsek Mts.

Geochemistry:

Only 3 samples (marl, siltstone and limonitic sandstone) were taken from the formation (Nos. 758, 776, 777. of Appendix 1). Ranges and medians are given below:

Au (<2–3)	<2 ppb	As (7.36–16.6)	10.6 ppm
Ag (0.4–1.26)	0.89 ppm	Hg (0.08–0.16)	0.10 ppm
Sb (0.1–0.89)	0.36 ppm	Tl (0.15–0.34)	0.26 ppm

No significant concentrations were found.

Hosszúhetény Marl (70)

Lithology: Grey marls and calcareous marls of “spotted marl” facies. The “spotted marl” character of the rocks reflects their marked bioturbation. In the lower part dark grey, spotted silty calcareous marls are characteristic. The silty marls contain millimetre size crinoidal and sandy lenses and crinoidal sandstone intercalations upsection. In the topmost part of the formation grey spotted marl and calcareous marl layers alternate.

Facies: the formation may have deposited in an open, relatively deep marine environment. Pelagic conditions are indicated by common occurrences of ammonites. It was probably formed in the deeper part of the open shelf, which was supplied of large amount of fine siliciclastics from distal sources.

Age: Upper Sinemurian–Lower Pliensbachian.

Thickness: 50–350 m, showing southward thickening trend in the Mecsek Mts.

Geochemistry:

2 samples (silty marl and limonitic marl) were analysed (Nos. 768, 774. of Appendix 1). Ranges are given below:

Au <2 ppb	As (6.84–13.2)
Ag (0.19–0.50)	Hg (0.12–0.16)
Sb (0.15–0.22)	Tl (0.17–0.20)

All concentrations are insignificant.

Mecseknádasd Sandstone (71)

“The formation consists of a rhythmic alternation of grey, bedded, fine-grained, mainly carbonate (crinoidal), graded sandstone, laminar calcareous siltstone, silty, spotted marl and calcareous marl (“Middle Liassic Sandstone Member”). The average grain size is decreasing upwards. The sandstone cement is calcareous, from the middle of the sequence with an increasing silica content, cherty lenses. The bioturbated, spotted calcareous marl in the upper part of the sequence contains ammonites. The facies is deep sublittoral, higher up it is shallow bathyal. The formation is divided into three (less frequently, four) units of member rank. The formation has a thickness ranging from a few tens of metres to 900 m” (HETÉNYI in CSÁSZÁR 1997).

Geochemistry:

One limonitic sandstone was sampled (No. 775. of Appendix 1). Gold was below detection limit, the other values (As 6.50 ppm, Ag 0.23 ppm, Hg 0.24 ppm, Sb 0.27 ppm and Tl 0.21 ppm) were insignificant.

Óbánya Siltstone (32)

Lithology: The lower part of the formation consists of grey, silty, bioturbated marl and siltstone. Its topmost part is made up by dark grey, black laminitic organic-rich shale with thin sandstone and crinoidal limestone inter-layers, pyritic limestone nodules. Thin-shelled bivalves and fish remnant are common.

Facies: Depositional environment of the lower part of the formation is a shallow bathial pelagic basin. The black shale member was formed under anoxic conditions. Since the anoxic layers show perfect correlation with the Toarcian anoxic event, establishment of the oxygen-depleted bottom-water conditions may be attributed to this wide spread event.

DULAI et al. (1992) reported 0.2 to 4.1% organic matter, pyrite and manganese with Cu (160 ppm), Pb (60 ppm), Mo (16 ppm), Ba (1600 ppm) and Mn (2500 ppm) from the Réka-völgy section.

Age: Upper Pliensbachian–Lower Toarcian

Thickness: 160 m as maximum. The thickness of the black shale member is about 10 m.

This formation was excluded from the predictive formation and no sampled after having negative results in 1996 from the similar Úrkút Manganese Ore.

Summary for the Mecsek Mountains:

The main geochemical features of the Mecsek Mountains are summarized in Table 5 and illustrated on Fig. 18. Here again we indicate that formations characterised by less than three samples are not plotted on Fig. 18. The Mecsek Mountains seem to have low potential as to gold and usually low maximum values for the other elements. There is only one formation above the established threshold for silver: the Hetvehely Dolomite (27).

Results and interpretations of stream sediment survey (Fig. 5) will be outlined in the following. Low to medium level additive anomalies are concentrated exclusively in the area of the Western Mecsek. Their internal architecture seems to follow both flanks of the Western Mecsek anticline. Major part of these anomalies are located over Triassic formations, indicated by the cells of No. 8026, 8027, 8032, 8038, 8043, 8044, 8045, 8046, 8051, 8053, 8054, 8055, and 8056. Some anomalous cells, like No. 8002, 8003, 8004, 8005, 8009 and 8013 are situated on Miocene clastic cover. The low level individual gold anomalies range between 2 and 72 ppb, but two cells over Triassic exhibit extrem high anomalies as follows: No.

Mecsek Mountains
Summary of geochemical parameters–median and maximum values.

Table 5

Form-code	Au (ppb)		Ag (ppm)		As (ppm)		Hg (ppm)		Sb (ppm)		Tl (ppm)		N
	Med.	Max.	Med.	Max.	Med.	Max.	Med.	Max.	Med.	Max.	Med.	Max.	
67	<2	3	0.29	0.91	2.32	19.2	0.05	0.08	0.125	0.13	0.21	1.09	4
27	<2	3	0.05	4.39	0.96	4.47	0.03	0.06	0.085	0.14	0.08	0.2	4
28	<2	3	0.15	0.62	3.03	38.5	0.06	0.08	0.11	0.21	0.12	0.45	7
30		<2	1.03m	5.1	7.99m	264	<0.02	2.1	0.22m	15.3	0.1m	0.17	2
31		<2	0.04	0.05	4.64	6.5	0.06	0.1	0.05	0.12	0.15	0.16	5
68	<2	7	0.07	0.39	13.7	29.2	0.14	0.3	0.56	1.79	0.25	0.93	6
69	<2	3	0.89	1.26	10.6	16.6	0.10	0.16	0.36	0.89	0.26	0.34	3
70		<2	0.19m	0.50	6.84m	13.2	0.12m	0.16	0.15m	0.22	0.17m	0.20	2

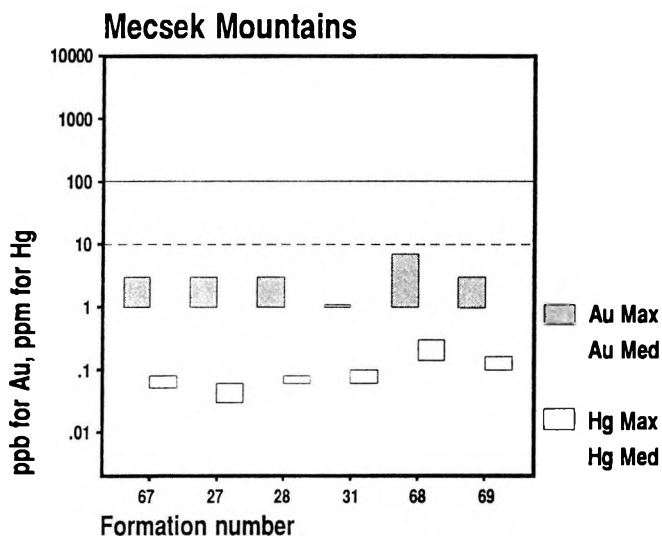
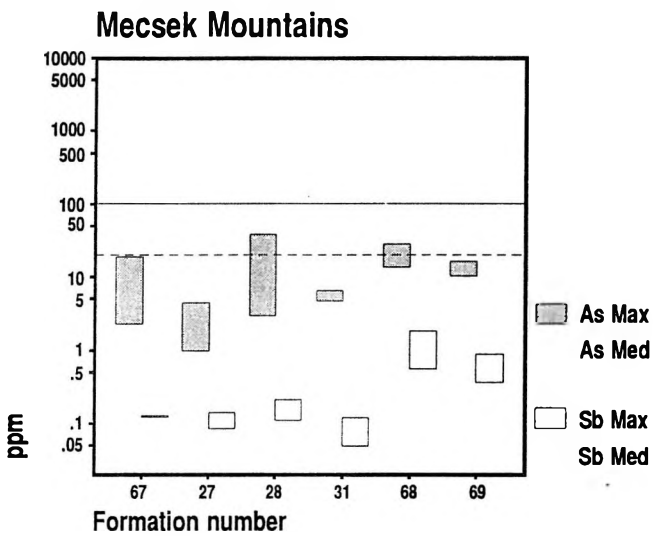
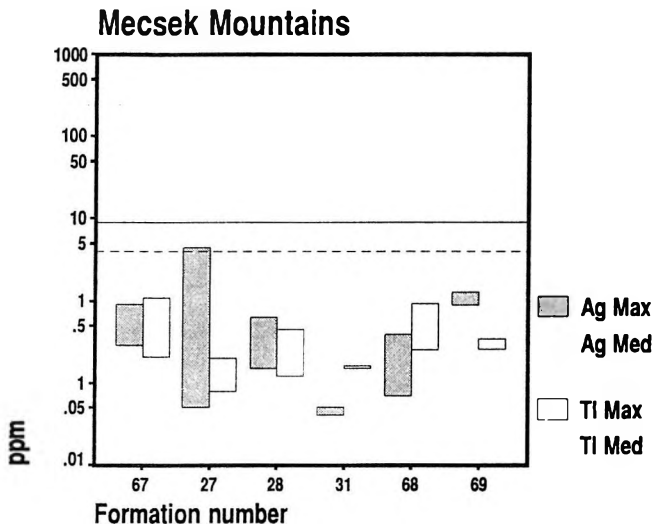
Remarks:

Formcode = the code number of the Formation:

67=Patacs Siltstone, 27=Hetvehely Dolomite, 28=Lapis Limestone, 30=Kozár Limestone, 31=Kantavár Fm., 68=Mecsek Coal, 69=Vasas Marl, 70=Hosszúhetény Marl

Med.=median value; Max.=maximum value; m=minimum values.

Fig. 18: The median (Med)–maximum (Max) concentration ranges of Au–Hg, As–Sb and Ag–Tl. Mecsek Mountains, Mesozoic formations



8045 with 1270 ppb Au near Mánfa and No. 8051 with 332 ppb Au near Magyarürög. Nature and host rock of these high level anomalies is unknown, although oreshows of malachite and azurite (Early Triassic: Patacs Siltstone, Magyarürög) and siderite (Late Triassic: Kantavár Formation, Mánfa Siderite Member) are known within the cells. Rock chip sampling of Triassic and Liassic formations (Appendix 1, Ns. 744–777) did not yield any gold anomalies.

Except of the anomalous stream sediment cells No. 8045 and 8051 of gold in the Mánfa and Magyarürög region, the entire Mecsek Mountains is considered unfavorable for Carlin-type gold mineralization.

3.4. Northeastern Range

The prospected areas and formations of the Northeastern Range will be evaluated using regional geological maps of Figs. 19 and 20 and regional stream sediment maps of Figs. 6 and 7.

3.4.1. Paleozoic

3.4.1.1. Silurian–Devonian–Carboniferous

Tapolcsány Formation (4)

The formation (Fig. 19) consists of grey, dark grey, black shale, siliceous shale and black, radiolarian lidite (jasper), with basic metavolcanite intercalations and graywackes at the basal horizons. It is rich in graphite and pyrite (up to 50%), and comprises of some iron ore and manganese bearing horizons (with hematite, goethite, siderite, pyrolusite and rodocrosite). The thickness of the anoxic deep-water sediments is about 400 m (FÜLÖP 1994).

Previous data of hard rock geochemistry (KORPÁS and HOFSTRA 1994): Ag (0.06–0.15 ppm), Ba (243–692 ppm), Cu (44–93 ppm), Mo (<2–18 ppm), Pb (7–27 ppm), Zn (74–203 ppm)

The thin iron ore lenses and related manganese are located in the radiolarian lidites (jaspers) and were mined between 1765 and 1779 (BALOGH and PANTÓ 1954, BALOGH 1964). Fe content of these lenses ranges between 14.98% and 45.86% with low values of Mn (0.36% to 8.08%) (BALOGH and PANTÓ 1954, ALFÖLDI et al. 1975). Fe- and Al phosphates, and jarosites (P₂O₅: 0.2 to 2.6%) are known both at the altered surface and within the formation (FÜLÖP 1994 and KOCH 1985). Reambulation of 22 adits and 11 small open pits including some reopenings between 1986 and 1991 resulted in low values of Fe: 12.77–15.43% and Mn: 5.28–6.96% (NAGY G. in FÜLÖP 1994).

Geochemistry:

60 samples have been collected to represent this formation (Nos. 1089–1091, 1094, 1096–1104, 1111–1146, 1175–1178, 1231–1234, 1260–1262. of Appendix 1). Limestones, pyritic limestones, sandstones, graphitic, pyritic and Mn-rich shales, dolomitic and jasper breccias were sampled. Ranges and medians are given below:

Au (<2–17)	<2 ppb	As (<0.2–468.0)	13.7 ppm
Ag (<0.02–44.0)	0.08 ppm	Hg (<0.02–2.30)	0.085 ppm
Sb (<0.1–79.7)	1.48 ppm	Tl (0.02–0.75)	0.145 ppm

The max. Au concentration is found in silicified dolomite breccia. Significant correlations have been determined for all pairs of elements except Tl–Au and Tl–Ag. Thresholds of anomalies have been detected for Au (12 ppb, five samples above it), As (70 ppm, 7 samples above it), Ag (2 ppm, one sample showing higher concentration) and Sb (7 ppm, with 20 samples above that limit). The formation was listed in the subanomalous group of formations.

Strázsahegy Formation (72)

The formation is made up by “green or greenish grey tholeitic basic metavolcanite, mainly volcanosedimentary schalstein, to a lesser extent lava with Silurian pelagic limestone and Lowermost Devonian crinoidal limestone olistolithes at one olistostroma level, and with frequent ferruginous metasomatism. Thickness: about 50 m” (KOVÁCS in CSÁSZÁR 1997).

Geochemistry:

Three tuff, pyroclastite and dolomite-quartzite samples (Nos. 1088, 1093 and 1095. of Appendix 1) were analysed. Ranges and medians are given below:

Au <2 ppb		As (1.01–9.05)	5.78 ppm
Ag (0.04–0.39)	0.06 ppm	Hg (<0.02–0.04)	0.02 ppm
Sb (0.17–0.62)	0.34 ppm	Tl (<0.02–0.11)	0.07 ppm

Gold was below detection limit in all samples.

Irota Formation (73)

It comprises of dark grey, black, graphitic, pyrite rich shales and metasandstones with horizons and lenses of lidites (jaspers) and veinlets of quartzite (FÜLÖP 1994). Slight hydrothermal alterations with traces of iron and manganese (up to 10,000 ppm) were reported by RAINCSÁKNÉ-KOSÁRY (1978) and uranium-shows explored in drillholes by KOVÁCS (1998) near to Irota and Gadna. Some ppb of Ag was detected in the basal horizons of the drillhole Alsóvadász 1. Thickness is about 350 m.

Geochemistry:

24 samples (limonitic, graphite shales, quartzites, quartz veins, cherty slate, breccias) were analyzed (Nos. 1278–1280, 1282–1286, 1309–1324. of Appendix 1). Ranges and medians are given below:

Au (<2–18)	<2 ppb	As (0.12–557.0)	3.39 ppm
Ag (<0.05–0.35)	0.07 ppm	Hg (<0.02–0.09)	<0.02 ppm
Sb (0.05–12.1)	0.38 ppm	Tl (<0.05–0.37)	0.115 ppm

The highest values appear in graphitic, limonitic and graphite shales within the formation. Significant correlation were found between Sb–As and Tl–Ag. Thresholds of anomalies were detected in the frequency distributions of Au, As and Sb. (Au 10 ppb/4 samples, As 50 ppm/5 samples and Sb 8 ppm/2 samples.) The formation was classified into the subanomalous group of formations.

Szendrőlád Limestone (2)

Characteristic rock-types of the formation are the following: 1) bioherm limestone of patchreef, b) limestone of basin facies, c) sandy and silty limestone of basin facies, d) metasandstone, metasiltstone and phyllite. The bioherm type consists of white and grey well bedded, massive, fine to coarse crystalline limestone rich in corals and crinoids. The limestone of basin facies is made up by bluish grey, massive, fine-crystalline, slightly argillaceous bedded limestone with conodonts. The sandy and silty limestone of basin facies is grey to dark grey in colour, and comprises of alternating beds of sandy or silty limestone and claystones, siltstones with some phyllites. Finally the group of metasandstones, metasiltstones and phyllites is built up by grey to dark grey, rhythmic and laminated metasiltstones and phyllites, intercalated with metasandstones and limestones. Slight syngenetic and early diagenetic dolomitization, furthermore presence of pyrite, kaolinite and few graphite is typical for every rock-types of the formation. Grade of metamorphism is: greenschist facies, quartz-albite-muscovite-chlorite subfacies. Thickness of the shelf and deep water intrashelf formation is about 400 m (FÜLÖP 1994).

Previous data of hard rock geochemistry (KORPÁS and HOFSTRA 1994): Ag (0.04–0.06 ppm), Ba (316–461 ppm), Cu (51–101 ppm), Mo (<2 ppm), Pb (5–13 ppm), Sb (2.5–16 ppm), Zn (5–83 ppm).

Small, partly underground iron ore deposit of some tens of tonnes was mined between 1913 and 1933 near to Szendrőlád. Fe content of the hematite and limonite ore is about 35–40% with 5–6% of Mn (FÜLÖP 1994). Jarosite was described at the contact with Late Miocene (Pannonian) sediments (JÁMBOR 1960).

Geochemistry:

15 samples (limestones, limonitic limestones, slate, limonitic sandstone, marble and phyllites) were sampled (Nos. 1273–1275, 1277, 1281, 1287–1289, 1291–1292, 1294–1296, 1306–1307. of Appendix 1). Ranges and medians are given below:

Au (<2–9)	<2 ppb	As (<0.02–22.7)	3.41 ppm
Ag (<0.05–0.35)	0.04 ppm	Hg (<0.02–0.12)	0.016 ppm
Sb (0.07–5.36)	0.58 ppm	Tl (<0.05–0.24)	0.04 ppm

Marble, limonitic limestone, limestone breccia and graphitic slate carry the relatively high concentrations within the formation. There are no anomalous values detected, except perhaps for Sb>2 ppm (there are 3 values above that). No correlation between any pairs of elements were found.

Uppony Limestone (3)

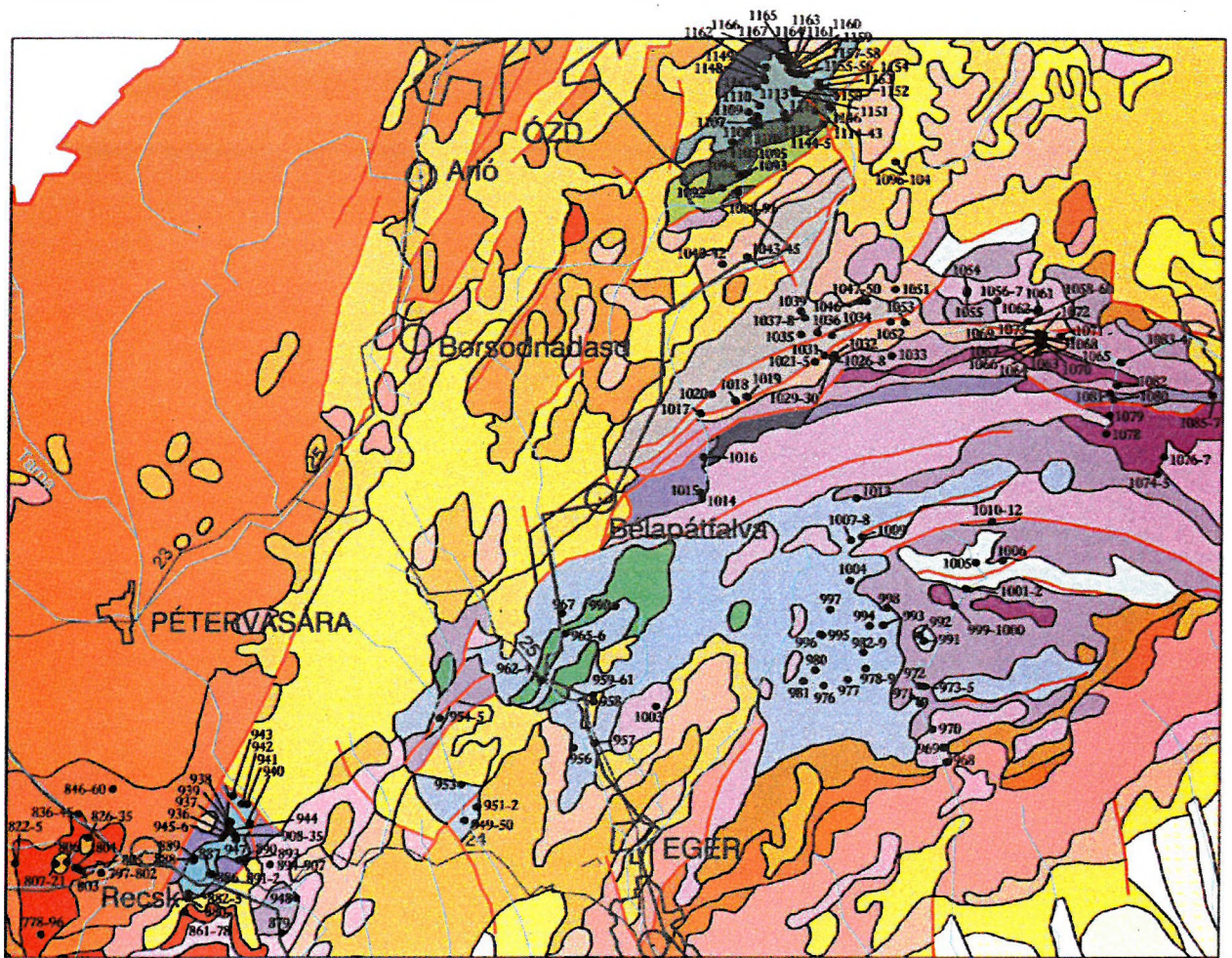
The formation consists of “light grey, sometimes light bluish grey bedded crystalline limestone of carbonate platform facies. Thickness: about 200 m” (KOVÁCS in CSASZÁR 1997).

Geochemistry:

Two samples (limestones) were only analysed (Nos. 1165. and 1167. of Appendix 1). Ranges are given below:

Au <2 ppb	As (1.51–9.73)
Ag (0.06–0.07)	Hg (0.06–0.09)
Sb (0.3–1.03)	Tl (0.03–0.04)

The concentrations are unimportant.



5 km

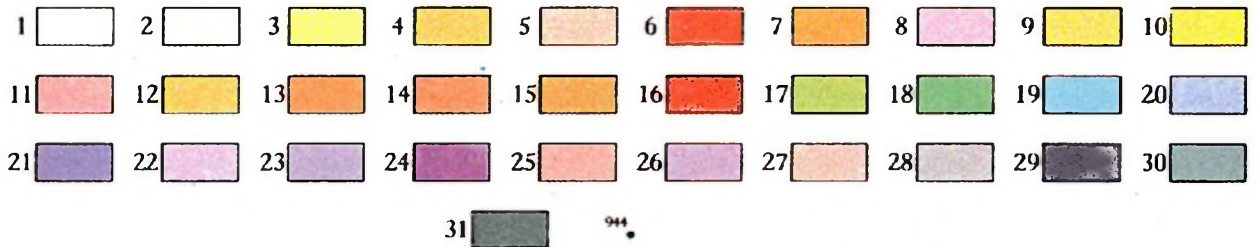
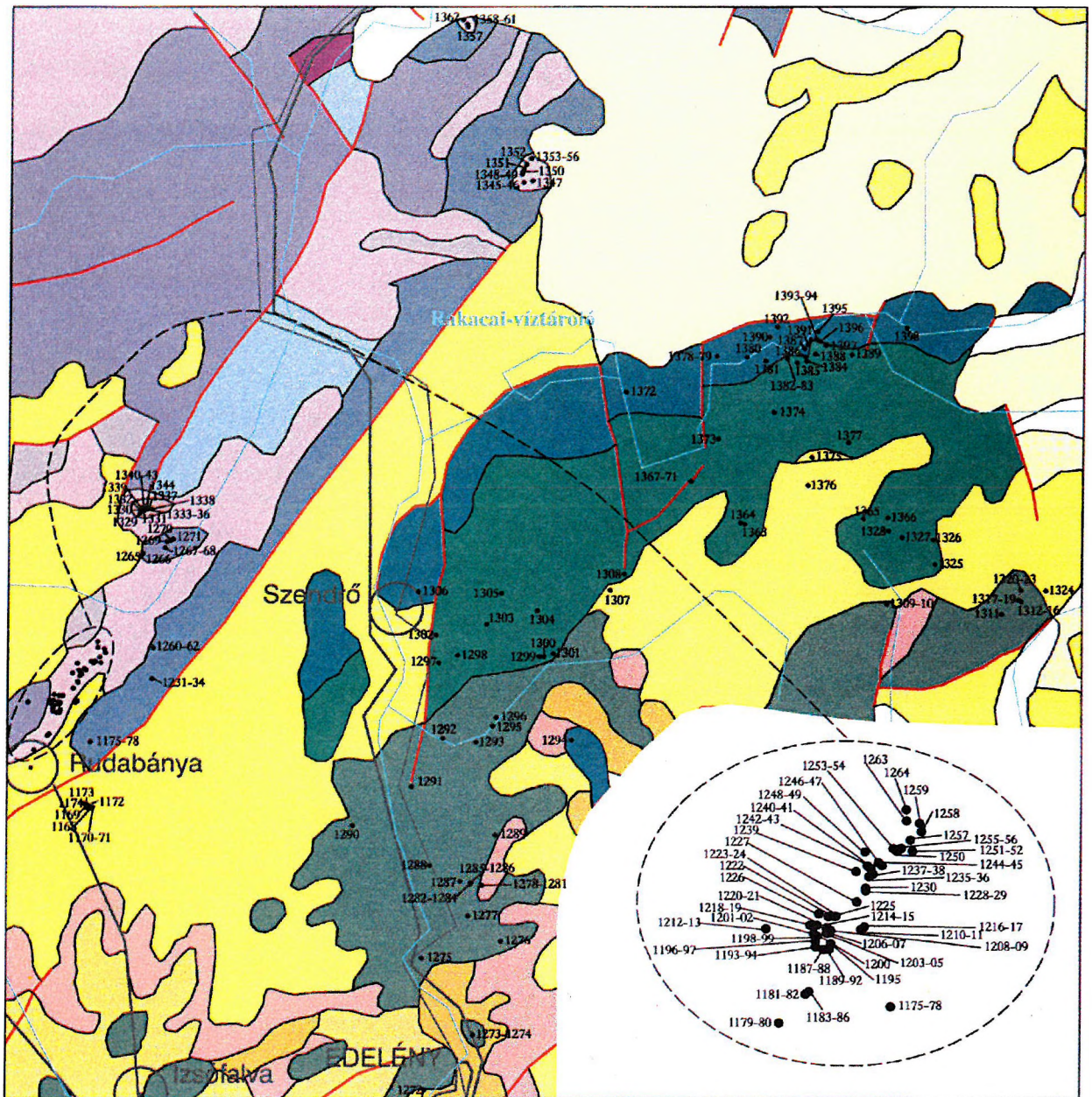


Fig. 19: Geological map of Recsk, Darnó Hill, Bükk Mountains and Uppony Mountains with Carlin gold sample sites

1. Holocene alluvial sediments, 2. Quaternary sediments, 3. Late Miocene–Pliocene sediments, 4. Middle–Late Miocene sediments, 5. Upper rhyolite tuff, 6. Mátra Andesite, 7. Middle Miocene calcareous sediments, 8. Middle rhyolite tuff, 9. Middle Miocene clastic sediments, 10. Early Miocene lignites, 11. Lower rhyolite tuff, 12. Early Miocene sediments, 13. Late Oligocene sediments, 14. Kiscell Clay, 15. Late Eocene sediments, 16. Recsk Andesite, 17. Senonian sediments, 18. Szarvaskő Basalt, 19. Darnóhegy Shale and Darnó Radiolarite, 20. Lökvolgy Shale, Monósbél Formation, Bányahegy Radiolarite and Oldalvolgy Formation, 21. Vesszős Shale, 22. Fehérkő Limestone, Berva Limestone, Kisfennsík Limestone, 23. Répáshuta Limestone, Rónabükk Limestone and Felsőtrárány Limestone, 24. Szentistvánhegy Metaandesite, Szinva Basalt, 25. Hámor Dolomite, 26. Gerennavár Limestone, Ablakoskövölgy Limestone and clastics, 27. Nagyvisnyó Limestone, Szentlélek Formation, 28. Szilvásszurdok Formation, Mályinka Formation and Tarófi Conglomerate, 29. Uppony Limestone, 30. Lázberc Formation, Abod Formation, 31. Tapolcsány Formation, Strázsahegy Formation, ●944 Carlin gold sample site



5 km

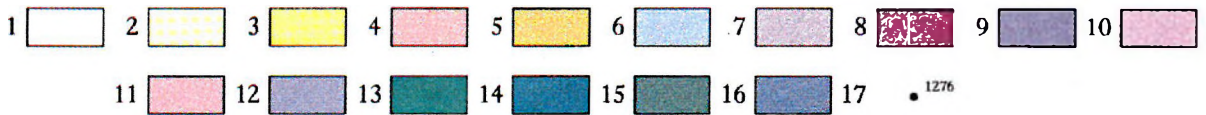


Fig. 20: Geological map of the Rudabánya and Szendrő Mountains with Carlin gold sample sites

1. Holocene alluvial sediments, 2. Quaternary sediments, 3. Edelény Clay, 4. Upper rhyolite tuff, 5. Early Miocene sediments, 6. Jurassic sediments, 7. Middle-Late Triassic sediments including Bodvarákó Formation and Tornaszentandrás Shale, 8. Middle Triassic ophiolites, 9. Gutenstein Dolomite, 10. Rudabánya Iron Ore, 11. Perkupa Anhydrite, 12. Early Triassic sediments, 13. Szendrő Phyllite, 14. Rakaca Marble, 15. Szendrőlad Limestone and Irota Formation, 16. Tapolcsány Formation, 17. •1180 Carlin gold sample site

Abod Limestone (74)

“..The formation is a white, bluish grey, violet grey, when weathered brownish yellow, metatuffitic limestone with typical chlorite-sericite mesh (“cipollino”), and with metatuffite and tuffitic calcareous schist, or basic metavolcanite intercalations. Its non-tuffitic variants are represented by bluish grey bedded limestone and brownish, flaser type limestone. (Partly corresponds to “Series II of Uppony” and “Series III of Szendrő”). Pelagic basin facies with conodonts. Thickness: approx. 200 m” (KOVÁCS in CSÁSZÁR 1997).

Geochemistry:

Three samples (limestones and a limonitic sandstone) were analysed (Nos. 1272, 1290. and 1304. of Appendix 1). Ranges and medians are given below:

Au (<2–6)	<2 ppb	As (3.03–15.0)	4.88 ppm
Ag (0.04–0.17)	0.06 ppm	Hg (<0.02–0.29)	<0.02 ppm
Sb (0.11–0.72)	0.49 ppm	Tl (0.06–0.12)	0.12 ppm

There are no significant concentrations of any element. The 6 ppb gold is in the limonitic sandstone.

Szendrő Phyllite (75)

The formation consists of “a turbiditic sequence (“Series II of Szendrő”), in the lower part of which (Meszes Member), graded sandstone, sandstone schist, limestone-olistostroma and allodapic limestone levels are intercalated into dark-grey, black phyllite. Its middle part is characterised by distal sandstone turbidites in the phyllite (Pestavölgy Member). Its upper part is formed by almost monotonous, dark-grey, black phyllite (Palabánya Member). It represents the Variscan “flysch” period. The major part of the limestone olistostromes derive from the Verebeshegy limestone (Rakaca Formation) and the Rakaca Marble. Thickness: 500 to 600 m” (KOVÁCS in CSÁSZÁR 1997).

Grade of metamorphism is: greenschist facies, quartz-albite-muscovite-chlorite subfacies. Veinlets of quartzite, presence of pyrite and metaanthracite-graphite (0.5–1.5%) was described by FÜLÖP (1994).

Geochemistry:

41 samples were collected from this Formation (the sampled mixed lithology: limonitic shales, limestones, quartzites, sandstones, see Nos. 1293, 1297–1303, 1305, 1308, 1325–1328, 1363–1365, 1367–1371, 1373–1374, 1377–1380, 1382–1389, 1391, 1393–1394, 1396–1397. of Appendix 1). Ranges and medians are given below:

Au (<2–7)	<2 ppb	As (0.26–25.0)	3.84 ppm
Ag (<0.02–0.38)	0.08 ppm	Hg (<0.02–0.34)	0.02 ppm
Sb (0.05–3.61)	0.39 ppm	Tl (<0.02–0.78)	0.09 ppm

Limestone, black shale and limonitic slate contain the relative high values within the Formation. Significant correlation was found for Sb–Au at significance level 0.01. Anomalous value was detected only for Sb (threshold = 3 ppm).

Rakaca Marble (76)

The formation consists of “white marble with bluish grey steaks, of carbonate platform facies (characterised by a lithology similar to that of the Rakacaszend Marble). The thickness of the formation is about 200 m. It interfingers through a transitional facies (“foamy marble”) with a dark bluish grey, finer crystalline limestone of basin facies (Verebeshegy Limestone Member)” (KOVÁCS in CSÁSZÁR 1997).

Geochemistry:

Marble, ankeritic, pyritic limestones and limestones were collected and analysed (8 samples altogether, see Nos. 1276, 1366, 1372, 1381, 1390, 1392, 1395, 1398. of Appendix 1). Ranges and medians are given below:

Au <2 ppb		As (0.39–23.0)	1.18 ppm
Ag (<0.02–0.11)	0.045 ppm	Hg (<0.02–0.1)	<0.02 ppm
Sb (0.21–2.87)	0.34 ppm	Tl <0.02–0.21	0.025 ppm

Gold is below detection limit in all samples. Highest values of other elements are found in ankeritic limestone and in pyritic limestone. There are no anomalous concentrations. No significant correlations were detected between any pairs of elements.

Lázbérc Formation (77)

The formation is made up by alternating strata of grey, dark grey well bedded sometimes laminated micritic limestone and of grey, dark grey calcareous shales with a single horizon of calcareous sandstone and of intraformational conglomerate and breccia. Content of organic matter and pyrite is about 1%. Thickness is about 200 to 300 m. (FÜLÖP 1994).

Geochemistry:

Predominantly limestones (limonitic limestones) and a shale were sampled (11 samples altogether, see Nos. 1152–1161, 1163. of Appendix 1). Ranges and medians are given below:

Au <2 ppb		As (1.17–14.6)	3.06 ppm
Ag (<0.02–0.06)	0.03 ppm	Hg (<0.02–0.14)	<0.02 ppm
Sb (0.0–1.0)	0.27 ppm	Tl (<0.02–0.08)	0.05 ppm

There are no anomalous values. There is a good and significant correlation between Sb–As.

Szilvásvár Formation (6)

The formation consists of “a series showing a fine rhythmic alternation of dark grey or black turbiditic sandstone, siltstone and clay, with intercalations of fine grained polymict conglomerate and sandstone with pebbles. The beds contain no fossils. The rock became foliated by the effect of anchizonal metamorphism. The thickness may exceed 1,000 m. The age is unknown. The formation underlies the Mályinka Formation” (PELIKÁN in CSÁSZÁR 1997). Small amount of dispersed organic matter (partly graphite) and veinlets of quartzite are common (FÜLÖP 1994).

Previous data of hard rock geochemistry (KORPÁS and HOFSTRA 1994): Ag (0.06–0.24 ppm), Ba (244–381 ppm), Cu (55–327 ppm), Mo (3 ppm), Pb (10 ppm), Zn (6–1047 ppm).

Geochemistry:

Shales, quartzites, conglomerates (9 samples) represent the formation (Nos. 1017–1020, 1034–1038. of Appendix 1). Ranges and medians are given below:

Au <2 ppb		As (4.96–24.6)	11.9 ppm
Ag (<0.1–0.24)	0.03 ppm	Hg (0.04–0.21)	0.08 ppm
Sb (0.24–1.61)	0.64 ppm	Tl (<0.05–0.34)	0.18 ppm

Conglomerates contain the highest values for Sb, As and Hg within the formation. Sb–As was found to be well correlated.

Mályinka Formation (6)

The formation is made up “by alternation of shallow marine, occasionally poorly stratified, terrigenous, fine-grained clastics and limestone. The clastics contain a mixture of dark-grey to black sand, silt and clay in a varying proportions, with polymict quartzite conglomerate lenses. The limestone bodies have a thickness of 10 to 50 m. The limestone is light or dark grey, with algal, coralline, crinoideal and fusunilida facies. The rock became foliated by the effect of anchizonal metamorphism. Maximum thickness: 400 m” (PELIKÁN in CSÁSZÁR 1997).

Previous data of hard rock geochemistry (KORPÁS and HOFSTRA 1994): Ag (0.06–0.24 ppm), Ba (244–381 ppm), Cu (55–327 ppm), Mo (3 ppm), Pb (10 ppm), Zn (6–1047 ppm).

Geochemistry:

15 samples (shales, bituminous shale, limestones, quartzites and sandstone) were analysed (Nos. 1027–1029, 1031, 1039, 1046–1050, 1052–1053, 1058–1060. of Appendix 1). Ranges and medians are given below:

Au <2 ppb		As (1.15–51.3)	5.32 ppm
Ag (<0.1–0.86)	0.03 ppm	Hg (<0.02–0.32)	0.0923 ppm
Sb (<0.1–1.22)	0.36 ppm	Tl (<0.05–0.2)	0.06 ppm

Gold was below detection limit in all samples. There were no anomalous values found. There is only an Sb–Ag correlation significant at 0.01 level.

Tarófü Conglomerate (78)

The some metres thick siliciclastic conglomerate lense is composed of well sorted and rounded quartz and quartzites, metasandstone, lidite with some volcanics and crystalline schist. Dominant grain-size of pebbles in the clast supported and silicified conglomerate is about 4–6 cm (FÜLÖP 1994).

Geochemistry:

5 conglomerate samples (Nos. 1021–1025. of Appendix 1) were analysed for this formation. Ranges and medians are given below:

Au <2 ppb		As (5.55–17.8)	13.4 ppm
Ag <0.1		Hg (0.0096–0.1727)	0.0372 ppm
Sb (0.13–0.28)	0.19 ppm	Tl (0.06–0.25)	0.09 ppm

Gold and silver are below detection limits in all samples. No anomalous values were found in this formation. The elements do not correlate with each other.

3.4.1.2. Permian

Perkupa Anhydrite (79)

The pyrite rich formation consists of light and dark grey bodies of gypsum and anhydrite, in alternance with grey brecciated dolomite, grey, greenish siltstones and dark grey to black shales (FÜLÖP 1994). In the melange zone of the abandoned Perkupa mine serpentinite and diabase-gabbro bodies (MÉSZÁROS 1954 and 1961) of ophiolites were described.

Geochemistry:

16 samples (shales with gypsum, pyritic shales, limonitic breccia, gypsum, anhydrite, veinlets of quartz) were collected and analysed (Nos. 1329–1344. of Appendix 1). Ranges and medians are given below:

Au (<2–5)	<2 ppb	As (0.74–84.6)	9.97 ppm
Ag (0.03–0.3)	0.065 ppm	Hg (0.08–4.63)	0.19 ppm
Sb (0.09–2.75)	0.555 ppm	Tl (0.06–0.19)	0.11 ppm

Pyritic shale and shale and limonitic breccia contain elevated concentrations within the formation. There are no anomalous values (with the exception of Hg). Good correlation was found for Tl–As.

Szentlélek Formation (80)

“Coastal plain sandstone, indicating an arid climate, and an evaporite sequence of sabkha facies. Its lower part with a thickness of 100 to 300 m includes whitish-grey, green or red sandstone and siltstone with violet spots (Farkasnyak Sandstone Member). The upper part is 120 to 150 m thick green mudstone, dolomite, gypsum-anhydrite (Garadnavölgy Evaporite Member). The top and bottom of this member is green mudstone with red strips. The rest of the member consists of frequently alternating layers of green mudstone, dolomite gypsum and anhydrite, with algal and foraminiferal limestone intercalations in the middle. The age of the formation is assumed (to be Middle Permian). It is located in the underlying of the Nagyvisnyó Formation” (PELIKÁN in CSÁSZÁR 1997).

Uranium ore shows with casolite, uranophane and uraninites in the green sandstones of the Farkasnyak Member were explored by the Mecsek Uran Ore Company between 1976 and 1982 in surface trenches and drillholes of the Bán-völgy area (FÜLÖP 1994). Rock chip sampling of the related polymetallic (chalcopyrite, galena, pyrite) mineralization resulted in the following metal concentrations: Cu: 0.03–0.13% (average of 12 samples: 0.06%), Pb: 0.37–5.10% (average of 75 samples: 0.74%), Zn: 0.01–0.71% (average of 75 samples: 0.01%), Ag 0–326 ppm (average of 75 samples: 69 ppm), As: 10–360 ppm (average of 75 samples: 90 ppm). Two samples from the malachite and azurite show in the Nagyvisnyó railroad cut section yielded the following results: Cu: 0.39–1.25%, Pb: 0.01–0.37%, Zn: 0.03–0.07%, Fe: 1.90–2.00%, S: 0.00% (PELIKÁN 1996).

Geochemistry:

6 samples (claystone with malachite, quartzite, limestone, sandstone) were analysed (Nos. 1026, 1030, 1032, 1040–1042. of Appendix 1). Ranges and medians are given below:

Au (<2–234)	<2 ppb	As (3.4–533.0)	22.0 ppm
Ag (<0.1–1.49)	0.55 ppm	Hg (0.0155–0.814)	0.31 ppm
Sb (<0.1–12.5)	2.43 ppm	Tl (<0.05–0.81)	0.37 ppm

There is only one positive value for gold (234 ppb) in a claystone with malachite. There are anomalous values (2) for arsenic, above 100 ppm.

Nagyvisnyó Limestone (5)

The formation consists of dark grey, black thin bedded, stylolitic, bituminous (0.6–0.8% TOC), pyritic, frequently dolomitized limestone with thin intercalations of claymarl and horizons of black chert-lenses. It is rich in fossils, like algae, foraminifera, bivalves, gastropods, nautiloids, trilobites, bryozoans, brachiopods, crinoids, echinoids, conodonts and ostracodes. Facies: restricted lagoon. Thickness: 200–270 m (FÜLÖP 1994).

Previous data of hard rock geochemistry (KORPÁS and HOFSTRA 1994): Ag (0.03–0.11 ppm), Ba (330 ppm), Cu (60–73 ppm), Mo (3 ppm), Pb (5–12 ppm), Zn (143–174 ppm).

Geochemistry:

Predominantly limestones, chert, shale and dolomite were sampled (20 samples, see Nos. 1033, 1043–1045, 1051, 1092, 1105–1110, 1147–1151, 1162, 1164, 1166. of Appendix 1). Ranges and medians are given below:

Au <2 ppb		As (<0.2–6.24)	2.1 ppm
Ag (<0.02–1.35)	0.3 ppm	Hg (<0.02–0.74)	0.02 ppm
Sb (0.08–2.02)	0.26 ppm	Tl (<0.02–0.15)	0.04 ppm

There is no positive value for gold. There is perhaps one anomalous value for Ag (threshold=1 ppm). No significant correlation was found between any pairs of elements.

3.4.2. Mesozoic

3.4.2.1. Triassic

Gerennavár Limestone (81)

The formation is made up by "light grey, greyish-brown, ooidic and laminar limestone formed in the outer, heavily agitated part of the shelf and its more protected basins, with beige marl intercalations. It has suffered anchizonal metamorphism. It forms the continuation of the Nagyvisnyó Limestone with a rapid transition. Thickness: 140 m" (PELIKÁN in CSÁSZÁR 1997).

Geochemistry:

There is only one sample (No. 1061 of Appendix 1) from this formation. Gold was below detection limit, As=1.07 ppm, Ag=0.07 ppm, Hg=0.04 ppm, Sb=0.08 ppm and Tl=0.02 ppm. These concentrations are insignificant.

Ablakoskővölgy Limestone (82)

"It consists of shallow sublittoral, bedded, variegated sandstone, laminar limestone, clay marl and calcareous marl. The formation suffered anchizonal metamorphism. The formation can be divided into four members which are as follows: at the bottom there is a variegated sandstone containing sandy limestone lenses (Ablakoskővölgy Sandstone Member), this is overlain by limestone with marl intercalations (Lillafüred Limestone Member), followed by the Savósvölgy Marl Member with frequent alternation of calcareous marl and marly limestone, and at the top there is dark-grey limestone with worm traces (Újmassa Limestone Member). Thickness: about 300 m" (PELIKÁN in CSÁSZÁR 1997).

Geochemistry:

Only one sample was collected (No. 1071 of Appendix 1). Gold was below detection limit, As=1.87 ppm, Ag=0.04 ppm, Hg=<0.02 ppm, Sb=0.19 ppm and Tl=0.11 ppm. These concentration values are insignificant.

Rudabánya Iron Ore (7)

The main host rocks (Bódvaszilás Sandstone, Szin Marl, Szinpetri Limestone and Gutenstein Dolomite) of the ore formation will be described as follows:

Bódvaszilás Sandstone

Lithology: It is made up by alternation of lilac-reddish locally greenish grey sandstone, siltstone and shale layers. On the bedding plains ripple marks and wrinkle marks are common. Ripple cross lamination also occurs. Bivalve coquinas are characteristics, generally on the bedding surfaces. In the sandstones the quartz grains are predominant with small amount of feldspar and muscovite. Ooidic limestone intercalations are common in the upper part of the formation.

Facies: shallow marine, intertidal–subtidal, storm dominated siliciclastic ramp facies.

Age: Lower Triassic (Induan)

Thickness: the formation is known in the Aggtelek Mts. in the Silice Nappe and in the Rudabánya Mts. in the Bódva Nappe. Its thickness is 200–300 m.

Szin Marl

Lithology: Grey marl, shale, calcareous marl. In the lower part of the formation, light brownish grey ooidic, sandy limestone and greyish brown cross-bedded sandstone and siltstone interbeds whereas its middle part lilac ooidic limestone interlayers with bivalve coquinas are characteristic. On the bedding plains of the marl layers, trace fossils are common. Ripple cross lamination also occurs.

Facies: shallow to deeper ramp facies with ooid sand shoals on the edge of the inner ramp. Behind the ooid shoals disaerobic conditions came into existence. On the mid-ramp crinoidal-ooidic storm sheets were deposited with outward decreasing grain size. The marl layers were formed on the deeper outer ramp under the storm wave base.

Age: Lower Triassic (Olenekian)

Thickness: It is known in the Aggtelek and Rudabánya Mts. in a thickness of 300–350 m.

Szinpetri Limestone

Lithology: It is composed of dark grey typically vermicular limestones. In its lower half marl and clay marl intercalations occur subordinately. The intense bioturbation masks the original sedimentary structures. Bivalve coquinas cover the bedding planes, occasionally. In the upper half vermicular limestones alternate with laminated ones. Lamination is expressed in an alternation of lighter and darker streaks. Slump structures are common in both rock types.

Facies: Shallow, restricted inner ramp–ramp lagoon. Weak circulation may have led to density layering and probably hypersaline bottom conditions came into being. This is reflected in the poverty of biota.

Age: Lower Triassic (Upper Olenekian)

Thickness: Its thickness in the Aggtelek facies unit of the Aggtelek Mts. is 150–200 m, whereas in the Bódva facies unit it is strongly reduced.

The history of mining, description of geological setting and ore deposits of the Rudabánya Iron Ore is discussed in details by HOFSTRA et al. (1999), therefore only the Carlin gold aspects will be outlined here. This formation was considered as the number one candidate for Carlin gold deposition in previous screening (KORPÁS and HOFSTRA 1994). This estimation was based on anomalous concentrations and distribution of almost all elements typical for the Carlin suite, like: Au (traces), Ag (2.7 ppm), Sb (25 ppm), Hg (16 ppm), As, Tl, with presence of Cd (0.7 ppm) and Se.

Geochemistry:

There are 96 data for Au, As, Ag and Sb and 67 data for Hg and Tl to characterise the formation (see Nos. 1179–1230, 1235–1259, 1263–1264, 1345–1346, 1348–1362. of Appendix 1). The lithology is not known for most parts of the samples. In other cases hematite, siderite, iron crusts infilling, dolomite, dolomite breccia, shale, cherty dolomite were sampled. Ranges and medians are given below:

Au (<2–630)	3 ppb	As (0.72–8110)	187.0 ppm
Ag (0.06–520)	18.35 ppm	Hg (0.07–3400)	11.4 ppm
Sb (0.27–13354.0)	154.0 ppm	Tl (0.03–9.46)	0.36 ppm

It was possible to establish thresholds for anomalies. Threshold values are the following. Au—15 ppb, As—130 ppm, Ag—22 ppm, Hg—20 ppm and Sb—35 ppm. Taking all samples into consideration good correlations were found for almost every pairs of elements. The exceptions are: Tl–Au, Tl–Ag and Tl–Sb.

The anomalous subpopulation for gold (Au >15 ppb) is characterised by the following parameters: range and median: (16–630), 50 ppb; mean=93.2 ppb. There is another subpopulation between 15–140 ppb. Four values seem really anomalous (of 220, 230, 560 and 630 ppb).

In the same population (Au >15 ppb) there are at least two different populations for Ag: one is from 22–164 ppm and the other is above Ag=164 ppm. The background for Ag can be characterised by the following parameters: range and median: (0.06–18.7), 1.75 ppm; mean: 4.36 ppm.

Several subpopulations can be distinguished for As above its threshold (130 ppm). The range and median values for the background are: (0.72–125.0), 37.0 ppm; the mean: 49.5 ppm.

There are many populations for Hg and Sb merging together. Background and main parameters for Hg are: background: <25 ppm; range and median: (0.07–22.2), 2.2 ppm; mean: 4.9 ppm. Background and main parameters for Sb: background: <35 ppm; range and median: (0.27–29.2), 7.73 ppm; mean: 10.25.

In the anomalous subpopulation of gold (Au >15 ppb) the following correlations were positive and significant: Sb–Ag, Hg–Au, Sb–Au and Sb–Hg. Tl has significant and negative correlations with all of the other four elements. The formation is classified into the anomalous group of formations and recommended for further, more detailed explorations.

Gutenstein Dolomite (24)

Lithology: It is made up by dark grey or black thin bedded, bituminous limestones or dolomites as well as alternation of limestone and dolomite layers. Lamination (fenestral laminated structure) is common in the dolomites. In addition to the most typical mudstone and bioclastic wackestone texture types, ooidic textures also occur. Centimetre thick grey marl interlayers are characteristic.

Facies: A large part of the formation (bituminous mudstones) represents restricted lagoon facies. The fenestral laminated carbonates were formed in a peritidal environment whereas the ooidic layers may have formed at the margin of the lagoon.

Age: Lower Anisian

Thickness: It is widely extended in the Aggtelek and Rudabánya Mts. It is known in the Aggtelek and Bódva facies units and also in the slightly metamorphosed structurally deeper nappes. Its thickness is about 250 m.

Previous data of hard rock geochemistry (KORPÁS and HOFSTRA 1994): Ag (1.7 ppm), As (≤10 ppm), Ba (3556 ppm), Cu (857 ppm), Mo (3.1 ppm), Pb (230 ppm), Sb (99.7 ppm), Tl (≤1 ppm), Zn (117 ppm).

Geochemistry:

Dolomite, bituminous dolomite and dolomite breccia (7 samples) were analysed (Nos. 1265–1271. of Appendix 1). Ranges and medians are given below:

Au <2 ppb		As (0.47–2.86)	0.74 ppm
Ag (0.69–80.02)	0.05 ppm	Hg (0.03–0.11)	0.05 ppm
Sb (0.23–1.41)	0.43 ppm	Tl (0.03–0.04)	0.04 ppm

Gold is below detection limit in all samples. The elevated concentrations within the formation are found in dolomite breccia. No correlation of elements was detected.

Bodvarákó Formation (25)

The formation represents “deep-water anoxic basin facies consisting of alternating medium to dark grey platy limestone and black chert beds, with intercalations of grey, cherty dolomarl, cherty siltstone, mudstone, marl and limestone layers. Thickness: about 50 m” (KOVÁCS–LESS–HAAS in CSÁSZÁR 1997).

It was canceled from the list of predictive formations and not sampled after studying the Carlin gold deposits in Nevada, in 1995.

Tornaszentandrás Shale (26)

The formation consists of “black shale and silty shale of pelagic basin facies, foliated to foliae of 2 to 10 mm, locally slightly calcareous, rarely with transverse schistosity. Thickness: 30 to 100 m” (LESS and HAAS in CSÁSZÁR 1997).

It was excluded from among the predictive formations and not sampled after studying the Carlin gold deposits in Nevada, in 1995.

Hámor Dolomite (22)

Lithology: Grey, locally dark grey dolomite. Massive or thick bedded parts alternates with fenestral laminated stromatolitic beds. In some cases, the original texture (mudstone, bioclastic wackestone) is recognisable but generally only dolosparites are visible as a consequence of the dolomitization.

Facies: shallow marine inner carbonate platform. The thick bedded rocks may have formed under subtidal conditions whereas the stromatolitic layers indicate peritidal environment.

Age: Lower–Middle Anisian

Thickness: It is widely extended in the Bükk unit. Its thickness is 350–450 m.

Previous data of hard rock geochemistry (KORPÁS and HOFSTRA 1994): Ag (2.4 ppm), As (16 ppm), Ba (170 ppm), Cu (47 ppm), Mo (≤ 2.5 ppm), Pb (280 ppm), Sb (62.7 ppm), Tl (≤ 1 ppm), Zn (403 ppm).

Geochemistry:

Bituminous and pyritic dolomites, dolomarls (11 samples) were collected and analysed from this Formation (Nos. 972, 1064–1070, 1072–1073, 1083. of Appendix 1). Ranges and medians are given below:

Au <2 ppb		As (0.56–8.7)	1.97 ppm
Ag (<0.02–0.14)	0.03 ppm	Hg (<0.02–2.22)	0.10 ppm
Sb (0.13–2.17)	0.45 ppm	Tl (<0.02–0.24)	0.12 ppm

Gold was below detection limit in all samples. Bituminous dolomite yielded almost all elevated values for the elements studied. There are no anomalous values. Good correlation was found for Tl–Sb.

Szentistvánhegy Metaandesite (83)

The formation is made up by “a stratovolcanic sequence mostly consisting of neutral, slightly acidic (andesitogenic-dacitogenic) lava and volcanoclastics of various origin (“Szentistvánhegy porphyryte”). Slightly more basic (basalto-andesite) or more acidic (rhyolite) versions are also occur in a minor capacity. Thickness: 200 to 350 m” (SZOLDÁN–PELIKÁN–HAAS in CSÁSZÁR 1997)

Geochemistry:

Quartz porphyries, porphyrites, andesite and tuff (6 samples) were analysed to represent the formation (Nos. 1057, 1063, 1074, 1076, 1077, 1084. of Appendix 1). Ranges and medians are given below:

Au <2 ppb		As (0.65–72.8)	2.04 ppm
Ag (<0.05–0.11)	0.025 ppm	Hg (<0.02–0.0294)	0.0072 ppm
Sb (0.08–0.78)	0.185 ppm	Tl (0.06–0.32)	0.11 ppm

Gold was below detection limit in all samples. The elevated values of most of the elements were found in quartz porphyry.

Parád Complex (84)

The formation will be described after FÖLDESSY JNÉ. (1975) and ZELENKA (1996). It consists of the following lithological units, from the top to the bottom: 1) Upper Shale, 2) Upper Quartzite, 3) Upper Limestone, 4) Middle Quartzite, 5) Lower Limestone, 6) Lower Quartzite, 7) Lower Shale. Total thickness is about 1,000 m.

The Upper Shale consists of thin bedded to laminated pyritic shales, with intercalations of cherty horizons, sandstone, marl, limestone, dolomite and dolomarl. It is strongly folded, with slump structures and related internal

breccias. The ooidic limestone horizons frequently contain fragments of molluscs, foraminifera, echinoids and ostracodes. Age: Carnian to Norian, thickness: 600 m.

The Upper Quartzite comprises of monotonous, shaly and laminated pyritic radiolarian chert with a few limestone and dolomite intercalations. Its thickness is about 40 to 250 m.

The Upper Limestone is made up by grey, flaser bedded micritic pyritic limestones interbedded with shales, marls, and in a smaller amount with dolomite and nodular stylolitic chert. Bivalve coquinas are characteristic, brachiopods, crinoids, echinoids, ostracodes and radiolarians also occur. Age: Ladinian, thickness: 100 to 400 m.

The Middle Quartzite is similar to the Upper Quartzite with a thickness of about 85 to 220 m.

The Lower Limestone is made up by grey, massive, micritic, stylolitic and pyritic limestones, interbedded frequently with shales and horizons of radiolarian chert, furthermore with thin dolomites and marls. In some ooidic horizons foraminifera, echinoids and ostracodes were encountered. Age: Ladinian, thickness: 100 m

The Lower Quartzite is about 50 m thick and consists of grey, massive, brecciated jasper with a few argillites.

Lithology of the Lower Shale is similar to the Upper Shale, but rich in organic matter. Its thickness surpasses 43 m.

The Parádk Complex is the host rock of the shallow intrusive body of the Late Eocene Recsk Andesite and the related large porphyry copper and skarn Cu–Zn deposit at Recsk (BAKSA 1975). According to BARTÓK and NAGY (1992) its estimated reserves are 159.3 Mt with Cu content of 1.14%. Above the porphyry copper deposit another disseminated gold deposit of high sulfidation type (with enargite and luzonite) was discovered recently in the old copper mine of Recsk–Lahóca. The proven reserves of this Late Eocene volcanic centre related deposit are 16.5 Mt with 2.01 ppm average content of gold (FÖLDESSY 1997).

Previous sporadic chip sampling of the formation in the drillhole cores of the Recsk copper deposit resulted in anomalies of Au (<1.05 ppm), Ag (<418 ppm), As (<580 ppm), Sb (<1080 ppm), Tl (<1 ppm), Se (<300 ppm) (ZELENKA 1996). Anomalies of arsenic (<1900 ppm), thalium (<15 ppm), antimony (<1600 ppm), selenium (<71 ppm), telur (<400 ppm) and barium (<15,000 ppm), furthermore traces of realgar and native sulfur in the formation were reported by CSILLAG (1975). Statistical analysis of geochemical data carried out by FÜGEDI et al. (1991) after complementary chip sampling on cores of the Recsk drillholes (Rm 10, 15, 26, 27, 33, 34, 37, 47, 48, 52, 53, 57, 58, 59, 63, 97, 124) resulted in discovery of further Au, Ag, As and Sb-anomalies. In the population of the almost 100 anomalous samples the gold ranges from some tens to 1210 ppb, the silver from some ppm to 50 ppm, the arsenic from some tens to 3000 ppm and antimony from 1 to 3000 ppm (Recsk ore analysis: pers. comm. of FÜGEDI U. in 1997).

Geochemistry:

Jasper breccias, shales, silicified and pyritic shales, limestones, limestone breccias, silicified limestone breccias, marl, tuff, skarn were sampled (66 samples, see Nos. 780–845. of Appendix 1). Ranges and medians are given below:

Au (<2–84)	3.5 ppb	As (<1.0–181.0)	19.9 ppm
Ag (<0.05–10.6)	0.05 ppm	Hg (0.0022–1.903)	0.0514 ppm
Sb (<0.1–108.0)	0.57 ppm	Tl (<0.05–0.82)	0.24 ppm

Jasper breccias and shale yielded the elevated concentrations and anomalies within the formation. Threshold values were established for Au, As, Ag and Sb. The threshold concentrations and the number of samples above these values are listed below: Au–17 ppb, 5 samples; As–100 ppm, 3 samples; Ag–2.5 ppm, 1 sample and Sb–10 ppm, 4 samples. Significant correlations were found for Au–As, Hg–As, Sb–As, Tl–As, Hg–Au, Sb–Au, Sb–Hg, Tl–Au and Tl–Hg.

Fehérkő Limestone (85)

The formation consists of “light-grey, massive or bedded limestone. Some parts are characterised by Lofer-cyclic carbonate platform facies. The grade of the metamorphism of the formation ranges from the deep diagenetic zone to the high temperature part of the anchizone, and varies from area to area. Thickness: about 400 m” (PELIKÁN and HAAS in CSÁSZÁR 1997).

Geochemistry:

One pyritic limestone was sampled (No. 1082 of Appendix 1). Gold was below detection limit, As=2.19 ppm, Ag=0.04 ppm, Hg=0.02 ppm, Sb=0.31 ppm and Tl=0.05 ppm. These values are insignificant.

Berva Limestone (86)

It is a “white, light-grey, grey platform limestone, with reef and cyclic lagoonal facies. Maximum thickness: 350 m” (HÍVES–VELLEDITS and HAAS in CSÁSZÁR 1997).

Geochemistry:

Limestone infilling and silicified limestone were sampled (2 samples, see Nos. 968, 1003. of Appendix 1).

Ranges are:

Au (<2–6) ppb	As (18.5–99.8) ppm
Ag (<0.1–0.13) ppm	Hg (0.17–6.04) ppm
Sb (0.37–6.34) ppm	Tl (<0.05–0.35) ppm

There are elevated values for As, Hg and Sb but limited number of samples does not allow a suitable evaluation.

Szinva Metabasalt (87)

The formation is made up by “a heavily deformed sequence consisting mainly of basalt lava and volcanoclastite, with siltstone, crinoidal limestone, or cherty limestone intercalations, lenses. (The sequence used to be included in the “Óhuta diabase”). It is partly intercalated into the Hollóstető Formation. Thickness: maximum 50 m” (SZOLDÁN–PELIKÁN–HAAS in CSÁSZÁR 1997).

Geochemistry:

Basalts and tuff (6 samples) were analysed (Nos. 973, 979, 989, 1002, 1078, 1079. of Appendix 1). Ranges and medians are given below:

Au (<2–6)	<2 ppb	As (1.19–9.98)	2.52 ppm
Ag (<0.05–0.10)	0.07 ppm	Hg (<0.02–0.19)	0.0079 ppm
Sb (0.07–0.32)	0.13 ppm	Tl (<0.02–0.17)	0.08 ppm

All concentrations are insignificant.

Kisfennsík Limestone (88)

“Predominantly light grey, in some areas whitish yellow limestone of carbonate platform facies, with *Megalontidae* bivalves. Generally it has a thick-bedded, or massive appearance. Laminated interbeds occur rarely. Occasionally *Lofer* cycles can be observed. Synsedimentary brecciation is comparatively frequent. The thickness is unknown but it is likely to be several hundreds of metres” (PELIKÁN and HAAS in CSÁSZÁR 1997).

Geochemistry:

Only one limestone sample was analysed from this formation No. 1055 of Appendix 1). Gold=<2 ppb, As=0.94 ppm, Ag=0.09 ppm, Hg=0.04 ppm, Sb=0.09 ppm and Tl=<0.02 ppm. The concentrations are insignificant.

Vesszős Shale (23)

Lithology: Black shale, locally with brownish sandstone interlayers. Greenish tuff horizons were encountered in several places within the formation. The slightly metamorphosed (anchi-epizonal) shales consist of quartz, muscovite and small amount of calcite and feldspar.

Facies: deeper marine facies which was probably formed in an intraplatform restricted basin receiving intense siliciclastic input.

Age: It is ambiguous because no fossil has been found in it. Taking into consideration the stratigraphic setting of the formation its Carnian age is the most probable, however according to other opinions it is Rhaetian–Lower Jurassic.

Thickness: It is known in some parts of the Bükk Mts. Its stratigraphic thickness is 150–200 m.

Geochemistry:

Shales, pyritic shale, limestone and dolomite were sampled (6 samples, see Nos. 1062, 1080, 1081, 1085–1087. of Appendix 1). Ranges and medians are given below:

Au <2 ppb	As (0.81–5.65)	2.52 ppm
Ag (0.03–0.05)	Hg (<0.02–0.34)	0.065 ppm
Sb (0.2–2.3)	Tl (<0.02–0.04)	<0.02 ppm

Gold was below detection limit in all samples. The elevated values are in the shale and pyritic shale samples. The elements are not correlated with each other. There are no anomalies.

Felsőtárkány Limestone (89)

Lithology: Light to dark grey, bedded locally cherty limestone with litoclastic (debrite) and laminated calciturbidite intercalations. Wackestone less frequently mudstone texture is characteristic with filaments, ossicles of planktonic crinoids, foraminifera, ostracods, and sponge spicules.

Facies: deeper intraplatform basin and toe-of-slope facies. The intraplatform basin was formed as a result of the Middle Triassic rifting. The debris and carbonate turbidites were accumulated near to the structurally controlled slopes between the platforms and the intraplatform basin.

Age: Based on radiolarians and conodonts it is Ladinian to Norian–Rhaetian.

Thickness: It is not known exactly, about 300–500 m.

Geochemistry:

Limestones, cherty limestones, dolomite, quartzite veinlet (7 samples) were analysed (Nos. 970, 971, 974, 975, 1000–1001, 1075. of Appendix 1). Ranges and medians are given below:

Au (<2–3)	<2 ppb	As (<0.5–24.1)	11.0 ppm
Ag (<0.1–0.34)	0.06 ppm	Hg (0.0043–0.2031)	0.0478 ppm
Sb (<0.1–0.56)	0.18 ppm	Tl (<0.05–0.18)	0.06 ppm

Neither correlations nor anomalous values were found in this formation.

Répáshuta Limestone (90)

Lithology: Yellow, pink, light grey, micritic limestones with crinoidal limestone intercalations and commonly with red chert nodules. Thickness of the crinoidal limestone beds may reach tens of meters, locally. Large olistolithes and olistostromes of platform carbonate origin are common, mainly in the lower part of the formation.

Facies: Slope, toe-of-slope and pelagic basin facies. The olistolithes and olistostromes may have been accumulated on the terraces of the slope and on the toe-of-slope taluses. The crinoidal limestones consist of redeposited crinoid fragments and represent distal toe-of-slope facies.

Age: Based on conodonts it is Norian–Rhaetian but probably continues in the Lower Jurassic

Thickness: It crops out in some parts of the Bükk Mts. Due to the strong tectonic deformation its thickness can hardly determine; 100–300 m can be estimated.

Geochemistry:

A limonitic limestone was sampled (No. 1007 of Appendix 1). All concentrations are low and insignificant: Au=<2 ppb, As=3.05 ppm, Ag=0.05 ppm, Hg=<0.02 ppm, Sb=0.47 ppm and Tl=0.13 ppm.

Rónabükk Limestone (91)

The formation consists of “grey cherty limestone of pelagic basin facies with marl intercalations which used to be included in the “Felsőtárkány Limestone Formation”. The originally bedded limestone became transverse schistose, foliated, in response to anchizonal metamorphism. Thickness: 10 to 300 m (PELIKÁN and HAAS in CSÁSZÁR 1997).

Geochemistry:

Cherty limestones (2 samples) were analysed (Nos. 1054, 1056. of Appendix 1). Ranges are given below:

Au <2 ppb	As (0.95–0.97) ppm
Ag (0.40–0.40) ppm	Hg (<0.02–0.02) ppm
Sb (0.11–0.12) ppm	Tl (0.50–0.50) ppm

The above concentrations are low and insignificant.

3.4.2.2. Jurassic

Darnóhegy Shale (92)

The formation consists of grey to black shales intercalated with limestones, sandstones, and some quartzites. The folded, often brecciated and turbiditic rocks exhibit internal slump structures. Horizons rich on pyrite and graphite occur frequently. Its thickness is about some hundred metres, estimated age Middle Jurassic.

Chalcopyrite bearing (Cu: 0.1–0.28%) black shale horizons were described by BAKSA et al. (1981) from the drillholes Recsk 131 and 135 on the Darnó-hegy.

Geochemistry:

87 samples (marls, pyritic breccias, clays, claystones, limestones, sideritic limestone breccias, sandstone, quartzite and graphytic shales) were analysed (Nos. 846–861, 863, 865, 866, 868–884, 886, 894–940, 944–945, 954. of Appendix 1). Ranges and medians are given below:

Au (<2–340)	<2 ppb	As (<0.2–177.6)	4.15 ppm
Ag (<0.05–0.42)	0.02 ppm	Hg (<0.02–6.49)	0.04 ppm
Sb (<0.1–6.2)	0.3 ppm	Tl (<0.02–10.5)	0.17 ppm

The relatively high concentrations of almost all elements are in a marl. Thresholds have been established for Au, As, Hg, Sb and Tl. Thresholds and number of samples above these values are the followings: Au–11 ppb, one sample; As–50 ppm, one sample; Hg–1 ppm, one sample; Sb–2 ppm, two samples and Tl–1 ppm, 2 samples. At significance level 0.01 the following pairs of elements show significant correlations: As–Hg, As–Sb, As–Tl, Hg–Sb, Hg–Tl and Sb–Tl.

Darnó Radiolarite (93)

Lithology: Red, yellowish red bedded radiolarites with red shale interlayers. Within the layers the radiolarians appear in lenses. In the radiolarian-rich layers, the tests show gradation. The Darnó Radiolarite is in an intimate relation with basic volcanites but nature of their relationship is ambiguous.

Facies: It was formed in deep sea, under the carbonate compensation depth. Gradation of the radiolarian tests indicates their redeposition by currents.

Presumed age: Middle Jurassic

Thickness: It was encountered in the environs of the Darnó Hill. Its estimated thickness is 20–30 m.

Geochemistry:

Radiolarites, quartzites, jasper, claystone and silicified claystone were sampled (8 samples, see Nos. 887, 890, 892, 893, 943, 946, 947, 955. of Appendix 1). Ranges and medians are given below:

Au (<2–5)	<2 ppb	As (<0.2–7.69)	0.8 ppm
Ag (<0.05–0.14)	0.065 ppm	Hg (0.008–0.522)	0.035 ppm
Sb (0.08–0.4)	0.2 ppm	Tl (0.02–0.33)	0.09 ppm

Silicified claystone, claystone and radiolarite samples yielded the highest but insignificant concentrations within the formation. No significant correlation have been found between the elements.

Szarvaskő Basalt (94)

“The formation consists of basaltic pillow lavas and hyaloclastics that came into being in the starting phase of the oceanic rifting. The older sediments show a gentle pyrometamorphic effect along the contact zone. The texture is vitroporphyrific-intersertal and often felsitised and chloritised. Thickness: 300 to 500 ” (PELIKÁN in CSÁSZÁR 1997). Shallow intrusive gabbro-bodies and dikes are also included.

Ore shows in quartzite dikes of native copper, chalkopyrite, cuprite, chalcocite and covellite with traces of galena (KISS 1958) in the Baj-patak and the Galambos-tanya are known for a long time. Similar occurrences were also detected in the quarries of the Nagy-Réz oldal and in the Polner-adit of the Darnó-hegy.

Geochemistry:

Gabbro, basalt, diabase, diabase tuff and radiolarite were sampled (16 samples, see Nos. 862, 864, 867, 885, 888, 889, 891, 941, 942, 949, 951, 956, 959, 962, 963, 966. of Appendix 1). Ranges and medians are given below:

Au (<2–5)	<2 ppb	As (<0.2–25.3)	1.51 ppm
Ag (<0.05–0.1)	0.03 ppm	Hg (<0.02–0.116)	0.017 ppm
Sb (<0.02–1.0)	0.135 ppm	Tl (<0.05–0.25)	0.075 ppm

The highest values of various elements are in the gabbro and diabase. There are no anomalous values at all. Sb–As, Tl–As and Tl–Sb show good correlation.

Bányahegy Radiolarite (95)

Lithology: Variegated (lilac, red, green, brown, grey, white) thin-bedded radiolarites and radiolarian shales, locally with allodapic limestone intercalations (crinoidal limestones) and olistolithes of carbonate platform origin. Slump structures are common.

Facies: Toe-of-slope and deep pelagic basin facies. It was deposited under the carbonate compensation depth. The olistolithes and allodapic limestones indicate the vicinity of slopes.

Age: Based on radiolarians it is Callovian to Oxfordian.

Thickness: It is known in the Bükk Mts. in a thickness of 10–30 m.

Geochemistry:

Predominantly radiolarites were sampled along with quartzites and iron-rich jasper breccias (14 samples, see Nos. 969, 978, 980, 981, 992, 996, 999, 1005, 1009–1014. of Appendix 1). Ranges and medians are given below:

Au (<2–3)	<2 ppb	As (0.87–405.0)	14.4 ppm
Ag (<0.02–0.09)	<0.02 ppm	Hg (<0.02–2.97)	0.1106 ppm
Sb (<0.2–15.2)	0.185 ppm	Tl (<0.02–4.03)	0.275 ppm

The highest concentrations are in the jasper breccia and radiolarite. Thresholds have been established for As, Hg and Sb. These and the number of anomalous values are listed below: As–60 ppm, 3 samples; Hg–1 ppm, 3 samples and Sb–3.5 ppm, one sample. The following pairs of elements show significant correlations: Hg–As and Tl–Sb.

Lökvölgy Shale (96)

Lithology: Dark grey clayey siltstone with thin sandstone layers and locally conglomerate lenses. From genetic point of view it is a distal turbidite series. In the lower part of the formation, thin black radiolarite intercalations occur. It was affected by anchizonal metamorphism which resulted in foliation.

Facies: Pelagic basin facies, site of deposition of distal turbidites. Deposition of the thick turbidite succession might be connected with the closure of the Neotethys oceanic basin.

Age: Upper Dogger–Malm.

Thickness: It is widely extended in the southern part of the Bükk Mts. Its thickness exceeds 1000 m.

Geochemistry:

Mainly shales, then olistolithes of basalt, jasper (after radiolarite), radiolarite and limestone skarn were sampled (16 samples, see Nos. 977, 982–988, 991, 993, 995, 997, 998, 1004, 1006, 1008. of Appendix 1).

Ranges and medians are given below:

Au (<2–11)	3 ppb	As (0.5–9.62)	2.06 ppm
Ag (<0.02–0.11)	0.03 ppm	Hg (<0.02–0.17)	0.052 ppm
Sb (<0.2–0.4)	0.2 ppm	Tl (<0.02–0.28)	<0.02 ppm

There are no anomalous values in this formation. There is only Hg–As correlation at the agreed upon significance level.

Mónosbél Formation (97)

Lithology: The formation is made up predominantly by black shale locally with fine sandstone, radiolarite, limestone and limestone olistostrome intercalations. Based mainly on the features of the carbonate intercalation, within the group the following units were distinguished:

Monosbél Formation – black shale, siltstone with limestone olistostrome bodies. Majority of the limestone fragments is of shallow marine facies and Upper Dogger to Malm in age.

Oldalvölgy Formation (see later) – black shale, siltstone with limestone interlayers and lenses.

Bükkzsérc Formation – black shale with thick-bedded limestone intercalations. The limestones are made up by redeposited ooids.

Csipkéstető Radiolarite – dark grey, greenish thin-bedded radiolarite interlayers within shales of the Monosbél Formation.

Facies: Toe-of-slope and pelagic deep basin facies. The Monosbél Formation represents a proximal toe-of-slope facies with debris flow deposits. The Bükkzsérc Formation may have deposited in the more distal part of the toe-of-slope belt. The ooids were redeposited by turbidity currents. The Oldalvölgy Formation is a deep, oxygen-depleted basin facies, while the Csipkéstető Radiolarite represents also a deep marine environment near to the calcite compensation depth.

Age: Upper Dogger–Malm

Thickness: The group occurs in the Bükk Mts. Its thickness may exceed 1000 m.

Geochemistry:

10 samples have been collected from the formation (the lithology: shales, hornfels, sandstone and quartzite). For details see Nos. 952, 957, 958, 960, 961, 964, 965, 967, 990, 1015. of Appendix 1 Ranges and medians are given below:

Au (<2–3)	<2 ppb	As (0.39–29.9)	7.06 ppm
Ag (<0.05–0.2)	0.005 ppm	Hg (<0.02–0.176)	0.094 ppm
Sb (<0.02–1.09)	0.3 ppm	Tl (<0.02–0.46)	0.086 ppm

There is only one positive value for gold (3 ppb). Shale seems to contain the elevated values of elements within the formation. There are no anomalous values. Correlation coefficients are significant for two pairs of elements: Sb–As and Sb–Tl.

Oldalvölgy Formation (98)

The formation consists of “black, schistose siltstone of deep-water facies, with mudstone type limestone beds or lenses. Thickness: several hundred metres” (PELIKÁN in CSÁSZÁR 1997). Veinlets of white quartzite are common.

Geochemistry:

Shale, limestone, sandstone and quartzite were sampled (6 samples) to represent the formation (Nos. 948, 950, 953, 976, 994, 1016. of Appendix 1). Ranges and medians are given below:

Au (<2–4)	<2 ppb	As (2.29–56.3)	3.89 ppm
Ag (0.03–0.24)	0.06 ppm	Hg (0.04–0.57)	0.063 ppm
Sb (0.1–0.75)	0.28 ppm	Tl (<0.02–0.24)	0.115 ppm

Shale, radiolarite and quartzite samples yielded the highest values of the formation. There are no anomalous values in the formation sampled. There is a very good correlation for Sb–As.

3.4.3. Cenozoic

3.4.3.1. Miocene

Edelény Clay (99)

“It consists of a dense alternation of grey and variegated clay, calcareous clayey silt, huminitic clay, carbonaceous clay, lignite, in the proximity of the base, vesicular sand and pebbly sand beds. It is a delta plain (fluvial, marshy, lacustrine) formation with a thickness of 50 to 300 m, near the top with freshwater limestone and clay marl (Szalonna Limestone Member)” (JÁMBOR in CSÁSZÁR 1997).

Geochemistry:

Limonic sandstones (2 samples) were analysed (Nos. 1375, 1376. of Appendix 1). Ranges are given below:

Au <2 ppb	As (605.0–806.0) ppm
Ag (0.02–0.04) ppm	Hg (0.10–0.13) ppm
Sb (2.59–2.94) ppm	Tl 0.10–0.15) ppm

The concentration of arsenic is high enough in both samples but otherwise there are no remarkable values for the other elements.

3.4.3.2. Holocene

Rudabánya Mine Dump (100)

Geochemistry:

Iron ore mine waste and base metal flotation waste were analysed (7 samples, see Nos. 1168–1174. of Appendix 1). Ranges and medians are given below:

Au (2–5)	3 ppb	As (28.9–117.0)	66.0 ppm
Ag (1.53–16.3)	4.09 ppm	Hg (1.92–4.5)	3.91 ppm
Sb (3.72–118.0)	45.2 ppm	Tl (0.46–1.17)	0.82 ppm

Threshold values are established for As, Ag, Hg and Sb. These values together with the number of samples above thresholds are listed: As–100 ppm, two samples; Ag–1 ppm, 7 samples; Hg–1 ppm, 7 samples and Sb–10 ppm, 5 samples. The correlation coefficient is significant only for Sb–Ag.

Martonyi Mine Dump (101)

Geochemistry:

One sample was collected representing a residual black shale (No. 1347 of Appendix 1).

All concentrations are low and insignificant: Au=<2 ppb, As=9.92 ppm, Ag=0.08 ppm, Hg=1.31 ppm, Sb=3.3 ppm and Tl=0.36 ppm.

Summary for the Northeastern Range:

The formations of this region show the following features. (Table 6, Figs. 21, 22 and 23) The figures showing the median to maximum characteristics of the formations are based on Table 6 but those characterised by less than three samples are not plotted. Using the established thresholds the following formations are worth mentioning:

Fig. 21 helps to draw attention to the high gold values of Szentlélek Formation (80), Rudabánya Iron Ore (7) and Darnóhegy Shale (92). Mercury appears to be anomalous only in the Rudabánya Iron Ore (7). Subanomalous gold values exhibit the Paleozoic Tapolcsány Formation and Irota Formation furthermore the Mesozoic Parád Complex.

Numerous anomalous maxima can be seen for As on Fig. 22 both for Paleozoic and Mesozoic formations: Tapolcsány Formation (4), Irota Formation (73), Szentlélek Formation (80), Rudabánya Iron Ore (7), Parád Complex (84), Darnóhegy Shale (92), Bányahégy Radiolarite (95) and Rudabánya Mine Dump (100). Anomalous Sb maxima can be found in fewer formations: in the Tapolcsány Formation (4), in the Rudabánya Iron Ore (7), in the Parád Complex (84) and in the Rudabánya Mine Dump (100). The anomalous values of silver (Fig. 23) appear in the same formations as those of antimony enumerated above. Tl maxima above the threshold (9 ppm) are few: the Rudabánya Iron Ore (7) and the Darnóhegy Shale seem to contain the high values of this element.

Northeastern Range
Summary of geochemical parameters – median and maximum values.

Table 6

Form-code	Au (ppb)		Ag (ppm)		As (ppm)		Hg (ppm)		Sb (ppm)		Tl (ppm)		N
	Med.	Max.	Med.	Max.	Med.	Max.	Med.	Max.	Med.	Max.	Med.	Max.	
4	<2	17	0.08	44	13.7	468	0.085	2.3	1.48	79.7	0.145	0.75	60
72		<2	0.06	0.39	5.78	9.05	0.02	0.04	0.34	0.62	0.07	0.11	3
73	<2	18	0.07	0.35	3.39	557	<0.02	0.09	0.38	12.1	0.115	0.37	24
2	<2	9	0.04	0.35	3.41	22.7	0.016	0.12	0.58	5.36	0.04	0.24	15
3		<2	0.06m	0.07	1.51m	9.73	0.06m	0.09	0.3m	1.03	0.03m	0.04	2
74	<2	6	0.06	0.17	4.88	15.0	<0.02	0.29	0.49	0.72	0.12	0.12	3
75	<2	7	0.08	0.38	3.84	25.0	0.02	0.34	0.39	3.61	0.09	0.78	41
76		<2	0.05	0.11	1.18	23.0	<0.02	0.1	0.34	2.87	0.025	0.21	8
77		<2	0.03	0.06	3.06	14.6	<0.02	0.14	0.27	1.0	0.05	0.08	11
601		<2	0.03	0.24	11.9	24.6	0.08	0.21	0.64	1.61	0.18	0.34	9
602		<2	0.03	0.86	5.32	51.3	0.092	0.32	0.36	1.22	0.06	0.20	15
78		<2		<0.1	13.4	17.8	0.037	0.173	0.19	0.28	0.09	0.25	5
79	<2	5	0.065	0.3	9.97	84.6	0.19	4.63	0.56	2.75	0.11	0.19	16
80	<2	243	0.55	1.49	22.0	5330	0.31	0.81	2.43	12.5	0.37	0.81	6
5		<2	0.3	1.35	2.1	6.24	0.02	0.74	0.26	2.02	0.04	0.15	20
7	3	630	18.35	520	187	8110	11.4*	3400	154	13354	0.36*	9.46	67*, 96
24		<2	0.05	0.69	0.74	2.86	0.05	0.11	0.43	1.41	0.04	0.04	7
22		<2	0.03	0.14	1.97	8.7	0.1	2.22	0.45	2.17	0.12	0.24	11
83		<2	0.025	0.11	2.04	72.8	0.007	0.029	0.185	0.78	0.11	0.32	6
84	3.5	84	0.05	10.6	19.9	181.0	0.051	1.903	0.57	108.0	0.24	0.82	66
86	<2m	6	<.1m	0.13	18.5m	99.8	0.17m	6.04	.37m	6.34	<.05m	0.35	2
87	<2	6	0.07	0.1	2.52	9.98	<0.02	0.19	0.13	0.32	0.08	0.17	6
23		<2	0.035	0.05	2.52	5.65	0.065	0.34	0.685	2.3	<0.02	0.04	6
89	<2	3	0.06	0.34	11.0	24.1	0.048	0.203	0.18	0.56	0.06	0.18	7
91		<2	0.40m	0.40	0.95m	0.97	<0.02	0.02	0.11m	0.12	0.50m	0.50	2
92	<2	340	0.02	0.42	4.15	177.6	0.04	6.49	0.3	6.2	0.17	10.5	87
93	<2	5	0.065	0.14	0.8	7.69	0.035	0.522	0.2	0.4	0.09	0.33	8
94	<2	5	0.03	0.1	1.51	25.3	0.017	0.116	0.135	1.0	0.075	0.25	16
95	<2	3	<0.02	0.09	14.4	405.0	0.111	2.97	0.185	15.2	0.275	4.03	14
96	3	11	0.03	0.11	2.06	9.62	0.052	0.17	0.2	0.4	<0.02	0.28	16
97	<2	3	0.005	0.2	7.06	29.9	0.094	0.176	0.3	1.09	0.086	0.46	10
98	<2	4	0.06	0.24	3.89	56.3	0.063	0.57	0.28	0.75	0.115	0.24	6
99		<2	0.02m	0.04	605m	806	0.1m	0.13	2.59m	2.94	0.1m	0.15	2
100	3	5	4.09	16.3	66.0	117.0	3.91	4.5	45.2	118.0	0.82	1.17	7

Remarks.

Formcode = the code of the Formation:

4=Tapolcsány Fm., 72=Strázsahegy Fm., 73=Irota Fm., 2=Szendrőlád Limestone, 3=Uppony Limestone, 74=Abod Limestone, 75=Szendrő Phyllite, 76=Rakaca Marble, 77=Lázberc Fm., 601=Szilvásvárad Fm., 602=Mályinka Fm., 78=Tarófü Fm., 79=Perkupa Anhydrite, 80=Szentlélek Fm., 5=Nagyvisnyó Limestone, 7=Rudabánya Iron Ore, 24=Gutenstein Fm., 22=Hámor Dolomite, 83=Szentistvánhegy Metaandesite, 84=Parád Complex, 86=Berva Limestone, 87=Szinva Metabasalt, 23=Vesszős Shale, 89=Felsőtárkány Limestone, 91=Rónabükk Limestone, 92=Darnóhegy Shale, 93=Darnó Radiolarite, 94=Szarvaskő Basalt, 95=Bányahegy Radiolarite, 96=Lökvölgy Shale, 97=Mónosbél Fm., 98=Oldalvölgy Fm., 99=Edelény Clay, 100=Rudabánya Mine Dump.

Med.=median value; Max.=maximum value; m=minimum value, when number of samples=2

67*, 96=number of analyzed samples for the components marked by *; number of samples for the other elements analyzed.

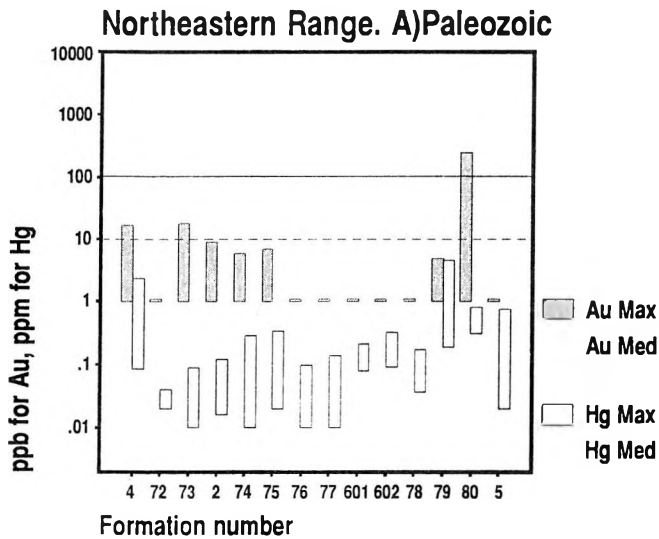
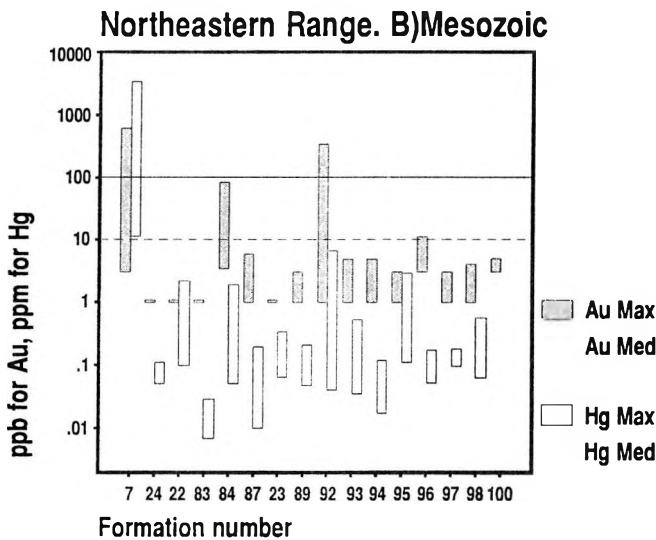


Fig. 21: The median (Med)–maximum (Max) concentration ranges of Au–Hg, Northeastern Range A/ Paleozoic formations, B/ Mesozoic formations



Results and interpretations of stream sediment survey will be outlined using Figs. 6 and 7. Almost all cells of low and medium level additive anomalies in the Bükk and Uppony Mountains are concentrated to S from the Bükk plateau (No. 2311, 2313, 2351, 2357, 2249, 2364, 2253, 2256, 2262, 2280, 2369, 2374, 2375, 2388 and 2390 on Fig. 6). They are located mainly over Jurassic shales with radiolarites, rarely over Triassic limestones. Gold content of the individual stream sediment cells is near to detection level and ranges between 2 and 22 ppb. More than 10 ppb Au was detected in the following cells of the Southern Bükk: No. 2341 (13 ppb), 2343 (10 ppb), 2357 (18 ppb), 2364 (22 ppb) and 2271 (13 ppb). Surface chip sampling has resulted only in two anomalies of gold. The first is related to the oreshow of malachite and azurite in the Permian Szentlélek Formation with 234 ppb Au in Nagyvisnyó, while the second “subanomalous” gold value (11 ppb) was detected in the Jurassic Lökvölgy Shale (Ns. 1040 and 1108 of Appendix 1).

Subsurface (drilling core and mining tunnel) chip sampling resulted in continuous low level gold anomalies in the Silurian to Carboniferous Tapolcsány Formation of the Uppony Mountains (10 to 14 ppb Au of the samples No. 1132, 1134, 1136, 1141 and 1142 of Appendix 1) and in the Middle to Late Triassic Parád Complex, furthermore in the Jurassic Darnóhegy Shale of the Recsk porphyry copper deposit area (11 to 340 ppb Au of the samples No. 782, 791, 792, 795, 797, 798, 799, 805, 817, 828, 832, 843, 847 and 895 of Appendix 1). Surface perspectives of the Bükk and Uppony Mountains are considered unfavorable for Carlin-type gold mineralization with exception of the single gold anomaly in the Szentlélek Formation.

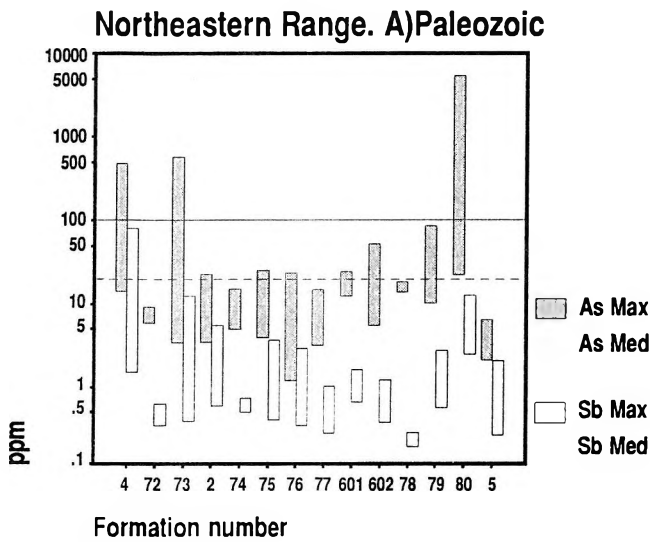
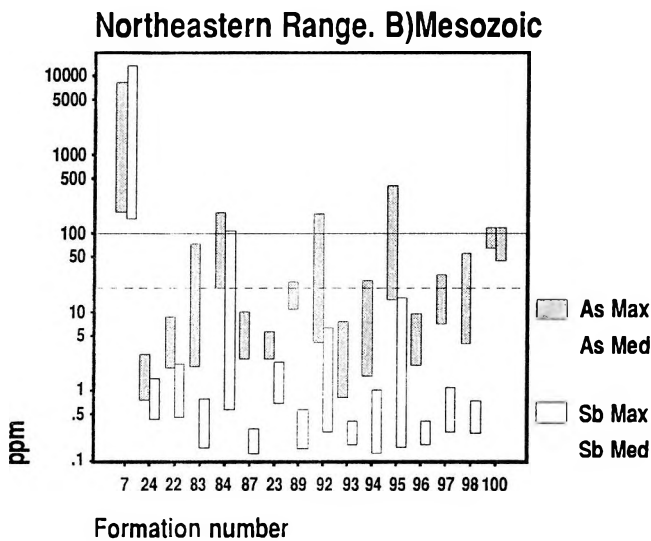


Fig. 22: The median (Med)–maximum (Max) concentration ranges of As–Sb, Northeastern Range A/ Paleozoic formations, B/ Mesozoic formations



In the Rudabánya and Szendrő Mountains are known only some low to medium level additive anomalies (Fig. 7), represented by the cells of No. 2573, 2576, 2577, 2583, 2585, 2587, 2588, 2601, 2602, 2603, 2689 and 2695. Gold values of the individual cells are also insignificant (2 to 4 ppb). Chip sampling of the Rudabánya Iron Ore in the Rudabánya and Martonyi abandoned open pit resulted in numerous gold anomalies, ranging between 16 and 630 ppb Au (No. 1177, 1180, 1182, 1184–1186, 1187–1188, 1189–1192, 1194, 1199, 1202, 1207, 1209, 1211, 1212–1213, 1215, 1217, 1218–1219, 1221, 1223–1224, 1228–1229, 1236, 1238, 1241, 1245, 1246–1247, 1252, 1254 and 1256 in Rudabánya and 1350 in Martonyi, Appendix 1). The Tapolcsány Formation at the eastern border of the Rudabánya Mountains shows low level anomalies with 11 to 16 ppb Au (No. 1231 and 1233 of Appendix 1). The Irota Formation in the Szendrő Mountains present similar subanomalous gold values, between 13 and 18 ppb (No. 1278, 1283, 1284 and 1322 of Appendix 1).

Both anomalous and subanomalous groups of formations in the Northeastern Range are related to the Darnó Zone. The Rudabánya Iron Ore showing typical anomalies for the Carlin suite is considered target of further explorations. Sporadic gold anomalies of the Darnóhegy Shale and continuous subanomalous gold values in the Parád Complex, both in the area of the Recsk porphyry copper deposit are also recommended for more detailed explorations. The subanomalous Tapolcsány Formation and Irota Formation with low level gold values and the Szentlélek Formation with sporadic high level gold anomaly are connected with uranium-shows and related to the second group in perspectivity. All other areas and formations are unfavorable for gold prospecting.

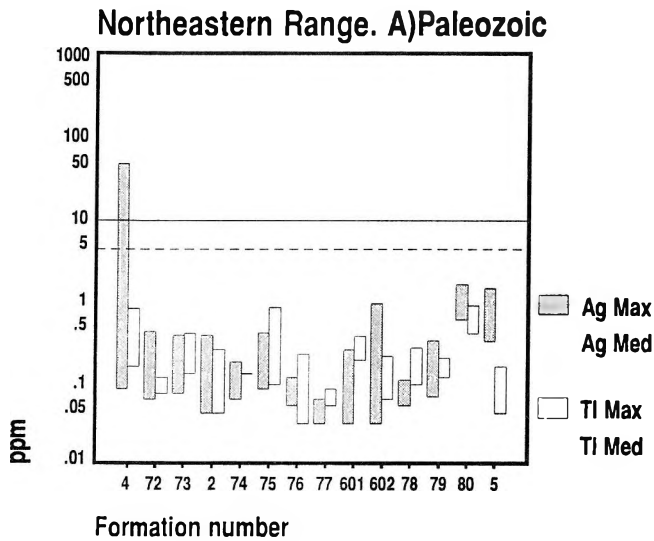
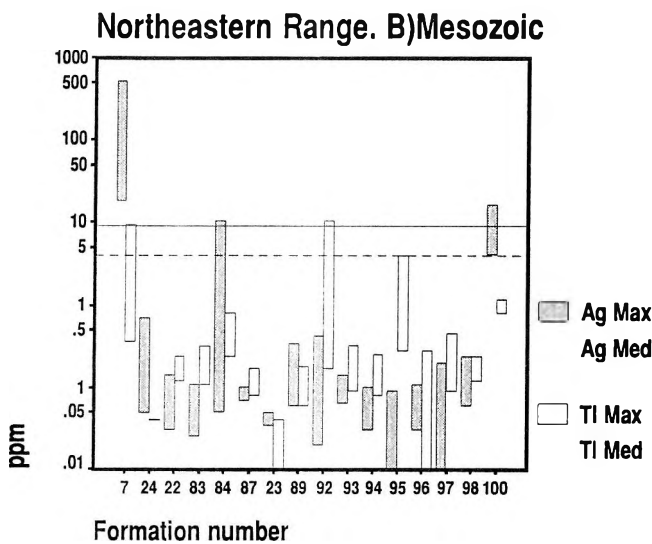


Fig. 23: The median (Med)–maximum (Max) concentration ranges of Ag–Tl, Northeastern Range A/ Paleozoic formations, B/ Mesozoic formations



4. DISCUSSION

Our data cannot stand alone, we should compare them to known deposits and to values of established indicators. It is not enough to have high values of let us say ten times that of the clark, some other features of these elements must also be known in order to make useful comparison.

Geochemical analyses of drillhole samples carried out in the USA indicate a large arsenic halo, >1000 ppm, that extends outward from gold mineralization. Antimony contents of >100 ppm are restricted to ore body. Hg does not correlate directly to gold, however, concentrations of 1–30 ppm occur within and adjacent to gold mineralization (PAUL et al. 1993). In Carlin-type deposits gold is associated with elevated values of As, Sb, Hg and Tl and low levels of Ag (THORESON 1993). According to DOYLE–KUNKEN (1993) a large halo of >500 ppm As surrounds the central alteration and mineralization zones. Upper level antimony anomalies are also common. Tl anomalies in the 0.5–25 ppm range are locally conformable with the ore horizons. Local concentrations of Ag are roughly correlative to gold.

The above results and especially the concentration limits for the indicator elements help us in evaluating our accidental hits, that is the chance anomalous values of the perhaps perspective formations. So with these limits in mind the geochemistry of the formations is further analyzed.

First we try to analyze the overall characteristics of elements independent of the formations containing them and of the regions they are situated in. That is we try to establish overall anomaly thresholds for the elements to

help to outline and to plot anomalies (especially for gold). This is an important step to separate background from anomaly. Then we try to investigate the influence of different factors on the concentration and distribution of elements (like lithology, geological age and geotectonic position of the groups of formation). Finally the results of an independent survey (stream sediment survey of the hilly and mountainous parts of Hungary) are also taken into consideration parallel with our findings in order to enlarge our means of evaluating the Carlin gold potential of the areas investigated.

4.1. Establishing anomaly thresholds

When it was possible (that is samples were available in necessary number) anomaly thresholds were established even for an individual formation. These threshold values are summarised for formations with $N > 20$ (Table 7). One can get an idea as to the range of concentrations of these threshold values, their reliability depending upon the number of samples used in the investigation. The number of anomalous samples in the formation is also given in this table to indicate the frequency of high values.

An other approach can also be used to determine these thresholds. By the use of all data for the 6 elements analysed the distribution characteristics can be studied. Histograms, boxplot diagrams and frequency tables were used of the SPSS PC+ software package to study the distribution of the concentrations. The results of all these procedures are summarised on Table 8. Because of the unevenness of the data, sample numbers used for geochemical characterization are different for the elements. There are of course uncertainties concerning the threshold of gold for example. On the boxplot diagram of gold, all values are outliers and extremes above 5 ppb. There is a break on the frequency distribution of gold concentrations at 10 ppb. (Fig. 24) It is not an entirely exact thing

Threshold values for the anomalies of the studied formations
(Formations with $N \geq 20$ are only summarized.)

Table 7

Form-code	Au (ppb)	auN	Ag (ppm)	agN	As (ppm)	asN	Hg (ppm)	hgN	Sb (ppm)	sbN	Tl (ppm)	tIN	N
37	-		-		>20	1	-		>10	4	-		20
39	>7	1	-		-		-		2	6	-		62
42	100*	5	5*	5	100	10	-		5	7	-		74*; 31
1	-		-		100	4	-		10	3	1	2	27
49	.*		0.5*	1	50	5	1	5	2	5	2	1	28*; 16
16	.*		.*		100	7	2	8	10	7	2	3	44*; 27
51	>20*	1	-		>10	2	>1	1	4	2	-		21*; 16
52	-		-		10	6	1	3	2	7	-		28
54	-		-		100	2	-		-		2	1	21
59	>100*	3	>3*	5	-		-		-		-		40*; 2
36	-		-		100	11	>5	2	20	4	>4	2	30
63	-		-		-		-		1.5	2	-		21
4	12	5	2	1	70	7	-		7	20	-		60
73	10	4	-		50	5	-		8	2	-		24
75	-		-		-		-		3	1	-		41
5	-		>1	1	-		-		-		-		20
7	15	35	22	47	130	56	20*	29	35	69	.*		96; 67*
84	17	5	2.5	1	100	3	-		10	4	-		66
92	>11	1	-		50	1	1	1	2	2	1	2	87

Remark:

Formcode = the code number of the Formation:

37=Köszeg Quartz Phyllite, 39=Velem Calc-Phyllite, 42=Lovas Slate, 1=Polgárdi Limestone, 49=Budaörs Dolomite, 16=Mátyáshegy Fm., 51=Földolomit Fm., 52=Dachstein Limestone, 54=Kisgerecse Marl, 59=Nadap Andesite, 36=Hárshegy Sandstone, 63=Källa Gravel, 4=Tapolcsány Fm., 73=Irota Fm., 75=Szendró Phyllite, 5=Nagyvisnyó Limestone, 7=Rudabánya Iron Ore, 84=Parád Complex, 92=Darnóhegy Shale

auN, agN, asN, hgN, sbN and tIN=number of anomalous samples above thresholds:

96;67*=number of samples analyzed; number of analyzed samples for the components marked by *

	Au (ppb)	As (ppm)	Ag (ppm)	Hg (ppm)	Sb (ppm)	Tl (ppm)
Thresholds for the anomalous population	100*	100	4	10	20	9
Thresholds for the subanomalous population	10*	40	0.6	1	4	1.5
Median	< 2	5.9	0.06	0.0501	0.42	0.13
75%	2	22.6	0.16	0.200	1.64	0.25
90%	6	117	0.89	1.292	15.17	0.53
95%	16	324	10.2	6.322	117.85	0.94
Maximum	4770	8110	520	3400	13354	33.7
N**	1398	1244	1336	1215	1242	1213

Remark:

*=The anomalous values above these thresholds are shown by the geochemical anomaly maps.

**=The data-set is uneven: not all samples (altogether 1398) were analysed for all 6 elements.

to put a certain limit as a threshold value. So we have decided to make a distinction between subanomalous and anomalous thresholds in order not to leave out any possibly interesting data from the anomalous population, from the geochemical anomaly map. The same was true for arsenic, where boxplot also indicated outliers and extremes above 40 ppm, so the 100 ppb for gold and 100 ppm for arsenic are somehow artificial thresholds for the anomalous population. There are many subpopulations on the histograms for silver and mercury indicating the composite nature of the distribution. The anomaly thresholds shown on Table 8 are used as reference lines on Figs. 9, 14, 15, 16, 18, 21, 22 and 23 together with subanomalous threshold for gold (10 ppb). These values for gold have also been used to plot the geochemical anomaly maps of the investigated regions.

A few parameters of the samples (sample No., formation number, lithology, geological age and gold content) considered anomalous (Au >100 ppb) and subanomalous (Au >10 ppb) are compiled in Table 9.

4.2. Influence of certain factors on the distribution of elements

Unfortunately we did not have the chance to have our samples analysed for components other than the six minor elements. All useful material and analytical data we've got can be found in Appendix 1 That is why it is not possible to look for relationships determined by factors like pyrite content, bitumen content of the analysed samples or degree of alteration reflected by some key mineral and so on. So our search for finding some factors determining the situation, position or value of anomalous samples for further follow-up surveys is limited to the investigation of those listed below.

Frequency distribution of gold concentrations (ppb)
(Values of Au <20 ppb are plotted)

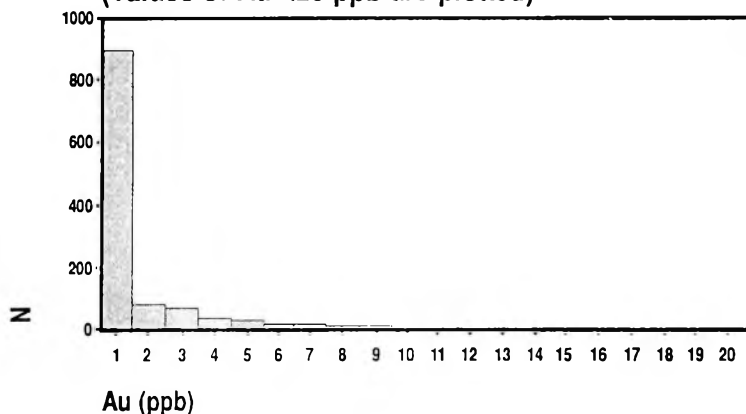


Fig. 24: Frequency distribution of gold concentrations (ppb)
(Values of Au < 20 ppb are only plotted)

Sample No.	Formations	Lithology	Age	Au (ppb)
Kőszeg Mountains				
8	Kőszeg Quartz Phyllite	quartz phyllite	J1(Mz21)	13
79	Cák Conglomerate	quartzite	J2(Mz22)	13
66	Velem Calc Phyllite	slate	J2-3(Mz25)	19
90	Felsőcsatár Greenschist	diabase	K1(Mz3)	310
Transdanubian Range				
284	Balatonfőkajár Quartz Phyllite	phyllite	O-S(Pz11)	27
349	Lovas Slate	limonitic quartzite	O-D(Pz12)	17
359	Lovas Slate	quartzite breccia	O-D(Pz12)	205
360	Lovas Slate	limonitic quartzite breccia	O-D(Pz12)	4770
361	Lovas Slate	quartzite breccia	O-D(Pz12)	48
363	Lovas Slate	quartzite breccia	O-D(Pz12)	81
364	Lovas Slate	quartzite	O-D(Pz12)	22
370	Lovas Slate	contact slate	O-D(Pz12)	20
371	Lovas Slate	contact slate	O-D(Pz12)	10
386	Lovas Slate	contact slate	O-D(Pz12)	200
388	Lovas Slate	contact slate	O-D(Pz12)	2200
389	Lovas Slate	contact slate	O-D(Pz12)	200
391	Lovas Slate	contact slate	O-D(Pz12)	200
455	Lovas Slate	limonitic slate	O-D(Pz12)	38
456	Lovas Slate	limonitic slate	O-D(Pz12)	15
362	Velence Granite	limonitic quartzite	C2(Pz21)	2090
365	Velence Granite	quartzite	C2(Pz21)	19
387	Velence Granite	microgranite	C2(Pz21)	600
541	Mátyáshegy F.	dolomite	T3(Mz13)	12
684	Födömit F.	brecciated dolomite	T3(Mz14)	25
671	Dachstein Limestone	limestone	T3(Mz15)	11
368	Nadap Andesite	intrusive breccia	E2-3	1000
369	Nadap Andesite	silicified intrusive breccia	E2-3	600
385	Nadap Andesite	intrusive breccia	E2-3	600
392	Nadap Andesite	intrusive breccia	E2-3	400
Northeastern Range				
1132	Tapolcsány F.	limestone	S-C1(Pz13)	13
1134	Tapolcsány F.	pyritic shale	S-C1(Pz13)	10
1136	Tapolcsány F.	pyritic limestone	S-C1(Pz13)	13
1141	Tapolcsány F.	pyritic shale	S-C1(Pz13)	14
1142	Tapolcsány F.	pyritic shale	S-C1(Pz13)	10
1177	Tapolcsány F.	silicified dolomite breccia	S-C1(Pz13)	17
1231	Tapolcsány F.	limonitic Mn rich shale	S-C1(Pz13)	16
1233	Tapolcsány F.	limonitic Mn rich shale	S-C1(Pz13)	11
1278	Irota F.	limonitic graphitic shale	D2(Pz14)	13
1283	Irota F.	graphitic limonitic shale	D2(Pz14)	18
1284	Irota F.	graphite shale	D2(Pz14)	15
1322	Irota F.	graphite shale	D2(Pz14)	17
1040	Szentlélek F.	claystone with malachite	P2(Pz22)	234
1350*	Rudabánya Iron Ore	limonite	T1-2(Mz11)	25
782	Parád Complex	jasper breccia	T2-3(Mz12)	16
791	Parád Complex	limestone breccia	T2-3(Mz12)	24
792	Parád Complex	limestone breccia	T2-3(Mz12)	13
795	Parád Complex	limestone breccia	T2-3(Mz12)	84
797	Parád Complex	marl, limestone	T2-3(Mz12)	15
798	Parád Complex	breccia	T2-3(Mz12)	60
799	Parád Complex	marl	T2-3(Mz12)	22
805	Parád Complex	bituminous limestone	T2-3(Mz12)	30
817	Parád Complex	limestone breccia	T2-3(Mz12)	12
828	Parád Complex	silicified limestone breccia	T2-3(Mz12)	12
832	Parád Complex	cherty limestone	T2-3(Mz12)	24
843	Parád Complex	silicified shale	T2-3(Mz12)	15
847	Darnóhegy Shale	marl	J2(Mz23)	340
895	Darnóhegy Shale	shale	J2(Mz23)	11
1008	Lökvölgy Shale	shale	J2(Mz24)	11

Table 9
continued

Sample No.	Formations	Age	Au (ppb)
1180	Rudabánya Iron Ore	T1-2(Mz11)	50
1182	Rudabánya Iron Ore	T1-2(Mz11)	70
1184	Rudabánya Iron Ore	T1-2(Mz11)	113
1185	Rudabánya Iron Ore	T1-2(Mz11)	60
1186	Rudabánya Iron Ore	T1-2(Mz11)	230
1187	Rudabánya Iron Ore	T1-2(Mz11)	40
1188	Rudabánya Iron Ore	T1-2(Mz11)	90
1189	Rudabánya Iron Ore	T1-2(Mz11)	630
1190	Rudabánya Iron Ore	T1-2(Mz11)	85
1191	Rudabánya Iron Ore	T1-2(Mz11)	220
1192	Rudabánya Iron Ore	T1-2(Mz11)	560
1194	Rudabánya Iron Ore	T1-2(Mz11)	30
1199	Rudabánya Iron Ore	T1-2(Mz11)	30
1202	Rudabánya Iron Ore	T1-2(Mz11)	50
1209	Rudabánya Iron Ore	T1-2(Mz11)	50
1211	Rudabánya Iron Ore	T1-2(Mz11)	50
1212	Rudabánya Iron Ore	T1-2(Mz11)	29
1213	Rudabánya Iron Ore	T1-2(Mz11)	80
1215	Rudabánya Iron Ore	T1-2(Mz11)	40
1217	Rudabánya Iron Ore	T1-2(Mz11)	140
1218	Rudabánya Iron Ore	T1-2(Mz11)	20
1219	Rudabánya Iron Ore	T1-2(Mz11)	100
1221	Rudabánya Iron Ore	T1-2(Mz11)	40
1223	Rudabánya Iron Ore	T1-2(Mz11)	36
1224	Rudabánya Iron Ore	T1-2(Mz11)	110
1228	Rudabánya Iron Ore	T1-2(Mz11)	16
1236	Rudabánya Iron Ore	T1-2(Mz11)	30
1238	Rudabánya Iron Ore	T1-2(Mz11)	50
1241	Rudabánya Iron Ore	T1-2(Mz11)	20
1246	Rudabánya Iron Ore	T1-2(Mz11)	27
1247	Rudabánya Iron Ore	T1-2(Mz11)	40
1252	Rudabánya Iron Ore	T1-2(Mz11)	20
1254	Rudabánya Iron Ore	T1-2(Mz11)	20
1256	Rudabánya Iron Ore	T1-2(Mz11)	60

* Data for TVX samples without lithology. Northeastern Range.

4.2.1. Lithology

We were mainly concerned with the behaviour of gold, with the possible influence of lithology on gold content. For this purpose we have used a subpopulation of samples with Au \geq 2 ppb. Rock types characterized by more than 2 samples have only been taken into consideration. The results are illustrated by Fig. 25. Out of the 17 rock types shown on the figure the following seven types seem to contain anomalous gold concentrations: slates and greenschists, shales, ophiolites, quartzites, marls and dolomarl, the Rudabánya Iron Ore and the intrusive

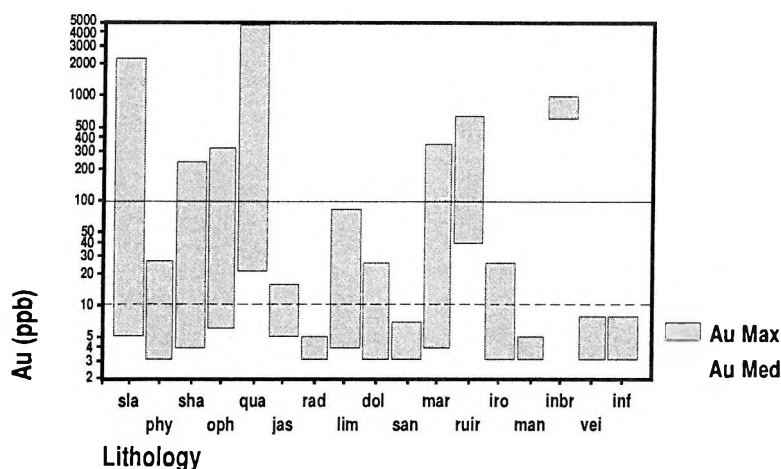


Fig. 25: Distribution of the median to maximum concentration ranges (ppb) of gold according to lithology
sla=slates and greenschists, phy=phyllites, sha=shales and clays, oph=ophiolites, qua=quartzites, jas=jasper and chert, rad=radiolarites, lim=limestone, dol=dolomite, san=sandstone and sand, mar=marl and dolomarl, ruir=rocks of Rudabánya Iron Ore, iro=iron ore and limonite, man=manganese ore, inbr=intrusive breccias, vei=veins, inf=infillings

Reference lines at 10 ppb and 100 ppb are given to indicate subanomalous and anomalous thresholds values of gold.

breccias. Slates, quartzites and intrusive breccias contain the three highest gold concentrations. All other rock types contain only subanomalous or background concentrations. To our surprise these include even the veins and infillings, which had previously been supposed to be enriched in the elements analyzed.

4.2.2. Geological age

Based on Table 9 the anomalous and subanomalous samples could be grouped according to their geological age. Using only samples with Au > 10 ppb could enhance the chance to make distinction between the age units (average values have been used for age units represented by more than one sample). Fig. 26 illustrates the gold concentrations for age units. It can be seen that Ordovician–Devonian (Pz12), Carboniferous–Permian (Pz21, Pz22), Early–Middle Triassic (Mz11), Middle Jurassic (Mz23), Early Cretaceous (Mz3) and Middle–Late Eocene (E2–3) formations give the highest gold concentrations in the subpopulation with Au > 10 ppb.

4.2.3. Geotectonic position

Many of the investigated formations can be grouped in distinct geotectonic units according to their palaeogeographic situation and stratigraphic position (HAAS et al. 1999). Others like the formations of the Mecsek Mountains are outside these geotectonic regions and can be used for comparison.

Two geotectonic situations have been distinguished. One is for formations situated and deposited at paleomargins, belonging to “A” paleotectonic situation (“A1” is for the Paleozoic formations of the Balatonfő–Velence–Hills region, in the Transdanubian Range, N=182; “A2” is for the Paleozoic formations of Uppony and Szendrő Mountains, in the Northeastern Range, N=196).

The other paleotectonic situation (“B”) is represented by ophiolitic oceanic basins (“B1” is for the Young Mesozoic formations of the Penninic basin, in the Kőszeg Mountains, West Hungary, N=91; “B2” is for the Young Mesozoic formations of the Meleata basin, in Darnó–hegy and Szarvaskő, Northeastern Range, N=223). For see the details in the caption of Fig. 27.

Because all median values were below detection limit for gold (2 ppb) it was not plotted in the upper part of Fig. 27. It can be seen that there are no great differences in the median values of these grouped formations, the ranges between lowest and highest medians are narrow.

If the paleotectonic situations are compared by their 95% values it can be said that “A1” geotectonic situation of paleomargins holds the highest concentrations for all elements (and especially for gold) and except for mercury it differs much from the other geotectonic situations. The differences, the ranges between highest and lowest 95% values, are greater (mainly for Au, Ag and As) than in case of medians. The “A2” geotectonic situation of paleomargins seems to be geochemically closer to the “B1” and “B2” geotectonic ones of the ophiolitic oceanic basins.

The different paleotectonic position of the Mecsek Mountains is reflected clearly by Carlin geochemistry too.

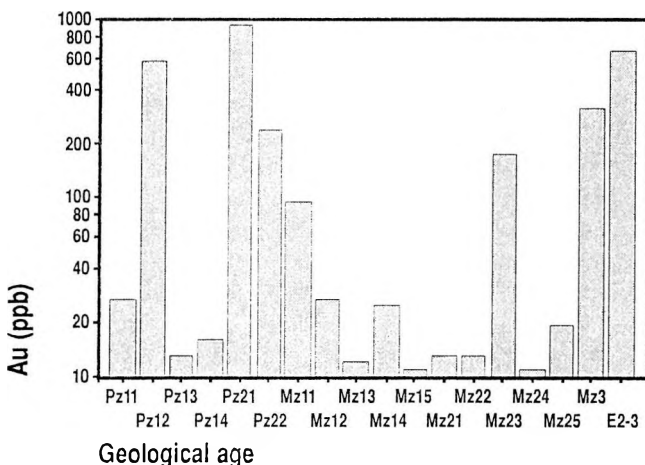


Fig. 26: Distribution in geological time of the average gold contents of anomalous and subanomalous groups of formations (Au > 10 ppb) For the explanation of geological ages see Table 7

Comparison of geotectonic situations (median values)

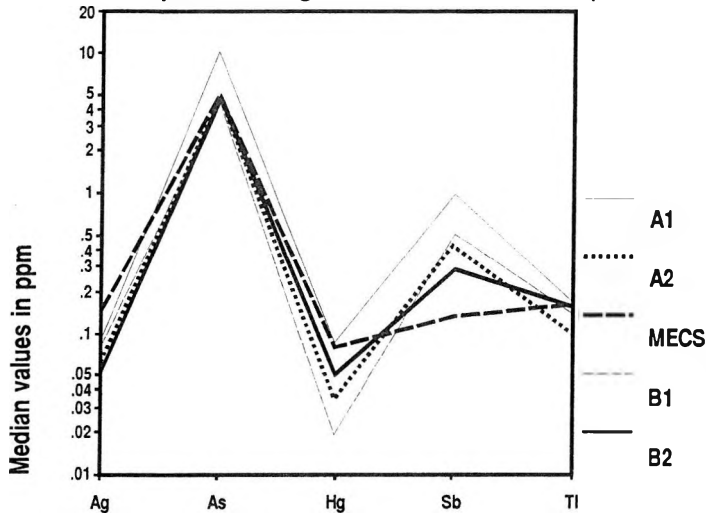
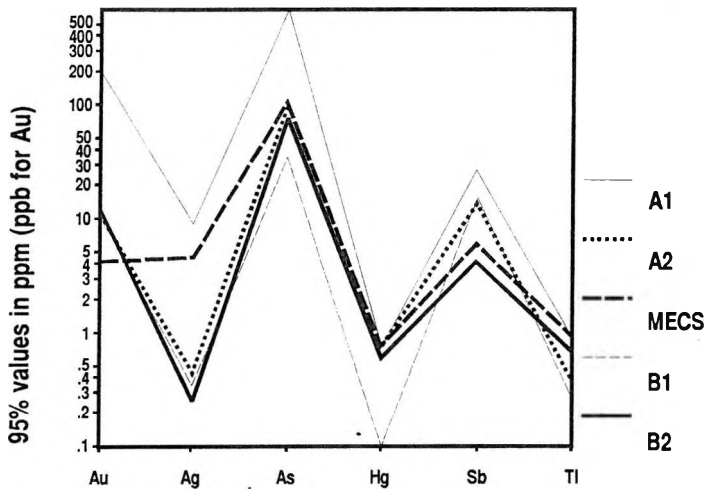


Fig. 27: Comparison of groups of formations according to their paleotectonic situations (A1, A2, Mecsek, B1 and B2) using median and 95 % values)

Comparison of geotectonic situations (95% values)



5. PERSPECTIVE AREAS AND FORMATIONS FOR FURTHER EXPLORATIONS

The perspective areas and formations for further explorations will be discussed using Figs. 24, 26, 27 and 28 and Table 7.

Frequency distribution of gold concentrations (Fig. 24) and gold content of anomalous and subanomalous sample-populations (Table 9) reflect clearly the rather low potential for Carlin-type gold mineralization in Hungary. 1398 analytical record of 604 sample sites resulted in detection of 92 subanomalous and anomalous gold values, representing about 6,6% of the total amount of the database. This modest gold potential is hosted mainly in Paleozoic sedimentary and intrusive formations, subordinately in Early Mesozoic sedimentary formations. High gold values of the Young Mesozoic metamorphic and sedimentary formations are represented by sporadic samples, while the peak of the Middle to Late Eocene indicate gold shows hosted in volcanics (Fig. 26). Distribution of the Carlin suite elements in function of paleotectonic position refers to that both rifting and collision are more suitable for enrichment of gold (Fig. 27) as stated by HAAS et al. (1999). The areal distribution of anomalous and subanomalous formations (Fig. 28) is tectonically controlled as well they are located along the master faults (Rába Line, Mid-Hungarian Line, Mecsekalja Line) and related shear zones (Balaton Line, Darnó Line and Pilis fault) separating the main tectonic units of Hungary. The ten predictive areas of about 2–190 km² (Fig. 28) will be evaluated in the following. The succession reflects their suggested order of perspectivity.

Fig. 28

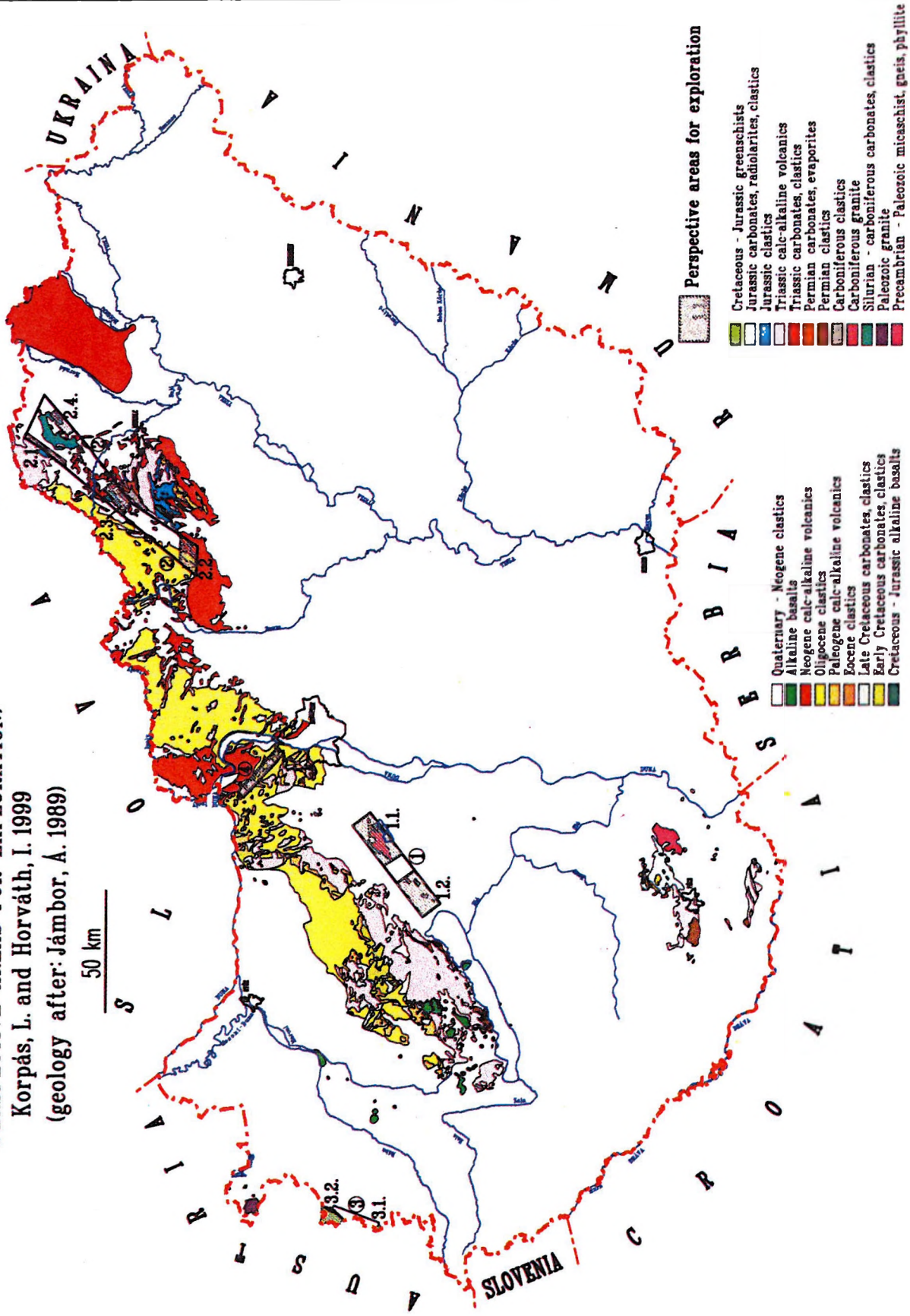
CARLIN ORE POTENTIAL MAP OF HUNGARY

(PERSPECTIVE AREAS FOR EXPLORATION)

Korpás, L. and Horváth, I. 1999

(geology after: Jámbor, A. 1989)

50 km



- Quaternary - Neogene clastics
- Alkaline basalts
- Neogene calc-alkaline volcanics
- Oligocene clastics
- Paleogene calc-alkaline volcanics
- Eocene clastics
- Late Cretaceous carbonates, clastics
- Early Cretaceous carbonates, clastics
- Cretaceous - Jurassic alkaline basalts

Perspective areas for exploration

- Cretaceous - Jurassic greenschists
- Jurassic carbonates, radiolarites, clastics
- Jurassic clastics
- Triassic calc-alkaline volcanics
- Triassic carbonates, clastics
- Permian carbonates, evaporites
- Permian clastics
- Carboniferous clastics
- Carboniferous granite
- Silurian - carboniferous carbonates, clastics
- Paleozoic granite
- Precambrian - Paleozoic mica-schist, gneis, phyllite

5. 1. Velence Hills–Balatonfő area, Transdanubian Range

The area in discussion is almost 430 km² (Fig. 28) and its great part is covered by Late Miocene to Quaternary sediments. Below these sediments are outcropping the predictive Paleozoic (meta)sedimentary group of formations (Balatonfőkajár Quartz Phyllite, Lovas Slate, Úrhida Limestone, Polgárdi Limestone, Szabadbattyán Limestone) intruded by the Late Carboniferous collisional Velence Granite and overprinted by the Middle to Late Eocene volcanic-plutonic complex of the Nadap Andesite. This is the geological and tectonic situation which should be considered in the first place favorable for Carlin-type gold mineralization.

5.1.1. Velence Hills

The area of about 190 km² includes favorable formations of the Paleozoic Lovas Slate, and Velence Granite, and the Middle to Late Eocene Nadap Andesite. High level gold anomalies up to 4770 ppb were detected in all formations. Extense zones of surface and near surface pneumatolitic and hydrothermal alterations are typical. The related basemetal mineralization accompanied by fluorite and barite was explored in many drillholes and trenches, and mined for a long time. Systematic metallometric and IP survey resulted in discovery of anomalies in the Eastern Velence Hills area, covering the Lovas Slate mantle over the Velence Granite and the volcanic centre of the Nadap Andesite.

The target of further explorations: selection of limited steep dipping gold rich zones of some 10 to 100 × 1000 m in size. This selection on the surface will be achieved at first by systematic soil and follow up rock chip sampling covering the whole area. The metallometric survey will be accompanied by the systematic rock sampling of drillhole-cores, available in the core depositories of the Geological Institute of Hungary. Surface anomalies of gold to the depth will be delineated by applying of IP survey and later on explored by some inclined drillholes.

5.1.2. Balatonfő

The anomalous and subanomalous formations (Balatonfőkajár Quartz Phyllite, Úrhida Limestone, Polgárdi Limestone, Szabadbattyán Limestone, Velence Granite and Nadap Andesite) of the Balatonfő area (about 150 km²) covered by a considerable thick Late Miocene to Quaternary sedimentary pile. They form small horstic blocks coming up below this cover. Consequently the detection of limited steep dipping gold rich horizons expected near the inferred contact with the Velence Granite or in volcanic centres seems to be rather difficult. The suggested method is the systematic seismic reflection and IP survey, complemented by dense soil and rock sampling in the area of the surface outcrops and accompanied by rock sampling of the available drillhole-cores. Typical IP anomalies near the surface will be explored by some inclined drillholes.

5.2. Darnó Zone area, Northeastern Range

The whole area of the extended Darnó Zone (Fig. 28) is about 930 km² including the surface and near surface subareas of the Rudabánya, Uppony and Szendrő Mountains and of the deep located Recsk porphyry copper and skarn deposit. The anomalous and subanomalous partly (meta)sedimentary formations (Tapolcsány Formation, Irota Formation, Szentlélek Formation, Rudabánya Iron Ore, Parád Complex, Darnóhegy Shale) are Paleozoic and Mesozoic in age. Their geologic and tectonic setting favorable for gold mineralization can be characterised by multiphase processes of rifting, subduction and collision, and related regional shear zones. The Rudabánya iron ore deposit, the Recsk porphyry copper and skarn deposit and the Recsk–Lahóca disseminated gold deposit are located in the Darnó shear zone too. These are the main features promising possibilities in the second place to discover Carlin-type gold mineralization.

5.2.1. Rudabánya Mountains

The area in consideration along the eastern border of the Rudabánya Mts. is about 35 km². The gold prospection on the Rudabánya Iron Ore including the abandoned open pits of Rudabánya, Martonyi and Esztramos mines has confirmed our estimations done during the previous screening (KORPÁS and HOFSTRA 1994). The formation as first candidate in that time of Carlin-type gold mineralization shows gold values up to 630 ppb and is considered favorable for further explorations. The surface and more detailed geochemical exploration will be developed on the following two main directions. Enrichment of gold in the open pits is expected in the upper parts of the mineralization, including the zones of secondary iron ore and the zone of base metals with barite. The size of the strata bounded or fault controlled potentially gold bearing zones is calculated about some 10 m × some 100 m.

Therefore the gold potential of the Rudabánya and Martonyi open pits will be controlled by a systematic soil and rock sampling, along a dense grid of geochemical profiles oriented from NW to SE. Distance of the individual profiles is 200 m, with 50 m steps of sampling. The detected gold bearing zones will be explored by trenches and reopening of old adits, furthermore by some normal and inclined drillholes. Subanomalous gold values (up to 16 ppb) of the Tapolcsány Formation and the additive stream sediment anomalies showing low level gold (2–4 ppb Au) will be checked by follow up rock chip sampling.

5.2.2. Recsk area

The area including the deep located porphyry copper and skarn deposit, the Lahóca gold deposit and the Darnó Hill is about 80 km². Continuous subanomalous gold values up to 84 ppb were known in the Parád Complex mantle of the shallow intrusive body hosting the porphyry copper and skarn deposit. A single anomaly with 340 ppb Au was discovered in the Darnóhegy Shale. Further explorations will be aimed at the detection of potentially gold bearing horizons by applying more dense rock chip sampling of the available drillhole cores (Recsk, Rm 1–136) deposited in the core lagers of the Geological Institute of Hungary. Gold analysis of the disposable pulver samples of the previous copper prospection period will be also involved.

5.2.3. Uppony Mountains

The area proposed for further explorations covers about 60 km² and includes the southern part of the Uppony Mts. and its foreland to S between Nagyvisnyó and Dédestapolcsány. Low level subanomalous gold values up to 17 ppb in the Tapolcsány Formation and a single gold anomaly with 234 ppb in the Szentlélek Formation were discovered. The target of the further explorations is to check these anomalies. This will be completed by applying of complementary stream sediment survey and follow up rock chip sampling in the Rágyincs–völgy, Csermely–völgy and Szalajka–patak area. Sampling and gold analysis of available cores of the drillholes Dédestapolcsány and Nagyvisnyó are also required.

5.2.4. Szendrő Mountains

The area located between Abod and Szendrőlád is about 40 km². Low level subanomalous gold values up to 18 ppb were detected in the Irota Formation. The area in discussion can be characterised by some additive stream sediment anomalies and two cells showing low level gold values (2–4 ppb) too. Further explorations will be aimed at the checking of these anomalies. This will be achieved by ways of complementary stream sediment survey and follow up rock chip sampling in the Irota–völgy, Nagy–Csákány–völgy Szén–völgy and Bódva–völgy area. Sampling and gold analysis of available cores of drillholes Szendrőlád, Abod, Irota and Felsővadász are also planned.

5.3. East Alpine units in West Hungary

Geologic and tectonic setting of the Penninic oceanic unit of the Rechnitz (Rohonc) window consisting of ophiolites and metasediments is considered favourable for enrichment of gold (HAAS et al. 1999). Partly mined ores of stibnite, chalkopyrite-azurite, manganese, siderite and pyrite and traces of gold in the metamorphites and ophiolites confirm this possibility. The area in discussion is about 45 km² and includes the Vas-hegy and the Kőszeg Mts. (Fig. 28).

5.3.1. Vas-hegy, Transdanubia

Our sporadic rock chip sampling on the small Vas-hegy plateau (~3 km²) resulted in discovery a single high level gold anomaly of 300 ppm in diabase of the abandoned Felsőcsatár talcum mine. Further systematic geochemical explorations will be aimed at the checking of this point-like anomaly. Stream sediment survey will be applied and complemented by follow up rock chip sampling.

5.3.2. Kőszeg Mountains, Transdanubia

The area in discussion covers 42 km² and can be characterised by some subanomalous gold values up to 19 ppb. A systematic stream sediment survey and complementary follow up rock chip sampling is required for to check these low level gold anomalies.

5.4. Pilis Mountains, Transdanubian Range

The area of 80 km² includes the Mesozoic, mainly Late Triassic horsts of the Kétágú-hegy, Fekete-hegy, Pilis-tető, Csévi-szirtek, Hosszú-hegy, Macska-hegy, Majdan and of the Kevély-hegy covered partly by Paleogene and Quaternary sediments (Fig. 28). This highland controlled by NW oriented dextral faults shows systematic additive stream sediment anomalies with gold values ranging between 2 and 27 ppb in the individual cells. Low level gold anomalies up to 25 ppb were detected in rock chip samples of the Triassic carbonates and related bauxites. Results of more than 75 Carlin samples have proven, that gold anomalies are hosted exclusively in the Triassic carbonates and/or related bauxites. Consequently further geochemical explorations will be concentrated for the 10 anomalous stream sediment cells and a systematic follow up rock chip sampling of the Triassic carbonates and related bauxites will be done within the anomalous cells

5.5. Mecsek Mountains, Transdanubia

The whole area of the Mecsek Mountains excepting the stream sediment cells of No. 8051 (near Magyarürög) and of No. 8045 (near Mánfa) was considered unfavorable for Carlin-type gold mineralization (Fig. 28). The additive anomalies of these two cells (1–1 km²) are accompanied by high level values of gold (332 ppb of the cell No. 8051 and 1270 ppb of the cell No. 8045). Oreshows of malachite and azurite in the Early Triassic Patacs Siltstone (near Magyarürög) and siderite in the Mánfa Siderite Member of the Late Triassic Kantavár Formation (near Mánfa) are known within the cell. Further geochemical explorations will be aimed at the checking of these cells by applying of a systematic follow up rock chip sampling.

6. CONCLUSIONS

Main results of the systematic geochemical explorations for to evaluate the potential of Carlin-type gold mineralization in Hungary can be summarized in the following:

1) Investigation of 97 formations resulted in estimation of a rather modest Carlin gold potential of Hungary. This potential is hosted mainly in Paleozoic, Early Mesozoic subordinately in Young Mesozoic and Paleogene formations.

2) Using threshold values for subanomalous (10–100 ppb Au) and anomalous (>100 ppb Au) groups remained 18 formations consisting of gold in subanomalous or anomalous concentration. In seven formations as well the Paleozoic Lovas Slate (max. 4770 ppb Au), Velence Granite (max. 2090 ppb Au) and Szentlélek Formation (max. 234 ppb Au), the Triassic Rudabánya Iron Ore (max. 630 ppb Au), the Jurassic Darnóhegy Shale (max. 340 ppb Au), the Cretaceous Felsőcsatár Greenschist (max. 300 ppb Au) and the Eocene Nadap Andesite (max. 1000 ppb Au) were detected anomalous values of gold.

3) Ten predictive areas of 2 to 190 km² for further explorations were separated as follows: Velence Hills (190 km²) and Balatonfő (150 km²) in the Transdanubian Range, Rudabánya Mountains (35 km²), Recsk area (80 km²), Uppony Mountains (60 km²) and Szendrő Mountains (40 km²) in the Northeastern Range, Vas-hegy (3 km²) and Kőszeg Mountains (42 km²) in Western Transdanubia, Pilis Mountains (80 km²) in the Transdanubian Range, Mecsek Mountains (2 km²) in South Transdanubia. Two of them in the Velence Hills and in the Rudabánya Mountains exhibit promising Carlin gold potential.

7. REFERENCES

- ALFÖLDI, L.–BALOGH, K.–RADÓCZ, GY.–RÓNAI, A. 1975: Magyarázó Magyarország 200 000-es földtani térképsorozatához. M–34–XXXIII. (Explanations to the geological map series of Hungary, scale 1:200 000. Sheet M–34–XXXIII. Miskolc). — Magyar Állami Földtani-Intézet, 277 p. (In Hungarian).
- BAKSA, CS. 1975: A recski mélyszintű szubvulkáni andezittest és telérei. (The subvolcanic andesite body of Recsk and its dikes). — Földtani Közlöny, 105: 612–624. (In Hungarian with English abstract).
- BAKSA, CS.–CSILLAG, J.–DOBOSI, G.–FÖLDESSY, J. 1981: Rézpala indikáció a Darnó-hegyen. (Copper-rich shale mineralization in the Darnó-hegy). — Földtani Közlöny, 111(1): 69–66. (In Hungarian with English abstract).
- BALOGH, K. 1964: A Bükkhegység földtani képződményei. (Geological formations of the Bükk Mountains). — Magyar Állami Földtani Intézet Évkönyve, 48(2): 245–719. (In Hungarian with German abstract).

- BALOGH, K.–PANTÓ, G. 1954: Földtani vizsgálatok Nekézseny környékén. (Geological investigations in the surroundings of Nekézseny). — Magyar Állami Földtani Intézet Évi Jelentése 1953: 17–27. (In Hungarian with French and Russian abstract).
- BERTALAN, É.–BARTHA, A. 1999: Analytical background of Carlin-type gold prospecting in Hungary. — *Geologica Hungarica Series Geologica* 24: 169–178.
- BARTÓK, A.–NAGY, I. 1992: Magyarország érchordozó ásványi nyersanyagai, színes és feketefémérc vagyona. (Ore deposits of Hungary. Reserves of polymetallic and iron-manganese ores). — Központi Földtani Hivatal, Budapest: 70 p. (In Hungarian).
- BENDA, L. 1932: A nyugatmagyarországi őskori bányászat és kohászat. (Prehistoric mining and metallurgy in West Hungary). — *Acta Sabariensia* 4: 1–19. (In Hungarian).
- BOHN, P. 1979: A Keszthelyi-hegység földtana. (The regional geology of the Keszthely Mountains). — *Geologica Hungarica Series Geologica*, 19: 197 p. (In Hungarian with English abstract).
- BÖJTÖSNÉ–VARRÓK, K. 1965: A nyugat-magyarországi kristályos palák geokémiai vizsgálata. (Geochemical survey of crystalline schist in western Hungary). — Magyar Állami Földtani Intézet Évi Jelentése 1963: 149–156. (In Hungarian with English and Russian abstract).
- BÖJTÖSNÉ–VARRÓK, K. 1967: A palaköpeny hidrotermális ércedése a Velencei-hegység keleti részén. (Hydrothermal ore mineralization in the schist mantle of the Eastern Velence Mts., Transdanubia, Hungary). — Magyar Állami Földtani Intézet Évi Jelentése 1965: 495–505. (In Hungarian with English and Russian abstract).
- BUDA, GY. 1985: Variszkuszi korú kollíziós granitoidok képződése Magyarország, Ny-Kárpátok és a Központi Cseh (Bohémiai) Masszívum granitoidjainak példáján. (Origin of collision-type Variscan granitoids in Hungary, West Carpathians and Central Bohemian Pluton). — Kandidátusi értekezés, Unpublished PhD Theses. (In Hungarian).
- CANDE, S. C.–KENT, D. V. 1992: Revised calibration of the geomagnetic polarity timescale for the Late Cretaceous and Cenozoic. — *Journal of Geophysical Research*, 100: 6093–6095.
- CHRISTENSEN, O. D. ed. 1993: Gold deposits of the Carlin Trend, Nevada. — Society of Economic Geologists, Guide Book Series 18, Lakewood, Colorado: 95 p.
- CSÁSZÁR, G. ed. 1997: Basic Lithostratigraphic Units of Hungary. Charts and short descriptions. — Geological Institute of Hungary, 114 p.
- CSILLAG, J. 1975: A recski terület magmás hatásra átalakult képződményei. (Rocks transformed upon magmatic effects in the Recsk area, Hungary). — *Földtani Közlöny*, 105: 646–671.
- DARIDA–TICHY, M.–HORVÁTH, I.–FARKAS, L.–FÖLDVÁRI, M. 1984: Az andezitmagmatizmushoz kapcsolódó kőzetelváltozások a Velencei-hegység K-i részén. (Rock alterations of andesitic magmatites on the eastern margin of the Velence Mts.). — Magyar Állami Földtani Intézet Évi Jelentése 1982: 271–288. (In Hungarian with English abstract).
- DEÁK, M. ed. 1981: Magyarázó Magyarország 200 000-es földtani térképsorozatához. L–33–V. Sopron. (Explanations to the geological map series of Hungary, scale 1:200 000. Sheet L–33–V. Sopron). — Magyar Állami Földtani Intézet, 132 p. (In Hungarian).
- DOYLE-KUNKEL, M. A. 1993: Geology of the Tusc Deposit, Nevada. In: Christensen O. D. ed.: Gold deposits of the Carlin Trend, Nevada. — Society of Economic Geologists, Guide Book Series 18: 79–87.
- DUDKO, A. 1988: A Balatonfő–Velencei terület szerkezetalakulása. (Tectonics of the Balatonfő–Velence area, Hungary). — *Földtani Közlöny*, 118(3): 207–218. (In Hungarian with English abstract).
- DUDKO, A.–MAJKUTH, T.–DARIDA–TICHY, M.–STOMFAI, R. 1989: A Kelet-Velencei paleovolcán szerkezete. (Structure of the paleovolcano east of Velence, Hungary). — *Általános Földtani Szemle* 24: 135–148. (In Hungarian).
- DULAI, A.–SUBA, ZS.–SZARKA, A. 1992: Toarci (alsójura) szervesanyagdús fekete pala a mecseki Rékavölgyben. (Toarcian (Lower Jurassic) organic-rich black shale in the Réka Valley (Mecsek Hills, Hungary). — *Földtani Közlöny*, 112(1): 67–87. (In Hungarian with English abstract).
- FÖLDESSY, J. 1997: A recski Lahóca aranyérc előfordulása. (The gold deposit of Recsk–Lahóca). — *Földtani Kutatás*, 34(2): 12–15. (In Hungarian).
- FÖLDESSY, JNÉ. 1975: A recski mélyszinti alaphegységi üledékes képződmények. (Deep-seated sedimentary rocks of the basement at Recsk). — *Földtani Közlöny*, 105: 598–609. (In Hungarian with English abstract).
- FÖLDVÁRI, A. 1947: A molibdén Velencei-hegységi előfordulásainak teleptani viszonyai. (Postvolcanic molybdenum traces in the Velence–Mountain). — *Beszámoló a Vitaülésekről*, 9(1–6): 39–58. (In Hungarian with English abstract).

- FÖLDVÁRI, A.–NOSZKY, J.–SZEBÉNYI, L.–SZENTES, F. 1948: Földtani megfigyelések a Kőszegi hegységben. (Geological observations in the Kőszeg Mountains). — Jelentés a Jövedéki Mélykutatás 1947–48. Évi Munkálatairól, 5–31. (In Hungarian).
- FÖLDVÁRINÉ–VOGL, M. 1970: Összefoglaló értékelő jelentés a területi ritkaelemkutatás tájékoztató jellegű kutatási fázisának eredményeiről. (Summary report about the results of the regional orientative rare element research). — Magyar Állami Földtani Intézet, 95 p. (In Hungarian).
- FÜGEDI, U.–SZEBÉNYI, G.–GASZTONYI, É.–CSILLAG, J.–BERTALAN, É.–CSALAGOVITS, I.–SÁSDI, L.–NÁDOR, A.–VÍG ANÉ. 1991: A recski mélyszinti színesfémérc-lelőhely geokémiai etalonvizsgálata. "Szkarnos" réz- és cinktelepek (É-i bányamező). (Geochemical standard-study of the Recsk deep-level base-metal deposit. "Skarn" copper and zinc orebodies of the orefield N). — Magyar Geológiai Szolgálat Országos Földtani és Geofizikai Adattára, Kézirat (Unpublished report in Hungarian).
- FÜLÖP, J. 1990: Magyarország geológiája. Paleozoikum I. (Geology of Hungary. Paleozoic I.). — Magyar Állami Földtani Intézet, Budapest, 325 p. (In Hungarian).
- FÜLÖP, J. 1994: Magyarország geológiája. Paleozoikum II. (Geology of Hungary. Paleozoic II.). — Akadémia Kiadó, Budapest, 447 p. (In Hungarian).
- HAAS, J. (ed). 1993: Magyarország litosztratigráfiai egységei. Triász. (Lithostratigraphic units of Hungary: Triassic). — Magyar Állami Földtani Intézet, Budapest, p. 278. (In Hungarian).
- HAAS, J.–HÁMOR, G.–KORPÁS, L. 1999: Geological setting and tectonic evolution of Hungary. — *Geologica Hungarica Series Geologica* 24: 179–196.
- HOFSTRA, A. H.–KORPÁS, L.–CSALAGOVITS, I.–JOHNSON, C. A.–CHRISTIANSEN, W. D. 1999: Stable isotopic study of the Rudabánya iron mine—a carbonate-hosted siderite, barite, base-metal sulfide replacement deposit. — *Geologica Hungarica Series Geologica* 24: 295–302
- HORVÁTH, I.–ÓDOR, L. 1989: A Polgárdi Mészke Formáció kontakt metamorf és metasomatikus jelenségei. (Contact metamorphic and metasomatic phenomena in the Polgárdi Limestone Formation, Transdanubia, Hungary). — Magyar Állami Földtani Intézet Évi Jelentése 1987: 137–143. (In Hungarian with English abstract).
- HORVÁTH, I.–ÓDOR, L.–Ó. KOVÁCS, L. 1989: A Velencei-hegységi gránit metallogéniai sajátosságai. (Metallogenic features of the Velence Mts. granitoids). — Magyar Állami Földtani Intézet Évi Jelentése 1987: 349–365. (In Hungarian with English abstract).
- HORVÁTH, I.–ÓDOR, L.–DARIDA–TICHY, M. 1990: Arany ércesedési nyomok a Velencei hegységi Nadap körzetében. (Gold shows in the Nadap area, Velence Hills). — Magyar Geológiai Szolgálat Országos Földtani és Geofizikai Adattára, Kézirat (Unpublished report in Hungarian).
- HORVÁTH, I.–GYALOG L.–ÓDOR, L.–DARIDA–TICHY, M.–DUDKO, A.–Ó. KOVÁCS, L. in press: Magyarázó a Velencei-hegység és környékének földtani térképeire. (Explanations to the geological maps of the Velence Hills and its surroundings). — Magyar Állami Földtani Intézet. (In Hungarian).
- JANTSKY, B. 1957: A Velencei-hegység földtana. (Geology of the Velence Mountains). — *Geologica Hungarica Series Geologica* 10: 1–170. (In Hungarian with French and Russian abstract).
- JÁGER, V. 1998: Ritkaságok a Keleti Mecsek ásványvilágából. (Rarities among the minerals of the Eastern Mecsek, Hungary). — *Földtani Kutatás*, 35 (2): 19–22. (In Hungarian).
- JÁMBOR, Á. 1960: Jarosit kötőanyagú homokkő a Szendrői-hegység DK-i peremén. (Jarosite bearing sandstone at the border SE of the Szendrő Mountains). — *Földtani Közlöny*, 90: 363–368. (In Hungarian with Russian abstract).
- JÁMBOR, Á. 1989: Földtan, M=1: 1,000 000. (Geology, scale: 1:1,000 000). — (Magyarország földtani térképe—Geological map of Hungary). Magyar Állami Földtani Intézet. (In Hungarian).
- KISS, J. 1951: A szabadbattyáni Szárhegy földtani és ércgenetikai adatai. (Geology and ore genesis of the Szárhegy, Szabadbattyán). — *Földtani Közlöny*, 81: 264–274. (In Hungarian with Russian and French abstract).
- KISS, J. 1958: Ércföldtani vizsgálatok a siroki Darnóhegyen. (Ore geological investigations at the Darnóhegy, Sirok). — *Földtani Közlöny*, 88: 27–41. (In Hungarian with German abstract).
- KOCH, S. 1985: Magyarország ásványai. (The minerals of Hungary). — Akadémia Kiadó, Budapest, 562 p. (In Hungarian).
- KORPÁS, L. 1998: Palaeokarst studies in Hungary. — *Occasional Papers of the Geological Institute of Hungary* vol. 195, Budapest, 140 p.
- KORPÁS, L.–HOFSTRA, A. 1994: Potential for Carlin-type gold deposits in Hungary. Carlin gold in Hungary. — Project JFNo 435. US–Hungarian Joint Fund, Budapest.
- KORPÁS, L.–CSILLAGNÉ–TEPLÁNSZKY, E.–HÁMOR, G.–ÓDOR, L.–HORVÁTH, I.–FÜGEDI, U.–HARANGI, SZ. 1998: Magyarázó a Börzsöny és a Visegrádi-hegység földtani térképéhez. (Explanations to the geological map of the Börzsöny and Visegrád Mountains). — Magyar Állami Földtani Intézet, Budapest, 216 p. (In Hungarian with English summary).

- KORPÁS, L.–LANTOS, M.–NAGYMAROSY, A. 1999: Timing and genesis of early marine caymanites in the hydrothermal palaeokarst system of Buda Hills, Hungary. — *Sedimentary Geology*, 123: 9–29.
- KOVÁCS, S. 1998: A Szendrői- és az Upponyi-hegység paleozóos képződményeinek rétegtana. (Stratigraphy of the Paleozoic formations of the Szendrő and Uppony Mountains). — in BÉRCZI, I.–JÁMBOR, Á. (eds.): Magyarország geológiai képződményeinek rétegtana. (Stratigraphy of geological formations in Hungary). — Budapest: 107–117. (In Hungarian).
- KUBOVICS, I. 1958: A sukorói Meleghegy hidrotermás ércesedése. (The hydrothermal ore genesis of the Meleg Hill, Sukoró, Velence Mountains, Hungary). — *Földtani Közöny* 88(3): 299–314. (In Hungarian with English abstract).
- LELKES–FELVÁRI, GY. 1978: A Balaton–vonal néhány permnél idősebb képződményének közettani vizsgálata. (Petrography of some pre-Permian formations along the Balaton Line). — *Geologica Hungarica Series Geologica*, 18: 193–295. (In Hungarian with German abstract).
- LELKES–FELVÁRI, GY. 1998a: Nyugat-Magyarországi metamorfitek. (Metamorphites of West Hungary). — in BÉRCZI, I.–JÁMBOR, Á. (eds.): Magyarország geológiai képződményeinek rétegtana. (Stratigraphy of geological formations in Hungary), Budapest: 55–71. (In Hungarian).
- LELKES–FELVÁRI, GY. 1998b: A Dunántúli-középhegység metamorf képződményeinek rétegtana. (Stratigraphy of the metamorphic formations in the Transdanubian Range). — in BÉRCZI, I.–JÁMBOR, Á. (eds.): Magyarország geológiai képződményeinek rétegtana. (Stratigraphy of geological formations in Hungary), Budapest: 73–86. (In Hungarian).
- MAJOROS, GY. 1998: A Dunántúli-középhegység újpaleozóos képződményeinek rétegtana. (Stratigraphy of the New Paleozoic formations of the Transdanubian Range). — in BÉRCZI, I.–JÁMBOR, Á. (eds.): Magyarország geológiai képződményeinek rétegtana. (Stratigraphy of geological formations in Hungary), Budapest: 119–147. (In Hungarian).
- MÉSZÁROS, M. 1954: Előzetes jelentés a perkupai gipszkutatásról. (Preliminary report of the exploration of gypsum, Perkupa). — *Magyar Állami Földtani Intézet Évi Jelentése* 1953(1): 277–286. (In Hungarian with French and Russian abstract).
- MÉSZÁROS, M. 1961: A perkupai gipsz–anhidrit előfordulás földtani viszonyai. (Geology of the gypsum-anhydrite deposit in Perkupa). — *Magyar Állami Földtani Intézet Évkönyve*, 49(4): 939–949. and 1157–1169. (In Hungarian).
- MOLNÁR, F. 1998: Újabb adatok a Velencei-hegység molibdenitjének genetikájához: ásványtani és folyadékzárvány vizsgálatok a Retezi–lejtakna ércesedésén. (Contributions to the genesis of molybdenite in the Velence Mts.: mineralogical and fluid inclusion studies on the mineralization of the Retezi adit). — *Földtani Közöny* 127(1–2): 1–17. (In Hungarian with English abstract).
- NAGY, B. 1980: Adatok a velencei-hegységi és szabadbattyáni ércesedések és ércindikációk ásványparageneziséhez és geokémiájához. (Contribution to the paragenesis and geochemistry of ore mineralizations and ore shows in the Velence Mountains and at Szabadbattyán). — *Magyar Állami Földtani Intézet Évi Jelentése* 1978: 263–289. (In Hungarian with English abstract).
- NAGY, E.–RAVASZNÉ–BARANYAI, L. 1968: Tufás kaolinit- és siderittelepek a mecseki ladini összlet alján. (Tuff bearing kaolinite and siderite deposits at the base of the Ladinian, Mecsek Mts., Hungary). — *Földtani Közöny*, 98(2): 213–217. (In Hungarian with German abstract).
- ÓDOR, L.–DUDKO, A.–GYALOG, L. 1982: A Velencei-hegység északkeleti részének metallometriai értékelése. (Metallometric evaluation of the NE Velence Mountains, W Hungary). — *Magyar Állami Földtani Intézet Évi Jelentése* 1980: 211–227. (In Hungarian with English abstract).
- ÓDOR, L.–WANTY, R. B.–HORVÁTH, I.–FÜGEDI, U. 1999: Environmental signatures of mineral deposits and areas of regional hydrothermal alterations in Northeastern Hungary. — *Geologica Hungarica Series Geologica* 24: 107–129.
- PAUL, E. K.–MUIRHEAD, E. M. M.–KUNKEL, K. W. 1993: Geology and gold mineralization of the Genesis deposit, Eureka County, Nevada. — In: CHRISTENSEN, O. D. ed.: *Gold deposits of the Carlin Trend, Nevada*, Society of Economic Geologists, Guide Book Series 18: 36–49.
- PELIKÁN, P. 1996: Geokémiai és földtani adatok a Bükk-hegységi Carlin aranyérc potenciál felméréséhez. (Geochemical and geological data for the estimation of Carlin gold ore potential of the Bükk Mountains). — *Magyar Geológiai Szolgálat Országos Földtani és Geofizikai Adattára, Kézirat* (Unpublished report in Hungarian).
- POLGÁRI, M. 1993: A Mn geokémiája a feketepala képződés és a diagenetikus folyamatok tükrében. Az úrkúti karbonátos mangánérc képződési modellje. (Manganese Geochemistry—reflected by black shale formation and diagenetic processes. Model of formation of the carbonatic manganese ore of Úrkút). — *Magyar Állami Földtani Intézet*, 211 p. (In Hungarian and English).

- RAINCSÁK, GY. 1984: Alsó triász sztratiform ércképződés lehetőségeinek vizsgálata Veszprém–Litér–Sóly között és az Iszka–hegy környékén. (A study on the possibility of Early Triassic stratiform ore mineralization in the Veszprém–Litér–Sóly zone and the vicinity of Iszka–hegy, Transdanubian Central Range). — Magyar Állami Földtani Intézet Évi Jelentése 1982: 245–262. (In Hungarian with English abstract).
- RAINCSÁK–KOSÁRY, ZS. 1978: A Szendrői-hegység devon képződményei. (The Devonian formations of the Szendrő Mountains). — *Geologica Hungarica Series Geologica* 18: 7–113. (In Hungarian with German abstract).
- ROTA, J. C. 1993: Geology and related studies at the Gold Quarry deposit, Nevada. — *in* CHRISTENSEN, O. D. ed.: Gold deposits of the Carlin Trend, Nevada, Society of Economic Geologists, Guide Book Series 18: 67–78.
- SZABÓ, Z.–GRASSELLY, GY.–CSEH NÉMETH, J. 1981: Some conceptual questions regarding the origin of manganese in the Úrkút deposit, Hungary. — *Chemical Geology*, 34: 19–29.
- SZEBÉNYI, L. 1948: A Vas-hegy magyarországi részének földtani viszonyai. (Geology of the Hungarian part of Vashegy). — Jelentés a Jövedéki Mélykutatás 1947–48 Évi Munkálatairól, 45–50. (In Hungarian).
- SZENTES, F. 1948: A kénkovand előfordulások földtani viszonyai a Keszthelyi-hegység környékén. (Geology of the pyrite and marcasite-occurrences in the surroundings of Keszthely Mountains.). — Jelentés a Jövedéki Mélykutatás 1947/48. Évi Munkálatairól, 51–103. (In Hungarian).
- SZENTES, F.–BARNABÁS, K.–CZABALAY, L.–DEÁK, M.–DÉR, I.–JUGOVICS, L.–KNAUER, J.–KOPEK, G.–KÓKAY, J.–MAJOROS, GY.–MARCZEL, FNÉ–NOSZK, Y J.–SZABÓ, I.–SZÜCS, L. 1972: Magyarázó Magyarország 200 000-es földtani térképsorozatához. L–33–XII. Veszprém. (Explanations to the geological map series of Hungary, scale 1:200 000. Sheet L–33–XII. Veszprém). — Magyar Állami Földtani Intézet, 271 p. (In Hungarian).
- THORESON, R. F. 1993: Geology of the Post deposit, Eureka county, Nevada. — *in* CHRISTENSEN, O. D. ed.: Gold deposits of the Carlin Trend, Nevada, Society of Economic Geologists, Guide Book Series 18: 50–66.
- TOKODY, L. 1952: A kozári azurit-előfordulás a Mecsek hegységben. (Occurrence of azurite at Kozár, Mecsek Mountains). — *Földtani Közlöny*, 82(7–9): 263–269. (In Hungarian with German abstract).
- VÁRSZEGI, K. 1965: Karbonátos rézászvány-előfordulás a mecseki Éger-völgy alsó triász rétegeiben. (Occurrence of carbonate copper minerals in the Lower Triassic beds of Éger-völgy, Mecsek Mts.). — *Földtani Közlöny*, 45(4): 437–438. (In Hungarian with German abstract).
- VETŐ, I. 1988: A Dunántúli-középhegység alsó-triász képződményeinek szervesanyaga. Szénhidrogén képződés és migráció. (Organic matter of Lower Triassic formations in the Transdanubian Mid-Mountains. Hydrocarbons and migration). — Magyar Állami Földtani Intézet Évkönyve 65(2): 323–330. (In Hungarian with English abstract).
- VETŐ, I.–DEMÉNY, A.–HERTELENDI, E.–HETÉNYI, M. 1997: Estimation of primary productivity in the Toarcian Tethys. — A novel approach based TOC, reduced sulfur and manganese contents. *Palaeogeography, Palaeoclimatology, Palaeoecology* 132: 355–371.
- WAKEFIELD, T. 1993: Geochemical exploration of the Carlin Trend. — *in* CHRISTENSEN, O. D. ed.: Gold deposits of the Carlin Trend, Nevada, Society of Economic Geologists, Guide Book Series 18: 88–92.
- ZELENKA, T. 1996: Carlin típusú aranyércesedés lehetőségei Recskén. (The possibility of Carlin-type gold mineralization at Recsk). — Magyar Geológiai Szolgálat Országos Földtani és Geofizikai Adattára, Kézirat (Unpublished report in Hungarian).

STABLE ISOTOPIC STUDY OF THE RUDABÁNYA IRON MINE. A CARBONATE-HOSTED SIDERITE, BARITE, BASE-METAL SULFIDE REPLACEMENT DEPOSIT

ALBERT H. HOFSTRA¹, LÁSZLÓ KÖRÖPÁS², IMRE CSALAGOVITS², CRAIG A. JOHNSON¹,
and WILLIAM D. CHRISTIANSEN¹

¹US Geological Survey, P. O. Box 25046, Denver, CO, 80225, USA

²Geological Institute of Hungary, H-1143 Budapest, Stefania út 14., Hungary

ABSTRACT

The Rudabánya iron mine is one of the oldest mines in Hungary. The deposit is hosted in Lower to Middle Triassic dolomites and siliciclastics. The stratabound replacement deposit is localized by faults produced during Middle Triassic rifting and is deformed by Late Cretaceous folds. The present day distribution of the ore is controlled by a large asymmetric and locally overturned dome. The primary massive replacement ores formed in 3 stages (1) hematite (\pm siderite) and (2) siderite, cut by (3) stockworks and veins of barite, galena, and chalcopyrite with anomalous Ag and Au. Mineral zoning in the ores from the surface to a depth of about 300 m consists of a zone of secondary limonite (40–50 m) that locally contains native copper and silver, followed by a zone of primary siderite (150 m) with chalcopyrite and galena and then hematite (>100 m) with lesser sulfides. The presence of marcasite in the ores is indicative of temperatures less than 240 °C and pH < 5. Results of stable isotope studies suggest (1) the host dolomite is diagenetic in origin, (2) the hydrothermal siderite has isotopic compositions similar to dolomite in MVT Zn-Pb deposits, (3) the SO₄ in barite was derived from Lower Paleozoic black shales underlying the deposit, (4) the sulfur in sulfides was derived from thermochemical reduction of Upper Permian sedimentary sulfate, and (5) sphalerite-galena geothermometry yields a temperature of 115 °C. The ore deposit formed where migrating, acidic, basinal brines containing Fe, base metals, and sulfate moved up faults produced by Middle Triassic rifting and encountered reactive carbonate rocks and indigenous ground waters containing Ba and H₂S.

1. INTRODUCTION

One of the oldest mines in Hungary, the Rudabánya iron mine is located in the Northeastern Range near the town Miskolc (Fig. 1). The deposit is hosted in Lower to Middle Triassic dolomites and siliciclastics where they are cut by a major NE-striking fault system called the Darnó Fault. Mining began about 2000 years ago for native copper. In the Middle Ages, Rudabánya was a free mining town and became one of the centers of copper and silver mining. Although mining declined during the 16th and 17th centuries, there was a resurgence with commencement of the first open pit iron mine in 1878. Intensive exploitation of the limonitic iron ores resulted in the opening of seven pits (Polyánka, Bruinmann, Andrásy I, II and III, Vilmos, Ruda-hegy and Deák pit) that together form a 5 km long by 1.5 km wide continuous mining belt. About 1,000 limonitic ore bodies were mined to depths of 50 to 60 m with maximum sizes of 500 × 40 × 10 m (PANTÓ 1956). Over 21 Mt of limonite ore with an iron content of 33–35% was produced. Surface operations were abandoned in 1953 but underground workings continued to extract siderite ore with 24% iron. About 50,000 t/year of copper ore was processed as a by-product. Iron mining ceased in 1985 after producing 11 Mt of siderite ore. Present day proven ore reserves according to BARTÓK and NAGY (1992) are as follows: 37.2 Mt of siderite ore (24.29% iron), 1.54 Mt of chalcopyrite ore (0.56% Cu and 1.2 ppm Ag) and 0.56 Mt of galena ore (1.42% Pb). At the current prices the average concentrations of the ores are insufficient to be mined economically. Gold concentrations are also low and generally <50 ppb (KÖRÖPÁS et al. 1999).

Rudabánya shares many features with carbonate-hosted siderite replacement deposits that form from basinal brines and are akin to MVT Pb-Zn deposits [e.g. Bilbao, Spain; Quenza, Algeria] (BOUZENOUNE and LECOLLE 1997).

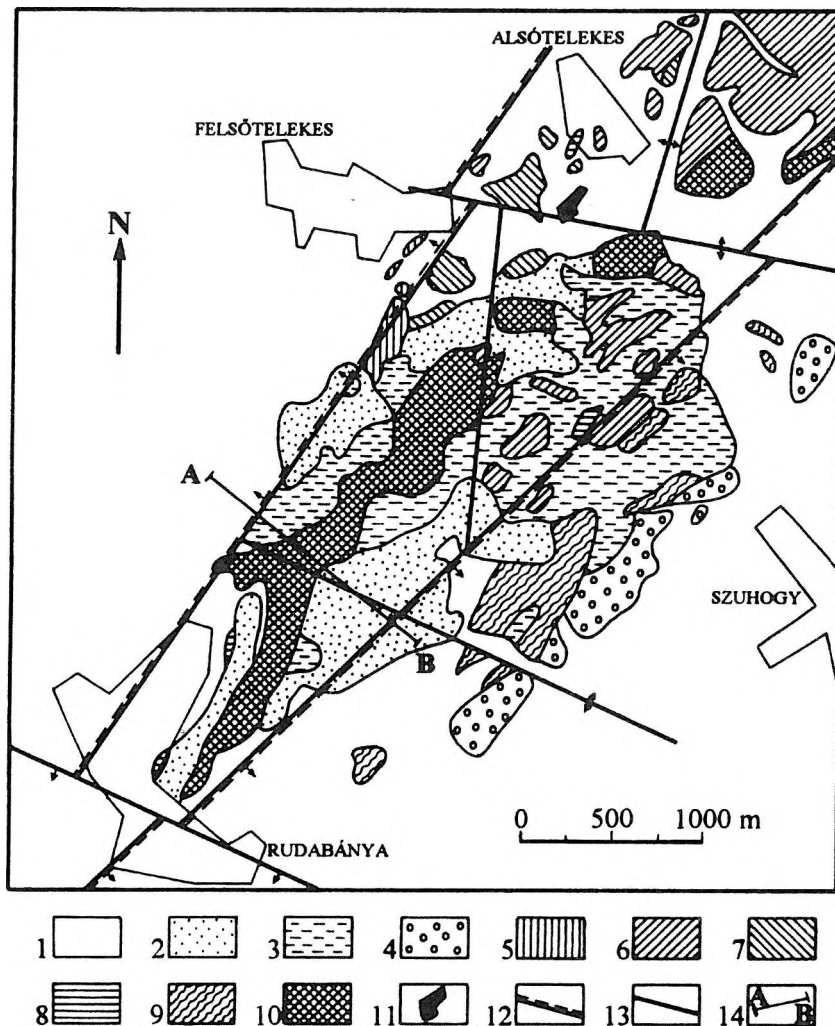


Fig. 1: Geologic map of the Rudabánya iron mine (after HERNYÁK 1977)

1. Quaternary sediments, 2. Mine waste, 3. Late Miocene clay, sand and gravel, 4. Early Miocene Szuhogy Conglomerate, 5. Jurassic shales, cherty limestone and radiolarite, 6. Middle Triassic Gutenstein Dolomite, 7. Lower Triassic Szin Marl and Szinpetri Limestone, 8. Lower Triassic Bódvaszilás Sandstone, 9. Paleozoic Tapolcsány Formation, 10. Limonite and siderite ore, 11. Hematite ore, 12. Reverse fault, 13. Normal fault, 14. Cross section.

Rudabánya also shares some features with polymetallic-siderite-quartz vein deposits hosted in clastic metasedimentary rocks that form from deep formation or metamorphic waters that ascend along major faults [e.g. Příbram, Czech Republic; Rudnany, Nizna Slana, and Dobsina in the Gemer Mountains, Slovakia; Bakalsk in the Ural Mountains, Russia; Kremikovci and Ciprovci in Sredna Gora, Bulgaria; Vares and Liubia, Bosnia; and Eiesenerz, Austria] (NAGY 1982; BEAUDOIN and SANGSTER 1992).

Previous investigations at Rudabánya by PANTÓ (1956), CSALAGOVITS (1973a,b) and NAGY (1982) resulted in the following conclusions regarding its origin. According to PANTÓ, the mineralization formed at shallow depths of up to 200 m, at temperatures of 100–150 °C, without any direct influence from magmatic activity. A Laramian age of mineralization was postulated by him based on evidence that the deposit was deformed during Late Cretaceous regional compression. Based on a systematic geochemical study of the mineralization and its footwall and hanging wall formations, CSALAGOVITS (1973a, b) concluded that the deposit formed from the mixing of two contrasting fluids. He thought that there were two major paleoaquifers in the region and that the replacement mineralization resulted from the mixing of a low temperature, reduced, descending water (rich in Ca, Mg, H₂S and HCO₃ with Fe, Mg, Ba) with a high temperature ascending thermal water (rich in Mg, Fe, Cl and SO₄ with Cu, Pb, Zn, Ag, As, Sb, Hg, Tl, Bi, Cd, In, and Ge). The source of the metals was considered by him to be the evaporites (Perkupa Anhydrite) and Paleozoic black shales below it. Moderate to deep burial subsidence, pre-ore tensional tectonics, and porosity controlled the localization of ore, which was sealed and trapped mainly by the Szin Marl. The mineralization predates compressional deformation. NAGY (1982) utilized fluid inclusion decrepitation temperatures from chalcopyrite (430 °C), galena (360 °C) and barite (350 °C and 260 °C) to estimate the temperature of ore formation and concluded that, in the absence of magmatic activity, these data require a long period of deep burial and/or elevated heat flow during ore formation.

During a field trip to Rudabánya in 1996, we collected nineteen representative samples from four sites in the Andrásy I. open pit. Samples were obtained from the dolomite host rock, siderite ores containing base metal sulfides and barite, and limonite ores containing supergene gypsum. Another sample was collected from the Alsótelekes gypsum-anhydrite open pit, which is in rocks representative of the foot wall of the Rudabánya Iron Mine. Polished pucks and thin sections were made of samples from the Andrásy I. pit and examined to document the paragenetic sequence. Minerals representative of the major stages of mineralization were separated and analyzed using standard stable isotopic methods. The goal of this study was to utilize new stable isotopic data along with previous geologic and geochemical information to improve understanding of the origin of the deposit.

2. GEOLOGIC SETTING AND TECTONIC EVOLUTION

The geologic setting and tectonic evolution of the area are described below based on information in GRILL et al. (1984), LESS and SZENTPÉTERY (1987), GRILL (1988), RÉTI (1988), KOVÁCS et al. (1989), HIPS (1996) and LESS (1998). The Late Permian to Middle Triassic pre-rift sedimentary sequences are representative of a continental to shallow ramp depositional system. Early evaporites (Perkupa Anhydrite) were followed by peritidal siliciclastics (Bodvaszilás Sandstone*), subtidal carbonates (Szin Marl*, Szinpetri Limestone*) and capped by dolomites of restricted lagoon (Gutenstein Formation*) or limestones of open lagoon (Steinalm Formation) environments. Rifting, accompanied by synchronous volcanism, was completed by Ladinian time and resulted in disintegration of the ramp system and opening of an oceanic basin between two continental units to the south and north. This oceanic basin was consumed partly during Middle Jurassic north-oriented subduction and closed during the Late Jurassic to Early Cretaceous collision of the two continental units. Coeval volcanism and emplacement of Gemer Granites far to the north can be related to the subduction and collision. A new depositional cycle started in the Middle Oligocene, after a long period of subaerial exposure, characterized by progressive nappe-formation to the south during the Late Cretaceous. Middle Oligocene to Early Miocene clastics were deposited in a narrow pull-apart basin oriented NNE-SSW controlled by sinistral movement along the Darnó Fault. Since then, the 25 km long iron ore belt (including the Rudabánya, Martonyi and Esztramos deposits) along the border east of the Rudabánya Mts. has been in its current position. Late Miocene to Quaternary alluvial, lake and eolian clastic sedimentation was the last depositional event, and was followed by subsequent uplift and erosion, yielding the present day picture.

3. DEPOSIT DESCRIPTION

The stratabound siderite replacement mineralization is hosted in the Bodvaszilás Sandstone, Szin Marl, Szinpetri Limestone and Gutenstein Dolomite (Fig. 2). The overlying Steinalm Limestone is unmineralized. The total thickness of these formations ranges from 800 to 1000 m. Siderite mineralization is known to a depth of 300 m, with mined ore to a depth of about 130 m (underground level +180 m, HERNYÁK 1977). Distribution of the ore is controlled by a large asymmetric and overturned dome that strikes NNE (PÁLFY 1924, BALOGH and PANTÓ 1952). This dome exhibits minor "roof structures" and is dissected by internal folds that verge to both the NW and SE (PANTÓ 1956).

Present day vertical zoning is outlined below after HERNYÁK (1977). The total thickness of mineralized rock is about 300 m and is divided from top to bottom in the following order:

Zone of secondary limonite: 40-50 m with variable basemetals,

Zone of primary siderite: 100 m of siderite that is rich in base metals (Cu, Pb) underlain by 50 m of silica-rich siderite that is poor in base metals (Cu),

Zone of primary hematite: >100 m of hematite that is poor in base metals (Cu).

Although siderite and Cu mineralization only extend to depths of about 300 to 400m, hematite mineralization has been encountered at the deepest levels explored by drilling (800m).

Three stages of mineralization were recognized by PANTÓ (1956), consisting of primary massive replacement ores with (1) hematite (\pm siderite) and (2) siderite, cut by (3) base metal stockworks and veins of barite, galena and chalcopyrite. The simple paragenesis of the primary iron ores, with ankerite, calcite and pyrite, was overprinted by a base metal sulfide-barite paragenesis accompanied by siderite, pyrite, pyrrhotite, bornite, chalcocite, tetrahedrite, stibnite, schwazite, pyrrargyrite, bourmonite, jamesonite and sphalerite with quartz, fluorite, sericite and other clay minerals (CSALAGOVITS 1973a, b and NAGY 1982). The secondary iron ore, consisting of massive

* Host rocks of the Rudabánya Iron Ore.

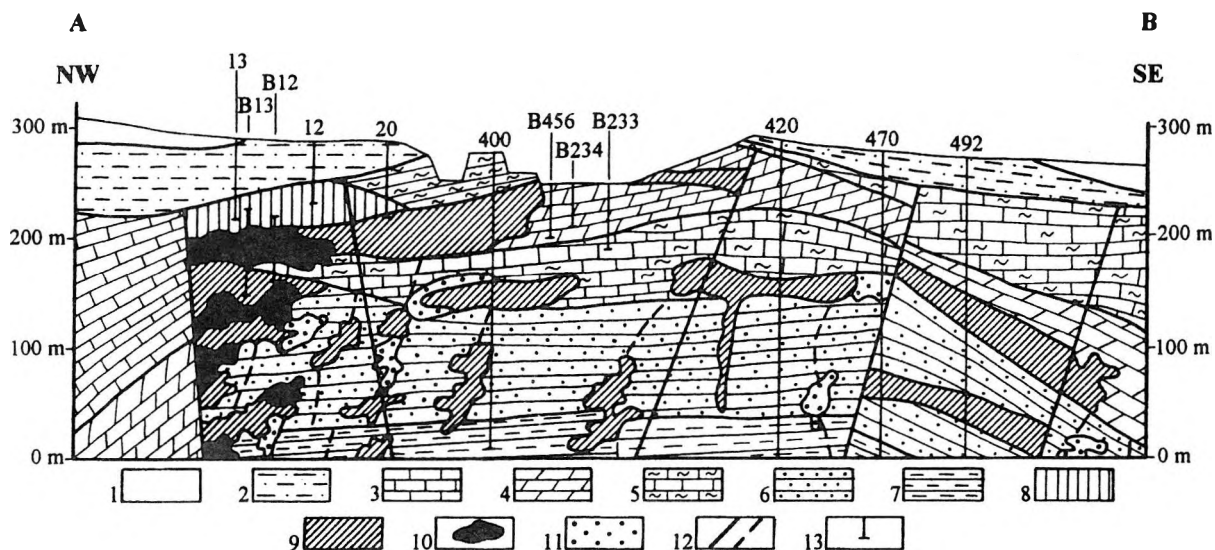


Fig. 2: Cross section of the Rudabánya iron mine (after HERNYÁK)

1. Mine waste, 2. Late Miocene clay, sand and gravel, 3. Jurassic shale, cherty limestone and radiolarite, 4. Middle Triassic Gutenstein Dolomite, 5. Lower Triassic Szin Marl and Szinpetri Limestone, 6. Lower Triassic Bódvaszilás Sandstone, 7. Black shales, 8. Limonite ore, 9. Siderite ore, 10. Polymetallic ore, 11. Barite (±sulfides), 12. Faults, 13. Drill holes.

limonite, goethite, hematite, sphaerosiderite, marcasite, and relict primary minerals, is rich in supergene Mn–(pirolusite, psilomelane, waad), Cu–(covellite, tenorite, cuprite, azurite, malachite, native copper), Ag–(native silver), Pb–(cerussite, anglesite), and Hg–minerals (cinabar, mercury), and also contains gypsum, epsomite, and melanterite. Traces of native gold were reported by PANTÓ (1956) and NAGY (1982).

Many of the primary hypogene minerals mentioned above were also observed in our samples. However, we observed textural features in the pyrite which indicate that it formed from a metastable marcasite precursor (MUROWCHICK 1992). We also think that the "secondary marcasite" described above may actually be primary. This is important because marcasite only forms at temperatures <240 °C from fluids with a pH <5 (MUROWCHICK 1992). The presence of marcasite in the ores suggests that the temperature of mineralization was much lower than that inferred from decrepitation temperatures of fluid inclusions (NAGY, 1982). The decrepitation temperatures are also unreliable because similar decrepitation temperatures are obtained from MVT Pb-Zn deposits in the United States that formed at temperatures <150 °C (D. LEACH and A. HOFSTRA unpublished data). The paragenetic sequence portrayed on Fig. 3 is based on crustification sequences and cross cutting relationships observed in polished pucks, thin sections, and field observations. It is similar to previous ones with precipitation of siderite followed by basemetal sulfides and barite. Episodes of brecciation or faulting are also indicated. As above, weathering and oxidation of the hypogene mineral assemblage resulted in the formation of limonite, gypsum, and a variety of supergene Cu, Pb, and Ag minerals.

Geochemical studies (CSALAGOVITS 1973a, b) have shown that the replacement mineralization is characterized by the introduction of Fe, Mg, Mn, Ba, Cu, Pb, Zn, Ag, As, Sb, Hg, Bi, Cd, In, Ge, and Tl. Previous Au and Ag analyses, conducted between 1971 and 1975, on 160 underground, surface and drillhole samples yield sporadic low level Au anomalies (traces to 0.2 ppm with a maximum of 1 ppm) and widespread Ag anomalies ranging from a few ppm to 20 ppm with a maximum of 451 ppm (RUDABÁNYA). New gold analyses of 50 grab samples from the mine ranged from <2 to 630 ppb, but only 5 samples contained more than 50 ppb Au (KORPÁS et al. 1999). Silver content ranges between 0.2 and 425 ppm with 11 samples containing more than 50 ppm Ag (KORPÁS et al. 1999).

4. STABLE ISOTOPES

The stable isotopic composition of brecciated host rock dolomite, evaporite gypsum, hydrothermal siderite, sulfides, and barite, and supergene gypsum are shown on Figs. 4 and 5. The brecciated dolomite host rock has $\delta^{13}\text{C}$ values (–0.8 to –1.7‰) typical of marine limestone and $\delta^{18}\text{O}$ values (18.2 to 18.8‰) that are at the low end for marine limestone. The isotopic data suggest that the dolomite is diagenetic in origin and was not substantially recrystallized by the hydrothermal fluids, although there may have been minor ^{18}O depletions. The isotopic com-

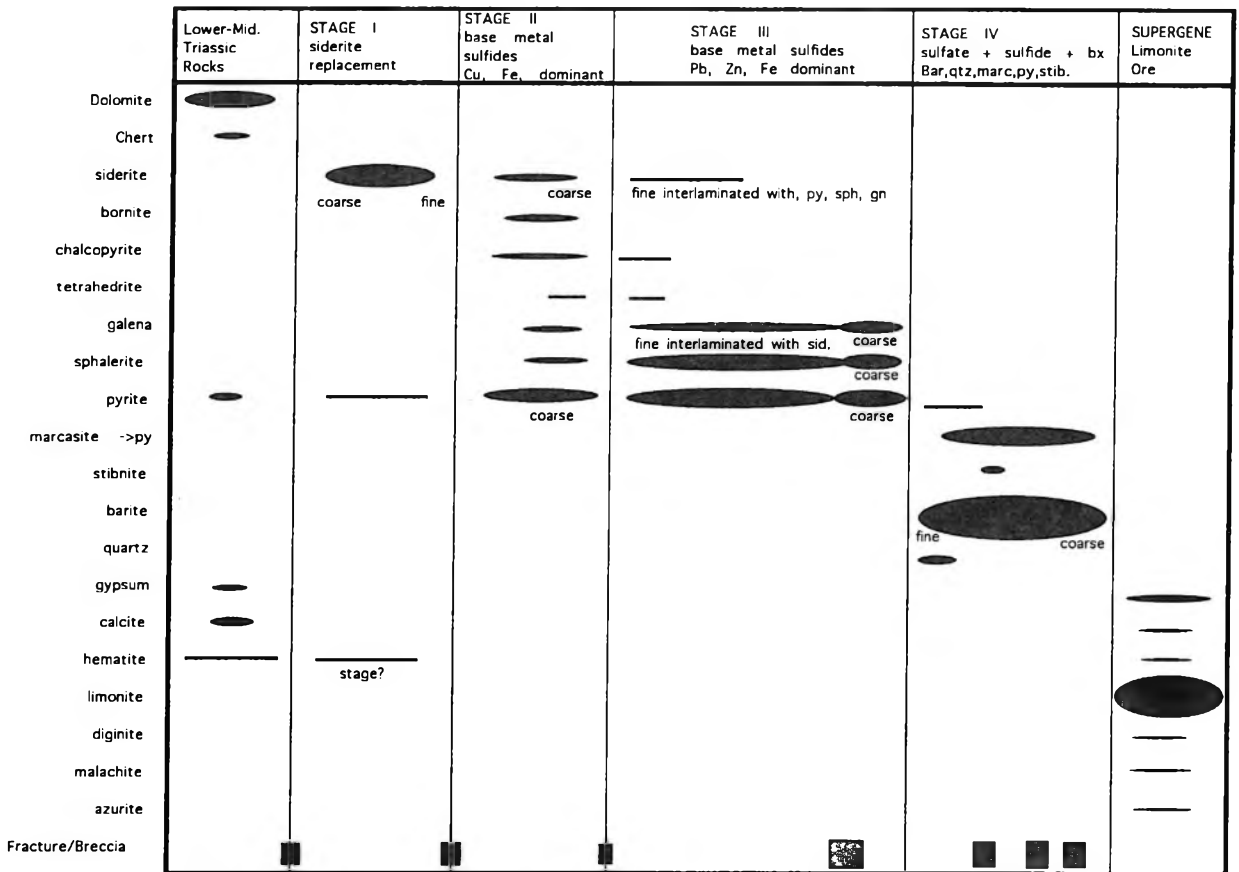
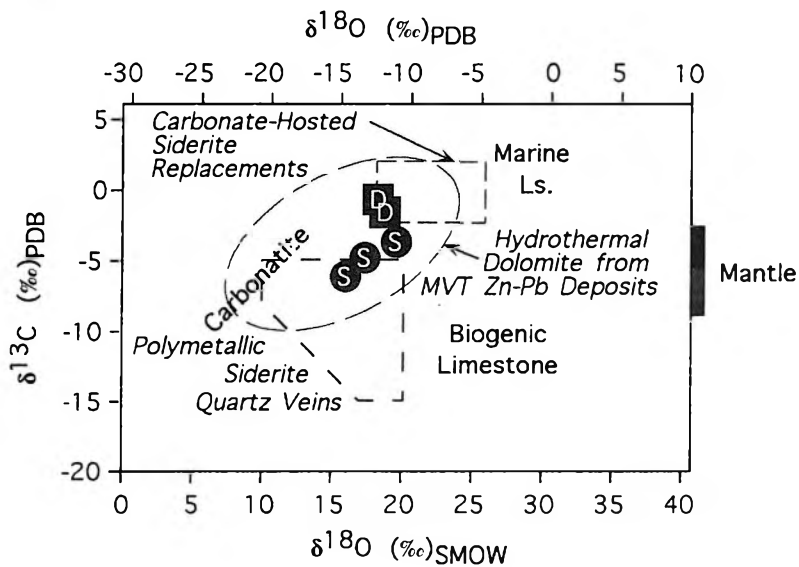


Fig. 3: Paragenetic sequence constructed from field observations and petrographic examination of polished pucks and thin sections
Fracturing and brecciation are also indicated

Fig. 4: Carbon and oxygen isotope composition of host rock dolomite (D) and hydrothermal siderite (S)
Results are shown relative to common ranges for marine limestone, biogenic limestone, carbonatite, and mantle carbon. The ellipse covers the common range of values for hydrothermal dolomite from MVT Zn-Pb deposits. The isotopic compositions of siderite in carbonate-hosted siderite replacement deposits (rectangle, BOUZENOUNE and LECOLLE 1997) and polymetallic siderite quartz veins (polygon, BEAUDOIN and SANGSTER 1992) are also shown



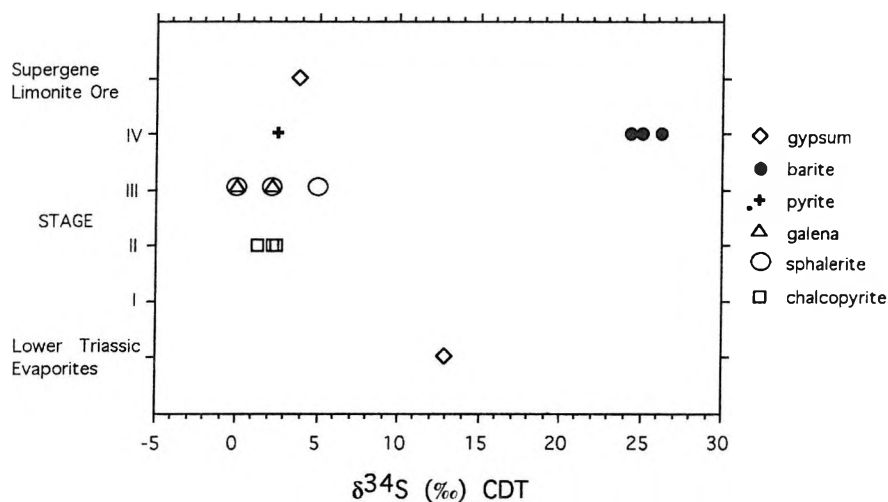


Fig. 5: Sulfur isotopic composition of sulfides and sulfates through the paragenetic sequence.

position of the siderite ($\delta^{13}\text{C} = -3.7$ to -6.1‰ , $\delta^{18}\text{O} = 16.0$ to 19.6‰) is lower than host rock dolomite, lower than carbonate-hosted siderite replacements, within the range of hydrothermal dolomite from MVT Zn-Pb deposits, and one value is within the range of polymetallic siderite quartz veins (Fig. 4). Although the $\delta^{13}\text{C}$ and $\delta^{18}\text{O}$ data do not permit a unique interpretation, the geology of the deposit is more similar to carbonate-hosted siderite replacements and MVT Zn-Pb deposits.

To determine whether the sulfate in ore fluids was derived from the Late Permian Perkupa Anhydrite, the sulfur isotopic composition of hydrothermal barite from Rudabánya was compared with evaporite gypsum from Alsótelekes. The $\delta^{34}\text{S}$ values of barite (24.3 to 26.2‰) and gypsum (13.0‰) are distinctly different (Figs. 3 and 5). The $\delta^{34}\text{S}$ composition of the gypsum is typical of Upper Permian and Lower Triassic marine evaporites while the barite is similar to marine sulfate in Late Devonian-Early Mississippian and Silurian rocks (CLAYPOOLE et al., 1980). The sulfate in the fluids that deposited barite may therefore have been derived from unexposed Lower Paleozoic rocks at deeper levels in the system. Rocks correlative with the Paleozoic black shales exposed in the Uppony and Szendrő Mts. are inferred to underlie the deposit.

Chalcopyrite, sphalerite, galena, and pyrite have $\delta^{34}\text{S}$ values that range between 0.3 and 5.1‰ (Figs. 3 and 5). The equilibrium sulfur isotopic fractionations between sphalerite and galena were used to estimate the temperature of ore formation (OHMOTO and RYE 1979). Sphalerite and galena from sample RB8-5 ($\Delta_{\text{sph-gn}} = 4.8\text{‰}$) yield a temperature of 115 °C that is well below the <240 °C temperature constraint provided by the presence of marcasite in the ores. This temperature estimate is also similar to those from other siderite replacement deposits and MVT Pb-Zn deposits world wide. The temperature of 115 °C was used to calculate the isotopic composition of H_2S in ore fluids. The $\delta^{34}\text{S}$ values calculated for H_2S range from -0.3 to 6.4‰ . H_2S produced by thermochemical sulfate reduction has $\delta^{34}\text{S}$ values 0 to 20‰ less than the sulfate source (OHMOTO and RYE 1979). The calculated range of $\delta^{34}\text{S}$ values for H_2S are 13.3 to 6.6‰ less than the sulfate in gypsum from the Alsótelekes evaporite deposit suggesting that H_2S was in fact derived from thermochemical reduction of Late Permian sedimentary sulfate. Although the calculated $\delta^{34}\text{S}$ values for H_2S are similar to those commonly observed in porphyry copper deposits (OHMOTO and RYE 1979), the lack of igneous intrusions in the area suggests that H_2S was derived from a local sedimentary source.

The sulfur isotopic composition of gypsum in the limonite ores was analyzed to determine whether sulfate was derived from oxidation of sulfides or from sulfate in evaporites. Because the isotopic fractionation associated with the oxidation of sulfides is very small, sulfate produced by oxidation of sulfides will have $\delta^{34}\text{S}$ values that are the same as the sulfides (OHMOTO and RYE, 1979). The gypsum analyzed has a $\delta^{34}\text{S}$ value of 3.8‰ that is similar to the sulfides but not the evaporites (Fig. 5). The $\delta^{34}\text{S}$ value of the gypsum in the limonite ores is therefore consistent with a supergene origin and is representative of the average isotopic composition of preexisting sulfides in siderite ore.

5. PROCESSES OF ORE FORMATION

Ore depositional processes were evaluated based on the geology of the deposit, temperature estimates, isotopic results, and solubilities of ore and gangue minerals. The introduction of Fe, basemetals, and SO_4 suggests

that the ore fluid was a relatively oxidized, acidic, saline, SO₄-rich fluid that transported Fe and basemetals as chloride complexes. The red bed sequence of the Perkupa Anhydrite and the Bódvaszilás Sandstone are the most obvious source for the Fe and basemetals. Surprisingly, the sulfur isotopic composition of barite suggests that SO₄ was derived from the Paleozoic black shales and not from Permian evaporites and siliciclastic rocks. Since siderite and most of the basemetal sulfides precipitated prior to barite, it is likely that Fe and basemetals were initially derived from fluids moving through red beds and that later on fluids containing SO₄ were derived from the black shales. The isotopic composition of the sulfides suggest that H₂S was generated locally by thermochemical reduction of Late Permian sedimentary sulfate by reaction with organic matter in the carbonate host rocks. Since Ba is relatively insoluble in SO₄-rich fluids, it must have been transported by the H₂S-rich fluid in the carbonates. Because quartz precipitates during cooling, the relative lack of hydrothermal quartz in the ores suggests that the ascending ore fluids were not appreciably hotter than the host rocks. The abundance of hematite, rather than siderite, in the deeper levels of the system suggests that the ore fluids lacked appreciable CO₂. Rather, the CO₂ in siderite was derived from the carbonate host rocks. These considerations suggest that Rudabánya formed along tensional faults where ascending ore fluids, derived from the Perkupa Anhydrite, Bódvaszilás Sandstone and Paleozoic black shales, reacted with dolomites and indigenous ground water. This model is essentially the same as that originally proposed by CSALAGOVITS (1973a, b) but is inconsistent with models for polymetallic-siderite-quartz veins (BEAUDOIN and SANGSTER 1992).

6. SUMMARY

The mineral paragenesis and stable isotopic data provide the following constraints on genetic models for Rudabánya:

1. The carbon and oxygen isotopic composition of the host dolomite is similar to normal marine limestones suggesting that the dolomite is diagenetic in origin and not a hydrothermal alteration product.
2. The carbon and oxygen isotopic composition of the siderite is consistent with results from MVT Zn-Pb deposits.
3. The sulfur isotopic composition of barite suggests that the SO₄ in ore fluids was derived from Lower Paleozoic sedimentary rocks correlative with the black shales of the Uppony and Szendrő Mts. and not from the Late Permian Perkupa Anhydrite.
4. The sulfur isotopic composition of the sulfides suggests that H₂S was derived from thermochemical reduction of Late Permian sedimentary sulfate.
5. The isotopic composition of sulfur in coeval sphalerite and galena yield a temperature of 115 °C.
6. The presence of marcasite in the ores is indicative of temperatures < 240 °C and pH < 5.
7. Ore precipitation took place along faults where ascending acidic, saline, sulfate-, Fe-, basemetal-rich fluids reacted with dolomite host rocks and indigenous Ba- and H₂S-rich ground waters.
8. The isotopic data confirm the mixing model of CSALAGOVITS (1973a, b) and suggest that Rudabánya formed where migrating basinal brines moved up faults produced by Middle Triassic rifting and encountered reactive carbonate rocks and indigenous ground waters.

7. REFERENCES

- BALOGH, K.–PANTÓ, G. 1952: A Rudabányai hegység földtana. (Geology of the Rudabánya Mountains). — Magyar Állami Földtani Intézet Évi Jelentése 1949: 135–154. (In Hungarian with French and Russian abstract)
- BARTÓK, A.–NAGY, I. 1992: Magyarország érchordozó ásványi nyersanyagai, színes és feketefémérc vagyona. (Ore deposits of Hungary. Reserves of polymetallic and iron-manganese ores). — Központi Földtani Hivatal, Budapest: 70 p. (In Hungarian).
- BEAUDOIN, G.–SANGSTER, D. F. 1992: A descriptive model for silver-lead-zinc veins in clastic metasedimentary terranes. — *Economic Geology* 87: 1005–1021.
- BOUZENOUNE, A.–LECOLLE, P. 1997: Petrographic and geochemical arguments for hydrothermal formation of the Ouenza siderite deposit (NE Algeria). — *Mineralium Deposita* 32: 189–196.
- CLAYPOOLE, G. E.–HOLSER, W. T.–KAPLAN, I. R.–SAKAI, H.–ZAK, I. 1980: The age curves of sulfur and oxygen isotopes in marine sulfate and their mutual interpretation. — *Chemical Geology* 28: 199–260.
- CSALAGOVITS, I. 1973a: Stratigraphically controlled Triassic ore mineralization. A genetic model based on Hungarian geochemical investigations. — *Acta Geologica Hungarica* 17(1-3): 39–48.

- CSALAGOVITS, I. 1973b: A Rudabánya környéki triász összlet geokémiai és ércgenetikai vizsgálatának eredményei. (Results of geochemical and ore genetical investigations of a Triassic sequence in the vicinity of Rudabánya). — Magyar Állami Földtani Intézet Évi Jelentése 1971: 61–90. (In Hungarian with English abstract).
- GRILL, J. 1988: A Rudabányai-hegység jura formációi. (Jurassic formations of the Rudabánya Mountains). — Magyar Állami Földtani Intézet Évi Jelentése 1986: 69–103. (In Hungarian with English abstract).
- GRILL, J.–KOVÁCS, S.–LESS, GY.–RÉTI, ZS.–RÓTH, L.–SZENTPÉTERY, I. 1984: Az Aggtelek–Rudabányai-hegység földtani felépítése és fejlődéstörténete. (Geological constitution and history of evolution of the Aggtelek–Rudabánya Range). — Földtani Kutatás 27(4): 49–56. (In Hungarian with English, German and Russian abstract).
- HIPS, K. 1996: Stratigraphic and facies evaluation of the Lower Triassic formations in the Aggtelek–Rudabánya Mountains, NE Hungary. — Acta Geologica Hungarica 39(4): 369–411.
- HERNYÁK, G. 1977: A Rudabányai-hegység szerkezeti elemzése az elmúlt 20 év kutatásai alapján. (Structural analysis of the Rudabánya Mountains in the light of the last twenty years of research). — Földtani Közöny 107: 368–374. (In Hungarian with English abstract).
- KORPÁS, L.–HOFSTRA, A. 1994: Potential for Carlin-type gold deposits in Hungary. Carlin gold in Hungary. — Project JFNo 435. US–Hungarian Joint Fund, Budapest
- KORPÁS, L.–HOFSTRA, A.–ÓDOR, L.–HORVÁTH, I.–HAAS, J.–ZELENKA, T. 1999a: Evaluation of the prospected areas and formations. — Geologica Hungarica Series Geologica 24: 197–293.
- KOVÁCS, S.–LESS, GY.–PIROS, O.–RÉTI, ZS.–RÓTH, L. 1989: Triassic formations of the Aggtelek–Rudabánya Mountains (North-eastern Hungary). Acta Geologica Hungarica 32(1–2): 31–63.
- LESS, GY. 1998: Földtani felépítés. (Geology). — in BAROSS, G. (ed.): Az Aggteleki Nemzeti Park (Aggtelek National Park): Mezőgazda Kiadó, Budapest: 26–66. (In Hungarian with English, German and Slovakian abstract).
- LESS, GY.–SZENTPÉTERY, I. (eds.) 1987: Az Aggtelek–Rudabányai hegység földtana. (Geology of the Aggtelek–Rudabánya Mountains). — Magyar Geológiai Szolgálat Adattára, Kézirat (Unpublished report in Hungarian).
- MUROWCHICK, J. B. 1992: Marcasite inversion and the petrographic determination of pyrite ancestry. — Economic Geology 87: 1141–1152.
- NAGY, B. 1982: A rudabányai ércesedés összehasonlító ércgenetikai vizsgálata. (A comparative metallogenic study of the Rudabánya mineralization, N Hungary). — Magyar Állami Földtani Intézet Évi Jelentése 1980: 45–58. (In Hungarian with English abstract).
- OHMOTO, H.–RYE, R.O. 1979: Isotopes of sulfur and carbon. — in BARNES H. L. (ed.): Geochemistry of Hydrothermal Ore Deposits: John Wiley and Sons; New York: 509–567.
- PANTÓ, G. 1956: A rudabányai vasércvonulat földtani felépítése. (Geology of the Rudabánya iron ore belt). — Magyar Állami Földtani Intézet Évkönyve 44(2): 329–637. (In Hungarian with French and Russian abstract).
- PÁLFY, M. 1924: A Rudabányai hegység geológiai viszonyai és vasérctelepei. (Geology and iron ore deposits of the Rudabánya Mountains). — Magyar Állami Földtani Intézet Évkönyve 26(2): 1–24. (In Hungarian).
- RÉTI, ZS. 1988: Triász időszaki óceáni kéregmaradványok az Aggtelek–Rudabányai-hegységben. (Triassic oceanic crust remains in the Aggtelek–Rudabánya Mountains). — Magyar Állami Földtani Intézet Évi Jelentése 1986: 45–52.
- RUDABÁNYA: Nemesfém vizsgálatok 1971–1975. (Precious metall analysis, 1971–1975). — Rudabányai Ércbánya Vállalat Adattára, Kézirat (Unpublished report in Hungarian).

Geochemical data for Carlin-type gold mineralization in Hungary
(compiled by S. LAJTOS 1999)

Appendix 1

Sample no.	Lithology	Formation	Age	Sample type (depth in m)	Elements						Analytical method	Coordinates	
					Au	Ag	As	Sb	Tl	Hg		X	Y
					ppb	ppm							
<i>1. KŐSZEG MOUNTAINS</i>													
1	phyllite	Kőszeg Quartz Phyllite	J ₁	outcrop	2	<0.05	8.88	1.42	0.190	0.0135	icpms	454657	232595
2	quartz phyllite	Kőszeg Quartz Phyllite	J ₁	outcrop	3	0.07	7.63	1.93	0.190	0.0226	icpms	456355	232221
3	quartz phyllite	Kőszeg Quartz Phyllite	J ₁	outcrop	<2	<0.05	5.94	0.97	0.130	0.0293	icpms	454349	230875
4	phyllite	Kőszeg Quartz Phyllite	J ₁	outcrop	2	0.08	13.7	6.42	0.300	0.0184	icpms	455722	231170
5	quartzite	Kőszeg Quartz Phyllite	J ₁	outcrop	<2	0.13	5.1	1.22	0.200	0.0054	icpms	455506	229724
6	quartz phyllite	Kőszeg Quartz Phyllite	J ₁	outcrop	5	0.19	17	20.00	0.110	0.0338	icpms	456485	229475
7	quartzite breccia	Kőszeg Quartz Phyllite	J ₁	outcrop	2	0.21	2.31	1.82	0.190	0.0205	icpms	456485	229475
8	quartz phyllite	Kőszeg Quartz Phyllite	J ₁	outcrop	13	0.19	286	22.10	0.140	0.0302	icpms	457273	230469
9	sencite phyllite	Kőszeg Quartz Phyllite	J ₁	outcrop	3	0.06	3.8	1.10	0.210	0.0147	icpms	457770	228352
10	calc phyllite	Kőszeg Quartz Phyllite	J ₁	outcrop	<2	0.08	3.22	1.28	0.130	0.0151	icpms	458359	229013
11	sencite phyllite	Kőszeg Quartz Phyllite	J ₁	outcrop	<2	0.11	2.06	28.70	0.210	0.0099	icpms	459887	228902
12	phyllite	Kőszeg Quartz Phyllite	J ₁	Kőszeg-1 182.3	2	0.14	4.8	0.7	0.07	<0.02	icpms	459893	229554
13	phyllite	Kőszeg Quartz Phyllite	J ₁	206.3	<2	<0.02	0.9	0.1	0.03	0.06	icpms	459893	229554
14	phyllite	Kőszeg Quartz Phyllite	J ₁	223.5-224.3	<2	<0.02	4.3	0.8	0.07	0.21	icpms	459893	229554
15	quartzite	Kőszeg Quartz Phyllite	J ₁	258.6-259.4	<2	<0.02	2.6	0.2	<0.02	<0.02	icpms	459893	229554
16	quartzite	Kőszeg Quartz Phyllite	J ₁	276.8-279.2	<2	<0.02	0.4	0.1	<0.02	0.1	icpms	459893	229554
17	phyllite	Kőszeg Quartz Phyllite	J ₁	301.9-302.5	5	0.04	2.5	0.3	0.06	0.04	icpms	459893	229554
18	phyllite	Kőszeg Quartz Phyllite	J ₁	304.0-304.9	<2	<0.02	1.9	0.3	<0.02	0.07	icpms	459893	229554
19	micaschist	Kőszeg Quartz Phyllite	J ₁	597.4-600.0	<2	<0.02	0.6	<0.1	0.09	<0.02	icpms	459893	229554
20	quartz phyllite	Kőszeg Quartz Phyllite	J ₁	outcrop	2	-0.050	2.23	119.00	0.140	0.0221	icpms	455950	226620
21	phyllite	Velem Calc-Phyllite	J ₂₋₃	outcrop	<2	-0.050	4.87	2.52	0.210	0.0168	icpms	455472	228026
22	phyllite	Velem Calc-Phyllite	J ₂₋₃	outcrop	<2	-0.050	24.80	0.87	0.350	0.0054	icpms	452629	226514
23	phyllite	Velem Calc-Phyllite	J ₂₋₃	outcrop	2	-0.050	5.52	3.18	0.120	0.007	icpms	453537	226020
24	quartz slate	Velem Calc-Phyllite	J ₂₋₃	outcrop	<2	0.060	3.52	0.52	-0.050	0.0093	icpms	453811	224805
25	quartzite	Velem Calc-Phyllite	J ₂₋₃	outcrop	3	0.070	2.85	10.70	0.140	0.009	icpms	453811	224805
26	slate	Velem Calc-Phyllite	J ₂₋₃	Velem-3 27.8	<2	0.08	11.9	2.71	0.27	0.0189	icpms	454698	225860
27	slate, quartzite	Velem Calc-Phyllite	J ₂₋₃	30.0	5	0.2	0.97	0.59	0.16	0.0241	icpms	454698	225860
28	slate	Velem Calc-Phyllite	J ₂₋₃	36.0-36.4	4	0.14	1.4	0.72	0.14	0.0432	icpms	454698	225860
29	slate	Velem Calc-Phyllite	J ₂₋₃	53.0	<2	0.19	10	0.31	0.2	0.0162	icpms	454698	225860
30	slate	Velem Calc-Phyllite	J ₂₋₃	57.5 m	<2	0.04	15.1	0.3	0.18	0.0178	icpms	454698	225860
31	slate	Velem Calc-Phyllite	J ₂₋₃	76.3-80.0	<2	0.1	0.4	0.6	0.19	0.0264	icpms	454698	225860
32	slate	Velem Calc-Phyllite	J ₂₋₃	77.7-80.0	<2	0.07	0.94	0.24	0.07	0.0098	icpms	454698	225860
33	limonitic slate	Velem Calc-Phyllite	J ₂₋₃	Velem-1 5.0-6.0	6	0.3	8.91	0.46	0.2	0.0294	icpms	455099	225790
34	graphite slate	Velem Calc-Phyllite	J ₂₋₃	23.0	3	0.33	0.74	1.21	0.09	0.0341	icpms	455099	225790
35	graphite slate	Velem Calc-Phyllite	J ₂₋₃	38.2	3	0.14	1.24	0.43	0.19	0.0255	icpms	455099	225790
36	graphite slate	Velem Calc-Phyllite	J ₂₋₃	39.0	3	0.13	3.59	0.28	0.16	0.0185	icpms	455099	225790
37	slate, quartzite	Velem Calc-Phyllite	J ₂₋₃	55.6-58.0	<2	0.08	0.98	0.09	0.04	0.0037	icpms	455099	225790
38	slate	Velem Calc-Phyllite	J ₂₋₃	60.0	<2	0.05	9.26	0.17	0.25	0.0094	icpms	455099	225790
39	graphitic slate	Velem Calc-Phyllite	J ₂₋₃	Velem-7 13.0-15.2	2	0.04	13.3	0.58	0.21	0.0201	icpms	455034	225915
40	graphitic slate	Velem Calc-Phyllite	J ₂₋₃	40.0-44.0	2	0.08	2.48	0.17	0.06	0.0103	icpms	455034	225915
41	graphitic slate	Velem Calc-Phyllite	J ₂₋₃	74.2-77.0	4	0.18	21.4	0.85	0.18	0.0276	icpms	455034	225915
42	graphite slate	Velem Calc-Phyllite	J ₂₋₃	Velem-2 49.2	2	0.17	2.15	0.45	0.21	0.0236	icpms	455216	226045
43	graphite slate	Velem Calc-Phyllite	J ₂₋₃	79.8	<2	0.04	17.6	0.23	0.18	0.0091	icpms	455216	226045
44	graphite slate	Velem Calc-Phyllite	J ₂₋₃	outcrop	<2	0.100	1.66	7.23	0.250	0.0139	icpms	455389	226175
45	phyllite	Velem Calc-Phyllite	J ₂₋₃	outcrop	<2	0.070	3.13	9.42	0.190	0.0082	icpms	455875	226251
46	slate, quartzite	Velem Calc-Phyllite	J ₂₋₃	Velem-4 7.0-8.5	<2	0.07	10.2	0.15	0.08	0.0143	icpms	455943	225884
47	slate	Velem Calc-Phyllite	J ₂₋₃	58.7-59.1	<2	0.14	15	0.45	0.14	0.0217	icpms	455943	225884
48	slate	Velem Calc-Phyllite	J ₂₋₃	78.0-80.0	<2	0.17	16.4	0.49	0.19	0.0218	icpms	455943	225884
49	graphitic slate	Velem Calc-Phyllite	J ₂₋₃	Velem-8 42.3-45.3	<2	0.22	8.53	0.29	0.17	0.0162	icpms	456037	225743
50	graphitic slate	Velem Calc-Phyllite	J ₂₋₃	96.0-97.0	4	0.11	17	0.24	0.1	0.0312	icpms	456037	225743

Sample no.	Lithology	Formation	Age	Sample type (depth in m)	Elements						Analytical method	Coordinates	
					Au	Ag	As	Sb	Tl	Hg		X	Y
					ppb	ppm							
51	graphite slate	Velem Calc-Phyllite	J _{2,3}	142.5-144.8	<2	<0.02	0.62	0.05	0.02	0.0163	icpms	456037	225743
52	graphite slate	Velem Calc-Phyllite	J _{2,3}	147.0	<2	<0.02	0.63	0.13	<0.02	0.0061	icpms	456037	225743
53	graphite slate	Velem Calc-Phyllite	J _{2,3}	182.0-185.0	7	0.15	34.9	1.33	0.2	0.0481	icpms	456037	225743
54	graphite slate	Velem Calc-Phyllite	J _{2,3}	221.8-224.6	5	0.38	2.85	0.52	0.17	0.0253	icpms	456037	225743
55	graphite slate	Velem Calc-Phyllite	J _{2,3}	248.7-250.7	2	0.11	6.81	0.38	0.16	0.0256	icpms	456037	225743
56	graphite slate	Velem Calc-Phyllite	J _{2,3}	295.0	<2	0.2	6.83	0.25	0.16	0.0203	icpms	456037	225743
57	graphite slate	Velem Calc-Phyllite	J _{2,3}	328.0	<2	0.13	4.37	0.22	0.15	0.0057	icpms	456037	225743
58	calc slate	Velem Calc-Phyllite	J _{2,3}	350.0	<2	0.03	3.04	0.76	0.05	0.0088	icpms	456037	225743
59	calc slate	Velem Calc-Phyllite	J _{2,3}	372.0	4	0.02	4.92	1.09	0.03	0.0123	icpms	456037	225743
60	calc slate	Velem Calc-Phyllite	J _{2,3}	410.0	<2	0.07	6.41	1.03	0.04	0.0156	icpms	456037	225743
61	calc slate	Velem Calc-Phyllite	J _{2,3}	420.0	<2	0.06	2.89	0.25	0.03	0.0082	icpms	456037	225743
62	graphitic slate	Velem Calc-Phyllite	J _{2,3}	479.0-480.0	2	0.13	1.74	0.22	0.07	0.0242	icpms	456037	225743
63	slate, quartzite	Velem Calc-Phyllite	J _{2,3}	Velem-5 22.0-24.1	3	0.08	21.3	0.56	0.17	0.0377	icpms	456604	226454
64	slate	Velem Calc-Phyllite	J _{2,3}	60.4-63.0	<2	0.17	0.64	0.6	0.16	0.0255	icpms	456604	226454
65	slate	Velem Calc-Phyllite	J _{2,3}	98.0-100.0	<2	0.19	9.13	0.43	0.19	0.0246	icpms	456604	226454
66	slate	Velem Calc-Phyllite	J _{2,3}	Velem-6 4.1-6.2	19	0.16	9.31	0.35	0.18	0.0298	icpms	456988	226745
67	graphite slate	Velem Calc-Phyllite	J _{2,3}	44.7-45.3	3	0.04	8.24	0.26	0.26	0.0197	icpms	456988	226745
68	slate, quartzite	Velem Calc-Phyllite	J _{2,3}	47.3-50.6	<2	0.08	9.77	0.25	0.1	0.0122	icpms	456988	226745
69	graphite slate	Velem Calc-Phyllite	J _{2,3}	73.3-76.0	<2	0.34	14.7	0.29	0.17	0.0247	icpms	456988	226745
70	slate	Velem Calc-Phyllite	J _{2,3}	Cák-3 54.0-72.6	2	0.2	5.6	0.4	0.21	0.1	icpms	458543	227133
71	graphite slate	Velem Calc-Phyllite	J _{2,3}	72.6-94.8	<2	0.12	0.8	0.3	0.16	0.08	icpms	458543	227133
72	slate	Velem Calc-Phyllite	J _{2,3}	94.8-120.3	<2	<0.02	5.8	0.1	0.13	0.03	icpms	458543	227133
73	graphite slate	Velem Calc-Phyllite	J _{2,3}	125.3-130.8	2	0.07	2.7	0.2	0.12	0.18	icpms	458543	227133
74	slate	Velem Calc-Phyllite	J _{2,3}	132.7-134.0	<2	0.2	28.4	1.2	0.22	0.09	icpms	458543	227133
75	slate	Velem Calc-Phyllite	J _{2,3}	134.4-147.4	<2	0.13	0.8	0.3	0.14	0.04	icpms	458543	227133
76	slate	Velem Calc-Phyllite	J _{2,3}	147.4-227.4	<2	0.07	2.4	0.3	0.04	0.04	icpms	458543	227133
77	graphite slate	Velem Calc-Phyllite	J _{2,3}	227.4-250.0	<2	0.06	12	0.4	0.08	0.15	icpms	458543	227133
78	graphite slate	Velem Calc-Phyllite	J _{2,3}	250.0-300.0	2	0.09	3.3	0.3	0.13	0.14	icpms	458543	227133
79	quartzite	Cák Conglomerate	J ₂	outcrop	13	0.650	245.00	6.27	0.530	0.0707	icpms	458631	227058
80	conglomerate	Cák Conglomerate	J ₂	outcrop	<2	<0.050	4.15	1.84	<0.05	0.0057	icpms	458631	227058
81	graphite slate	Velem Calc-Phyllite	J _{2,3}	outcrop	9	<0.050	3.03	1.03	0.280	0.0089	icpms	455495	224936
82	phyllite	Velem Calc-Phyllite	J _{2,3}	outcrop	<2	0.130	1.97	0.18	<0.05	0.0041	icpms	455199	224204
83	vein of quartzite	Velem Calc-Phyllite	J _{2,3}	outcrop	<2	<0.050	0.64	0.27	-0.050	0.0076	icpms	455199	224204
84	phyllite	Velem Calc-Phyllite	J _{2,3}	outcrop	<2	0.070	7.78	1.91	0.160	0.0125	icpms	456608	224281
85	greenschist	Felsőcsatár Greenschist	Cr ₁	outcrop	<2	<0.05	3.63	0.51	<0.050	0.0016	icpms	451098	210313
86	greenschist	Felsőcsatár Greenschist	Cr ₁	outcrop	<2	<0.050	2.63	0.38	<0.050	0.0025	icpms	451711	210385
87	calc phyllite	Felsőcsatár Greenschist	Cr ₁	outcrop	<2	<0.050	3.76	0.88	0.080	0.027	icpms	451991	209943
88	quartz phyllite	Felsőcsatár Greenschist	Cr ₁	outcrop	3	0.360	33.50	6.49	0.100	0.0074	icpms	452630	209550
89	greenschist	Felsőcsatár Greenschist	Cr ₁	outcrop	<2	<0.05	1.70	3.98	<0.050	0.0015	icpms	453248	210395
90	diabase	Felsőcsatár Greenschist	Cr ₁	underground	310	0.140	71.30	0.78	<0.050	0.0076	icpms	453342	210052
91	serpentinite	Felsőcsatár Greenschist	Cr ₁	underground	7	0.760	17.10	0.87	<0.050	0.003	icpms	453342	210052
<i>2 KESZTHELY MOUNTAINS, BALATON-FELVIDÉK, BAKONY MOUNTAINS</i>													
92	clay	Veszprém Marl	T ₃	Hévíz H-6 177.6-178.6	<2	<0.02	4.3	0.5	0.71	<0.02	icpms	506965	161269
93	marl	Veszprém Marl	T ₃	197.5-198.4	<2	<0.02	7.2	0.4	0.32	<0.02	icpms	506965	161269
94	marl	Veszprém Marl	T ₃	222.7-223.7	<2	0.05	6.6	0.3	0.29	0.06	icpms	506965	161269
95	limestone	Veszprém Marl	T ₃	233.7-234.7	<2	<0.02	6	0.2	0.15	<0.02	icpms	506965	161269
96	dolomarl	Veszprém Marl	T ₃	245.7-246.7	<2	0.04	8.3	0.7	0.15	0.04	icpms	506965	161269
97	dolomite	Veszprém Marl	T ₃	249.0	<2	<0.02	7.8	0.6	0.39	0.02	icpms	506965	161269
98	dolomite	Veszprém Marl	T ₃	383.2-383.6	<2	<0.02	0.8	<0.1	0.03	<0.02	icpms	506965	161269
99	marl	Veszprém Marl	T ₃	410.0-411.0	<2	<0.02	7.8	0.3	0.24	0.02	icpms	506965	161269
100	marl	Veszprém Marl	T ₃	432.0-432.9	<2	<0.02	8.8	0.4	0.17	<0.02	icpms	506965	161269
101	marl	Veszprém Marl	T ₃	455.3-454.3	<2	<0.02	5.1	0.2	0.12	<0.02	icpms	506965	161269
102	marl	Veszprém Marl	T ₃	472.1-473.0	<2	<0.02	5	0.3	0.15	0.06	icpms	506965	161269

Sample no.	Lithology	Formation	Age	Sample type (depth in m)	Elements						Analytical method	Coordinates	
					Au	Ag	As	Sb	Tl	Hg		X	Y
					ppb	ppm							
103	marl	Veszprém Marl	T ₃	492.0–491.0	<2	<0.02	7.5	0.4	0.16	0.02	icpms	506965	161269
104	marl	Veszprém Marl	T ₃	529.9–530.9	<2	<0.02	12.2	0.4	0.2	<0.02	icpms	506965	161269
105	sandstone	Szák Clay Marl	M ₃	Cserszegtomaj-196	<2	0.08	2.32	0.22	0.12	0.0129	icpms	510084	162424
106	marl	Szák Clay Marl	M ₃	12.6–12.7	<2	0.09	2.52	0.31	0.22	0.0501	icpms	510084	162424
107	sandstone	Szák Clay Marl	M ₃	15.6–15.7	<2	0.09	1.44	0.18	0.14	0.0154	icpms	510084	162424
108	marl	Szák Clay Marl	M ₃	17.3–17.8	<2	0.08	1.18	0.28	0.29	0.0371	icpms	510084	162424
109	sandstone	Szák Clay Marl	M ₃	20.4–20.7	<2	0.04	1.55	0.22	0.17	0.0173	icpms	510084	162424
110	paleosol	Szák Clay Marl	M ₃	21.7–21.9	<2	0.11	16.4	0.81	0.22	0.0939	icpms	510084	162424
111	sand	Szák Clay Marl	M ₃	22.9–23.2	3	0.06	4.76	0.39	0.22	0.0374	icpms	510084	162424
112	limonitic sand	Kálla Gravel	M ₃	25.0–25.4	<2	0.09	3.62	0.27	0.21	0.0612	icpms	510084	162424
113	pyritic sand	Kálla Gravel	M ₃	52.1–52.6	<2	0.09	9.98	0.19	0.26	0.2078	icpms	510084	162424
114	silicified sandstone	Kálla Gravel	M ₃	52.7–53.0	<2	0.04	1.59	0.11	0.11	0.0373	icpms	510084	162424
115	pyritic sand	Kálla Gravel	M ₃	53.9–62.7	<2	0.12	2.9	0.3	0.22	0.0633	icpms	510084	162424
116	pyritic sand	Kálla Gravel	M ₃	62.7–63.9	3	0.16	7.19	0.43	0.43	0.1686	icpms	510084	162424
117	pyritic sand	Kálla Gravel	M ₃	63.9–64.1	2	0.18	9.46	0.32	0.67	0.2098	icpms	510084	162424
118	pyritic sand	Kálla Gravel	M ₃	64.1–64.3	7	0.17	9.36	0.36	1.4	0.127	icpms	510084	162424
119	pyritic sand	Kálla Gravel	M ₃	64.3–64.5	4	0.2	10.5	0.36	0.57	0.1583	icpms	510084	162424
120	pyritic sand	Kálla Gravel	M ₃	64.5–64.8	2	0.16	37.9	0.49	2.18	0.1333	icpms	510084	162424
121	pyritic sand	Kálla Gravel	M ₃	64.8–65.5	2	0.14	25.3	0.33	1.79	0.2202	icpms	510084	162424
122	pyritic sand	Kálla Gravel	M ₃	65.5–66.8	<2	0.06	11.8	0.42	0.97	0.273	icpms	510084	162424
123	pyritic sand	Kálla Gravel	M ₃	66.8–67.6	4	0.16	16.3	0.65	1.3	0.3593	icpms	510084	162424
124	pyritic sand	Kálla Gravel	M ₃	67.8–68.0	<2	0.06	7.58	0.46	0.8	0.1592	icpms	510084	162424
125	pyritic sand	Kálla Gravel	M ₃	68.0–68.7	<2	0.4	5.15	0.48	0.48	0.1069	icpms	510084	162424
126	pyritic sand	Kálla Gravel	M ₃	68.7–69.5	<2	0.04	3.99	0.11	0.04	0.0664	icpms	510084	162424
127	pyritic sand	Kálla Gravel	M ₃	69.5–69.8	2	0.06	11	4.89	0.39	0.1819	icpms	510084	162424
128	sand	Kálla Gravel	M ₃	77.8	3	0.03	2.15	0.41	0.08	0.1451	icpms	510084	162424
129	sand	Kálla Gravel	M ₃	78.7	<2	0.07	11.1	5.48	0.09	0.1123	icpms	510084	162424
130	sand	Kálla Gravel	M ₃	83.8	3	0.04	2.5	0.37	0.22	0.1201	icpms	510084	162424
131	dolomite	Rezi Dolomite	T ₃	96.0	<2	0.23	1.02	0.11	0.05	0.0085	icpms	510084	162424
132	marl	Szák Clay Marl	M ₃	Cs-28 29.0–72.0	<2	0.23	5.71	0.37	0.36	0.0428	icpms	510728	162830
133	silicified sandstone	Kálla Gravel	M ₃	Kútbarlang undergr	<2	-0.050	4.38	1.19	1.190	0.0262	icpms	510414	163665
134	marl	Szák Clay Marl	M ₃	Cs-18 24.9–44.1	<2	0.07	4.48	0.3	0.35	0.0331	icpms	511306	163297
135	marl	Szák Clay Marl	M ₃	Cs-16 16.6–76.3	<2	0.07	6.84	0.28	0.57	0.0391	icpms	511301	162875
136	marl	Szák Clay Marl	M ₃	Cs-25 47.3–65.8	<2	0.14	6.81	0.38	0.37	0.0424	icpms	511086	162500
137	marl	Szák Clay Marl	M ₃	Cs-20 11.0–48.7	<2	0.06	4.49	0.3	0.31	0.0351	icpms	511489	162299
138	marl	Szák Clay Marl	M ₃	Cs-27 21.4–59.4	<2	0.14	4.74	0.35	0.32	0.0395	icpms	511699	162102
139	marl	Szák Clay Marl	M ₃	Cs-26 22.7–58.0	<2	0.13	5.68	0.35	0.25	0.0366	icpms	511925	162103
140	marl	Szák Clay Marl	M ₃	Cs-23 29.4–58.4	<2	0.14	3.85	0.22	0.2	0.0359	icpms	511698	162298
141	marl	Szák Clay Marl	M ₃	Cs-19 22.1–55.0	<2	0.09	21.6	2.11	3.41	0.0484	icpms	511925	162290
142	limestone, marl	Kössen Formation	T ₃	outcrop	<2	<0.050	<1.00	<0.10	0.120	0.0059	icpms	511364	165904
143	dolomite	Rezi Dolomite	T ₃	outcrop	<2	<0.050	<1.00	<0.10	<0.05	0.0159	icpms	510684	167223
144	dolomarl	Rezi Dolomite	T ₃	Rezi Rzt-1 11.0	<2	0.08	0.9	1.11	0.07	0.012	icpms	511166	167155
145	bituminous dolomite	Rezi Dolomite	T ₃	40.0	<2	0.1	0.29	0.47	0.09	0.0069	icpms	511166	167155
146	dolomarl	Rezi Dolomite	T ₃	55.4	<2	0.05	1.28	0.36	0.08	0.0044	icpms	511166	167155
147	bituminous dolomite	Rezi Dolomite	T ₃	75.0	<2	0.08	1.21	1.48	0.03	0.0093	icpms	511166	167155
148	bituminous dolomite	Rezi Dolomite	T ₃	102.5	<2	0.07	0.65	1.36	<0.02	0.0101	icpms	511166	167155
149	marl	Rezi Dolomite	T ₃	130.0	<2	0.07	2.65	0.78	0.08	0.0116	icpms	511166	167155
150	dolomite	Rezi Dolomite	T ₃	169.0	<2	0.1	1.16	0.34	<0.02	0.0119	icpms	511166	167155
151	dolomite	Rezi Dolomite	T ₃	outcrop	<2	-0.050	<1.00	<0.10	<0.050	0.0057	icpms	517002	167014
152	dolomite	Rezi Dolomite	T ₃	outcrop	<2	-0.050	<1.00	0.25	<0.050	0.0071	icpms	518812	164404
153	pyritic matrix	Kálla Gravel	M ₃	outcrop	<2	n.a	n.a	n.a	n.a	<0.02	aas	521221	172673
154	marl	Kössen Formation	T ₃	Sümeg Sp-3 327.5–330.8	<2	0.09	5.2	0.2	0.53	<0.02	icpms	514262	185575

Sample no.	Lithology	Formation	Age	Sample type (depth in m)	Elements						Analytical method	Coordinates	
					Au	Ag	As	Sb	Tl	Hg		X	Y
					ppb	ppm							
155	limestone	Kössen Formation	T ₃	378.6	<2	0.03	1.9	0.1	0.15	0.02	icpms	514262	185575
156	limonitic limestone	Kössen Formation	T ₃	Szóc Sct-1 8.0-8.2	<2	0.04	10.2	3.34	0.1	0.0063	icpms	533613	187420
157	dolomite	Kössen Formation	T ₃	51.4-51.7	<2	0.05	1.25	0.21	0.05	0.0033	icpms	533613	187420
158	marl	Kössen Formation	T ₃	74.1-74.5	<2	0.04	1.07	0.14	0.26	0.0034	icpms	533613	187420
159	marl	Kössen Formation	T ₃	112.0-113.0	<2	0.08	6.06	0.31	0.17	0.0248	icpms	533613	187420
160	limestone	Kössen Formation	T ₃	160.0-166.5	<2	0.16	5.38	0.4	0.22	0.0088	icpms	533613	187420
161	dolomite	Födolomit Formation	T ₃	211.8-218.1	<2	0.05	0.81	0.37	0.08	0.0069	icpms	533613	187420
162	limestone	Eplény Limestone	J ₁₋₂	Ajka A-97 198.4-212.8	<2	0.12	0.5	0.1	0.15	0.0038	icpms	539214	192393
163	marl	Kisgerecse Marl	J ₁	Úrkút Ú-108 32.5-35.1	<2	0.31	14.7	0.88	1.17	0.1897	icpms	543002	193314
164	marl	Kisgerecse Marl	J ₁	35.1-38.0	<2	0.16	15.1	0.82	0.69	0.112	icpms	543002	193314
165	marl	Kisgerecse Marl	J ₁	38.0-40.6	<2	0.05	5.29	0.35	0.09	0.0829	icpms	543002	193314
166	marl	Kisgerecse Marl	J ₁	Úrkút Ú-111 1.6-6.2	<2	0.28	35.1	0.85	1.62	0.3511	icpms	542976	193394
167	marl	Kisgerecse Marl	J ₁	6.2-11.6	2	0.15	44.4	0.67	3.18	0.401	icpms	542976	193394
168	Mn ore	Úrkút Manganese Ore	J ₁	underground, level 175, 326 m	<2	0.1	1.66	0.59	0.11	0.0169	icpms	541538	194440
169	Mn ore	Úrkút Manganese Ore	J ₁	underground, shaft III., level 175	5	0.07	13.8	0.88	0.11	0.14	icpms	541222	194446
170	Mn ore	Úrkút Manganese Ore	J ₁	underground, level 175, end	<2	0.29	5.1	0.22	0.04	0.1	icpms	541222	194446
171	Mn ore	Úrkút Manganese Ore	J ₁	200 m	<2	0.12	59.1	0.59	0.11	0.1249	icpms	541644	194469
172	radiolarian marl	Kisgerecse Marl	J ₁	165 m	3	0.38	23.5	1.3	0.97	0.28	icpms	541708	194468
173	radiolarian marl	Kisgerecse Marl	J ₁	162 m	4	0.36	24.3	1.12	0.63	0.28	icpms	541708	194468
174	radiolarian marl	Kisgerecse Marl	J ₁	167 m	<2	0.24	17.1	1.06	0.64	0.24	icpms	541708	194468
175	radiolarian marl	Kisgerecse Marl	J ₁	175 m	7	0.26	28.1	1.17	0.32	0.18	icpms	541708	194468
176	radiolarian marl	Kisgerecse Marl	J ₁	175 m	4	0.45	9.41	1.6	0.18	0.66	icpms	541708	194468
177	radiolarian marl	Kisgerecse Marl	J ₁	177 m	5	0.76	13.5	1.8	0.38	0.38	icpms	541708	194468
178	radiolarian marl	Kisgerecse Marl	J ₁	173 m	3	0.53	13.7	1.33	0.23	0.36	icpms	541708	194468
179	radiolarian marl	Kisgerecse Marl	J ₁	179 m	5	0.68	26.2	2	0.76	0.4	icpms	541708	194468
180	radiolarian marl	Kisgerecse Marl	J ₁	170 m	2	0.46	12.8	1.43	0.12	0.22	icpms	541708	194468
181	Mn ore	Úrkút Manganese Ore	J ₁	162 m	2	0.31	33.4	0.83	0.7	0.2367	icpms	541708	194468
182	Mn ore	Úrkút Manganese Ore	J ₁	underground, shaft III., level 175, 20-25 m, second orebed	<2	0.11	11.9	0.14	0.18	0.09	icpms	541813	194435
183	Mn ore	Úrkút Manganese Ore	J ₁		<2	0.38	13.4	0.16	0.21	0.17	icpms	541813	194435
184	Mn ore	Úrkút Manganese Ore	J ₁		<2	0.54	7.5	0.19	0.16	0.1	icpms	541813	194435
185	Mn ore	Úrkút Manganese Ore	J ₁		<2	0.33	19	0.57	0.24	0.14	icpms	541813	194435
186	Mn ore	Úrkút Manganese Ore	J ₁		3	0.35	21.9	0.37	0.33	0.12	icpms	541813	194435
187	Mn ore	Úrkút Manganese Ore	J ₁		2	1.08	15.4	0.41	0.26	<0.02	icpms	541813	194435
188	radiolarian marl	Kisgerecse Marl	J ₁		<2	0.42	147	2.63	0.17	0.28	icpms	541813	194435
189	radiolarian marl	Kisgerecse Marl	J ₁		<2	0.9	127	1.75	0.22	0.32	icpms	541813	194435
190	radiolarian marl	Kisgerecse Marl	J ₁		<2	0.4	24.3	0.27	0.21	0.06	icpms	541813	194435
191	Mn ore	Úrkút Manganese Ore	J ₁		4	0.05	11	0.83	0.15	0.18	icpms	541833	194404
192	Mn ore	Úrkút Manganese Ore	J ₁	<2	0.12	7.62	0.9	0.13	0.12	icpms	541833	194404	
193	Mn ore	Úrkút Manganese Ore	J ₁	<2	0.06	7.92	0.56	0.11	0.24	icpms	541833	194404	
194	Mn ore	Úrkút Manganese Ore	J ₁	level 175, 246 m	<2	0.11	2.46	0.43	0.12	0.0068	icpms	541402	194461
195	marl	Kisgerecse Marl	J ₁	Úrkút Ú-106 159.8-163.7	8	0.31	17.5	0.8	0.45	0.1085	icpms	542011	194921
196	marl	Kisgerecse Marl	J ₁	163.7-166.5	<2	0.18	47.6	0.68	0.74	0.177	icpms	542011	194921
197	marl	Kisgerecse Marl	J ₁	166.7-169.2	<2	<0.02	60.9	0.77	0.22	0.2907	icpms	542011	194921
198	marl	Kisgerecse Marl	J ₁	169.2-172.9	<2	0.02	31.7	0.5	0.33	0.2022	icpms	542011	194921
199	limestone	Kössen Formation	T ₃	Szentgál Szg-7 47.7-50.1	<2	0.05	0.6	<0.1	0.05	0.08	icpms	548993	205700
200	marl	Veszprém Marl	T ₃	Bakonyszücs Szü-1 69.0-72.0	<2	<0.02	4.2	0.3	0.13	0.38	icpms	546798	224417
201	marl	Veszprém Marl	T ₃	160.5-164.0	<2	0.02	6.2	<0.1	0.36	0.26	icpms	546798	224417

Sample no.	Lithology	Formation	Age	Sample type (depth in m)	Elements						Analytical method	Coordinates	
					Au	Ag	As	Sb	Tl	Hg		X	Y
					ppb	ppm							
205	marl	Veszprém Marl	T ₃	196.2–200.0	<2	<0.02	5.4	0.1	0.18	0.07	icpms	546798	224417
206	limestone	Veszprém Marl	T ₃	247.1–250.6	<2	0.07	5.2	0.2	0.08	0.15	icpms	546798	224417
205	marl	Veszprém Marl	T ₃	302.8–305.5	<2	<0.02	11.4	0.2	0.22	0.06	icpms	546798	224417
206	marl	Veszprém Marl	T ₃	343.9–345.0	<2	0.06	10.2	0.3	0.18	0.09	icpms	546798	224417
207	marl	Veszprém Marl	T ₃	484.4–488.2	<2	<0.02	6.1	0.2	0.17	0.24	icpms	546798	224417
208	marl	Veszprém Marl	T ₃	658.8–662.0	<2	<0.02	7.1	0.3	0.2	0.33	icpms	546798	224417
209	marl	Veszprém Marl	T ₃	693.4–696.5	<2	<0.02	8.3	0.2	0.25	0.21	icpms	546798	224417
210	marl	Veszprém Marl	T ₃	798.0–801.5	4	<0.02	7.4	0.4	0.28	0.14	icpms	546798	224417
211	marl	Veszprém Marl	T ₃	838.0–842.0	<2	<0.02	10.5	0.3	0.22	0.13	icpms	546798	224417
212	marl	Veszprém Marl	T ₃	944.3–948.3	<2	<0.02	11.9	0.2	0.27	0.11	icpms	546798	224417
213	marl	Veszprém Marl	T ₃	1044.0–1048.0	<2	0.07	3.6	0.2	0.29	0.4	icpms	546798	224417
214	marl	Veszprém Marl	T ₃	1099.0–1102.8	<2	<0.02	6.4	0.1	0.36	0.42	icpms	546798	224417
215	limestone	Eplény Limestone	J ₁₋₂	Eplény E-64 93.6–96.1	<2	0.12	1.56	0.14	0.08	0.0408	icpms	562354	207335
216	limestone	Eplény Limestone	J ₁₋₂	98.0–98.1	<2	0.04	0.95	0.1	0.06	0.0126	icpms	562354	207335
217	limestone	Eplény Limestone	J ₁₋₂	98.1–103.3	5	0.42	24.6	1.23	0.58	0.3214	icpms	562354	207335
218	marl	Úrkút Manganese Ore	J ₁	Eplény E-2 145.2–148.1	4	0.39	20.5	1.14	0.28	0.3164	icpms	563317	208025
219	marl	Úrkút Manganese Ore	J ₁	148.1–155.7	2	0.3	31.9	1.06	0.42	0.3258	icpms	563317	208025
220	marl	Úrkút Manganese Ore	J ₁	155.7–156.5	2	0.41	42.2	0.87	0.6	1.671	icpms	563317	208025
221	limestone	Eplény Limestone	J ₁₋₂	Eplény E-69 243.3–248.4	<2	0.29	0.56	0.05	0.08	0.0288	icpms	563055	208255
222	limestone	Eplény Limestone	J ₁₋₂	248.4–257.0	3	0.19	24.8	1.02	0.5	0.4492	icpms	563055	208255
223	bituminous marl	Veszprém Marl	T ₃	Veszprém-1 330.0	<2	0.05	4.18	0.19	0.16	0.0116	icpms	563347	197092
224	marl	Veszprém Marl	T ₃	350.0	<2	0.09	3.26	0.27	0.15	0.0123	icpms	563347	197092
225	dolomite	Veszprém Marl	T ₃	370.0	<2	0.08	0.92	0.11	<0.02	0.002	icpms	563347	197092
226	dolomite	Veszprém Marl	T ₃	401.0	<2	0.04	1.65	0.13	<0.02	0.0023	icpms	563347	197092
227	dolomite	Veszprém Marl	T ₃	450.0	<2	0.06	5.28	0.25	<0.02	0.0076	icpms	563347	197092
228	marl	Veszprém Marl	T ₃	454.0	<2	0.06	4.97	0.23	0.19	0.016	icpms	563347	197092
229	marl	Veszprém Marl	T ₃	480.0	<2	0.05	1.8	0.12	0.09	0.0071	icpms	563347	197092
230	marl	Veszprém Marl	T ₃	500.0	<2	0.07	3.3	0.22	0.17	0.0187	icpms	563347	197092
231	marl	Veszprém Marl	T ₃	520.0	<2	0.08	2.42	0.18	0.15	0.0124	icpms	563347	197092
232	marl	Veszprém Marl	T ₃	565.0	<2	0.48	3.34	0.16	0.15	0.0138	icpms	563347	197092
233	marl	Veszprém Marl	T ₃	580.0	<2	0.08	5.9	0.7	0.05	0.0198	icpms	563347	197092
234	marl	Veszprém Marl	T ₃	585.0	<2	0.06	2	0.11	0.08	0.0066	icpms	563347	197092
235	marl	Veszprém Marl	T ₃	587.0	<2	0.06	2.87	0.15	0.12	0.0095	icpms	563347	197092
236	dolomite	Veszprém Marl	T ₃	606.0	<2	0.09	6.82	0.22	0.1	0.0096	icpms	563347	197092
237	dolomite	Veszprém Marl	T ₃	650.0	<2	0.05	0.96	0.17	0.03	0.0035	icpms	563347	197092
238	dolomite	Megyehégy Dolomite	T ₂	outcrop	<2	0.011	2.25	0.19	0.02	<0.02	icpms	569671	197022
239	lim. dolom. breccia	Megyehégy Dolomite	T ₂	outcrop	<2	0.024	12.3	1.12	0.12	0.06	icpms	569671	197022
240	dolomite	Megyehégy Dolomite	T ₂	outcrop	<2	0.035	4.62	0.41	0.04	0.02	icpms	569711	197032
241	lim dolom breccia	Megyehégy Dolomite	T ₂	outcrop	<2	0.012	5.85	0.5	0.01	0.02	icpms	569771	197032
242	lim dolom breccia	Megyehégy Dolomite	T ₂	outcrop	<2	0.015	31.5	3.54	0.11	0.2	icpms	569691	197052
243	lim dolom breccia	Megyehégy Dolomite	T ₂	outcrop	<2	0.021	25.7	1.83	0.19	0.08	icpms	572080	199652
244	ankeritic limestone	Csopak Marl	T ₁	outcrop	<2	0.03	9.78	0.28	0.02	0.04	icpms	573450	199042
245	limestone	Felsőörs Limestone	T ₁	outcrop	<2	0.12	3.13	0.64	0.43	0.0103	icpms	547955	180443
246	limestone	Buchenstein Formation	T ₂	Vöröstó-8 38.0	<2	0.07	2.15	0.08	0.09	0.0032	icpms	548599	180914
247	tuff	Buchenstein Formation	T ₂	59.0	<2	0.08	0.31	0.07	0.17	0.0022	icpms	548599	180914
248	limestone	Buchenstein Formation	T ₂	78.0	<2	0.05	0.71	0.13	0.11	0.0019	icpms	548599	180914
249	limestone	Buchenstein Formation	T ₂	110.0	<2	0.1	2.3	0.21	0.13	0.0338	icpms	548599	180914
250	limestone	Buchenstein Formation	T ₂	140.0	<2	0.03	1.74	0.13	0.1	0.0101	icpms	548599	180914
251	dolomite	Veszprém Marl	T ₃	Barnag-2 7.5	<2	0.14	1.27	0.08	0.03	0.0024	icpms	553012	182438
252	clay	Veszprém Marl	T ₃	12.0	<2	0.15	10.9	0.31	0.82	0.0775	icpms	553012	182438
253	marl	Veszprém Marl	T ₃	41.0	<2	0.04	3.41	0.07	0.11	0.0055	icpms	553012	182438

Sample no.	Lithology	Formation	Age	Sample type (depth in m)	Elements						Analytical method	Coordinates	
					Au	Ag	As	Sb	Tl	Hg		X	Y
					ppb	ppm							
254	limestone	Veszprém Marl	T ₃	67.0	<2	0.08	2.9	0.13	0.05	0.0027	icpms	553012	182438
255	marl	Veszprém Marl	T ₃	97.0	<2	0.08	6.15	0.11	0.09	0.0043	icpms	553012	182438
256	marl	Veszprém Marl	T ₃	138.0	<2	0.11	4.06	0.3	0.23	0.0088	icpms	553012	182438
257	limestone	Veszprém Marl	T ₃	169.0	<2	0.06	5.6	0.36	0.48	0.0327	icpms	553012	182438
258	marl	Veszprém Marl	T ₃	192.0	<2	0.07	4.66	0.14	0.13	0.0121	icpms	553012	182438
259	marl	Buchenstein Formation	T ₂	Vászoly-1 25.0	<2	0.09	5.29	0.21	0.27	0.0253	icpms	551719	176804
260	limestone	Buchenstein Formation	T ₂	53.0	<2	0.11	0.36	0.1	0.03	0.0051	icpms	551719	176804
261	tuff	Buchenstein Formation	T ₂	96.0	<2	0.1	1.18	0.09	0.12	0.0016	icpms	551719	176804
262	marl	Buchenstein Formation	T ₂	103.5	<2	0.12	22.7	1.16	0.13	0.0474	icpms	551719	176804
263	limestone	Buchenstein Formation	T ₂	outcrop	<2	0.21	3.25	0.46	0.12	0.003	icpms	553635	176814
264	dolomite	Aszófő Dolomite	T ₂	outcrop	<2	0.14	1.12	0.25	0.1	0.0035	icpms	556934	176205
265	limestone	Füred Limestone	T ₃	outcrop	<2	0.1	1.69	0.18	0.08	0.0095	icpms	558574	180194
266	bituminous limest.	Veszprém Marl	T ₃	Balatonfüred-2 34.0	<2	0.1	4.29	0.39	0.05	0.0021	icpms	562916	182188
267	bituminous limest.	Veszprém Marl	T ₃	73.0	<2	0.1	3.64	0.27	0.05	0.0105	icpms	562916	182188
268	dolomitic limestone	Veszprém Marl	T ₃	101.0	<2	0.07	5.55	0.39	0.13	0.0018	icpms	562916	182188
269	breccia	Veszprém Marl	T ₃	148.0	<2	0.1	14.3	0.99	0.3	0.0071	icpms	562916	182188
270	limestone	Veszprém Marl	T ₃	193.5	<2	0.11	7.08	0.25	0.07	0.0048	icpms	562916	182188
271	dolomite	Veszprém Marl	T ₃	225.0	<2	0.1	0.85	0.12	0.03	0.0021	icpms	562916	182188
272	marl	Veszprém Marl	T ₃	268.0	<2	0.09	3.82	0.24	0.08	0.0049	icpms	562916	182188
273	marl	Veszprém Marl	T ₃	300.0	<2	0.07	2.62	0.22	0.04	0.002	icpms	562916	182188
274	marl	Veszprém Marl	T ₃	347.0	<2	0.1	22.4	0.72	0.86	0.0063	icpms	562916	182188
275	dolomite	Hidegkút Formation	T ₁	outcrop	<2	0.21	23.8	3.14	0.13	0.0043	icpms	563303	181004
276	slate	Lovas Slate	O-D	outcrop	<2	0.03	2.5	0.2	0.04	<0.02	icpms	567702	182614
277	slate	Lovas Slate	O-D	outcrop	5	0.03	5.6	0.4	0.38	0.02	icpms	567702	182614
278	slate	Lovas Slate	O-D	outcrop	<2	0.12	3	0.23	0.22	0.0313	icpms	567702	182614
279	bituminous limest.	Sándorhegy Formation	T ₃	outcrop	<2	0.1	0.63	0.15	0.06	0.0065	icpms	563732	184784
280	bituminous limest.	Felsőörs Limestone	T ₁	outcrop	<2	0.09	2.36	0.24	0.09	0.0534	icpms	566012	186654
281	tuff	Buchenstein Formation	T ₂	outcrop	<2	0.06	0.8	0.24	0.21	0.0241	icpms	566012	186654
282	dolomite	Megyehégy Dolomite	T ₂	outcrop	<2	0.03	0.57	0.07	0.02	0.0089	icpms	566012	186654
3. BALATONFŐ													
283	quartz phyllite	Balatonfőkajár Quartz Ph.	O-S	outcrop	<2	0.09	7.53	0.86	0.11	0.0048	icpms	587549	187325
284	phyllite	Balatonfőkajár Quartz Ph.	O-S	Balatonfőkajár-1 8.0	27	0.09	13.8	4.4	0.33	0.2	icpms	587598	187355
285	phyllite	Balatonfőkajár Quartz Ph.	O-S	37.0	<2	0.22	3.9	1.6	0.05	0.22	icpms	587598	187355
286	phyllite	Balatonfőkajár Quartz Ph.	O-S	59.9	<2	<0.02	2	0.5	0.08	0.18	icpms	587598	187355
287	phyllite	Balatonfőkajár Quartz Ph.	O-S	99.1	<2	0.07	2.5	0.7	0.2	0.28	icpms	587598	187355
288	phyllite	Balatonfőkajár Quartz Ph.	O-S	120.8-121.0	2	0.03	0.4	0.2	0.12	0.3	icpms	587598	187355
289	phyllite	Balatonfőkajár Quartz Ph.	O-S	147.4-147.5	<2	0.52	3.3	1.5	0.25	0.23	icpms	587598	187355
290	phyllite	Balatonfőkajár Quartz Ph.	O-S	172.0-172.1	<2	0.06	10.2	1	0.21	0.18	icpms	587598	187355
291	phyllite	Balatonfőkajár Quartz Ph.	O-S	196.2-196.4	<2	<0.02	1.9	0.2	0.09	0.17	icpms	587598	187355
292	shale	Füle Conglomerate	C ₂	Füle-3 126.2-126.8	<2	0.15	1.46	0.33	0.48	0.0308	icpms	589586	191889
293	sandstone	Füle Conglomerate	C ₂	163.0-165.2	<2	0.07	5.54	0.62	0.11	0.0242	icpms	589586	191889
294	sandstone	Füle Conglomerate	C ₂	186.4-190.0	<2	0.05	0.57	0.2	0.16	0.0401	icpms	589586	191889
295	shale	Füle Conglomerate	C ₂	269.4-269.5	<2	0.05	0.57	0.22	0.25	0.0372	icpms	589586	191889
296	shale	Füle Conglomerate	C ₂	294.0-294.2	<2	0.04	1.47	0.18	0.22	0.0596	icpms	589586	191889
297	limestone	Polgárdi Limestone	D ₂	Polgárdi Po-2 109.0-110.2	<2	0.11	4.61	0.27	0.22	0.1217	icpms	591883	193934
298	limestone	Polgárdi Limestone	D ₂	141.1-142.0	<2	0.05	10.1	0.77	0.06	0.0619	icpms	591883	193934
299	limestone	Polgárdi Limestone	D ₂	166.9-168.7	<2	0.07	7.25	0.33	0.06	0.2188	icpms	591883	193934
300	limestone	Polgárdi Limestone	D ₂	219.6-220.3	<2	0.06	2.76	0.18	0.04	0.016	icpms	591883	193934
301	clay	Polgárdi Limestone	D ₂	274.9-279.2	3	0.13	7.76	0.49	0.45	0.5839	icpms	591883	193934
302	limonitic infilling	Polgárdi Limestone	D ₂	outcrop	5	0.333	596	12.9	0.62	0.3	icpms	594408	194205
303	vein of calcite	Polgárdi Limestone	D ₂	outcrop	2	0.11	2.67	0.23	0.12	0.38	icpms	594518	194305
304	breccia	Polgárdi Limestone	D ₂	outcrop	<2	0.1	18.8	0.7	0.13	0.44	icpms	594518	194305

Sample no.	Lithology	Formation	Age	Sample type (depth in m)	Elements						Analytical method	Coordinates	
					Au	Ag	As	Sb	Tl	Hg		X	Y
					ppb	ppm							
305	ankeritic sideritic dolomite (infilling)	Polgárdi Limestone	D ₂	outcrop	2	0,29	67,5	2,64	0,27	0,2	icpms	594498	194315
306	granite porphyry	Velence Granite	C ₂	outcrop	<2	0.008	16.8	0.22	0.17	0.12	icpms	594398	194525
307	granite porphyry	Velence Granite	C ₂	outcrop	<2	0.041	38.5	2.72	0.17	0.24	icpms	594398	194525
308	ankeritic limestone	Polgárdi Limestone	D ₂	outcrop	8	0.049	24.9	1.58	0.05	0.3	icpms	594398	194525
309	granite porphyry	Velence Granite	C ₂	outcrop	<2	0.039	2.95	0.37	0.16	0.14	icpms	594458	194525
310	dolomitic limestone	Polgárdi Limestone	D ₂	outcrop	<2	0.014	2.09	0.27	0.02	0.18	icpms	594458	194525
311	Mn rich infilling	Polgárdi Limestone	D ₂	outcrop	7	0.2	336	23.1	6.56	2.76	icpms	594898	194885
312	lim. limest breccia	Polgárdi Limestone	D ₂	outcrop	<2	0.08	9.93	1.25	0.18	0.32	icpms	594898	194885
313	drusy calcite	Polgárdi Limestone	D ₂	outcrop	4	0.06	3.85	0.62	0.12	0.34	icpms	594868	194965
314	brucite	Polgárdi Limestone	D ₂	outcrop	2	0.16	3.33	0.27	0.1	0.85	icpms	594868	194965
315	limestone breccia	Polgárdi Limestone	D ₂	outcrop	<2	0.41	52.2	2.7	0.23	0.16	icpms	595188	195025
316	slate	Lovas Slate	O-D	outcrop	5	0.2	885	2.03	0.58	0.34	icpms	595158	195065
317	limonitic infilling	Polgárdi Limestone	D ₂	outcrop	<2	0.1	18.4	0.98	0.48	0.22	icpms	595158	195065
318	ankeritic limestone	Polgárdi Limestone	D ₂	outcrop	8	0.06	70.3	1.16	0.08	0.22	icpms	595108	195105
319	ankeritic limestone	Polgárdi Limestone	D ₂	outcrop	6	0.057	41.3	2.11	0.19	0.26	icpms	595108	195105
320	andesite	Buchenstein Formation	T ₂	outcrop	<2	0.009	14.8	0.5	0.02	0.1	icpms	595108	195105
321	limonitic infilling	Polgárdi Limestone	D ₂	outcrop	3	1.22	591	15.8	6.23	0.4	icpms	595118	195175
322	limonitic limestone	Polgárdi Limestone	D ₂	outcrop	<2	0.08	94.9	2.87	0.36	0.3	icpms	595148	195215
323	ironcrust	Polgárdi Limestone	D ₂	outcrop	7	0.2	140	5.8	0.93	1.34	icpms	595148	195215
324	limonitic limestone	Polgárdi Limestone	D ₂	Szabadbattyán Szb-9 97.8–100.0	2	0.13	11.1	4.3	0.13	0.6751	icpms	595254	195980
325	limestone	Polgárdi Limestone	D ₂	122.0–124.5	<2	0.03	7.08	1.04	0.09	0.0218	icpms	595254	195980
326	limonite breccia	Polgárdi Limestone	D ₂	165.1–169.1	<2	0.15	6.87	0.76	<0.02	0.0461	icpms	595254	195980
327	limonitic limestone	Polgárdi Limestone	D ₂	200.8–204.2	<2	0.12	28.6	6.36	0.18	0.0678	icpms	595254	195980
328	limestone	Polgárdi Limestone	D ₂	223.8–232.0	<2	0.16	3.2	0.86	<0.02	0.0348	icpms	595254	195980
329	limonitic shale	Szabadbattyán Limestone	C ₁	246.0–249.0	2	0.16	99.7	5.28	0.1	0.1283	icpms	595254	195980
330	limestone	Szabadbattyán Limestone	C ₁	285.5–290.3	<2	0.03	2.57	0.15	<0.02	0.0158	icpms	595254	195980
331	limestone	Szabadbattyán Limestone	C ₁	310.0–313.0	<2	0.03	17.7	1.16	0.23	0.1357	icpms	595254	195980
332	slate quartzite	Lovas Slate	O-D	348.8–356.9	<2	<0.02	3.78	0.1	0.06	0.0121	icpms	595254	195980
333	slate	Lovas Slate	O-D	381.6–382.1	<2	0.03	6.11	1.16	0.1	0.0684	icpms	595254	195980
334	graphite slate	Lovas Slate	O-D	404.4	<2	0.21	43.3	8.91	0.1	0.18	icpms	595254	195980
335	limonitic quartzite	Lovas Slate	O-D	404.5–405.0	<2	1.42	21.6	3.25	0.04	0.1131	icpms	595254	195980
336	slate, quartzite	Lovas Slate	O-D	407.0–407.6	9	0.14	128	2.01	0.35	0.0719	icpms	595254	195980
337	limonitic limestone	Lovas Slate	O-D	422.1–424.0	<2	0.08	1.17	0.11	<0.02	0.0068	icpms	595254	195980
338	sandstone	Lovas Slate	O-D	432.7–433.0	<2	<0.02	5.71	0.16	0.1	0.0093	icpms	595254	195980
339	slate	Lovas Slate	O-D	549.3–554.1	<2	0.12	6.04	0.07	0.19	0.008	icpms	595254	195980
340	slate	Lovas Slate	O-D	584.6–591.4	<2	0.1	4.81	0.1	0.22	0.0082	icpms	595254	195980
341	limestone	Úrhida Limestone	D ₁₋₂	Úrhida Ú-4 179.0–179.5	<2	0.03	21.4	2.95	0.29	0.48	icpms	595701	199095
342	limestone	Úrhida Limestone	D ₁₋₂	203.8–204.5	<2	0.03	5.07	1.1	0.06	0.09	icpms	595701	199095
343	limestone	Úrhida Limestone	D ₁₋₂	250.0–251.0	<2	0.04	23.3	4.23	0.26	0.51	icpms	595701	199095
344	limestone	Úrhida Limestone	D ₁₋₂	277.0–278.8	<2	0.19	1.85	0.26	0.04	0.04	icpms	595701	199095
345	limestone	Úrhida Limestone	D ₁₋₂	301.5–302.0	<2	0.04	1.06	0.16	<0.02	0.06	icpms	595701	199095
346	limestone	Úrhida Limestone	D ₁₋₂	307.0–308.0	5	0.09	1.81	1.18	0.05	0.07	icpms	595701	199095
347	limestone	Úrhida Limestone	D ₁₋₂	318.0–319.0	<2	0.09	33.7	3.38	0.29	0.26	icpms	595701	199095
348	limestone	Úrhida Limestone	D ₁₋₂	420.5–421.0	<2	1.35	2.37	0.53	0.04	0.05	icpms	595701	199095
4. VELENCE HILLS													
349	limonitic quartzite	Lovas Slate	O-D	outcrop	17	<0.050	16.10	0.41	0.120	0.1596	icpms	608950	213200
350	slate	Lovas Slate	O-D	outcrop	<2	0.380	92.70	1.67	0.360	0.0131	icpms	608950	213200
351	silicified slate	Lovas Slate	O-D	outcrop	5	0.090	77.70	4.19	0.160	0.1357	icpms	612090	214415
352	bituminous slate	Lovas Slate	O-D	outcrop	5	<1	n.a	n.a	n.a	n.a	aas	612090	214415
353	limonitic quartzite	Lovas Slate	O-D	outcrop	<2	0.520	1189.0	20.20	0.110	0.0825	icpms	614231	213969
354	limonitic quartzite	Lovas Slate	O-D	outcrop	<2	<0.050	2.92	0.22	<0.050	0.0034	icpms	614358	214030

Sample no.	Lithology	Formation	Age	Sample type (depth in m)	Elements						Analytical method	Coordinates	
					Au	Ag	As	Sb	Tl	Hg		X	Y
					ppb	ppm							
355	lim quartzite br.	Lovas Slate	O-D	outcrop	<2	<0.050	14.90	1.02	0.050	0.0151	icpms	614400	214091
356	slate	Lovas Slate	O-D	outcrop	<2	0.150	37.80	0.79	0.370	0.0117	icpms	614400	214091
357	flintslate	Lovas Slate	O-D	outcrop	<2	0.080	5.97	0.43	0.050	0.0052	icpms	614400	214091
358	granite	Velence Granite	C ₂	outcrop	<2	-0.050	4.71	0.38	0.190	0.0097	icpms	614149	214247
359	quartzite breccia	Lovas Slate	O-D	outcrop	214	1.370	357.00	50.70	0.110	0.0417	icpms	615444	212911
360	lim. quartzite br.	Lovas Slate	O-D	outcrop	5005	38.100	1255.0	791.00	0.380	0.9655	icpms	615381	212943
361	quartzite breccia	Lovas Slate	O-D	outcrop	48	0.510	792.00	13.80	0.180	0.1488	icpms	615339	212974
362	limonitic quartzite	Velence Granite	C ₂	outcrop	2090	18	n.a.	n.a.	n.a.	n.a.	aas	615335	212974
363	quartzite breccia	Lovas Slate	O-D	outcrop	81	0.410	180.00	29.60	0.130	0.054	icpms	615277	213036
364	quartzite	Lovas Slate	O-D	outcrop	22	0.600	251.00	52.80	0.840	0.0416	icpms	615803	213187
365	quartzite	Lovas Slate	C ₂	outcrop	19	2	n.a.	n.a.	n.a.	n.a.	aas	615772	213296
366	intrusive breccia	Nadap Andesite	E _{2,3}	Nadap Nt-2 66.8	<2	2.9	n.a.	n.a.	n.a.	n.a.	fa	616001	213381
367	intrusive breccia	Nadap Andesite	E _{2,3}	94.7	<2	0.6	n.a.	n.a.	n.a.	n.a.	fa	616001	213381
368	intrusive breccia	Nadap Andesite	E _{2,3}	97.5-98.9	1000	142	n.a.	n.a.	n.a.	n.a.	fa	616001	213381
369	silicified intr. br.	Nadap Andesite	E _{2,3}	98.9-99.5	600	23.9	n.a.	n.a.	n.a.	n.a.	fa	616001	213381
370	contact slate	Lovas Slate	O-D	outcrop	20	0.150	159.00	4.34	0.800	0.0324	icpms	616015	213402
371	contact slate	Lovas Slate	O-D	outcrop	10	<1	n.a.	n.a.	n.a.	n.a.	aas	616015	213402
372	silicified slate	Lovas Slate	O-D	outcrop	<2	-0.050	26.80	0.40	0.250	0.0058	icpms	616057	213464
373	intrusive breccia	Nadap Andesite	E _{2,3}	outcrop	3	0.080	173.00	1.35	0.440	0.0162	icpms	616057	213464
374	slate, breccia	Lovas Slate	O-D	outcrop	<1	<1	n.a.	n.a.	n.a.	n.a.	aas	616057	213464
375	intrusive breccia	Nadap Andesite	E _{2,3}	Nadap Nt-4 4.0-5.6	<2	<0.02	n.a.	n.a.	n.a.	n.a.	fa	616064	213626
376	contact slate	Lovas Slate	O-D	5.6-6.5	<2	<0.02	n.a.	n.a.	n.a.	n.a.	fa	616064	213626
377	intrusive breccia	Nadap Andesite	E _{2,3}	6.5-8.0	<2	0.6	n.a.	n.a.	n.a.	n.a.	fa	616064	213626
378	contact slate, br.	Lovas Slate	O-D	8.0-10.4	<2	<0.02	n.a.	n.a.	n.a.	n.a.	fa	616064	213626
379	intrusive breccia	Nadap Andesite	E _{2,3}	10.4-10.9	<2	0.2	n.a.	n.a.	n.a.	n.a.	fa	616064	213626
380	contact slate	Lovas Slate	O-D	10.9-12.2	<2	0.2	n.a.	n.a.	n.a.	n.a.	fa	616064	213626
381	intrusive breccia	Nadap Andesite	E _{2,3}	12.2-12.9	<2	<0.02	n.a.	n.a.	n.a.	n.a.	fa	616064	213626
382	contact slate, br.	Lovas Slate	O-D	12.9-16.0	<2	<0.02	n.a.	n.a.	n.a.	n.a.	fa	616064	213626
383	intrusive breccia	Nadap Andesite	E _{2,3}	16.0-16.8	<2	2	n.a.	n.a.	n.a.	n.a.	fa	616064	213626
384	contact slate	Lovas Slate	O-D	16.8-18.1	<2	9	n.a.	n.a.	n.a.	n.a.	fa	616064	213626
385	intrusive breccia	Nadap Andesite	E _{2,3}	18.1-18.3	600	5.8	n.a.	n.a.	n.a.	n.a.	fa	616064	213626
386	contact slate	Lovas Slate	O-D	18.3-19.2	200	11.6	n.a.	n.a.	n.a.	n.a.	fa	616064	213626
387	microgranite	Velence Granite	C ₂	19.2-20.8	600	13	n.a.	n.a.	n.a.	n.a.	fa	616064	213626
388	contact slate	Lovas Slate	O-D	20.8-21.7	2200	140	n.a.	n.a.	n.a.	n.a.	fa	616064	213626
389	contact slate	Lovas Slate	O-D	21.7-23.5	200	2.8	n.a.	n.a.	n.a.	n.a.	fa	616064	213626
390	intrusive breccia	Nadap Andesite	E _{2,3}	23.5-26.0	<2	2.4	n.a.	n.a.	n.a.	n.a.	fa	616064	213626
391	contact slate	Lovas Slate	O-D	26.0-27.7	200	6.6	n.a.	n.a.	n.a.	n.a.	fa	616064	213626
392	intrusive breccia	Nadap Andesite	E _{2,3}	27.7-28.5	400	11.2	n.a.	n.a.	n.a.	n.a.	fa	616064	213626
393	contact slate, br.	Lovas Slate	O-D	28.8-34.4	<2	1.6	n.a.	n.a.	n.a.	n.a.	fa	616064	213626
394	intrusive breccia	Nadap Andesite	E _{2,3}	34.4-39.3	<2	0.4	n.a.	n.a.	n.a.	n.a.	fa	616064	213626
395	contact slate	Lovas Slate	O-D	39.3-46.5	<2	<0.02	n.a.	n.a.	n.a.	n.a.	fa	616064	213626
396	intrusive breccia	Nadap Andesite	E _{2,3}	46.5-47.0	<2	1	n.a.	n.a.	n.a.	n.a.	fa	616064	213626
397	contact slate	Lovas Slate	O-D	47.0-51.0	<2	<0.02	n.a.	n.a.	n.a.	n.a.	fa	616064	213626
398	intrusive breccia	Nadap Andesite	E _{2,3}	51.0-52.6	<2	<0.02	n.a.	n.a.	n.a.	n.a.	fa	616064	213626
399	contact slate, br.	Lovas Slate	O-D	52.6-57.4	<2	<0.02	n.a.	n.a.	n.a.	n.a.	fa	616064	213626
400	intrusive breccia	Nadap Andesite	E _{2,3}	57.4-57.8	<2	<0.02	n.a.	n.a.	n.a.	n.a.	fa	616064	213626
401	contact slate, br.	Lovas Slate	O-D	57.8-58.9	<2	<0.02	n.a.	n.a.	n.a.	n.a.	fa	616064	213626
402	contact slate, br.	Lovas Slate	O-D	58.9-60.2	<2	1.6	n.a.	n.a.	n.a.	n.a.	fa	616064	213626
403	intrusive breccia	Nadap Andesite	E _{2,3}	60.2-60.4	<2	<0.02	n.a.	n.a.	n.a.	n.a.	fa	616064	213626
404	contact slate, br.	Lovas Slate	O-D	60.4-68.1	<2	1.4	n.a.	n.a.	n.a.	n.a.	fa	616064	213626
405	intrusive breccia	Nadap Andesite	E _{2,3}	68.1-68.5	<2	<0.02	n.a.	n.a.	n.a.	n.a.	fa	616064	213626
406	contact slate, br.	Lovas Slate	O-D	68.5-70.7	<2	<0.02	n.a.	n.a.	n.a.	n.a.	fa	616064	213626
407	intrusive breccia	Nadap Andesite	E _{2,3}	70.4-71.2	<2	0.6	n.a.	n.a.	n.a.	n.a.	fa	616064	213626

Sample no.	Lithology	Formation	Age	Sample type (depth in m)	Elements						Analytical method	Coordinates	
					Au	Ag	As	Sb	Tl	Hg		X	Y
					ppb	ppm							
408	contact slate, br	Lovas Slate	O-D	71.2-78.8	<2	<0.02	n.a.	n.a.	n.a.	n.a.	fa	616064	213626
409	intrusive breccia	Nadap Andesite	E _{2,3}	78.8-79.5	<2	<0.02	n.a.	n.a.	n.a.	n.a.	fa	616064	213626
410	contact slate, br	Lovas Slate	O-D	79.5-81.4	<2	0.4	n.a.	n.a.	n.a.	n.a.	fa	616064	213626
411	contact slate	Lovas Slate	O-D	81.4-83.1	<2	<0.02	n.a.	n.a.	n.a.	n.a.	fa	616064	213626
412	contact slate, br	Lovas Slate	O-D	83.1-84.6	<2	<0.02	n.a.	n.a.	n.a.	n.a.	fa	616064	213626
413	contact slate	Lovas Slate	O-D	84.6-85.7	<2	<0.02	n.a.	n.a.	n.a.	n.a.	fa	616064	213626
414	intrusive breccia	Nadap Andesite	E _{2,3}	85.7-87.6	<2	<0.02	n.a.	n.a.	n.a.	n.a.	fa	616064	213626
415	contact slate, br	Lovas Slate	O-D	87.6-89.5	<2	0.2	n.a.	n.a.	n.a.	n.a.	fa	616064	213626
416	contact slate	Lovas Slate	O-D	89.5-92.2	<2	0.6	n.a.	n.a.	n.a.	n.a.	fa	616064	213626
417	intrusive breccia	Nadap Andesite	E _{2,3}	92.2-93.0	<2	1	n.a.	n.a.	n.a.	n.a.	fa	616064	213626
418	contact slate	Lovas Slate	O-D	93.0-95.8	<2	0.2	n.a.	n.a.	n.a.	n.a.	fa	616064	213626
419	intrusive breccia	Nadap Andesite	E _{2,3}	95.8-96.7	<2	1.2	n.a.	n.a.	n.a.	n.a.	fa	616064	213626
420	contact slate, br	Lovas Slate	O-D	96.7-98.3	<2	<0.02	n.a.	n.a.	n.a.	n.a.	fa	616064	213626
421	intrusive breccia	Nadap Andesite	E _{2,3}	98.3-98.6	<2	<0.02	n.a.	n.a.	n.a.	n.a.	fa	616064	213626
422	contact slate, br	Lovas Slate	O-D	98.6-100.3	<2	<0.02	n.a.	n.a.	n.a.	n.a.	fa	616064	213626
423	intrusive breccia	Nadap Andesite	E _{2,3}	100.3-100.6	<2	<0.02	n.a.	n.a.	n.a.	n.a.	fa	616064	213626
424	contact slate	Lovas Slate	O-D	100.6-102.2	<2	<0.02	n.a.	n.a.	n.a.	n.a.	fa	616064	213626
425	intrusive breccia	Nadap Andesite	E _{2,3}	102.2-102.9	<2	<0.02	n.a.	n.a.	n.a.	n.a.	fa	616064	213626
426	contact slate, br	Lovas Slate	O-D	102.9-105.2	<2	<0.02	n.a.	n.a.	n.a.	n.a.	fa	616064	213626
427	intrusive breccia	Nadap Andesite	E _{2,3}	105.2-109.4	<2	<0.02	n.a.	n.a.	n.a.	n.a.	fa	616064	213626
428	contact slate, br	Lovas Slate	O-D	109.4-111.3	<2	<0.02	n.a.	n.a.	n.a.	n.a.	fa	616064	213626
429	intrusive breccia	Nadap Andesite	E _{2,3}	111.3-112.7	<2	<0.02	n.a.	n.a.	n.a.	n.a.	fa	616064	213626
430	contact slate, br	Lovas Slate	O-D	112.7-115.0	<2	0.4	n.a.	n.a.	n.a.	n.a.	fa	616064	213626
431	intrusive breccia	Nadap Andesite	E _{2,3}	115.0-117.0	<2	1	n.a.	n.a.	n.a.	n.a.	fa	616064	213626
432	contact slate	Lovas Slate	O-D	117.0-118.9	<2	<0.02	n.a.	n.a.	n.a.	n.a.	fa	616064	213626
433	intrusive breccia	Nadap Andesite	E _{2,3}	118.9-119.8	<2	0.6	n.a.	n.a.	n.a.	n.a.	fa	616064	213626
434	contact slate, br	Lovas Slate	O-D	119.8-120.3	<2	<0.02	n.a.	n.a.	n.a.	n.a.	fa	616064	213626
435	intrusive breccia	Nadap Andesite	E _{2,3}	120.3-121.1	<2	<0.02	n.a.	n.a.	n.a.	n.a.	fa	616064	213626
436	contact slate	Lovas Slate	O-D	121.1-121.5	<2	<0.02	n.a.	n.a.	n.a.	n.a.	fa	616064	213626
437	intrusive breccia	Nadap Andesite	E _{2,3}	121.5-122.0	<2	1.2	n.a.	n.a.	n.a.	n.a.	fa	616064	213626
438	contact slate, br	Lovas Slate	O-D	122.0-123.8	<2	1.2	n.a.	n.a.	n.a.	n.a.	fa	616064	213626
439	silicified intr. br	Nadap Andesite	E _{2,3}	123.8-124.4	<2	<0.02	n.a.	n.a.	n.a.	n.a.	fa	616064	213626
440	contact slate	Lovas Slate	O-D	124.4-126.4	<2	2	n.a.	n.a.	n.a.	n.a.	fa	616064	213626
441	intrusive breccia	Nadap Andesite	E _{2,3}	126.4-126.8	<2	8.4	n.a.	n.a.	n.a.	n.a.	fa	616064	213626
442	contact slate	Lovas Slate	O-D	126.8-127.7	<2	0.8	n.a.	n.a.	n.a.	n.a.	fa	616064	213626
443	granite porph., br	Velence Granite	C ₂	127.7-130.1	<2	0.6	n.a.	n.a.	n.a.	n.a.	fa	616064	213626
444	breccia	Lovas Slate	O-D	130.1-132.0	<2	3	n.a.	n.a.	n.a.	n.a.	fa	616064	213626
445	microgranite	Velence Granite	C ₂	132.0-132.7	<2	<0.02	n.a.	n.a.	n.a.	n.a.	fa	616064	213626
446	intrusive breccia	Nadap Andesite	E _{2,3}	132.7-135.6	<2	<0.02	n.a.	n.a.	n.a.	n.a.	fa	616064	213626
447	granite	Velence Granite	C ₂	135.6-136.5	<2	0.2	n.a.	n.a.	n.a.	n.a.	fa	616064	213626
448	intrusive breccia	Nadap Andesite	E _{2,3}	136.5-137.3	<2	<0.02	n.a.	n.a.	n.a.	n.a.	fa	616064	213626
449	granite, breccia	Velence Granite	C ₂	137.3-144.2	<2	<0.02	n.a.	n.a.	n.a.	n.a.	fa	616064	213626
450	granite	Velence Granite	C ₂	144.2-146.9	<2	<0.02	n.a.	n.a.	n.a.	n.a.	fa	616064	213626
451	intrusive breccia	Nadap Andesite	E _{2,3}	146.9-147.1	<2	0.2	n.a.	n.a.	n.a.	n.a.	fa	616064	213626
452	intrusive breccia	Nadap Andesite	E _{2,3}	148.1-149.1	<2	0.4	n.a.	n.a.	n.a.	n.a.	fa	616064	213626
453	granite	Velence Granite	C ₂	149.1-150.5	<2	1.6	n.a.	n.a.	n.a.	n.a.	fa	616064	213626
454	granite	Velence Granite	C ₂	169.0-170.3	<2	<0.02	n.a.	n.a.	n.a.	n.a.	fa	616064	213626
455	limonitic slate	Lovas Slate	O-D	outcrop	38	0.130	151.00	1.88	0.530	0.0253	icpms	618778	211257
456	limonitic slate	Lovas Slate	O-D	outcrop	15	<1	n.a.	n.a.	n.a.	n.a.	aas	618778	211257
457	andesite	Nadap Andesite	E _{2,3}	outcrop	3	0.690	80.40	2.20	1.370	0.0188	icpms	618191	211600
458	limonitic slate	Lovas Slate	O-D	outcrop	2	0.680	38.20	1.72	1.060	0.006	icpms	618191	211600
459	limonitic slate	Lovas Slate	O-D	outcrop	2	2	n.a.	n.a.	n.a.	n.a.	aas	618191	211600
460	diabase	Litér Metabasalt	S	outcrop	1	<1	n.a.	n.a.	n.a.	n.a.	aas	618381	211630

Sample no.	Lithology	Formation	Age	Sample type (depth in m)	Elements						Analytical method	Coordinates	
					Au	Ag	As	Sb	Tl	Hg		X	Y
					ppb	ppm							
461	dolomite	Budaörs Dolomite	T _{2,3}	Vál-3 275 0	<2	0.08	27.2	0.26	0.2	0.008	icpms	620821	225180
462	dolomite	Budaörs Dolomite	T _{2,3}	300.0	<2	0.14	13.1	0.15	0.35	0.003	icpms	620821	225180
463	dolomite	Budaörs Dolomite	T _{2,3}	325.0	<2	0.04	19.6	0.17	0.3	0.0034	icpms	620821	225180
464	dolomite	Budaörs Dolomite	T _{2,3}	350.0	<2	0.11	11.4	0.37	0.05	0.0032	icpms	620821	225180
465	dolomite	Budaörs Dolomite	T _{2,3}	375.0	<2	0.14	4.32	0.31	0.03	0.0033	icpms	620821	225180
466	dolomite	Budaörs Dolomite	T _{2,3}	400.0	<2	0.08	4.16	0.14	<0.02	0.0024	icpms	620821	225180
467	dolomite	Budaörs Dolomite	T _{2,3}	422.0	<2	0.12	706	0.76	2.63	0.0086	icpms	620821	225180
468	dolomite	Budaörs Dolomite	T _{2,3}	450.0	<2	0.17	9.87	0.16	0.06	0.0019	icpms	620821	225180
469	dolomite	Budaörs Dolomite	T _{2,3}	475.0	<2	0.56	7.4	0.15	0.06	0.0021	icpms	620821	225180
470	sandstone	Csopak Marl	T ₁	500.0	<2	0.06	41.5	0.26	0.34	0.0038	icpms	620821	225180
471	siltstone	Csopak Marl	T ₁	526.0	<2	0.12	9.04	0.27	0.13	0.0063	icpms	620821	225180
472	sandstone	Csopak Marl	T ₁	555.0	<2	0.07	5.32	0.42	0.03	0.0046	icpms	620821	225180
473	limestone	Csopak Marl	T ₁	575.0	<2	0.06	5.25	0.16	0.17	0.0033	icpms	620821	225180
474	siltstone	Csopak Marl	T ₁	599.0	<2	0.09	11.9	0.7	0.31	0.0024	icpms	620821	225180
475	limestone	Csopak Marl	T ₁	625.0	<2	0.05	2.19	0.11	0.15	0.0042	icpms	620821	225180
476	siltstone	Csopak Marl	T ₁	650.0	<2	0.05	4.94	0.45	0.25	0.0017	icpms	620821	225180
477	limestone	Csopak Marl	T ₁	675.0	<2	0.1	3.72	0.18	0.1	0.0034	icpms	620821	225180
478	limestone	Csopak Marl	T ₁	700.0	<2	0.06	3.19	0.13	0.06	0.0025	icpms	620821	225180
479	limestone	Csopak Marl	T ₁	725.0	<2	0.05	5.77	0.12	0.09	0.0021	icpms	620821	225180
480	siltstone	Csopak Marl	T ₁	749.0	<2	0.09	3.76	0.19	0.21	0.0034	icpms	620821	225180
481	dolomite	Hidegkút Formation	T ₁	775.0	<2	0.1	6.84	0.08	0.02	0.0009	icpms	620821	225180
482	dolomite	Hidegkút Formation	T ₁	801.0	<2	0.1	16.6	0.38	0.09	0.0064	icpms	620821	225180
483	sandstone	Hidegkút Formation	T ₁	825.0	<2	0.09	11	0.45	0.24	0.0043	icpms	620821	225180
484	dolomite	Hidegkút Formation	T ₁	851.0	<2	0.09	4.92	0.15	0.07	0.0028	icpms	620821	225180
485	sandstone	Hidegkút Formation	T ₁	873.0	<2	0.07	16.1	0.4	0.23	0.0189	icpms	620821	225180
486	siltstone	Hidegkút Formation	T ₁	888.6	<2	0.04	1.52	0.39	0.3	0.0007	icpms	620821	225180
487	shale	Lovas Slate	O-D	890.0	<2	0.04	3.56	0.1	0.08	0.0026	icpms	620821	225180
488	diabase	Litér Metabasalt	S	899.0	<2	0.07	1	0.08	0.18	0.0055	icpms	620821	225180
<i>5. BUDA HILLS, PILIS MOUNTAINS</i>													
489	limonitic dolomite	Buda Marl	E ₃ -O ₁	outcrop	<2	0.016	265	16.2	0.21	5.28	icpms	642840	235544
490	limonitic marl	Buda Marl	E ₃ -O ₁	outcrop	5	0.097	1296	31.1	4.42	66.8	icpms	642810	235564
491	limonitic sandstone	Buda Marl	E ₃ -O ₁	outcrop	2	0.075	65.6	13.7	1.06	6.28	icpms	642810	235564
492	lim. silicified marl	Buda Marl	E ₃ -O ₁	outcrop	<2	0.098	210	46.7	2.1	11.1	icpms	641450	235514
493	dolomite	Budaörs Dolomite	T _{2,3}	outcrop	<2	0.012	74.7	8.67	0.96	2.6	icpms	641540	235664
494	limonitic breccia	Budaörs Dolomite	T _{2,3}	outcrop	<2	0.087	88.3	18.1	0.69	10.7	icpms	642220	235814
495	limonitic infilling	Budaörs Dolomite	T _{2,3}	outcrop	<2	0.013	111	12.8	0.09	5.2	icpms	642500	236044
496	silicified marl	Budaörs Dolomite	T _{2,3}	outcrop	<2	0.059	36.8	5.86	1.11	3.19	icpms	643221	235815
497	dolomite	Budaörs Dolomite	T _{2,3}	outcrop	<2	0.025	87.8	11.6	0.13	2.16	icpms	643300	235824
498	dolomite	Budaörs Dolomite	T _{2,3}	Budaörs-1 135 0	2	n.a.	n.a.	n.a.	n.a.	n.a.	icpms	644538	236353
499	dolomite	Budaörs Dolomite	T _{2,3}	256.0	5	n.a.	n.a.	n.a.	n.a.	n.a.	icpms	644538	236353
500	dolomite	Budaörs Dolomite	T _{2,3}	323.4	<2	n.a.	n.a.	n.a.	n.a.	n.a.	icpms	644538	236353
501	dolomite	Budaörs Dolomite	T _{2,3}	418.0	2	n.a.	n.a.	n.a.	n.a.	n.a.	icpms	644538	236353
502	dolomite	Budaörs Dolomite	T _{2,3}	472.0	<2	n.a.	n.a.	n.a.	n.a.	n.a.	icpms	644538	236353
503	dolomite breccia	Budaörs Dolomite	T _{2,3}	702.0	2	n.a.	n.a.	n.a.	n.a.	n.a.	icpms	644538	236353
504	dolomite	Budaörs Dolomite	T _{2,3}	715.0	<2	n.a.	n.a.	n.a.	n.a.	n.a.	icpms	644538	236353
505	dolomite	Budaörs Dolomite	T _{2,3}	787.3	4	n.a.	n.a.	n.a.	n.a.	n.a.	icpms	644538	236353
506	dolomarl	Budaörs Dolomite	T _{2,3}	945.0	<2	n.a.	n.a.	n.a.	n.a.	n.a.	icpms	644538	236353
507	dolomarl	Budaörs Dolomite	T _{2,3}	998.0-999.7	<2	n.a.	n.a.	n.a.	n.a.	n.a.	icpms	644538	236353
508	marl	Budaörs Dolomite	T _{2,3}	1004.7	<2	n.a.	n.a.	n.a.	n.a.	n.a.	icpms	644538	236353
509	dolomite	Budaörs Dolomite	T _{2,3}	1024.5	<2	n.a.	n.a.	n.a.	n.a.	n.a.	icpms	644538	236353
510	dolomite	Csopak Marl	T ₁	1144.0	<2	n.a.	n.a.	n.a.	n.a.	n.a.	icpms	644538	236353
511	dolomite	Csopak Marl	T ₁	1156.0	<2	n.a.	n.a.	n.a.	n.a.	n.a.	icpms	644538	236353
512	limonitic sand	Zámor Gravel	M ₃	outcrop	<2	0.06	1810	48.4	0.525	25.63	aas	645330	237524

Sample no.	Lithology	Formation	Age	Sample type (depth in m)	Elements						Analytical method	Coordinates	
					Au	Ag	As	Sb	Tl	Hg		X	Y
					ppb	ppm							
513	cherty dolomite	Mátyáshegy Formation	T ₃	outcrop	<2	0.03	12.7	9.8	0.205	0.49	aas	645090	237644
514	clay	Tard Clay	Ol ₁	Budapest Kv-1 300.0-300.3	<2	0.23	52.9	14.5	1.83	0.2019	icpms	651644	235493
515	limestone	Szépvolgy Limestone	E ₃	304.0	<2	0.16	5.75	0.25	0.09	0.0485	icpms	651644	235493
516	breccia	Mátyáshegy Formation	T ₃	368.9	3	0.09	1.15	0.29	0.07	0.0103	icpms	651644	235493
517	vein of calcite	Mátyáshegy Formation	T ₃	393.5	<2	0.07	216	8.46	1.97	1.836	icpms	651644	235493
518	marl	Mátyáshegy Formation	T ₃	448.7	<2	0.08	16.9	1.16	0.09	0.0183	icpms	651644	235493
519	pyritic breccia	Mátyáshegy Formation	T ₃	500.0	<2	0.08	20.9	1.11	0.15	0.092	icpms	651644	235493
520	limestone	Mátyáshegy Formation	T ₃	558.8	<2	0.07	0.95	0.16	0.06	0.002	icpms	651644	235493
521	marl	Tard Clay	Ol ₁	Engels tér-1 453.0	<2	0.15	13.8	1.17	0.72	0.0905	icpms	650336	239377
522	marl	Buda Marl	E ₃ -Ol ₁	501.0	<2	0.1	2.64	0.33	0.14	0.0253	icpms	650336	239377
523	marl	Buda Marl	E ₃ -Ol ₁	551.0	<2	0.1	3.25	0.4	0.14	0.0349	icpms	650336	239377
524	marl	Buda Marl	E ₃ -Ol ₁	603.0	<2	0.09	5.27	0.74	0.12	0.0415	icpms	650336	239377
525	limestone	Mátyáshegy Formation	T ₃	Vérhalom-1 51.4-79.4	<1	n.a	n.a	n.a	n.a	n.a	icpms	648302	241914
526	limestone	Mátyáshegy Formation	T ₃	91.0-94.1	2	n.a	n.a	n.a	n.a	n.a	icpms	648302	241914
527	marl	Mátyáshegy Formation	T ₃	98.3-101.5	1	n.a	n.a	n.a	n.a	n.a	icpms	648302	241914
528	cherty limestone	Mátyáshegy Formation	T ₃	106.9-115.6	3	n.a	n.a	n.a	n.a	n.a	icpms	648302	241914
529	marl	Mátyáshegy Formation	T ₃	128.2-129.9	<1	n.a	n.a	n.a	n.a	n.a	icpms	648302	241914
530	marl	Mátyáshegy Formation	T ₃	145.3-145.8	2	n.a	n.a	n.a	n.a	n.a	icpms	648302	241914
531	marl	Mátyáshegy Formation	T ₃	148.4-157.4	1	n.a	n.a	n.a	n.a	n.a	icpms	648302	241914
532	dolomarl	Mátyáshegy Formation	T ₃	168.2-174.3	1	n.a	n.a	n.a	n.a	n.a	icpms	648302	241914
533	marl	Mátyáshegy Formation	T ₃	193.2-193.6	2	n.a	n.a	n.a	n.a	n.a	icpms	648302	241914
534	dolomarl	Mátyáshegy Formation	T ₃	201.0-201.4	3	n.a	n.a	n.a	n.a	n.a	icpms	648302	241914
535	dolomarl	Mátyáshegy Formation	T ₃	209.1-227.4	2	n.a	n.a	n.a	n.a	n.a	icpms	648302	241914
536	dolomarl	Mátyáshegy Formation	T ₃	231.0-234.0	2	n.a	n.a	n.a	n.a	n.a	icpms	648302	241914
537	dolomarl	Mátyáshegy Formation	T ₃	235.5-236.2	2	n.a	n.a	n.a	n.a	n.a	icpms	648302	241914
538	dolomite	Mátyáshegy Formation	T ₃	242.3-243.8	3	n.a	n.a	n.a	n.a	n.a	icpms	648302	241914
539	dolomarl	Mátyáshegy Formation	T ₃	243.8-245.1	1	n.a	n.a	n.a	n.a	n.a	icpms	648302	241914
540	dolomite	Mátyáshegy Formation	T ₃	243.8-245.1	<1	n.a	n.a	n.a	n.a	n.a	icpms	648302	241914
541	dolomite	Mátyáshegy Formation	T ₃	248.5-250.0	12	n.a	n.a	n.a	n.a	n.a	icpms	648302	241914
542	silicified marl	Buda Marl	E ₃ -Ol ₁	outcrop	<2	0.06	160	19.1	1.109	20.12	aas	641471	236865
543	dolomite	Mátyáshegy Formation	T ₃	outcrop	<2	0.05	8.54	3.4	0.064	0.57	aas	641841	236675
544	silicified marl	Buda Marl	E ₃ -Ol ₁	outcrop	<2	0.08	49.6	4.5	3.39	20.56	aas	641841	236675
545	limonitic sand	Zámor Gravel	M ₃	outcrop	<2	0.11	152	3.9	0.071	0.05	aas	642501	236955
546	cherty dolomite	Mátyáshegy Formation	T ₃	outcrop	<2	<0.02	274	43.7	0.445	58.07	aas	641230	237324
547	dolomite	Mátyáshegy Formation	T ₃	outcrop	<2	<0.02	463	15	0.795	8.19	aas	641560	237494
548	cherty dolomite	Mátyáshegy Formation	T ₃	outcrop	<2	0.06	97.6	8.6	1.8	6.51	aas	641560	237494
549	limy mudstone	Travertine Formation	Pa-Q ₁	outcrop	<2	0.03	36.8	<0.02	0.172	0.1	aas	642090	237564
550	bitum travertine	Travertine Formation	Pa-Q ₁	outcrop	<2	0.02	5.06	0.4	<0.02	0.27	aas	642090	237564
551	limonitic travertine	Travertine Formation	Pa-Q ₁	outcrop	<2	0.06	500	48.4	4.88	12.24	aas	642090	237564
552	dolom. br. (infilling)	Mátyáshegy Formation	T ₃	outcrop	<2	<0.02	291	19.6	0.188	10.39	aas	641770	237894
553	dolomite	Mátyáshegy Formation	T ₃	outcrop	<2	<0.02	5.65	1.7	<0.02	1.28	aas	641770	237894
554	cherty dolomite (infilling)	Mátyáshegy Formation	T ₃	outcrop	<2	0.02	3.87	0.7	<0.02	0.8	aas	642020	238384
555	chert	Mátyáshegy Formation	T ₃	outcrop	<2	0.02	4.26	0.8	<0.02	0.74	aas	642020	238384
556	dolomite	Mátyáshegy Formation	T ₃	outcrop	<2	0.02	9.89	1.4	<0.02	0.8	aas	642020	238384
557	lim. cherty dolomite	Mátyáshegy Formation	T ₃	outcrop	<2	0.06	91.7	788	0.81	28.95	aas	640551	239014
558	chert (infilling)	Mátyáshegy Formation	T ₃	outcrop	<2	0.05	78.1	21.1	33	7.19	aas	640831	238864
559	limonitic dolomite	Mátyáshegy Formation	T ₃	outcrop	<2	0.05	160	1760	29.4	30.73	aas	640831	238864
560	limonitic infilling	Mátyáshegy Formation	T ₃	outcrop	<2	0.04	235	1220	33.7	111.37	aas	640831	238864
561	dolomite	Födolomit Formation	T ₃	outcrop	<2	0.28	6.09	1.6	<0.02	0.61	aas	636630	240284
562	sandstone	Hárshegy Sandstone	Ol ₁	outcrop	<2	0.03	426	50.2	0.938	7.14	aas	636630	240284
563	sandstone	Hárshegy Sandstone	Ol ₁	outcrop	<2	0.21	80.1	31.2	4.9	11.54	aas	637360	241354

Sample no.	Lithology	Formation	Age	Sample type (depth in m)	Elements						Analytical method	Coordinates	
					Au	Ag	As	Sb	Tl	Hg		X	Y
					ppb	ppm							
564	limonitic sandstone	Hárshegy Sandstone	Ol ₁	outcrop	<2	0.07	338	176	8.86	0.3	aas	637540	242753
565	dolomite	Födolomit Formation	T ₃	outcrop	<2	<0.02	3.13	6.8	0.025	0.05	aas	637560	242933
566	limonitic sandstone	Hárshegy Sandstone	Ol ₁	outcrop	<2	0.04	74.4	7.1	0.122	0.36	aas	638690	242784
567	dolomitic limestone	Dachstein Limestone	T ₃	outcrop	<2	<0.02	5.44	0.6	<0.02	<0.02	aas	639050	243084
568	bauxitic clay	Bauxite Formation	Cr ₃ -E ₁	outcrop	<2	0.09	28.4	5.2	0.157	0.05	aas	639050	243084
569	dolomite	Födolomit Formation	T ₁	Adyliget-1 398.5	4	n.a.	n.a.	n.a.	n.a.	n.a.	icpms	640010	243509
570	dol. with kaolinite	Födolomit Formation	T ₁	417.9-418.0	<2	n.a.	n.a.	n.a.	n.a.	n.a.	icpms	640010	243509
571	dolomite breccia	Födolomit Formation	T ₃	446.0-446.3	2	n.a.	n.a.	n.a.	n.a.	n.a.	icpms	640010	243509
572	dol. with kaolinite	Födolomit Formation	T ₃	471.9-472.0	<2	n.a.	n.a.	n.a.	n.a.	n.a.	icpms	640010	243509
573	dolomite	Födolomit Formation	T ₃	497.6	<2	n.a.	n.a.	n.a.	n.a.	n.a.	icpms	640010	243509
574	limestone	Szépvolgy Limestone	E ₃	outcrop	<2	0.03	0.82	1.7	<0.02	0.15	aas	642470	240014
575	pyritic clay	Tard Clay	Ol ₁	Városmajor-1 62.5-68.4	<2	0.18	15.1	0.99	0.43	0.103	icpms	644489	240491
576	marl	Tard Clay	Ol ₁	113.7-116.4	<2	0.16	8.82	1.32	0.21	0.0562	icpms	644489	240491
577	clay	Tard Clay	Ol ₁	156.0-156.5	<2	0.08	2.48	0.37	0.13	0.0271	icpms	644489	240491
578	cherty limestone	Mátyáshegy Formation	T ₃	313.5-318.3	<2	0.08	0.86	0.29	0.08	0.0314	icpms	644489	240491
579	marl	Buda Marl	E ₃ -Ol ₁	outcrop	<2	0.04	3.9	0.8	0.033	0.08	aas	643340	241234
580	dolomite (infilling)	Dachstein Limestone	T ₃	outcrop	<2	0.03	5.69	1	0.035	0.1	aas	643480	241504
581	dolomite	Födolomit Formation	T ₃	outcrop	<2	0.03	1.84	3.3	0.021	0.26	aas	643540	241524
582	sandstone	Hárshegy Sandstone	Ol ₁	outcrop	<2	0.07	1.23	0.3	<0.02	0.02	aas	642960	242884
583	limestone (infilling)	Dachstein Limestone	T ₃	outcrop	<2	0.05	1.72	0.4	0.025	0.04	aas	642960	242884
584	sandstone	Hárshegy Sandstone	Ol ₁	outcrop	<2	0.04	112	8.7	0.045	0.41	aas	642960	242884
585	lim br (infilling)	Dachstein Limestone	T ₃	outcrop	2	0.03	2.13	0.4	<0.02	0.06	aas	642960	242884
586	limestone	Dachstein Limestone	T ₃	outcrop	<2	<0.02	0.22	<0.02	<0.02	<0.02	aas	642960	242884
587	sandstone	Hárshegy Sandstone	Ol ₁	outcrop	<2	0.05	1065	11.7	<0.02	4.01	aas	643000	243244
588	iron ore	Hárshegy Sandstone	Ol ₁	outcrop	2	0.04	813	26.6	<0.02	2.82	aas	643050	243254
589	iron ore	Hárshegy Sandstone	Ol ₁	outcrop	<2	0.04	1020	15.1	<0.02	1.32	aas	643050	243254
590	microgabbro	Budakeszi Picrite	Cr ₃	outcrop	<2	<0.02	1.53	0.1	0.377	<0.02	aas	637160	244743
591	bauxitic clay	Bauxite Formation	Cr ₃ -E ₁	outcrop	<2	0.03	5.42	1.1	0.026	<0.02	aas	637420	245203
592	limestone breccia	Dachstein Limestone	T ₃	outcrop	<2	<0.02	12.53	0.6	0.023	<0.02	aas	637420	245203
593	limestone	Dachstein Limestone	T ₃	outcrop	<2	<0.02	1.69	0.2	0.07	<0.02	aas	637420	245203
594	dolomite	Födolomit Formation	T ₃	outcrop	<2	<0.02	4.74	0.3	<0.02	<0.02	aas	635250	247033
595	sandstone	Hárshegy Sandstone	Ol ₁	outcrop	<2	0.05	984	19.6	1.342	0.12	aas	635140	248353
596	dolomite	Budaörs Dolomite	T ₂₋₃	outcrop	<2	0.19	0.69	0.1	<0.02	0.07	aas	634450	249373
597	sandstone	Hárshegy Sandstone	Ol ₁	outcrop	<2	0.07	7.81	1.4	<0.02	0.09	aas	636160	249423
598	dolomite	Budaörs Dolomite	T ₂₋₃	outcrop	<2	<0.02	1.04	0.3	<0.02	0.09	aas	636160	249423
599	dolomite	Veszprém Marl	T ₃	Zsámbék-14 313.1-314.0	<2	0.07	0.83	0.14	0.03	0.0037	icpms	624467	246133
600	marl	Veszprém Marl	T ₃	350.4-351.8	<2	0.07	27.5	0.59	0.75	0.0048	icpms	624467	246133
601	dolomitic limestone	Veszprém Marl	T ₃	395.2-401.0	4	0.21	1.3	<0.1	0.04	0.05	icpms	624467	246133
602	dolomite breccia	Veszprém Marl	T ₃	424.2-425.1	<2	0.04	7.7	0.7	0.06	0.1	icpms	624467	246133
603	marl	Veszprém Marl	T ₃	463.3-464.2	<2	0.07	4.4	0.2	0.11	0.02	icpms	624467	246133
604	limestone	Veszprém Marl	T ₃	507.1-507.8	<2	0.03	1.2	0.1	0.05	0.04	icpms	624467	246133
605	marl	Veszprém Marl	T ₃	554.7-555.8	<2	0.06	3	0.3	0.06	<0.02	icpms	624467	246133
606	limestone	Veszprém Marl	T ₃	604.0-605.1	<2	0.06	1.96	0.11	0.04	0.0068	icpms	624467	246133
607	marl	Veszprém Marl	T ₃	650.1-654.2	<2	0.05	8.5	0.3	0.28	<0.02	icpms	624467	246133
608	marl	Veszprém Marl	T ₃	705.0-706.4	<2	0.05	1.6	<0.1	0.1	0.1	icpms	624467	246133
609	marl	Veszprém Marl	T ₃	750.2-751.2	<2	0.05	6.8	0.4	0.16	0.1	icpms	624467	246133
610	dolomite	Veszprém Marl	T ₃	796.4-796.5	<2	0.16	0.8	<0.1	<0.02	<0.02	icpms	624467	246133
611	limonitic limestone	Buda Marl	E ₃ -Ol ₁	outcrop	<2	0.11	56.3	5.83	0.11	5.149	icpms	645689	246754
612	marl	Buda Marl	E ₃ -Ol ₁	outcrop	<2	0.04	3.15	0.35	0.05	0.242	icpms	645689	246754
613	dolomite breccia	Mátyáshegy Formation	T ₃	outcrop	<2	0.02	3.94	0.31	0.02	0.0967	icpms	646079	246364
614	lim dolomite br	Mátyáshegy Formation	T ₃	outcrop	<2	0.39	50.8	5.67	0.09	0.2623	icpms	646079	246364
615	dolomite breccia	Mátyáshegy Formation	T ₃	outcrop	<2	0.03	258	4.2	<0.02	0.49	aas	646139	245504

Sample no.	Lithology	Formation	Age	Sample type	Elements						Analytical method	Coordinates	
					Au	Ag	As	Sb	Tl	Hg		X	Y
					ppb	ppm							
616	dolomite breccia	Mátyáshegy Formation	T ₃	outcrop	<2	0.18	5.29	0.42	0.04	0.4138	icpms	646559	245974
617	cherty dolomite	Mátyáshegy Formation	T ₃	outcrop	<2	0.21	8.61	1.36	0.05	1.005	icpms	647089	245024
618	cherty dolomite	Mátyáshegy Formation	T ₃	outcrop	<2	0.08	5.22	0.35	0.02	0.0422	icpms	647259	245054
619	siliciclastic sandstone (infilling)	Mátyáshegy Formation	T ₃	outcrop	<2	0.11	7.63	0.63	0.14	0.1184	icpms	647259	245054
620	limonitic clay	Hárshegy Sandstone	Ol ₁	outcrop	<2	0.03	670	13.4	1.77	3.891	icpms	644771	245764
621	limestone	Szépvolgy Limestone	E ₃	outcrop	<2	<0.02	3.79	0.5	0.024	0.1	aas	646150	244634
622	vein of calcite	Szépvolgy Limestone	E ₃	outcrop	<2	0.02	0.78	0.2	0.024	0.08	aas	646150	244634
623	marl	Buda Marl	E ₃ -Ol ₁	outcrop	<2	0.02	2.03	0.4	0.027	0.04	aas	646150	244634
624	calcite with cinnabar	Szépvolgy Limestone	E ₃	outcrop	3	<0.3	<2.5	n.a.	n.a.	58.2	icpms	645810	244224
625	sandstone	Hárshegy Sandstone	Ol ₁	outcrop	<2	0.22	21.6	<0.02	<0.02	<0.02	aas	646810	251904
626	dolomarl	Födolomit Formation	T ₃	outcrop	<2	0.02	3.17	0.3	0.021	0.04	aas	637379	252863
627	dolomite	Födolomit Formation	T ₃	outcrop	<2	<0.02	1.33	0.8	<0.02	0.06	aas	637279	252913
628	dolomite	Födolomit Formation	T ₃	outcrop	<2	0.1	3.5	2.7	<0.02	<0.02	aas	637079	253043
629	dolomite	Födolomit Formation	T ₃	outcrop	<2	<0.02	1.12	0.7	<0.02	<0.02	aas	636989	253163
630	dolomite	Födolomit Formation	T ₃	outcrop	<2	0.02	3.24	0.9	0.03	<0.02	aas	637050	253203
631	dolomite	Födolomit Formation	T ₃	outcrop	<2	<0.02	0.63	0.6	<0.02	0.05	aas	637090	253263
632	dolomite	Födolomit Formation	T ₃	outcrop	<2	<0.02	85.4	<0.02	0.218	1.76	aas	637130	253303
633	dolomite	Födolomit Formation	T ₃	outcrop	<2	0.02	8.46	3.1	0.093	0.07	aas	637210	253323
634	limonitic sandstone	Hárshegy Sandstone	Ol ₁	outcrop	<2	<0.02	2.62	0.6	0.023	0.07	aas	636279	255613
635	dolomitic limestone	Dachstein Limestone	T ₃	outcrop	<2	<0.02	7.54	1.7	0.175	0.14	aas	636359	255933
636	limonitic limestone	Dachstein Limestone	T ₃	outcrop	<2	0.02	69	6.2	0.95	2.65	aas	634759	255912
637	limestone	Dachstein Limestone	T ₃	outcrop	<2	<0.02	5.64	4.5	<0.02	0.4	aas	634239	256922
638	limestone	Dachstein Limestone	T ₃	outcrop	<2	<0.02	3.3	3.6	<0.02	0.22	aas	635039	258512
639	sand	Mány Formation	Ol ₂	outcrop	<2	0.08	5.21	1.2	<0.02	0.07	aas	633799	258762
640	sandstone	Hárshegy Sandstone	Ol ₁	outcrop	<2	0.16	9.88	1.3	0.021	0.47	aas	646259	252223
641	sandstone	Dachstein Limestone	T ₃	outcrop	<2	<0.02	0.87	0.2	0.032	0.13	aas	645649	252783
642	sandstone	Hárshegy Sandstone	Ol ₁	outcrop	<2	<0.02	12.4	2.6	0.025	2.06	aas	645649	252783
643	sandstone	Hárshegy Sandstone	Ol ₁	outcrop	<2	0.02	65.3	3.3	1.067	1.44	aas	645709	252813
644	travertine	Travertine Formation	Pa-Q ₁	outcrop	<2	<0.02	2.87	0.4	0.04	0.04	aas	647559	253174
645	dolomitic limestone	Dachstein Limestone	T ₃	outcrop	<2	<0.02	13.01	2.9	<0.02	0.5	aas	645239	253183
646	sandstone	Hárshegy Sandstone	Ol ₁	outcrop	<2	0.03	10.61	4.5	<0.02	0.51	aas	645489	253553
647	limestone	Dachstein Limestone	T ₃	outcrop	<2	<0.02	3.94	0.6	0.124	0.04	aas	645820	253254
648	sandstone	Hárshegy Sandstone	Ol ₁	outcrop	<2	0.03	22.2	<0.02	0.376	0.54	aas	645820	253254
649	sandstone	Hárshegy Sandstone	Ol ₁	outcrop	<2	<0.02	60.9	5.3	0.051	2.93	aas	644759	254793
650	limestone	Dachstein Limestone	T ₃	outcrop	<2	0.02	3.47	0.3	0.066	0.09	aas	645199	255103
651	limestone	Dachstein Limestone	T ₃	outcrop	<2	0.05	1.66	0.3	0.065	0.07	aas	645849	256063
652	sandstone	Hárshegy Sandstone	Ol ₁	outcrop	<2	0.03	15.78	1.3	0.919	0.09	aas	645039	256073
653	limestone	Szépvolgy Limestone	E ₃	outcrop	<2	<0.02	64.3	5.4	0.674	4.36	aas	644259	256473
654	amphibole andesite	Börzsöny and Visegrád Andesite	M ₂	outcrop	<2	0.02	0.69	0.2	0.07	0.03	aas	644669	257183
655	amphibole andesite	Börzs. and Vis. And.	M ₂	outcrop	<2	<0.02	0.83	0.2	0.093	0.04	aas	644929	257633
656	sandstone	Hárshegy Sandstone	Ol ₁	outcrop	<2	0.04	300	5.7	1.182	0.66	aas	638829	259443
657	sandstone	Hárshegy Sandstone	Ol ₁	outcrop	<2	0.03	1.13	0.3	0.096	<0.02	aas	638829	259443
658	limestone	Dachstein Limestone	T ₃	outcrop	<2	<0.02	1.04	0.6	<0.02	0.05	aas	639279	259893
659	sandstone	Hárshegy Sandstone	Ol ₁	outcrop	<2	0.04	24.7	<0.02	0.222	2.33	aas	639259	259913
660	limestone	Dachstein Limestone	T ₃	outcrop	<2	<0.02	15.74	3	0.137	2.9	aas	640659	259633
661	sandstone	Hárshegy Sandstone	Ol ₁	outcrop	<2	<0.02	8.28	2.1	0.482	2.44	aas	640659	259633
662	limestone	Dachstein Limestone	T ₃	outcrop	<2	<0.02	4.69	0.9	0.067	0.06	aas	640329	260023
663	andesite pyroclastite	Börzs. and Vis. And.	M ₂	outcrop	<2	0.08	2.24	0.19	0.19	0.0076	icpms	642089	260173
664	andesite pyroclastite	Börzs. and Vis. And.	M ₂	outcrop	<2	0.06	0.69	0.14	0.15	0.0108	icpms	643059	259683
665	limestone	Dachstein Limestone	T ₃	outcrop	<2	0.08	1.64	0.09	0.04	0.0733	icpms	636149	261392
666	limestone	Dachstein Limestone	T ₃	outcrop	<2	0.1	2.17	0.14	0.03	0.0268	icpms	636569	261882
667	limonitic sandstone	Hárshegy Sandstone	Ol ₁	outcrop	<2	0.07	250	1.63	0.61	1.607	icpms	637119	262242

Sample no.	Lithology	Formation	Age	Sample type (depth in m)	Elements						Analytical method	Coordinates	
					Au	Ag	As	Sb	Tl	Hg		X	Y
					ppb	ppm							
668	amphibole andesite	Börzs. and Vis. And.	M ₂	outcrop	<2	0.02	4.17	0.05	0.11	0.0184	icpms	637119	262242
669	limestone	Dachstein Limestone	T ₃	outcrop	<2	0.15	1.16	0.14	<0.02	0.0958	icpms	636979	262632
670	amphibole andesite	Börzs. and Vis. And.	M ₂	outcrop	<2	0.3	0.59	0.06	0.07	0.0117	icpms	638675	262602
671	limestone	Dachstein Limestone	T ₃	outcrop	11	0.05	198	6.92	0.37	0.719	icpms	634695	262102
672	clay	Bauxite Formation	Cr ₃ -E ₄	outcrop	<2	0.02	24.2	0.22	0.4	0.0517	icpms	634699	262102
673	limonitic sandstone	Hárshegy Sandstone	Ol ₁	outcrop	2	0.07	13.2	0.37	2.57	0.3007	icpms	634699	262102
674	bauxitic clay	Bauxite Formation	Cr ₃ -E ₄	outcrop	6	0.15	9.11	0.7	1.59	0.3294	icpms	634719	262172
675	sandstone	Hárshegy Sandstone	Ol ₁	outcrop	<2	0.03	12.4	0.43	0.21	0.2583	icpms	634719	262172
676	limestone	Dachstein Limestone	T ₃	outcrop	2	<0.02	2.9	0.07	0.05	0.024	icpms	634719	262252
677	dolomite	Dachstein Limestone	T ₃	outcrop	<2	0.13	6.11	0.25	0.04	0.1999	icpms	634269	262342
678	sandstone	Hárshegy Sandstone	Ol ₁	outcrop	<2	0.07	320	5.27	0.99	1.244	icpms	634349	262592
679	andesite breccia	Börzs. and Vis. And.	M ₂	outcrop	<2	<0.02	4.7	0.12	0.2	0.0138	icpms	633749	262722
680	sandstone	Hárshegy Sandstone	Ol ₁	outcrop	<2	0.03	4.04	0.08	0.12	0.0316	icpms	633619	262752
681	limestone	Dachstein Limestone	T ₃	outcrop	<2	0.14	2.76	0.12	0.02	0.067	icpms	635719	263112
682	limestone	Dachstein Limestone	T ₃	outcrop	<2	<0.02	25	3.1	0.198	2.38	aas	631729	264412
683	br. dol. (infilling)	Földolmit Formation	T ₃	outcrop	5	<0.02	4.48	1.2	0.032	0.27	aas	634989	263772
684	brecciated dolomite	Földolmit Formation	T ₃	outcrop	25	0.16	401	11.3	0.183	0.98	aas	634989	263772
685	limestone	Pisznice Limestone	J ₁	outcrop	<2	<0.02	1.05	0.3	<0.02	<0.02	aas	631939	264682
686	limestone breccia	Pisznice Limestone	J ₁	outcrop	<2	0.03	4.62	0.5	0.252	0.09	aas	631939	264682
687	radiolarite	Lókút Radiolarite	J ₂₋₃	outcrop	5	0.08	152	4.7	0.15	1.35	aas	631609	264762
688	radiolarite breccia	Lókút Radiolarite	J ₂₋₃	outcrop	<2	0.04	126	3.5	0.404	1.43	aas	631609	264762
689	limestone	Szépölggy Limestone	E ₃	outcrop	<2	<0.02	5.53	1.2	<0.02	0.56	aas	631999	265182
690	limestone	Dachstein Limestone	T ₃	outcrop	<2	<0.02	0.6	0.1	<0.02	0.04	aas	631979	265442
691	limestone	Feketehegy Formation	T ₃	outcrop	<2	0.03	3.08	0.15	<0.02	0.1435	icpms	632979	264982
692	bitum. limestone	Feketehegy Formation	T ₃	outcrop	<2	0.05	5.64	0.94	0.03	0.1505	icpms	633339	264892
693	dolomite	Feketehegy Formation	T ₃	outcrop	3	0.06	2.9	0.34	<0.02	0.0484	icpms	633629	264742
694	dolomite	Feketehegy Formation	T ₃	outcrop	3	0.02	31.9	4.58	0.28	0.1552	icpms	633629	264742
695	bituminous dolomite	Feketehegy Formation	T ₃	outcrop	<2	0.08	5.36	1.11	0.07	0.0799	icpms	633799	264662
696	dolomite breccia	Földolmit Formation	T ₃	outcrop	<2	<0.02	5.42	1.6	0.415	0.48	aas	634139	264592
697	biotite dacite	Börzs. and Vis. And.	M ₂	outcrop	<2	0.05	1.86	0.08	0.07	0.0159	icpms	635309	264762
698	biotite dacite	Börzs. and Vis. And.	M ₂	outcrop	<2	<0.02	0.43	<0.02	0.058	<0.02	aas	630439	266182
699	biotite dacite	Börzs. and Vis. And.	M ₂	outcrop	<2	<0.02	0.81	0.4	0.146	0.04	aas	631499	266362
700	biotite dacite	Börzs. and Vis. And.	M ₂	outcrop	<2	<0.02	1.18	0.1	0.046	<0.02	aas	631879	266662
701	andesite tuff	Börzs. and Vis. And.	M ₂	outcrop	<2	0.03	1.68	0.06	0.08	0.0142	icpms	634079	266462
702	biotite dacite	Börzs. and Vis. And.	M ₂	outcrop	<2	<0.02	1.25	0.07	0.06	0.009	icpms	634949	265842
<i>6. CSÖVÁR HORST</i>													
703	limestone	Buda Marl	E ₃ -Ol ₁	outcrop	<2	0.4	2.6	1.06	0.04	4.32	icpms	669557	274884
704	vein of calcite	Buda Marl	E ₃ -Ol ₁	outcrop	2	<0.3	5.7	0.51	<0.02	0.12	icpms	669557	274884
705	limestone	Buda Marl	E ₃ -Ol ₁	outcrop	<2	0.4	<2.5	0.42	0.03	0.78	icpms	669557	274884
706	limestone	Csővár Limestone	T ₃ -J ₁	outcrop	<2	0.4	3	1.04	0.03	0.26	icpms	669557	274884
707	limestone	Csővár Limestone	T ₃ -J ₁	outcrop	<2	<0.3	<2.5	<0.02	<0.02	0.08	icpms	669297	275054
708	limestone	Csővár Limestone	T ₃ -J ₁	Csővár-1 13 0	3	n.a.	n.a.	n.a.	n.a.	n.a.	icpms	669360	275062
709	limestone	Csővár Limestone	T ₃ -J ₁	74 0	2	n.a.	n.a.	n.a.	n.a.	n.a.	icpms	669360	275062
710	cherty limestone	Csővár Limestone	T ₃ -J ₁	100.0	<2	n.a.	n.a.	n.a.	n.a.	n.a.	icpms	669360	275062
711	limestone	Csővár Limestone	T ₃ -J ₁	124.3-130.3	<2	n.a.	n.a.	n.a.	n.a.	n.a.	icpms	669360	275062
712	limestone	Csővár Limestone	T ₃ -J ₁	150.8-154.3	4	n.a.	n.a.	n.a.	n.a.	n.a.	icpms	669360	275062
713	limestone	Csővár Limestone	T ₃ -J ₁	174.3-175.3	<2	n.a.	n.a.	n.a.	n.a.	n.a.	icpms	669360	275062
714	marl	Csővár Limestone	T ₃ -J ₁	209.0	<2	n.a.	n.a.	n.a.	n.a.	n.a.	icpms	669360	275062
715	limestone	Csővár Limestone	T ₃ -J ₁	240.5	<2	n.a.	n.a.	n.a.	n.a.	n.a.	icpms	669360	275062
716	limestone	Csővár Limestone	T ₃ -J ₁	267.0	<2	n.a.	n.a.	n.a.	n.a.	n.a.	icpms	669360	275062
717	limestone	Csővár Limestone	T ₃ -J ₁	280.0	<2	n.a.	n.a.	n.a.	n.a.	n.a.	icpms	669360	275062
718	marl	Csővár Limestone	T ₃ -J ₁	300.0	3	n.a.	n.a.	n.a.	n.a.	n.a.	icpms	669360	275062
719	limestone	Csővár Limestone	T ₃ -J ₁	327.5	<2	n.a.	n.a.	n.a.	n.a.	n.a.	icpms	669360	275062

Sample no.	Lithology	Formation	Age	Sample type (depth in m)	Elements						Analytical method	Coordinates	
					Au	Ag	As	Sb	Tl	Hg		X	Y
					ppb	ppm							
726	marl	Csővár Limestone	T ₃ -J ₁	343.0	<2	n.a.	n.a.	n.a.	n.a.	n.a.	icpms	669360	275062
721	limestone breccia	Csővár Limestone	T ₃ -J ₁	392.0	<2	n.a.	n.a.	n.a.	n.a.	n.a.	icpms	669360	275062
722	limestone breccia	Csővár Limestone	T ₃ -J ₁	412.0	<2	n.a.	n.a.	n.a.	n.a.	n.a.	icpms	669360	275062
723	limestone	Csővár Limestone	T ₃ -J ₁	433.5	<2	n.a.	n.a.	n.a.	n.a.	n.a.	icpms	669360	275062
724	limestone	Csővár Limestone	T ₃ -J ₁	458.0	<2	n.a.	n.a.	n.a.	n.a.	n.a.	icpms	669360	275062
725	limestone	Csővár Limestone	T ₃ -J ₁	477.6	<2	n.a.	n.a.	n.a.	n.a.	n.a.	icpms	669360	275062
726	limestone	Csővár Limestone	T ₃ -J ₁	505.9	<2	n.a.	n.a.	n.a.	n.a.	n.a.	icpms	669360	275062
727	limestone	Csővár Limestone	T ₃ -J ₁	520.2	<2	n.a.	n.a.	n.a.	n.a.	n.a.	icpms	669360	275062
728	limestone	Csővár Limestone	T ₃ -J ₁	544.0	<2	n.a.	n.a.	n.a.	n.a.	n.a.	icpms	669360	275062
729	dolomite	Csővár Limestone	T ₃ -J ₁	578.5	2	n.a.	n.a.	n.a.	n.a.	n.a.	icpms	669360	275062
730	dolomitic limestone	Csővár Limestone	T ₃ -J ₁	600.8	<2	n.a.	n.a.	n.a.	n.a.	n.a.	icpms	669360	275062
731	dolomite	Csővár Limestone	T ₃ -J ₁	627.0	<2	n.a.	n.a.	n.a.	n.a.	n.a.	icpms	669360	275062
732	dolomite	Csővár Limestone	T ₃ -J ₁	703.0	<2	n.a.	n.a.	n.a.	n.a.	n.a.	icpms	669360	275062
733	bitum limestone	Csővár Limestone	T ₃ -J ₁	outcrop	<2	<0.3	6.3	1.1	0.09	0.08	icpms	669297	275084
734	cherty limestone	Csővár Limestone	T ₃ -J ₁	outcrop	<2	1	8.3	0.61	0.07	0.26	icpms	669477	275124
735	cherty limestone	Csővár Limestone	T ₃ -J ₁	outcrop	<2	<0.3	3.8	0.41	0.04	0.18	icpms	669467	275184
736	cherty limestone	Csővár Limestone	T ₃ -J ₁	outcrop	<2	0.3	<2.5	0.53	0.04	0.18	icpms	669457	275224
737	cherty limestone	Csővár Limestone	T ₃ -J ₁	outcrop	<2	0.4	11.4	0.98	0.11	0.34	icpms	669457	275264
738	vein of calcite	Csővár Limestone	T ₃ -J ₁	outcrop	<2	0.4	<2.5	0.2	0.06	0.7	icpms	669427	275304
739	limonitic infilling	Csővár Limestone	T ₃ -J ₁	outcrop	3	0.6	17.3	0.41	0.17	0.16	icpms	669347	275324
740	cherty limestone	Csővár Limestone	T ₃ -J ₁	outcrop	<2	<0.3	<2.5	0.32	0.38	0.06	icpms	669347	275354
741	vein of calcite	Vashegy Dolomite	T ₂	outcrop	3	<0.3	3.5	0.23	0.22	1.66	icpms	669017	275854
742	dolomite	Vashegy Dolomite	T ₂	outcrop	<2	0.4	<2.5	0.53	<0.02	0.06	icpms	669017	275854
743	limonitic dolomite	Vashegy Dolomite	T ₂	outcrop	<2	<0.3	9.4	0.54	0.36	0.3	icpms	668957	275904
<i>7. MECSEK MOUNTAINS</i>													
744	sandstone	Patacs Siltstone	T ₂	outcrop	3	0.08	1.91	0.07	0.24	0.04	icpms	582217	80688
745	silty marl	Patacs Siltstone	T ₂	outcrop	3	0.33	19.2	0.13	1.09	0.08	icpms	582420	81520
746	clayst. and limestone	Kantavár Formation	T _{2,3}	outcrop	<2	0.04	4.64	0.05	0.16	0.02	icpms	585627	85963
747	limestone	Kantavár Formation	T _{2,3}	outcrop	<2	0.03	1.23	0.04	0.11	0.04	icpms	585627	85963
748	claystone	Kantavár Formation	T _{2,3}	outcrop	<2	0.02	2.05	0.04	0.15	0.06	icpms	585627	85963
749	limestone	Lapis Limestone	T ₂	outcrop	<2	0.07	7.97	0.1	0.08	0.06	icpms	586618	84254
750	limestone	Lapis Limestone	T ₂	outcrop	<2	0.15	3.03	0.21	0.45	0.08	icpms	586554	84286
751	limestone	Lapis Limestone	T ₂	outcrop	<2	0.08	3.67	0.1	0.21	0.08	icpms	583149	85218
752	bituminous dolomite	Hetvehely Dolomite	T ₂	outcrop	3	4.39	0.7	0.05	0.09	0.02	icpms	583344	85380
753	limestone	Lapis Limestone	T ₂	outcrop	<2	0.08	1.32	0.09	0.12	0.08	icpms	584252	85947
754	limestone and marl	Hetvehely Dolomite	T ₂	outcrop	<2	0.06	4.47	0.14	0.2	<0.02	icpms	576504	86345
755	dolomite	Hetvehely Dolomite	T ₂	outcrop	<2	0.04	1.11	0.08	0.07	0.04	icpms	571256	87430
756	dolomite breccia	Hetvehely Dolomite	T ₂	outcrop	<2	0.03	0.8	0.09	0.06	0.06	icpms	570742	87560
757	limestone (infilling)	Lapis Limestone	T ₂	outcrop	<2	0.62	2.46	0.13	0.13	0.06	icpms	580345	87935
758	marl	Vasas Marl	J ₁	Pécs-XI 352.0	<2	1.26	7.36	0.89	0.34	0.08	icpms	584355	87640
759	limestone	Lapis Limestone	T ₂	559.0	3	0.53	2.46	0.11	0.1	0.02	icpms	584355	87640
760	limestone	Kozár Limestone	T ₂	outcrop	<2	1.03	7.99	0.22	0.1	<0.02	icpms	587043	87893
761	limestone breccia with azurite	Kozár Limestone	T ₂	outcrop	<2	5.1	264	15.3	0.17	2.1	icpms	587043	87893
762	marl with coal	Mecsek Coal	T ₃ -J ₁	outcrop	2	0.06	11.7	0.15	0.52	0.12	icpms	592389	87994
763	pyritic bitum. marl	Kantavár Formation	T _{2,3}	outcrop	<2	0.04	6.5	0.12	0.15	0.08	icpms	589566	89072
764	limestone	Kantavár Formation	T _{2,3}	outcrop	<2	0.05	5.22	0.12	0.09	0.1	icpms	589526	89257
765	limestone	Lapis Limestone	T ₂	Pécs-XVI 198.6	<2	0.54	38.5	0.15	0.07	0.06	icpms	597707	89487
766	claystone	Patacs Siltstone	T ₂	965.0	<2	0.24	2.73	0.12	0.17	0.04	icpms	597707	89487
767	shale with anhydrite	Patacs Siltstone	T ₂	1196.0	<2	0.91	1.81	0.13	0.16	0.06	icpms	597707	89487
768	silty marl	Hosszúhetény Calcareous Marl	J ₁	outcrop	<2	0.5	13.2	0.22	0.17	0.16	icpms	596487	90088
769	pyritic coal	Mecsek Coal	T ₃ -J ₁	outcrop	2	0.14	26.1	1.79	0.93	0.3	icpms	593638	90731
770	coal and trachydole.	Mecsek Coal	T ₃ -J ₁	outcrop	<2	0.39	11.5	0.77	0.27	0.18	icpms	593638	90731

Sample no.	Lithology	Formation	Age	Sample type (depth in m)	Elements						Analytical method	Coordinates	
					Au	Ag	As	Sb	Tl	Hg		X	Y
					ppb	ppm							
771	pyritic siltstone	Mecsek Coal	T ₃ -J ₁	outcrop	<2	0.05	29.2	0.86	0.15	0.16	icpms	593638	90731
772	tuff	Mecsek Coal	T ₃ -J ₁	outcrop	7	0.07	3.52	0.19	0.22	0.08	icpms	593638	90731
773	sphaeroiderite	Mecsek Coal	T ₃ -J ₁	outcrop	<2	0.07	15.7	0.34	0.17	0.1	icpms	593638	90731
774	limonitic marl	Hosszúhetény Calcareous Marl	J ₁	outcrop	<2	0.19	6.84	0.15	0.2	0.12	icpms	595680	91052
775	limonitic sandstone	Mecseknádasd Sandstone	J ₁	outcrop	<2	0.23	6.5	0.27	0.21	0.24	icpms	604482	97340
776	siltstone	Vasas Marl	J ₁	outcrop	<2	0.4	10.6	0.36	0.26	0.16	icpms	611572	96551
777	limonitic sandstone	Vasas Marl	J ₁	outcrop	3	0.89	16.6	0.1	0.15	0.1	icpms	611572	96551
<i>8. RECSK, DARNÓ HILL, BÜKK MOUNTAINS AND UPPONY MOUNTAINS</i>													
778	limestone	Szépvölgy Limestone	E ₃	Recsk Rm-79 419 8	3	<0.100	22.50	0.63	0.870	0.0098	icpms	725347	285329
779	basal breccia	Szépvölgy Limestone	E ₃	425.5	4	<0.100	32.70	0.75	0.750	0.1094	icpms	725347	285329
780	breccia	Parád Complex	T ₂₋₃	432.0	2	<0.100	24.30	1.27	0.320	0.1436	icpms	725347	285329
781	jasper	Parád Complex	T ₂₋₃	440.0	4	<0.100	46.20	1.51	0.310	0.0766	icpms	725347	285329
782	jasper breccia	Parád Complex	T ₂₋₃	470.0	16	<0.100	46.50	5.08	0.080	0.4184	icpms	725347	285329
783	jasper breccia	Parád Complex	T ₂₋₃	535.0	2	<0.100	9.87	4.72	0.060	0.1153	icpms	725347	285329
784	shale	Parád Complex	T ₂₋₃	550.0	6	<0.100	76.10	2.59	0.470	0.2595	icpms	725347	285329
785	shale	Parád Complex	T ₂₋₃	581.0	4	<0.100	74.40	3.04	0.610	0.33	icpms	725347	285329
786	limestone	Parád Complex	T ₂₋₃	600.0	<2	<0.100	10.30	0.21	0.120	0.0231	icpms	725347	285329
787	limestone breccia	Parád Complex	T ₂₋₃	650.00	7	1.330	73.20	1.13	0.240	1.534	icpms	725347	285329
788	cherty limestone	Parád Complex	T ₂₋₃	725.6	<2	<0.100	3.02	<0.10	<0.050	0.0091	icpms	725347	285329
789	shale	Parád Complex	T ₂₋₃	766.5	6	<0.100	19.90	2.00	0.400	0.0121	icpms	725347	285329
790	limestone	Parád Complex	T ₂₋₃	812.5	4	<0.100	12.20	<0.10	0.270	0.0044	icpms	725347	285329
791	limestone breccia	Parád Complex	T ₂₋₃	861.0	24	0.820	59.90	25.00	0.100	0.0652	icpms	725347	285329
792	limestone breccia	Parád Complex	T ₂₋₃	921.0	13	<0.100	31.40	108.00	<0.050	0.0096	icpms	725347	285329
793	silicified limest. br.	Parád Complex	T ₂₋₃	961.0	5	0.860	41.30	0.39	0.060	0.0076	icpms	725347	285329
794	silicified limestone	Parád Complex	T ₂₋₃	985.0	5	<0.100	5.63	0.21	0.400	0.0022	icpms	725347	285329
795	limestone breccia	Parád Complex	T ₂₋₃	1030.0	84	2.460	117.00	3.32	0.220	0.2231	icpms	725347	285329
796	marble	Parád Complex	T ₂₋₃	1090.0	2	0.680	2.54	<0.10	<0.050	0.1413	icpms	725347	285329
797	marl. limestone	Parád Complex	T ₂₋₃	Recsk Rm-VI 566.2	15	<0.050	26.70	1.23	0.330	0.0524	icpms	727670	287757
798	breccia	Parád Complex	T ₂₋₃	678.8	60	<0.050	85.40	2.15	0.820	0.1669	icpms	727670	287757
799	marl	Parád Complex	T ₂₋₃	705.0	22	<0.050	48.40	0.10	0.530	0.0622	icpms	727670	287757
800	marl	Parád Complex	T ₂₋₃	731.0	9	<0.050	21.80	0.31	0.520	0.0508	icpms	727670	287757
801	tuff	Parád Complex	T ₂₋₃	770.0	9	<0.050	35.10	4.32	0.540	0.1243	icpms	727670	287757
802	breccia	Parád Complex	T ₂₋₃	775.0	2	<0.050	3.76	2.76	<0.050	0.0233	icpms	727670	287757
803	silicified limestone	Parád Complex	T ₂ -J ₂	1790	<2	0.1	4.19	0.35	0.04	0.014	icpms	726912	287840
804	limestone	Parád Complex	T ₂ -J ₂	underground, 1520	2	0.18	3.88	0.32	0.08	0.0184	icpms	726662	287961
805	bitum. limestone	Parád Complex	T ₂₋₃	level -900, 1700	30	<2	<100	n.a.	n.a.	n.a.	aas	726808	287901
806	skarn	Parád Complex	T ₂ -J ₂	1118	8	0.12	1.35	0.14	0.06	0.0101	icpms	726347	288203
807	shale	Parád Complex	T ₂₋₃	Recsk Rm-XXXI 224.0	8	0.070	130.00	6.58	0.660	1.888	icpms	725884	288121
808	jasper breccia	Parád Complex	T ₂₋₃	263.0	3	<0.050	24.30	0.76	0.510	0.4018	icpms	725884	288121
809	silicified shale	Parád Complex	T ₂₋₃	307.0	2	<0.050	1.70	0.24	0.340	0.0272	icpms	725884	288121
810	jasper breccia	Parád Complex	T ₂₋₃	369.0	2	<0.050	7.29	0.60	0.240	1.903	icpms	725884	288121
811	jasper	Parád Complex	T ₂₋₃	393.0	<2	<0.050	12.10	<0.10	0.340	0.0222	icpms	725884	288121
812	jasper	Parád Complex	T ₂₋₃	430.0	2	<0.050	11.40	0.41	0.310	0.0245	icpms	725884	288121
813	jasper breccia	Parád Complex	T ₂₋₃	469.0	7	<0.050	42.40	8.54	0.280	0.441	icpms	725884	288121
814	jasper breccia	Parád Complex	T ₂₋₃	492.0	5	1.270	96.30	85.90	0.780	1.239	icpms	725884	288121
815	shale	Parád Complex	T ₂₋₃	525.0	4	10.600	181.00	0.23	0.380	0.0433	icpms	725884	288121
816	limestone	Parád Complex	T ₂₋₃	557.0	<2	0.290	6.81	1.82	0.130	0.0894	icpms	725884	288121
817	limestone breccia	Parád Complex	T ₂₋₃	591.0	12	<0.050	66.60	0.99	0.210	0.5234	icpms	725884	288121
818	limestone	Parád Complex	T ₂₋₃	694.0	<2	<0.050	-1.00	<0.10	0.160	0.0104	icpms	725884	288121
819	limestone breccia	Parád Complex	T ₂₋₃	711.4	<2	<0.050	1.83	0.50	0.070	0.0055	icpms	725884	288121
820	silicified limestone	Parád Complex	T ₂₋₃	750.0	2	<0.050	6.82	0.21	0.140	0.0338	icpms	725884	288121
821	limestone	Parád Complex	T ₂₋₃	893.0	<2	<0.050	7.48	<0.10	0.220	0.0047	icpms	725884	288121

Sample no.	Lithology	Formation	Age	Sample type (depth in m)	Elements						Analytical method	Coordinates	
					Au	Ag	As	Sb	Tl	Hg		X	Y
					ppb	ppm							
822	limestone	Parád Complex	T _{2,3}	Recsk Rm-XXVIII 779.0	<2	<0.050	20.60	0.53	0.220	0.0328	icpms	724335	288146
823	shale	Parád Complex	T _{2,3}	793.0	3	<0.050	18.10	0.57	0.330	0.0818	icpms	724335	288146
824	shale	Parád Complex	T _{2,3}	825.0	<2	<0.050	3.37	<0.10	0.260	0.0383	icpms	724335	288146
825	silicified shale	Parád Complex	T _{2,3}	859.0	<2	<0.050	1.88	<0.10	0.170	0.0514	icpms	724335	288146
826	jasper breccia	Parád Complex	T _{2,3}	Recsk Rm-VIII 602.8	6	0.100	35.90	1.44	0.260	0.0393	icpms	727164	289162
827	silicified limestone	Parád Complex	T _{2,3}	680.0	2	<0.050	6.84	<0.10	0.390	0.0111	icpms	727164	289162
828	silicified limest. br	Parád Complex	T _{2,3}	750.5	12	0.990	28.50	0.40	0.280	0.1225	icpms	727164	289162
829	silicified limest. br	Parád Complex	T _{2,3}	789.5	8	<0.050	40.50	29.40	0.110	0.1801	icpms	727164	289162
830	limestone breccia	Parád Complex	T _{2,3}	831.9	2	0.140	-1.00	<0.10	<0.050	0.0221	icpms	727164	289162
831	cherty limest. br	Parád Complex	T _{2,3}	897.3	4	<0.050	9.59	<0.10	0.150	0.04	icpms	727164	289162
832	cherty limestone	Parád Complex	T _{2,3}	947.5	24	0.240	29.60	1.33	0.090	0.1347	icpms	727164	289162
833	silicified limestone	Parád Complex	T _{2,3}	985.2	2	0.100	9.13	1.92	0.110	0.0047	icpms	727164	289162
834	silicified limestone	Parád Complex	T _{2,3}	1020.6	<2	<0.050	1.46	<0.10	<0.050	0.0037	icpms	727164	289162
835	silicified limestone	Parád Complex	T _{2,3}	1066.4-1066.5	2	<0.050	-1.00	<0.10	0.110	0.0066	icpms	727164	289162
836	cherty limestone	Parád Complex	T _{2,3}	Recsk Rm-XVIII 484.0	9	<0.050	25.30	<0.10	0.320	0.5196	icpms	726775	290087
837	jasper	Parád Complex	T _{2,3}	510.0	6	<0.050	14.10	0.98	0.280	0.1247	icpms	726775	290087
838	shale	Parád Complex	T _{2,3}	555.0	3	<0.050	57.80	0.79	0.230	0.1143	icpms	726775	290087
839	breccia	Parád Complex	T _{2,3}	637.0	3	<0.050	6.33	0.27	0.300	0.0803	icpms	726775	290087
840	pyritic shale	Parád Complex	T _{2,3}	657.0	9	<0.050	54.40	3.34	0.590	0.106	icpms	726775	290087
841	limestone breccia	Parád Complex	T _{2,3}	728.3	3	<0.050	21.90	<0.10	0.260	0.0234	icpms	726775	290087
842	silicified shale	Parád Complex	T _{2,3}	809.6	2	0.060	29.10	0.94	0.360	0.1801	icpms	726775	290087
843	silicified shale	Parád Complex	T _{2,3}	839.5	15	<0.050	117.00	2.38	0.670	0.2181	icpms	726775	290087
844	cherty limestone	Parád Complex	T _{2,3}	961.2	<2	<0.050	<1.00	0.55	<0.050	0.0149	icpms	726775	290087
845	cherty limestone	Parád Complex	T _{2,3}	994.00	<2	<0.050	<1.00	0.59	<0.050	0.0122	icpms	726775	290087
846	marl	Darnóhegy Shale	J ₂	Recsk Rm-118 394.0	9	0.05	30.4	0.4	0.76	0.4	icpms	728106	291060
847	marl	Darnóhegy Shale	J ₂	411.0	340	0.05	177.6	6.2	10.5	6.49	icpms	728106	291060
848	breccia	Darnóhegy Shale	J ₂	476.0	<2	<0.02	7.7	0.4	0.17	0.37	icpms	728106	291060
849	breccia	Darnóhegy Shale	J ₂	488.4	<2	<0.02	10	0.3	0.52	0.28	icpms	728106	291060
850	breccia	Darnóhegy Shale	J ₂	506.0	<2	<0.02	14.2	0.4	0.32	0.83	icpms	728106	291060
851	pyritic breccia	Darnóhegy Shale	J ₂	538.0	2	<0.02	20.2	0.6	0.24	0.14	icpms	728106	291060
852	breccia	Darnóhegy Shale	J ₂	550.7	<2	<0.02	4.3	0.1	0.07	0.08	icpms	728106	291060
853	brecciated clay	Darnóhegy Shale	J ₂	618.2	<2	0.42	4.2	0.3	1.42	0.16	icpms	728106	291060
854	pyritic breccia	Darnóhegy Shale	J ₂	632.6	<2	<0.02	24.8	0.5	0.66	0.11	icpms	728106	291060
855	marl	Darnóhegy Shale	J ₂	726.5	5	0.06	1.4	0.1	0.18	<0.02	icpms	728106	291060
856	marl	Darnóhegy Shale	J ₂	766.0	7	<0.02	0.7	<0.1	0.22	0.02	icpms	728106	291060
857	clay	Darnóhegy Shale	J ₂	790.6	<2	<0.02	11.4	0.2	0.21	0.14	icpms	728106	291060
858	clay	Darnóhegy Shale	J ₂	827.5	2	<0.02	18.4	0.5	0.26	0.14	icpms	728106	291060
859	clay	Darnóhegy Shale	J ₂	846.5	<2	0.05	0.3	<0.1	0.1	0.04	icpms	728106	291060
860	breccia	Darnóhegy Shale	J ₂	950.0	<2	0.06	0.8	<0.1	0.05	0.08	icpms	728106	291060
861	clay	Darnóhegy Shale	J ₂	Recsk Rm-131 106.0	<2	0.11	26.8	1	0.28	0.06	icpms	730939	286201
862	diabase	Szarvaskő Basalt	J ₂	289.0	<2	0.02	1.2	0.1	0.05	<0.02	icpms	730939	286201
863	claystone	Darnóhegy Shale	J ₂	335.0	4	<0.02	2.5	0.1	0.31	0.04	icpms	730939	286201
864	diabase	Szarvaskő Basalt	J ₂	474.0	<2	<0.02	2.7	0.3	0.13	<0.02	icpms	730939	286201
865	claystone	Darnóhegy Shale	J ₂	503.0	3	<0.02	4.6	0.2	0.13	<0.02	icpms	730939	286201
866	claystone	Darnóhegy Shale	J ₂	597.0	<2	<0.02	16	1.3	0.33	0.43	icpms	730939	286201
867	diabase	Szarvaskő Basalt	J ₂	688.0	<2	0.02	1.8	0.1	0.13	0.02	icpms	730939	286201
868	silicified dolomite	Darnóhegy Shale	J ₂	696.0	<2	0.02	0.3	<0.1	0.16	<0.02	icpms	730939	286201
869	limest. (olistholith)	Darnóhegy Shale	J ₂	736.0	<2	<0.02	0.5	0.1	<0.02	<0.02	icpms	730939	286201
870	limestone	Darnóhegy Shale	J ₂	787.5	<2	<0.02	1.6	0.2	0.1	0.04	icpms	730939	286201
871	shale	Darnóhegy Shale	J ₂	818.0	3	<0.02	3.8	0.2	0.2	<0.02	icpms	730939	286201
872	limestone	Darnóhegy Shale	J ₂	886.0	<2	<0.02	0.6	0.1	0.2	0.06	icpms	730939	286201
873	graphite shale	Darnóhegy Shale	J ₂	903.0	2	<0.02	8.5	0.4	0.17	0.08	icpms	730939	286201

Sample no.	Lithology	Formation	Age	Sample type (depth in m)	Elements						Analytical method	Coordinates	
					Au	Ag	As	Sb	Tl	Hg		X	Y
					ppb	ppm							
874	breccia, quartzite	Darnóhegy Shale	J ₂	927.0	<2	<0.02	3	0.3	0.05	<0.02	icpms	730939	286201
875	limestone	Darnóhegy Shale	J ₂	989.0	<2	<0.02	6.7	0.6	0.21	0.1	icpms	730939	286201
876	shale	Darnóhegy Shale	J ₂	1005.0	<2	<0.02	25.7	2.3	0.33	0.3	icpms	730939	286201
877	limestone	Darnóhegy Shale	J ₂	1062.5	<2	<0.02	5.1	0.7	<0.02	0.04	icpms	730939	286201
878	limestone	Darnóhegy Shale	J ₂	1178.0	3	<0.02	0.5	0.1	<0.02	0.06	icpms	730939	286201
879	shale	Darnóhegy Shale	J ₂	outcrop	<2	0.08	0.6	0.15	0.12	0.025	icpms	734774	285385
880	shale	Darnóhegy Shale	J ₂	outcrop	<2	0.13	4.13	0.21	0.23	0.0131	icpms	731079	286753
881	limonite breccia	Darnóhegy Shale	J ₂	outcrop	<2	0.07	0.69	0.14	0.06	0.037	icpms	731079	286753
882	limestone	Darnóhegy Shale	J ₂	outcrop	<2	0.15	3.46	0.14	0.03	0.014	icpms	731076	286938
883	silicified claystone	Darnóhegy Shale	J ₂	outcrop	<2	0.08	3.52	0.33	0.15	0.0064	icpms	731076	286938
884	sideritic limest. br.	Darnóhegy Shale	J ₂	outcrop	<2	0.12	11.1	0.24	0.11	0.0213	icpms	731076	286938
885	gabbro	Szarvaskő Basalt	J ₂	outcrop	5	0.08	0.32	0.13	0.04	0.0146	icpms	731076	286938
886	claystone	Darnóhegy Shale	J ₂	outcrop	5	0.07	4.15	0.32	0.2	0.1369	icpms	731999	287693
887	radiolarite	Darnó Radiolarite	J ₂	outcrop	<2	0.100	7.69	0.40	0.180	0.0082	icpms	731937	287723
888	diabase	Szarvaskő Basalt	J ₂	outcrop	<2	0.08	4.17	0.14	0.08	0.0814	icpms	731287	288239
889	diabase tuff	Szarvaskő Basalt	J ₂	outcrop	<2	0.08	6.76	0.28	0.14	0.0751	icpms	731307	288332
890	quartzite	Darnó Radiolarite	J ₂	outcrop	<2	0.06	<0.2	0.08	0.02	0.0089	icpms	733071	288264
891	diabase	Szarvaskő Basalt	J ₂	outcrop	<2	0.1	<0.2	0.14	0.08	0.0093	icpms	733238	288204
892	silicified claystone	Darnó Radiolarite	J ₂	outcrop	5	0.14	<0.2	0.22	0.15	0.06	icpms	733238	288204
893	radiolarite	Darnó Radiolarite	J ₂	outcrop	<2	0.08	<0.2	0.17	0.06	0.024	icpms	733299	288298
894	shale	Darnóhegy Shale	J ₂	Recsk Rm-135 422.5	4	0.05	11.2	0.5	0.24	0.13	icpms	734266	288107
895	shale	Darnóhegy Shale	J ₂	675.0	11	<0.02	1.2	0.1	0.12	0.04	icpms	734266	288107
896	shale	Darnóhegy Shale	J ₂	725.0	<2	<0.02	3.9	0.3	0.23	0.09	icpms	734266	288107
897	shale	Darnóhegy Shale	J ₂	764.0	<2	0.02	3.6	0.6	0.17	0.04	icpms	734266	288107
898	shale	Darnóhegy Shale	J ₂	834.0	9	<0.02	0.7	<0.1	0.09	<0.02	icpms	734266	288107
899	shale	Darnóhegy Shale	J ₂	885.0	<2	<0.02	4.3	0.2	0.13	<0.02	icpms	734266	288107
900	limestone	Darnóhegy Shale	J ₂	903.5	<2	<0.02	0.5	<0.1	0.05	0.04	icpms	734266	288107
901	shale	Darnóhegy Shale	J ₂	933.0	<2	<0.02	4.1	0.5	0.11	0.1	icpms	734266	288107
902	sandstone	Darnóhegy Shale	J ₂	939.5	<2	<0.02	0.8	<0.1	0.02	<0.02	icpms	734266	288107
903	shale	Darnóhegy Shale	J ₂	983.0	<2	0.02	4.7	0.4	0.05	0.09	icpms	734266	288107
904	limestone	Darnóhegy Shale	J ₂	1052.0	<2	<0.02	1.3	0.2	<0.02	<0.02	icpms	734266	288107
905	shale	Darnóhegy Shale	J ₂	1109.0	2	<0.02	2.5	0.3	0.13	0.04	icpms	734266	288107
906	limestone	Darnóhegy Shale	J ₂	1149.0	4	<0.02	2.5	0.2	0.04	0.04	icpms	734266	288107
907	shale	Darnóhegy Shale	J ₂	1187.0	3	<0.02	3	0.4	0.24	0.08	icpms	734266	288107
908	shale	Darnóhegy Shale	J ₂	Recsk Rm-136 56.8	<2	0.05	13.5	0.4	0.26	0.08	icpms	732893	289239
909	shale	Darnóhegy Shale	J ₂	121.6	<2	<0.02	1.3	0.2	0.28	<0.02	icpms	732893	289239
910	shale	Darnóhegy Shale	J ₂	190.2	<2	<0.02	3.6	0.2	0.08	<0.02	icpms	732893	289239
911	shale, sandstone	Darnóhegy Shale	J ₂	344.1	3	0.03	8.7	0.4	0.16	0.1	icpms	732893	289239
912	shale	Darnóhegy Shale	J ₂	372.5	<2	0.06	1.4	<0.1	0.13	0.04	icpms	732893	289239
913	limestone	Darnóhegy Shale	J ₂	400.1	5	0.07	7.7	0.7	0.06	0.02	icpms	732893	289239
914	sandstone	Darnóhegy Shale	J ₂	456.3	<2	0.03	3.5	0.3	0.09	0.02	icpms	732893	289239
915	quartzite, shale	Darnóhegy Shale	J ₂	506.5	<2	0.04	8.2	0.2	0.3	0.04	icpms	732893	289239
916	limest. (olistholith)	Darnóhegy Shale	J ₂	527.6	3	0.07	8	0.3	0.03	<0.02	icpms	732893	289239
917	shale	Darnóhegy Shale	J ₂	552.7	<2	0.02	2.7	<0.1	0.32	0.04	icpms	732893	289239
918	dolomite, sandstone	Darnóhegy Shale	J ₂	578.5	<2	0.06	7.8	0.7	0.19	0.14	icpms	732893	289239
919	limestone	Darnóhegy Shale	J ₂	583.4	<2	0.04	1.3	0.1	0.09	0.04	icpms	732893	289239
920	shale	Darnóhegy Shale	J ₂	618.0	<2	0.2	31.56	1.3	0.82	0.79	icpms	732893	289239
921	shale	Darnóhegy Shale	J ₂	548.0	2	0.07	6.5	0.4	0.29	0.04	icpms	732893	289239
922	limestone	Darnóhegy Shale	J ₂	584.0	<2	0.07	1.7	<0.1	0.09	<0.02	icpms	732893	289239
923	claystone	Darnóhegy Shale	J ₂	696.0	<2	0.06	12.2	0.2	0.21	0.19	icpms	732893	289239
924	shale	Darnóhegy Shale	J ₂	750.0	<2	0.03	1.1	<0.1	0.27	<0.02	icpms	732893	289239
925	claystone	Darnóhegy Shale	J ₂	791.0	2	0.05	5.3	0.5	0.07	0.08	icpms	732893	289239
926	claystone, limestone	Darnóhegy Shale	J ₂	836.0	6	0.08	32.7	0.9	0.35	<0.02	icpms	732893	289239

Sample no.	Lithology	Formation	Age	Sample type (depth in m)	Elements						Analytical method	Coordinates	
					Au	Ag	As	Sb	Tl	Hg		X	Y
					ppb	ppm							
927	limonitic limestone	Darnóhegy Shale	J ₂	869.0	<2	0.04	11	0.2	0.36	0.09	icpms	732893	289239
928	limestone	Darnóhegy Shale	J ₂	905.0	<2	0.06	4.7	0.3	0.2	0.08	icpms	732893	289239
929	chert, limestone br.	Darnóhegy Shale	J ₂	953.4	<2	0.08	16.4	1.8	0.48	0.61	icpms	732893	289239
930	shale, quartzite	Darnóhegy Shale	J ₂	976.0	<2	0.02	7.7	0.2	0.19	0.04	icpms	732893	289239
931	graphite shale	Darnóhegy Shale	J ₂	1020.0	2	0.04	11.8	0.4	0.25	0.02	icpms	732893	289239
932	graph. sh., quartzite	Darnóhegy Shale	J ₂	1061.0	<2	0.04	4.7	1.1	0.1	0.55	icpms	732893	289239
933	graphite shale	Darnóhegy Shale	J ₂	1105.0	<2	0.03	7.5	0.4	0.26	0.05	icpms	732893	289239
934	quartzite	Darnóhegy Shale	J ₂	1165.0	<2	0.02	1.9	0.4	0.07	0.03	icpms	732893	289239
935	siltstone, quartzite	Darnóhegy Shale	J ₂	1205.0	<2	<0.02	6.6	0.7	0.08	0.2	icpms	732893	289239
936	silicified sandstone	Darnóhegy Shale	J ₂	outcrop	<2	<0.02	1.54	0.09	0.05	0.0599	icpms	732518	289306
937	shale	Darnóhegy Shale	J ₂	outcrop	<2	0.08	9.27	0.34	0.26	0.0768	icpms	732618	289555
938	limestone	Darnóhegy Shale	J ₂	outcrop	<2	0.07	2.09	0.17	0.04	0.042	icpms	732719	289742
939	shale	Darnóhegy Shale	J ₂	outcrop	6	0.14	0.42	0.16	0.25	0.1787	icpms	732656	289772
940	claystone	Darnóhegy Shale	J ₂	outcrop	<2	0.09	<0.2	0.73	0.19	0.0318	icpms	733446	289721
941	diabase	Szarvaskő Basalt	J ₂	outcrop	2	0.06	4.77	0.24	0.14	0.0132	icpms	733352	290461
942	diabase	Szarvaskő Basalt	J ₂	outcrop	<2	0.1	4.11	0.22	0.1	0.1158	icpms	733144	290489
943	jasper	Darnó Radiolarite	J ₂	outcrop	<2	0.06	5.97	0.36	0.03	0.0177	icpms	732787	290793
944	limest. (olistolith)	Darnóhegy Shale	J ₂	outcrop	<2	0.05	2.14	0.18	0.03	0.0566	icpms	732765	289402
945	claystone, sandstone	Darnóhegy Shale	J ₂	outcrop	<2	0.03	8.91	0.46	0.28	0.0838	icpms	732395	289150
946	quartzite	Darnó Radiolarite	J ₂	outcrop	<2	0.02	1.09	0.12	0.03	0.0465	icpms	732395	289150
947	claystone	Darnó Radiolarite	J ₂	outcrop	<2	0.07	0.51	0.26	0.33	0.5219	icpms	732936	289065
948	shale, sandstone	Oldalvölgy Formation	J ₃	outcrop	<2	0.070	2.90	0.24	0.110	0.0665	icpms	735316	286753
949	basalt, radiolarite	Szarvaskő Basalt	J ₂	outcrop	<2	0.080	0.86	0.10	-0.050	0.0077	icpms	741891	289818
950	limestone	Oldalvölgy Formation	J ₃	outcrop	<2	0.050	56.30	0.75	0.120	0.2582	icpms	741891	289818
951	diabase	Szarvaskő Basalt	J ₂	outcrop	<2	-0.050	3.41	0.16	0.070	0.0313	icpms	742380	290350
952	shale	Mónosbél Formation	J ₃	outcrop	<2	-0.050	22.30	0.40	0.160	0.097	icpms	742380	290350
953	quartzite	Oldalvölgy Formation	J ₃	outcrop	3	0.060	3.18	0.26	0.240	0.0589	icpms	741764	291236
954	shale	Darnóhegy Shale	J ₂	outcrop	2	-0.050	2.18	0.10	0.170	0.0246	icpms	740894	293848
955	radiolarite, quartzite	Darnó Radiolarite	J ₂	outcrop	<2	-0.050	2.35	0.11	0.120	0.0548	icpms	740894	293848
956	basalt	Szarvaskő Basalt	J ₂	outcrop	<2	<0.02	0.73	0.1	<0.02	0.06	aas	746098	292665
957	shale	Mónosbél Formation	J ₃	outcrop	<2	-0.050	3.36	0.19	0.100	0.0171	icpms	746987	292865
958	sandstone	Mónosbél Formation	J ₃	outcrop	<2	0.090	21.30	1.09	0.340	0.1756	icpms	746877	294501
959	gabbro	Szarvaskő Basalt	J ₂	outcrop	<2	<0.02	1.22	0.1	<0.02	<0.02	aas	746852	294748
960	hornfels	Mónosbél Formation	J ₃	outcrop	<2	<0.02	0.39	0.1	<0.02	<0.02	aas	746852	294748
961	hornfels	Mónosbél Formation	J ₃	outcrop	<2	<0.02	1.82	<0.02	0.045	0.09	aas	746852	294748
962	gabbro	Szarvaskő Basalt	J ₂	outcrop	<2	0.02	25.3	1	0.254	0.06	aas	744852	295332
963	gabbro	Szarvaskő Basalt	J ₂	outcrop	<2	0.03	1.19	<0.02	<0.02	0.04	aas	744852	295332
964	shale, quartzite	Mónosbél Formation	J ₃	outcrop	<2	0.03	4.15	0.3	<0.02	0.1	aas	744852	295332
965	hornfels	Mónosbél Formation	J ₃	outcrop	<2	<0.02	0.58	<0.02	0.029	<0.02	aas	745755	297201
966	limonitic gabbro	Szarvaskő Basalt	J ₂	outcrop	<2	0.03	0.32	<0.02	<0.02	<0.02	aas	745755	297201
967	shale, sandstone	Mónosbél Formation	J ₃	outcrop	<2	0.05	9.97	0.3	0.071	0.17	aas	745617	298002
968	limestone (infilling)	Érva Limestone	T ₂₋₃	outcrop	<2	<0.100	99.80	0.37	<0.050	0.1723	icpms	760734	292121
969	radiolarite	Bányahegy Radiolarite	J ₂	outcrop	2	<0.100	18.70	<0.10	0.090	0.0178	icpms	760579	292674
970	cherty limestone	Felsőtárkány Limestone	T ₃	outcrop	<2	0.340	7.37	0.55	0.180	0.1367	icpms	760150	293408
971	cherty limestone	Felsőtárkány Limestone	T ₃	outcrop	<2	<0.100	11.00	0.42	0.100	0.2031	icpms	759675	294418
972	bituminous dolomite	Hámor Dolomite	T ₂	outcrop	<2	0.060	8.70	0.23	0.060	0.0513	icpms	759641	295097
973	basalt	Szinva Metabasalt	T ₃	outcrop	<2	<0.050	2.73	0.07	0.060	0.0084	icpms	759807	295100
974	dolomite	Felsőtárkány Limestone	T ₃	outcrop	<2	0.090	24.10	0.18	0.060	0.0478	icpms	759807	295100
975	veinlet of quartzite	Felsőtárkány Limestone	T ₃	outcrop	<2	0.070	-0.50	<0.05	<0.050	0.0043	icpms	759807	295100
976	shale	Oldalvölgy Formation	J ₃	outcrop	<2	0.03	2.29	0.1	<0.02	0.04	icpms	755887	295121
977	shale	Lökvölgy Shale	J ₂₋₃	outcrop	5	0.04	2.02	0.2	0.024	0.12	aas	756837	295355
978	radiolarite	Bányahegy Radiolarite	J ₂	outcrop	3	<0.02	0.87	0.1	0.033	0.07	aas	757534	295800
979	basalt	Szinva Metabasalt	T ₃	outcrop	6	0.08	2.36	0.2	<0.02	0.19	aas	757534	295800

Sample no.	Lithology	Formation	Age	Sample type (depth in m)	Elements						Analytical method	Coordinates	
					Au	Ag	As	Sb	Tl	Hg		X	Y
					ppb	ppm							
980	radiolarite	Bányahegy Radiolarite	J ₂	outcrop	<2	<0.02	405	3.2	0.71	2.24	aas	755523	295732
981	jasper breccia	Bányahegy Radiolarite	J ₂	outcrop	<2	0.09	302	15.2	4.03	2.97	icpms	755056	295291
982	basalt with jasper (olistholith)	Lökvölgy Shale	J _{2,3}	outcrop	<2	0.03	1.57	0.3	<0.02	<0.02	icpms	757439	296447
983	limestone skarn (olistholith)	Lökvölgy Shale	J _{2,3}	outcrop	<2	0.03	0.6	0.3	<0.02	0.04	icpms	757439	296447
984	radiolarite	Lökvölgy Shale	J _{2,3}	outcrop	3	<0.02	1.08	0.2	<0.02	0.07	icpms	757439	296447
985	radiolarite	Lökvölgy Shale	J _{2,3}	outcrop	2	<0.02	0.5	0.1	<0.02	0.04	icpms	757439	296447
986	jasp. after radiolarite	Lökvölgy Shale	J _{2,3}	outcrop	<2	<0.02	1.01	<0.2	<0.02	<0.02	icpms	757439	296447
987	basalt (olistholith)	Lökvölgy Shale	J _{2,3}	outcrop	4	0.11	2.09	0.4	<0.02	0.05	icpms	757439	296447
988	shale	Lökvölgy Shale	J _{2,3}	outcrop	4	0.04	1.11	0.1	0.03	<0.02	icpms	757439	296447
989	basalt	Szinva Metabasalt	T ₃	outcrop	<2	0.07	1.19	0.32	0.17	0.08	icpms	757440	296447
990	shale	Mónosbél Formation	J ₃	outcrop	<2	0.19	29.9	0.35	0.12	0.0024	icpms	747685	298284
991	shale	Lökvölgy Shale	J _{2,3}	outcrop	<2	0.050	5.29	0.14	0.220	0.0537	icpms	759773	296922
992	radiolarite, quartzite	Bányahegy Radiolarite	J ₂	outcrop	<2	0.060	8.41	0.17	1.200	0.0056	icpms	759623	297136
993	shale, quartzite	Lökvölgy Shale	J _{2,3}	outcrop	4	0.04	3.07	0.2	<0.02	0.17	aas	758227	297542
994	shale, radiolarite, quartzite	Oldalvölgy Formation	J ₃	outcrop	4	0.24	5.42	0.3	<0.02	0.57	aas	757668	297502
995	shale	Lökvölgy Shale	J _{2,3}	outcrop	3	0.03	4.56	0.2	<0.02	0.08	icpms	755809	297128
996	radiolarite	Bányahegy Radiolarite	J ₂	outcrop	<2	0.05	56.4	<0.2	<0.02	0.24	icpms	755726	297157
997	shale	Lökvölgy Shale	J _{2,3}	outcrop	3	0.04	9.62	0.26	0.2	0.16	icpms	756122	298153
998	shale	Lökvölgy Shale	J _{2,3}	outcrop	<2	0.03	8.58	0.3	<0.02	0.12	aas	758338	298224
999	radiolarite with hematite	Bányahegy Radiolarite	J ₂	outcrop	<2	<0.02	234	1.03	1.74	1.71	aas	760949	298304
1000	bitum. limestone	Felsőtárkány Limestone	T ₃	outcrop	3	<0.10	16.50	-0.10	<0.050	0.0168	icpms	760949	298304
1001	limestone	Felsőtárkány Limestone	T ₃	outcrop	<2	0.060	1.79	0.14	<0.050	0.0125	icpms	761391	298993
1002	basalt	Szinva Metabasalt	T ₃	outcrop	<2	0.070	2.67	0.11	0.080	0.0074	icpms	761391	298993
1003	silicified limestone	Berva Limestone	T _{2,3}	outcrop	6	0.130	18.50	6.34	0.350	6.042	icpms	749308	294295
1004	shale	Lökvölgy Shale	J _{2,3}	outcrop	4	<0.02	3.07	0.17	0.28	0.04	icpms	756888	299310
1005	radiolarite	Bányahegy Radiolarite	J ₂	outcrop	<2	<0.05	5.61	0.15	0.140	0.0201	icpms	761786	300020
1006	shale	Lökvölgy Shale	J _{2,3}	outcrop	<2	<0.05	1.51	0.12	0.140	0.0233	icpms	762821	300102
1007	limonitic limestone	Répáshuta Limestone	T ₃	outcrop	<2	0.05	3.05	0.47	0.13	<0.02	icpms	756900	300917
1008	shale	Lökvölgy Shale	J _{2,3}	outcrop	11	0.08	5.91	0.38	0.24	0.09	icpms	756900	300917
1009	radiolarite	Bányahegy Radiolarite	J ₂	outcrop	3	0.03	7.1	0.31	0.24	0.05	icpms	757353	301110
1010	Fe rich breccia	Bányahegy Radiolarite	J ₂	Répáshuta-3 43.7-57.0	<2	<0.100	43.10	2.48	0.410	0.1511	icpms	762376	301670
1011	radiolarite	Bányahegy Radiolarite	J ₂	57.0-63.9	<2	<0.100	19.00	0.79	0.410	0.3881	icpms	762376	301670
1012	radiolarite	Bányahegy Radiolarite	J ₂	63.9-67.7	<2	<0.100	10.10	0.15	0.290	0.2111	icpms	762376	301670
1013	quartzite, radiolarite, shale	Bányahegy Radiolarite	J ₂	outcrop	<2	<0.02	4.68	0.2	0.029	<0.02	aas	757119	302588
1014	radiolarite	Bányahegy Radiolarite	J ₂	outcrop	<2	<0.02	2.14	0.14	0.26	0.07	icpms	751030	302572
1015	shale	Mónosbél Formation	J ₃	outcrop	3	0.2	17.1	0.97	0.46	0.16	icpms	750985	302788
1016	shale	Oldalvölgy Formation	J ₃	outcrop	<2	0.06	4.59	0.55	0.21	0.05	icpms	751084	304211
1017	shale	Szilvásvár Formation	C ₂	outcrop	<2	0.04	5.54	0.32	0.21	0.08	icpms	751122	305571
1018	quartzite	Szilvásvár Formation	C ₂	outcrop	<2	<0.02	11.9	1.01	0.07	0.21	icpms	752328	306457
1019	shale	Szilvásvár Formation	C ₂	outcrop	<2	0.03	6.3	0.42	0.34	0.08	icpms	752781	306589
1020	conglomerate	Szilvásvár Formation	C ₂	outcrop	<2	<0.02	24.6	1.61	0.18	0.16	icpms	751413	306688
1021	conglomerate	Tarófi Conglomerate	C ₂	outcrop	<2	<0.100	13.40	0.14	0.090	0.0242	icpms	755426	307964
1022	conglomerate	Tarófi Conglomerate	C ₂	outcrop	<2	<0.100	8.14	0.19	0.060	0.0096	icpms	755426	307964
1023	conglomerate	Tarófi Conglomerate	C ₂	outcrop	<2	<0.100	14.20	0.28	0.120	0.0372	icpms	755426	307964
1024	conglomerate	Tarófi Conglomerate	C ₂	outcrop	<2	<0.100	17.80	0.21	0.250	0.1727	icpms	755426	307964
1025	conglomerate	Tarófi Conglomerate	C ₂	outcrop	<2	<0.100	5.55	0.13	0.070	0.0868	icpms	755426	307964
1026	sandstone	Szentlélek Formation	P ₂	outcrop	<2	1.400	533.00	12.50	0.190	0.8137	icpms	756126	308162
1027	limestone	Mályinka Formation	C ₂	outcrop	<2	<0.100	51.30	0.13	<0.050	0.117	icpms	756126	308162
1028	limestone, quartzite	Mályinka Formation	C ₂	outcrop	<2	<0.100	5.21	-0.10	<0.050	0.0305	icpms	756126	308162

Sample no.	Lithology	Formation	Age	Sample type (depth in m)	Elements						Analytical method	Coordinates	
					Au	Ag	As	Sb	Tl	Hg		X	Y
					ppb	ppm							
1029	limestone	Mályinka Formation	C ₂	outcrop	<2	0.860	24.30	0.79	0.050	0.0944	icpms	756104	308193
1030	limestone	Szentlélek Formation	P ₂	outcrop	<2	0.330	6.45	0.99	0.240	0.0398	icpms	756104	308193
1031	shale, sandstone	Mályinka Formation	C ₂	outcrop	<2	0.340	7.36	0.68	0.180	0.0923	icpms	755773	308217
1032	quartzite	Szentlélek Formation	P ₂	outcrop	<2	<0.100	3.40	<0.10	<0.050	0.0155	icpms	756166	308194
1033	limestone	Nagyvisnyó Limestone	P ₂	outcrop	<2	0.03	2.51	0.11	0.06	<0.02	icpms	758463	308206
1034	shale	Szilvsvárad Formation	C ₂	outcrop	<2	<0.100	9.55	0.40	0.180	0.0647	icpms	756111	308996
1035	shale, quartzite	Szilvsvárad Formation	C ₂	outcrop	<2	0.03	4.96	0.24	0.24	0.08	icpms	754890	309036
1036	shale, quartzite	Szilvsvárad Formation	C ₂	outcrop	<2	0.03	12.7	0.76	0.16	0.04	icpms	755509	309110
1037	shale	Szilvsvárad Formation	C ₂	outcrop	<2	0.240	19.50	1.04	0.200	0.0772	icpms	755009	309702
1038	quartzite	Szilvsvárad Formation	C ₂	outcrop	<2	0.110	14.00	0.64	<0.050	0.0701	icpms	755009	309702
1039	shale, quartzite	Mályinka Formation	C ₂	outcrop	<2	0.05	4.84	0.49	0.1	0.02	icpms	754874	309932
1040	claystone with malachite	Szentlélek Formation	P ₂	outcrop	234	1.49	116	1.96	0.81	0.22	icpms	751758	311854
1041	claystone	Szentlélek Formation	P ₂	outcrop	<2	0.4	13	2.9	0.5	<1	icpms	751758	311854
1042	claystone with malachite	Szentlélek Formation	P ₂	outcrop	<2	0.7	31	3.6	0.5	<1	icpms	751758	311854
1043	limestone	Nagyvisnyó Limestone	P ₂	outcrop	<2	0.41	4.13	0.18	0.1	0.28	icpms	752745	312149
1044	limest., chert, shale	Nagyvisnyó Limestone	P ₂	outcrop	<2	0.41	6.24	0.28	0.09	<0.02	icpms	752745	312149
1045	dolomite	Nagyvisnyó Limestone	P ₂	outcrop	<2	0.36	2.24	0.24	0.04	<0.02	icpms	752745	312149
1046	limestone	Mályinka Formation	C ₂	outcrop	<2	0.02	3.13	0.33	0.06	0.08	icpms	757203	310376
1047	limestone	Mályinka Formation	C ₂	outcrop	<2	0.02	2.75	0.34	0.12	<0.02	icpms	757431	310349
1048	limestone breccia	Mályinka Formation	C ₂	outcrop	<2	0.03	1.15	0.22	0.05	<0.02	icpms	757431	310349
1049	quartzite	Mályinka Formation	C ₂	outcrop	<2	0.02	2.4	0.42	0.02	0.07	icpms	757431	310349
1050	shale	Mályinka Formation	C ₂	outcrop	<2	0.03	11	0.99	0.16	0.18	icpms	757431	310349
1051	limestone	Nagyvisnyó Limestone	P ₂	outcrop	<2	0.03	3.28	0.18	0.06	0.04	icpms	758559	310833
1052	shale	Mályinka Formation	C ₂	outcrop	<2	0.05	5.32	0.35	0.2	<0.02	icpms	758378	309502
1053	limestone	Mályinka Formation	C ₂	outcrop	<2	0.11	27.3	1.22	0.06	0.32	icpms	758936	309512
1054	cherty limestone	Rónabükk Limestone	T ₃	outcrop	<2	0.04	0.95	0.11	0.05	0.02	icpms	761352	310793
1055	limestone	Kisfennsík Limestone	T ₃	outcrop	<2	0.09	0.94	0.09	<0.02	0.04	icpms	761333	310700
1056	cherty limestone	Rónabükk Limestone	T ₃	outcrop	<2	0.04	0.97	0.12	0.05	<0.02	icpms	762498	310383
1057	tuff	Szentistvánhegy Metaandesite	T ₂	outcrop	<2	0.03	2.29	0.3	0.06	0.02	icpms	762498	310383
1058	dolomitic shale	Mályinka Formation	C ₂	outcrop	<2	0.03	2.81	0.25	0.06	0.22	icpms	763733	309573
1059	shale	Mályinka Formation	C ₂	outcrop	<2	0.09	8.34	0.36	0.13	0.23	icpms	763733	309573
1060	bituminous shale	Mályinka Formation	C ₂	outcrop	<2	0.06	11.7	0.54	0.18	0.2	icpms	763733	309573
1061	bitum. limestone	Gerennavár Limestone	T ₁	outcrop	<2	0.07	1.07	0.08	0.02	0.04	icpms	764077	309950
1062	pyritic shale	Vesszős Formation	T ₃	outcrop	<2	0.05	0.81	0.2	0.04	0.04	icpms	764138	310013
1063	pyritic porphyrite	Szentistván Metaand	T ₂	outcrop	<2	0.02	1.85	0.08	0.11	<0.02	icpms	764131	308314
1064	dolomite	Hámor Dolomite	T ₂	outcrop	<2	0.02	0.56	0.13	<0.02	0.04	icpms	764249	308625
1065	pyritic dolomite	Hámor Dolomite	T ₂	outcrop	<2	0.07	0.79	0.27	0.02	0.1	icpms	764330	308688
1066	dolomarl	Hámor Dolomite	T ₂	outcrop	<2	0.03	1.41	0.45	0.13	0.17	icpms	764247	308718
1067	bituminous dolomite	Hámor Dolomite	T ₂	outcrop	<2	0.06	2.97	0.68	0.12	0.08	icpms	764143	308747
1068	dolomite	Hámor Dolomite	T ₂	outcrop	<2	0.03	0.8	0.18	<0.02	<0.02	icpms	764266	308811
1069	bituminous dolomite	Hámor Dolomite	T ₂	outcrop	<2	0.14	1.97	0.64	0.24	0.04	icpms	764182	308871
1070	bituminous dolomite	Hámor Dolomite	T ₂	outcrop	<2	0.12	5.46	2.17	0.23	2.22	icpms	764200	308964
1071	limestone	Ablakoskövölgy Form	T ₁	outcrop	<2	0.04	1.87	0.19	0.11	<0.02	icpms	764966	308967
1072	bitum. pyritic dol	Hámor Dolomite	T ₂	outcrop	<2	0.03	3.53	0.96	0.21	0.25	icpms	764303	309028
1073	pyritic dolomite	Hámor Dolomite	T ₂	outcrop	<2	<0.02	5.15	0.61	0.17	0.14	icpms	764136	309086
1074	andesite	Szentistván. Metaand	T ₂	outcrop	<2	-0.050	1.73	0.24	0.110	0.0068	icpms	768801	303526
1075	limestone	Felsőtárkány Limestone	T ₃	outcrop	<2	-0.050	11.70	0.56	0.060	0.1959	icpms	768801	303526
1076	quartz porphyry	Szentistván Metaand	T ₂	outcrop	<2	-0.050	72.80	0.78	0.210	0.0294	icpms	769056	304211
1077	quartz porphyry	Szentistván Metaand	T ₂	outcrop	<2	0.110	2.23	0.13	0.070	0.0076	icpms	769056	304211
1078	basalt	Szinva Metabasalt	T ₃	outcrop	<2	0.04	1.45	0.09	0.08	<0.02	icpms	766760	305153
1079	tuff	Szinva Metabasalt	T ₃	outcrop	<2	0.1	9.98	0.15	0.17	<0.02	icpms	766891	305866

Sample no.	Lithology	Formation	Age	Sample type (depth in m)	Elements						Analytical method	Coordinates	
					Au	Ag	As	Sb	Tl	Hg		X	Y
					ppb	ppm							
1080	limestone	Vesszős Formation	T ₃	outcrop	<2	0.03	0.87	0.27	<0.02	<0.02	icpms	767022	306518
1081	dolomite	Vesszős Formation	T ₃	outcrop	<2	0.04	2.96	0.24	0.02	<0.02	icpms	766935	306732
1082	pyritic limestone	Fehérvölgy Limestone	T _{2,3}	outcrop	<2	0.04	2.19	0.31	0.05	0.02	icpms	767157	307046
1083	dolomite	Hámor Dolomite	T ₂	outcrop	<2	0.02	0.57	0.29	0.04	0.1	icpms	767346	307915
1084	porphyrite	Szentistvánhi Metaand	T ₂	outcrop	<2	0.03	0.65	0.12	0.32	<0.02	icpms	767346	307915
1085	shale	Vesszős Formation	T ₃	Miskolc-14 46.0	<2	0.03	2.07	1.1	<0.02	0.09	aas	770949	306629
1086	shale	Vesszős Formation	T ₃	48.8	<2	0.04	5.65	2.2	<0.02	0.13	aas	770949	306629
1087	shale	Vesszős Formation	T ₃	58.8	<2	0.03	3.66	1.5	<0.02	0.34	aas	770949	306629
1088	tuff	Strázsahegy Formation	D ₂	outcrop	<2	0.06	5.78	0.34	0.11	<0.02	icpms	752306	314737
1089	shale	Tapolcsány Formation	S-C ₁	outcrop	<2	0.07	25.5	2.88	0.64	0.04	icpms	752306	314737
1090	quartzite	Tapolcsány Formation	S-C ₁	outcrop	<2	0.04	42.8	21.5	0.21	0.09	icpms	752306	314737
1091	vein of quartzite	Tapolcsány Formation	S-C ₁	outcrop	8	0.160	83.00	12.70	0.340	0.714	icpms	752306	314737
1092	limest. with hematite	Nagyvisnyó Limestone	P ₂	outcrop	<2	0.07	1.57	0.39	0.02	0.02	icpms	751685	314849
1093	pyroclastite	Strázsahegy Formation	D ₂	outcrop	<2	0.04	9.05	0.62	0.07	0.02	icpms	752522	315389
1094	arkosic sandstone	Tapolcsány Formation	S-C ₁	outcrop	<2	0.03	10.2	0.27	0.1	<0.02	icpms	752377	315418
1095	dolomite, quartzite	Strázsahegy Formation	D ₂	outcrop	<2	0.39	1.01	0.17	<0.02	0.04	icpms	752584	315421
1096	limestone	Tapolcsány Formation	S-C ₁	Dédestapolcsány-11 372.5	<2	0.06	3.6	0.2	0.14	0.04	icpms	758544	315871
1097	limestone	Tapolcsány Formation	S-C ₁	400.0	<2	0.09	18.9	0.7	0.07	0.07	icpms	758544	315871
1098	graphite shale	Tapolcsány Formation	S-C ₁	430.0	<2	0.3	23.6	1	0.28	0.03	icpms	758544	315871
1099	graphite shale	Tapolcsány Formation	S-C ₁	460.0	<2	0.1	21	1	0.19	0.1	icpms	758544	315871
1100	limestone	Tapolcsány Formation	S-C ₁	490.0	<2	0.05	2.2	0.1	0.06	0.13	icpms	758544	315871
1101	shale	Tapolcsány Formation	S-C ₁	520.0	<2	0.08	5.2	0.3	0.07	0.13	icpms	758544	315871
1102	limestone	Tapolcsány Formation	S-C ₁	550.0	<2	0.13	3.3	0.2	0.06	0.17	icpms	758544	315871
1103	limestone	Tapolcsány Formation	S-C ₁	575.0	<2	0.06	1.4	<0.1	0.03	0.1	icpms	758544	315871
1104	limestone	Tapolcsány Formation	S-C ₁	600.0	<2	0.08	2.8	0.2	0.07	0.08	icpms	758544	315871
1105	limestone	Nagyvisnyó Limestone	P ₂	outcrop	<2	0.04	2.66	0.2	0.04	<0.02	icpms	752108	316680
1106	limestone	Nagyvisnyó Limestone	P ₂	outcrop	<2	1.35	2.89	0.97	0.02	<0.02	icpms	753004	317375
1107	pyritic limestone	Nagyvisnyó Limestone	P ₂	outcrop	<2	<0.02	2.23	0.46	0.04	0.02	icpms	752921	317436
1108	limestone	Nagyvisnyó Limestone	P ₂	outcrop	<2	0.03	0.67	0.1	<0.02	<0.02	icpms	753019	317715
1109	limestone	Nagyvisnyó Limestone	P ₂	outcrop	<2	<0.02	1.97	1.05	0.03	<0.02	icpms	752747	317896
1110	limestone	Nagyvisnyó Limestone	P ₂	outcrop	<2	<0.02	1.16	0.45	0.03	0.16	icpms	753176	318151
1111	shale	Tapolcsány Formation	S-C ₁	outcrop	2	0.29	87.9	53.7	0.32	1.25	icpms	754198	317643
1112	shale	Tapolcsány Formation	S-C ₁	outcrop	5	0.35	97.6	58.8	0.31	1.14	icpms	754239	317644
1113	shale	Tapolcsány Formation	S-C ₁	outcrop	7	0.59	160	79.7	0.7	2.3	icpms	754070	317857
1114	pyritic shale	Tapolcsány Formation	S-C ₁	Dédestapolcsány-8 34.5-34.6	<2	0.03	3.33	0.19	0.14	<0.02	icpms	755330	317880
1115	pyritic shale	Tapolcsány Formation	S-C ₁	37.3	<2	0.11	3.13	1.77	0.26	0.06	icpms	755330	317880
1116	pyritic shale	Tapolcsány Formation	S-C ₁	86.0-88.5	<2	<0.02	5.49	0.25	0.12	<0.02	icpms	755330	317880
1117	pyritic shale	Tapolcsány Formation	S-C ₁	107.7	<2	0.08	24.2	0.51	0.19	0.04	icpms	755330	317880
1118	pyritic shale	Tapolcsány Formation	S-C ₁	139.2-139.3	<2	0.08	18.2	0.29	0.2	<0.02	icpms	755330	317880
1119	pyritic shale	Tapolcsány Formation	S-C ₁	160.0-160.1	<2	0.1	<0.2	0.37	0.12	0.05	icpms	755330	317880
1120	pyritic shale	Tapolcsány Formation	S-C ₁	161.4-161.5	2	0.05	1.27	0.15	0.06	0.04	icpms	755330	317880
1121	pyritic shale	Tapolcsány Formation	S-C ₁	181.2-181.3	<2	0.21	2.6	0.46	0.18	0.04	icpms	755330	317880
1122	sandstone	Tapolcsány Formation	S-C ₁	212.1	<2	0.1	17.7	0.25	0.11	<0.02	icpms	755330	317880
1123	limestone	Tapolcsány Formation	S-C ₁	211.6-211.7	2	0.04	4.53	1.78	0.1	<0.02	icpms	755330	317880
1124	sandstone	Tapolcsány Formation	S-C ₁	237.8	2	0.08	5.55	0.99	0.18	<0.02	icpms	755330	317880
1125	pyritic shale	Tapolcsány Formation	S-C ₁	254.2	3	0.05	11.5	0.84	0.14	0.04	icpms	755330	317880
1126	pyritic sandstone	Tapolcsány Formation	S-C ₁	280.2	<2	0.04	3.39	0.66	0.16	0.3	icpms	755330	317880
1127	pyritic sandstone	Tapolcsány Formation	S-C ₁	312.9	<2	0.04	3.68	0.35	0.11	<0.02	icpms	755330	317880
1128	limestone	Tapolcsány Formation	S-C ₁	372.3-372.4	<2	0.06	1.13	1.66	0.75	0.06	icpms	755330	317880
1129	pyritic limestone	Tapolcsány Formation	S-C ₁	395.0-395.0	2	0.07	4.86	0.65	0.18	<0.02	icpms	755330	317880
1130	limestone	Tapolcsány Formation	S-C ₁	399.0	<2	0.04	18.4	1.3	0.38	0.06	icpms	755330	317880
1131	limestone	Tapolcsány Formation	S-C ₁	402.3-402.4	<2	0.05	0.22	0.92	0.57	<0.02	icpms	755330	317880

Sample no.	Lithology	Formation	Age	Sample type (depth in m)	Elements						Analytical method	Coordinates	
					Au	Ag	As	Sb	Tl	Hg		X	Y
					ppb	ppm							
1132	limestone	Tapolcsány Formation	S-C ₁	405.6–406.6	13	0.68	98.6	11	0.28	0.56	icpms	755330	317880
1133	pyritic limestone	Tapolcsány Formation	S-C ₁	411.1	<2	0.43	15.5	2.11	0.23	0.4	icpms	755330	317880
1134	pyritic shale	Tapolcsány Formation	S-C ₁	429.7	10	0.08	270	28.5	0.26	0.46	icpms	755330	317880
1135	pyritic limestone	Tapolcsány Formation	S-C ₁	431.9–432.5	3	0.05	59.3	8.85	0.16	0.16	icpms	755330	317880
1136	pyritic limestone	Tapolcsány Formation	S-C ₁	441.3–441.4	13	0.18	72.9	30.9	0.29	0.57	icpms	755330	317880
1137	pyritic limestone	Tapolcsány Formation	S-C ₁	444.1–444.2	4	0.11	61.1	2.24	0.31	0.1	icpms	755330	317880
1138	pyritic shale	Tapolcsány Formation	S-C ₁	450.6	<2	0.1	21.7	15	0.12	0.18	icpms	755330	317880
1139	pyritic shale	Tapolcsány Formation	S-C ₁	458.1–458.2	<2	0.09	16.6	8.42	0.09	0.33	icpms	755330	317880
1140	pyritic shale	Tapolcsány Formation	S-C ₁	460.5–460.6	9	0.79	98.7	20.1	0.09	1.01	icpms	755330	317880
1141	pyritic shale	Tapolcsány Formation	S-C ₁	470.1	14	0.68	79.3	12.1	0.15	1.02	icpms	755330	317880
1142	pyritic shale	Tapolcsány Formation	S-C ₁	474.2–474.4	10	0.69	139	20.6	0.21	1.9	icpms	755330	317880
1143	pyritic shale	Tapolcsány Formation	S-C ₁	475.6–475.7	8	0.49	62.7	9.61	0.14	1.5	icpms	755330	317880
1144	sandstone	Tapolcsány Formation	S-C ₁	outcrop	<2	0.03	2.6	0.26	0.05	<0.02	icpms	755627	317422
1145	quartzite breccia	Tapolcsány Formation	S-C ₁	outcrop	<2	<0.02	5.58	0.22	0.04	<0.02	icpms	755627	317422
1146	quartzite	Tapolcsány Formation	S-C ₁	outcrop	<2	0.04	5.15	0.22	0.07	<0.02	icpms	755863	318075
1147	limestone	Nagyvisnyó Limestone	P ₂	outcrop	<2	0.04	1.15	0.23	0.03	0.2	icpms	753080	318921
1148	limestone	Nagyvisnyó Limestone	P ₂	outcrop	<2	<0.02	0.4	0.08	0.03	0.02	icpms	753303	319142
1149	limestone	Nagyvisnyó Limestone	P ₂	outcrop	<2	0.04	0.73	0.21	0.15	0.18	icpms	753281	319203
1150	br. cherty limestone	Nagyvisnyó Limestone	P ₂	outcrop	<2	0.07	2.71	0.82	0.02	0.04	icpms	754467	318730
1151	limestone	Nagyvisnyó Limestone	P ₂	outcrop	<2	0.02	1.81	0.36	0.04	<0.02	icpms	754510	318669
1152	limestone	Lázberc Formation	C	outcrop	<2	0.03	1.97	0.37	<0.02	0.04	icpms	755517	318903
1153	limestone	Lázberc Formation	C	outcrop	<2	0.03	1.47	0.19	0.05	<0.02	icpms	755496	318933
1154	limonitic limestone	Lázberc Formation	C	outcrop	<2	0.03	4.89	0.44	0.08	<0.02	icpms	755433	318994
1155	limestone	Lázberc Formation	C	outcrop	<2	0.02	14.6	0.65	0.06	<0.02	icpms	754682	319382
1156	limestone	Lázberc Formation	C	outcrop	<2	0.02	6.71	0.26	0.05	<0.02	icpms	754909	319386
1157	limestone	Lázberc Formation	C	outcrop	<2	0.02	9.22	1	0.04	0.02	icpms	754475	319409
1158	limestone	Lázberc Formation	C	outcrop	<2	0.03	3.06	0.27	0.06	0.14	icpms	754599	319411
1159	limestone	Lázberc Formation	C	outcrop	<2	0.03	1.55	0.2	0.03	<0.02	icpms	754392	319469
1160	limestone	Lázberc Formation	C	outcrop	<2	0.03	1.17	0.1	0.03	<0.02	icpms	754288	319498
1161	limestone	Lázberc Formation	C	outcrop	<2	<0.02	1.8	0.14	0.06	0.04	icpms	754307	319560
1162	limestone	Nagyvisnyó Limestone	P ₂	outcrop	<2	0.03	<0.2	0.21	0.04	0.32	icpms	753356	319637
1163	shale	Lázberc Formation	C	outcrop	<2	0.06	4.92	0.6	0.08	0.04	icpms	754326	319684
1164	limestone	Nagyvisnyó Limestone	P ₂	outcrop	<2	0.02	2.93	0.75	0.04	0.74	icpms	754259	319962
1165	limestone	Uppony Limestone	D _{2,3}	outcrop	<2	0.06	9.73	1.03	0.04	0.09	icpms	754237	320023
1166	limestone	Nagyvisnyó Limestone	P ₂	outcrop	<2	0.03	1.94	2.02	0.09	0.26	icpms	753968	320050
1167	limestone	Uppony Limestone	D _{2,3}	outcrop	<2	0.07	1.51	0.3	0.03	0.06	icpms	754032	319957
<i>9 RUDABÁNYA MOUNTAINS AND SZENDRŐ MOUNTAINS</i>													
1168	mine waste	Rudabánya Mine Dump	H	outcrop	4	5	65.5	45.2	0.9	3.95	icpms	767873	336907
1169	mine waste	Rudabánya Mine Dump	H	outcrop	4	9.39	117	106	0.9	1.92	icpms	767811	336937
1170	flotation waste	Rudabánya Mine Dump	H	outcrop	5	1.53	31.2	3.72	0.46	3.04	icpms	767955	336940
1171	flotation waste	Rudabánya Mine Dump	H	outcrop	3	1.95	28.9	6.49	0.46	3.03	icpms	767955	336940
1172	mine waste	Rudabánya Mine Dump	H	outcrop	2	16.3	66	118	0.68	4.5	icpms	767872	336969
1173	mine waste	Rudabánya Mine Dump	H	outcrop	3	4.09	105	56.4	0.82	3.91	icpms	767830	336999
1174	mine waste	Rudabánya Mine Dump	H	outcrop	2	4.01	89	36.1	1.17	4	icpms	767768	337028
1175	dol. jasper breccia	Tapolcsány Formation	S-C ₁	outcrop	6	0.26	5.26	5.04	0.03	1.2	icpms	767884	338390
1176	silicified dol. breccia	Tapolcsány Formation	S-C ₁	outcrop	9	0.38	5	5.64	0.03	0.97	icpms	767884	338390
1177	silicified dol. breccia	Tapolcsány Formation	S-C ₁	outcrop	17	1.2	9.6	5.3	0.5	<1	icpms	767884	338390
1178	quartz	Tapolcsány Formation	S-C ₁	outcrop	3	0.11	2.87	2.23	0.05	0.38	icpms	767884	338390
1179	TVX samples, lithology not known	Rudabánya Iron Ore	T _{1,2}	outcrop	7	24.5	181	59.6	0.3	58	icpms	766673	338211
1180	TVX samples, lithology not known	Rudabánya Iron Ore	T _{1,2}	outcrop	50	70	166	173	n.a.	n.a.	aas	766673	338211
1181	TVX samples, lithology not known	Rudabánya Iron Ore	T _{1,2}	outcrop	<2	7.3	93.4	243	0.32	13.8	icpms	766955	338526

Sample no.	Lithology	Formation	Age	Sample type (depth in m)	Elements						Analytical method	Coordinates	
					Au	Ag	As	Sb	Tl	Hg		X	Y
					ppb	ppm							
1182	TVX samples, lithology not known	Rudabánya Iron Ore	T ₁₋₂	outcrop	70	30	106	287	n.a.	n.a.	aas	766955	338526
1183	TVX samples, lithology not known	Rudabánya Iron Ore	T ₁₋₂	outcrop	4	18	32	84.5	0.17	58	icpms	766995	338558
1184	TVX samples, lithology not known	Rudabánya Iron Ore	T ₁₋₂	outcrop	113	112	478	1640	0.14	207	icpms	766995	338558
1185	TVX samples, lithology not known	Rudabánya Iron Ore	T ₁₋₂	outcrop	60	352	43	183	n.a.	n.a.	aas	766995	338558
1186	TVX samples, lithology not known	Rudabánya Iron Ore	T ₁₋₂	outcrop	230	423	705	2943	n.a.	n.a.	aas	766995	338558
1187	TVX samples, lithology not known	Rudabánya Iron Ore	T ₁₋₂	outcrop	40	65	4420	5990	1.05	460	icpms	767150	339024
1188	TVX samples, lithology not known	Rudabánya Iron Ore	T ₁₋₂	outcrop	90	164	5827	1050	n.a.	n.a.	aas	767150	339024
1189	TVX samples, lithology not known	Rudabánya Iron Ore	T ₁₋₂	outcrop	630	425	8110	7490	0.04	1600	icpms	767212	339026
1190	TVX samples, lithology not known	Rudabánya Iron Ore	T ₁₋₂	outcrop	85	390	1300	1770	0.32	480	icpms	767212	339026
1191	TVX samples, lithology not known	Rudabánya Iron Ore	T ₁₋₂	outcrop	220	94	797	1408	n.a.	n.a.	aas	767212	339026
1192	TVX samples, lithology not known	Rudabánya Iron Ore	T ₁₋₂	outcrop	560	342	8083	13354	n.a.	n.a.	aas	767212	339026
1193	TVX samples, lithology not known	Rudabánya Iron Ore	T ₁₋₂	outcrop	7	36.1	108	711	0.24	360	icpms	767067	339053
1194	TVX samples, lithology not known	Rudabánya Iron Ore	T ₁₋₂	outcrop	30	48	112	752	n.a.	n.a.	aas	767067	339053
1195	limonitic dolomite	Rudabánya Iron Ore	T ₁₋₂	outcrop	3	1.75	331	697	0.19	5.7	icpms	767231	339088
1196	TVX samples, lithology not known	Rudabánya Iron Ore	T ₁₋₂	outcrop	8	10.8	196	356	0.21	1000	icpms	767066	339115
1197	TVX samples, lithology not known	Rudabánya Iron Ore	T ₁₋₂	outcrop	<2	47	259	487	n.a.	n.a.	aas	767066	339115
1198	TVX samples, lithology not known	Rudabánya Iron Ore	T ₁₋₂	outcrop	<2	31.2	851	389	1.53	132	icpms	767065	339177
1199	TVX samples, lithology not known	Rudabánya Iron Ore	T ₁₋₂	outcrop	30	42	845	451	n.a.	n.a.	aas	767065	339177
1200	galena	Rudabánya Iron Ore	T ₁₋₂	outcrop	<2	125	16.5	149	0.52	3400	icpms	767086	339177
1201	TVX samples, lithology not known	Rudabánya Iron Ore	T ₁₋₂	outcrop	8	57.5	925	286	2.34	340	icpins	767044	339207
1202	TVX samples, lithology not known	Rudabánya Iron Ore	T ₁₋₂	outcrop	50	243	1444	498	n.a.	n.a.	aas	767044	339207
1203	limonite with barite	Rudabánya Iron Ore	T ₁₋₂	outcrop	<2	9.35	282	44.3	0.13	33.1	icpms	767188	339210
1204	limonite	Rudabánya Iron Ore	T ₁₋₂	outcrop	3	18.7	556	391	2.25	110	icpms	767188	339210
1205	limonitic dolomite	Rudabánya Iron Ore	T ₁₋₂	outcrop	2	0.43	125	124	0.18	2.55	icpms	767188	339210
1206	TVX samples, lithology not known	Rudabánya Iron Ore	T ₁₋₂	outcrop	<2	25.7	2030	182	0.85	42	icpms	767208	339211
1207	TVX samples, lithology not known	Rudabánya Iron Ore	T ₁₋₂	outcrop	<20	43	1991	233	n.a.	n.a.	aas	767208	339211
1208	TVX samples, lithology not known	Rudabánya Iron Ore	T ₁₋₂	outcrop	4	13.1	571	165	0.39	50	icpms	767228	339242
1209	TVX samples, lithology not known	Rudabánya Iron Ore	T ₁₋₂	outcrop	50	70	1218	289	n.a.	n.a.	aas	767228	339242
1210	TVX samples, lithology not known	Rudabánya Iron Ore	T ₁₋₂	outcrop	8	3	106	119	0.19	0.86	icpms	767557	339249
1211	TVX samples, lithology not known	Rudabánya Iron Ore	T ₁₋₂	outcrop	50	11	67	126	n.a.	n.a.	aas	767557	339249
1212	TVX samples, lithology not known	Rudabánya Iron Ore	T ₁₋₂	outcrop	29	15.5	1720	829	2.1	113.5	icpms	766528	339259
1213	TVX samples, lithology not known	Rudabánya Iron Ore	T ₁₋₂	outcrop	80	33	1710	1215	n.a.	n.a.	aas	766528	339259
1214	TVX samples, lithology not known	Rudabánya Iron Ore	T ₁₋₂	outcrop	<2	84	52	49.9	0.98	68	icpms	767186	339272

Sample no.	Lithology	Formation	Age	Sample type (depth in m)	Elements						Analytical method	Coordinates	
					Au	Ag	As	Sb	Tl	Hg		X	Y
					ppb	ppm							
1215	TVX samples, lithology not known	Rudabánya Iron Ore	T ₁₋₂	outcrop	40	241	65	120	n.a.	n.a.	aas	767186	339272
1216	TVX samples, lithology not known	Rudabánya Iron Ore	T ₁₋₂	outcrop	5	45	95	117	0.36	124	icpms	767598	339281
1217	TVX samples, lithology not known	Rudabánya Iron Ore	T ₁₋₂	outcrop	140	77	96	113	n.a.	n.a.	aas	767598	339281
1218	TVX samples, lithology not known	Rudabánya Iron Ore	T ₁₋₂	outcrop	20	6.6	183	121	0.51	35.2	icpms	767001	339299
1219	TVX samples, lithology not known	Rudabánya Iron Ore	T ₁₋₂	outcrop	100	31	225	230	n.a.	n.a.	aas	767001	339299
1220	TVX samples, lithology not known	Rudabánya Iron Ore	T ₁₋₂	outcrop	<2	10.6	2390	430	3.96	44	icpms	767083	339301
1221	TVX samples, lithology not known	Rudabánya Iron Ore	T ₁₋₂	outcrop	40	42	2199	574	n.a.	n.a.	aas	767083	339301
1222	siderite	Rudabánya Iron Ore	T ₁₋₂	outcrop	<2	8.58	326	46.5	0.36	45	icpms	767205	339396
1223	TVX samples, lithology not known	Rudabánya Iron Ore	T ₁₋₂	outcrop	36	368	1750	3210	1.27	280	icpms	767266	339397
1224	TVX samples, lithology not known	Rudabánya Iron Ore	T ₁₋₂	outcrop	110	56	1967	7028	n.a.	n.a.	aas	767266	339397
1225	lim. with malachite	Rudabánya Iron Ore	T ₁₋₂	outcrop	<2	0.61	475	28.1	0.26	1.6	icpms	767287	339398
1226	limonite	Rudabánya Iron Ore	T ₁₋₂	outcrop	3	0.9	198	236	0.78	2.2	icpms	767101	339425
1227	limonitic dolomite with malachite	Rudabánya Iron Ore	T ₁₋₂	outcrop	4	0.97	25.6	38.3	0.3	3.3	icpms	767510	339557
1228	TVX samples, lithology not known	Rudabánya Iron Ore	T ₁₋₂	outcrop	16	100	3850	450	0.22	7	icpms	767610	339683
1229	TVX samples, lithology not known	Rudabánya Iron Ore	T ₁₋₂	outcrop	<20	319	3043	456	n.a.	n.a.	aas	767610	339683
1230	limonite	Rudabánya Iron Ore	T ₁₋₂	outcrop	6	3.04	645	220	0.53	22.2	icpms	767610	339713
1231	lim. Mn rich shale	Tapolcsány Formation	S-C ₁	outcrop	16	0.07	46.7	8.46	0.18	0.16	icpms	769234	339778
1232	lim. Mn rich shale	Tapolcsány Formation	S-C ₁	outcrop	<2	44	46	9.3	0.6	<1	icpms	769234	339778
1233	lim. Mn rich shale	Tapolcsány Formation	S-C ₁	outcrop	11	0.4	88	13	0.5	<1	icpms	769234	339778
1234	chert	Tapolcsány Formation	S-C ₁	outcrop	9	0.140	34.40	10.80	0.110	0.2016	icpms	769234	339778
1235	TVX samples, lithology not known	Rudabánya Iron Ore	T ₁₋₂	outcrop	3	44	25	4.65	0.06	7	icpms	767648	339838
1236	TVX samples, lithology not known	Rudabánya Iron Ore	T ₁₋₂	outcrop	30	3	17	12	n.a.	n.a.	aas	767648	339838
1237	TVX samples, lithology not known	Rudabánya Iron Ore	T ₁₋₂	outcrop	<2	118	104	107	0.42	500	icpms	767689	339870
1238	TVX samples, lithology not known	Rudabánya Iron Ore	T ₁₋₂	outcrop	50	449	148	184	n.a.	n.a.	aas	767689	339870
1239	dolomite breccia with barite	Rudabánya Iron Ore	T ₁₋₂	outcrop	<2	0.41	8.01	3.27	0.07	0.8	icpms	767503	339897
1240	TVX samples, lithology not known	Rudabánya Iron Ore	T ₁₋₂	outcrop	<2	60	105	21.9	0.61	440	icpms	767667	339931
1241	TVX samples, lithology not known	Rudabánya Iron Ore	T ₁₋₂	outcrop	20	352	177	73	n.a.	n.a.	aas	767667	339931
1242	siderite	Rudabánya Iron Ore	T ₁₋₂	outcrop	<2	0.89	256	67.3	0.17	2.8	icpms	767630	339961
1243	dolomite with siderite and barite	Rudabánya Iron Ore	T ₁₋₂	outcrop	<2	6.48	27.1	10.4	0.07	9.9	icpms	767630	339961
1244	TVX samples, lithology not known	Rudabánya Iron Ore	T ₁₋₂	outcrop	<2	5.4	181	500	2.72	62	icpms	767790	339964
1245	TVX samples, lithology not known	Rudabánya Iron Ore	T ₁₋₂	outcrop	<20	10	194	803	n.a.	n.a.	aas	767790	339964
1246	TVX samples, lithology not known	Rudabánya Iron Ore	T ₁₋₂	outcrop	27	40.4	367	233	1.9	50	icpms	767748	339994
1247	TVX samples, lithology not known	Rudabánya Iron Ore	T ₁₋₂	outcrop	40	66	420	309	n.a.	n.a.	aas	767748	339994
1248	silicified breccia	Rudabánya Iron Ore	T ₁₋₂	outcrop	<2	0.37	146	14.3	0.38	0.4	icpms	767601	340115
1249	dolomite with veinlets of quartz	Rudabánya Iron Ore	T ₁₋₂	outcrop	<2	0.21	32.1	7.73	0.16	0.39	icpms	767601	340115
1250	sideritic sandstone	Rudabánya Iron Ore	T ₁₋₂	outcrop	3	0.55	319	105	0.15	8.5	icpms	767951	340122

Sample no.	Lithology	Formation	Age	Sample type (depth in m)	Elements						Analytical method	Coordinates	
					Au	Ag	As	Sb	Tl	Hg		X	Y
					ppb	ppm							
1251	TVX samples, lithology not known	Rudabánya Iron Ore	T ₁₋₂	outcrop	<2	12.7	231	429	0.37	19.2	icpms	768116	340126
1252	TVX samples, lithology not known	Rudabánya Iron Ore	T ₁₋₂	outcrop	20	372	265	574	n.a.	n.a.	aas	768116	340126
1253	TVX samples, lithology not known	Rudabánya Iron Ore	T ₁₋₂	outcrop	3	7.4	182	59.6	0.42	11.4	icpms	767909	340152
1254	TVX samples, lithology not known	Rudabánya Iron Ore	T ₁₋₂	outcrop	20	27	191	100	n.a.	n.a.	aas	767909	340152
1255	TVX samples, lithology not known	Rudabánya Iron Ore	T ₁₋₂	outcrop	<2	140	72.1	159	0.54	198	icpms	767992	340154
1256	TVX samples, lithology not known	Rudabánya Iron Ore	T ₁₋₂	outcrop	60	520	86	199	n.a.	n.a.	aas	767992	340154
1257	gossan	Rudabánya Iron Ore	T ₁₋₂	outcrop	<2	10.2	206	18	0.72	3.2	icpms	768093	340249
1258	dol. with veinlets of quartz and covellite	Rudabánya Iron Ore	T ₁₋₂	outcrop	3	39.1	258	864	0.05	7	icpms	768214	340344
1259	siderite	Rudabánya Iron Ore	T ₁₋₂	outcrop	<2	0.2	491	22.2	0.37	0.19	icpms	768192	340436
1260	dolomite	Tapolcsány Formation	S-C ₁	outcrop	<2	0.03	0.53	0.3	0.02	0.16	icpms	769261	340458
1261	limonitic infilling	Tapolcsány Formation	S-C ₁	outcrop	3	0.08	468	9.07	0.05	0.57	icpms	769261	340458
1262	silicified dol. breccia	Tapolcsány Formation	S-C ₁	outcrop	<2	0.05	1.5	0.18	0.03	<0.02	icpms	769261	340458
1263	limonite	Rudabánya Iron Ore	T ₁₋₂	outcrop	2	3.51	44.8	25.8	9.46	7.09	icpms	768047	340464
1264	limonite	Rudabánya Iron Ore	T ₁₋₂	outcrop	<2	1.96	969	11.8	0.98	0.9	icpms	768044	340588
1265	dolomite breccia	Gutenstein Dolomite	T ₂	outcrop	<2	0.69	2.86	1.41	0.04	0.11	icpms	768993	342523
1266	dolomite	Gutenstein Dolomite	T ₂	outcrop	<2	0.06	0.81	0.39	0.04	0.07	icpms	769033	342555
1267	dolomite	Gutenstein Dolomite	T ₂	outcrop	<2	0.04	0.74	0.73	0.03	0.07	icpms	769504	342688
1268	dolomite breccia	Gutenstein Dolomite	T ₂	outcrop	<2	0.06	0.54	0.49	0.04	0.03	icpms	769504	342688
1269	bituminous dolomite	Gutenstein Dolomite	T ₂	outcrop	<2	0.05	1.35	0.43	0.04	0.03	icpms	769542	342813
1270	bituminous dolomite	Gutenstein Dolomite	T ₂	outcrop	<2	0.02	0.47	0.23	0.04	0.03	icpms	769624	342845
1271	bitum. br dolomite	Gutenstein Dolomite	T ₂	outcrop	<2	0.03	0.55	0.39	0.03	0.05	icpms	769685	342877
1272	limestone	Abod Limestone	D ₃	outcrop	<2	0.17	3.03	0.49	0.06	<0.02	icpms	775255	330666
1273	phyllite	Szendrölád Limestone	D ₂₋₃	outcrop	<2	0.03	1.38	0.35	0.04	0.04	icpms	776294	331875
1274	limestone	Szendrölád Limestone	D ₂₋₃	outcrop	<2	0.14	4.31	0.65	<0.02	<0.02	icpms	776294	331875
1275	dolomite breccia	Szendrölád Limestone	D ₂₋₃	outcrop	<2	<0.02	1.03	4.22	<0.02	<0.02	icpms	775172	333569
1276	pyritic limestone	Rakaca Marble	C	outcrop	<2	0.04	0.95	0.29	0.05	<0.02	icpms	776896	333946
1277	marble	Szendrölád Limestone	D ₂₋₃	outcrop	<2	0.03	3.41	3.17	0.04	0.04	icpms	776182	334517
1278	lim. graphitic shale	Irota Formation	D ₂	outcrop	13	0.1	43.4	2.33	0.15	<0.02	icpms	776475	335203
1279	lim. graphitic shale	Irota Formation	D ₂	outcrop	3	0.07	46.6	4.18	0.27	<0.02	icpms	776475	335203
1280	lim. graphitic shale	Irota Formation	D ₂	outcrop	2	0.05	328	2.47	0.18	<0.02	icpms	776475	335203
1281	flintshale	Szendrölád Limestone	D ₂₋₃	outcrop	4	0.04	5.09	0.86	0.11	<0.02	icpms	776475	335203
1282	graphite shale	Irota Formation	D ₂	outcrop	4	0.34	557	4.93	0.22	0.02	icpms	776228	335229
1283	graphitic lim. shale	Irota Formation	D ₂	outcrop	18	0.31	115	12.1	0.23	<0.02	icpms	776228	335229
1284	graphite shale	Irota Formation	D ₂	outcrop	15	0.07	195	1.62	0.14	<0.02	icpms	776228	335229
1285	graphite shale	Irota Formation	D ₂	outcrop	<2	0.050	160.00	8.85	0.160	0.0098	icpms	776248	335260
1286	quartzite breccia	Irota Formation	D ₂	outcrop	<2	-0.050	4.84	1.28	-0.050	0.013	icpms	776248	335260
1287	marble	Szendrölád Limestone	D ₂₋₃	outcrop	9	-0.050	22.70	5.36	-0.050	0.0156	icpms	776000	335286
1288	limestone breccia	Szendrölád Limestone	D ₂₋₃	outcrop	<2	0.23	0.46	0.37	<0.02	0.07	icpms	775333	335643
1289	limestone	Szendrölád Limestone	D ₂₋₃	outcrop	<2	<0.02	1.26	0.47	0.02	<0.02	icpms	776761	336322
1290	limonitic sandstone	Abod Limestone	D ₃	outcrop	6	0.04	4.88	0.72	0.12	<0.02	icpms	773647	336533
1291	limestone	Szendrölád Limestone	D ₂₋₃	outcrop	<2	0.03	0.58	0.08	0.08	0.05	icpms	774925	337395
1292	limonitic limestone	Szendrölád Limestone	D ₂₋₃	outcrop	<2	0.06	21.1	1.36	0.2	<0.02	icpms	775604	338462
1293	marble	Szendrő Phyllite	C	outcrop	<2	0.03	3.59	0.4	<0.02	0.2	icpms	776324	338383
1294	limonitic limestone with quartzite	Szendrölád Limestone	D ₂₋₃	outcrop	2	0.35	4.97	0.58	0.04	<0.02	icpms	778402	338429
1295	limonitic sandstone	Szendrölád Limestone	D ₂₋₃	outcrop	<2	0.04	0.9	0.36	0.14	0.05	icpms	776686	338731
1296	graphitic slate	Szendrölád Limestone	D ₂₋₃	outcrop	<2	0.19	5.15	0.07	0.11	0.12	icpms	776765	338917
1297	black shale	Szendrő Phyllite	C	outcrop	3	0.09	0.51	0.42	0.42	0.34	icpms	775504	340127
1298	massive quartzite with limonite	Szendrő Phyllite	C	outcrop	<2	0.11	0.26	0.05	0.06	0.02	icpms	775912	340290

Sample no.	Lithology	Formation	Age	Sample type (depth in m)	Elements						Analytical method	Coordinates	
					Au	Ag	As	Sb	Tl	Hg		X	Y
					ppb	ppm							
1295	quartzite with Fe and Mn crust	Szendrő Phyllite	C	outcrop	2	0.08	3.96	1.39	0.21	0.04	icpms	777682	340267
1300	limestone	Szendrő Phyllite	C	outcrop	3	0.03	2.26	2.38	0.09	0.04	icpms	777786	340270
1301	limonitic quartzite	Szendrő Phyllite	C	outcrop	<2	0.07	16.4	1.92	0.11	0.08	icpms	777989	340336
1302	limonitic shale	Szendrő Phyllite	C	outcrop	<2	0.34	11.3	0.29	0.21	0.22	icpms	775449	340744
1303	limonitic limestone	Szendrő Phyllite	C	outcrop	<2	0.12	1.98	0.21	0.03	<0.02	icpms	776534	340983
1304	limestone	Abod Limestone	D ₃	outcrop	<2	0.06	15	0.11	0.12	0.29	icpms	777640	341286
1305	pyritic lim. limest	Szendrő Phyllite	C	outcrop	<2	0.1	9.16	0.23	0.03	<0.02	icpms	776849	341670
1306	limestone	Szendrőlád Limestone	D _{2,3}	Szendrő-23 11.0	<2	0.02	<0.2	0.27	0.24	<0.02	icpms	775051	341704
1307	limestone	Szendrőlád Limestone	D _{2,3}	outcrop	<2	0.07	3.66	0.69	0.08	0.02	icpms	779236	341734
1308	silicified slate	Szendrő Phyllite	C	outcrop	<2	0.07	21.8	0.14	<0.02	<0.02	icpms	779535	342101
1309	jasper breccia	Irota Formation	D ₂	outcrop	<2	0.14	3.26	0.55	0.06	0.03	icpms	785270	341428
1310	marble	Irota Formation	D ₂	outcrop	<2	0.18	0.12	0.35	<0.02	0.04	icpms	785270	341428
1311	pyritic graphite shale	Irota Formation	D ₂	outcrop	<2	0.05	5.15	0.12	0.21	<0.02	icpms	787765	341209
1312	pyritic limestone	Irota Formation	D ₂	outcrop	<2	<0.02	3.51	0.48	0.03	0.07	icpms	788190	341498
1313	vein of quartz	Irota Formation	D ₂	outcrop	<2	0.04	2.58	0.4	0.03	0.03	icpms	788190	341498
1314	cherty slate	Irota Formation	D ₂	outcrop	<2	0.02	0.82	0.31	0.03	<0.02	icpms	788190	341498
1315	pyritic silic. shale	Irota Formation	D ₂	outcrop	<2	0.06	1.85	0.15	0.02	<0.02	icpms	788190	341498
1316	jasper	Irota Formation	D ₂	outcrop	4	0.070	4.28	0.45	-0.050	0.0901	icpms	788190	341498
1317	quartzite	Irota Formation	D ₂	outcrop	<2	0.03	0.15	0.05	0.03	<0.02	icpms	788128	341527
1318	quartzite	Irota Formation	D ₂	outcrop	<2	0.080	2.33	0.23	0.060	0.0101	icpms	788128	341527
1319	quartzite	Irota Formation	D ₂	outcrop	<2	<0.02	0.92	0.05	<0.02	<0.02	icpms	788185	341745
1320	lim. graphitic shale	Irota Formation	D ₂	outcrop	<2	0.08	2.01	0.17	0.09	<0.02	icpms	788185	341745
1321	shale	Irota Formation	D ₂	outcrop	6	0.09	0.99	0.19	0.14	<0.02	icpms	788185	341745
1322	graphite shale	Irota Formation	D ₂	outcrop	17	0.09	1.35	0.36	0.37	0.02	icpms	788185	341745
1323	graphite shale	Irota Formation	D ₂	outcrop	<2	0.35	3.62	0.24	0.35	0.04	icpms	788185	341745
1324	graphite shale	Irota Formation	D ₂	outcrop	<2	0.14	0.57	0.28	0.17	0.02	icpms	788741	341727
1325	massive quartzite	Szendrő Phyllite	C	outcrop	<2	0.03	0.78	0.11	<0.02	<0.02	icpms	786298	342318
1326	limonitic limestone	Szendrő Phyllite	C	outcrop	<2	0.22	5.02	0.32	0.1	0.03	icpms	786265	342873
1327	pyritic limestone	Szendrő Phyllite	C	outcrop	<2	0.06	1.81	0.3	0.03	<0.02	icpms	785585	342919
1328	sandstone	Szendrő Phyllite	C	outcrop	<2	0.03	5.62	1.08	0.09	<0.02	icpms	785293	343066
1329	siltstone	Perkupa Anhydrite	P ₂	outcrop	<2	0.11	12.3	1.42	0.1	0.08	icpms	768953	343449
1330	dolomitic siltstone	Perkupa Anhydrite	P ₂	outcrop	<2	0.3	22.6	0.56	0.17	0.09	icpms	768972	343511
1331	limonitic breccia	Perkupa Anhydrite	P ₂	outcrop	<2	0.15	33.2	0.53	0.18	0.15	icpms	769034	343513
1332	shale with gypsum	Perkupa Anhydrite	P ₂	outcrop	<2	0.06	7.63	0.55	0.1	0.22	icpms	768951	343542
1333	shale with veinlets of quartz	Perkupa Anhydrite	P ₂	outcrop	<2	0.04	1.79	0.09	0.12	0.1	icpms	769054	343544
1334	shale	Perkupa Anhydrite	P ₂	outcrop	<2	0.05	84.6	2.75	0.19	0.18	icpms	769054	343544
1335	anhydrite	Perkupa Anhydrite	P ₂	outcrop	<2	0.04	2.57	0.34	0.07	0.1	icpms	769054	343544
1336	gypsum	Perkupa Anhydrite	P ₂	outcrop	<2	0.07	2.98	0.52	0.08	0.44	icpms	769054	343544
1337	pyritic sandstone	Perkupa Anhydrite	P ₂	outcrop	<2	0.06	15.4	0.27	0.18	0.59	icpms	769116	343545
1338	gypsum	Perkupa Anhydrite	P ₂	outcrop	<2	0.1	6.71	2.08	0.08	4.63	icpms	769218	343547
1339	silicified limestone	Perkupa Anhydrite	P ₂	outcrop	4	0.05	14	1.19	0.16	0.15	icpms	768971	343573
1340	shale with veinlets of quartz	Perkupa Anhydrite	P ₂	outcrop	<2	0.07	1.36	0.63	0.07	0.29	icpms	769033	343574
1341	veinlet of quartz	Perkupa Anhydrite	P ₂	outcrop	<2	0.07	1.52	0.13	0.06	0.13	icpms	769033	343574
1342	pyritic shale	Perkupa Anhydrite	P ₂	outcrop	5	0.05	39.7	0.83	0.19	0.25	icpms	769033	343574
1343	veinlet of quartz	Perkupa Anhydrite	P ₂	outcrop	2	0.03	0.74	0.3	0.08	0.2	icpms	769033	343574
1344	pyritic shale	Perkupa Anhydrite	P ₂	outcrop	2	0.2	13.3	0.9	0.15	0.9	icpms	769094	343607
1345	chert in dolomite	Rudabánya Iron Ore (Martonyi)	T _{1,2}	outcrop	<2	0.32	10.9	1.2	0.45	0.4	icpms	777274	350794
1346	black shale	Rud. Iron Ore (Martonyi)	T _{1,2}	outcrop	<2	0.41	15.1	2.29	0.5	0.23	icpms	777274	350794
1347	residual black shale	Martonyi Mine Dump	H	outcrop	<2	0.08	9.92	3.3	0.36	1.31	icpms	777470	350831
1348	br. cherty dolomite	Rud. Iron Ore (Martonyi)	T _{1,2}	outcrop	4	0.2	41.9	29.2	0.45	9.67	icpms	777241	350980
1349	limonitic shale	Rud. Iron Ore (Martonyi)	T _{1,2}	outcrop	<2	0.57	12.3	3.75	0.45	1.64	icpms	777241	350980

Sample no.	Lithology	Formation	Age	Sample type (depth in m)	Elements						Analytical method	Coordinates	
					Au	Ag	As	Sb	Tl	Hg		X	Y
					ppb	ppm							
1350	limonite	Rud. Iron Ore (Martonyi)	T ₁₋₂	outcrop	<2	55.1	551	1580	0.22	239	icpms	777260	351042
1351	bitum. dol. breccia	Rud. Iron Ore (Martonyi)	T ₁₋₂	outcrop	<2	0.08	1.44	0.27	0.09	0.1	icpms	777279	351104
1352	dolomitic siderite	Rud. Iron Ore (Martonyi)	T ₁₋₂	outcrop	<2	4.31	64.6	4.45	0.12	2.05	icpms	777338	351198
1353	siderite and limonite	Rud. Iron Ore (Martonyi)	T ₁₋₂	outcrop	<2	2.46	267	51.8	0.45	17.7	icpms	777438	351324
1354	bitum. dol. breccia	Rud. Iron Ore (Martonyi)	T ₁₋₂	outcrop	<2	0.07	0.72	0.98	0.03	0.26	icpms	777438	351324
1355	limonite (infilling)	Rud. Iron Ore (Martonyi)	T ₁₋₂	outcrop	8	0.27	12.3	1.04	0.2	0.4	icpms	777438	351324
1356	siderite with bante	Rud. Iron Ore (Martonyi)	T ₁₋₂	outcrop	<2	0.37	54.9	14.7	0.16	15.4	icpms	777438	351324
1357	iron crust infilling	Rudabánya Iron Ore (Esztramos)	T ₁₋₂	outcrop	3	0.25	12.9	2.23	1.09	0.26	icpms	776039	354230
1358	hematite ore	Rud. Iron Ore (Esztr.)	T ₁₋₂	outcrop	<2	0.06	31.4	13.7	0.05	0.07	icpms	776017	354291
1359	hematite siderite br	Rud. Iron Ore (Esztr.)	T ₁₋₂	outcrop	<2	0.07	7.27	2.08	0.11	0.43	icpms	776017	354291
1360	siderite hematite ore	Rud. Iron Ore (Esztr.)	T ₁₋₂	outcrop	<2	0.06	10.2	1.72	0.15	0.21	icpms	776017	354291
1361	hematite ore	Rud. Iron Ore (Esztr.)	T ₁₋₂	outcrop	<2	0.13	23.2	18.1	0.23	0.54	icpms	776017	354291
1362	siderite	Rud. Iron Ore (Esztr.)	T ₁₋₂	outcrop	<2	0.7	12.1	1.01	0.23	2.59	icpms	775933	354382
1363	limonitic limestone	Szendró Phyllite	C	outcrop	<2	0.1	5.23	0.73	0.02	<0.02	icpms	782163	343210
1364	slate	Szendró Phyllite	C	outcrop	<2	0.14	3.9	1.1	0.08	0.04	icpms	782080	343239
1365	massive quartzite	Szendró Phyllite	C	outcrop	<2	0.29	1.53	0.06	<0.02	<0.02	icpms	784752	343333
1366	limestone breccia	Rakaca Marble	C	outcrop	<2	0.06	2.37	0.3	0.02	<0.02	icpms	785280	343356
1367	pyritic sandstone	Szendró Phyllite	C	outcrop	<2	<0.02	1.27	0.39	0.15	<0.02	icpms	780989	344172
1368	sandstone	Szendró Phyllite	C	outcrop	<2	0.02	6.05	0.53	0.2	0.04	icpms	780989	344172
1369	pyritic limestone	Szendró Phyllite	C	outcrop	<2	0.02	1.2	0.74	0.03	0.04	icpms	780989	344172
1370	limonitic quartzite	Szendró Phyllite	C	outcrop	<2	<0.02	0.83	0.25	0.03	0.02	icpms	780989	344172
1371	sandstone	Szendró Phyllite	C	outcrop	<2	0.33	3.17	0.19	0.78	<0.02	icpms	780989	344172
1372	marble	Rakaca Marble	C	outcrop	<2	0.02	0.45	1.04	<0.02	<0.02	icpms	779547	346149
1373	pyritic sandstone	Szendró Phyllite	C	outcrop	<2	0.38	11.1	0.23	0.19	<0.02	icpms	781564	345113
1374	limonitic slate	Szendró Phyllite	C	outcrop	<2	0.03	0.47	0.72	0.26	0.04	icpms	782785	345697
1375	limonitic sandstone	Edelény Clay	M ₃	outcrop	<2	0.02	605	2.94	0.15	0.13	icpms	783630	344697
1376	limonitic sandstone	Edelény Clay	M ₃	outcrop	<2	0.04	806	2.59	0.1	0.1	icpms	783542	344077
1377	sandstone	Szendró Phyllite	C	outcrop	<2	0.07	8.02	0.31	0.19	0.04	icpms	784404	345024
1378	slate	Szendró Phyllite	C	outcrop	<2	0.02	1.67	0.38	0.04	<0.02	icpms	781523	346935
1379	limestone	Szendró Phyllite	C	outcrop	7	0.16	3.84	1.74	0.04	0.03	icpms	781523	346935
1380	silicified limestone	Szendró Phyllite	C	outcrop	<2	0.09	13.6	0.95	<0.02	0.03	icpms	782181	346919
1381	ankeritic limestone	Rakaca Marble	C	outcrop	<2	0.04	23	2.87	0.21	0.1	icpms	782594	346836
1382	sandstone and slate	Szendró Phyllite	C	outcrop	<2	0.12	12	0.38	0.2	<0.02	icpms	783066	346878
1383	pyritic slate	Szendró Phyllite	C	outcrop	<2	0.09	7.56	0.26	0.18	0.04	icpms	783066	346878
1384	pyritic limestone	Szendró Phyllite	C	outcrop	<2	0.08	2.17	1.31	0.03	<0.02	icpms	783478	346826
1385	limonitic limestone	Szendró Phyllite	C	outcrop	<2	0.04	2.31	2.14	0.05	<0.02	icpms	783274	346790
1386	slate	Szendró Phyllite	C	outcrop	<2	0.06	7.83	0.56	0.2	0.02	icpms	783456	346918
1387	limestone	Szendró Phyllite	C	outcrop	<2	0.09	0.35	0.29	0.06	<0.02	icpms	783431	347103
1388	limestone with quartzite and siderite	Szendró Phyllite	C	outcrop	<2	0.08	3.11	1.14	0.12	<0.02	icpms	783680	346985
1389	sandstone	Szendró Phyllite	C	outcrop	<2	0.03	2.01	0.57	0.14	0.2	icpms	784462	346972
1390	limestone	Rakaca Marble	C	outcrop	<2	<0.02	0.81	0.21	<0.02	<0.02	icpms	782685	347357
1391	limonitic slate	Szendró Phyllite	C	outcrop	<2	0.06	6.95	0.43	0.16	<0.02	icpms	783511	347197
1392	pyritic limestone	Rakaca Marble	C	outcrop	<2	0.05	2.19	0.44	0.03	<0.02	icpms	782844	347584
1393	graphitic slate	Szendró Phyllite	C	outcrop	<2	0.11	13.6	0.25	0.25	<0.02	icpms	783570	347291
1394	sideritic limestone	Szendró Phyllite	C	outcrop	<2	0.08	2.45	0.24	0.02	<0.02	icpms	783693	347325
1395	limestone	Rakaca Marble	C	outcrop	<2	0.11	1.4	0.38	0.02	0.04	icpms	783730	347481
1396	limonitic slate	Szendró Phyllite	C	outcrop	5	0.37	25	3.61	0.38	0.02	icpms	783777	347265
1397	graphitic slate	Szendró Phyllite	C	outcrop	<2	0.1	12.8	0.34	0.2	0.04	icpms	783902	347176
1398	limestone	Rakaca Marble	C	outcrop	<2	0.06	0.39	0.26	0.03	<0.02	icpms	785661	347556

Explanations and remarks:

1. Age codes: O=Ordovician, S=Silurian, D=Devonian, C=Carboniferous, P=Permian, T=Triassic, J=Jurassic, Cr=Cretaceous, E=Eocene, Ol=Oligocene, M=Miocene, Q=Quaternary, H=Holocene.
2. Methods: icpms=infra colour plasma mass spectrometry, aas=atomabsorption spectrometry, fa=fire assay. Gold was analyzed by AAS method.
3. Coordinates: Egységes Országos Vetületi Rendszer (Unified National Projection System).
4. Items 1180, 1182, 1185, 1186, 1188, 1191, 1192, 1194, 1197, 1199, 1202, 1207, 1209, 1211, 1213, 1215, 1217, 1219, 1221, 1224, 1229, 1236, 1238, 1241, 1245, 1247, 1252, 1254, 1256 were analyzed at the SGS Lab. Ind. France and Don Mills, Ontario, Canada. (Courtesy of I. VÖRÖS, TVX).
5. Items 352, 362, 365, 371, 374, 456, 459, 460 were analyzed at the Analabs Pty. Ltd., Welshpool, Western Australia. (Courtesy of J. FÖLDESSY, Enargit).
6. Items 1041, 1042, 1177, 1232, 1233 were analyzed at the Laboratory of USGS, Denver. (Courtesy of A. HOFSTRA, USGS).
7. Item 805 was analyzed at the Analabs Pty. Ltd., Welshpool, Western Australia. (Courtesy of G. SZEBÉNYI, Recski Ércbányák/Recsk Ore Mine Company/).
8. Items 366–369 and 375–454 were analyzed in 1982–1983 at the Országos Érc- és Ásványbányák Rézérc Művei, Recsk, Laboratórium (National Ore and Mineral Mining Company, Copper Ore Mine Recsk, Laboratory)

